SENSITIVE RHYOLITIC PYROCLASTIC DEPOSITS IN THE TAURANGA REGION:

MINERALOGY, GEOMECHANICS AND MICROSTRUCTURE OF PEAK AND REMOULDED STATES

A thesis submitted in partial fulfilment

of the requirements for the degree

of

Master of Science in Earth Sciences

at

The University of Waikato

by

Michael J. Cunningham

THE UNIVERSITY OF
WAIKATO
Te Whare Wānanga o Waikato

The University of Waikato

2012

ABSTRACT

Soil sensitivity has previously been recognised as a significant contributor to soil failures both internationally and within New Zealand, particularly in the Tauranga region. Sensitive soils are characterised by initial high peak shear strength, yet very low remoulded shear strength. While international sensitive soils have been well characterised, the nature of sensitivity in rhyolitic deposits in New Zealand is poorly understood. This study characterises both sensitive and non-sensitive rhyolitic tephra derived soil samples from the Tauranga region in order to identify the fundamental differences in the materials between states of peak and remoulded strength.

Field and laboratory investigations were undertaken to analyse sensitivity. Field investigations included shear vane testing for the quantification of sensitivity, and stratigraphic profiling. Laboratory testing comprised geotechnical testing (particularly shear strength and Atterberg limits), petrographic observations through scanning electron microscopy (SEM) and X-ray diffraction (XRD), and measurement of the rheology of remoulded sensitive materials.

Five localities were used in this study. Three sites were considered sensitive (Omokoroa, Te Puna and Pahoia Peninsula), while the remaining two (Rangataua Bay and Tauriko) were considered non-sensitive on the basis of the Milne *et al.* (Milne, J.D.G.; Clayden, B.; Singleton, P.L.; Wilson, A.D. 1995: *Soil description handbook.* Manaaki Whenua Press, Lincoln, Canterbury) sensitivity test. Field observations showed sensitive material is of tephric origin, likely associated with the Te Puna Ignimbrite (~ 0.93 Ma). The deposits considered generally classify as sensitive to extra sensitive (7-15) with no samples being identified as quick. The non-sensitive material has characteristically different field behaviour where the material does not release moisture, or flow, upon remoulding. The non-sensitive material is associated with the Te Ranga Ignimbrite (~ 0.27 Ma).

Moisture contents are typically high for the sensitive materials, always exceeding their respective liquid limits (liquidity indices > 1), while the opposite is true for the non-sensitive samples. Porosity is also high for the sensitive materials (> 61 %), whereas non-sensitive materials return lower porosity values of < 60 %. Characterising the peak strength state of the sensitive materials, triaxial testing show consistent effective cohesion and friction angles ranging between 8–16 kPa and 28–41 ^{0}, respectively. Viscometric flow characteristics indicate that pH adjustment has a critical impact on remoulded sensitive material: typically as the pH becomes more alkaline, clay particle association is reduced and the soil weakens further, while with increased acidity there is a small increase in yield stress.

XRD indicates that all materials are dominated by halloysite. The wet to saturated rhyolitic materials promote a silica-rich environment that is slow draining, leading to favourable conditions for halloysite formation over other clay minerals. Most commonly, halloysite was observed in sphere, tube and to a lesser extent, plate morphologies. SEM, XRD and EDX analyses revealed previously undocumented, large (~ 60 µm–~ 1.5 mm) halloysite books in selected sensitive materials. The books are hypothesised to have formed from the incorporation of iron into the halloysite unit cell to form plate morphologies, followed by Ostwald ripening under conditions of low iron in the soil solution, and coalescence during a relatively dry period to form the large books.

The soil microstructure of the sensitive materials in comparison with the non-sensitive soils appears to provide the critical distinction in determining the variation between the peak to remoulded strength characteristics for the sensitive material. The sensitive

material is comprised of similar sized small spheres and short, stubby tubular halloysite morphologies. These pack inefficiently, producing a low density of packing. Such an arrangement produces many small micropores which facilitate the development of high moisture contents, producing liquidity indices > 1. The primary microstructure is matrix-skeletal for sensitive samples. The non-sensitive samples are comprised of large spheres and long, thin tubular halloysite morphologies. These particles pack much more efficiently, where the tubes fill the voids produced between large spherical formations. The result is a much tighter structural arrangement in the clay fraction, with reduced potential for high moisture contents to build up, leading to liquidity indices < 1. The non-sensitive material typically displays a matrix microstructure.

Upon remoulding, the structure of the sensitive material was broken down and appeared continuous. Connectors were typically destroyed, while tubes, plates and books were broken into smaller remnants. The similar sized spherical and tubular particles appeared to be easily mobilised following disturbance where they would fail in a fluidised manner from the high moisture held within the sample. The non-sensitive material, however, indicated very little change upon remoulding. The clay particle interactions were still arranged in a tight structure, which did not breakdown sufficiently to become entrained within the available moisture.

The sensitivity of rhyolitic tephra, therefore, is primarily attributed to the relative size and packing of the halloysite particle morphologies. The low density of packing produced an open structure, allowing for high moisture contents to develop, which following remoulding, leads to irreversible structural breakdown and release of stored water, promoting flow characteristics of the soil and thus high sensitivity.

ACKNOWLEGEMENTS

Firstly, I would like to acknowledge the support and dedication I have received from my supervisors Dr. Vicki Moon and Professor David Lowe. Vicki, from the first meeting to the end of this project, your enthusiasm and tireless efforts in helping to put this project together have been inspirational. Thanks for providing an excellent topic at the drop of a hat and allowing me to undertake all of the aspects I wanted in this project. David, thank you for all of the time and effort you have provided throughout. Your encouragement and expert knowledge have helped me greatly and your input to this project has been invaluable. Also to Dr. Jock Churchman, thank you for all of your help over the duration of this project and for taking the time to discuss the interesting world of halloysite clay minerals with me.

I am greatly appreciative of the financial support I have received for this thesis from the University of Waikato Masters' Research Scholarship and from the Broad Memorial Fund. The support allowed me to place all my efforts into this thesis project and undertake my fieldwork in the Tauranga region and I am very grateful to have had that opportunity. I also thank Peter Blakely from A&R Earthmovers at Tauriko for allowing me access to the pumice pit to collect samples.

I am very grateful to the staff from the Department of Earth and Ocean Sciences who helped me out during all stages of this project. Renat Radosinsky, your help through many parts of my laboratory testing was much appreciated and I thank you for taking the time to show me ropes of the triaxial apparatus. Thanks also go to Janine Ryburn, Helen Turner, Jacinta Parenzee and Annette Rodgers for all of the help provided in laboratory analyses of my samples. Thanks are due to Dr. Ganqing Xu for scanning my many samples with the XRD machine. Also, thanks to Associate Professor Roger Briggs for helping me to understand the complex stratigraphy of the Tauranga region. Professor Cam Nelson, thanks for helping me to grasp the concepts of clay mineral crystal structure analysis – your support was much appreciated.

I acknowledge and thank my fellow students in the Department of Earth and Ocean Sciences for all the bits and pieces along the way. Courtney, thank you for your help with Illustrator; and Kate many thanks for helping out with some of the finishing touches towards the end.

To Lisa, thanks for being there throughout all parts of this project and more. You were a superb field assistant, rain or shine, expert editor, and gave more to this project than I could have imagined (or put down here). Thanks for listening to my general ramblings and ideas about soil sensitivity and providing helpful advice along the way.

Finally, grateful thanks are extended to my family and friends who have been very supportive throughout this project. Mum and Dad, thanks for having me back around the house and for all of the encouragement throughout my years of study and for this project.

TABLE OF CONTENTS

LIST OF FIGURES

Chapter One

Chapter Two

Chapter Three

Chapter Four

Chapter Five

Chapter Six

Chapter Seven

Chapter Eight

LIST OF TABLES

Chapter Two

Chapter Three

Chapter Four

Chapter Five

Chapter Six

Chapter Seven

Chapter Eight

Chapter 1

INTRODUCTION

1.1 Background

Soil sensitivity has long been recognised as a significant contributor to the instability of slopes, primarily in post-glacial clay soils of the Northern Hemisphere. More recently, however, sensitivity has been documented locally in New Zealand (Jacquet 1987; 1990; Cong 1992; Keam 2008; Wyatt 2009; Arthurs 2010), giving rise to the importance of understanding the behaviour of such materials. Soil sensitivity is characterised by an initial high peak strength which, upon failure, is substantially reduced, leading to remoulding and flow. Given these characteristics, sensitivity is defined by the ratio of the undisturbed strength to the remoulded strength of a soil at constant moisture content (Skempton and Northey 1952; Gillot 1979). Sensitive soils are particularly hazardous because soil materials with only a relatively minor sensitive constituent can remain stable for a long period yet fail catastrophically resulting in infrastructure damage and potential loss of life.

Sensitivity of clay soils was initially reported in Northern Hemisphere regions such as Canada, Norway, Sweden, Japan and North America (Skempton and Northey 1952; Egashira and Ohtsubo 1982; Rankka *et al.* 2004; Mitchell and Soga 2005). These extensive deposits are primarily located in regions that were glaciated during the Pleistocene period. The sensitive clays, otherwise known as ‘quick clays’, are strictly of sedimentary origin and formed as a result of salts leaching from marine sediments deposited in a pro-glacial environment. Typically, these sensitive soil deposits produce landslides with very long run out distances, which often regress following initial failure. The formation and development of such highly sensitive materials have been extensively described, although the nature of sensitive soils recognised from New Zealand is poorly understood. This lack of understanding is compounded by the difference in

depositional environment and material source, where sensitivity in New Zealand is associated with rhyolitic pyroclastic deposits rather than pro-glacial sedimentary environments. Notwithstanding this difference, exceptionally high sensitivities have still been recorded, where in some cases quick clay behaviour has been observed in sensitive rhyolitic soil materials (Smalley *et al.* 1980; Arthurs 2010).

Although recent authors have attempted to characterise the formation of sensitive soils in New Zealand (Smalley *et al.* 1980; Jacquet 1990; Wyatt 2009; Arthurs 2010), a general consensus regarding the mechanism of sensitivity across multiple sensitive soils is yet to be achieved. Furthermore, a fundamental understanding of the changes inherent in the structural breakdown between the peak undisturbed state and remoulded state of sensitive material is not well established for rhyolitic sensitive soil. One location where landsliding events have occurred as the result of soil sensitivity is in the Tauranga region.

The Tauranga region (Figure 1.1) has continually proven to be a problem location for sensitive soil failures (Gulliver and Houghton 1980; Smalley *et al*. 1980; Burns and Cowbourne 2003; Wesley 2007; Keam 2008; Wyatt 2009; Arthurs 2010). Sensitive failures have been reported in a variety of locations within the region, including Omokoroa Peninsula, Otumoetai and Ruahihi. Each event has been considerable enough to produce substantial damage, prompting a serious land management issue for the region. Developing a comprehensive knowledge of sensitive soils from the region is thus of paramount importance. Furthermore, with this understanding, the development of possible mitigation methods and land planning stipulations based on sensitive soil hazards can then be produced, providing possible assurance for the communities within the region.

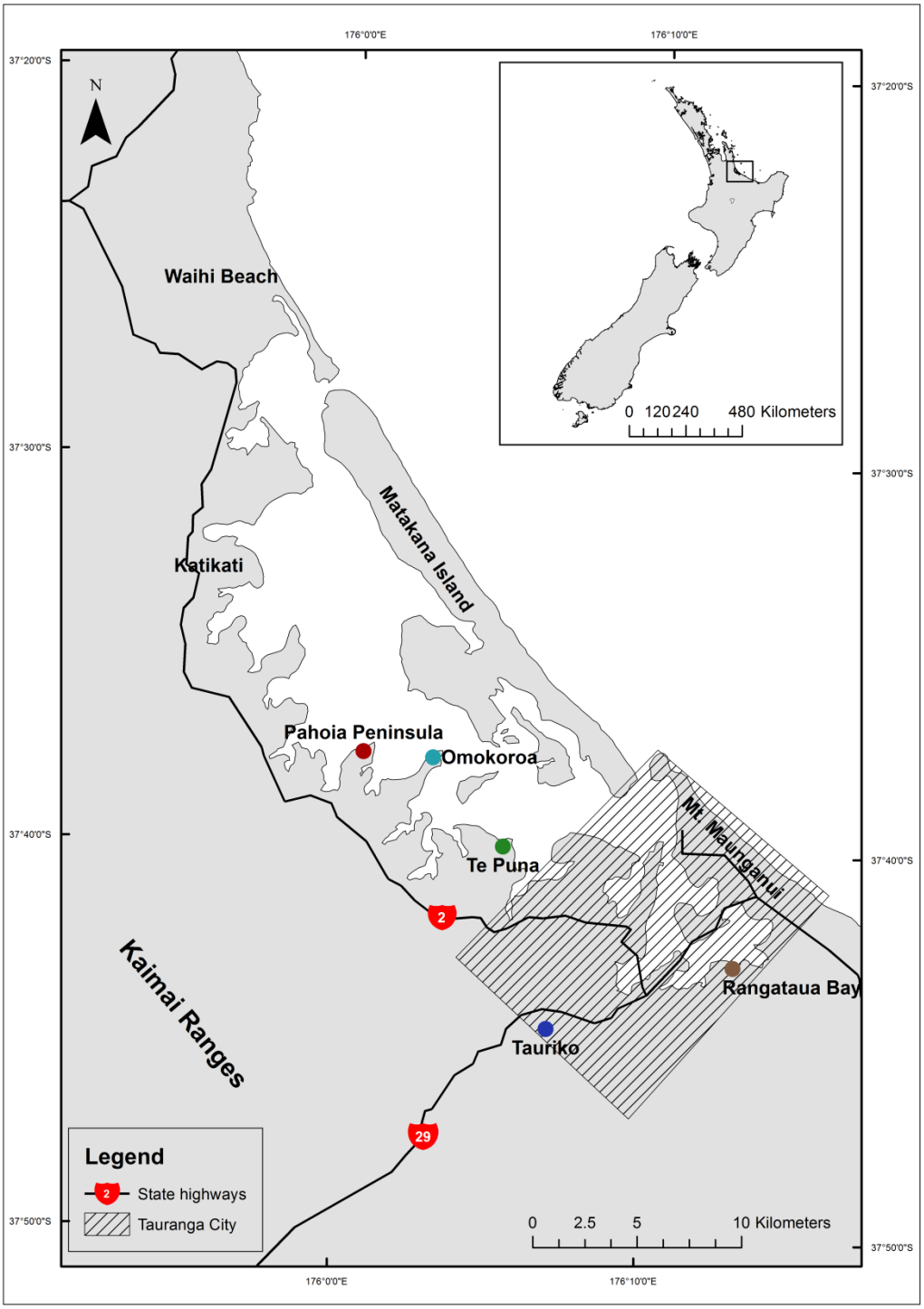

Figure 1.1: Map of the Tauranga region showing the locations of the sites chosen for this study (large dots).

1.2 Aim and objectives

The primary aim of this study is to understand the structural changes inherent in the breakdown of sensitive rhyolitic soils from the Tauranga region. This aim will be achieved through the following objectives:

1. Document the stratigraphy and engineering geologic properties of sensitive and non-sensitive materials.

2. Determine the peak and remoulded geomechanical properties of sensitive and non-sensitive materials.

3. Determine the petrography and microstructural variation between the peak and remoulded state of sensitive and non-sensitive soils.

4. Statistically examine relationships between various sensitive soil properties.

5. Characterise what structural variation leads to the development of sensitivity in rhyolitic soils from the Tauranga region.

To do this, five sites including examples of both sensitive and non-sensitive soils have been sampled and described to establish what key characteristics change between peak and remoulded states to determine what factors make a soil sensitive in the Tauranga region.

1.3 Thesis layout

Chapter 2 reviews the literature describing research previously undertaken on characterising sensitivity both internationally and more specifically in New Zealand. Clay mineralogy previously attributed to the sensitivity of volcanic and pyroclastic soil materials is then reviewed, as well as a summary of the relevant stratigraphic sequence found in the Tauranga region. Landslide geomorphology of sensitive soils is then identified, characterising previous failure events as the result of sensitive or general mass wasting processes. Chapter 3 describes all field and

laboratory methods used in this thesis. Chapter 4 discusses site selection and documents stratigraphic and engineering geologic descriptions at the selected sampling sites (objective 1). Field sensitivity summaries of all chosen locations are also presented. Chapter 5 presents all geotechnical related data, including Atterberg limits, particle size, triaxial shear strength and viscometric assessments on the soil materials (objective 2). Chapter 6 provides an assessment of the petrographic observations, covering both mineralogical and microstructural characteristics of the sensitive soils encountered (objective 3).Chapter 7 presents a linear regression statistical analysis of the data collected throughout this study (objective 4). Chapter 8 then discusses all of the main results from this study, including explanations of the differences between sensitive and non-sensitive material and their associated undisturbed and remoulded characteristics. Following this, an hypothesis for the development of sensitivity in rhyolitic tephra is given (objective 5). Chapter 9 summarises the main research findings from this study and gives recommendations for future research. All original data are presented in the appendices.

Chapter 2

LITERATURE REVIEW

2.1 Introduction

Sensitive soils have been identified in many environments both locally in New Zealand and internationally (Smalley *et al.* 1980; Jacquet 1990). Predominantly, sensitive clay materials have been identified in northern latitudes, where large failures have been identified (Gillott 1979; Gregersen 1981). Several studies have also identified volcanic derived soils in New Zealand to be sensitive in nature (Torrance 1983; Jacquet 1990; Wyatt 2009; Arthurs 2010). Sensitive soils are identified as soil materials that lose substantial strength upon remoulding, where previously stable soils fail catastrophically after disturbance. Characteristically, the transition from well-structured soil material to a failed state can occur with little or no rise in moisture content and low levels of applied stress (Selby 1993; Mitchell and Soga 2005). Understanding the critical characteristics which predispose these soils to failure is, therefore, essential in reducing landslide hazard.

2.2 Sensitive soils

The sensitivity of soils is defined as the ratio of the undisturbed shear strength to the remoulded shear strength (Jacquet 1990; Selby 1993; Lefebvre 1996):

$$Sensitivity = \frac{Undisturbed, undrained\ strength}{Remoulded, undrained\ strength} \tag{2.1}$$

The behaviour of sensitive material failures differ from non-sensitive material in many ways. Lefebvre (1996) identifies that non-sensitive material tends to stop at the bottom of the slope from which it has failed, and act as a

stabilising mass in the new geometry of the slope. Sensitive soil, in comparison, is far more dilatant and liquid-like, leading to very long runout zones (Torrance 1987; Selby 1993). The remoulding process involved in the mass movement consequently results in a significant decline in shear resistance, causing the material to behave in a viscous liquid-like form, and flow, leaving the slope unsupported (Lefebvre 1996; Mitchell and Soga 2005). Soil sensitivity is generally measured with the use of a shear vane, for both the intact peak and remoulded strength determinations.

Several different schemes exist for the classification of sensitive soils (Skempton and Northey 1952; New Zealand Geotechnical Society 2005), where terms defining sensitivity vary slightly. However, these classifications do conform to a general pattern where values less than 2 are considered insensitive, while values greater than 16 are considered quick (Table 2.1). In New Zealand the New Zealand Geotechnical Society (2005) classification is the recommended method for analysis, and will be hence used in this study.

Table 2.1: Soil sensitivity classification values as identified by (A) Skempton and Northey (1952) and (B) The New Zealand Geotechnical Society (2005)

A

Sensitivity values	Sensitivity categories
1	Insensitive clays
1-2	Clays of low sensitivity
2-4	Clays of medium sensitivity
4-8	Sensitive clays
8-16	Extra-sensitive clays
> 16	Quick clays

B

Descriptive term	Shear strength ratio (Undisturbed strength/Remoulded strength)
Insensitive, normal	< 2
Moderately sensitive	2-4
Sensitive	4-8
Extra sensitive	8-16
Quick	> 16

2.3 International sensitive soils

Sensitive materials have been widely observed in post-glacial marine environments in the Northern Hemisphere, typically in Canada and Scandinavia, but also in Japan (Ohtsubo *et al.* 1982; Lefebvre 1996; Locat *et al.* 2011). Sensitive clay deposits residing in the northern hemisphere are recognised as geologically young, having been deposited by the Wisconsin ice sheet retreat between 18,000 and 6,000 years before present (Lefebvre 1996). Furthermore, in Canada it is suggested that the largest deposits of post-glacial marine clays were formed in the Champlain Sea, which 12,500 to 10,000 years before present occupied the Gulf of St. Lawrence to the region around the city of Ottawa (Lefebvre 1996). Isostatic rebound from the last deglaciation has seen the uplift of certain sections of land masses, bringing these deposited clays to the surface (Liebling and Kerr 1965; Torrance 1978; Lefebvre 1996; Rankka *et al.* 2004).

Sensitive clays are characterised by low liquid limits, which are often less than 40%, while moisture contents are typically high, giving liquidity indices > 1 (Gillott 1979; Mitchell and Soga 2005). Dominant minerals in quick clays are generally low activity non-swelling clays and include illite, smectite and chlorite with non-clay constituents comprising quartz, feldspar, amphibole, and hydrous mica (Bentley and Smalley 1979; Egashira and Ohtsubo 1982; Torrance 1983; Mitchell and Soga 2005). Torrance (1983) suggests that the existence of high activity clays increases the liquid limits during leaching and in turn averts the development of high sensitivities. Torrance (1983) additionally advocates that the mineralogical requirement for quick clays to develop is for low activity minerals to dominate in the sediment.

The high sensitivity in Northern Hemisphere sensitive soils has primarily been attributed to the leaching of salt from pore water within the dominantly clay soil materials, together with the formation of a flocculated microstructure (Lefebvre 1996; Torrance 1992). For such flocculated conditions to arise, initially, soil particles must have a very slow settling velocity during formation (Smalley 1971). Additional to the slow sedimentation rate, inefficiently packed particle groups form in an initial strong flocculated structure (Torrance 1987) with edge-to-edge and face-to-edge particle interaction or in what Goldschmidt (1926)

termed a 'cardhouse' formation. The development of the flocculated structure is critical as it encourages a high moisture content, meaning sufficient water is available for fluidisation upon remoulding (Torrance 1983; 1992). The initial high salt concentration within the structure, however, is removed, where water introduced by rainfall or snowmelt percolates through the deposit, reducing the salt content (Rankka *et al.* 2004). Salt leaching can also occur by artesian water pressures in underlying soil or rock forcing water upward, or by the diffusion of salts towards areas of lower ion concentrations (Rankka *et al.* 2004). The leaching of salt is important where saline water is replaced with freshwater, weakening clay bonding and encouraging easily disturbed, short range inter-particle bonds (Smalley 1971). Furthermore, leaching reduces the ability of the particles to re-form their original structure after remoulding, meaning that the reduction in strength cannot be regained (Torrance 1992). Leaching of salts also tends to decrease the soil liquid limit of low activity clays, which also reduces the remoulded strength while maintaining a constant void ratio, thus increasing sensitivity (Mitchell and Soga 2005). Tavenas (1984) suggests that sensitive soil failures occur when salt content is less than 3 g l^{-1}. The impact of salt concentrations in Northern Hemisphere sensitive soils is illustrated in Figure 2.1.

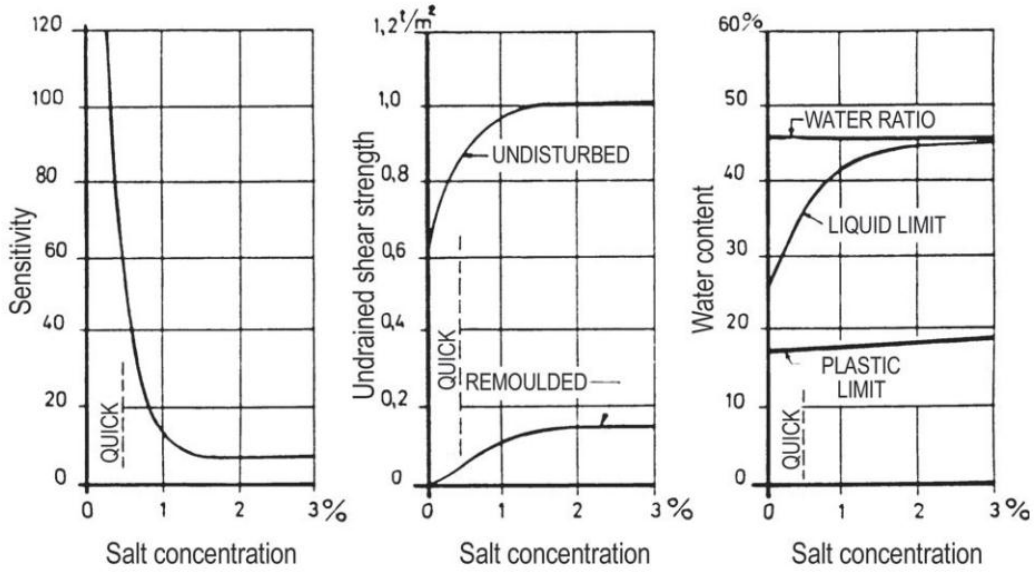

Figure 2.1: The impact of salt concentration leaching on sensitivity, undrained shear strength and consistency limits (Rankka *et al.* 2004 from Bjerrum 1954)

In relation to salt leaching, Mitchell and Soga (2005) also advocate that ion composition of the pore water is another key factor for the development of quick clays. Mitchell and Soga (2005) suggest that while leaching of salt causes little change to the microstructure of a sensitive soil, the interparticle forces are altered

which facilitate the low remoulded strength. Primarily, the large proportion of monovalent ions present in sensitive soils encourages a large double diffuse layer around clay particles (Rankka *et al*. 2004). Larger diffuse double layers result in greater repulsive forces between particles so upon remoulding of sensitive soils these forces prevent the reflocculation of clay particles and the primary structure is lost. As a result the soil becomes fluidised promoting failure (Rankka *et al*. 2004).

Although the leaching of salt is important for sensitivity, several authors indicate that it is not the sole controlling variable for the development of sensitive soils (Torrance 1992; Mitchell and Soga 2005). Other important factors include the cementation of aggregates by the precipitation of carbonates, iron oxide, alumina or organic matter at inter-particle contacts. Cementation increases the undisturbed strength which in turn increases sensitivity, as upon disturbance these cemented bonds are destroyed leading to a loss of strength (Mitchell and Soga 2005). Torrance (1983), however, adds that cementation alone would not produce a quick clay as the formation of a low remoulded strength is not altered by the presence of cementing compounds. Torrance (1983) attributes the role of cementation to increasing the undisturbed strength meaning that cementation only plays a secondary role to leaching in the development of quick clays.

Sensitivity in glaciomarine environments has previously been associated with flat, plate-like particle shapes, which easily form a flocculated sensitive structure (Pusch 1970). Aside from forming the edge to edge and face to edge structures, the particles are said to become easily separated upon remoulding, rather than a soil structure that is dominated by uniformly sized particles, allowing for fluidised soil characteristics (Rankka *et al.* 2004).

Volcanic ash has similarly been identified as a source of sensitive soils, primarily in Indonesia (Yong and Warkentin 1966; Wesley 1977). Unlike the sedimentary sensitive clays from Canada and Scandinavia, the explanation of sensitivity in volcanic sourced materials is yet to be mutually agreed upon. Yong and Warkentin (1966) suggested that high sensitivity was due to the presence of allophane, yet other Indonesian sensitive soils were found to have low levels of allophane (Wesley 1973). These contradictory conclusions suggest that sensitivity

born out of volcanic ash is highly variable in relation to parent materials and formation.

2.4 Soil sensitivity in New Zealand

Sensitive soils have also been recognised in New Zealand (Table 2.2), yet their origin and sensitive characteristics are quite different. Jacquet (1990) outlines that some fine grained volcanic ash deposits display a large loss in shear strength following remoulding. Typically these volcanic ash materials have been found in the Bay of Plenty, although several other deposits have been recognised from various sites in the North Island (Huntly, New Plymouth and Auckland) (Jacquet 1990; Arthurs 2010). The composition of pyroclastic soils in New Zealand generally consists of pumices and crystal fragments, clay minerals (such as halloysite, kaolinite and allophane), crystal fragments and glass shards (Wada 1987; Parfitt 1990; Arthurs 2010).

The presence of soil sensitivity within New Zealand has been recognised primarily through development and infrastructure works by various authors (Birrell 1951; Gradwell and Birrell 1954; Wesley 1968; Bullen and Campbell 1972; Campbell 1972; Aves 1973; Fullarton 1978; Prebble 1983). Jacquet (1987) compiled a bibliography of the physical and engineering properties of volcanic ash in New Zealand, which primarily identified sensitive volcanic soils in New Plymouth. The sensitive volcanic soils from the Taranaki region were of andesitic origin, where sensitivities ranged from sensitive to quick (4 – 21). Primarily mineralogy was identified to be mostly allophane with a gel like structure (Fullarton 1978), while halloysite comprised only a minor constituent. Gradwell and Birrell (1954) suggested that allophane allows a high moisture content to develop, which along with high void ratios leads to sensitivity. Jacquet (1987) was more conservative, suggesting that the presence of such mineralogical components along with microstructural characteristics were important for the unique properties of these soils, however indicated that the reasons for sensitivity were unknown.

As with international examples the explanation of sensitivity has led to much debate. In New Zealand the presence of pyroclastic sensitive soils has led to speculation that the presence of halloysite and allophane promote porous

structures which release water upon remoulding were keys to sensitivity. In following up this lack of understanding into sensitivity, Jacquet (1990) investigated a series of sensitive materials from the Taranaki and Waikato region. Jacquet (1990) encountered sensitivities between 5 and 55 in volcanic materials at or near saturation. Principally, Jacquet (1990) stated that the relative proportions of halloysite and allophane seem unrelated to sensitivity (on the basis that sensitivity was encountered in samples with both minerals). Rather, microstructural characteristics were suggested to be of most importance where sensitivity was primarily the result of the destruction of imogolite fibres between particles (Jacquet 1990). The irreversible destruction of these bonds on remoulding results in a large decrease in strength and thus the high sensitivity encountered.

2.4.1 **Sensitivity in the Tauranga region**

Several well documented examples of sensitive soils have occurred within the Tauranga region, primarily the Ruahihi Canal failure and the Omokoroa landslide of 1979. The Ruahihi Canal failure occurred in September 1981, 6 months following the completion of the Ruahihi Hydro Electric Project. Crucial to the cause of the failure was the widespread distribution of sensitive weathered Waimakariri Ignimbrite, which was identified as a major determining factor for the failure (Burns and Cowbourne 2003). The construction of the fill covering the Waimakariri Ignimbrite is suggested to have likely prevented free drainage from the Waihou Ignimbrite (underlying the Waimakariri Ignimbrite) (Burns and Cowbourne 2003). Preventing the drainage was recognised as leading to raised groundwater levels, promoting further cavities and piping erosion. Furthermore, the build-up of pore pressures was identified as destabilising the fill and allowing it to separate from the natural ground, furthering the sensitive nature and failure of the canal (Burns and Cowbourne 2003). Analysis of the sensitive material itself revealed very high moisture contents, which gave liquidity indices greater than 1. Sensitivity values were as high as 60, where a porous halloysitic structure was identified as the likely contributor (Oborn *et al*. 1982; Prebble 1986).

The August 1979 landslide failure in Omokoroa was a large event which was classified as a highly sensitive flowslide (Smalley *et al*. 1980; Gulliver and Houghton 1980). Following an investigation into the failure, Gulliver and

Houghton (1980) described the volcanic ashes of the soil profile as deeply weathered leading to extreme sensitivity. Smalley *et al*. (1980) identify that sensitivities of up to 140 were observed. Following analysis of the material, it was found that the clay mineralogy consisted of 80% hydrated halloysite and minor amounts of quartz and cristobalite (Smalley *et al*. 1980). Additionally, when plotted on the Casagrande Plasticity Chart all of the samples collected plotted below the A line, indicating that they had the properties of silt (Smalley *et al*. 1980). Critical to the 1979 failure, it was established that the natural water contents of the sensitive ash soils were exceptionally high at 60-100% and were repeatedly above their liquid limits (Smalley *et al*. 1980). Smalley *et al*. (1980) offers that the initial brittle failure at Omokoroa occurred due to the lack of long range bonds in the material, also known as the inactive-particle, short-range-bond theory. Effectively, this is due to very few active clay minerals in the soils and so although materials may have a high clay content, they do not display a high plasticity as may be expected (Smalley *et al*. 1980). Following failure of such materials, the clays become disaggregated and the abundant water supports the separated particles leading to long run out distances.

As part of a wider study on the engineering geological features of the Omokoroa Peninsula, Keam (2008) investigated the failure mechanisms of the Bramley Drive failure. Keam (2008) reported that excess pore water pressure from both natural and anthropogenic sources is the primary mechanism for the loss of strength for the sensitive rhyolitic ash unit. Initially, negative pore water pressures provide some stability within the soils allowing for a high undisturbed strength, however, once the pressure increases, the soil loses all strength and flows (Keam 2008).

On the 11th of May 2011, the Omokoroa failure of 1979 was reactivated (Tonkin and Taylor 2011). According to a subsequent consulting report on the failure, it was concluded that both the prolonged period of heavy rainfall which preceded the failure and the presence of highly sensitive material resulted in the failure (Tonkin and Taylor 2011). The Tonkin and Taylor (2011) report similarly suggests that the soils that were exposed from the initial August 1979 failure were weakened over time due to weathering of the slope. The report suggests that

headscarp regression is likely to continue by up to 10 metres over the next 10 years (Tonkin and Taylor 2011).

The presence of sensitive rhyolitic material was also encountered following a landslip in Otumoetai, Tauranga from a large storm event in May 2005 (Wesley 2007). Wesley (2007) reported long run-out distances for the landslides at Otumoetai, suggesting that the abundant supply of water lubricated the failure surface along with the sensitive soil. Sensitivities up to 97 were encountered below the Hamilton Ash sequence. Sensitivity was highly variable, yet was most prominent in pale silty CLAY to CLAY material. The soil mineralogy was again considered to be predominantly halloysite. Like Keam (2008), Wesley (2007) suggested that the failure was the result of the rise in pore pressure from the percolating rainfall, which at a critical point would lose all strength and liquefy. The typical presence of liquidity indices greater than 1 suggested that such fluidised behaviour upon remoulding was to be expected.

In another recent study, Wyatt (2009) attempted to characterise the sensitivity of rhyolitic tephra derived sensitive soils from Otumoetai and Tauriko in Tauranga. Wyatt (2009) suggested that key controls on sensitivity for the Tauranga region of New Zealand were primarily due to halloysite mineral composition of the clays. Importantly, Wyatt (2009) found that allophane was sparse in the Tauranga region and halloysite was the dominant clay mineral in the sensitive soils. Due to the slow draining environment, halloysite formation was promoted, where the water within the soil microstructure could be released upon remoulding. Furthermore, the presence of halloysite would typically be expected in a slow draining rhyolitic environment rather than allophane (further discussed in section 2.5.2). It was noted that the electrostatic bonds supporting the halloysite minerals increased, the undisturbed soil strength allowing the natural moisture contents to be exceeded. Furthermore, it is suggested that the high natural moisture content of the clays could exceed the liquid limits, where the water held in the pores dilutes the plasticity and suspends the aggregates of clay and larger grains following disturbance (Wyatt 2009). Wyatt (2009) therefore proposed that similar to international sensitive clays, liquidity indexes greater than 1 are an essential component of rhyolitic sensitive material. In contrast to previous studies from Jacquet (1990) and Torrance (1992) he indicated that sensitivity in Tauranga

region was manifested in low remoulded strengths, rather than particularly high material peak strengths.

Arthurs (2010) similarly identified sensitive soils in the Tauranga region, but also looked in a wider sense, attempting to correlate soil sensitivity solely within the Kidnappers Ignimbrite and associated tephra deposits. He suggested that Kidnappers Ignimbrite deposits could be identified both in Tauranga and Auckland and found that soil sensitivity ranged from 5 (moderately sensitive) to 24 (quick). The identification of the Kidnappers Ignimbrite in the Tauranga region, however, is somewhat contentious. Arthurs (2010) stated that the Kidnappers Ignimbrite is correlative of the Te Puna Ignimbrite, originally identified by Harmsworth (1983), on the basis of field mineral identification, the presence of accretionary lapilli and stratigraphic position. Considering both deposits are sourced from the Taupo Volcanic Zone, the field similarities between the Te Puna and Kidnappers ignimbrites are not surprising. Furthermore, the similar age range between the two deposits (0.97-1.08 Ma Kidnappers Ignimbrite and 0.93 Ma Te Puna Ignimbrite; Wilson *et al.* 1995; Briggs *et al.* 2005) does imply consistencies between the two deposits. Critically, however, the deposits are distinguished by their magnetic polarity. Wilson *et al.* (1995) identify that the Kidnappers Ignimbrite has normal magnetic polarity, interpreted to lie within the 0.99-1.07 Jaramillo Subchron. Conversely, the primary magnetisation of the Te Puna Ignimbrite is suggested to be reversed (Briggs *et al.* 1996), yet still interpreted to still lie within the Matuyama Chron (Briggs *et al*. 2005). This evidence indicates that the Kidnappers and Te Puna ignimbrites cannot be correlatives of each other and thus are not the same unit. Other field evidence for disputing the correlation includes previously identified characteristics. Whitbread-Edwards (1994) suggested that the Te Puna Ignimbrite is non-welded to partially welded, while Wilson *et al.* (1995) indicate that the Kidnappers Ignimbrite is completely non-welded. While the collation of this evidence does not rule out the potential sensitivity of the Kidnappers Ignimbrite, it does indicate that sensitivity in the Tauranga region is potentially associated with the Te Puna Ignimbrite, and not the Kidnappers ignimbrite.

Nevertheless, Arthurs (2010) advocated that weathering of Kidnappers/Te Puna Tephra to produce low activity clays (particularly halloysite and kaolinite)

promoted sensitivity. Furthermore, Arthurs (2010) noted that sensitivity was established by high natural water contents which often exceeded the liquid limit of the soil. He suggested that this required the soil to have high porosity and that the soil is located at or below the water table. Arthurs (2010) concludes that in addition to the aforementioned criteria, materials prone to sensitivity are distal pyroclastic deposits, as opposed to proximal deposits, as they have smaller grain size and have a slower, shallower burial.

Table 2.2: Summary of studies on soil sensitivity in New Zealand

			Geomechanical Properties								
	Locations	**Materials**	**Peak Strength (kPa)**	**Remoulded Strength (kPa)**	**Liquid Limit (%)**	**Plastic Limit (%)**	**Plasticity Index (%)**	**Liquidity Index (%)**	**Sensitivity**	**Mineralogy**	**Structure**
Gulliver and Houghton (1980)	Tauranga (Omokoroa)	clayey SILT, red yellowish brown with black speckles	80-42	2-11	-	-	-	-	7-140	halloysite	-
Smalley *et al.* (1980)	Tauranga (Omokoroa)	Silty CLAY	-	-	-	-	-	-	Up to 140	halloysite, quartz, feldspar, cristobalite	-
Jacquet (1990)	Huntly, New Plymouth	Volcanic ash, massive, firm, sticky, varying colours (light pink, reddish yellow, dark brown, yellowish brown), clayey SILT and silty CLAY ferromagnesian crystals.	80-380	3-19	99-133	43-84	20-48	0.49-0.78	5-55	halloysite, allophane	Imogolite fibre networks, aggregates of halloysite tubes
Wesley (2007)	Tauranga (Otumoetai)	CLAY, silty CLAY, pale yellowish brown, homogeneous, black specks	72-107	1-4	60-96	48-66	5-44	0.78-2.7	24-72	-	-
Wyatt (2009)	Tauranga (Tauriko, Otumoetai)	**Tauriko:** Clayey SILT, trace fine sand, light pink with black flecks (MnO_2) coarse pebbles representing pumiceous flecks. **Otumoetai:** Sity CLAY, Clayey SILT, CLAY, dark greyish brown to dark yellowish brown with black flecks, (MnO_2).	45-172	2-34	51-96	32-57	13-42	0.27-2.41	**Tauriko:** 5-22, **Otumoetai:** 5-14	**Tauriko:** halloysite, quartz feldspar **Otumoetai:** halloysite, kaolinite, quartz, feldspar	**Tauriko:** halloysite tubes, books, irregular plates and polygonal spheres. **Otumoetai:** Halloysite tubes, plates and spheres.
Arthurs (2010)	Tauranga (Pahoia, Omokoroa, Te Puna, Otumoetai), Auckland (Ahitu, Mangatawhiri, Ohuka), Matata	**Tauranga:** White clayey SILT, pink orange, brown clayey SILT. **Auckland:** Pink clayey SILT, white clayey SILT. **Matata:** Greyish blue clayey SILT	**Tauranga:** 53-260. **Auckland:** 71-112. **Matata:** -	**Tauranga:** 3-22. **Auckland:** 4-18. **Matata:** -	42-98	30-66	12-48	0.88-2.39	**Tauranga:** 7-23. **Auckland:** 7-17. **Matata:** -	**Tauranga:** halloysite dominated, some kaolinite. **Auckland:** halloysite and kaolinite. **Matata:** smectite-illite, chlorite, kaolinite	**Tauranga:** skeletal-matrix, matrix skeletal. **Auckland:** skeletal matrix, matrix. **Matata:** skeletal

2.5 **Clay minerals**

Within the North Island landscape of New Zealand, pyroclastic deposits provide a suitable environment for the weathering and formation of clay minerals. Deposits of volcanic ash and pumice are typically weathered and form a variety of clay minerals by dissolution and precipitation (Wada 1987). Typical crystalline clay minerals formed in volcanic derived materials in New Zealand include halloysite, kaolinite and allophane (Parfitt *et al.* 1984; Lowe and Percival 1993). On the basis of the clay mineral identifications made in previous studies into sensitivity both from the Tauranga region and other locations around New Zealand (Jacquet 1990; Wesley 2007; Wyatt 2009; Arthurs 2010), the formation of these three clay minerals are reviewed in the following section. A summary of the clay mineral properties is presented in Table 2.3.

2.5.1 **Halloysite**

Halloysite is recognised as a 1:1 phyllosilicate clay mineral with 1 tetrahedral sheet to 1 octahedral sheet of the kaolin group (Joussein *et al.* 2005) (Figure 2.2). The unit layers in halloysite are separated by a monolayer of water molecules where hydrated halloysite has a basal spacing of spacing of 10 Å. Joussein *et al*. (2005) however notes that the interlayer of water in halloysite is weakly held, and the mineral therefore can irreversibly dehydrate giving a dehydrated halloysite form with a basal spacing of 7 Å.

Halloysite particles are identified in various morphologies (Table 2.2), of which most commonly recognised is tubular (Joussein *et al.* 2005). Other morphologies include, plates, spheres and most recently discovered in New Zealand, books (Bailey 1990; Singer *et al.* 2004; Etame *et al.* 2009; Wyatt 2009). Halloysite morphology, chemical composition and conditions are closely linked (Parfitt *et al*. 1984; Singer *et* al. 2004; Joussein *et* al. 2005). Tube morphologies dominate halloysite formation, primarily due to the interlayer water present in the structure as well as the apparent lack of Fe. The interlayer water prevents rotation of the tetrahedral sheet, while a lack of Fe in the octahedral sheet means that the larger tetrahedral sheet curls around the outside of the octahedral sheet, forming the tube shape (Churchman 2000; Churchman and Lowe 2012). Moreover,

Joussein *et al.* (2005) suggest that the relationship between the three main morphologies of halloysite (tube, spherical, and platy) and Fe content display conclusive trends. Typically platy forms of halloysite contain large amounts of Fe. Initially halloysite is formed with an unmatching octahedral Al sheet and tetrahedral sheet of Si. Where Fe^{3+} is incorporated, it substitutes for the Al^{3+} in the octahedral sheet (Churchman and Lowe 2012). The Fe^{3+} to Al^{3+} substitution allows for the correction of the unmatching tetrahedral and octahedral sheets and thus produces flat plates and reduces curvature. Where the situation arises of low Fe content in halloysite minerals as previously mentioned, tube curvature and thus formation is common (Churchman and Lowe 2012). Singer *et al.* (2004) identify that spheroidal halloysite particles have higher SiO_2/Al_2O_3 ratios compared to other morphologies and typically varying Fe content, ranging from very low to very high. The varying iron content indicates that it content does not have specific control over the spheroidal morphology (Joussein *et* al. 2005).

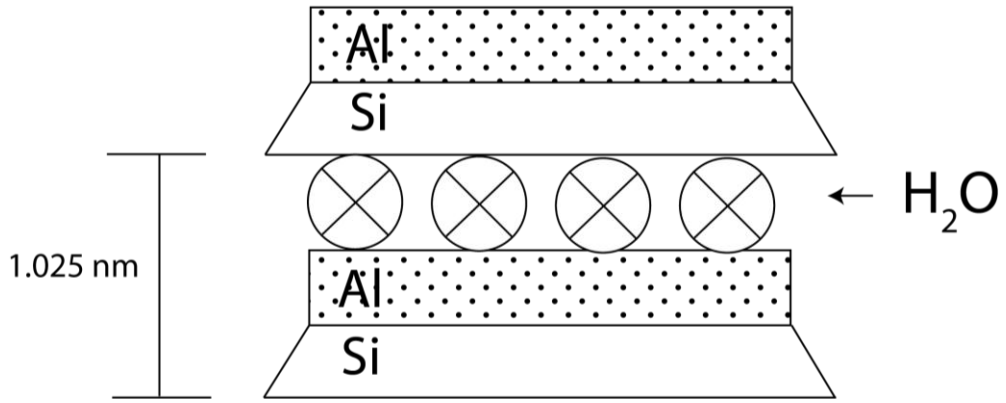

Figure 2.2: Schematic representation of the layers forming halloysite, after Selby (1993).

Halloysite is formed by a range of parent materials, but perhaps most important in New Zealand is the weathering of pumice and volcanic glass (Joussein *et al.* 2005; Jacquet 1990). Fieldes (1955) suggest that halloysite is typically formed via the weathering of volcanic ash to allophane to hydrated halloysite. Parfitt *et al.* (1984) subsequently suggested that volcanic ash can weather by dissolution and precipitation directly to halloysite from primary minerals, as well as to allophane, imogolite and ferrihydrite.

Influencing the conditions for halloysite formation directly from primary materials is the presence of a silica rich environment (Churchman 2000; Churchman *et al.* 2010). Joussein *et al*. (2005) identify that high rainfall events promote higher silica exposure in tephra material, where the leaching of silica is great through the profile. Furthermore, conditions where moisture is retained within a soil profile is also favoured for halloysite formation, where silica is not leached out of a profile and so the potential for halloysite formation remains high (Wada 1989). Therefore suggested that the abundance of water is critical to halloysite formation and thus halloysite is common in more saturated sections of a soil profile (Churchman 1990).

The behaviour of halloysite is strongly linked to its morphology. In plate form, halloysite has strong inter-particle interaction due to Van Der Waals bonds, however in tube and spherical form, it is suggested to have lower activity with weaker interactions (Smalley *et al.* 1980; Joussein *et al.* 2005). Contacts between morphologies of halloysite can also be a significant factor. Edge-to-edge, face-to-face and edge-to-face are the types of contacts between the clay morphologies, which have a impact strength (Selby 1993). Face-to-face contacts are recognised as having the greatest strength while edge-to-edge have the least due to the decreased surface area for bonding.

Specifically in the Tauranga region, several authors have encountered halloysite morphologies in sensitive soils identified (Smalley *et al.* 1980; Keam 2008; Wyatt 2009; Arthurs 2010). The dominant presence of halloysite indicates that it is important for the development of sensitive rhyolitic deposits.

2.5.2 **Allophane**

Allophane is a short range order aluminosilicate which is characterised by small, hollow, porous spheres between ~ 3 – 5 nm (van der Gaast *et al.* 1985; Kaufold *et al.* 2010). Allophane can be recognised as one of the first mineral adaptation products from volcanic ash where it can be found in weathered pumices, making it particularly important in a New Zealand soil context given the volcanic environment (Kaufold *et al.* 2010). Allophane spherules are also recognised to interact with each other strongly, especially if they are dried where

they can form silt and sand sized aggregates (Parfitt 1990). Parfitt (1990) identified that allophanic soils have a high undisturbed strength. Additionally, he adds that on remoulding allpphane soils lose significant strength, making them comparable to quick clays. The high undisturbed strength is attributed to the electrostatic and physical bonds which form between allophanic spherules (Parfitt 1990).

Allophane is established as a mineral which is relatively stable in soils, where it forms rapidly from fine grained glass particles (Parfitt 1990). Three types of allophane can be recognised in New Zealand, namely Al-rich allophane, Si-rich allophane and stream deposit allophane (Parfitt 1990; Lowe and Percival 1993; Lowe 1995). Al-rich allophane has an Al:Si ratio of 2:1 and has been named proto-imogolite allophane because of its imogolite inter-connections (Lowe 1995). Si-rich allophane has an Al:Si ratio of 1:1. The silica in these soils is primarily controlled by drainage and leaching in the soil (Parfitt 1990). Stream deposit allophanes have Al:Si ratios between 0.9-1.8. They differ from other allophonic particles because they appear as hollow spherules, which form globular aggregates (Wells *et al*. 1977). The formation of Al-rich allophane is typically favoured in andesitic materials as opposed to rhyolitic materials. Lowe (1995) suggests that the dissolution of andesitic glass is much faster than volcanic glass of rhyolitic origin, meaning that Si in solution is easily lost through rainfall leaching and so the predominance of Al remains in the soil. Conversely, the slower rate of Si leaching from rhyolitic glass promotes halloysite formation (Nanzyo 2002).

2.5.3 **Kaolinite**

The clay mineral kaolinite is a 1:1 phyllosilicate clay which, unlike halloysite, is resistant to expanding, remaining at its original size when water is present (Figure 2.3) (Selby 1993; Mirabella *et al*. 2005). Instead of water molecules occupying the interlayer space, typically hydrogen is present (Selby 1993). Kaolinite therefore, forms where some profile dehydration occurs rather than the wet conditions required for halloysite (Churchman *et al.* 2010). Kaolinite has a basal spacing of 7 Å and is typically characterised by a platy morphology (Jouissen *et al*. 2005; Ekosse 2010). Kaolinite minerals consist of one octahedral

Si^{4+} sheet and one tetrahedral Al^{3+} sheet. These sheets, however, have a dimensional misfit but are corrected by the rotation of the alternative tetrahedra in opposite directions (Jouissen *et al*. 2005). Kaolinite has been intermittently observed in recent studies in New Zealand sensitive soils, however, allophane and halloysite formations appear more dominant (Jacquet 1990; Wyatt 2009; Arthurs 2010).

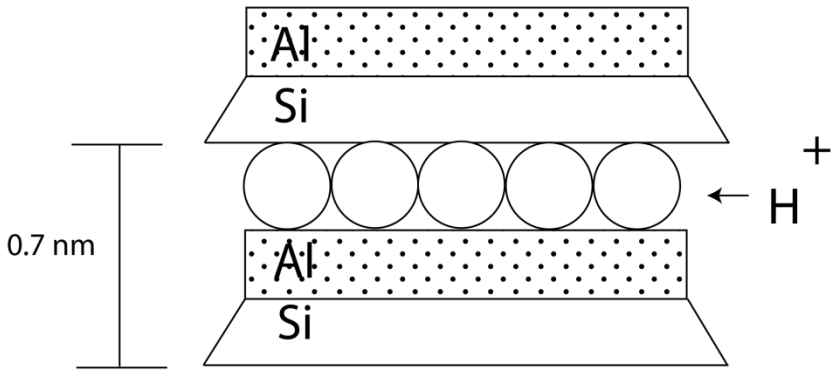

Figure 2.3: Schematic representation of the layers forming kaolinite after Selby (1993).

Table 2.3: Summary of types of clays typically associated with sensitivity in New Zealand

	Clay type	**Morphology**	**Formation**	**Locations found in New Zealand**
Halloysite	1:1 layer clay mineral	Tubes, spheres, plates, books (Selby 1993; Joussein *et al.* 2005; Wyatt 2009)	Direct weathering of volcanic ash (Parfitt *et al.* 1984)	Auckland, Huntly, New Plymouth, Tauranga (Arthurs 2010; Jacquet 1990; Wyatt 2009)
Allophane	Short range order aluminosilicate	Hollow porous spheres (Selby 1993; Lowe 1995)	Where Si is low, Al rich allophane is formed or where Si is high Si rich allophane may form (Lowe 1995)	North Island, NZ (Huntly, Auckland, Mt Ruapehu, New Plymouth, Ohaewai) (Jacquet 1990; Parfitt 1990)
Kaolinite	1:1 layer clay mineral	Hexagonal plates (Selby 1993)	Direct precipitation with $Al(OH)_3$ and SiO_2 forming sheet structures	New Zealand wide (e.g. Waikato, Tauranga, Auckland) (Ward 1967; Wyatt 2009; Arthurs 2010)

2.6 **Tauranga geology**

The geologic setting of the Tauranga Basin comprises of late Pliocene to Pleistocene sedimentary material, situated on the western fringe of the Bay of Plenty region (Briggs *et al*. 1996). The basin consists of a multifaceted sequence of volcanic, pyroclastic and sedimentary deposits, situated between the Coromandel Volcanic Zone (CVZ) and the Taupo Volcanic Zone (TVZ) (Briggs *et al*. 1996; 2005). The western boundary of the Tauranga Basin is characterised by the Kaimai Ranges, from where it extends east over an area of 570 km^2 to the Pacific Ocean (Briggs *et al*. 1996). Aside from the early Otawa Volcanics (andesitic lavas), the primary and reworked volcanic materials observed in the Tauranga Basin are characterised as predominantly rhyolitic in composition (Briggs *et al*. 1996).The volcanic events and subsequent pyroclastic flows resulted in large ignimbrites which were typically reworked via estuarine and fluvial processes, eventually deposited in alternating sequences with primary volcanic deposits (Figure 2.4) (Briggs *et al*. 1996; Briggs *et al.* 2005). The following section will describe each unit within the Tauranga stratigraphy in order of age.

GENERALISED STRATIGRAPHY OF THE TAURANGA REGION

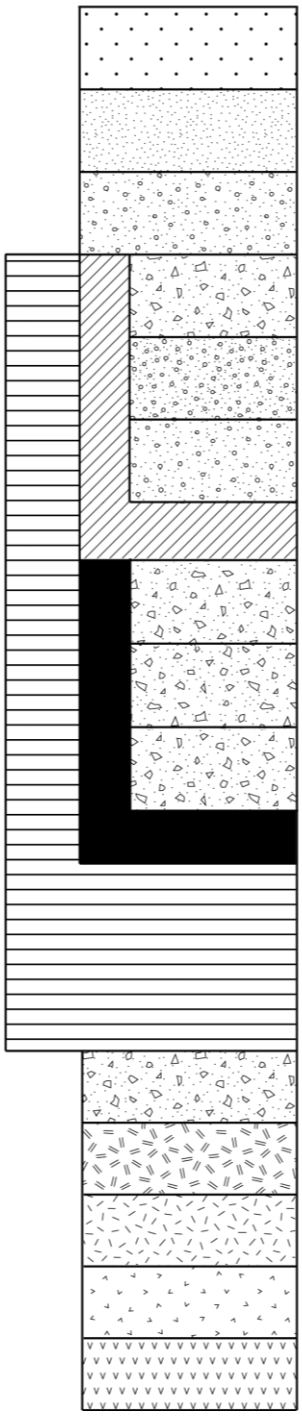

	Age
Holocene alluvium and dunes	
Holocene and Late Pleistocene tephras	< ~ 50 ka
Rotoehu Ash	~ 60 ka
Mamaku Ignimbrite	0.22 Ma
Waimakariri Ignimbrite	< 0.27 Ma
Te Ranga Ignimbrite	0.27 Ma
Hamilton Ash	0.1 - 0.35 Ma
Te Puna Ignimbrite	0.93 Ma
Ongatiti Ignimbrite	1.34 Ma
Papamoa Ignimbrite	1.9 - 2.4 Ma
Pahoia Tephra	0.35 - 2.18 Ma
Matua Subgroup (fluviatile sands and gravels, lignites, estuarine sands, lucustrine silts)	~ 60 ka - 2.09 Ma
Waitetariki Ignimbrite	2.09 Ma
Kopukairua Dacite	2.20 Ma
Matakana Basalt	2.7 Ma
Mindin Rhyolite	1.95 - 2.89 Ma
Otawa Volcanics	2.54 - 2.95 Ma

Figure 2.4: Stratigraphy of the Tauranga region compiled from Briggs *et al.* (1996); Briggs *et al.* (2005); Briggs *et al.* (2006); Wilson *et al.* (2007).

2.6.1 **Waitearikí Ignimbrite**

Several ignimbrite sheets are prominent in the Tauranga region, of which the Waitearikí Ignimbrite (2.09 Ma) forms the foundation of the Tauranga Basin at depths of 50-150 m (Briggs *et al*. 1996). The Waitearikí Ignimbrite was established before the uplift of the Kaimai Range, after which it was tilted and uplifted 3-5 º NE towards the Tauranga Basin. The Waitearikí Ignimbrite is overlain by multiple layers of volcanic, pyroclastic and sedimentary deposits, which, following episodes of erosion and redeposition, form the present setting (Briggs *et al*. 1996; Arthurs 2010). Briggs *et al.* 2005 identifies that the Waitearikí Ignimbrite is a large volume welded ignimbrite, which in places is greater than 220 m thick. The Waitearikí Ignimbrite can be subdivided into three sections, namely: (a) a lower 3-5 m non-welded pumice-rich foundation, (b) a middle portion consisting of 150 m of welded ignimbrite which incorporates medium to very densely welded glass lenses and finally (c) an upper welded to non welded soft unit approximately 50-70 m thick (Briggs *et al*. 1996). Exposed outcrops in the Tauranga region typically consist of the upper to middle portion (Briggs *et al*. 1996). Waitearikí Ignimbrite samples differ in composition from rhyolitic to dacitic (Briggs *et al*. 1996).

2.6.2 **The Matua Subgroup**

The Matua Subgroup is a major constituent of the Tauranga stratigraphy (Briggs *et al.* 1996), originally defined as part of the Tauranga Group by Kear and Schofield (1978). All terrestrial and estuarine deposits that postdate the Waitearikí Ignimbrite are defined as the Matua Subgroup (0.22 - 2.09 Ma) (Briggs *et al.* 2005; 2006). Furthermore, the upper boundary of the Matua Subgroup was originally recognised as the Mamaku Ignimbrite (Briggs *et al*. 1996; 2005), while Briggs *et al.* (2006) suggest that the most upper unit is the Rotoiti Tephra, which would include the Rotoehu Ash (~ 60 ka). The Matua Subgroup incorporates a broad range of lithologies, including pumiceous and rhyolitic silts, sands and gravels, estuarine muds, peats, lignites and air fall tephra which vary rapidly vertically and laterally (Briggs *et al.* 1996; 2005; 2006). Sedimentary deposits are defined as those which post-date the Waitearikí Ignimbrite (2.09 Ma) and pre-date the Hamilton Ash (0.35 Ma). Sediments found in the Matua Subgroup have an assortment of structures such as cross bedding, planar stratified and massive units

(Briggs *et al.* 2006). Other structures include post depositional slump and water escape structures (Briggs *et al*. 1996). The Matua Subgroup sediments are suggested to be derived from erosion, transportation and redeposition of reworked ignimbrites, tephras and lava flows from the Tauranga volcanic centre and the TVZ (Briggs *et al.* 1996; 2005). The Matua Subgroup deposits have been observed at depths of approximately 150 m in the Tauranga Basin (Briggs *et al*. 1996), while terraces, approximately 80 m in height, formed by the sediments of the Matua Subgroup are observed (Briggs *et al.* 2005). Importantly, Briggs *et al.* (2006) suggests that the Matua Subgroup is very susceptible to marine cliff erosion and landslides, especially where wet conditions prevail.

2.6.3 **Pahoia Tephras**

Pahoia Tephras (2.18 - 0.35 Ma) are highly weathered ashes of rhyolitic composition which lie below the Hamilton Ash Formation (Harmsworth 1983; Briggs *et al.* 1996). Halloysite formed from rhyolitic Pahoia Tephra beds was observed by Kirkman (1977), near Opotiki (Bay of Plenty). Briggs *et al.* (1996) describe the Pahoia Tephra as a group of several tephras, which may correlate to the Kauroa Ash Formation, which is characterised as severely weathered, clay rich rhyolitic tephra observed under the Hamilton Ash in the Waikato region. Within the Pahoia tephra sequence are sediments of fluvial origin as well as distal ignimbrites (Briggs *et al.* 1996).

Exposed sections of Pahoia Tephras have been observed in coastal areas at Greerton, Maungatapu, Matapihi, Matua, Omokoroa and the base of Mt Maunganui in the Tauranga region (Briggs *et al.* 1996).

2.6.4 **Papamoa Ignimbrite**

The Papamoa Ignimbrite (1.9 – 2.4 Ma) is distributed in the north-eastern Tauranga region. Outcrops can be identified at the foothills of the Papamoa Ranges (Briggs *et al*. 1996). Where the ignimbrite extends north from the Papamoa Ranges, it gently dips and thins in a fan-like distribution (Briggs *et al*. 1996). The Papamoa Ignimbrite can be characterised as a medium to strong rock with wide joint spacing (Briggs *et al*. 1996). Additionally the Papamoa Ignimbrite

is made up of numerous flow and interbedded fall deposits, however the source of the ignimbrites is unknown (Briggs *et al.* 2005).

2.6.5 **Ongatiti Ignimbrite**

The Ongatiti Ignimbrite (1.34 Ma) originated from the Mangakino Volcanic Centre and is one of the largest eruptive units from the Taupo Volcanic Zone (Briggs *et al.* 2005). The Ongatiti Ignimbrite is characterised as being partially to densely welded rhyolitic material. Depending on the welding, the Ongatiti Ignimbrite varies from weak to very strong rock with joints ranging from 0.3 m to 4 m in width (Briggs *et al.* 1996). The voluminous ignimbrite extends from Mangakino to the west coast of the North Island, but is only locally recognised in the Tauranga region (Briggs *et al.* 1996).

2.6.6 **Te Puna Ignimbrite**

The Te Puna Ignimbrite (0.93 Ma) is recognised as a small volume ignimbrite (< 5 km^3). Briggs *et al.* (2005) recognises that the Te Puna Ignimbrite corresponds to either locally derived eruptive events only in the Tauranga Basin, or of widespread formation from currently unidentified ignimbrites from the Taupo Volcanic Zone. The Te Puna Ignimbrite varies in character from non-welded weak rock to partially welded rock of medium strength, typically with no joints, which weathers to a firm clay (Briggs *et al*. 1996). At both Omokoroa and Pahioa Peninsula the ignimbrite is sequenced with Matua Subgroup fluvial and estuarine sands and Pahioa Tephras. Briggs *et al.* (1996) establishes that this intercalation leads the material to be very prone to shallow and deep landsliding under wet conditions, which can be observed in these areas.

2.6.7 **Hamilton Ash**

The Hamilton Ash Formation (0.35 – 0.1 Ma) has been recognised throughout the Waikato, Auckland and Tauranga regions (Ward 1967; Pain 1975; Briggs *et al.* 1996). Typically Hamilton Ash is characterised by a sequence of highly weathered, clay-textured tephra beds and paleosols usually between 3 – 5 m thick (Ward 1967; Lowe and Percival 1993). Briggs *et al*. (1996) describe the

Hamilton Ash sequence in eight divisions (H1-H8), however all eight units are not expected at any one site. The unobserved units are often due to the erosion of beds and the existence of paleosols visible on profiles (Briggs *et al.* 1996). The H1 unit has been identified as the Rangitawa Tehpra. The Rangitawa Tephra is thought to be a distal correlative of the Whakamaru group, originating from the Whakamaru caldera (Briggs *et al.* 1996; Lowe *et al.* 2001). The remaining units of Hamilton Ash (H2-H8) are of unknown source, yet Lowe *et al*. (2001) suggests that they are likely to be of rhyolitic origin, with younger volcanic centres in the TVZ potential sources. Briggs *et al*. (1996) identify the Hamilton Ash to be approximately 2.5 m thick at Omokoroa, where it can be identified as orange-brown at its base with a developed dark brown paleosol on the upper surface.

2.6.8 **Te Ranga Ignimbrite**

The Te Ranga Ignimbrite (0.27 Ma) is a local ignimbrite, confined to the Tauranga Basin, suggesting a Tauranga source (Briggs *et al*. 1996). The Te Ranga Ignimbrite is non-welded and unconsolidated in formation and only covers an area of approximately 30 km^2 with a thickness ranging from 6 m to 26 m (Briggs *et al*. 1996).

2.6.9 **Waimakariri Ignimbrite**

The Waimakariri Ignimbrite is a voluminous semi-welded ignimbrite with a speculated source in the Rotorua Volcanic Centre (Briggs *et al.* 2005). The age of the Waimakariri Ignimbrite is still unknown, however is thought to be < 0.27 Ma (Briggs *et al.* 2005). The Waimakariri Ignimbrite is large with a volume of approximately 100 km^2 (Houghton *et al.* 1995). Both the Waimakariri Ignimbrite and the Mamaku Ignimbrite form the Mamaku Plateau which is characterised as gently dipping (1-2 º) towards the Tauranga Basin (Briggs *et al*. 2005).

2.6.10 **Mamaku Ignimbrite**

The Mamaku Ignimbrite is the upper component of the Mamaku Plateau. The ignimbrite is very large in size (300 km^3) and extends from Lake Rotorua to the southern Tauranga region (Briggs *et al.* 1996). The Mamaku Ignimbrite is

approximately 70-80 m thick in the Tauranga region (Briggs *et al.* 1996); it varies in strength from very weak to medium rock strength, and is partially to densely welded (Briggs *et al.* 1996).

2.6.11 Rotoehu Ash

The Rotoehu Ash (~ 60 ka) is a distinctive younger tephra which overlies the Hamilton Ash sequence (Briggs *et al.* 1996; Wilson *et al*. 2007). The Rotoehu Ash can be characterised as being a widespread, shower bedded tephra-fall deposit, which varies in the Tauranga region from 0.3 to 2.4 m in thickness (Briggs *et al.* 1996). Walker (1979) suggests that the Rotoehu Ash was deposited when the Rotoiti Ignimbrite entered the sea causing a large phreatomagmatic eruption. The Rotoehu Ash is identified as whitish-grey, with fine to coarse ash.

2.6.12 Post Rotoehu Ash

Post Rotoehu Ash tephras over-lie the Rotoehu Ash in the Tauranga Basin; these tephras are the dominant parent material of the productive soils in the Tauranga region (Briggs *et al*. 1996). Briggs *et al*. (1996) identify the various tephras comprising the Post Rotoehu Ash as: Mangone Tephra, Kawakawa Tephra, Te Rere Tephra, Okareka Tephra, Rotorua Tephra, Mamaku Tephra, Tuhua Tephra, Waimihia Tephra, Taupo Tephra and Kaharoa Tephra. All of the identified tephras making up the Post Rotoehu Ash are derived from the TVZ apart from the Tuhua Tephra which is derived from Mayor Island (Briggs *et al.* 1996).

2.7 Holocene and late Pleistocene Tephras

Holocene sediments represent the sedimentary deposits from the large barrier enclosed Tauranga harbour. Similarly, Holocene sediments include the alluvium and peat deposits formed on low terraces of Holocene and late Pleistocene age. The composition of the material is typically of silts, sands, clays, gravels and carbonaceous material (Briggs *et al.* 1996).

2.7.1 **Pyroclastic landslide characteristics**

Pyroclastic deposits are often prone to landsliding events where they are exposed. Typically the high porosity, low strength and low density of particles promote the susceptibility of pyroclastic materials to landsliding (Arthurs 2010). Furthermore, the crushability of low density particles such as pumice, and the high pore water that can be held within the open voids, leads to landslide susceptible conditions (Borja-Baeza *et al.* 2006; De Vita *et al.* 2006). Arthurs (2010) suggests that low density particles also tend to create longer runout distances, in comparison to landslides in denser soils. Pyroclastic deposits typically bury prevailing topography, which can result in steep soil geometries, promoting landsliding (Arthurs 2010).

2.8 **Tauranga landslide geomorphology**

Various studies spanning several decades have characterised the geomorphology of landsliding in the Tauranga region (Houghton and Hegan 1980; Gulliver and Houghton 1980; Bird 1981; Oliver 1997; Bell *et al*. 2001; Keam 2008; Wyatt 2009; Arthurs 2010). In analysing coastal landsliding on the Maungatapu Peninsula, studies by Bird (1981) and Oliver (1997) have identified geomorphological features that were associated with the landsliding events in the area. Bird (1981) inferred that the coastal cliff landslide events of the Maungatapu Peninsula were typically the result of coastal wave processes on the cliffs, causing erosion and over steepening of the exposed cliffs. Bird (1981) proposed that the pore water pressures increased in a silty lens material overlying an impermeable unit. He suggested that these elevated pore water pressures developed during prolonged wet periods and promoted failure. Bird (1981) suggested that circular failures were typically not encounted, concluding that the failure mechanisms can be better analysed as non-circular. Oliver (1997) divided the types of failure into large block failures, block failures triggered by piping erosion, wave cut block failure and shallow regolith failures. He concluded that the method of establishing a geotechnical hazard zone using a 2H:1V profile was not accurate in representing the types of failure dwellings on cliff tops are exposed to. Bell *et al.* (2001), however was critical of the analyses in determining failure mechanisms as part of the work undertaken by Bird (1981) and Oliver (1997). Bell *et al.* (2001),

suggest Bird (1981) and Oliver (1997) do not account for water pressures present in tension cracks, only considering phreatic water pressures. Furthermore, Bell *et al.* (2001) suggest that while the failure mechanism of horizontal blocks sliding on clay seams of low residual shear strength is generally a common failure type, it is not appropriate to assume this is the case for Maungatapu as Oliver (1997) suggested.

Bell *et al.* (2001) looked to compare the slope failures observed at Maungatapu by Oliver (1997) with those recorded at the 1979 Bramley Drive failure at Omokoroa. Bell *et al.* (2001) note that the slide geometry at Maungatapu is considerably different from that at Bramley Drive, and suggest that the 2H:1V design suggestion cannot be used universally around Tauranga due to the variability of Tauranga landslip geomorphology. Furthermore, Bell *et al.* (2001) identify that the Maungatapu landslides are characterised by much steeper backslopes (> 60 º) even after five years following the landslides, while those at Bramley Drive are much lower (22 º - 28 º). It is suggested that this slope difference is due to Omokoroa being more sheltered from wave action than Maungatapu (Bell *et al.* 2001). It should also be noted that the Maungatapu landslides were not attributed to sensitive material, whereas the Bramley Drive failure was (Gulliver and Houghton 1980).

In his review of the Otumoetai landslips following the May 2005 storm event, Wesley (2007) suggested that where sensitive material is present, a factor of safety of ~ 1.8 would be more appropriate as opposed to the 1.5 standard used for non-sensitive material. Moreover, Wesley (2007) suggests that at a factor of safety of < 1.7 allows for overstressed zones within a slope, which could potentially lead to failure in highly sensitive material.

The identification of previous landslide events has also been undertaken by identifying the characteristic geomorphology types. Houghton and Hegan (1980) identified approximately 250 relic landslides in the Tauranga City area. On review, Bell *et al.* (2001) identified approximately 2000 relic landslide events. Of the 2000 landslide events identified, Bell *et al*. (2001) characterise the geomorphology types into four geomorphological features: (1) poorly defined headscarps with no associated debris (> 800), (2) poorly defined headscarps with

associated debris (< 100), (3) clearly defined headscarp with no associated debris (> 700) and (4) clearly defined headscarp with associated debris (> 250). This characterisation of landsliding events identified that slope failure is common throughout the Tauranga region, however, it was interpreted that less than 1 % of those identified displayed recent activity.

2.8.1 New Zealand sensitive landslide geomorphology and comparison with international quick clays

While the landslide morphologies in 'quick clays' internationally in Canada, Norway and Scandinavia have been characterised by large retrogressive failures, which continually flake away at the edges (Gregersen 1981), generally pyroclastic soil failures in New Zealand take on different morphologies (Gulliver and Houghton 1980; Keam 2008; Arthurs 2010). New Zealand landslides typically tend to be slides of varying depths that rarely retrogress and especially not to the same degree as international quick clays (Selby 1993). Arthurs (2010) identifies that associated with New Zealand landslides, the shear strength of stratigraphic layers influences the undulating nature of the landslide scar. He adds that the differences in geologic origin and geotechnical properties of soils are the primary contributors to the landslide morphology (Arthurs 2010). The contrasting geotechnical properties of New Zealand soils are attributed to the intercalation of pyroclastic and sedimentary materials that typically make up the landscape (Arthurs 2010).

2.9 Summary

The sensitivity of soils to failure following remoulding has been reviewed. Sensitivity is defined as the ratio between the peak to remoulded strength of a soil. Therefore, the level of strength decrease a soil will undergo after remoulding will determine its sensitivity. Typically, sensitive materials become fluidised, which often leads to catastrophic failures. The nature of sensitivity is well understood internationally, where salt leaching within a flocculated glaciomarine clay structure leads to high sensitivity or 'quick' soil behaviour. The formation and behaviour of sensitive materials within a New Zealand context, however, is not as

well characterised. While several recent studies have attempted to identify various contributing factors to sensitivity, no clear understanding remains about the fundamental characteristics of the soil as it is altered from its peak strength state. Previous studies have identified that halloysite is a key component of sensitive material, while allophane and kaolinite are also present. Within the Tauranga region, sensitive material has been identified at several locations in weathered rhyolitic tephra deposits. The sensitivity has been attributed to high pore water contents, leading to liquidity indexes greater than 1, while sensitivity is manifested in low remoulded strength rather than high undisturbed peak strength.

Chapter 3

METHODS

3.1 Introduction

The methods of research conducted for this study required a multi-stage approach of characterising field properties along with geomechanical and geotechnical testing. Field and laboratory methods of the 17 techniques used in this study are hence described in this chapter. All methods were typically based on set standards from previous studies, standards, guidelines or set precedents. Any variation from such published methods is explained, with an appropriate basis for doing so.

3.2 Soil description

Soil descriptions were undertaken at all sites considered for analysis in this study. The soil descriptions of the potential sites were developed following the guidelines issued by the New Zealand Geotechnical Society (2005). The descriptions were systematically ordered to allow for simplistic comparisons while still retaining a comprehensive characterisation. Aspects considered for the characterisations included soil group, colour, plasticity, presence of coarse material, strength, moisture condition, weathering and sensitivity. A field test for ferrous iron was undertaken using the method proposed by Childs (1981) which is further discussed in Section 3.4.2.1.

3.3 Field sampling

Field sampling was conducted at three sites which were chosen following the positive identification of sensitive soil materials (see Chapter 4). At each site a series of samples were taken. Bulk samples were extracted for particle size analysis, viscometry, Atterberg limits, moisture content, X-Ray diffraction and

SEM analysis. Three 50 mm by 60 mm cores were extruded from the sites for bulk density and laboratory shear vane tests, while larger 97 mm by 48 mm cores were sampled for triaxial testing.

3.4 Soil properties

3.4.1 Moisture content

Moisture content for the field samples was determined following the New Zealand Standard Methods of Testing Soils for Engineering Purposes (NZS 4402: 1986) Test 2.1. The soil samples analysed were all considered to be ≤ 2 mm in grain size, so were tested using the method for fine soil analysis. Soil samples were dried at 105 ^{0}C to avoid data discrepancies from heating temperatures outside of a 105 ^{0}C to 110 ^{0}C temperature range as noted in Note 2 of NZS 4402 (2.1) (1986).

Moisture content is given by:

$$Moisture\ content = \frac{Mass\ of\ container\ and\ wet\ soil - mass\ of\ container\ and\ dried\ soil}{Mass\ of\ container\ and\ dried\ soil - mass\ of\ container} \times 100\ (\%) \quad (3.1)$$

3.4.2 Bulk density

Bulk density testing was undertaken with slight methodological differences to that stated in NZS 4402 (1986) (5.1.3). With respect to apparatus variations, the dolly, guide rod and drive collar were not used as part of the sampling technique. Replacing this, the sampling tube was carefully hammered into the soil face, ensuring that the soil filled the entire sampling tube which could then be trimmed to size.

Bulk density is given by:

$$\rho = \frac{Mass\ of\ tube\ and\ core - Mass\ of\ sampling\ tube}{Volume\ of\ tube}\ (kgm^{-3}) \quad (3.2)$$

Dry bulk density is also established from the bulk density cores using the equation:

$$\rho_d = \frac{100\rho}{100 + water\ content\ of\ the\ soil}\ (kgm^{-3}) \quad (3.3)$$

3.4.3 **Particle density**

The density or specific gravity of soil particles was established using the method outlined in NZS 4402 (1986) (2.7.1), Vickers (1978) and Head (1992), whereby particle density was determined by the use of density bottles. Considering all authors followed the same principles of density calculation, the method from Head (1992) was chosen given that it was the most recently published method and was easily implemented. Head (1992) suggests the density bottle method is the traditional method for accurate measurement of particle density. The density bottle method was also recognised for its applicability and ease of use for fine grained soils making it a suitable method. The method involved determining the weight of the weighing bottle, the de-aired distilled water and bottle weight and finally the de-aired distilled water, soil and the bottle. Following which the weight determinations could be applied to the following equation to establish particle density:

$$\rho_s = \frac{Soil, bottle\ and\ stopper\ weight - Bottle\ and\ stopper\ weight}{(Bottle, stopper\ and\ deaired\ water - Bottle\ and\ stopper\ weight) - (Bottle, stopper\ and\ deaired\ water - Soil, bottle\ and\ stopper\ weight)}\ (kgm^{-3}) \quad (3.4)$$

3.4.4 **Porosity**

Porosity was determined by dividing the dry bulk density by the average particle density (McLaren and Cameron 1996) which is expressed as a percentage:

$$Porosity\ (n) = 1 - \left(\frac{Dry\ bulk\ density\ (kgm^{-3})}{Particle\ density}\right) \times 100\ (\%) \quad (3.5)$$

3.4.5 Voids ratio

Void Ratio is given as the inverse of porosity (Lancellota 1995) by:

$$e = \frac{V_v}{V} = \frac{n}{1-n} \tag{3.6}$$

3.4.6 Atterberg limits

Atterberg limits, offer a standard of soil behaviour characteristics, from which comparisons can be made between various soil types (Selby 1993; Wesley 2003; Mitchell and Soga 2005). Atterberg limits are important for characterising soil behaviour and in turn identify a soil type based on those characteristics (Selby 1993).

Atterberg limits are measured from remoulded soil paste. The preparation of the soil paste involved using two steel spatulas to thoroughly remould the soil on a glass plate until the material was of an approximately even consistency.

3.4.6.1 Liquid limit

Liquid limit was tested by cone penetration as set out in NZS 4402 (1986) (2.5), Head (1992) and Vickers (1978). The liquid limit describes the water content at which the soil behaviour passes from a plastic to liquid state (Head 1992). The liquid limit is derived from the moisture content at which the drop cone penetrates 20 mm into remoulded soil (Sherwood and Ryley 1970; Campbell 1975; Head 1992; Selby 1993). The determination of the liquid limit by means of cone penetration was preferred over the original Casagrande apparatus method as cone penetration reduced many of the significant limitations of the Casagrande method (Campbell 1975; Wires 1984). Campbell (1975) offers that the cone penetration test is ideally suited over the Casagrande test as the ease of use is greatly enhanced and thus the reproducibility between operators can be significantly improved. Moreover, it has been suggested that the cone penetration test gives a narrower range of liquid limit values over the Casagrande method and thus greater precision can be achieved (Wires 1984; Selby 1993). The procedure involved recording a series of cone penetration readings at various moisture contents and plotting a graph of penetration against moisture content. From the

resulting graph the moisture content at 20 mm penetration could be determined, which would correspond to the liquid limit of that soil.

3.4.6.2 **Plastic limit**

The plastic limit was determined following the procedure outlined by the NZS 4402 (1986) (2.3). The plastic limit describes the state at which a soil transitions from a plastic to solid state and becomes too dehydrated to be in plastic form (Head 1992). The procedure involved rolling the soil evenly into 3 mm threads, by which the natural heat from the operator's hand slowly dries out the soil until it shears laterally and longitudinally, reaching a crumbling like condition. At this point the soil can be considered to be at its plastic limit and the resulting moisture content is the soil plastic limit (Head 1992; NZS 4402 1986). The standard method for the plastic limit is, however, contentious (Selby 1993). Several studies have pursued that again determining the plastic limit by cone penetration offers greater accuracy in determining the plastic limit and is also less subjective on the part of the operator (Towner 1973; Campbell 1976). More specifically, it is suggested that at low penetrations such as 2.8 mm the plastic limit is identified with greater precision. However, considering that the NZS 4402 (1986) and other comparative studies (Keam 2008; Wyatt 2009; Arthurs 2010) preferred the hand rolling method, this method chosen for this study.

3.4.6.3 **Plasticity index**

The plasticity index identifies the water content range between the liquid limit and plastic limit (Selby 1993; Head 1992). The plasticity index was calculated under the guidelines set in NZS 4402 (1986) (2.4). The plasticity index is particularly useful in helping to construct the plasticity or 'A-line' chart along with the liquid limit to help identify in what characteristic manner the soil is behaving. Plasticity index is given by:

$$Plasticity\ index\ (PI) = liquid\ limit\ (LL) - plastic\ limit\ (PL)(\%) \quad (3.7)$$

3.4.6.4 **Activity**

Soil activity is the ratio of the plasticity index to the percentage of clay size particles. It is useful for samples which are considered to have significant

influence from clays such as sensitive soils (Selby 1993). Activity can be calculated by the following equation (Selby 1993):

$$Activity = \frac{PI}{\%\ soil < 0.002mm} \tag{3.8}$$

3.4.6.5 Liquidity index

The liquidity index (LI) describes the relationship of the field moisture content to the liquid and plastic limits (Head 1992; Selby 1993). Consequently, if the liquidity index of a soil is 1 the natural soil is at its liquid limit, however, if the liquidity index is at 0 then the soil is at its plastic limit (Selby 1993). The liquidity index can be expressed as (NZS 4402 1986):

$$Liquidity\ Index\ (LI) = \frac{Natural\ Moisture\ Content - PL}{PI} \tag{3.9}$$

3.4.7 Viscometric assessment of remoulded soil

Viscometric properties of remoulded soils, particularly sensitive soils, have previously been noted to play an important role in the behaviour of landslides (Edgers and Karlsrud 1985; Torrance 1987; Budhu and Mahajan 2008). Viscosity describes the friction between two fluid layers and the force required to generate movement between the layers (i.e. shear) (Tadros 2010). Therefore, reduced friction between layers reduces viscosity which is important for characterising the remoulded properties of a soil (Torrance 1987; Budhu and Mahajan 2008). Viscosity is simply defined by the following equation:

$$Viscosity\ (\eta) = \frac{Shear\ Stress\ (\tau)}{Shear\ Rate\ (D)}\ (Pa.s) \tag{3.10}$$

The characterisation of sensitive material has primarily been analysed by the yield stress (Bentley 1979; Torrance 1987; Locat and Demers 1988). Yield stress is a function of the relationship between shear stress and shear rate. Yield stress describes the shear stress required to promote flow behaviour of a material

(further discussed in section 3.4.7.4), and will be the primary determinant used to analyse the flow behaviour of sensitive soils in this study.

Viscometric properties of the sensitive soil deposits from this study were measured using a Brookfield R/S+ Rheometer incorporating a V3-40-20 vane spindle (Brookfield 2012). The rheometer measures shear resistance as a result of the torque applied to a remoulded soil specimen (Torrance 1987).

3.4.7.1 **Apparatus description**

The Brookfield R/S+ Rheometer is comprised of three main components: the electronic measuring drive, the vane spindle (V3-40-20), and the computer system for controlling the measurement (Figure 3.1). The electronic measuring drive was the SST model which was suitable for automatic shear rate (torque) adjustment during testing. The SST has an operating range of 0 – ~ 1200 sec^{-1} (Brookfield 2012). With the vane spindle attached the SST has a shear stress range of 51 – 1700 Pa (Brookfield 2012). All control of the machine is made by programming commands into the RHEO3000 software which transmits the specified operations for test requirements to the SST electronic measuring device. All shear stress, shear rate and viscosity measurements are calculated automatically by the RHEO3000 software. The housing for the specimen itself is not incorporated into the design for a vane spindle as may be expected for a coaxial setup. Instead a 150 ml glass beaker was used. The manufacturing guidelines for the vanes recommend that the sample container diameter should be two times the vane diameter, while the depth should provide a vane diameter clearance to the bottom of the container (Brookfield 2012). All of these specifications were met by the beaker.

Figure 3.1: Image displaying the Brookfield R/S+ Rheometer, where (A) is the electronic measuring drive, (B) is the vane spindle (V3-40-20) and (C) is computer system for controlling the measurement The sample beaker was clamped in on the base plate beneath the vane spindle during operation (not shown).

3.4.7.2 **Sample preparation**

Sample preparation for analysis in the Brookfield R/S+ Rheometer involved initially thoroughly remoulding the sample into a paste. A subsample of approximately 300 g was then placed in the 150 ml beaker ready for testing. Moisture content has historically proven to be critical to the outcome of the viscometry tests (Bentley 1979). Therefore, to account for soil moisture loss during sample preparation, ~ 1 ml – 2 ml of water was added to each soil material tested, to ensure that moisture content could be consistently maintained between the samples. The moisture content was ensured to be kept within ± 7 % of the natural moisture content for each sample at the time of testing, by taking a subsample and analysing the moisture content. Following sample preparation, samples were kept within multiple sealed plastic bags and tested immediately to prevent further moisture evaporation.

3.4.7.3 **General test protocol**

The method for determining the viscometric properties of sensitive soils has been consistent between several previous studies (Bentley 1979; Torrance 1987; Locat and Demers 1988). Bentley (1979) proposed a method which has been replicated several times in subsequent studies (Torrance 1987; Locat *et al*. 1988; Locat and Demers 1988). The method involved initially increasing the shear

rate to the maximum of 200 s^{-1} and allowing the shear stress value to stabilise. Following stabilisation, the shear rate was decreased one step lower to the next shear rate, where a reading could be attained, and then increased back to maximum shear rate, where a stable value could again be recorded. The shear rate would then be reduced down two steps where a reading could be attained, and again following this, the rate would be increased back to the maximum. The stepwise process was repeated until the lowest shear rate was applied, and then the whole sequence was applied, but in reverse, increasing the shear rate back to a maximum (the sequence was therefore 200, 150, 200, 100, 200, 75, 200, 50, 200, 200, 25, 200, 12, 200, 6, 200, 3, 200, 1.5 s^{-1} and then 1.5, 200, 3, 200… 200, 100, 200 s^{-1}). Torrance (1987) commented that the test sequence was suitable for use as it produced readily reproducible results even for materials which displayed hysteresis. Wells and Childs (1988), however, undertook viscosity measurements by accelerating the shear rate constantly from the lowest programmable rate to the maximum, and then again decelerating at the same constant rate to zero.

For this study, the Bentley (1979) method was adopted, while also recording the initial increase as Wells and Childs (1988) offer (Figure 3.2). The analysis of results and yield stress values, however, were recorded by considering only the Bentley (1979) method. The Bentley (1979) method allowed for the stabilisation of the shear stress which appeared to be essential for attaining a credible value. When simply increasing the shear rate without waiting for a constant value to be reached, as indicated by the Wells and Childs (1988) method, the shear stress value reaches a peak and then steadily decreases over time while the shear rate remains the same (Figure 3.2). The decreasing values mean that the determination of the actual value is somewhat open to interpretation and increases the operator error. It appeared that these decreasing values were the result of the soil sample moving and adjusting within the beaker, until a time at which the soil particles were rearranged to a point where it would no longer significantly change position within the beaker. Allowing for this rearrangement of the soil paste to occur (as the Bentley (1979) method sanctions) is considered essential for stable values to be reached and should be done before taking any measurements. It is recognised, however, that Wells and Childs (1988) were using a Haake Rotovisco RV3 sensor system as opposed to the Brookfield R/S+ Rheometer used in this study, and so the individual method variation is not accounted for.

Notwithstanding this, it was still concluded that the Bentley (1979) method was preferred due to it being the established precedent, its reproducibility, and the ability to compare the results with previous studies.

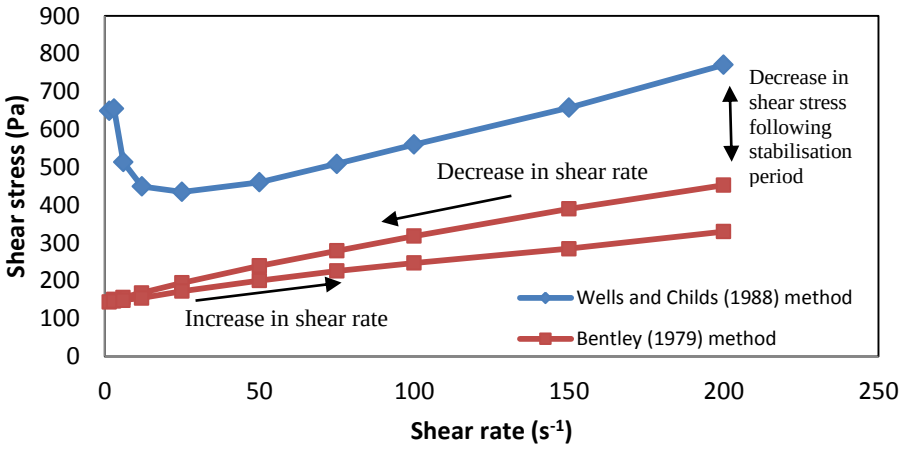

Figure 3.2: Viscosity curve for sample PS2 following both the Wells and Childs (1988) method and the Bentley (1979) method. A significant drop in shear stress can be seen between the initial shear rate increase from the Wells and Childs (1988) method, following the mandatory stabilisation period imposed from the Bentley (1979) method. This drop illustrates the importance of allowing the soil to reach an equilibrium shear stress at the maximum shear rate before commencing a viscosity test to ensure the reliability and comparability between results.

Soil temperature was monitored with a temperature probe to ensure that during test conditions the sample did not alter significantly. Temperature conditions were always 20 ± 0.5 º C which is common for *in-situ* New Zealand soil temperatures. This allowed for any test by test variation from temperature changes to be ruled out and similarly give consistency and comparability between the tests.

3.4.7.4 **Yield stress**

As mentioned earlier, yield stress is an important characteristic of sensitive soils and their flow properties upon remoulding, which can be attained by viscometric analysis. The yield stress of a material is the stress which must be surpassed to force a structured material in 'solid' form, to flow (Moller 2006). Bentley (1979) suggested that yield stress can be identified as the 'y' intersection of a shear stress against shear rate curve. Torrance (1987), however, suggests that where properties of a Bingham plastic or shear thinning are present (as in this study) the yield stress should be calculated "as the intercept on the shear stress (y)

axis, of the best fit line, for the five fastest shear rates" (Torrance 1987). The Torrance (1987) method of determination has also been used by Locat and Demers (1988). Although Torrance (1987) do not give a reason as to why the slow shear rates are not included, it appears to be because the high shear rate portion is the most consistent, reliable and repeatable section of the test, whereas at low shear rates, stress fluctuation could skew the test away from the general trend. To account for the slight variation between the increase and decrease in shear rate which the Bentley (1979) method produced, a linear regression line was added to the shear stress values including both the decrease and increase in shear rate (Figure 3.3).

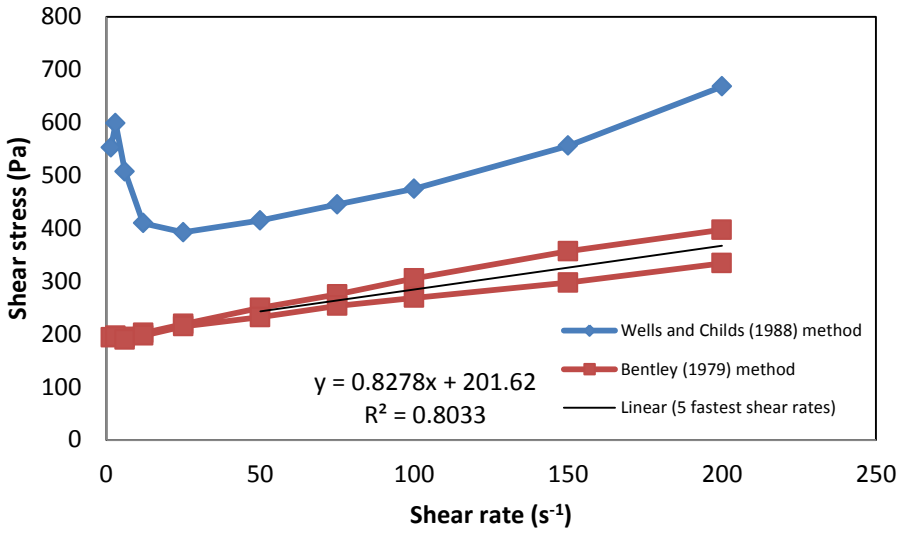

Figure 3.3: Viscosity curve for the sample PS1. Yield stress is denoted as the y-intercept of the linear regression line from the top five fastest shear rates.

3.4.7.5 Alteration of soil pH using NaOH and HCL for analysis with the Brookfield Rheometer

Alterations in soil pH were undertaken to determine the effects of pH on yield stress and thus the importance of soil pH for rhyolitic sensitive soil. To adjust the pH, sodium hydroxide (NaOH 4 %) was used to increase the soil pH and hydrochloric acid (HCL 1 M 10 %) was used to decrease the soil pH, keeping with the technique applied by Bentley (1979). Relatively consistent variations in pH were followed, to allow for clear determinations of yield stress disparity observed between this study and those previously undertaken (Bentley 1979; Yong *et al.* 1979). The pH adjustments tested were ~ 4, ~ 5, ~ 6 (natural pH), ~ 7,

~ 8. This range was deemed to provide a suitable cover from acidic to alkaline soil conditions.

3.4.7.6 Sensitivity to shear measurement by viscometric shear stress assessment

Wells and Theng (1985) suggested that the sensitivity of soil pastes to shear could be determined from viscometric assessment using the ratio of the maximum shear stress (T_i) to the minimum shear stress (T_f). Maximum and minimum shear stress are suggested to be measures of strength before and after shear, giving rise to the classical ratio of peak to remoulded strength for sensitivity (Wells and Theng 1985). Maximum shear stress was identified to be the peak shear stress during shear rate acceleration (Figure 3.4). Minimum shear stress was considered problematic following the dramatic drop in shear stress at low shear rates. Wells and Theng (1985) identify that the sudden drop of the shear stress resembles "pseudoplastic material" and that the minimum shear stress can be derived from the linear portion of the curve which would intersect the Y axis (Figure 3.4).

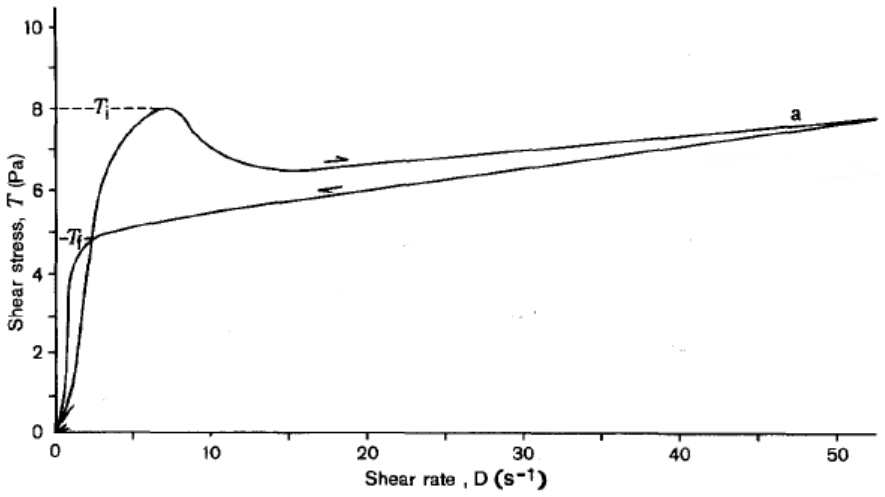

Figure 3.4: Establishment of a maximum peak shear stress (T_i) and minimum shear stress (T_f) for sensitivity assessment (Wells and Theng 1985). Wells and Theng (1985) suggest that maximum peak shear stress represents maximum peak strength, while minimum shear stress represents the strength of the material after shear. The ratio T_i/T_f is suggested to represent the sensitivity of the paste.

Sensitivity measurements under this method were determined to establish how pH affected the values of sensitivity and also how sensitive pastes of the rhyolitic material from this study were to shear. The maximum peak shear stress

(T_i) was taken from the maximum value attained during the initial increase (Wells and Childs (1988) method) (Figure 3.3). The minimum shear stress (T_f) was taken as the y-intercept from the five fastest shear rates (both decelerating and accelerating shear rates) and also used to determine yield stress following the Torrance (1987) method (Figure 3.3).

3.4.8 **Particle size**

Particle size was measured using the Malvern Mastersizer laser particle sizer. Soil samples were obtained from the field as bulk samples and then air dried and passed through a 2 mm sieve (the sample was typically fine grained and so no analysis of > 2 mm material was required), before a representative sample was taken for pre-treatment preparation. Pre-treatment preparation required the removal of all organic matter by hydrogen peroxide soaking, and then the deflocculation of particles with sodium hexametaphosphate. Sonication was undertaken immediately before the analysis to ensure particles were separated. Both the pre-treatment and sonication techniques used for this study have been proven successful in previous studies (McCave *et al.* 1986; Singer *et al.* 1988).

Following appropriate pre-treatment the samples were analysed in the Malvern Mastersizer. The Malvern Mastersizer operates under the Mie theory, determining particle size by predicting the light scattering behaviour of the particles. As a requirement of the Mie theory, the indices of refraction and absorption are known. Sperazza (2004) suggests that the operations under the Mie theory are less susceptible to grain size miscalculations, and thus is the optimal theory to use in relation to laser particle size analysis. The Mie theory is used to adapt the scatter of light to grain size, which is represented as a volume by the Malvern Mastersizer (Sperazza 2004).

For the measurement of particle size the indices of refraction and absorption relate to the particles being analysed and the medium which is used to suspend the particles (which in this case is water) (Sperazza 2004). The choice of the refractive index (RI) and absorption (A) are critical in the use of the Mie theory (Wyatt 2009). The refractive index and absorption values are based on the types of soil particles which are being analysed. The RI and A values which the University of Waikato Malvern Mastersizer defaults to are 1.56 and 0.0

respectively (Wyatt 2009). An A value of 0.0, however, suggests that the particles under analysis are expected to be perfectly rounded and semi-transparent under the Mie theory, which is unrealistic (Wyatt 2009). Loizeau *et al.* (1994) suggests that, for analyses under the Mie theory, the refractive index must be set with a unique value. Wyatt (2009) explored the use of various RI and A values to estimate the percentage of < 2 µm materials in a soil. He concluded that by reducing the refractive index, the apparent percentage of < 2 µm material significantly increased where in one example, a RI value of 1.56 yielded 4.81 % of clay size material, while a RI value of 1.38 gave 80.75 % clay size material. Wyatt (2009) noted that where the RI was changed to 1.38, the residuals on the data were very wide. To correct for the absorption assumption, Wyatt (2009) adjusted the A value to 0.01 which was concluded to be a representative value for the soil samples. Wyatt (2009) studied all samples at RI values between 1.52 and 1.57, with A values of 0.01 consistently.

Considering the need for specific refractive and absorption values, and to achieve consistency between results, a specified soil standard operating procedure (SOP) was utilised as part of the Malvern Mastersizer. The specified soil SOP set specific RI and A values which were 1.52 and 0.01 respectively. Using these RI and A values offers a greater comparability between the various sites and similarly between various studies. Furthermore, the use of SOPs is recognised as an important tool in producing consistent results between various studies (Jones 2003). Jones (2003) suggests that SOPs reduce operator variability and allow greater reproducibility and comparability between studies.

Obscuration of the laser for the particle sizer is based on the amount of sample added to the Mastersizer. The Mastersizer pre-set values give a good range of obscuration between 10 % and 20 % to avoid the rescattering of light (Sperazza 2004). Light rescattering typically occurs over 30 % obscuration (Wyatt 2009). Sperazza (2004) suggests that the most reproducible results are achieved at 20 % obscuration. Given this, operating obscuration levels were consistently between 17 % and 20 %.

3.4.8.1 **Comparison with NZS 4402 (1986) Pipette Method**

Initial particle size recordings using the Malvern Mastersizer delivered low recordings of the clay size fraction in the sensitive soil samples analysed, contrary to what was expected based on previous studies (Jacquet 1990; Wesley 2007; Wyatt 2009). On this basis a pipette method particle size analysis was undertaken in accordance with NZS 4402 (1986) (Test 2.8.3) to compare whether the results achieved with the laser sizer were consistent with another known method. The results (Table 3.1) indicate that the laser sizer offers a suitable estimate for the clay size fraction in comparison with the pipette method. It was concluded that the laser sizer offered the best and most up to date method for analysing particle size over the pipette method, where it has been suggested that the latter method can result in error in excess of 40 % (Sperazza 2004; Eshel *et al.* 2004). In light of this evidence, the laser sizer was continued as the method for particle size analysis.

Table 3.1: Clay size fraction estimates by the Malvern Mastersizer and pipette method

Sample	**Malvern Mastersizer < 2 % grain size estimation**	**NZS 4402 Pipette method < 2 % grain size estimation**
Omokoroa (OS2)	2.16 %	1.65 %

3.4.9 **Field shear vane**

The field shear vane was employed to determine undrained shear strength of the *in-situ* soil outcrops. A Geotechnics shear vane apparatus was used along with the shearing procedure offered by the New Zealand Geotechnical Society (2001). The shear vane is a simple apparatus which operates by increasing torsion spring resistance as the vane is rotated (New Zealand Geotechnical Society 2001). The vane head includes a graduated scale which is readily converted to shear strength in kPa with the use of a calibration constant, determined during the calibration procedure. Field shear strength tests were conducted typically at 150 to 300 mm intervals vertically down the exposed soil face of interest, however this also depended on the variability/homogeneity in soil layers in the profile. The shear vane was inserted at least 60 mm into the soil to reduce error and ensure that shearing would only be on the vertical edges of the blade. The vane was then

slowly rotated at approximately one revolution per minute. Two shear vane blades were available for use – 19 mm and 33 mm. The 19 mm shear vane was used as this had greater success penetrating to the required depth into the soil surface as opposed to the 33 mm vane.

3.4.9.1 **Soil remoulding for sensitivity analysis**

Once the soil had sheared, remoulding of the soil was undertaken to determine the sensitivity ratio. The method for remoulding the soil was chosen following consideration of the various methods used both in comparative studies and official standards and guidelines (Table 3.2). The method used in this study for remoulding followed the ASTM D2573 – 08 Standard Test Method for Field Vane Shear Test in Cohesive Soil. The ASTM shear vane test involves rapidly rotating the vane 5 – 10 times following shearing of the soil, and then repeating the steps of initial shear testing to gain a remoulded strength. In comparing the various methods used to determine remoulded shear strength of soils, several inconsistencies between methods were recognised. Most of the methods looked to remould the soil by rotating the vane either quickly or slowly while it was still *in-sit*u from the initial shear strength measurement (Table 3.2).

Wyatt (2009) compared the New Zealand Geotechnical Society (2001) method to an innovative method of removing the soil of interest, physically remoulding it by hand, replacing it, and then undertaking shear vane strength analysis on that sample. Wyatt (2009) concluded that the innovative method appeared more sensitive to variation, yet because it ensured that the soil specimen was completely destroyed it offered greater understanding of the remoulded strength for the types of failures which sensitive soils display. However, undertaking this method incorporates many limitations and error which are not quantified. For example, the length of time and amount of pressure placed on the sample during remoulding, the amount of compaction when replacing the soil sample and the impacts of boundary changes and friction. The innovative method was trailed in the field at the Omokoroa sites. Following remoulding, however, it became apparent that when trying to replace the soil in its original position, the soil could not hold its own structure, meaning that consistently replicating the field method between measurements was difficult. While the method does offer an attempt to expose a well remoulded specimen to shear strength testing, the error

associated renders it impractical to be used consistently as a field shear strength test. For these reasons, again, the consistency that could be achieved with the ASTM D2573 – 08 test meant that it was preferred over other methods.

Table 3.2: Methods used for remoulding soil materials by comparative studies and published standards/guidelines

Study	Remoulded Soil Method
New Zealand Geotechnical Society (2001)	*In-situ* remoulding of 5 rotations at 10 seconds per rotation
Wyatt (2009)	Two methods: (1): 5 rotations at 10 seconds per rotation (2): Soil remoulded in a bag and then either replaced or placed in a ring and sheared again with shear vane
Arthurs (2010)	*In-situ* remoulding by rotating the vane rapidly through a minimum of 5 to 10 revolutions
Craig (1997)	*In-situ* remoulding by rapidly rotating the vane through several revolutions
Keam (2008)	*In-situ* remoulding by rotating the vane rapidly 30 times and then allowing pore pressures to build up for 30 seconds
Lancellotta (1995)	*In-situ* remoulding by rotating the vane rapidly 25 times
ASTM D 257301 (2008)	*In-situ* remoulding by rotating the vane rapidly through a minimum of 5 to 10 revolutions
This Study (2012)	*In-situ* remoulding by rapidly rotating the vane 10 times to completely destroy the structure of the soil, thus remoulding it.

3.4.9.2 Inherent limitations of field shear strength testing using the *in-situ* shear vane method

The field shear vane test for soil strength employed throughout the official standards and guidelines by the New Zealand Geotechnical Society (2001) and the ASTM D 257301 (2008) are expected to be used both nationally and internationally to regulate field shear vane tests. The tests, however, appear to be limited in determining how remoulded strength is quantified. Remoulding the soil sample by simply rotating the vane in the zone of initial shear does not appear to completely represent the same immersed conditions that the initial peak shear strength test is subjected to. The vane head is already in a zone of soil which has been disturbed and moved from its original position. The remoulding process only impacts the small layer of soil which is between the edges of the vane blade,

rather than the whole vane blade being immersed in remoulded material and the shear plane has not already been defined (Figure 3.5). The situation where a shear plane has not been already defined would appear to more accurately represent the remoulded strength of the soil. It appeared that even for soil materials which typically did not exhibit sensitive properties upon remoulding, such as an inability to support light applied pressure and not smearing upon disturbance, were still classed as sensitive to highly sensitive. Although Wyatt (2009) attempted to rectify these issues, too many limitations and inconsistencies between sites could not be accounted for.

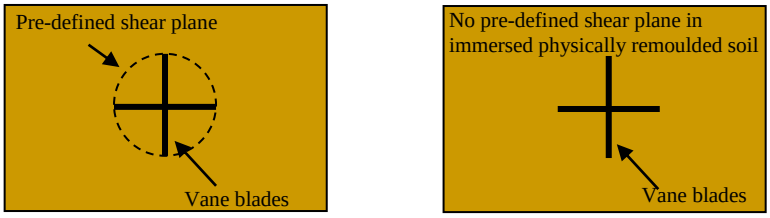

Figure 3.5: Illustration of the pre-defined shear plane in the shear vane method of remoulding currently used as a standard for the establishment of sensitivity (left) compared to the more realistic situation where no predefined shear plane has been established, i.e. if the shear vane was tested in physically remoulded soil (right).

Based on inconsistencies between shear vane observations and behavioural observations, each soil which was classed as sensitive with the hand shear vane was also subjected to a hand shear test as described by Milne *et al*. (1995). The procedure involved applying a moderate to weak shear force (20 kPa – 40 kPa) between thumb and finger to the soil. Following the application of pressure it was observed whether the soil suddenly changed to a fluid where it smeared and water could be detected on the fingers. A soil that did not smear or become fluidised was considered "non-sensitive" and thus this term was adopted for such materials encountered in this study (Table 3.3). Only following this step would a soil be conclusively identified as a sensitive soil and further hand shear vane tests following the ASTM 257301 (2008) method were carried out.

Table 3.3: Sensitivity classes and descriptions adapted from Milne *et al.* (1995). The test was primarily used to characterise non-sensitive material where the shear vane was inappropriate.

Class	Relative strength loss onremoulding (class decrease)	Reaction to shear test
Non-sensitive	0-1	On applying shear force between thumb and forefinger, the soil material does not soften and smear or softens only slightly.
Weakly sensitive	2	On applying moderate (20 – 40 kPa) shear force between thumb and forefinger, the soil material softens, fingers skid and the soil smears.
Sensitive	3	On applying moderate (20 – 40 kPa) shear force between thumb and forefinger, the soil material suddenly changes to fluid, fingers skid and the soil smears. After the soil smears some free water can be detected on fingers.
Strongly sensitive	> 3	On applying weak (20 kPa) shear force between thumb and forefinger, the soil material suddenly changes to a fluid, fingers skid and the soil smears and is slippery. After the soil smears free water is easily seen on the fingers.

3.4.10 Laboratory shear vane

The laboratory shear vane was used to make accurate determinations of peak and remoulded shear strength of the soil. The laboratory shear vane allows for a controlled constant rate of shear on the soil, thus reducing the operator error of the field shear vane. The laboratory shear vane apparatus used was a VJ Tech VJT5300 which was based on the original Transport and Road Research Laboratory (TRRL) design, and also conforms to the requirements of the British Standard 1377-7 (1990). The laboratory shear vane operates by applying torsional load via calibrated springs to a 12.7 mm by 12.7 mm vane and thus onto the

sample (VJ Tech 2011). Failure is recorded at the maximum angular deflection of the torsion spring which is then converted to kPa by the equation:

$$\tau_v = \frac{1000M}{K}\ (kPa) \tag{3.11}$$

where:

$$M = Maximum\ angular\ rotation\ \times calibration\ factor\ (N\ mm)$$

and

$$K = \pi D^2 \left(\frac{12.7}{2} + \frac{12.7}{6}\right)\ (mm^3) \tag{3.12}$$

The apparatus includes a motorised attachment which allows for a constant shear rate of 12 degrees of rotation per minute in accordance with BS 1377-7 (1990).

Cylindrical cores (60 mm diameter x 50 mm height) were used to extract field samples for laboratory shear vane use in the lab. The samples were placed below the vane, and the vane lowered 25 mm into the sample to ensure that the vane was influenced by the sample on all sections of the blade. The vane motor was engaged, and torque was applied until the soil sheared at which a value could be attained. Remoulding of the specimen was achieved in accordance with BS 1377-7 (1990) by rotating the vane rapidly through two revolutions without adjusting the vane from the sheared zone. Torque was again applied and a value was attained from the shearing of the remoulded specimen. The test was repeated 3 times within separate cores to ensure reproducibility and reliability of results.

3.4.11 Oxidising and reducing conditions

Oxidising soil conditions are present where soils are not saturated and oxygen can pass into and through the soils (Birkeland 1999). Oxidation is recognised as an important weathering process occurring in soil where oxygen supply is greater than the biological demand (Buol *et al.* 2003). Oxidation is the elemental loss of electrons, which results in the disintegrative weathering process in common minerals containing ferrous iron such as clay minerals (Buol *et al*. 2003). As a result of the oxidation of primary minerals, manganese is released into free form (Buol *et al*. 2003).

Soils are considered to be under reducing conditions when they are anaerobic and hold chemically reduced forms of either N, Mn, Fe, or S rather than just the depletion of oxygen (Vepraskas 1994). Reduction, also known as the gain of electrons, occurs under the proviso of 3 conditions: (1) the soil is saturated, (2) oxygen supply is low and (3) biological oxygen demand is high (Buol *et al.* 2003). The effect of these conditions is the process of reducing iron to a highly mobile form (gleization) (Buol *et al.* 2003). Following the conditions of soil saturation, the oxygen in the water and soil must be removed by microbial respiration. The organic substrate is also the electron donor, which is oxidised during the reduction process. The oxidisation subsequently drives metabolic reactions that synthesise high energy compounds within the microorganisms (Buol *et al*. 2003). Following the depletion of oxygen, the microbes reduce Mn (III) and finally Fe (III) to leave iron in its reduced form Fe (II) (Vepraskas 1994; Buol *et al*. 2003).

Any method which indicates the presence of reduced Fe (Fe^{2+}) is considered suitable for testing for reduced soil conditions (Vepraskas 1994). Therefore, to test for ferrous iron at each site (and therefore reducing conditions), the Childs Test (Childs 1981) was employed.

3.4.11.1 Childs' Test

A test for ferrous iron (Fe^{2+}) in soils was carried out at each of the sensitive site locations using a 10 % 1 M solution of ammonium acetate containing 1 g of α,α-dipyridyl. The method was originally published by Childs (1981) who further details the test preparation. The spray test method was employed for this study. A soil surface was freshly exposed using a block of wood and then sprayed with the solution. Care was taken not to clear the surface with a steel object, such as a spade, as contact of this manner can give a weak positive test (Childs 1981). When soluble ferrous iron is present in the exposed soil following the spray test, a red colour develops. Depending on the level of soluble ferrous iron in the soil, a range of red colouring is distinguishable and interpreted accordingly (Table 3.4).

Table 3.4: Sensitivity of the ferrous iron test (from Childs 1981)

Solution Colour	Total solution concentration of ferrous iron			
	moles/l	**ppm**	**mmoles/ 100 g soil***	**m.e./ 100 g soil***
Red to deep red	$> 7 \times 10^{-5}$	> 4	> 0.02	> 0.04
Pale pink to pink	$3 \times 10^{-6} – 7 \times 10^{-5}$	0.2 – 4.0	$1 \times 10^{-3} – 2 \times 10^{-2}$	$2 \times 10^{-3} – 4 \times 10^{-2}$
Not detectable	$< 3 \times 10^{-6}$	< 0.2	$< 1 \times 10^{-3}$	$< 2 \times 10^{-3}$

*Based on 1 g of soil placed in vial containing 2.2 ml of reagent.

After spraying the surface, Childs (1981) recommends observing colour development within a "few" minutes. Initial testing revealed that at least 15 minutes was required to ascertain whether any colour development was present, and a final description of the colour change was recorded following 30 minutes. Care was taken to ensure that during the 30 minute development period shade was provided to the site as the α,α-dipyridyl solution is sensitive to light, and intense sunlight can produce a potentially false reading (Vepraskas 1994).

3.5 **Geomechanical properties**

3.5.1 **Triaxial**

The triaxial apparatus was employed to determine the shear strength of the soil specimen under laboratory conditions. Principally, effective stress was determined with the triaxial apparatus which involved subjecting the specimen to controlled stresses on all planes, while attempting to replicate the *in-situ* properties the soil would be exposed to (Head 1998). The triaxial apparatus offers several advantages over other methods of soil strength measurements, including control of the size of the principal stress, and control over drainage and pore water pressure conditions (Bishop and Henkel 1962; Head 1998). Consolidation and permeability, therefore, can be derived from the triaxial test, furthering the ability to understand soil characteristics and behaviour (Craig 1997; Head 1998). The method of testing undertaken strictly followed the British Standard 1377 (1990) Part 8: Shear strength tests (effective stress). The standard offers an established method of determining effective stress for both consolidated undrained (CU) and consolidated drained (CD) tests, both of which were used in this study. Only soils

in an undisturbed state could be measured with the triaxial as remoulded specimens displayed an inability to support themselves in a cylindrical shape, which previous authors have noted as a limitation of quantifying shear strength of remoulded sensitive soil (Bishop and Henkel 1962; Wyatt 2009).

3.5.2 **The triaxial apparatus**

The triaxial apparatus used in this study was a VJ Technology Triplex Multitester triaxial. The triaxial system was fully automated with the ability to accurately control the amount of load placed on the specimen. A MM linear displacement sensor was attached to the top of the triaxial cell to automatically measure strain as load was increased on the specimen. Pore water pressure and volume change were also digitally measured with the use of inbuilt transducers. Cell pressure and back pressure were controlled using two butyl rubber bladders inside de-aired water cell chambers. Compressed air was used in the system to increase the air pressure inside the bladders therefore allowing the cell or back pressure levels to increase. A 2:1 in-line air amplifier was installed to ensure that great enough air pressures could be derived for the various triaxial tests. De-aired water, as required by BS 1377 (1990) was provided to the system by first distilling the water with a Merrit Water Still 4000. The distilled water was then transferred to a Nold Deaerator where it was de-aired before it was to be used in the triaxial cell. Figure 3.6 illustrates a simplified diagram of the triaxial set up used.

All data from the triaxial system was recorded via a 16 channel VJ Technology MPX3000 data logger. To display and control the triaxial rate of strain WINCLISP software was used. The WINCLISP software was further used to duplicate the data recorded from the data logger and then could be graphed and analysed accordingly.

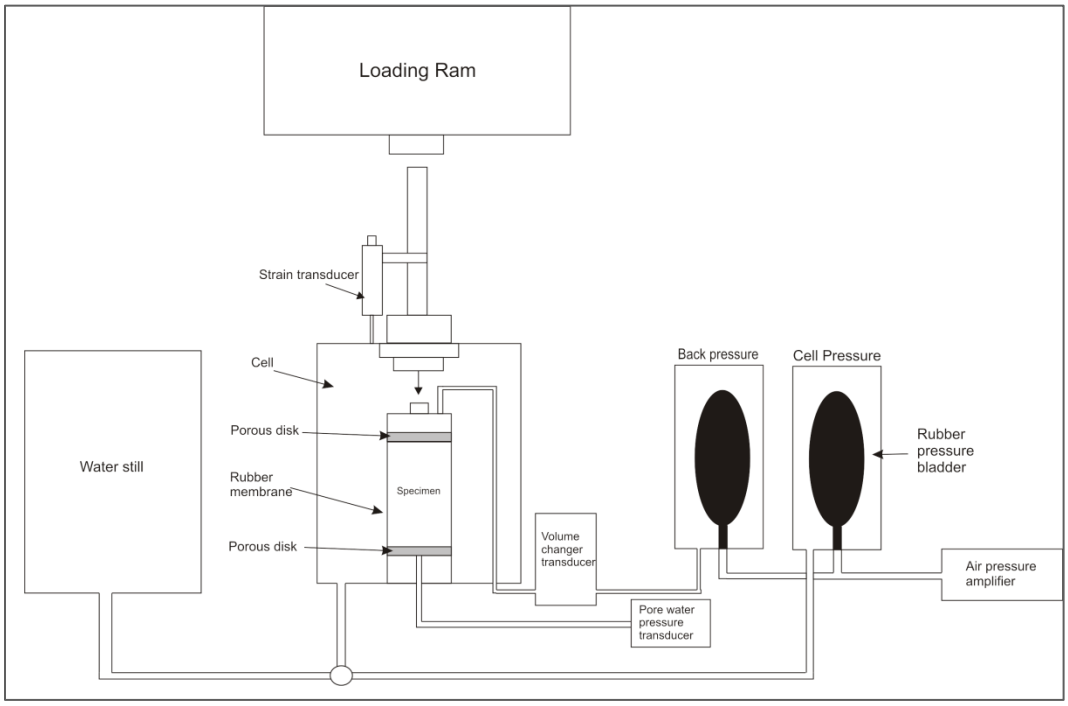

Figure 3.6: Simplified diagram of the triaxial apparatus setup

3.5.3 **Triaxial tests**

Triaxial tests undertaken in this study included consolidated drained (CD) and consolidated undrained (CU). Both tests were undertaken in accordance with BS 1377 (1990). The variations between the test types are outlined in Table 3.5.

Table 3.5: Types of triaxial test undertaken in this study (based on Fratta *et al*. (2007))

Consolidated-undrained (CU) Tests	**Consolidated-drained (CD) Tests**
Stage 1: Confining (under hydrostatic pressure)	*Stage 1: Confining (under hydrostatic pressure)*
Increasing cell pressure (σ_3)	Increasing cell pressure (σ_3)
Volume change varies	Volume change is not permitted
Stage 2: Shearing	*Stage 2: Shearing*
Increasing cell pressure (σ_3)	Increasing cell pressure (σ_3)
Volume change is not permitted	Volume change varies
Pore pressure varies	Pore pressure is not permitted

3.5.3.1 **Consolidated drained (CD)**

Only one consolidated drained (CD) test was undertaken in this study. The consolidated drained test, otherwise known as the 'slow' test, provides long term values of shear strength (Selby 1993). Selby (1993), however, suggests that the

results of this test are similar to the consolidated undrained test, but are more useful for slow, progressive failures. The types of failures which sensitive soils produce are considered rapid, which generally suits a consolidated undrained test (Selby 1993). Primarily determining the length of the test is the coefficient F, which is used in the determination of testing time depending on the drainage conditions of the test type (i.e. consolidated drained or consolidated undrained).

3.5.3.2 **Consolidated undrained (CU)**

Consolidated undrained (CU) tests were undertaken on all sample sites. The tests were undertaken using 3 sample specimens for one site to allow for a suitable Mohr Coulomb plot to be produced. Each test sample took a minimum of 3 days to complete with the saturation stage taking ~ 8 hours, consolidation taking ~ 16 hours and finally the compression stage taking between 16 to 24 hours to complete. Primarily determining the length of the triaxial test is the coefficient F, which is dependent on the type of drainage and based on 95 % dissipation of excess pore pressure induced by shear (BS 1377 1990). Generally consolidated undrained tests are significantly faster than consolidated drained tests, given that the coefficient F is for CU tests 0.53 instead of 8.5 for CD tests as stipulated in the BS 1377 (1990). The coefficient F of 0.53, however, only applies to non-sensitive soils and so Head (1998) suggests that for sensitive soils, the same coefficient F for consolidated drained tests should also be used for consolidated undrained tests.

3.5.4 **Test procedure**

The test procedure followed for both the consolidated drained and undrained tests were undertaken in accordance with the standard set by BS 1377 (1990). Both the consolidated drained test and the consolidated undrained test undergo the same saturation and consolidation stages. The only alteration between the two methods is during the compression stage, where the consolidated drained test is allowed to drain during compression, while consolidated undrained tests are restricted from doing so.

3.5.4.1 **Saturation stage**

The saturation stage of the triaxial test ensures that all voids in the specimen are filled with water (BS 1377 1990). Even 50kPa increments of cell

pressure followed by increments of back pressure, no less than 10 kPa below the cell pressure, were used to slowly increase the pore water pressure of the sample. The resulting increase in pore water pressure is continued until a B value of 0.95 or greater is achieved and the pore water pressure is greater than or equal to 300 kPa. The B value describes the change in pore pressure over the increase in cell pressure during saturation. Therefore when the difference in pore pressure from the cell pressure is $\leq$ 5 % the sample is considered saturated. A pore water pressure of 300 kPa or greater is critical as that is the pressure air within water is dissolved at, ensuring any air bubbles that may have remained following cell preparation do not impose on the success of the test (BS 1377 1990). Following the saturation stage the cell pressure is raised to the required effective pressure. The required effective pressure is based on the *in-situ* conditions of the sample. The required effective pressure was determined from the multiplication of the unit weight of the sample by the sample depth. Following this determination, the depth to the water table was multiplied by the force of gravity and deducted from the required effective pressure so that only the volume unit weight of the materials above the sample were accounted for.

3.5.4.2 **Consolidation stage**

The consolidation stage followed immediately after the saturation stage. The consolidation stage was initiated after a stable required effective pressure value had been reached. Consolidation of the specimens was continued until 95 % of the pore water pressure had been dissipated. The samples placed under consolidation consistently needed between 8 and 16 hours before 95 % pore water pressure dissipation was reached. Following pore water pressure dissipation, the specimen volume change is plotted against the square root time ($\sqrt{T100}$) to determine the testing time according to the BS1377 (1990) (for the detailed process of the determination of the T100, see BS1377 1990 Section 6.3). The significant testing time could then be established from multiplying the T100 by the coefficient F. Applying the consolidation time resulted in a slow rate of strain, with triaxial speeds between 0.014 to 0.019 mm min^{-1}. Head (1998) suggests that for sensitive soils a slow rate of compression is required, as this allows for pore water pressure to be equalised across the specimen during the compression/shearing stage.

3.5.4.3 **Compression stage**

In accordance with BS 1377 (1990), compression was applied immediately following consolidation. Compression was run until 20 % axial strain was reached (BS 1377 1990). For a consolidated drained test the back pressure drain remained open to allow for drainage during compression. During consolidated undrained tests, the back pressure drain was closed, restricting any drainage from occurring (BS 1377 1990). Measurements were recorded every 2 minutes to ensure that the failure curves were well documented and to enhance the accuracy of the plots. Approximately 800 points were recorded for each specimen test. Following test completion a membrane correction was required to account for the restraining effect of the membrane. A third order polynomial equation from Wyatt (2009) was implemented to determine the membrane correction required. The correction was subtracted from the measured deviator stress values. The equation was:

$$Mc = 4 \times 10^{-5} (\varepsilon^3) - 4.7 \times 10^{-3} (\varepsilon^2) + 0.1596 \times \varepsilon \qquad (3.13)$$

Where: *Mc* = membrane correction
ε = strain (%)

3.6 **Mineralogical properties**

3.6.1 **X-Ray Diffraction**

For each soil sample studied, an X-ray diffraction analysis was undertaken to establish what minerals were present in each sample. The X-ray diffraction technique works on the principle that crystals within the microstructure of the soil diffract in characteristic patterns (Whitton and Churchman 1987; Mitchell and Soga 2005).

X-ray diffraction offers a particularly effective technique for identifying clay minerals within soil samples which are not visible via most optical means. While no single identification procedure is flawless in its ability, X-ray diffraction offers a technique that distinguishes between various clay minerals which may be present in a soil sample (Brindley and Brown 1980). Further, the XRD method is

non-destructive and requires only small amounts of material (Whitton and Churchman 1987).

X-ray diffraction, however, is limited by extremely small and poorly crystalline clay materials such as allophane (Mitchell and Soga 2005). Allophane is identified as X-ray amorphous, and so other methods are generally employed to determine allophane content (Mitchell and Soga 2005). Previous studies in the Tauranga Region (Keam 2008; Wyatt 2009; Wyatt *et al*. 2010) have found little to no allophane was present in the soils. Arthurs (2010) speculated that halloysite or allophane was present in the soils he studied in the Tauranga region, however did not make a determination to distinguish between them. Considering the lack of allophane previously encountered at Tauranga, aside from SEM analysis, separate allophane determinations were not undertaken in this study.

The XRD analyses were undertaken with a Philips PW analytical defractometer. The scanning range chosen was 2^0 to 40^0 2θ. To make determinations between the minerals in the samples as well as identifying particular clay minerals, separate investigations were undertaken. Bulk samples were crushed with a porcelain mortar and pestle before scanning. Clay fractions were separated by a centrifuge. The samples were initially treated with sodium hexametaphosphate and then run in a centrifuge at 800 rpm for three minutes (Whitton and Churchman 1987). The remaining particles in suspension were removed with a pipette, and placed in a separate beaker for MgCl treatment. MgCl was used to flocculate the sample (Whitton and Churchman 1987). Following flocculation the sample was pipetted onto a ceramic tile and allowed to dry over distilled water for 24 hours (Lowe and Nelson 1983). Drying samples over distilled water has been found to be important for the determination of halloysite in its actual field state and similarly to prevent irreversible halloysite dehydration to its 7 Å state (Kirkman and Pullar 1978). Ceramic tiles were preferred over glass tiles, which have been known to crack following sample placement (Lowe and Nelson 1983).

The scanning regime employed was based on that of Wyatt (2009) and Whitton and Churchman (1987) to ensure comparability and reproducibility between results. Following an initial scan on the bulk and clay fraction samples, the clay samples were heated to 110 ^{0}C for 1 hour and then scanned again.

Subsequently, the samples were heated to 550 ^{0}C for 1 hour and scanned again. Heating the samples clarifies halloysite presence, where following heating, halloysite should dehydrate from a basal spacing of ~ 10 Å to ~ 7 Å. To distinguish between dehydrated halloysite and kaolinite minerals, 1 drop of formamide was added and the sample rescanned (Churchman *et al*. 1984).

Interpretation of the results was undertaken by initially converting the basal spacing from ° 2 θ to Å. Mineral correlations of these Å values were made following the work of Brindley and Brown (1980) to positively identify each significant peak identified.

3.6.2 **Scanning Election Microscope (SEM)**

Scanning electron microscopy (SEM) was undertaken on all of the samples tested in this study. SEM analysis permits the observation and classification of organic and inorganic materials at a scale of nanometres to micrometres (Goldstein *et al.* 2003). The electron microscope produces a point by point reconstruction of the specimen from a signal emitted from the specimen when it is illuminated by the high energy electron beam (Lee 1993). The SEM was used to analyse microstructural characteristics of the specimens sampled in this study.

As the SEM requires samples to be placed in a vacuum chamber, all samples had to be thoroughly air dried. Following drying the intact samples were lightly broken down by hand to leave little intact blocks. Remoulded specimens were also air dried and lightly broken down by hand. The intact and remoulded blocks were mounted to a steel mount by carbon paint. A platinum coating was finally added to minimise sample charging and increase electron conductivity.

Samples were examined between 3 kV to 5 kV to ensure that the level of charging was minimised, enhancing the clarity of the images. Energy dispersive X-ray (EDX) analyses were undertaken, however, the samples were required to be scanned at 20 kV. Scanning at this voltage resulted in an unclear image, which would often be blurry when still shots were taken. The picture was clear enough, however, to ensure that an accurate EDX analyses could be taken for the particles in question.

Chapter 4

FIELD OBSERVATIONS AND STRATIGRAPHY

4.1 Introduction

Much of the Tauranga region is underlain by a series of pyroclastic deposits including ignimbrite and tephra-fall deposits, sedimentary deposits consisting mainly of reworked pyroclastic materials, and buried soils (paleosols). Most of the deposits are encompassed by the Matua Subgroup (see Chapter 2 for generalised stratigraphy of Tauranga). The deposits typically display weathering to varying extents. Furthermore, paleotopography and paleoerosion contribute to the multifarious stratigraphic distribution between sites which promotes a non-idealistic complexity in the region (Briggs *et al*. 1996). Initial site selection for this study was based on the accessibility to soil outcrops, geomorphic indicators (such as previous landsliding events) and those areas previously recognised as sensitive (Gulliver and Houghton 1980; Smalley *et al.* 1980; Wyatt 2009; Arthurs 2010). The following chapter will describe the process for identification of sensitive and non-sensitive field localities, and the resulting site selection from those investigations. Each suitable site is subsequently described, identifying the stratigraphic distribution and geomorphic observations for each site. The engineering geological descriptions used to characterise each site were based on the guidelines issued by the New Zealand Geotechnical Society (2005).

4.2 Initial field observations and site selection

An initial field scout for exposed soil outcrops was undertaken to establish whether sensitive soils were present or not. As previously identified in Chapter 3, the field shear vane and the hand shear test (from Milne *et al.* 1995), were used to quantify sensitivity. These tools provided the basis for identification of suitable sensitive or non-sensitive sites. Primarily, coastal areas were explored because

sections were exposed through erosion and thus were readily accessible. Coastal sites investigated included Omokoroa (6392592.4N 2779197.7E), Pahoia Peninsula (6392862.6N 2776074.9E and 6392458.4N 2775311.3E), Te Puna (6388572.0N 2782693.9E), Rangataua Bay (6382764.4N 2794147.9E), Plummers Point (6389822.4N 2779066.9E) and Maungatapu (6382272.0N 2791366.5E). Of these coastal locations investigated, sensitive material was identified at Omokoroa, Te Puna and Pahoia Peninsula, while the outcrops at Rangataua Bay and Maungatapu did not exhibit any sensitive stratigraphic layers. The non-sensitive nature of the soil materials from Maungatapu was somewhat surprising, given Bird (1981) previously identified interstratified sensitive clay at Maungatapu. Plummers Point did not offer any suitable exposed outcrops for analysis. At Rangataua Bay the deposits seemed similar in appearance, and at a similar stratigraphic position, as sensitive materials identified at Omokoroa, Te Puna and Pahoia Peninsula. The soil material at Rangataua Bay, however, did not exhibit sensitive properties and so was analysed to establish how it differed from sensitive materials.

Investigations into sensitivity away from the coast were also attempted. This proved problematic given that much of the Tauranga region is heavily developed, and exposures are uncommon. A pumice excavation pit at Tauriko (6378656.1N 2783169.1E) provided a large open profile, where potentially sensitive material could be found. Soil material at this site was similar in appearance to the sensitive materials found at Omokoroa, Te Puna and Pahoia Peninsula, but upon closer inspection had different characteristics (as described later in Section 4.3.4). As with Rangataua Bay, this material was analysed to determine how non-sensitive material was different from sensitive material.

On the basis of these field investigations, five sites were chosen for this study, three (Omokoroa, Te Puna and Pahoia Peninsula) which displayed sensitive properties and two (Rangataua Bay and Tauriko) which did not appear to exhibit sensitive attributes (Figure 4.1).

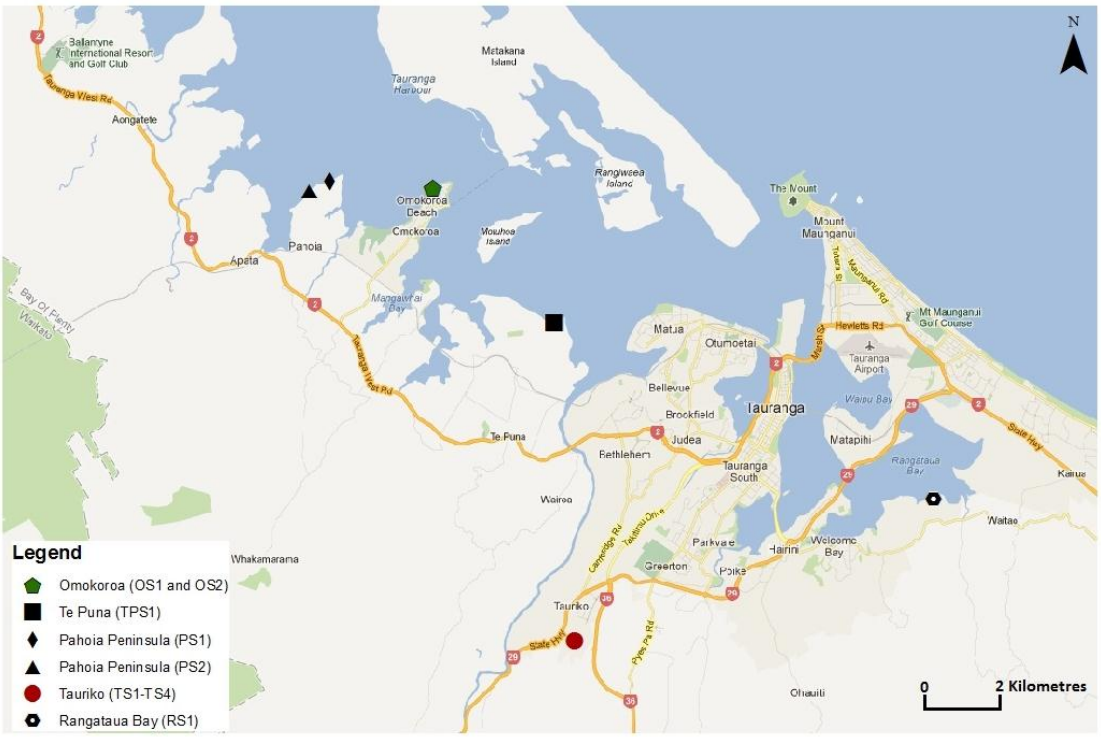

Figure 4.1: Map showing locations of the sample sites used in this study (Google Earth 2012)

4.3 Stratigraphy and site location properties

4.3.1 Omokoroa

The stratigraphic column described for Omokoroa (Figure 4.2) was recorded from a relict landslip immediately adjacent to the sampling sites chosen, which provided an open profile readily accessible for documentation. The sensitive soil materials studied at Omokoroa were identified close to the shore platform and were confined within a 1.2 m section. A hand auger was used to identify layers below the shore platform enabling the correlation of layer observations in this study with previously recognised deposits (Gulliver and Houghton 1980; Briggs *et al*. 1996; Keam 2008; Arthurs 2010).

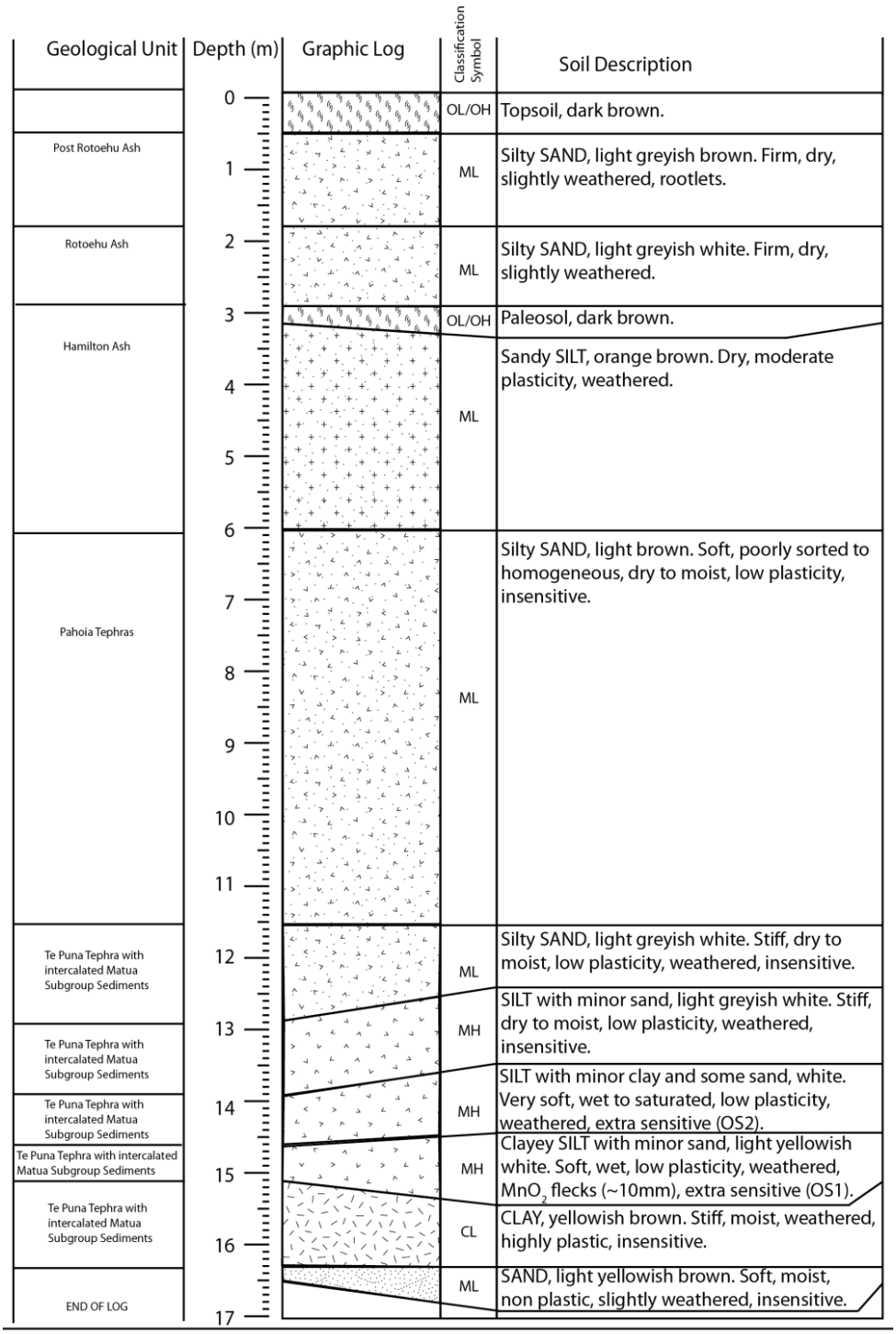

Figure 4.2: Complete stratigraphic log of the Omokoroa sampling site exposure

Two intact samples were collected from the sensitive soil exposure at Omokoroa. These were recorded as OS1 and OS2. The two separate samples were positioned immediately above/below each other, but were characteristically discernible yet both displayed sensitive properties. The engineering geological properties of the materials are described in the following section.

4.3.1.1 Engineering geological description at Omokoroa Sample One (OS1)

OS1 (Fig. 4.10) was identified as moderately weathered clayey SILT. The *in-situ* material was wet and a distinct cream white colour, which did not appear to have a sharp upper boundary, but was rather indistinct to diffuse. OS1 was considered sensitive to extra sensitive (field sensitivities ~ 11) and became dilatant upon remoulding. Manganese-rich nodules and concretions were abundant, covering ~ 5-10 % of the sample in any given area within the layer and were medium (10-20 mm) sized. Orange mottles were also observed near the top of the layer (~5-~10% of the matrix). This soil unit likely represents undifferentiated tephra fall deposits and rhyolitic silts and sands of the Matua Subgroup in association with the Te Puna ignimbrite eruptive sequence (0.93 Ma; Briggs *et al*. 2005; Arthurs 2010). Under the OS1 layer was a yellowish brown CLAY layer, clearly distinguishable. The clay layer extended to the shore platform, and a further 1.4 m below. Because of the high level of clay in this material, permeability was considered low, and the material was moist to wet. Briggs *et al.* (1996) suggest that at Omokoroa, the Te Puna ignimbrite can be observed as a weathered brown clay layer which appears to correlate to the clay layer observed (Figure 4.3). Immediately above OS1 was OS2, with a boundary approximately 0.6 m above the shore platform.

Within the OS1 layer, two distinguishable perched water tables could be seen where the impermeable weathered Te Puna clay layer acts as an aquaclude resulting in a variable water table position (Figure 4.3). The perched water tables suggest fluctuating levels of saturation for the material, indicating the sensitive layer was completely saturated on more than one occasion. This variation between saturation and partial saturation of the soil again tends to support the formation and presence of manganese dioxide (probably pyrolusite) concretions as observed in the sample.

4.3.1.2 Engineering geological description at Omokoroa Sample Two (OS2)

OS2 (Figure 4.3) was recognised as a weathered SILT with minor sand. The material was close to saturation, and extremely dilatant upon remoulding. The colour was characterised as white with imbedded manganese dioxide nodules and

concretions. These concretions covered ~ 10 % of the sample and were medium (10-20 mm) in size. The layer was considered to be sensitive to extra sensitive (field sensitivities ~ 15). As aforementioned, OS2 is immediately positioned above OS1 and is likely to be within the Matua Subgroup sequence of undifferentiated tephra-fall beds and rhyolitic silts and sands in association with the Te Puna ignimbrite eruptive sequence (0.93 Ma; Briggs *et al.* 1996; Briggs *et al.* 1996; Arthurs 2010). Atop the OS2 layer was another SILT layer, considerably drier and too hard for shear vane determinations. The material represented an undifferentiated tephra-fall deposit associated with the Matua Subgroup.

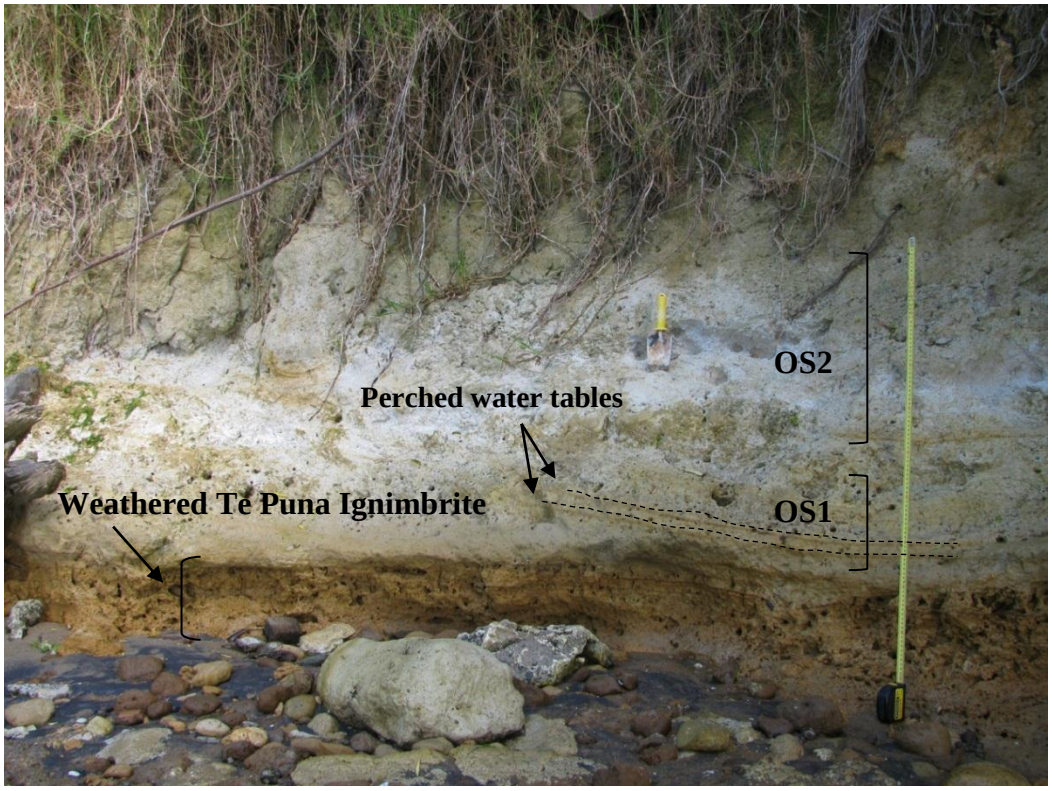

Figure 4.3: Omokoroa sampling location. Sample locations are identified as OS1 and OS2. Perched water tables can be observed near the bottom of OS1 at approximately 0.35 m and 0.40 m above the shore platform. The tape measure was extended approximately 1.2 m for scale.

4.3.1.3 **Childs' Test observations at Omokoroa**

The soil materials at the Omokoroa exposure were further investigated with Childs' Test at both sample sites. At OS2, a pale pink colour developed, following the appropriate rest period after the test reagent was sprayed (Figure 4.4). The pale pink colour appeared in blotches over the exposed area and remained the same pale pink colour even after a further 30 minutes. Childs (1981) suggested that a pale pink to pink reaction corresponds to ~ 0.2 - 4.0 ppm of ferrous iron in the soil solution. OS1 displayed a similar reaction, only even paler, yet was still considered to be pale pink. The result indicates between 0.2-4.0 ppm of ferrous iron was present in the soil solution (Childs 1981). The paler pink colour observed here suggests that the ferrous iron concentration in solution is likely to be closer to 0.2 ppm than c. 4.0 ppm. Nevertheless, both layers were thus considered to be under reducing conditions.

Figure 4.4: Results of Childs' Test (Childs 1981) undertaken at OS2. A pale pink colour is visible in blotches (circled) on the surface, indicating that low levels of ferrous iron (Fe^{2+}) were present in the soil solution.

4.3.1.4 Geomorphic observations associated with Omokoroa

4.3.1.4.1 Primary features

Omokoroa Peninsula is recognised for land instability and landsliding features, which have affected coastal cliff properties for over 30 years .The geomorphic observations, therefore, are similar to those presented by Gulliver and Houghton (1980), Keam (2008) and Arthurs (2010). Several landsliding features are recognised, primarily on the north western side of the peninsula. Main failure features include landslides on the coastal boundary of Ruamoana Place (6392503.7N 2779083.3E), Walnut Grove (6392726.0N 2779384.1E), Gerald Place (6392730.1N 2779472.5E) and the largest relict slip off Bramley Drive (6392397N.7 2778965.4E) (Figure 4.5). Significantly, the Bramley Drive failure, which initially occurred in 1979, was reactivated in May 2011 (Tonkin and Taylor 2011). The failure was again large and resulted in a large landslide runout deposit (Figure 4.6). The Bramley Drive failure has been previously identified as the result of the sensitive soil failure, following increased heavy rainfall loading in the area (Keam 2008; Tonkin and Taylor 2011).

Figure 4.5: Map of the northern tip of Omokoroa Peninsula. A steep coastal cliff is generally continuous on the north western side of the peninsula (Google 2012).

Figure 4.6: The Bramley Drive failure, which originally failed in 1979. The slide was reactivated in 2011, exposing the landslide scarp. In the foreground, hummocky features associated with the long landslide runout can be seen.

4.3.1.4.2 **Small scale features**

The exposed coastal cliff face at the sampled section (OS1 and OS2) appeared to have experienced some coastal landsliding, with large intact units transported from high on the face to approximately 3 m above the shore platform (Figure 4.7). Tides and coastal processes had removed any runout lobe or failed material from this event meaning that no post-failure analysis of failed material was possible. The impact of coastal erosion by wave undercutting on the landsliding events, however, has been suggested to be limited because the majority of large failures observed have been attributed to the presence of sensitive soil layers (Keam 2008). The primary impact of marine transportation appears to be in the removal of the landslide buttress by wave action, thereby keeping landslides active with the removal of basal support to the cliffs (Keam 2008).

Figure 4.7: Intact unit (above the dashed line) that has been transported from higher on the coastal cliff to approximately 3 m above the shore platform. The lower unit (below dashed line) comprises in situ deposits.

At the top of the coastal cliffs, particularly above the Omokoroa sampling site, soil cracking covered by grass was observed (Figure 4.8). Many areas on the north western coastline of Omokoroa are cordoned by setback fences to reduce risk associated with the gradual retreat of the coastal cliffs, which likely begin with such cracking features. The soil close to the edge of the coastal cliff (above the location of OS1 and OS2) appeared to be gradually moving downslope (Figure 4.8). This feature appears to emulate a similar pattern to what may have occurred at Slip 1 and Slip 2 (Figure 4.9) which are immediately adjacent to the slope cracking shown in Figure 4.8, before they detached from the edge of the cliff. It is likely that as the cracking increases, the slope will retreat further and fail in a similar way.

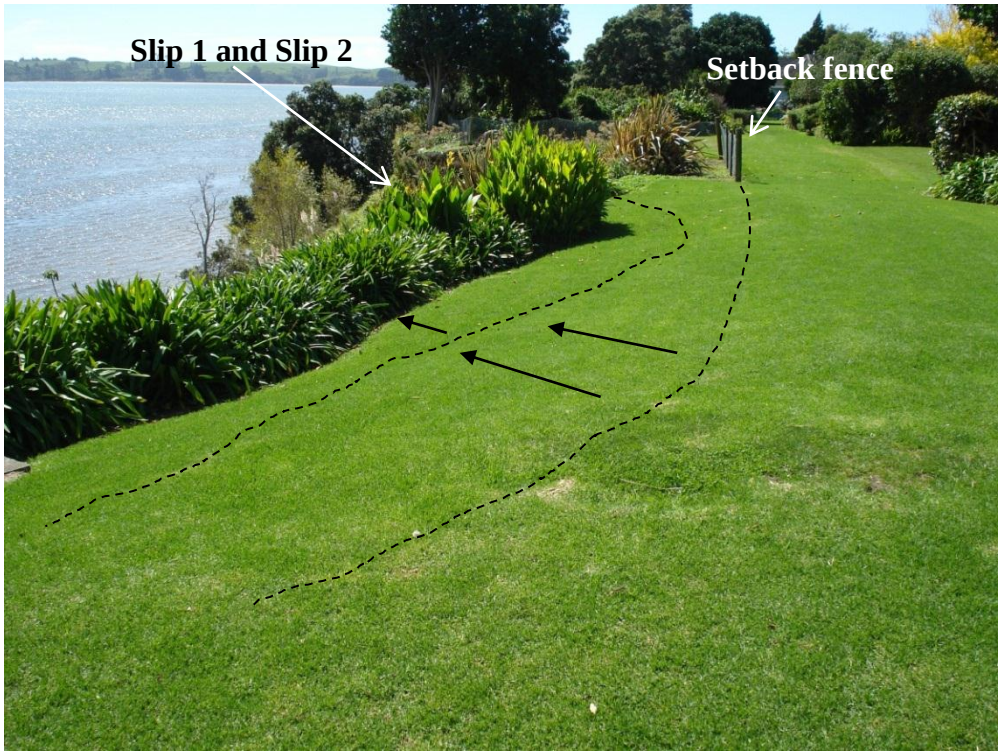

Figure 4.8: Cracking at the edge of the coastal cliffs at Omokoroa (changes in slope and cracking covered by grass indicated by the dashed lines and arrows). Note the setback fence in the background, which indicates the retreat positioning of neighbouring slopes, suggesting the cracking could lead to failure in line with some of those that have previously occurred.

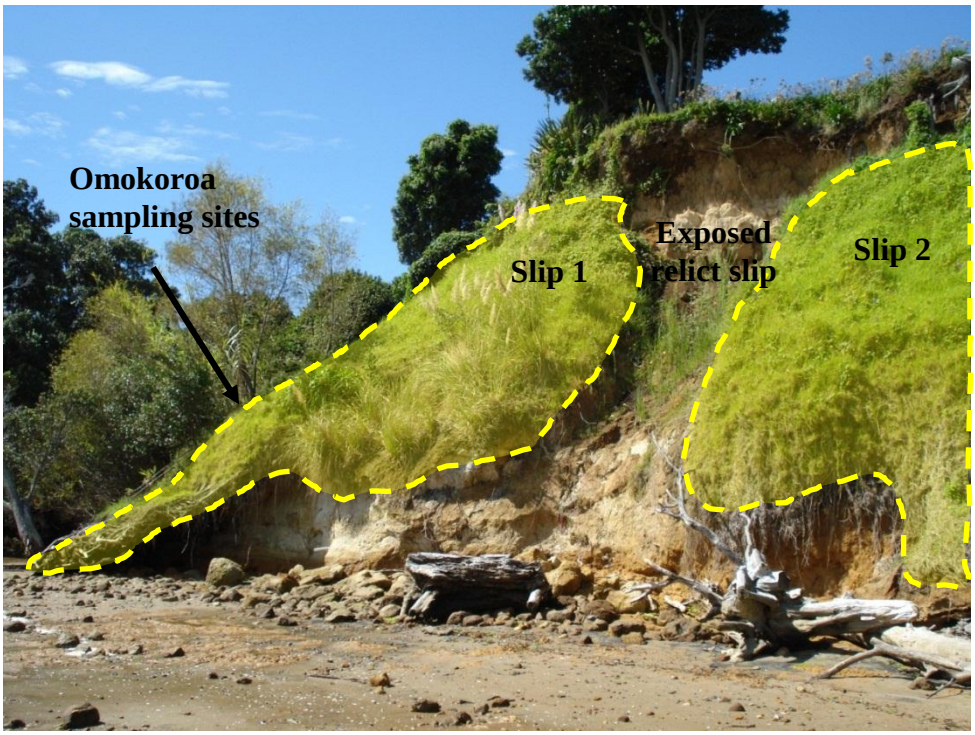

Figure 4.9: Two slowly progressive landslips either side of an exposed relict slip near the Omokoroa sampling site. The intact upper unit evident in Fig. 4.7 is associated with Slip 1. Both Slip 1 and Slip 2 have gradually detached from the uppermost soil at the edge of the coastal cliff, indicating they are prone to further failure.

4.3.1.4.3 **Post-failure landslide runout zones**

At the base of both the Bramley Drive and Ruamoana Place landslides, are geomorphic features consistent with sensitive soil failures. Particularly noteworthy are the long runout lobes extending from the landslides (Figure 4.10). Significant landslide debris was intermixed within these runout lobes including disfigured trees and other displaced foliage. The runout lobe was not uniform or smooth and completely covered any previous natural features that were at the base of the coastal cliff. The further distance from the cliff the runout material spread, the more obvious it was a "single" material, rather than a series of units intermixed during failure. A thin sand layer of ~ 0.02 m had been deposited over much of the runout lobe, likely during the tidal fluctuations. Beneath this sand cover, the runout lobe material was comprised of white, naturally remoulded soil material (Fig. 4.11). The material behaved in a dilatant manner, consistent with that observed at OS1 and OS2 upon remoulding. Considering sensitive failures have previously been recognised with characteristically long runout lobe features (Wyatt 2009; Quinn *et al.* 2011), the material furthest out from the landslide is likely to be the sensitive material derived from the basal units of the deposits that failed, generating the sensitive landslide event. This material therefore was characterised as naturally remoulded sensitive material.

Figure 4.10: Landslide runout deposits from the failures at Ruamoana Place and Bramley Drive.

Figure 4.11: Remoulded white material uncovered on the Ruamoana Place landslide runout lobe. The material was widespread at the end of the runout lobe underneath a thin (~ 0.02 m) sand layer likely deposited by wave action following the landslide.

On the basis of the naturally remoulded sensitive soil material being exposed, a second sample site was chosen, namely the material uncovered in this runout lobe. This site was recorded as the Omokoroa landslide runout (OLRO). The description and analysis of this material allow for the unique characterisation of naturally remoulded sensitive soil. Figure 4.12 illustrates where OLRO was sampled in relation to the other sampling sites and major geomorphology features previously identified.

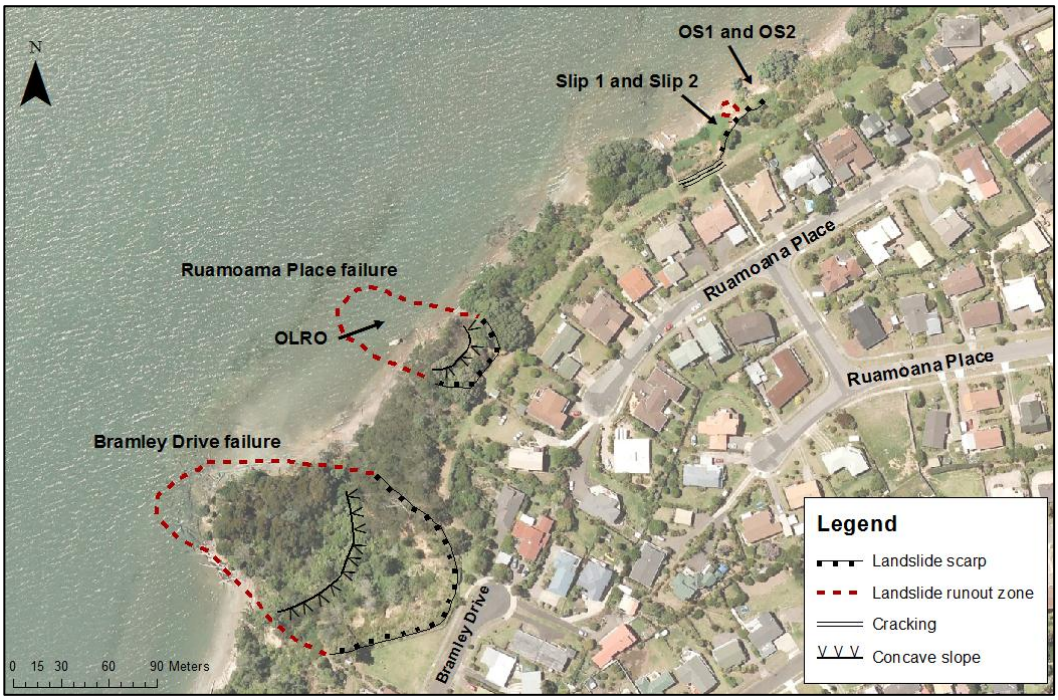

Figure 4.12: Geomorphic map of the study area from Omokoroa. The image was captured in 2007 (from Google Earth 2012) and so does not have the most recent 2011 Bramley Drive landslide reactivation, nor the Ruamoana Place landslide deposit. The landslide runout zones are drawn at the approximate locations and areas that they were occupying during this study.

4.3.1.5 Engineering geological description of the Omokoroa Landslide Runout (OLRO)

OLRO was described as clayey SILT with sand. The soil was a homogenous white colour with no visible variations or manganese concretions. The material had been deposited away from its original deposition location following the landslide, meaning sand contamination during (and after) the landslide process and variations in moisture content could not be adequately accounted for. The sensitive material appeared (in both colour and texture) similar to that of OS1 and so was speculated to be a part of the Matua Subgroup as a tephra deposit associated with the Te Puna Ignimbrite eruptive sequence.

4.3.1.6 Field sensitivity observations

Field sensitivities at both OS1 and OS2 were considered extra sensitive (New Zealand Geotechnical Society 2005) with average sensitivities of 11 and 15, respectively (Table 4.1, Figure 4.12). Both materials were dilatant under pressure with thumb and finger. Considering no intact material for OLRO could be obtained, no suitable quantitative sensitivity measurements could be undertaken

on that soil material. Figure 4.13 illustrates the profile variability of sensitivity for both OS1 and OS2. The peak vane shear strength typically decreases with depth in OS2, but recovers at the boundary with OS1. This pattern is mimicked with the remoulded strength. However, where remoulded strength decreases significantly at approximately 14.3 m and 14.55 m depth, the sensitivity is heavily impacted, increasing to the highest and second highest value attained throughout the profile. These low strengths demonstrate the significance of the remoulded strength at low values on the determination of sensitivity.

Table 4.1: Field sensitivity observations undertaken at the Omokoroa sample sites.

	Peak Vane Shear Strength Range	**Mean Peak Vane Shear Strength (kPa)**	**Remoulded Shear Strength Range**	**Mean Remoulded Vane Shear Strength (kPa)**	**Sensitivity (kPa)**
OS1	78 – 106	92 ± 6	6 – 11	8 ± 0.6	11 ± 0.6
OS2	53 – 109	74 ± 4	3 – 8	5 ± 0.6	15 ± 1.5

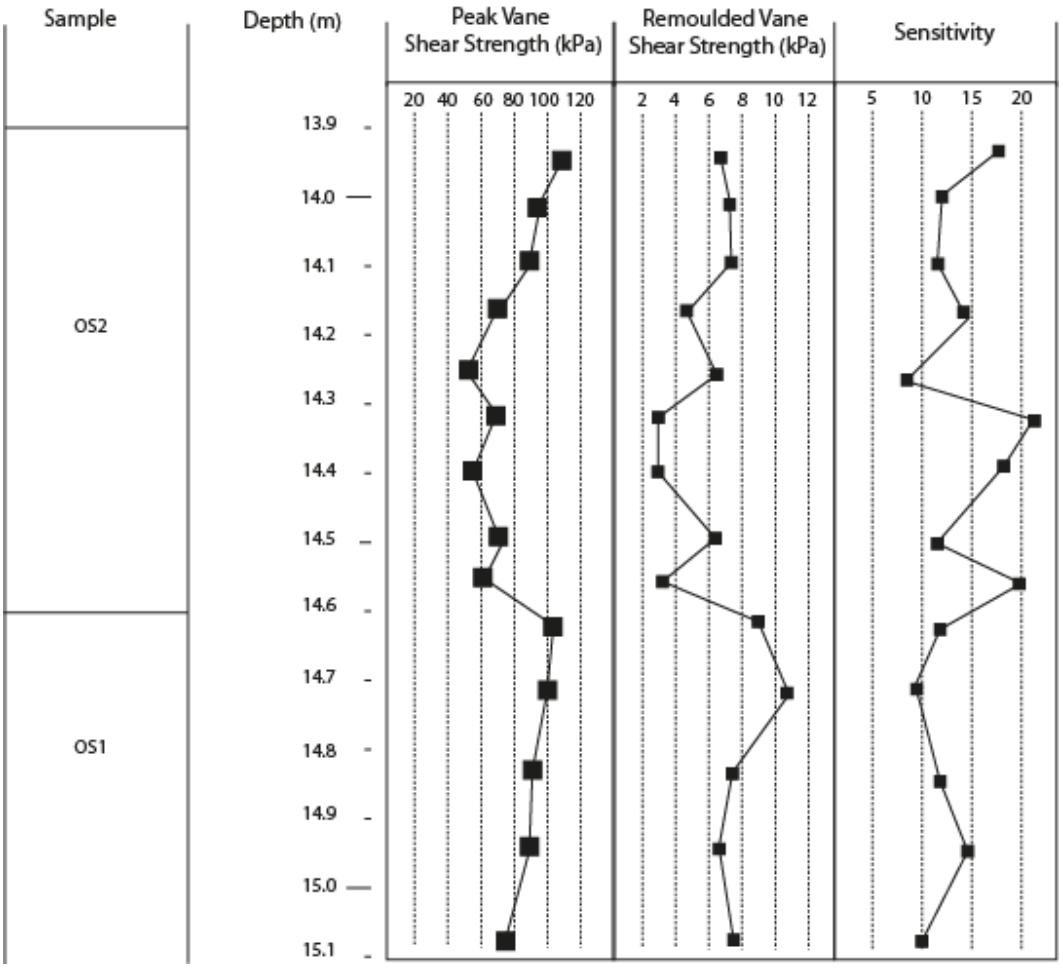

Figure 4.13: Complete shear vane strength and sensitivity log of the Omokoroa sampling site exposure (OS1 and OS2).

4.3.2 **Te Puna**

The second sample site was located at Te Puna, which provided a ~ 3 m high exposure, for which a sensitive layer immediately above the shore platform was characterised. Only one homogenous sensitive layer within the stratigraphy was recognised, meaning that only one sample was taken from this site, named TPS1. Although the exposure was comparatively small compared to that at Omokoroa, a generalised stratigraphy could still be recognised (Figure 4.14).

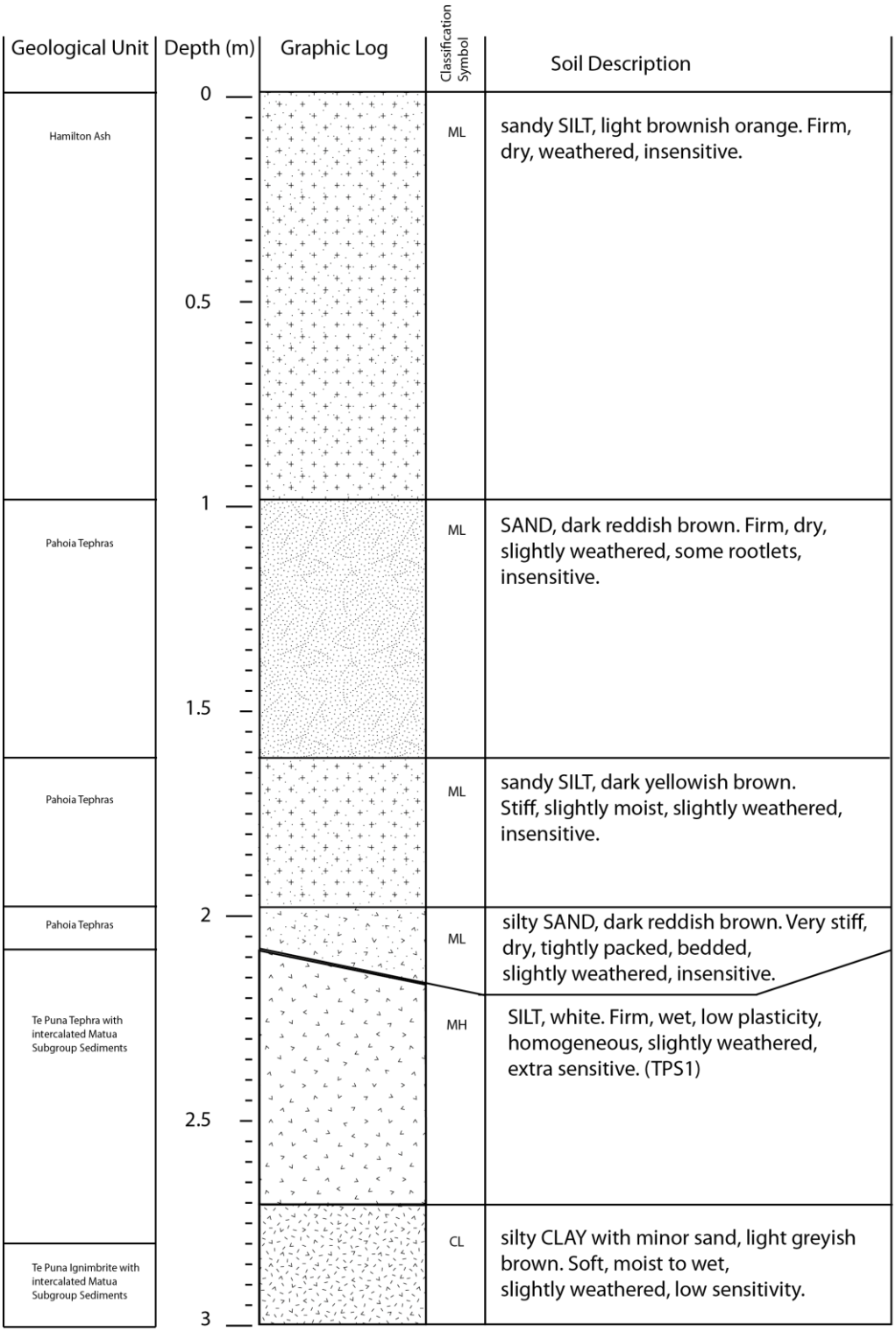

Figure 4.14: Complete stratigraphic log of the Te Puna sampling site exposure.

4.3.2.1 Engineering geological description of Te Puna (TPS1)

The Te Puna sensitive layer was identified primarily as a SILT deposit that was slightly weathered. The material was very dilatant upon remoulding

indicating high sensitivity. Furthermore, the soil was very wet and close to saturation. The soil was a homogenous white colour, with almost no variations across the distribution (Figure 4.15). In contrast to the material from Omokoroa, manganese concretions or nodules were not observed. This sensitive material likely represents undifferentiated tephras and rhyolitic silts and sands of the Matua subgroup in probable association with the Te Puna ignimbrite eruptive sequence (Briggs *et al.* 1996; Arthurs 2010). The sensitive layer was positioned immediately above the shore platform, which was a light greyish brown layer of silty CLAY. The depth of this layer was unknown, yet again appeared to be weathered Te Puna ignimbrite intercalated with the Matua Subgroup sediments as suggested by previous authors (e.g Arthurs 2010). Additionally above the sensitive layer was a silty SAND layer which was dark red to brown and weathered. This layer was interpreted as being associated with the Pahoia tephras as part of the Matua Subgroup classification (Briggs *et al.* 1996; Arthurs 2010).

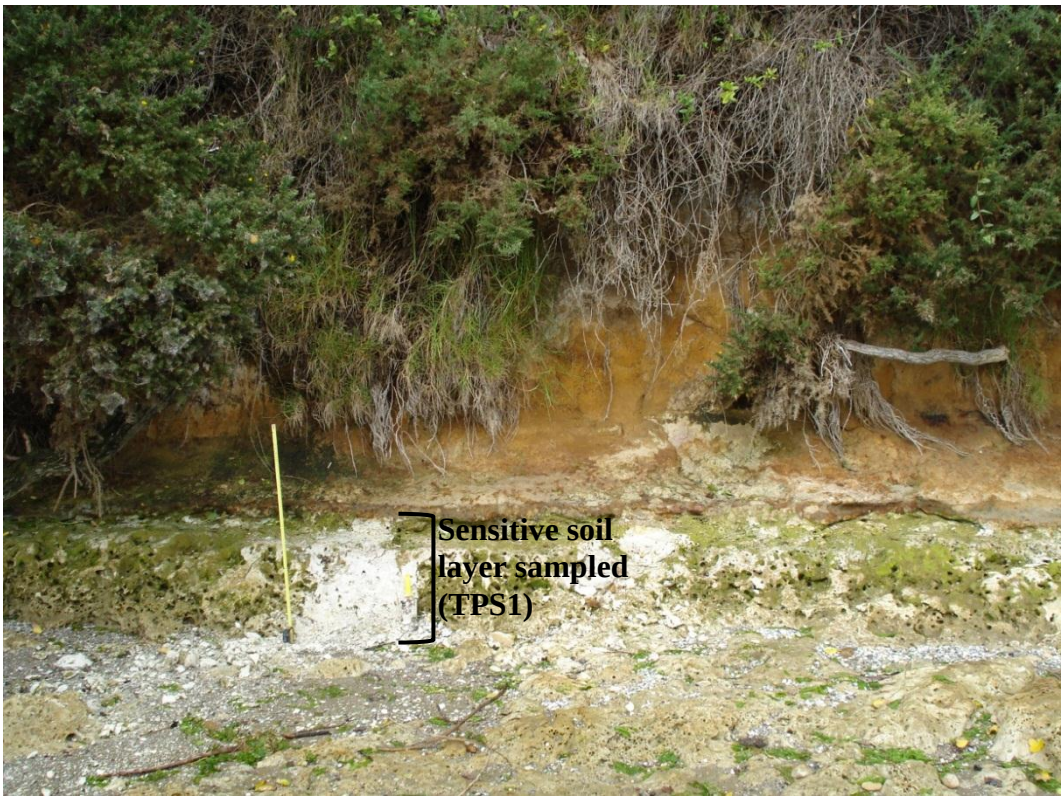

Figure 4.15: Te Puna sensitive soil outcrop. Note that the sensitive soil layer appears to stop at the shore platform. The tape measure was extended approximately 1.2 m for scale.

4.3.2.2 Childs' Test observations at Te Puna

The Childs' Test at TPS1 yielded similar results to those at Omokoroa. The colour development started in blotches of pink, which became more homogenous

across the sample with time (Figure 4.16). The colour was described as pale pink to pink. In reference to Childs (1981) the resulting colour suggests between 0.2-4.0 ppm of ferrous iron was available in solution. As the colour development was closer to pink than pale pink, the concentration of ferrous iron was considered to be between ~ 2.0-4.0 ppm. The results showed that the soils contained reduced forms of Fe^{2+} and so the soil itself was considered to be under reducing conditions (Vepraskas 1994).

Figure 4.16: The Childs' Test result at Te Puna. A pale pink to pink colour development is obvious on the normally white soil surface. This development suggests ~ 2.0 - 4.0 ppm of ferrous iron is present in the soil solution.

4.3.2.3 **Geomorphic observations**

Aside from the profile exposure used to categorise TPS1, only one other small (~ 2.5 m depth) erosive event c. 30 m south west of TPS1 was recognised (Figure 4.17) . The failure was along a sloping incline, meaning that the sensitive layer had dipped below the shore platform. Nearby a prominent Hamilton Ash paleosol could be seen protruding midway up the profile, with the Rotoehu Ash exposed above it.

The top of the coastal cliff areas at Te Puna were typically masked by overlying vegetation with some foliage sprouting from the exposures themselves. This vegetation potentially masked previous small landsliding events from the higher coastal exposures. However, given the density of the vegetation, it was apparent that no significant failures had occurred within the recent past. Considering the close proximity to the shore platform, any previously failed material is likely to have been promptly transported from the area leaving no talus or fan-type relict deposits.

The sensitive layer exposed at Te Puna was covered by green algae, suggesting a significantly wet environment. However this could have been partially due to tidal fluctuations, where a MHWS of 0.89 m (Civil Defence 2010) suggests that the high tide level generally covers the sensitive layer during an incoming tide. As mentioned earlier the sensitive material deposit was characteristically different from material on the shore platform, which could be seen to extend approximately 10 m from the coastal cliff.

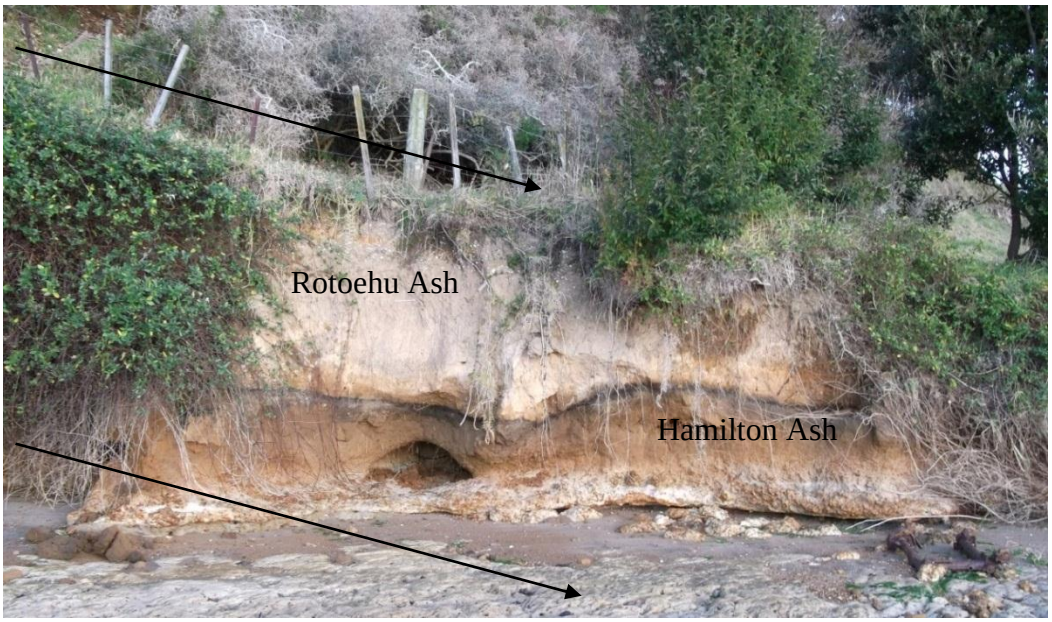

Figure 4.17: Small coastal exposure at Te Puna. The sensitive layer cannot be seen as it has dipped below the shore platform (indicated by the arrows). The prominent paleosol midway up the profile indicates the Hamilton Ash, above which the Rotoehu Ash in exposed.

4.3.2.4 **Field sensitivity observations**

Te Puna field sensitivity observations were extra sensitive according to the scale of the New Zealand Geotechnical Society (2005). Peak vane strength was

typically high, while remoulded vane strength was low, giving rise to high sensitivity measurements (Table 4.2).The material displayed characteristic sensitivity observations including dilatancy upon physical remoulding of the sample under hand pressure. The material did have a high enough intact strength to support cores and could be extracted in blocks, yet it remoulded and flowed immediately upon the application of pressure. The sensitive unit displayed relatively uniform sensitivity over the 0.6 m exposure (Figure 4.18). The remoulded strength was generally variable across the profile, which was typically mimicked by the peak strength, giving a relatively uniform sensitivity value.An exception is observed at approximately 0.2 m above the shore platform. The sensitivity increases dramatically where the peak strength increases and instead of the remoulded strength replicating the change, it decreased giving rise to such a large sensitivity value of 25.

Table 4.2: Field sensitivity observations undertaken at the Te Puna sample site.

	Peak Vane Shear Strength Range (kPa)	**Mean Peak Vane Shear Strength (kPa)**	**Remoulded Vane Shear Strength Range (kPa)**	**Mean Remoulded Vane Shear Strength (kPa)**	**Sensitivity (kPa)**
TPS1	94 – 156	122 ± 5.7	6 – 19	12 ± 1.3	11 ± 1.4

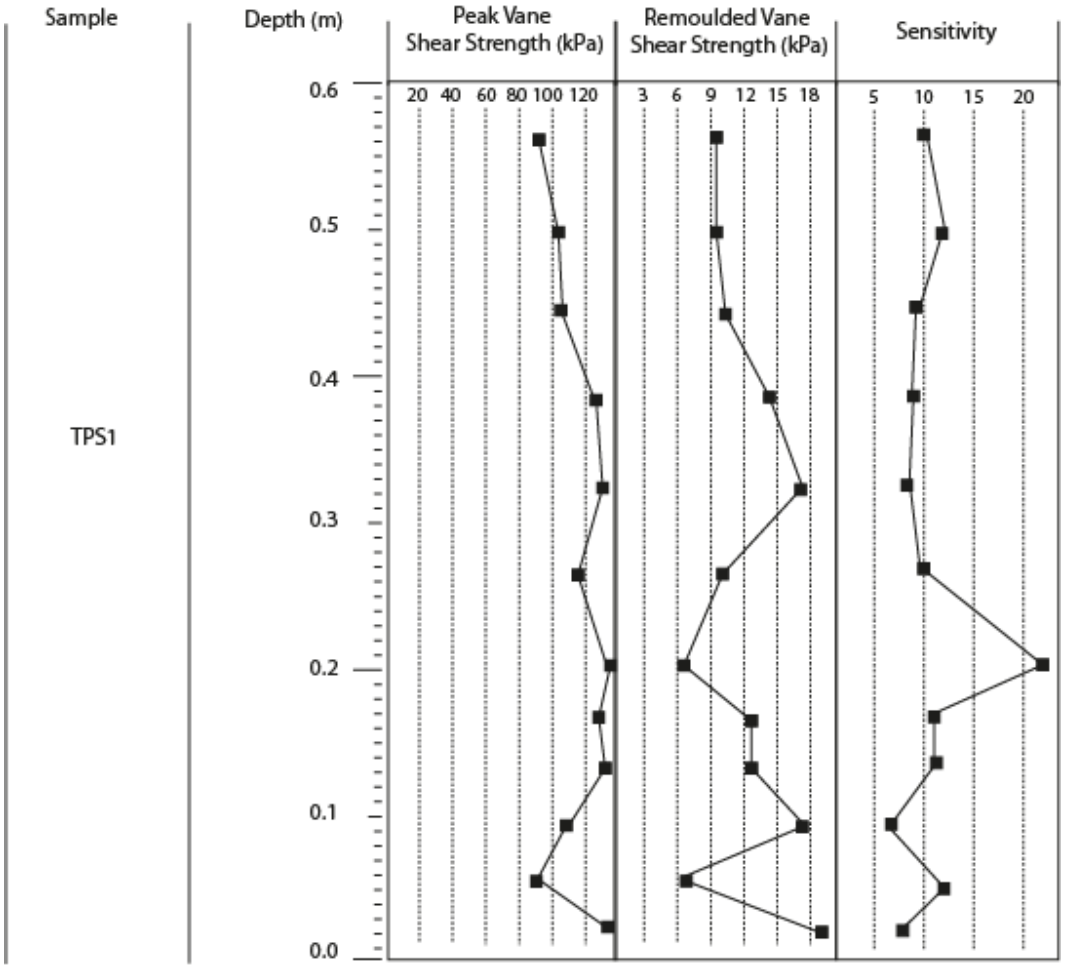

Figure 4.18: Complete shear vane strength and sensitivity log of the Te Puna sampling exposure.

4.3.3 **Pahoia Peninsula**

Soil sensitivity was identified at Pahoia Peninsula in two separate locations, approximately 1 kilometre apart. The two locations were subsequently named PS1 and PS2. Both sample sites were identified immediately above the shore platform (as was observed at Te Puna). The height of the exposure was also similar to that at Te Puna, ranging between ~ 0.85 to 2 m in height. PS1 was an isolated section limited in size and had topsoil immediately above, meaning a detailed stratigraphic log could not be obtained (Figure 4.19). PS2 offered a larger exposure, allowing for the description of overlying deposits (Figure 4.20).

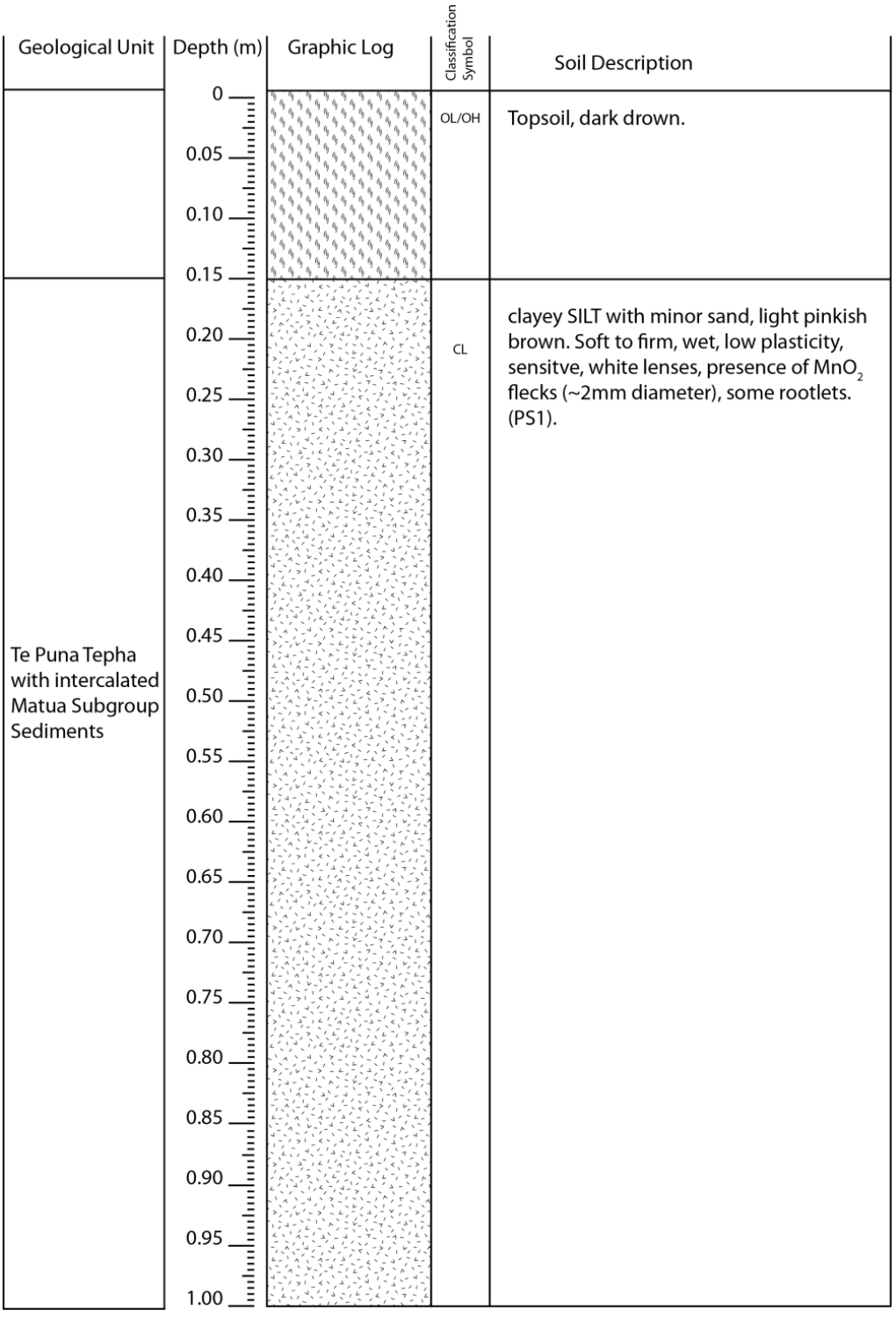

Figure 4.19: Complete stratigraphic log of PS1 from Pahoia Peninsula

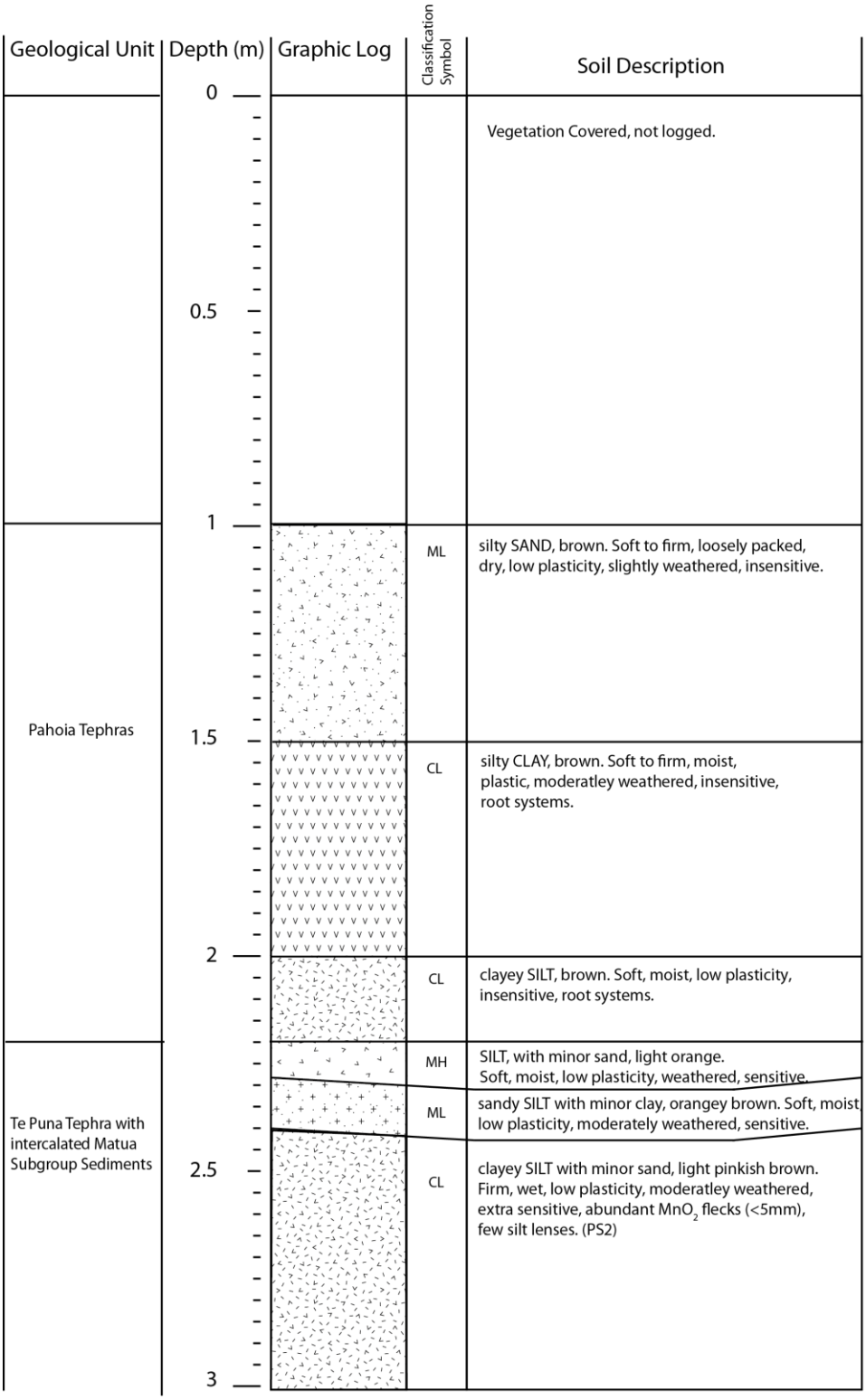

Figure 4.20: Complete stratigraphic log of PS2 from Pahoia Peninsula.

4.3.3.1 Engineering geological description of Pahoia Sample One (PS1)

PS1 was characterised as moderately weathered clayey SILT with minor sand. As with the previous sensitive sites, the material was extremely dilatant upon remoulding. The material colour was light pinkish brown. Furthermore, large abundant manganese concretions were present, covering ~ 10 % of the sample (Figure 4.21). Silt lenses approximately 30 mm wide were also observed in the soil and covered ~ 2 % of the sample. The soil was very wet and close to saturation. The sensitive soil material appeared to be of tephric origin, likely associated with the Te Puna Ignimbrite with intercalated terrestrial and fluvial deposits of the Matua Subgroup (Briggs *et al.* 1996; Arthurs 2010). Immediately above the sensitive layer was top soil with extensive vegetation (Figure 4.21). Some organic matter (plant and tree roots) appeared to penetrate into the uppermost layer of the sensitive material, but it did not infiltrate further than ~ 50 mm. The material below on the shore platform had consistent sensitive properties as that within the sampling range, suggesting the sensitive layer extended onto and below the shore platform (Figure 4.22).

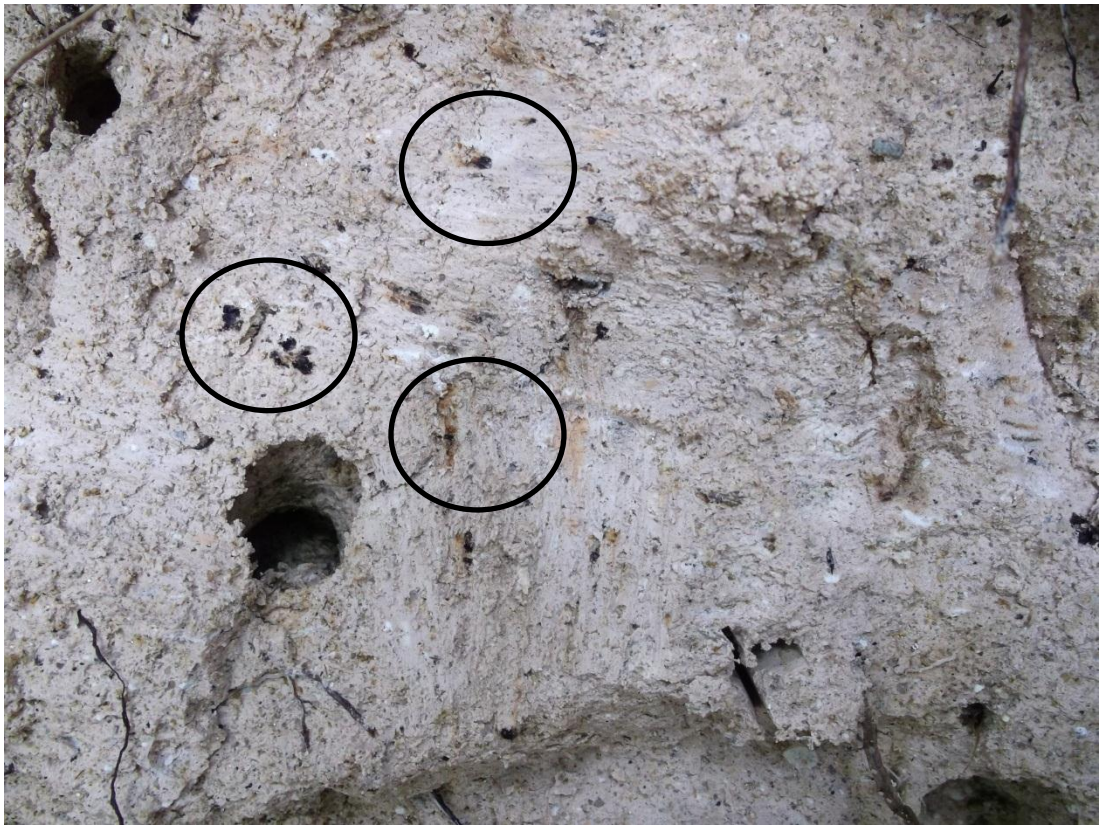

Figure 4.21: Abundance of large manganese concretions (some indicated by circles) present at PS1.

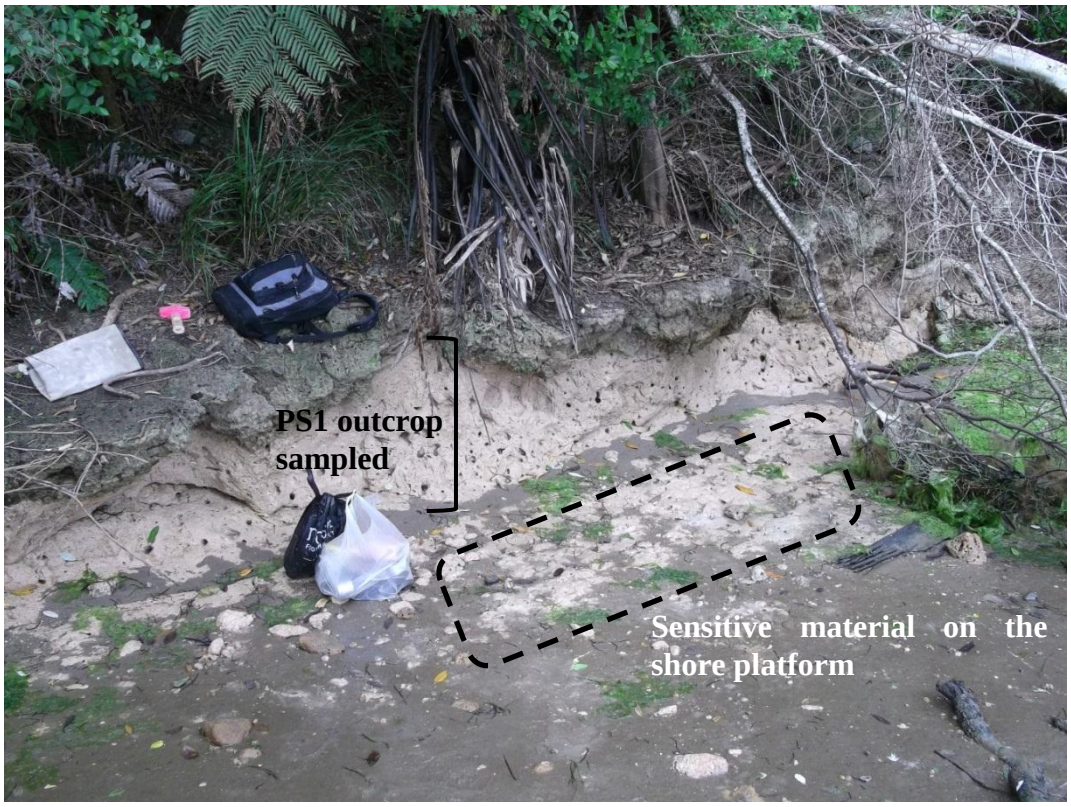

Figure 4.22: The sensitive soil outcrop at PS1. The sensitive material appeared to extend below the shore platform.

4.3.3.2 Engineering geological description of Pahoia Sample Two (PS2)

The sensitive layer at PS2 appeared to be very similar to that of PS1 possibly suggesting they were distal correlatives. Different from PS1, PS2 had exposed younger deposits sitting on top of it (Figure 4.23). The material was weathered clayey SILT, with minor sand. As with PS1, a similar light pinkish brown colour was observed. The soil was very wet to saturated. The soil material also had an abundance of manganese concretions, which included two consistent lines of manganese concretions protruding through the sample spaced approximately 20 mm apart (Figure 4.24). Furthermore, the soil had very similar sensitivity values to those of PS1, with 11 for PS1 and 9 for PS2. Given these consistencies and characteristics the material was again interpreted to be a tephra-fall deposit with intercalated Matua Subgroup sands and silts associated with the Te Puna Ignimbrite eruptive sequence. The sensitive layer was immediately above the shore platform, with no exposed units below it. Immediately above the extra sensitive unit was a sandy SILT with minor clay deposit. This unit was also extra

sensitive and displayed many similar properties as evident for PS2, including low plasticity and high saturation level. The material was still considered to be of tephric origin within the Matua Subgroup, but was possibly further reworked following deposition and thus it has a greater sand constituent than the PS2 sample.

Figure 4.23: Sensitive soil outcrop at PS2. The tape measure was extended approximately 1.5 m for scale.

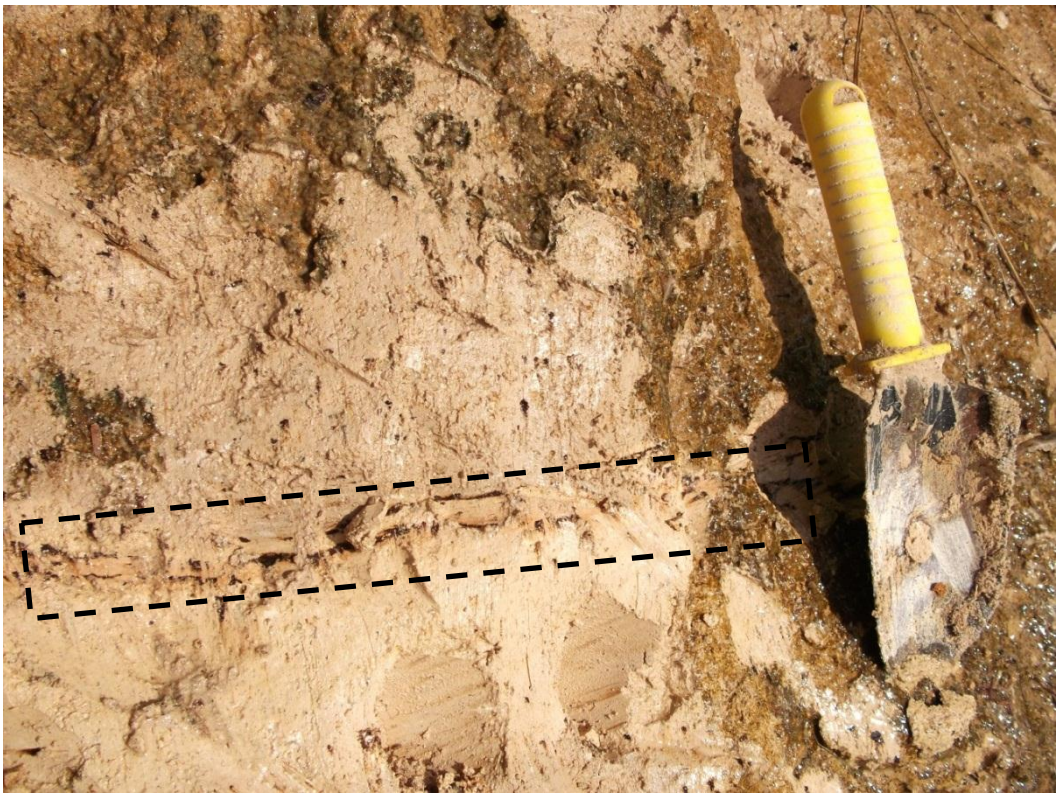

Figure 4.24: Sensitive soil layer at PS2. The thin lines of manganese concretions are indicated within the dashed box. Note the wet nature of the undisturbed soil at the right of the picture. The soil was observed to be very wet to saturated. The sun position at the time of the photo suggests the material is of an orange brown colour, but it was actually pinkish brown in colour.

4.3.3.3 Childs' Test observations at Pahoia Peninsula

Results of Childs' Test at Pahoia Peninsula differed from those at Omokoroa and Te Puna, in that the material was naturally a light pinkish brown colour (Figure 4.25). After undertaking Childs' Test, no credible distinction in colour change could be recognised at either location. The original colour of the soil made it difficult to ascertain whether a reaction had occurred or not. This soil colour issue, therefore, appeared to affect the ability to gauge a result from Childs' Test, which, as indicated by the results at both Omokoroa and Te Puna, has only a subtle colour development effect on the soil. It should be noted, however, that a lack of visible distinction in colour development does not necessarily mean reducing conditions were not present in the soils (Childs 1981). A small reaction could have taken place, albeit only a weak one, which was not visible on the pinkish brown background, suggesting that a low level of ferrous iron may have been present in the sample, at a similar level (~ 0.2 ppm) to that at

Omokoroa. Conversely, no reaction is also a possibility, suggesting that there was no ferrous iron in the soil solution.

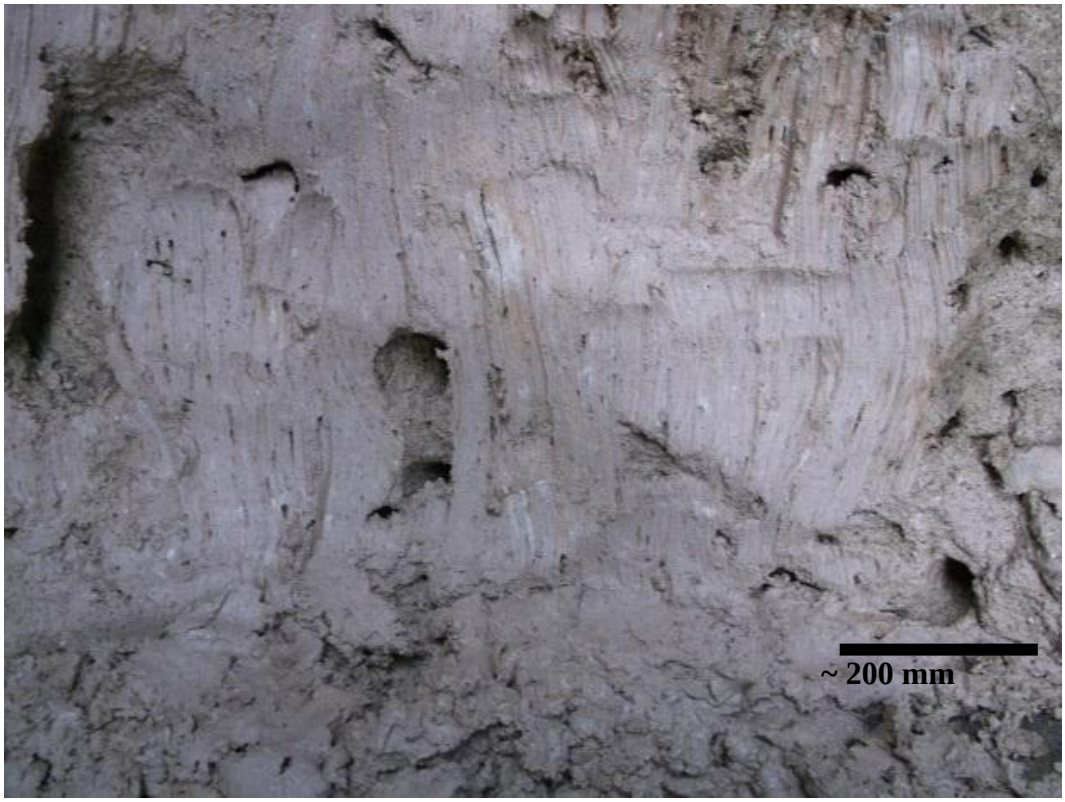

Figure 4.25: The results of Childs' Test undertaken at PS1. It was difficult to establish whether there was any colour development at either location at Pahoia Peninsula as the original colour of the soil was a light pinkish brown, blending with any possible reaction.

4.3.3.4 **Geomorphic observations**

No significant landsliding events were observed at the Pahoia Peninsula coast, where only small outcrops were exposed. Approximately 10 m north of PS1 was a large exposed ignimbrite block (Figure 4.26). This ignimbrite was a prominent feature at certain parts of Pahoia Peninsula and is likely to be partially welded top welded Te Puna Ignimbrite (Briggs *et al.* 1996; Arthurs 2010). The beach platform varied between steep coastal cliffs to gradually inclined and flat lying sections of coast. PS1 was situated beneath an area of gradual inclination, and thus no younger materials were observed above it, while PS2 was exposed at a more abrupt steep faced slope. Because the sensitive soil outcrops at Pahoia Peninsula were exposed close to the shore platform, tide and marine processes likely increased erosion and removed any slope buttressing at the base of the exposed cliffs. Other regions of the peninsula were densely vegetated, with some fallen trees. These may have been the result of landsliding features. However, the

vegetation was so heavily matted that no slope debris could be recognised. The dense vegetation cover also suggest that any landsliding events are not recent and the slopes have remained stable for some time.

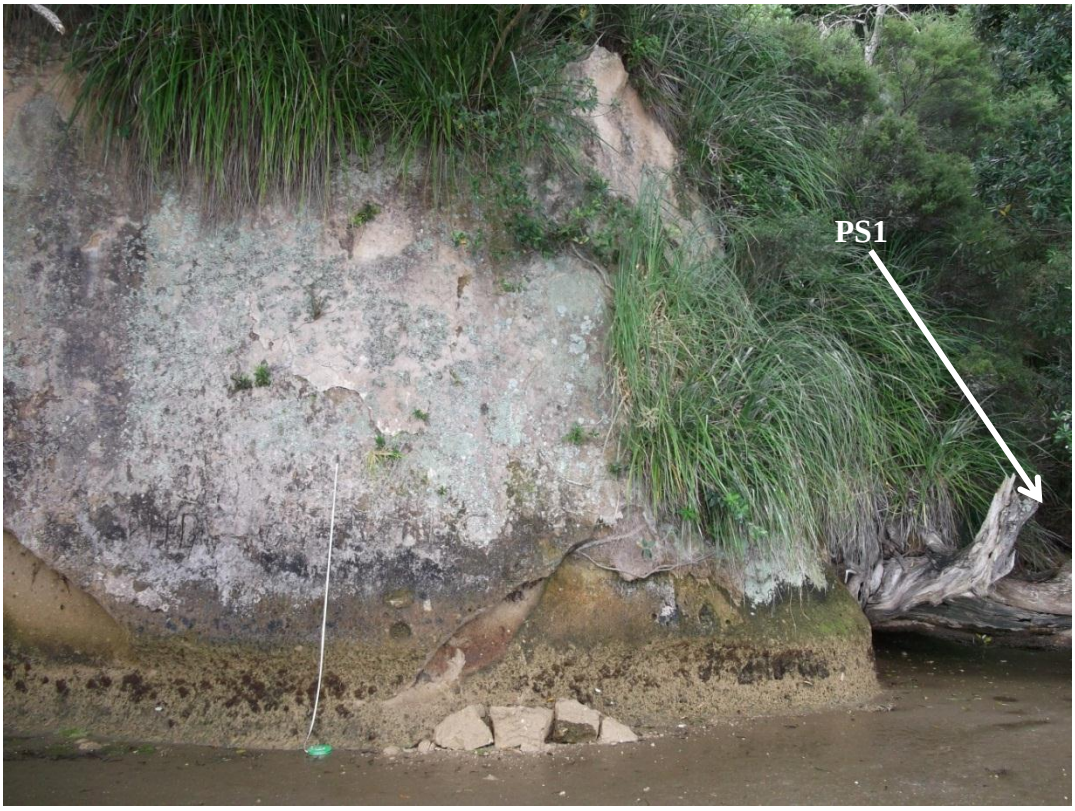

Figure 4.26: Exposed Te Puna Ignimbrite block approximately 10 m to the left of PS1. The tape measure was extended approximately 1.2 m for scale.

4.3.3.5 **Field sensitivity observations**

Pahoia Peninsula field sensitivity observations were characterised as extra sensitive (Table 4.3) (New Zealand Geotechnical Society 2005). The remoulded material at both locations behaved very similarly, where it remoulded under low applied pressure and had a very dilatant nature. Sensitivity values occurred over a smaller range than that typically observed at other sample sites, providing readily reproducible shear vane determinations across the units. PS1 indicated that sensitivity increased slightly with depth (Figure 4.27). This feature was the result of a marginally lower remoulded strength lower in the profile, but the variation was only minor and so did not detract significantly from the mean sensitivity of 11. PS2 did not display any particular sensitivity variation with height, with the values slightly fluctuating above and below ~ 10 (Figure 4.28). Sensitivity values

for the extra sensitive material situated above PS2 exhibited similar shear vane determinations as those within the defined unit (Figure 4.28).

Table 4.3: Field Sensitivity observations undertaken at both the Pahoia sample locations.

	Peak Vane Shear Strength Range (kPa)	Mean Peak Vane Shear Strength (kPa)	Remoulded Vane Shear Strength Range (kPa)	Mean Remoulded Vane Shear Strength (kPa)	Sensitivity (kPa)
PS1	47 – 78	69 ± 1.5	5 – 9	6 ± 0.3	11 ± 0.5
PS2	31 – 81	67 ± 1.9	6 – 11	8 ± 0.3	9 ± 0.4

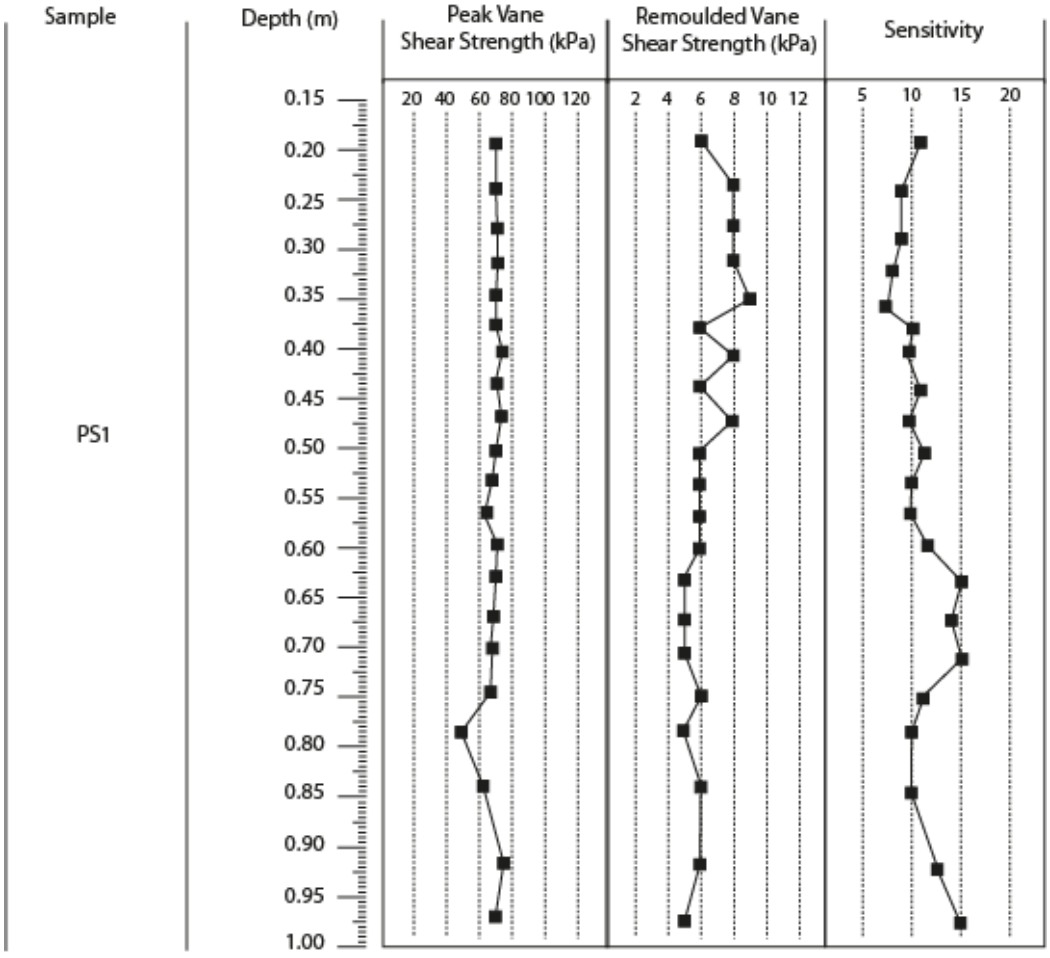

Figure 4.27: Complete shear vane strength and sensitivity log from PS1

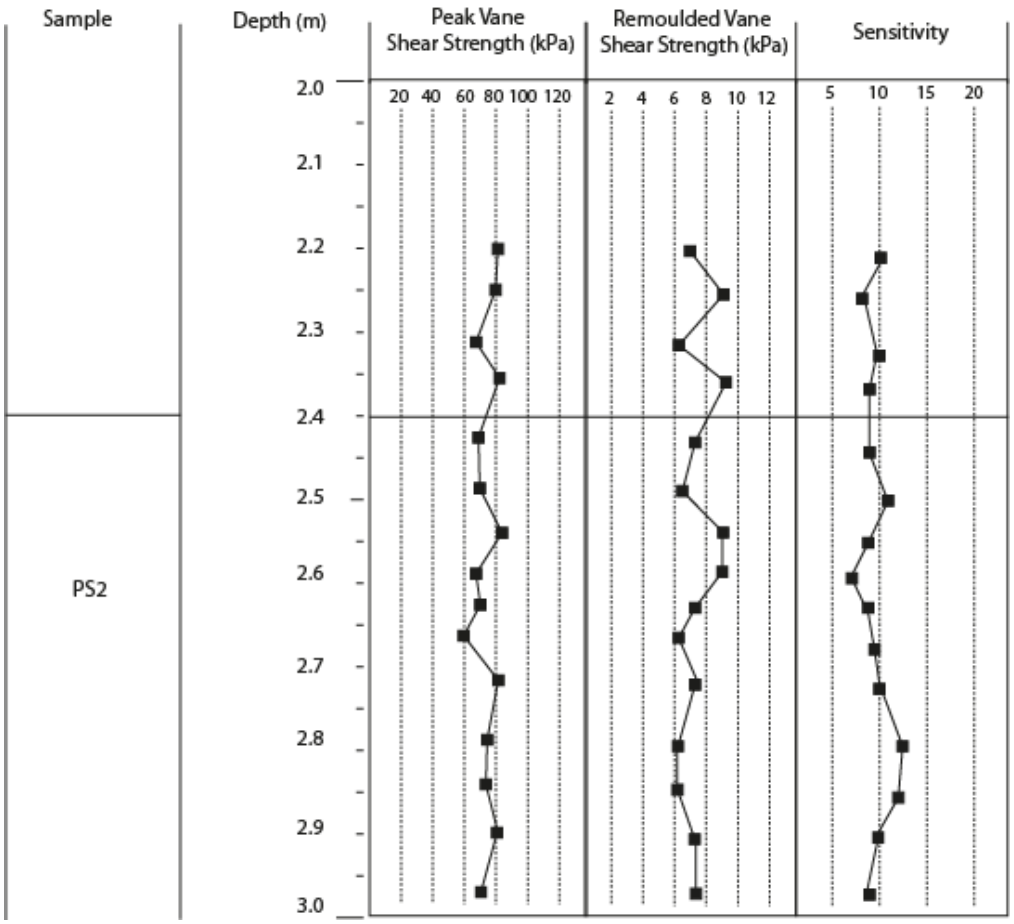

Figure 4.28: Complete shear vane strength and sensitivity log of PS2

4.3.4 **Tauriko**

The pumice pit at Tauriko appeared to also contain materials with similar physical characteristics, such as colour and stratigraphic location, as those sensitive materials from Omokoroa (Figure 4.29, 4.30). Furthermore, considering previous studies had indicated sensitivity in exposed soils at Tauriko (Wyatt 2009), sensitive materials were expected. Upon investigation, however, little to no sensitive material was encountered. Four locations (TS1, TS2, TS3, TS4) were sampled to account for any individual location variability and to establish whether sensitivity varied spatially across the exposure (Figure 4.29). The exposed profile was uniformly dry and so the samples were extracted from 1 m behind the face to discount any immediate sun-drying effect. With consideration of the apparent non-sensitivity of the site, the location was further sampled with the goal of comparing non-sensitive materials at similar stratigraphic locations to those found at Omokoroa, Te Puna and Pahoia.

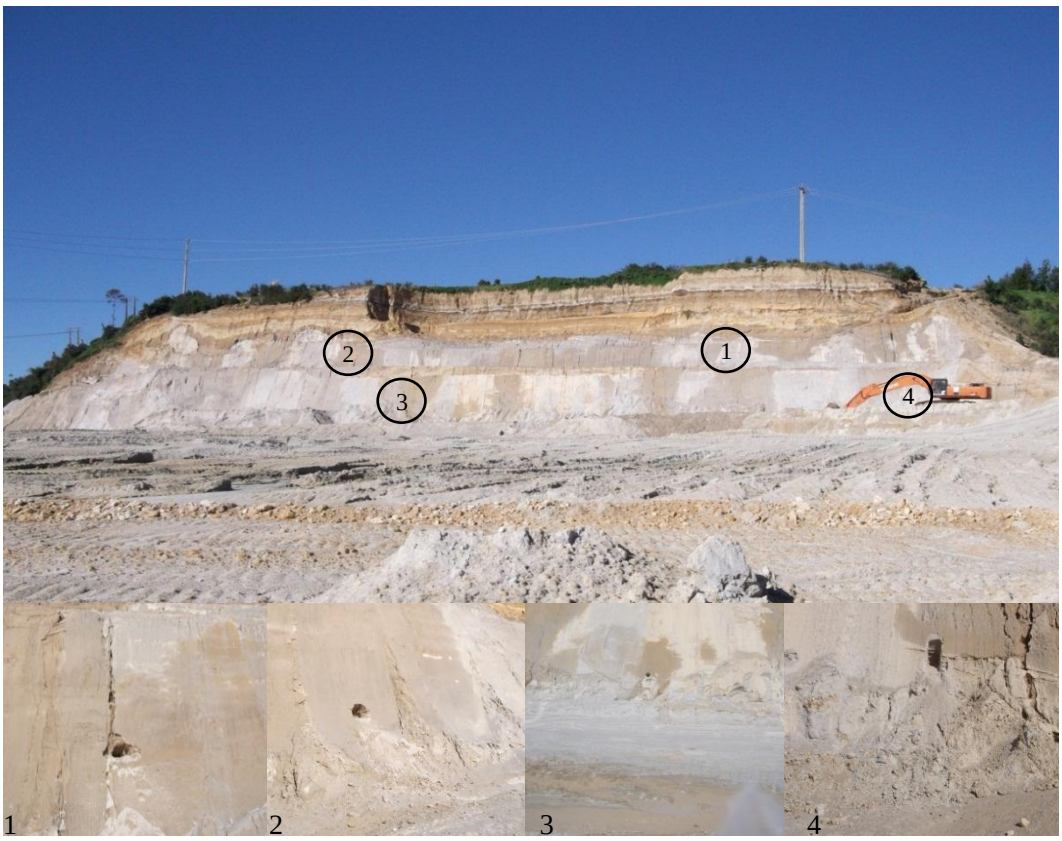

Figure 4.29: Tauriko pumice pit location. The white material comprising the bottom half of the exposed sequence is similar to white material observed at Omokoroa and Te Puna. The numbered circles indicate the various sample locations.

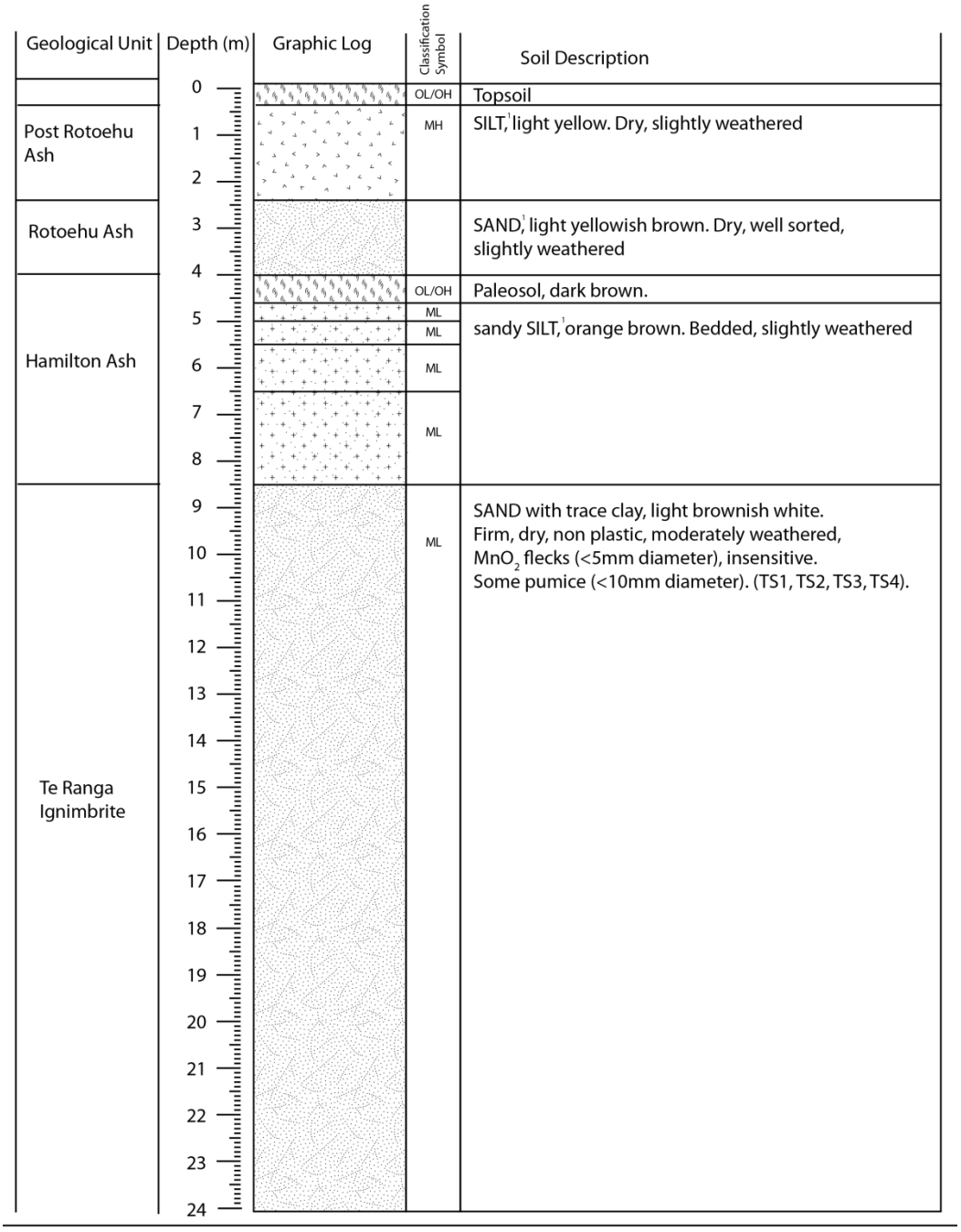

Figure 4.30: Complete stratigraphic log of the Tauriko sampling locations

4.3.4.1 Engineering geological description for all four sample sites at Tauriko

The layer sampled at Tauriko was primarily SAND with trace clay. The material was moderately weathered and classified as massive in a homogenous distribution. The soil appeared to be a light brownish white colour and was brittle. Furthermore, the soil was dry to moist and had very limited cohesion. Based on the characterisation by Briggs *et al.* (1996), the deposits were correlated with the Te Ranga Ignimbrite with intercalated Matua Subgroup sediments, and were

approximately 22 m thick. Considering the non-cohesive and brittle nature of the material, no shear vane measurements, and thus sensitivity analysis, could be undertaken. Upon applying manual pressure (as per Milne *et al.* 1995) to the sample, the soil crumbled and did not release water or smear as is characteristic of a sensitive soil (Milne *et al.* 1993). Manganese concretions and nodules were abundant within the soil comprising approximately 10-15 % of the matrix. The soil contained no roots or other organic matter. The layer immediately above the sampled Te Ranga Ignimbrite was the Hamilton Ash, where a prominent paleosol (Hamilton Ash Paleosol) was evident. No material could be observed below the Te Ranga Ignimbrite (Figure 4.29) and so the lowest boundary of the deposit was not established.

4.3.4.2 **Geomorphic observations**

The natural land features at the Tauriko pumice pit were extensively altered, and so no immediate determinations could be attained as to whether previous land sliding events had occurred. Extensive subdivisions covered any relict landsliding events or minor failures in the surrounding area. The wider Tauriko site itself appeared to undulate between hills and wide valleys. The cutting sampled was into a hillside, which plateaued giving a relatively uniform exposure approximately 40 m in width.

4.3.4.3 **Field sensitivity observations**

Considering the inability to determine sensitivity with the shear vane, no quantitative sensitivity determinations were made, but, the material was clearly not sensitive following the Milne *et al.* (1995) field test and so was classified as a non-sensitive material.

4.3.5 **Rangataua Bay**

Rangataua Bay offered another location to study material which appeared similar to that of the sensitive materials at Omokoroa, Te Puna and Pahoia Peninsula. The material, however, was determined to be non-sensitive (following the Milne *et al.* 1995 test) (Figure 4.31). One location was sampled to establish its characteristics of non-sensitivity.

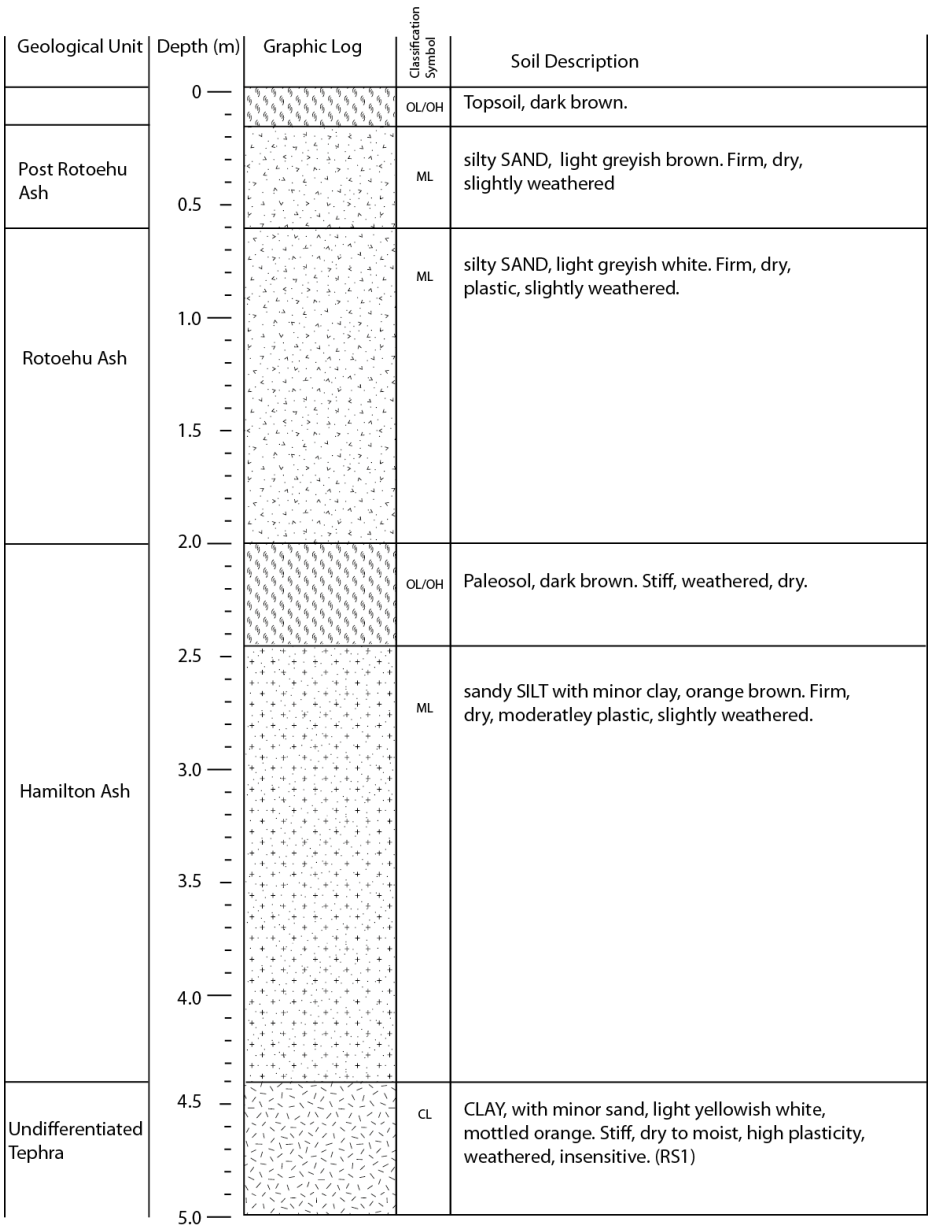

Figure 4.31: Complete stratigraphic log of RS1 from Rangataua Bay.

4.3.5.1 Engineering geological description of Rangataua Bay (RS1)

The sampled layer at Rangataua Bay was CLAY with minor sand. The material was homogenous in formation with few embedded roots (Figure 4.32). The material was stiff and plastic, where it could easily form a ball upon remoulding (Figure 4.33). The soil had orange mottles near the top of the unit comprising ~ 30 % of the sample (Figure 4.31). Few manganese concretions were present, (~ 1 %). The unit was identified as an undifferentiated tephra associated with the Te Ranga Ignimbrite, with intercalated Matua Subgroup sediments

(Briggs *et al.* 1996). The layer immediately above that sampled was an orange brown sandy SILT, which likely represented part of the Hamilton Ash sequence. The dark uppermost paleosol represented the top of the Hamilton Ash, above which the Rotoehu Ash was represented by a light greyish white fine to coarse material (Briggs *et al.* 1996). Below the sample area was a wetter silty CLAY layer. The depth of this unit was unknown, but it appeared to be a correlative of the unit above (undifferentiated tephra associated with the Te Ranga Ignimbrite and intercalated Matua Subgroup sediments). Differentiating this material from the sampled unit was that it appeared to be below the water table and so remained permanently saturated.

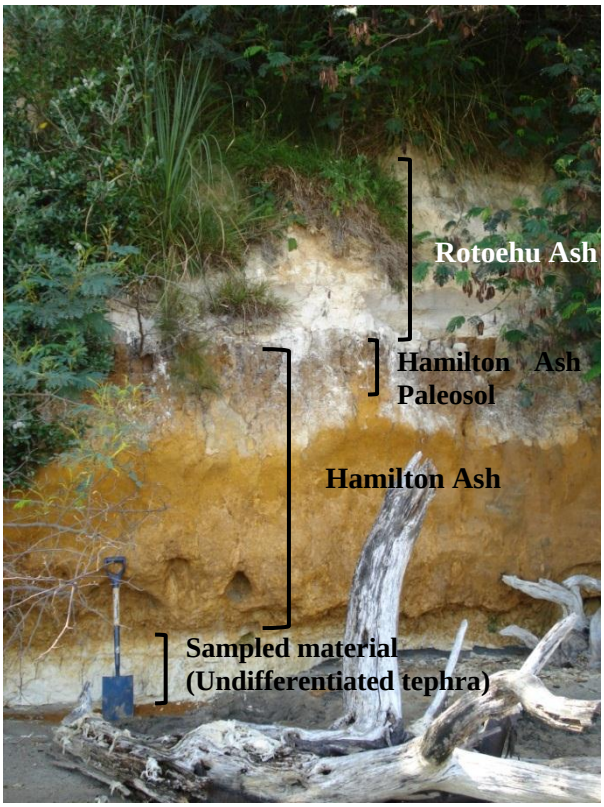

Figure 4.32: Exposed outcrop at Rangataua Bay. The sample site tested is indicated. The material indicated appears similar to that of Omokoroa, and Te Puna, but was not considered sensitive.

Figure 4.33: The sampled unit at Rangataua Bay. Note the well formed ball of remoulded material (left), with the undisturbed material next to it (right). The material did not significantly reduce in strength upon remoulding. Orange mottles were present at the top of the unit.

4.3.5.2 **Geomorphic observations**

Rangataua Bay appeared to have experienced some small to medium sized landslide events. Translational and rotational slips were present, with no buttressing at the base of the slips. The lack of landslide buttress indicated that tidal fluctuations and wave action had transported the landslide deposits away, thus keeping the site active and susceptible to further failure (Figure 4.33). Vegetation was consistently seen to have been disturbed or felled as a result of the cliff erosion, suggesting the landslides were not infrequent. Slope angles were generally very steep, indicating that the slopes would continue to undergo post-failure relaxation and regression until a sustainable slope angle is achieved.

Figure 4.34: Exposed coastal cliff face at Rangataua Bay. Noteworthy is the lack of landslide buttress, meaning that following failure any base support that may have strengthened or reduced the effects of tidal processes have been removed. This subsequently keeps the landslide active, meaning more failures and regression is likely.

4.3.5.3 Field sensitivity observations

Because of the stiff nature of the soil unit, no sensitivity values with the shear vane could be attained. Applying hand pressure (as per the Milne *et al.* 1995 method) yielded plastic deformation, which could easily be remoulded into a ball rather than smearing or becoming fluidised as a sensitive or highly sensitive soil would. The soil material therefore was considered to be non-sensitive, and was further investigated on this basis.

4.4 Summary

An investigation into sensitivity in the Tauranga region revealed soil sensitivity to be limited to deposits at Omokoroa, Te Puna and Pahoia Peninsula whereas deposits at Tauriko and Rangataua Bay appeared non-sensitive. The materials from Omokoroa, Te Puna and Pahoia Peninsula appear to be

undifferentiated tephras in association with the Te Puna Ignimbrite. The materials from both Tauriko and Rangataua Bay, however, appear to be ignimbrite and tephra-fall deposits, respectively, in association with the Te Ranga Ignimbrite eruptive sequence. Mean sensitivities ranged from 9 to 15 at the three sensitive sites, indicating that on average they were all classed as extra sensitive. Omokoroa, Te Puna and Pahoia Peninsula sample locations displayed sensitivity upon physical remoulding and were characteristically dilatant in the disturbed form. Deposits at the two non-sensitive sites, Tauriko and Rangataua Bay, did not display dilatant properties. Tauriko deposits exhibited limited cohesion while Rangataua Bay had excellent cohesion, but remained plastic and did not flow on disturbance.

Chapter 5

GEOMECHANICAL PROPERTIES

5.1 Introduction

Geomechanical data derived from Omokoroa, Te Puna, Pahoia Peninsula, Tauriko and Rangataua Bay is presented. Basic characterisation analyses undertaken on all samples included the determination of Atterberg limits, particle size and density, and moisture content. Measurements only undertaken on the sensitive soil samples included laboratory shear vane strength, triaxial shear strength and soil viscosity. The differentiation in testing regimes for sensitive and non-sensitive soils was undertaken because data relating to shear strength was only useful for cohesive soil (which the Tauriko samples were not) while the sample from Rangataua Bay was too firm for triaxial sample extraction.

5.2 Moisture content, bulk density, porosity and void ratio

Moisture content, bulk density and porosity analyses were undertaken for all sensitive material studied, while only moisture content was investigated for OLRO (Table 5.1). All raw and calculated values can be found in Appendix 5.1.

Table 5.1: Moisture content, bulk density and porosity measurements for the soil materials analysed in this study. Moisture content was analysed for all soils, both sensitive and non-sensitive, while bulk density, porosity and void ratio were only analysed for the sensitive soils.

Sample	Moisture Content (%)	Wet Bulk Density (kgm^{-3})	Dry Bulk Density (kgm^{-3})	Porosity (%)	Void Ratio (%)
OS1	84.00 ± 4	1535.00 ± 26	834.24 ± 14	65.38	1.89
OS2	89.30 ± 1	1475.00 ± 27	779.19 ± 14	67.80	2.11
OLRO	42.44 ± 0.3	–	–	–	–
TPS1	108.83 ± 7	1436.30 ± 12	687.78 ± 6	69.02	2.23
PS1	67.50 ± 2	1633.40 ± 3	975.16 ± 2	61.46	1.59
PS2	70.00 ± 2	1618.90 ± 14	952.29 ± 8	63.51	1.74
RS1	46.27 ± 1	1721.00 ± 15	1176.59 ± 10	50.77	1.03
TS1	31.61 ± 0.1	1289.80 ± 93	980.02 ± 70	58.69	1.42
TS2	23.38 ± 0.2	1346.90 ± 15	1091.67 ± 12	53.51	1.15
TS3	23.25 ± 0.1	1124.80 ± 19	912.62 ± 9	59.59	1.47
TS4	26.07 ± 0.2	1133.80 ± 20	899.34 ± 16	59.48	1.47

Moisture contents for sensitive soils were generally high, ranging from ~ 68 % to ~ 109 %. The OLRO material had a low moisture content compared with the other sensitive materials. Considering the foreign depositional environment of OLRO, its moisture content characteristics could not be measured as original values because after the material had been deposited as a relatively thin layer, and also was covered with sand from tidal influences. The moisture contents for non-sensitive soils were considerably lower between ~ 23 % and ~ 46 %.

Wet bulk density values of the sensitive material typically increased as moisture content reduced (Figure 5.1), where values ranged from approximately 1475 kg m^{-3} to 1619 kg m^{-3}. Such a relationship describes that where less void spaces within the sample are available, the moisture content is lower, thus reducing the site bulk density. Samples from PS1 and PS2 typically displayed the highest bulk densities (1633 kg m^{-3} and 1619 kg m^{-3}), while TPS1 had the lowest bulk density.

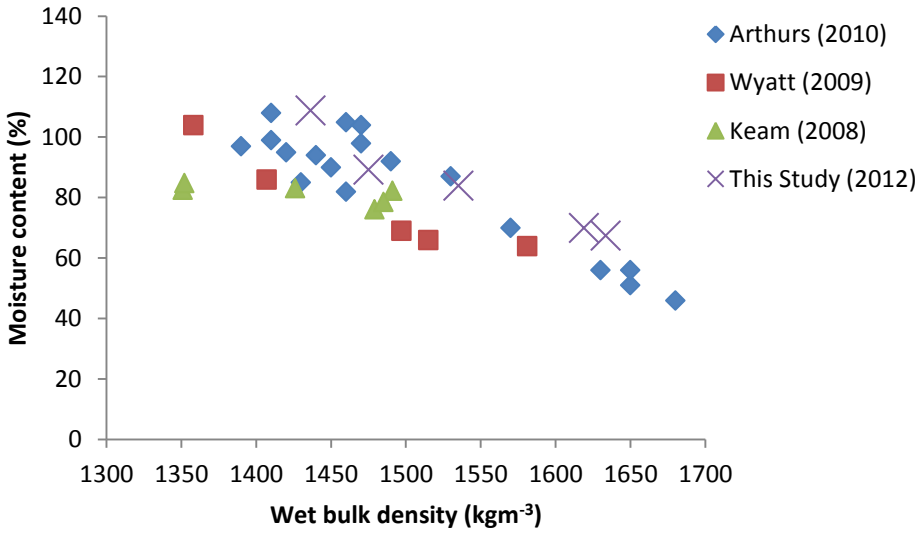

Figure 5.1: Inverse relationship between moisture content and wet bulk density. The negative relationship is consistent with other studies from the Tauranga region (Keam 2008, Wyatt 2009, Arthurs 2010).

Porosity was relatively consistent between sensitive samples, ranging from ~ 61 % to 69 %. Selby (1993) suggested porosities for unconsolidated silt materials to be between 20 % – 40 % while unconsolidated clay sediments have a porosity of approximately 45 % – 60 %. Given this, the results from the sensitive sites studied indicate high porosity values similar to that of unconsolidated clay. In analysing porosity variation with dry bulk density for sensitive samples, a clear negative trend is apparent, where porosity decreases with increasing dry bulk density (Figure 5.2). The development of the negative trend is typical of most soils and not confined to sensitive materials (Selby 1993; Lancelotta 1995; Craig 1997). It indicates that as pore spaces decrease, the sample is more tightly packed and the bulk density of the sample is increased, consistent with the moisture content variation (Arthurs 2010). Mitchell and Soga (2005) stated that soils with higher porosity values indicate spherical shaped particles, which induce lower density packing, while ellipsoidal shaped particles are more tightly packed giving a lower porosity and higher bulk density. The two clusters (given in circles A and B in Figure 5.2) were recorded by Arthurs (2010) from Pahoia Peninsula and Te Puna. The samples recorded by Arthurs (2010) from Pahoia Peninsula were typically in line with the general negative trend, while samples from Te Puna were outliers with low porosities and low bulk densities. Considering they were not

consistent with the recordings from Te Puna recorded in this study, the outliers were not considered important in reducing the reliability of the relationship.

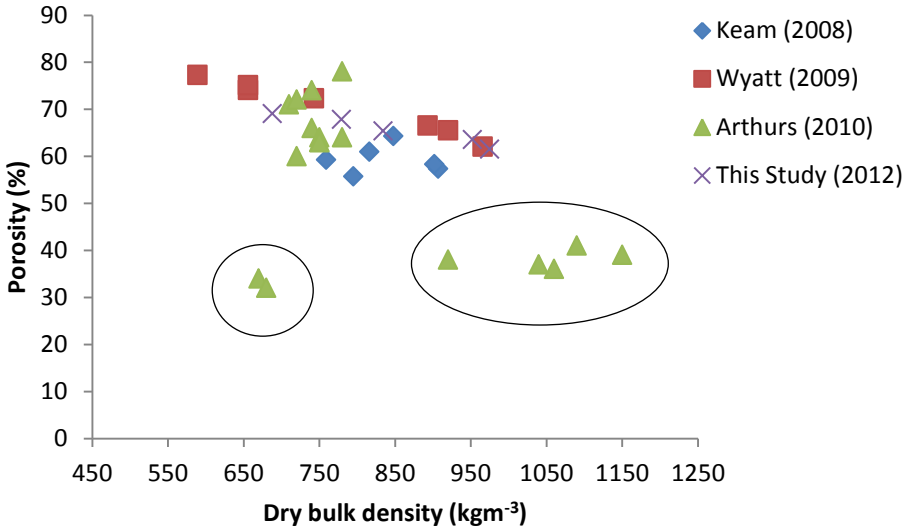

Figure 5.2: Relationship between porosity and dry bulk density. It can be seen that as porosity decreases, dry bulk density increases. Circle A represents samples from Te Puna, and circle B represents samples from Pahoia Peninsula from Arthurs (2010).

5.3 Particle size and density

Particle size and density analysis was undertaken on all sampling sites and locations in this study (Table 5.2). Particle size fractions were divided into clay size (< 2 µm), silt size (2 – 63 µm) and sand size (63 – 2000 µm). The following section presents the particle size and density analysis determined from the samples in this study, along with comparisons with other sensitive soil studies from both New Zealand and internationally. All raw data can be found in Appendix 5.2.

Table 5.2: Particle density and particle size determinations from Omokoroa, Te Puna, Pahoia Peninsula, Rangataua Bay and Tauriko.

Sample	Particle Density (kg m^{-3})	Clay (%)	Silt (%)	Sand (%)
OS1	2410.00 ± 5	10.29	49.11	40.60
OS2	2420.00 ± 3	2.17	73.40	24.43
OLRO	2550.00 ± 17	10.74	26.93	62.33
TPS1	2220.00 ± 7	2.96	76.14	20.90
PS1	2530.00 ± 19	4.97	84.62	10.40
PS2	2610.00 ± 18	6.75	69.54	23.71
RS1	2390.00 ± 6	30.36	59.58	10.06
TS1	2372.23 ± 23	5.05	22.52	72.43
TS2	2348.37 ± 34	4.35	24.66	70.98
TS3	2258.42 ± 32	2.40	14.12	83.48
TS4	2219.29 ± 19	3.25	17.40	79.35

Particle density variation between all sites ranged from ~ 2219 kg m^{-3} at TPS1 to ~ 2610 kg m^{-3} at PS2. Both Omokoroa samples were very similar in particle density, only varying by ~ 10 kg m^{-3}. The OLRO material displayed a higher particle density than the two *in-situ* samples at ~ 2550 kg m^{-3}. Again this variation of OLRO from OS1 and OS2 is likely due to the sample disturbance and intermixing of other material during deposition. Both PS1 and PS2 were also very comparable with only 80 kg m^{-3} difference in particle density. The particle density of the sensitive material (mean = 2457 kg m^{-3}) from this study was comparable to other sensitive studies in the Tauranga region (Wyatt 2009). Sensitive materials at both Tauriko and Otumoetai have previously been reported to have mean particle densities of ~ 2560 kg m^{-3} and ~ 2660 kg m^{-3} respectively (Wyatt 2009). Sensitive material in other New Zealand locations and internationally, however, has been reported at higher densities than those found in Tauranga. Jacquet (1990) reported sensitive soil particle densities between ~ 2720 kg m^{-3} – ~ 2890 kg m^{-3} from Huntly and New Plymouth sample sites. Wesley (1973) reported that Indonesian weathered volcanic latsol and andisol halloysite dominated materials had particle densities ranging between ~ 2730 kg m^{-3} and ~ 2840 kg m^{-3}.

Of the non-sensitive locations, the particle density variation (mean = 2317 kg m^{-3}) was smaller, ranging between ~ 2219 kg m^{-3} at TS4 to ~ 2390 kg m^{-3} at RS1. Depth variation at Tauriko was again apparent, where both the samples taken from ~ 23 m depth (TS3 and TS4) had lower, consistent particle densities, while the samples at approximately 17 m depth (TS1 and TS2) had slightly higher particle densities.

Particle size variation indicated that all of the sensitive locations, excluding OLRO, were dominated by silt size particles (≥ 49 %). In contrast, OLRO appeared to be dominated by sand sized grains. Considering the OLRO material was not *in-situ* and appeared to have been reworked during failure, a higher sand content was likely incorporated into the soil. Silt content was highest at PS1 (~ 85 %), while OS1 contained the lowest (~ 49 %). Sand sized fractions ranged between 10 % – 40 % across all *in-situ* sensitive sites. Clay size fractions of the sensitive material were relatively low, ranging from ~ 2 % to ~ 11 %. Jacquet (1990) reported clay size fractions in sensitive soil from Huntly and New Plymouth between ~ 21 % – ~ 56 %. Sensitivity has, however, been reported in soil materials of relatively low clay concentrations previously in Tauranga. Wyatt (2009) indicated materials with limited clay size fractions (~ 2 % – ~ 10 %) were typically extra-sensitive, while material of higher clay content was of lower sensitivity.

Non-sensitive material at Rangataua Bay was characterised by a high clay content (> 30 %) and a higher silt content (> 59 %). The sand fraction was comparatively low compared to all other materials examined at ~ 10 %. The non-sensitive soil at Tauriko was primarily sand sized materials (~ 71 % – ~ 83 %). All clay sized fraction samples from Tauriko were low at ~ 2 %.

5.4 Atterberg limits

Atterberg limits were investigated for all sample sites. The data values are presented in Table 5.3. Due to the non-plastic (NP) properties of the non-sensitive Tauriko samples, only the liquid limit could be determined. The definition of a non-plastic sample as stipulated by the NZS 4402 (1986) (2.3) is given as a thread

that cannot be rolled down to a 3 mm diameter. At best, the Tauriko samples could be rolled to ~ 6 mm. All raw data is presented in Appendix 5.3.

Table 5.3: Atterberg limit results for the five sites sampled. Omokoroa (OS1, OS2), Te Puna (TPS1) and Pahoia (PS1, PS2) were sensitive, while Tauriko (TS1, TS2, TS3, TS4) and Rangataua Bay (RS1) were non-sensitive. The Omokoroa landslide runout (OLRO) material represents the properties of naturally remoulded sensitive soil material. NP denotes that the soil materials were non-plastic. Clay content values used to calculate activity are given in Table 5.2.

Sample	Liquid Limit (%)	Plastic Limit (%)	Plasticity Index (%)	Liquidity Index (%)	Activity
OS1	72.3	45.7	26.6	1.4	2.6
OS2	73.6	51.5	22.1	1.7	10.2
OLRO	39.9	24.1	15.8	1.2	1.5
TPS1	89.4	45.7	43.6	1.4	14.7
PS1	52.9	34.3	18.6	1.8	3.7
PS2	53.6	35.8	17.9	1.9	2.7
RS1	52.7	37.1	15.5	0.6	0.6
TS1	39.4	NP	NP	–	–
TS2	44.4	NP	NP	–	–
TS3	59.4	NP	NP	–	–
TS4	58.1	NP	NP	–	–

The liquid limits for all sampled materials varied from 39.4 % to 89.4 %. The liquid limits for the sensitive soil materials were typically high, ranging from 52.9 % (PS1) to 89.4 % (TPS1). The liquid limit values at Omokoroa did not vary greatly between OS1 (72.3 %) and OS2 (73.6 %), however, the OLRO deposit displayed a considerably lower liquid limit of 39.9 %. The OLRO material was considered separate to the sensitive material as it was altered from its original depositional state and likely incorporated more sand during failure. Consequently, the OLRO Atterberg values are expectedly different from the *in-situ* properties considering the variation in (or lack of) loading conditions, moisture content and permeability of overlying materials.

The plastic limit for the Omokoroa sampling sites followed a similar pattern, where again OS2 had the highest (51.5 %) and OLRO had the lowest (24.1 %) plastic limit. Both Pahoia Peninsula samples displayed strong similarities between each other for both liquid limits and plastic limits indicating the high likelihood of the samples being distal correlatives. Mitchell and Soga (2005) suggest that liquid limits between 30 % – 110 % and plastic limit values between

25 % – 40 % indicate kaolinitic dominated materials which would account for the Omokoroa and Te Puna samples. Wesley (1973), however, suggests that halloysite dominated soil from Indonesia has liquid limits between 70 % – 110 % and plastic limits ranging from 55 % – 75 %, implying the clay fraction materials from Omokoroa and Te Puna could be halloysite dominated, which is expected considering both minerals are from the kaolin group. The Pahoia Peninsula samples sit within the dehydrated halloysite bracket, where liquid limits are between 35 % – 55 % and plastic limits between 30 % – 45 % (Mitchell and Soga 2005).

Soil samples from Tauriko and Rangataua Bay displayed relatively consistent liquid limit values, ranging from ~ 40 % to 59 %. Samples from Tauriko indicated similarities between sample positions in the profile. TS1 and TS2 (at ~ 17 metres profile depth) were comparable at 39.4 % and 44.4 % respectively, while TS3 and TS4 (23 metres depth), displayed higher liquid limit values of 59.4 % and 58.1 % respectively. This possibly indicates that as the consolidation pressure increases, the liquid limit is similarly increased.

Plasticity indexes ranged between 15.5 % and 43.6 % for all materials. The plasticity index for OLRO was again significantly lower than OS1 and OS2 at 15.8 %. RS1 was the only quantifiable non-sensitive plasticity index that could be measured which gave a value of ~ 16 %.

The liquidity index for all sensitive materials was always above 1, but did not exceed 2, while the only recorded non-sensitive location at Rangataua Bay was below 1 at 0.6. The samples from this study had high activity values. Typically in the sensitive material, where clay content was high (Table 5.2), activity was low. Previous studies from the Tauranga region have exhibited similar behaviour for sensitive material (Wyatt 2009). Two samples (OS2 and TPS1) displayed exceptionally high activity values. This was primarily attributed to their low recorded clay content, yet moderate to high plasticity index. Selby (1993) indicates that these properties represent allophonic or smectite behaviour in soils. Interestingly, RS1 which had the highest clay content, also had the lowest activity, at ~ 0.6. This latter observation correlates well with halloysitic clays,

which in New Zealand, are characteristically low activity clays (Egashira and Ohtsubo 1982).

Presenting the Atterberg limit data on a Casagrande Plasticity Chart (Figure 5.3) indicates that all of the soil materials except for OLRO behaved as a highly or very highly compressed silt and were placed below the A line. Highly sensitive volcanic derived material is commonly reported to be plotted below the A line both internationally and in the Tauranga region (Wesley 1973; 1979; Jacquet 1990; Wyatt 2009; Arthurs 2010). OLRO was placed on the A line, suggesting its behaviour was comparable to either an intermediate clay or intermediate silt. The non-sensitive site of RS1 appeared to behave in a similar manner to PS1 and PS2, as a highly compressed silt material, even considering its large clay component (Table 5.2). The low plasticity indices indicate that the cohesive nature of the clay is not sufficient enough to produce clay like behaviour.

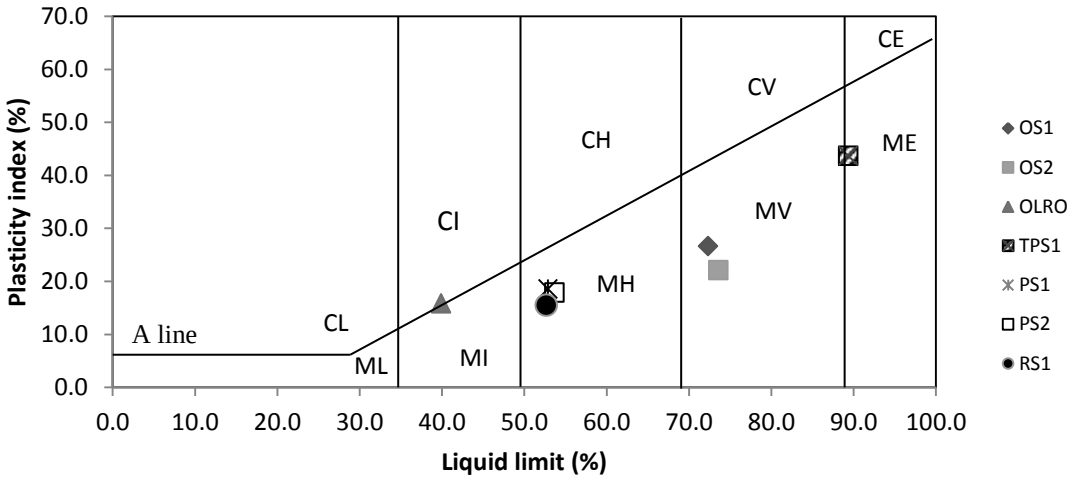

Figure 5.3: Casagrande classification chart with samples from Omokoroa, Te Puna, Pahoia Peninsula and Rangataua Bay plotted. The chart describes what likely constituents (clay, C or silt, M) compose the samples based on their Atterberg limit behaviour. Compressibility of clay or silt are given as low (L), intermediate (I), high (H), very high (V), or extremely high (E). As the Tauriko samples were considered non-plastic, no plot is given for them.

A comparison of Atterberg limits was undertaken with other studies in the Tauranga region (Table 5.4).

Table 5.4: Comparison of Atterberg limits of various studies undertaken in the Tauranga Region. (*) denotes that the sample was considered to be sensitive. NP denotes that the material was non-plastic, while NA indicates that the value was not applicable for that material.

Study	Location	Material	Liquid Limit (%)	Plastic Limit (%)	Plasticity Index (%)	Liquidity Index (%)
Bird (1981)	Maungatapu	CLAY, silty, SAND, SAND	28–57	27–31	1–32	0.94–14.27
Oliver (1997)	Maungatapu	CLAY, silty SAND	51–103	30–53	6–68	–
Wesley (2007)	Otumoetai*	CLAY, silty CLAY, sandy SILT	76–116	48–66	5–58	0.09–1.22
Keam (2008)	Omokoroa*	sandy SILT	55–72	39–48	10–33	1.01–2.06
Wyatt (2009)	Otumoetai*	silty CLAY, clayey SILT	57–96	32–54	25–43	0.27–1.46
	Tauriko*	clayey SILT	52–81	39–57	13–26	1.88–2.41
Arthurs (2011)	Otumoetai*	clayey SAND	98	66	32	0.5
	Te Puna*	clayey SILT	93	52	40	1.2
	Pahoia Peninsula*	sandy CLAY	42–59	29–36	12–23	0.86–2.23
This Study (2012)	Omokoroa*	SILT with clay	74	52	22	1.71
	Omokoroa*	Clayey SILT	72	46	27	1.44
	Te Puna*	SILT	89	46	44	1.2
	Pahoia Peninsula*	Clayey SILT	53–54	34–36	18–19	1.80–1.90
	Rangataua Bay	silty CLAY	53	37	16	0.6
	Tauriko	silty SAND	39–59	NP	NA	NA

Various studies have indicated similar Atterberg limit results in the Tauranga region, particularly between sensitive locations. The results of this study typically resided within the ranges presented from other comparable studies, however, the value ranges were wide, indicating sensitive material is not simply confined within recognisable boundaries. While no sensitive samples from the sites used in this study reached liquid limits over 100 % (as was observed by Wesley (2007)), Arthurs (2010) indicates that liquid limits of rhyolitic sensitive soils can be as low as ~ 42 %. Importantly, liquidity indexes are almost always above 1, indicating that sensitive material in the Tauranga region typically becomes fluidised upon remoulding. In distinguishing between the non-sensitive material studied from Maungatapu (Bird 1981; Oliver 1997) and those considered sensitive from the Tauranga region no definite variations could be distinguished from the Atterberg limits results.

5.5 Laboratory shear vane strength and sensitivity

Laboratory shear vane strength data was undertaken at a controlled rate on all sensitive sample locations. All shear strength data was recorded in kPa, with a sensitivity ratio established following the remoulded strength determination (see Chapter 3). As with the field shear vane, samples from Tauriko could not be analysed due to their non-cohesive nature, while RS1 was too hard for shear vane penetration. Table 5.5 presents the mean peak and remoulded strength data for the sample sites tested.

Table 5.5: Mean laboratory peak and remoulded shear vane strength from the sensitive locations sampled. Each mean peak strength, remoulded strength and sensitivity was calculated from the individual trials for peak strength, remoulded strength and sensitivity. The mean sensitivity is not derived from the ratio of the mean peak strength to the mean remoulded strength. All raw data can be found in Appendix 5.4.

Sample	Mean Peak Strength (kPa)	Mean Remoulded Strength (kPa)	Mean Sensitivity
OS1	56 ± 8	6 ± 1	10 ± 1
OS2	25 ± 4	4 ± 1	7 ± 1
OLRO	–	–	–
TPS1	80 ± 3	9 ± 3	11 ± 2
PS1	26 ± 2	2 ± 0.2	13 ± 2
PS2	57 ± 9	8 ± 3	10 ± 4

Mean peak shear vane strength ranged from 25 kPa at OS2 to 80 kPa recorded at TPS1. Remoulded shear vane strength ranged between 2 kPa at PS1 to 9 kPa at both TPS1 and OS1. All samples were considered sensitive to extra sensitive (New Zealand Geotechnical Society 2005). Mean sensitivity values were, typically, consistent with the field shear vane (see Chapter 4) where most of the calculated sensitivities between the methods were within ± 2 of each other for each site. The exception was OS2, where the field shear vane was considerably different from the laboratory shear vane measurements. A mean sensitivity of 15 was recorded with the field shear vane, while a mean sensitivity ratio of only 7 was calculated from the laboratory shear vane.

Typically, mean peak strengths measured using the field shear vane and the laboratory shear vane were not consistent. The peak strength recorded with the laboratory shear vane was lower than that of the field shear vane. A similar variation between field and laboratory shear vane has previously been reported by Perlow (1977). He found that field shear vane strengths were always higher than those encountered with the laboratory shear vane which was due to variations in vane size and rotation rate. Furthermore, other inconsistent measurements were particularly evident at Pahoia Peninsula, where the two sampled sites (PS1 and PS2) were thought to be correlatives of each other, however, mean peak strengths recorded with the laboratory shear vane were considerably different from one another. PS1 was recorded with a mean peak strength of 26 kPa, while PS2 had a mean peak strength of 57 kPa. On the contrary, the field shear vane gave close mean peak strength readings between the sites of 69 kPa for PS1 and 67 kPa for PS2. Whether the problem in consistency between methods is due to the field shear vane or the laboratory shear vane or some sample disturbance during transportation is unknown.

5.6 Triaxial

Effective stress triaxial testing was undertaken on all *in-situ* sensitive samples from Omokoroa, Te Puna and Pahoia Peninsula. Consolidated drained testing was undertaken only on OS1, while consolidated undrained tests were undertaken on all sensitive samples. Analysis of testing conditions, compression results, pore water pressure characteristics, stress path properties, Mohr-Coulomb plots and specimen condition will be presented in the following sections. All raw data can be found in Appendix 5.5.

5.6.1 Sample pre-test conditions

Initial sample test conditions for the triaxial test involved determining sample moisture content and bulk density conditions to ensure that the samples were the same as those analysed in Section 5.3.

Moisture contents of the triaxial samples were typically slightly below (1 % – 3 %) those which were encountered in the field with the exception of OS2

(2 % higher). This typical reduction in moisture content is likely the result of partial drying during the trimming and preparation of the sample. Nevertheless, considering the samples were completely saturated before compressing the sample, small variation in initial moisture content was disregarded.

Wet bulk density indicated a relatively minor difference (< 5 %) between those measured with the triaxial specimens and those attained in Section 5.3. Given the consistency between results, the samples were confirmed to be from the same sample set.

Saturation times (following the BS1377 (1990)) for each sample varied: OS2, PS1 and PS2 saturated very quickly, only taking approximately three hours, while OS1 and TPS1 required longer for a > 0.90 B value to be reached for each increase of back pressure, totalling approximately 5 hours for satisfactory saturation. This longer time suggested that the pore water did not permeate as well through OS1 and TPS1 as the other three materials allowed.

5.6.2 **Compression stage characteristics**

The compression stage determined several key factors which were used to describe the specimen stress conditions during the application of axial strain. The measured variables included deviator stress, stress path, pore water pressure and Mohr-Coulomb characteristics. Each parameter is presented separately in the following sections. Each sample was tested over a different effective stress range based on its depth within the stratigraphic profile (see Chapter 3 Section 3.5.4). Samples from Omokoroa were at an approximate depth of 18 m, and bulk density of ~ 1535 kg m^{-3}, giving an *in-situ* overburden of 114 kPa. Te Puna had an overburden stress of 31 kPa. PS2 indicated a similar overburden at 49 kPa, however the small exposure at PS1 indicated a very low overburden at ~ 6 kPa. The required effective pressures for triaxial testing were based on these *in-situ* overburden values and ranged to simulate a range of higher conditions for failure. The effective pressures used are summarised in Table 5.6.

Table 5.6: Required effective/confining pressure employed for each sample. The required effective pressure was reached following the saturation stage.

Effective/confining pressure (kPa)	OS1	OS2	TPS1	PS1	PS2
50			●	●	●
100	●	●	●	●	●
150			●	●	●
200	●	●			
300	●	●			

5.6.2.1 Stress versus Strain

5.6.2.1.1 OS1 consolidated drained, consolidated undrained

OS1 was tested under both consolidated drained and consolidated undrained conditions where clear variations were observed between the deviator stress characteristics (Figures 5.4, 5.5). The consolidated drained test indicated very gradual failure, where peak deviator stress was either not achieved or occurred just before the 20 % end of test termination point. Confining pressures at 200 kPa and 300 kPa indicated that the sample behaved as an over consolidated clay given that a peak deviator stress was not achieved before the test finished at 20 % axial strain (Head 1998). The 100 kPa run achieved peak deviator stress at approximately 18 %, just before the test termination point was reached. A peak deviator stress reached between 15 % and 20 % strain is suggested to be representative of normally consolidated clays (Head 1998). Bishop and Henkel (1962), however, previously reported that normally consolidated London clay reached peak deviator stress between 20 % and 24 % strain, perhaps indicating that the 20 % strain termination point presented by the BS1377 (1990) is not suitable at high confining pressures for this material.

The consolidated undrained test, conversely, behaved in a similar pattern across all three effective confining pressures. Furthermore, peak deviator stress was achieved between 5 % and 9 % strain for each sample. Head (1998) suggests that failure strains between 8 % and 15% (200 kPa and 300 kPa confining pressures) indicate compacted sandy silt materials while failure strains under 8 % (100 kPa runs) suggest plastic to brittle behaviour. The primary difference between the tests undertaken was characterised by consolidated undrained tests

rapidly reaching a peak deviator stress, while consolidated drained tests did not. In an analysis of the Bramley Drive failure at Omokoroa, Gulliver and Houghton (1980) previously observed peak deviator stress to rapidly increase and reach a peak within 4 % (consolidated undrained test) at confining pressures of 150 kPa and 300 kPa, while at higher confining pressures (450 kPa) ~ 6 % of axial strain was required for failure.

The consolidated undrained test displayed very minor decrease in deviator stress following the peak, alternatively known as strain softening (Prevost and Hoeg 1975; Wood 1990). The feature is prominent in saturated undrained compression conditions where the soil is incapable of contracting, leading to the development of positive pore pressures, giving the strain weakening behaviour (Fell *et al.* 2007). Strain softening typically characterises soils as dense sands or over consolidated clay (Wyatt 2009) which are considered prone to progressive failures (Powrie 2004).

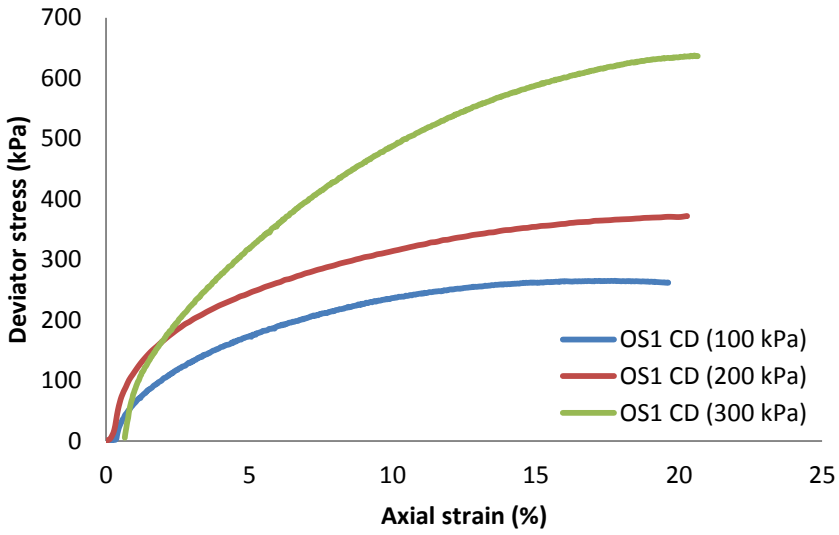

Figure 5.4: Deviator Stress characteristics for the consolidated drained test of OS1. Confining pressures of 100 kPa, 200 kPa and 300 kPa were employed.

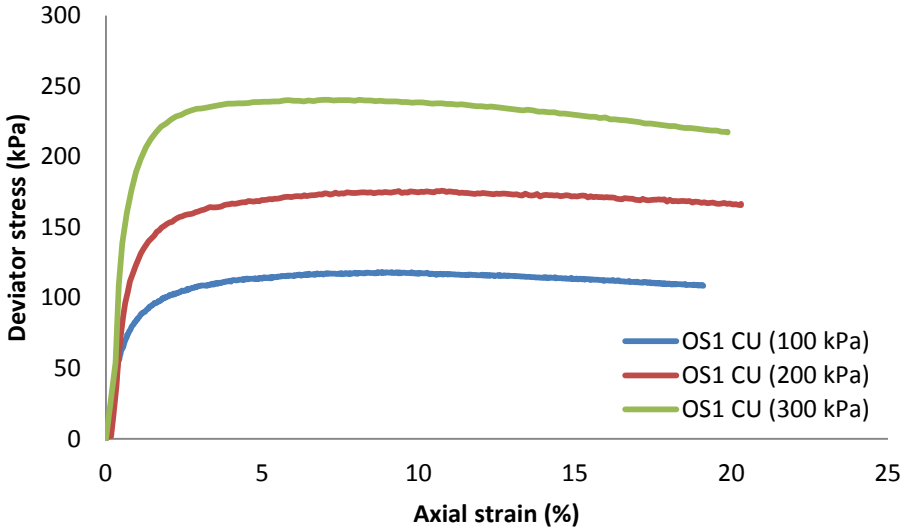

Figure 5.5: Deviator Stress characteristics for the consolidated undrained test of OS1. Confining pressures of 100 kPa, 200 kPa and 300 kPa were employed.

5.6.2.1.2 OS2 consolidated undrained

OS2 showed that peak deviator stress for all three effective confining pressures occurred at less than 5 % axial strain in consolidated undrained testing (Figure 5.6). According to Head (1998), peak deviator stress below 5 % suggests brittle soil behaviour. The first two sample runs at confining pressures of 100 kPa and 200 kPa displayed peak deviator stresses within approximately 25 kPa of each other, while the difference between the 200 kPa and 300 kPa confining pressure was approximately 93 kPa. Strain softening was characteristic of all OS2 specimens, especially at higher confining pressures (300 kPa).

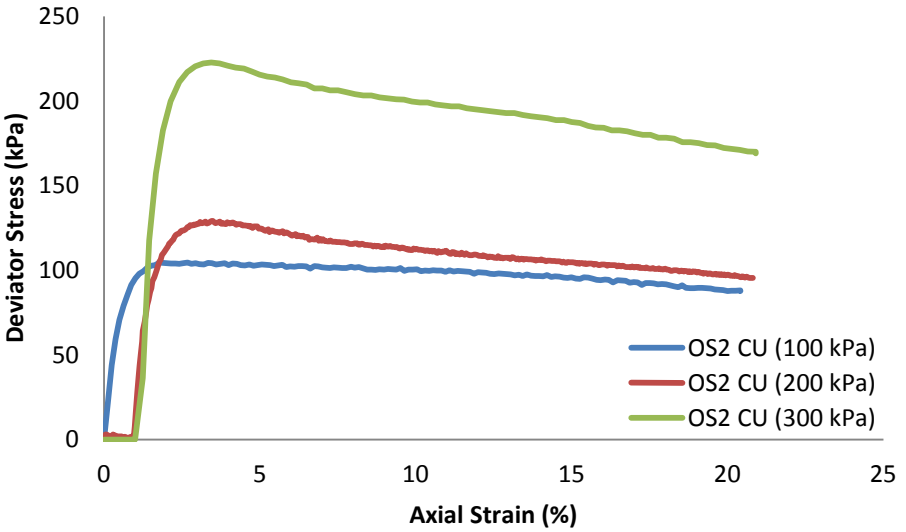

Figure 5.6: Deviator Stress characteristics for the consolidated undrained test of OS2. Confining pressures of 100 kPa, 200 kPa and 300 kPa were employed. The decrease in deviator stress following the peak (particularly evident at 300 kPa confining pressure) represents strain softening of the sample.

5.6.2.1.3 **TPS1 consolidated undrained**

The consolidated undrained samples from TPS1 (Figure 5.7) again indicated peak deviator stresses between 4 % and 8 % of axial strain, suggesting plastic to brittle soil behaviour (Head 1998). The TPS1 sample displayed very minor reduction in strength following peak deviator stress (strain softening), where the curves flattened and decreased slowly which is expected for CU triaxial tests (Bishop and Henkel 1962).

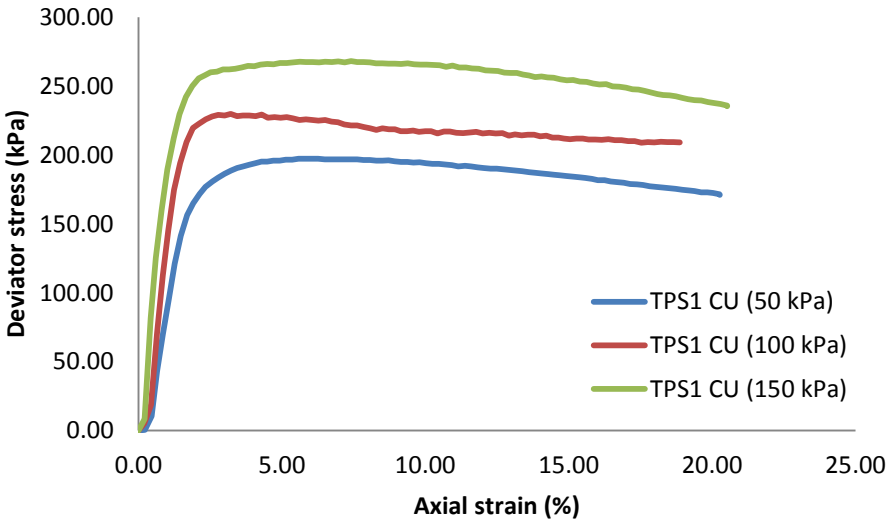

Figure 5.7: Deviator Stress characteristics for the consolidated undrained test of TPS1. Confining pressures of 50, 100 and 150 kPa were employed.

5.6.2.1.4 **PS1 and PS2 consolidated undrained**

Both PS1 and PS2 displayed very similar deviator stress characteristics as axial strain increased (Figure 5.8, 5.9). Two PS1 specimens tested at 50 kPa and 100 kPa confining pressures indicated compacted sandy silt behaviour (Head 1998). The remaining samples, however, reached peak deviator stress at $\leq$ 5 % strain, indicating a brittle soil nature (Head 1998). PS1 and PS2 displayed the most prominent strain softening of all samples tested, with a significant reduction in deviator stress following failure at all confining pressures.

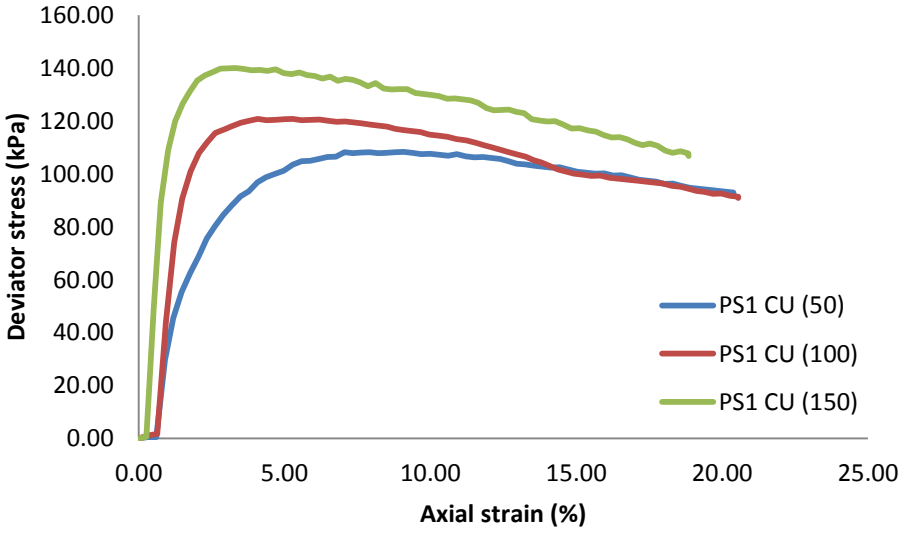

Figure 5.8: Deviator Stress characteristics for the consolidated undrained test of PS1. Confining pressures of 50, 100 and 150 kPa were employed.

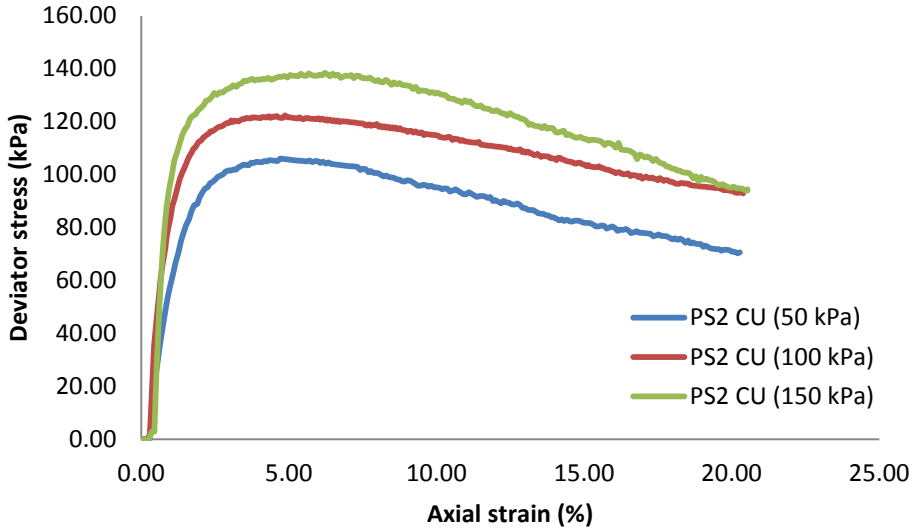

Figure 5.9: Deviator Stress characteristics for the consolidated undrained test of PS2. Confining pressures of 50, 100 and 150 kPa were employed.

Table 5.7 summarises the stress strain results from the consolidated undrained tests from this study.

Table 5.7: Summary of the stress strain characteristics from the consolidated undrained tests from this study.

Sample	Effective confining pressure	Strain at failure (%)	Peak deviator stress (kPa)	Post-failure response
OS1 (1) CU	100	8	118.23	Minor strain softening
OS1 (2) CU	200	9	175.74	Minor strain softening
OS1 (3) CU	300	5	240.24	Minor strain softening
OS2 (1) CU	100	1	104.50	Moderate strain softening
OS2 (2) CU	200	4	129.04	Moderate strain softening
OS2 (3) CU	300	4	222.70	High strain softening
TPS1 (1) CU	50	5	197.38	Minor strain softening
TPS1 (2) CU	100	4	229.84	Minor strain softening
TPS1 (3) CU	150	8	268.28	Minor strain softening
PL1 (1) CU	50	3	106.07	High strain softening
PL1 (2) CU	100	4	122.39	High strain softening
PL1 (3) CU	150	7	138.55	High strain softening
PL2 (1) CU	50	5	106.07	High strain softening
PL2 (2) CU	100	4	122.39	High strain softening
PL2 (3) CU	150	6	138.55	High strain softening

5.6.2.2 Pore water pressure and volume change characteristics

Post peak pore water pressure characteristics varied both between sample confining pressures and between sampling locations (Table 5.8). Observed characteristics were typically negative trending (decreasing) curves, levelling curves and increasing curves (where no maximum pore water pressure was reached before 20 % strain) (Figure 5.10). Negative trending behaviour following peak pore water pressure is referred to as dilation (Wesley 2010). Wyatt (2009) identified dilatation behaviour in sensitive Tauranga samples at low confining pressures, where pore pressures would often decrease to a negative state, possibly classifying the samples as over-consolidated clays. Supporting this, the results of the pore water pressure characteristics during compression from this study suggest over-consolidation of specimens from Te Puna, and both Pahoia Peninsula samples at low confining pressures. Other behaviours observed were at OS1 which indicated that following the peak, pore water pressure would level off.

Some sample specimens, however, displayed increasing pore water pressure meaning no peak was produced, possibly suggesting normally consolidated clay (Head 1998). Wesley (2010) also recognised such increasing post peak-pore water pressure for undisturbed silt samples from Indonesia. This suggests that such behaviour is not unrecognised for silt dominated samples as suggested by particle size analysis (see Section 5.3) from this study.

Table 5.8: Post-peak pore water pressure characteristics of all consolidated undrained triaxial specimens tested.

Required Pressure (kPa)	OS1	OS2	TPS1	PS1	PS2
50	-	-	Decrease	Decrease	Decrease
100	Level	Level	Decrease	Increase	Increase
150	-	-	Decrease	Increase	Increase
200	Level	Increase	-	-	-
300	Level	Increase	-	-	-

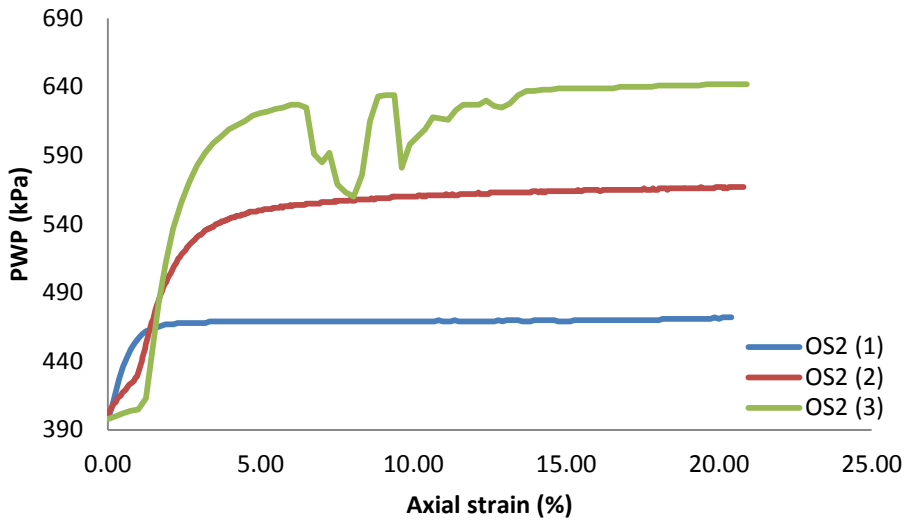

Figure 5.10: Pore water pressure characteristics of OS2. Pore water pressure is observed to level off at a confining pressure of 100 kPa. At higher confining pressures the pore water pressure is observed to increase. It should be noted that the fluctuation at 300 kPa is due to instrument error, and thus ignored in terms of the overall line trend.

The addition of drainage for the consolidated drained samples (OS1 only) appeared to indicate a key differentiation between sample behaviours during the compression stage. Volume change in the consolidated drained samples showed that as axial strain increased, pore water pressure was gradually dissipated (Figure 5.11), instead of increasing as with the undrained tests where volume change was

restricted. Head (1998) suggests that volume change during compression on a consolidated drained test which gradually rises and does not dip represents normally consolidated clay which was expected for all confining pressures, considering all tests were at or above the calculated *in-situ* confining pressure.

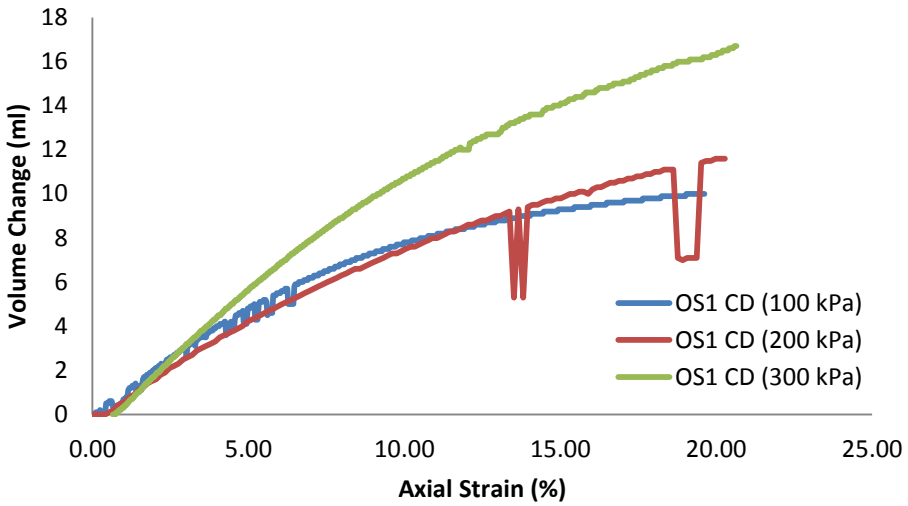

Figure 5.11: Volume change characteristics for the consolidated drained test from OS1.

5.6.2.3 **Effective stress path characteristics**

A stress path analysis describes the change in stress conditions during compression of a soil specimen (Head 1998). Stress paths are particularly useful in depicting normal consolidation where stress curves trend left, or in the opposite condition where stress curves trend right suggests over-consolidated clay characteristics (Head 1998; Powrie 2004; Wyatt 2009). Soil specimen consolidation characteristics were split evenly between normal and over-consolidation. OS1 indicated opposing results depending on whether the consolidated drained test or consolidated undrained test was carried out. The consolidated drained test displayed properties of over-consolidation for all specimens tested while the undrained test suggested the specimens were normally consolidated at all confining pressures (Figure 5.12). OS2 similarly indicated normal consolidation and compaction characteristics at all confining pressures, while TPS1 displayed over-consolidation and dilation characteristics (Table 5.9). Both Pahoia Peninsula samples indicated variations between confining pressures. At low pressures, the Pahoia Peninsula samples displayed properties of over-

consolidation and dilation, while at high confining pressures normal consolidation and compaction characteristics were observed. Both samples were not, however, identical where at the intermediate confining pressure of 100 kPa, PS1 behaviour suggested a normally consolidated clay while PS2 indicated over-consolidated clay characteristics.

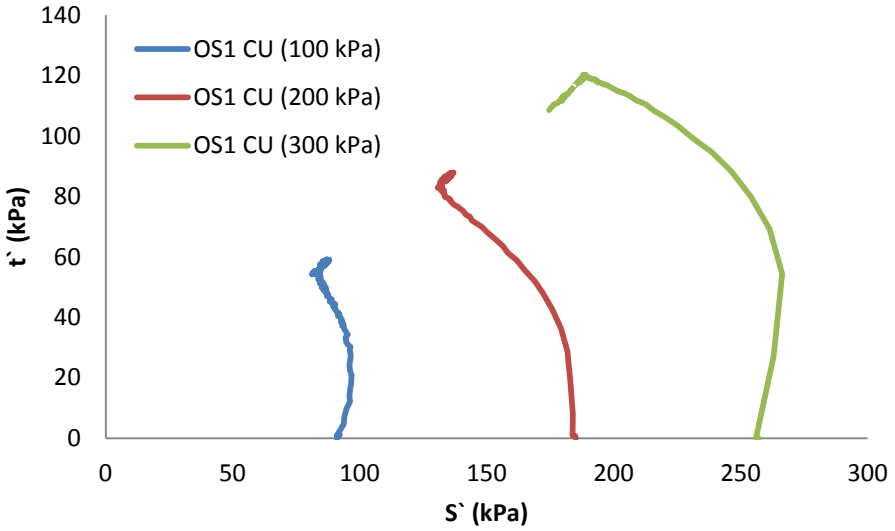

Figure 5.12: Stress path characteristics from the OS1 consolidated undrained test. All stress paths trend left indicating normal consolidation and compaction

Over-consolidation at low confining pressures has previously been reported by Wyatt (2009), who suggested that such behaviour was likely to occur in sensitive soil samples tested below their *in-situ* confining pressures. Results of the triaxial tests from this study further support that statement, where all samples tested with the lowest confining pressure of 50 kPa exhibited over-consolidated and dilatant clay behaviour (Table 5.9).

Table 5.9: Consolidation condition interpretations for each sample test.

Required Effective Pressure (kPa)	OS1 CU	OS2 CU	TPS1 CU	PS1 CU	PS2 CU
50			Over consolidation	Over consolidation	Over consolidation
100	Normal consolidation	Normal consolidation	Over consolidation	Normal consolidation	Over consolidation
150			Over consolidation	Normal consolidation	Normal consolidation
200	Normal consolidation	Normal consolidation			
300	Normal consolidation	Normal consolidation			

5.6.2.4 **Effective Mohr-Coulomb Failure Criterion**

Mohr-Coulomb failure criteria were determined based on effective cohesion (c') and effective friction angle (φ') on the basis of PWP measurement during triaxial compression. Peak deviator stress was the key criterion used to establish a point of sample failure as recommended by several previous authors (Bishop and Henkel 1962; BS1377 1990; Head 1998). Effective cohesion (c') and effective friction angle (φ') values are summarised in Table 5.10:

Table 5.10: Summary of effective cohesion and friction angle values for both the consolidated drained and consolidated undrained tests undertaken in this study.

Sample	Effective cohesion (c')	Effective friction angle (φ')
OS1 (CD)	19	32
OS1 (CU)	8	37
OS2 (CU)	16	28
TPS1 (CU)	16	41
PS1 (CU)	15	32
PS2 (CU)	10	36

Immediately apparent are the similarities and differences between the consolidated drained and consolidated undrained tests undertaken on OS1. Effective friction angles for both samples are comparable. Effective cohesion between the tests, however, is markedly different. On the basis of these results, the drained test displays a cohesion and friction angle that would represent silty CLAY type behaviour (Waltham 2002). The undrained test conversely appears to display properties closer to that of a clayey SILT, where a small amount of clay is providing limited cohesion and the higher friction angle suggesting silt like behaviour (Waltham 2002). The remaining sample sites appeared to indicate clayey SILT behaviour with the exception of TPS1. TPS1 displayed the most characteristic silt-like behaviour with a very high friction angle of 41^{o} and a low relatively low cohesion of 16 kPa. All of the consolidated undrained tests were comparable with the inferred textures from the field investigations (see Chapter 4).

Previous triaxial strength determinations on Tauranga sensitive soils, indicate wide ranging, typically inconsistent cohesion and friction angle values (Table 5.11).

Table 5.11: Effective cohesion and friction angle values for sensitive material from the Tauranga region.

Study	Location	Materials	Effective Cohesion (kPa)	Effective Friction Angle (°)	Dominat clay mineral (Selby 1993)
Keam (2008)	Omokoroa	sandy SILT	- 4.95 – 42.77	49.57 – 56.21	Halloysite, allophane
Wyatt (2009)	Tauriko, Otumoetai	silty CLAY, clayey SILT	4.7 – 34.5	25.7 – 38.5	Halloysite, allophane
Arthurs (2010)	Otumoetai, Te Puna, Pahoia Peninsula, Omokoroa	clayey SAND, clayey SILT, sandy CLAY, SILT with clay	0 – 81	12 – 37	Halloysite, allophane
This study (2012)	Omokoroa, Te Puna, Pahoia Peninsula	Clayey SILT, SILT	8 – 19	28 – 41	Halloysite, allophane

The results from this study, however, give consistent values for sensitive materials, with some comparable results with Wyatt (2009). Keam (2008) and Arthurs (2010), conversely, all indicated a wide range of cohesion values and varying friction angles, suggesting sensitive material cannot be easily quantified through the analysis of Mohr-Coulomb parameters.

5.6.2.5 Post triaxial test specimen condition

The specimen failure condition following a triaxial test is an important characteristic as the type of failure is not predetermined and it gives some idea as to what loading and confining conditions particular failure types occur under for a given soil type. Characterising specimen failure type for this study was done by classifying the failure type into four distinct groups; shear, barrel, intermediate and wedge failure. Shear failure describes a soil material shearing or failing along a single shear plane. Barrel failure is where no distinct shear plane is identified and the resulting specimen shape is barrel like in nature. Intermediate failure is the combination between shear and barrel failure, while wedge failure is the situation of shear failure occurring along two shear planes. The classification types are presented in Figure 5.13.

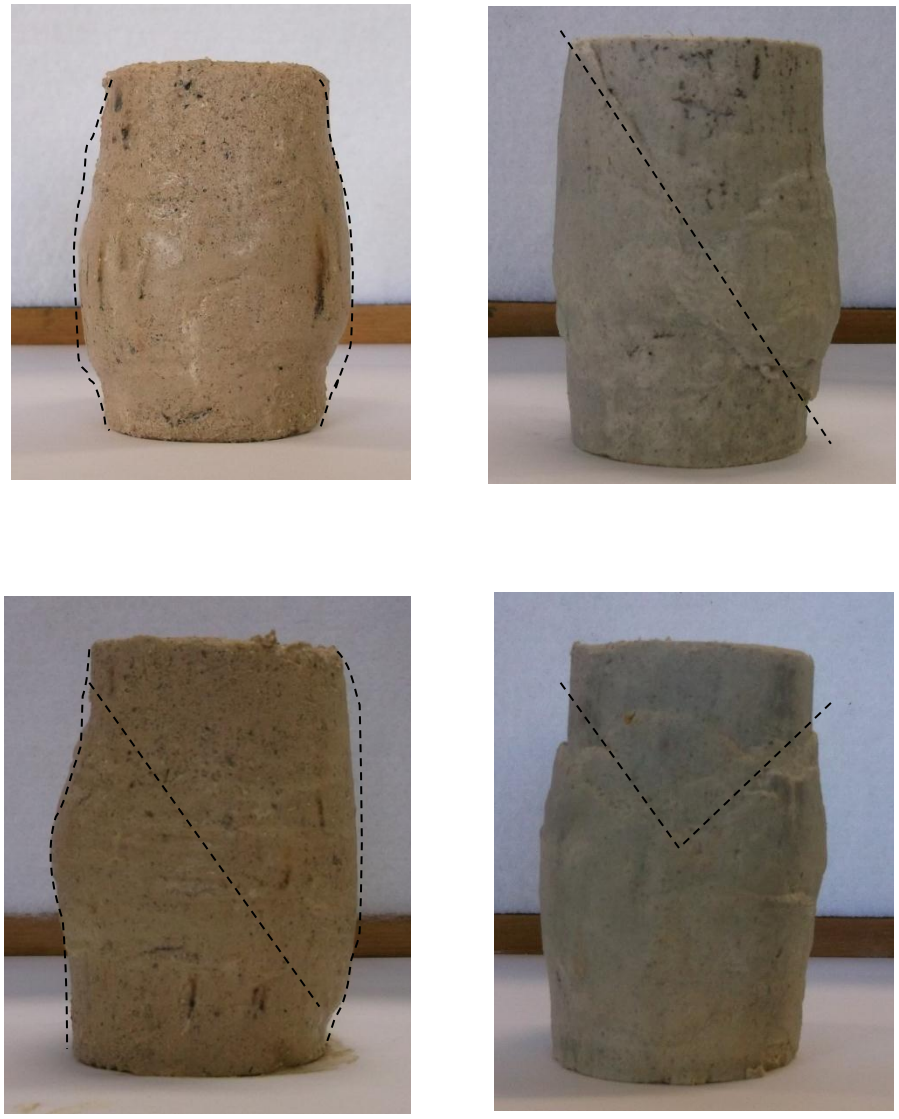

Figure 5.13: Types of specimen failure observed in this study; (A) Barrel failure, (B) Shear failure, (C) Intermediate failure and (D) Wedge failure.

A mixture of failure type was observed over all confining pressures from this study (Table 5.12). The least common failure was wedge failure, which only occurred at the lowest confining pressure in the Te Puna sample. OS1 indicated under consolidated undrained test conditions that intermediate and shear failures were most common, where no barrelling failures were observed. OS2, however, indicated much different results, with barrel type failures occurring at the two highest confining pressures. TPS1 displayed distinct shear planes for all three specimens, while the Pahoia Peninsula samples were primarily barrel and shear type failures.

Table 5.12: Specimen failure types observed in this study; Barrel failure (B), Shear failure (S), Intermediate failure (I) and Wedge failure (W).

Required effective pressure (kPa)	OS1 CU	OS2 CU	TPS1 CU	PS1 CU	PS2 CU
50			W	B	S
100	S	I	S	I	S
150			S	B	B
200	I	B			
300	I	B			

Wyatt (2009) reported that no distinct trends between confining pressures were apparent for samples from the Tauranga region. The results from this study tend to indicate that shear failure is dominant for samples that are over-consolidated based on the stress path behaviour (Table 5.9). Conversely, intermediate and barrel failure is more common for normally-consolidated samples based on the stress path characteristics. Aside from these trends, no other correlation between confining pressures and failure type was obvious.

5.7 Viscometric assessment of remoulded sensitive soils

Viscometric assessment was undertaken on remoulded specimens from OS1, OS2, OLRO, TPS1, PS1 and PS2. Each sample was initially analysed under the Wells and Childs (1988) method for initial shear rate acceleration. Following the initial shear rate increase, the Bentley (1979) method was employed to establish a yield stress based on the shear stress of the five fastest shear rates. Changes in yield stress at a variety of pH levels were also determined. Shear stress, yield stress and viscosity variation characteristics of the sensitive samples are presented along with appropriate comparisons with international examples. All raw data is presented in Appendix 5.6.

5.7.1 **Test sample conditions**

Pre-test sample characteristics were measured to ensure comparability in sample preparation between different samples, field conditions and pH variations for the tests undertaken. The pre-test sample conditions are presented in Table 5.13.

Table 5.13: Pre-test sample conditions for the viscometrically assessed samples.

Sample	Additive	Amount of additive (ml)	pH	Moisture Content (%)
OS1	HCl (1M 10%)	2.40	3.58	84.80
OS1	HCl (1M 10%)	1.00	4.68	87.90
OS1	Nil (natural pH)	–	6.20	84.74
OS1	NaOH (4%)	0.35	6.98	86.16
OS1	NaOH (4%)	1.00	8.19	85.77
OS2	HCl (1M 10%)	2.40	3.64	86.16
OS2	HCl (1M 10%)	1.00	4.71	83.57
OS2	Nil (natural pH)	–	6.19	83.63
OS2	NaOH (4%)	0.35	6.94	89.79
OS2	NaOH (4%)	0.95	7.96	81.72
OLRO	HCl (1M 10%)	2.40	3.75	59.20
OLRO	HCl (1M 10%)	1.00	4.81	55.18
OLRO	Nil (natural pH)	–	6.01	59.76
OLRO	NaOH (4%)	0.35	7.04	61.64
OLRO	NaOH (4%)	0.95	8.02	64.60
TPS1	HCl (1M 10%)	2.20	4.04	109.99
TPS1	HCl (1M 10%)	0.90	4.95	111.94
TPS1	Nil (natural pH)	–	6.21	112.95
TPS1	NaOH (4%)	0.37	7.30	107.20
TPS1	NaOH (4%)	1.00	8.01	112.23
PS1	HCl (1M 10%)	2.20	3.86	58.26
PS1	HCl (1M 10%)	0.90	4.91	62.38
PS1	Nil (natural pH)	–	6.23	62.85
PS1	NaOH (4%)	0.37	7.12	59.47
PS1	NaOH (4%)	1.00	8.12	51.54
PS2	HCl (1M 10%)	2.20	3.80	63.91
PS2	HCl (1M 10%)	0.90	4.82	63.61
PS2	Nil (natural pH)	–	6.52	64.10
PS2	NaOH (4%)	0.37	7.17	66.74
PS2	NaOH (4%)	1.00	8.22	65.73

The adjustment of pH indicated that a reasonable consistency between samples could be attained, with a very similar addition of either HCL or NaOH. Natural pH levels were also very similar between samples which was expected. Typically natural pH was ~ 6.2, however OLRO indicated a slightly lower pH at ~ 6.01 and PS2 indicated a slightly higher pH at ~ 6.52. These subtle differences did not impact the pH adjustment process considerably.

Moisture content was recorded for each sample before testing and compared to the field conditions (Table 5.13). This was done to ensure approximately even testing conditions were recorded for each pH variation and that the samples were as close to field moisture conditions as possible. This was achievable for all samples, with the exception of OLRO, which had a higher moisture content than originally recorded in Section 5.2. This is because the samples were collected on different occasions and due to the position of OLRO on the shore platform, which is heavily impacted by tidal fluctuations, moisture content was expected to be highly variable. The variation in OLRO moisture content was not considered important because all pH variations were tested at approximately similar moisture contents. Moisture content has been previously identified as having a significant impact on soil viscometric assessment (Bentley 1979), and so care was taken to ensure moisture content was similar across pH variations. OS1 had a moisture content variation range of ~ 3.1 % between samples, while OS2 had a range of ~ 8 %. TPS1 had a range of approximately 5.75 % between pH variations while PS1 and PS2 had a range of ~ 4.59 % and ~ 3.13 % respectively.

5.7.2 **Shear stress characteristics**

Shear stress profile characteristics typically varied between the Wells and Childs (1988) method used for the initial shear rate increase and the Bentley (1979) method employed following a state of shear stress equilibrium (at maximum rpm of ~ 850 – see Chapter 3). Over all samples it was apparent that both methods followed a broad pattern of shear stress increase with shear rate as would be expected (Figure 5.15). For the majority (66 %) of samples, a high shear stress was initially observed for the lowest shear rates, which would quickly decrease, followed by a gradual increase in shear stress with shear rate (Figure

5.14). This slight increase at very low shear rates was most prominent from the Wells and Childs (1988) method and was typically observed only at shear rates below ~ 25 s^{-1}. The presence of this high initial shear stress is interpreted as representing the shear stress required to originally shear the soil paste when it had settled in the sample cup. This phenomenon was not observed by Wells and Childs (1988) during their original study. The initial shear rate increase was not considered an important factor in affecting the overall results attained from these series of rheological determinations. The effect was primarily observed at very low shear rates of the Wells and Childs (1998) method, and only the 5 fastest shear rates (from the Bentley (1979) method) were accounted for in the yield stress determination (see Chapter 3) meaning shear stress values at lower shear rates were not important.

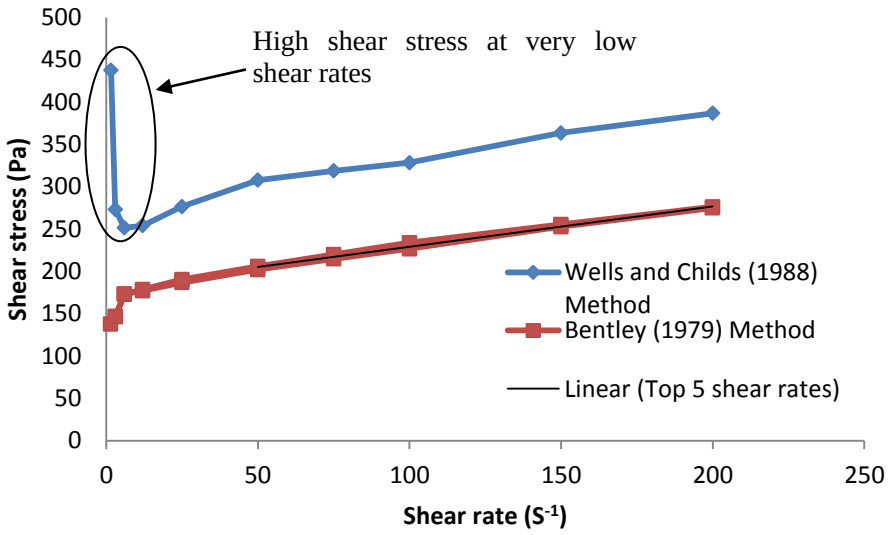

Figure 5.14: Shear stress curve for OS1 at pH 6.98. The shear stress curve is observed to be the highest at the lowest pH, however reduces rapidly as the shear rate increases, where it begins to increase linearly. The Wells and Childs (1988) method follows a very similar pattern to the Bentley (1979) method, however displays a significantly larger shear stress value for each shear rate.

Following initial shear rate increase to the fastest shear rate as per the Wells and Childs (1988) method, two minutes was allowed for all samples before an equilibrium maximum shear stress value was reached. Shear rate deceleration and acceleration (as per the Bentley (1979) method) characteristics yielded little (< 70 Pa) variation between the initial maximum shear stress and the final maximum shear stress, with the exception of PS1 and PS2. This indicated that the equilibrium established at the fastest shear rate was acceptable for regulating a

consistency between both the decrease in shear rate and the increase in shear rate across the whole test run. PS1 and PS2 showed ~ 130 Pa variations between the initial and final maximum shear stress (Figure 5.15). This may suggest that the Pahoia Peninsula samples required longer than two minutes for an equilibrium shear stress to have been attained. Nevertheless, the yield stress determination from the linear average between the increasing and decreasing shear rate was still believed to provide an accurate determination of yield stress for the sample.

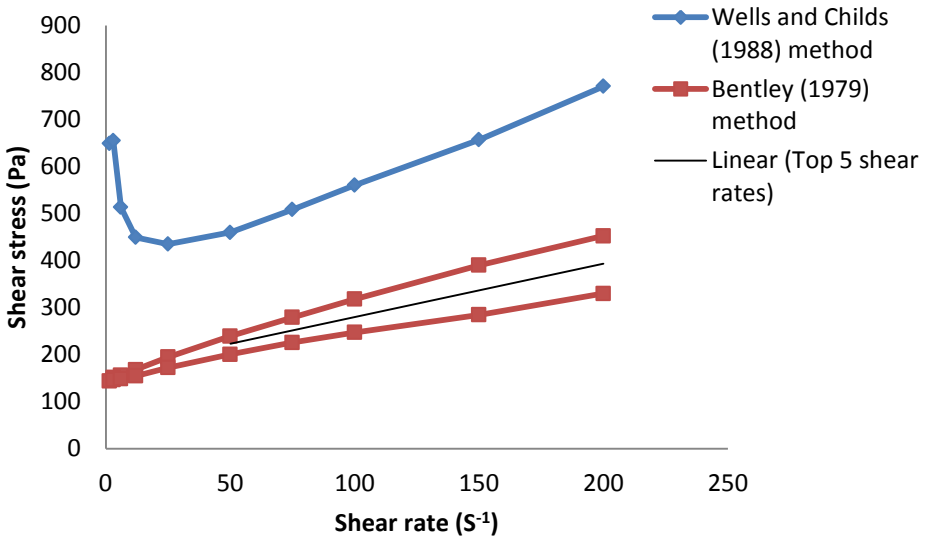

Figure 5.15: Shear stress curve for PS2 at natural pH. A difference of ~ 130 Pa in shear stress is observed between the initial and final maximum shear stress values. This result was typical for both Pahoia Peninsula samples across the range of pH values.

Following the state of equilibrium, the Bentley (1979) method typically displayed a gradual linear trend for shear stress from low shear rates to high shear rates, which was consistent between samples. The slope of the shear stress change with shear rate under the five fastest shear rates of the Bentley (1979) method indicated varying slope gradients (Table 5.14). Slope gradients from PS1, PS2 and OLRO were relatively steep. Conversely OS1, OS2 and TPS1 indicated shallow gradients. Theng and Wells (1995) suggest that differences in slope are related to the size and shape of micro-aggregates and their propensity to flow. For example, a suspension concentration of larger blocky micro-aggregates offer greater resistance and thus highest slope gradient, than smaller plate-like micro-aggregates which typically have small gradients (Theng and Wells 1995).

Table 5.14: Mean shear stress slope gradients (Bentley (1979) method) at natural pH for each sample analysed in this study.

Sample	Mean shear stress gradient (Bentley (1979) method)
OS1	0.51 ± 0.08
OS2	0.48 ± 0.01
OLRO	0.71 ± 0.02
TPS1	0.23 ± 0.003
PS1	0.77 ± 0.06
PS2	1.12 ± 0.01

As a general trend, the Wells and Childs (1988) method displayed consistently higher shear stress values than the Bentley (1979) method (Figure 5.14). Once a peak shear stress was reached, the Wells and Childs (1988) method would not re-establish its original maximum shear stress which could be seen after the period of equilibrium was allowed. On the contrary, the Bentley (1979) method would often be very close to its original maximum shear rate following deceleration and then acceleration to maximum shear, confirming the importance of allowing an equilibrium shear stress point to be established before analysis. Shear stress profiles for all samples are available in Appendix 5.6.

5.7.3 **Viscosity and yield stress at natural pH**

Viscosity indicated some variation across all samples (Table 5.15). Initially TPS1 had the highest viscosity, while PS2 had the lowest viscosity. This observation is surprising, given that the clay particle analysis (see Section 5.3) indicated that TPS1 had a very low clay content (2.96 %) compared to the majority of other samples. Increasing clay content would typically be expected to increase the viscosity of the soil paste.

International sensitive ‘quick’ clays have indicated viscosities ranging from 0.01 Pa.s to 0.9 Pa.s (Locat and Demers 1988), suggesting that viscosities determined in this study are considerably higher (more viscous) than international quick clays. Considering the *in-situ* behaviour of the material studied was not classified as ‘quick’ (according to the New Zealand Geotechnical Society 2005) and also had a high proportion of large grained material within the suspension, the

higher viscosity values are expected. The high proportion of larger silt grained material in the sensitive materials from this study (see Section 5.4) compared to the predominantly clay composition of international sensitive clays increases the frictional resistance between grains when the material is remoulded so a higher viscosity is promoted.

Yield stress values at natural pH also indicated OLRO and TPS1 had the highest values, while PS1 and PS2 had the lowest yield stress values (Table 5.15). These results indicate that samples from PS1 and PS2 required less applied stress to flow, while OLRO required a higher applied stress. The high proportion of sand in OLRO (likely incorporated during remoulding process – see Chapter 4) is likely responsible for the higher yield stress, however, it is not markedly higher than the in-situ derived materials.

Table 5.15: Viscosity and yield stress values at natural pH for all sensitive samples analysed in this study.

Sample	Viscosity (Pa.s)	Yield Stress (Pa)
OS1	22.20 ± 0.6	213.40 ± 2.6
OS2	21.08 ± 0.1	214.69 ± 7.3
OLRO	30.03 ± 0.9	253.41 ± 8.6
TPS1	30.80 ± 1.9	219.86 ± 3.6
PS1	18.96 ± 2.6	181.51 ± 23.4
PS2	15.20 ± 1.5	154.03 ± 9.9

5.7.4 Viscosity and liquidity index variation with yield stress

Viscosity variation with yield stress was analysed across all samples at natural pH values and the viscosities calculated from the Bentley (1979) method. The results indicated that viscosity was positively correlated with yield stress (Figure 5.16). This relationship indicates that as yield stress increases, viscosity will also increase. The relationship is not surprising given that yield stress is determined from the shear stress to shear rate viscosity curve. The results do indicate that the behaviour is consistent with international sensitive clays from Canada as reported by Locat and Demers (1988).

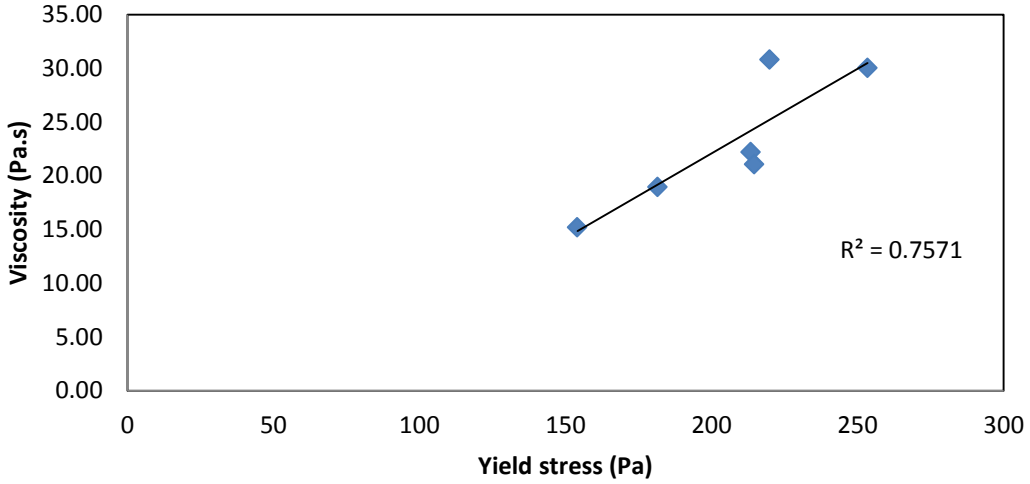

Figure 5.16: Viscosity variation with yield stress. A positive linear relationship was plotted, which is expected considering shear stress is a function of viscosity.

Liquidity index has previously been reported to decrease with yield stress for sensitive clay material from Canada (Locat and Demers 1988). The sensitive material from this study also indicated a similar linear trend at natural pH (Figure 5.17). Effectively, the relationship describes that yield stress increases as the liquidity index decreases. The natural high moisture content of the sensitive materials promotes high liquidity indexes, therefore reducing the yield stress of the samples which is consistent with previous studies (Bentley 1979). Therefore, it can be deduced that soil materials with lower liquidity indexes will have a higher yield stress, and be less prone to flow behaviour upon remoulding as would be expected. PS2 had the lowest yield stress of 154.03 Pa where the liquidity index was observed to be the highest at 1.91 %. The highest yield stress at natural pH was 253.41 Pa measured at OLRO, which also had the lowest liquidity index of 1.16 %.

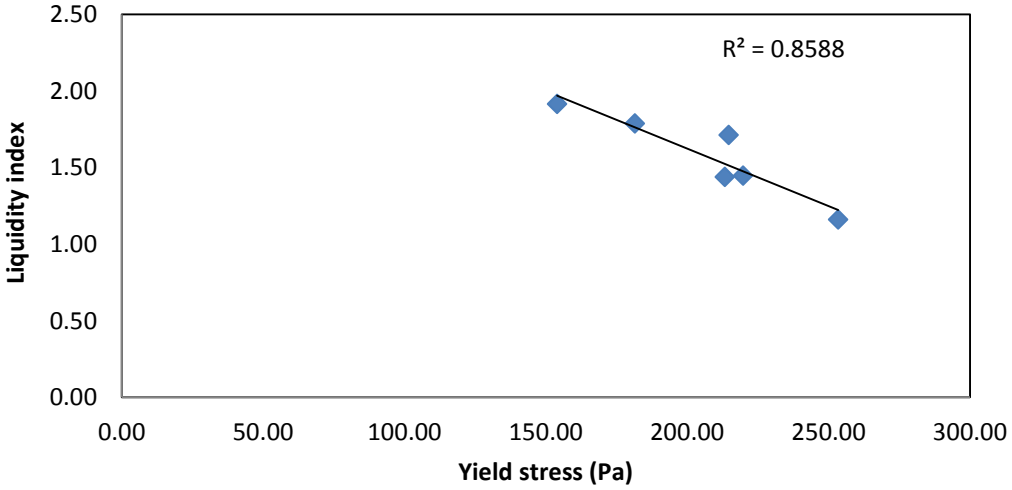

Figure 5.17: Liquidity index variation with yield stress. The relationship indicates a similar pattern as that observed by Locat and Demers (1988).

5.7.5 Yield stress variation with pH

Yield stress variation with pH indicated a difference in behaviour across all samples. Initially, the natural pH of all samples only varied slightly between ~ 6 – ~ 6.5. The yield stress response to pH adjustment, however, was not consistent (Figure 5.18).

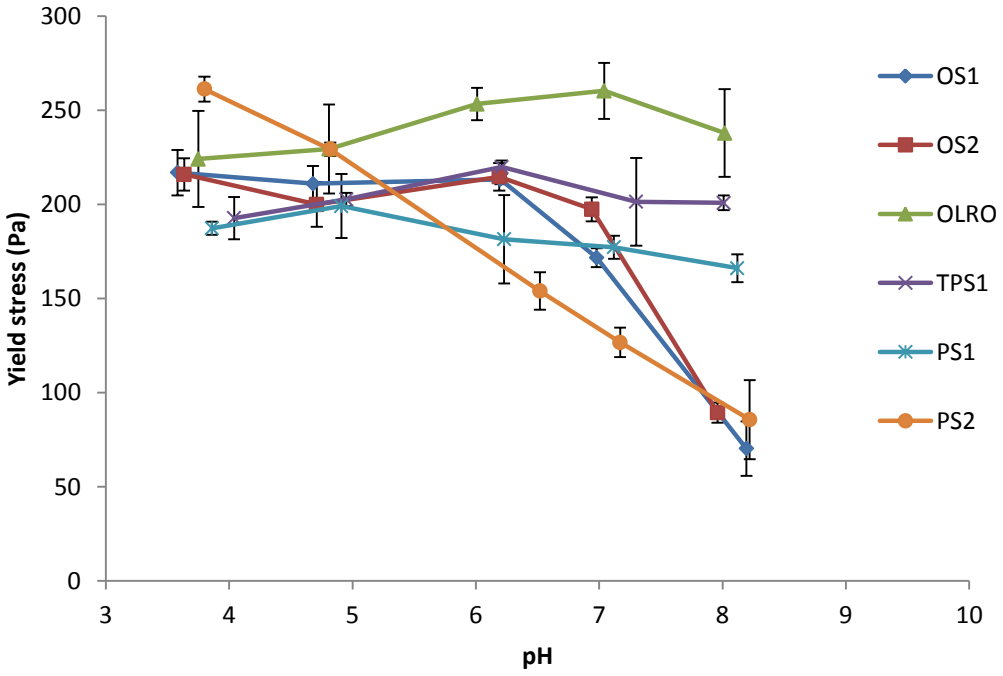

Figure 5.18: pH impact on yield stress variation. Samples varied in response to the pH variation, however generally the sensitive material would decrease with pH, and always be below the natural yield stress value at pH ~ 8.

Initially, OS1, OS2, PS1 and PS2 typically displayed a decreasing yield stress value with pH indicating the majority trend for the sensitive sample response with pH. PS1 indicated that the yield stress was highest at pH ~ 5 and slightly lower at pH ~ 4. OS2 and OS1 indicated the opposite conditions at lower pH to PS1 and PS2, where the yield stress slightly decreased at pH ~ 5, however increased again to its maximum at pH ~ 4. PS2 was consistently higher with each decrease in pH and also displayed the most dramatic increase. The dramatic yield stress variation with PS2 was apparent from a visual inspection of the sample as well (Figure 5.19). The high pH sample is seen to be much more dilatant, with no physical soil 'peaks' which can be seen in the lower pH sample. Furthermore, the pH ~ 4 sample maintained a continuous edge, indicating a greater cohesion between clay particle grains in the sample, whereas the pH ~ 8 flowed out at the edges.

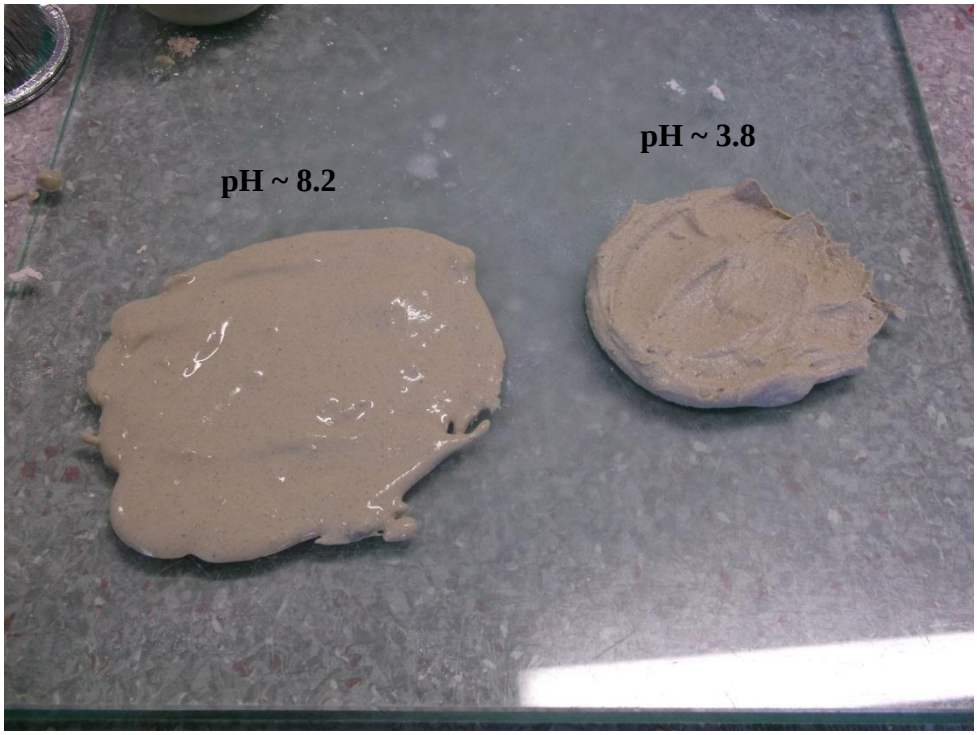

Figure 5.19: Remoulded soil pastes from PS2. The sample on the left is at pH ~ 8.2 which indicated the lowest yield stress, while the sample on the right is at pH ~ 3.8 (highest yield stress). Both samples were at approximately similar moisture contents (< ± 2 %).

At pH values above the natural pH, OS1, OS2 and PS2 all indicated rapid decreases in yield stress from pH ~ 7 – 8, where OS1 indicated a decrease of a third of its original yield stress at 70.31 Pa. PS1 indicated a less intense yield

stress decrease. All of OS1, OS2, PS1 and PS2 indicated that the lowest measured yield stress was at pH ~ 8.

TPS1 and OLRO did not conform to the same negative trend with pH as was typical for the aforementioned samples. TPS1 decreased in yield stress as pH was both increased and decreased. OLRO, also decreased in yield stress as pH was lowered, however when pH was increased to ~ 7, the yield stress increased slightly. With further pH increase the yield stress decreased. The decrease in pH at ~ 8 was consistent across all samples, indicating that pH increase to ~ 8 would decrease the yield stress capability of sensitive material from the Tauranga region.

The typical decrease of yield stress with increased pH that was observed across several samples in this study has previously been characterised for halloysite suspensions by Theng and Wells (1995). Theng and Wells (1995) suggested that the variation of pH with HCl and NaOH predominantly impacts the charge characteristics of clay particles. Hence, samples that contained higher proportions of clay may have been expected to respond more strongly to the pH treatments. This did not appear to be the complete case, however, where the sample with the highest clay content (OS1) did not have a strong change in yield stress with HCl, yet with the addition of NaOH, it did respond strongly, decreasing by ~101 Pa from pH ~ 7 to pH ~ 8. OS2 however, which had the lowest clay content at ~ 2.17 %, indicated a stronger response in comparison with OS1 with a ~ 108 Pa difference between the pH ~ 7 to pH ~ 8 range. Similar inconsistencies between clay content variations were apparent with other samples tested, suggesting that the relative abundance of clay is not a determinant for yield stress variation with pH.

5.7.6 **Sensitivity assessment**

The sensitivity calculation based on the Wells and Theng (1985) method for determination on viscometrically assessed remoulded soils suggested (with the exception of PS2) low sensitivities to shear in all samples analysed (Table 5.16).

Table 5.16: Sensitivity to shear assessment based on the Wells and Theng (1985) method. Sensitivity was assessed as the ratio of maximum shear stress from shear rate acceleration to the y-intercept of the linear portion of the deceleration shear stress to shear rate curve i.e. yield stress (Wells and Theng 1985).

Sample	pH	Yield Stress (Pa)	Max Shear Stress Wells and Childs (Pa)	Sensitivity (Wells and Theng Method)
OS1	3.58	216.92	334.33	2
OS1	4.68	211.04	416.67	2
OS1	6.20	213.40	616.67	3
OS1	6.98	171.77	443.90	3
OS1	8.19	70.31	278.68	4
OS2	3.64	215.96	400.38	2
OS2	4.71	200.03	366.39	2
OS2	6.19	214.69	441.15	2
OS2	6.94	197.43	412.22	2
OS2	7.96	89.47	313.84	4
OLRO	3.75	224.19	607.83	3
OLRO	4.81	229.47	598.22	3
OLRO	6.01	253.41	617.49	2
OLRO	7.04	260.36	579.73	2
OLRO	8.02	237.94	517.98	2
TPS1	4.04	192.77	396.28	2
TPS1	4.95	202.74	400.00	2
TPS1	6.21	219.86	436.55	2
TPS1	7.30	201.44	384.30	2
TPS1	8.01	200.88	401.44	2
PS1	3.86	187.37	502.41	3
PS1	4.91	199.12	523.95	3
PS1	6.23	181.51	580.83	3
PS1	7.12	177.30	624.97	4
PS1	8.12	166.16	552.80	3
PS2	3.80	261.27	589.20	2
PS2	4.82	229.38	627.44	3
PS2	6.52	154.03	714.58	5
PS2	7.17	126.73	586.69	5
PS2	8.22	85.69	805.14	9

Sensitivity to shear according to the Wells and Theng (1985) method indicated that the majority of samples displayed consistent sensitivity values of between 2 and 4 over all pH values. With the exception of OLRO and TPS1 (which displayed low sensitivities to shear) all samples tended to increase in sensitivity at higher pH levels. PS2 was considerably sensitive to shear at higher pH values, where a sensitivity of 5 was recorded at pH ~ 6.5 and 7.2, while a sensitivity of 9 was recorded at pH ~ 8.22. Under the Wells and Theng (1985) method, Wells and Childs (1988) have previously reported sensitivities ranging between 1.0 and 7.8 for allophonic materials collected from the base of the Ohinewai formation in Te Kuiti. This would suggest that the sensitivity to shear of the samples from this study is comparable with allophanic materials.

5.8 Geomechanical properties summary

Geomechanical properties of sensitive and non-sensitive soil deposits from the Tauranga region have been characterised in this chapter. Atterberg limits indicated a reasonably clear distinction between sensitive and non-sensitive soil properties. Liquid limits of the *in-situ* sensitive material were consistently below the corresponding moisture contents, producing liquidity indexes greater than 1, while the opposite conditions were true for the non-sensitive material. Plastic limits indicated that the non-sensitive sites at Tauriko were non-plastic, while no clear distinction could be determined between the remaining sensitive and non-sensitive sites. Plotting the sensitive materials on the Casagrande Plasticity chart indicated that the material behaved predominantly in a silt like manner.

Moisture contents were high for all sensitive samples, while non-sensitive samples displayed relatively low values. Bulk density for the sensitive samples was negatively correlated with moisture content. Particle size variations indicated low levels of clay (≤ 11 %) with the exception of Rangataua Bay. *In-situ* sensitive soils were largely comprised of silt (> 49 %) whereas non-sensitive material from Rangataua Bay had high clay and silt contents while the material from Tauriko was largely comprised of sand. The OLRO material proved problematic in interpretation considering its post failure transportation before deposition. The material was likely intermixed with sand during failure resulting in an inconsistent

moisture content between collection times and also indicating a relatively high sand content.

Laboratory shear vane assessments indicated that the materials were extra sensitive which was mostly consistent with the field shear vane. Triaxial testing suggested that the sensitive materials behaved as both over-consolidated and normally consolidated clays. Over-consolidation was typical at low confining pressures (50 kPa) while normal consolidation was common for high consolidation pressure (150 – 300 kPa). Shear failure was most common from over-consolidated conditions, while intermediate and barrel failures were typical of normally consolidated conditions. Mohr-Coulomb failure criterion indicated cohesion values < 20 kPa and friction angles of 28 º– 41 º, implying halloysite and allophane clay behaviour.

Viscometric assessment indicated that typically viscosities from the sensitive materials in this study were much higher than those observed in international quick clays. Viscosity was observed to increase with yield stress, while the liquidity index decreased. Yield stress variation with pH was not consistent, however indicated a general decreasing trend with increasing pH. At high pH values, the yield stress was always reduced from its corresponding natural pH value.

Chapter 6

PETROGRAPHY

6.1 Introduction

The roles of clay mineralogy and microstructure have previously been identified as critical factors for soil sensitivity (Collins and McGown 1974; Smalley *et al.* 1980; Jacquet 1990; Selby 1993; Keam 2008; Wyatt 2009; Arthurs 2010). Understanding which clay minerals encourage sensitive behaviour in the soils observed from the Tauranga region is an important facet for classifying the structural and behavioural characteristics of the sensitive material. Furthermore, determining how these minerals are assembled and their interactions within the overall soil microstructure is critical for determining their sensitive nature. X-ray diffraction (XRD) and scanning electron microscopy (SEM) were the two methods employed to establish the primary clay and non-clay mineral constituents comprising the soil. Scanning electron microscopy was also utilised in microstructure analysis. Samples from all five sites (Omokoroa, Te Puna, Pahoia Peninsula, Tauriko and Rangataua Bay) were analysed by both XRD and SEM methods.

6.2 Petrographic observations

6.2.1 X-Ray Diffraction (XRD)

Both bulk and clay size (< 2 μm) samples were examined with XRD. Bulk samples were used to analyse all minerals present in the sample material, whereas the clay size analyses were used to specifically isolate clay mineral assemblages in each sample. A ceramic slide was used for analysis of the clay fraction (see Chapter 3, Section 3.6.1). A scan of a blank ceramic slide was undertaken, which revealed small reflections of quartz, plagioclase feldspar and cristobalite minerals.

This meant that the relative intensities of these three minerals observed in the clay fraction may not have been accurate where an insufficiently thick spread of the clay solution was applied. The analysis of the bulk sample was, therefore, used to ensure that no misinterpretation between minerals in the ceramic plate and the actual sample was made. Furthermore, these small reflections were not considered to be significant because the primary purpose of scanning clay size fractions was to distinguish between clay species rather than analyse non-clay minerals. All XRD diffractograms are presented in Appendix 6.1.

6.2.1.1 **Omokoroa (OS1, OS2, OLRO)**

Mineralogical analyses from all bulk Omokoroa samples indicated a strong similarity in mineral composition between them. Table 6.1 summarises the clay, silt and sand size mineral compositions of the three samples.

Table 6.1: Bulk mineralogical summary for OS1, OS2 and OLRO from Omokoroa. The samples include minerals from the clay, silt and sand fraction of each sample.

Sample	Mineralogy
OS1	Hydrated halloysite, plagioclase feldspar, quartz, cristobalite
OS2	Hydrated halloysite, plagioclase feldspar, quartz, cristobalite, feldspar
OLRO	Hydrated halloysite, dehydrated halloysite/kaolinite (see text), quartz, plagioclase feldspars, cristobalite, halite

Bulk sample mineralogy of the Omokoroa samples indicated a general characterisation of hydrated halloysite, plagioclase feldspar and quartz. Both OS1 and OS2 were very similar in composition with the most prominent feature illustrated by the large halloysite 001 peak at ~ 10 Å (Figures 6.1 and 6.2). The primary peak for halloysite is at least double the intensity of the quartz and plagioclase feldspar peaks, suggesting the relative abundance of halloysite in the bulk samples is high. Quartz typically reflects very well from XRD, so for halloysite to reflect so strongly suggests the sample had abundant halloysite. A secondary peak of halloysite is also recognised at ~ 4.42 Å in both OS1 and OS2, which is characteristic of the 02, 11 band of dehydrated halloysite (Brindley and Brown 1980; Wyatt 2009). Furthermore, OS1 displays a pronounced peak at

2.52 Å representing the 13, 20 band of halloysite further confirming halloysite dominance of the sample.

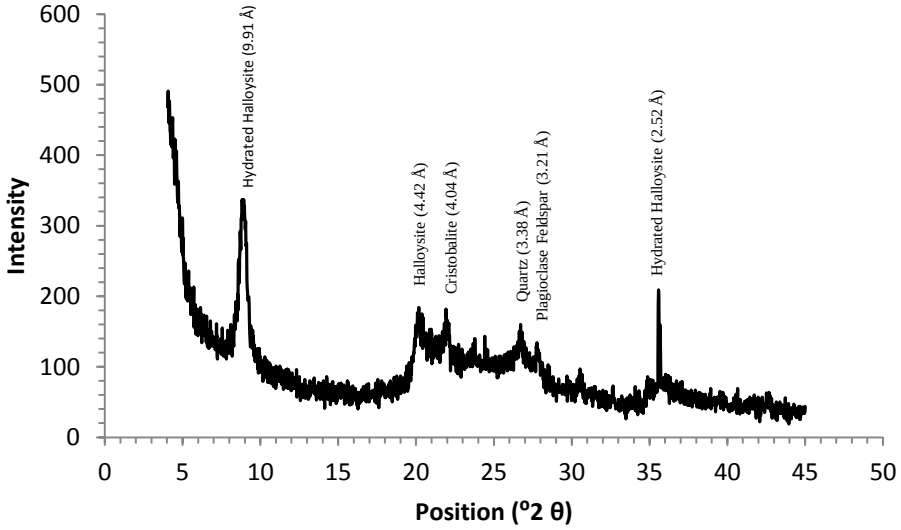

Figure 6.1: XRD bulk sample diffractogram for OS1. Peak/mineral associations are labelled on the plot.

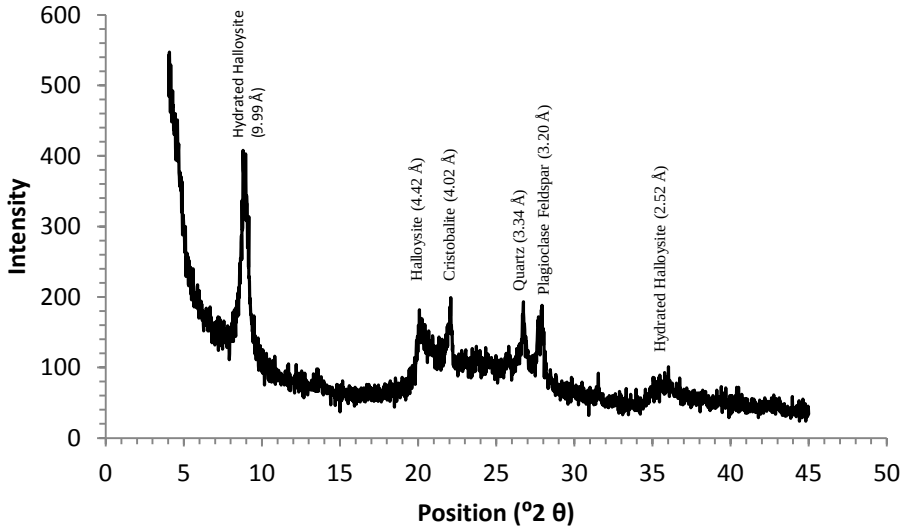

Figure 6.2: XRD bulk sample diffractogram for OS2. Peak/mineral associations are labelled on the plot.

OLRO indicates halloysite at the ~ 10.02 Å, ~ 4.44 Å and ~ 2.56 Å peaks. However, they are slightly less intense than for the OS1 and OS2 samples (Figure 6.3), indicating a lower concentration of halloysite. Dehydrated halloysite is represented by a broad peak at ~ 7.29 Å, and at ~ 4.44 Å. The identification of the

~ 7.29 Å peak as dehydrated halloysite as opposed to kaolinite (which has a basal reflection of 7.14 Å) is supported by the findings reported by Joussein *et al.* (2005), who indicate that 7 Å halloysite is characterised by very broad and weak peaks between 7.2 – 7.6 Å, but never as low as 7.14 Å. The presence of any small amount of kaolinite that may be present at 7.14 Å is masked by the dehydrated halloysite. A small broad peak at ~ 2.35 Å may suggest that kaolinite is present in very low concentrations but this 003 peak also represents dehydrated halloysite and so the evidence for kaolinite is equivocal.

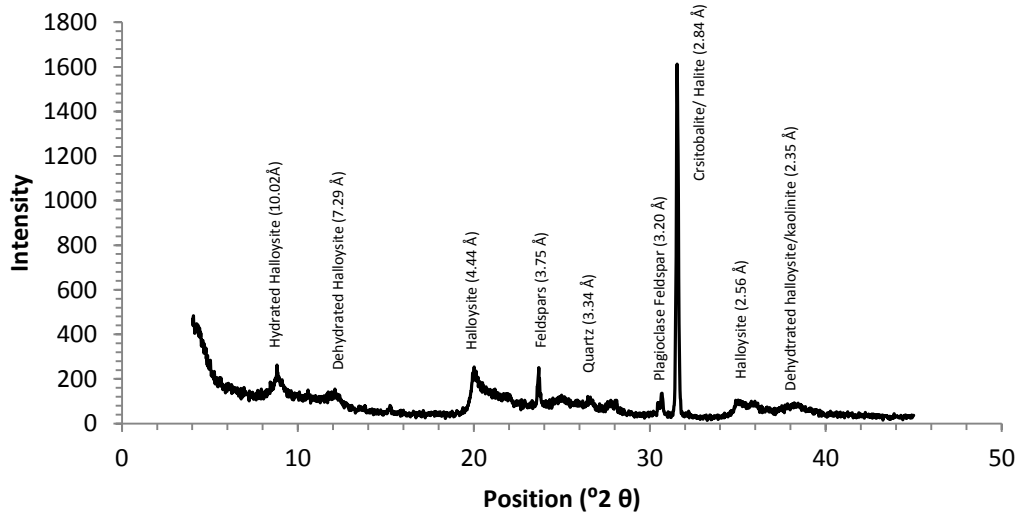

Figure 6.3: XRD bulk sample diffractogram for OLRO. Peak/mineral associations are labelled on the plot.

Of the non-clay constituents recognised in the bulk sample scans, plagioclase feldspar and quartz were present in similar amounts in all three samples. Cristobalite was also common in OS1, OS2 and OLRO. Cristobalite is a silica group mineral, common in volcanic materials (e.g. Lowe 1986; Mizota *et al.*, 1987; Mizota and Itoh 1993; Wallace, 1991) and so is not unexpected in the XRD traces from the Tauranga region. Furthermore, cristobalite has previously been reported in the Tauranga region by Wyatt (2009) as well as in the Hamilton Ash beds that are also present in the Tauranga region (Salter 1979; Wallace 1991; Lowe and Percival 1993). OLRO indicated a peak at ~ 3.34 Å which Brindley and Brown (1980) associate with feldspar. However, this peak was not considered to represent plagioclase given the reflection was not within the range 3.18 – 3.22 Å (Brindley and Brown 1980).Instead it is likely to be quartz. The largest peak from

all three samples was recorded in the OLRO sample with a strong reflection at 2.84 Å. This peak could have likely represented both cristobalite and/or halite, which may not be considered surprising since the material was sampled from a coastal area. Given the high solubility of halite (NaCl) and that the Tauranga region does undergo periods of significant rainfall, the possibility of halite does seem low. Considering the intertidal fluctuations overtop of the sampled area, halite was not unequivocally ruled out, but more likely present due to surficial salt spray.

The analyses of the clay fractions indicated a very similar pattern of minerals, which further supported the relatively high abundance of halloysite in the Omokoroa samples (Table 6.2).

Table 6.2: Clay fraction mineralogical summary for OS1, OS2 and OLRO from Omokoroa. The samples include only minerals of clay size or smaller (< 2 μm).

Sample	Mineralogy
OS1	Hydrated halloysite, feldspars, quartz, plagioclase feldspar, cristobalite
OS2	Hydrated halloysite, quartz, plagioclase feldspar, cristobalite
OLRO	Hydrated halloysite, dehydrated halloysite, quartz, plagioclase feldspar

Hydrated halloysite is abundant in the clay fraction. Upon heating the samples, all three depicted interlayer water loss with peaks shifting from ~ 10 Å to ~ 7 Å (Figure 6.4), confirming that hydrated halloysite is present in all samples. The 550 ^{0}C heated sample indicated no peak at ~ 10 Å or ~7 Å which is characteristic of halloysite (as it becomes X-ray amorphous). The lack of a ~ 10 Å peak also indicated that no micas were present in the sample, because a ~ 10 Å peak reflecting mica would have persisted following sample heating to 550 ^{0}C (Lowe and Nelson 1983). The 02, 11 band halloysite peak (~ 4.42 Å) is observed to become X-ray amorphous following 550 ^{0}C sample heating, confirming halloysite.

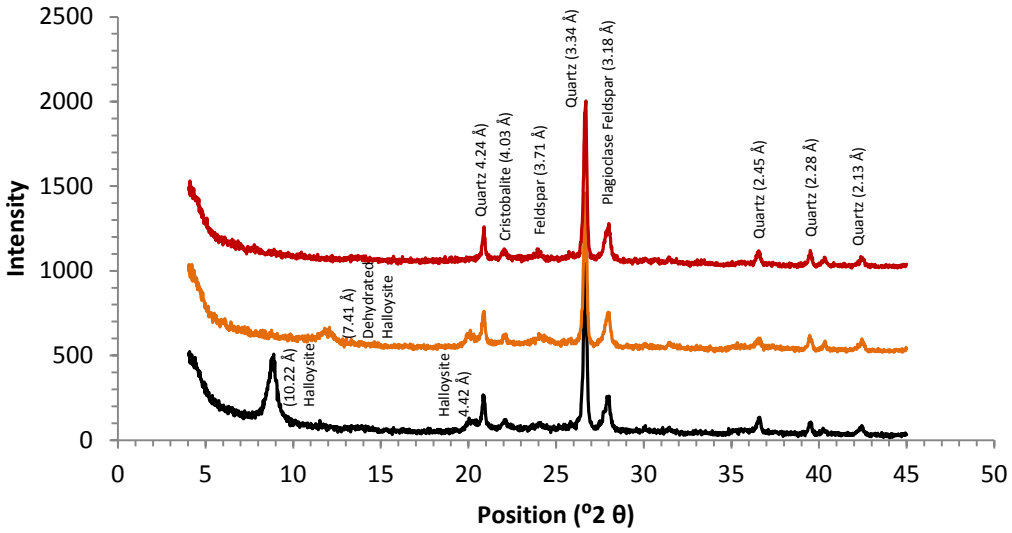

Figure 6.4: OS1 unheated clay fraction sample diffractogram (black), heated to 110 ^{0}C (orange) and heated to 550 ^{0}C (red). Hydrated halloysite can be seen to peak at ~ 10 Å in the unheated sample, while the 110^{0}C heated sample indicates the dehydrated form of halloysite, where the interlayer water is removed and the peak collapses to ~ 7 Å. Following 550 ^{0}C heating the ~ 10 Å peak becomes X-ray amorphous, further confirming halloysite. Note each intensity data point for the 110 ^{0}C heated data set has been offset/increased by 500 points each while the 550 ^{0}C dataset has been offset by 1000 points to differentiate between scans. OS1 is characteristic of all Omokoroa sample sites.

Consistent with the analyses of bulk samples, the clay fraction OLRO XRD diffractogram displayed peaks at both ~ 10 Å and ~ 7 Å. The ~ 7.29 Å peak observed in the OLRO bulk sample is represented as a 'shoulder' in the clay fraction diffractogram, which upon the addition of formamide expanded to ~ 10.18 Å, confirming that dehydrated halloysite rather than kaolinite is present (Figure 6.5). The presence of a 'shoulder' tapering off the ~ 10 Å halloysite position is characteristic of halloysite in a form where the interlayer water has only been partially dehydrated and thus is not completely differentiated from the primary peak (Churchman *et al.* 1972).

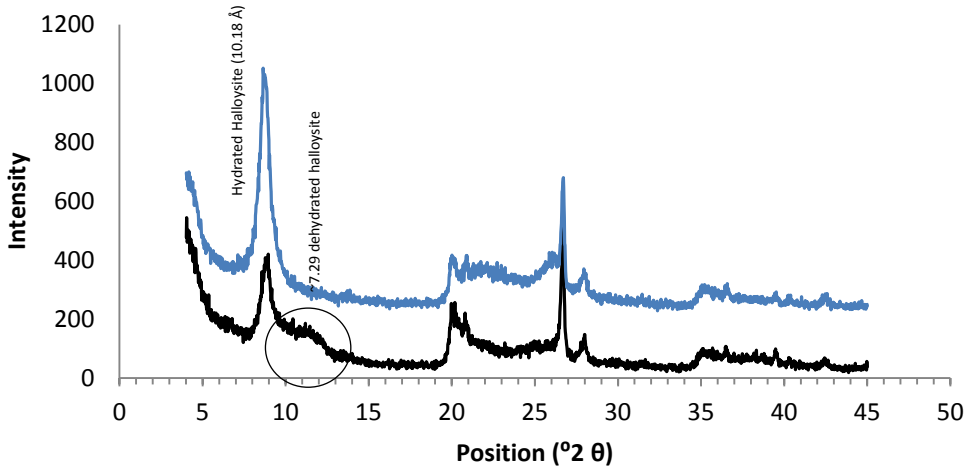

Figure 6.5: OLRO before the addition of formamide (black) and after formamide treatment (blue). The ~ 7 Å dehydrated halloysite 'shoulder' peak is indicated by the circle. Upon the treatment of formamide it expands and shifts to ~ 10 Å, indicating the ~ 7 Å peak is halloysite and not kaolinite. Note each intensity data point for the formamide-treated set has been offset/increased by 200 points each.

The remaining minerals at < 2 µm are recognised as quartz and plagioclase feldspar as found in the larger bulk samples. Heating the samples had no significant effect on the non-clay minerals. The 003 peak for halloysite is represented by a peak between 3.32 – 3.35 Å, which initially coincided with the quartz peak, potentially masking the quartz as halloysite or vice versa. The heating had no effect on the peak (pattern not shown), and hence the reflection could not be halloysite because a halloysite peak would have moved after dehydration, thus confirming the peak represents quartz (Brindley and Brown 1980).

6.2.1.2 **Te Puna (TPS1)**

Bulk and clay mineral compositions of samples from TPS1 indicated a very similar pattern to that of the Omokoroa samples. Table 6.3 summarises the minerals observed from both analyses of the bulk and clay-size samples from TPS1. The minerals observed in both analyses were identical and are therefore described together.

Table 6.3: Bulk and clay-size sample mineralogy for TPS1 from Te Puna. No mineralogical difference was observed between the bulk sample scan and the clay size scan and so the analyses are given as a combination of both scans.

Sample	Mineralogy
TPS1	Hydrated halloysite, feldspars, quartz, plagioclase feldspar, cristobalite

As observed at Omokoroa, the TPS1 bulk mineral composition was predominantly hydrated halloysite, plagioclase feldspar, cristobalite and quartz (Figure 6.6). The halloysite 001 peak is seen to be the dominant mineral represented in the sample. Furthermore, halloysite is observed at its 02, 11 band at ~ 4.44 Å and again at ~ 2.5 Å. The prevalence of halloysite and not any other clay minerals suggest that it is the dominant clay mineral in the sample. Furthermore, no dehydrated peak at ~ 7 Å is observed, suggesting that the interlayer water was not lost in sample preparation and that only hydrated halloysite is present (Churchman *et al*. 1972; Churchman and Lowe 2012).

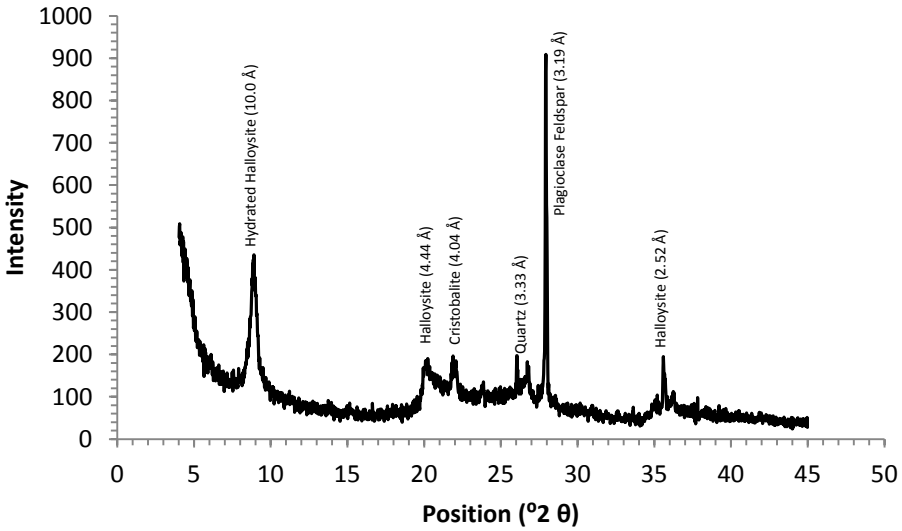

Figure 6.6: Bulk XRD diffractogram for TPS1. The sampled material included clay, silt, and sand size minerals.

The non-clay minerals were recognised as plagioclase feldspar and quartz. The peak at ~ 3.18 Å is a typical common indication of plagioclase feldspar (Brindley and Brown 1980). The quartz peaks were relatively small in comparison, but were still clearly discernible.

The analyses of the clay size fraction further confirmed the presence of hydrated halloysite: after heating to 110 ^{0} C and 550 ^{0} C, the ~ 10 Å peak initially shifted and then disappeared completely (Figure 6.7). The addition of formamide (pattern not shown) only proved to enhance the peak slightly, with no other differences observed.

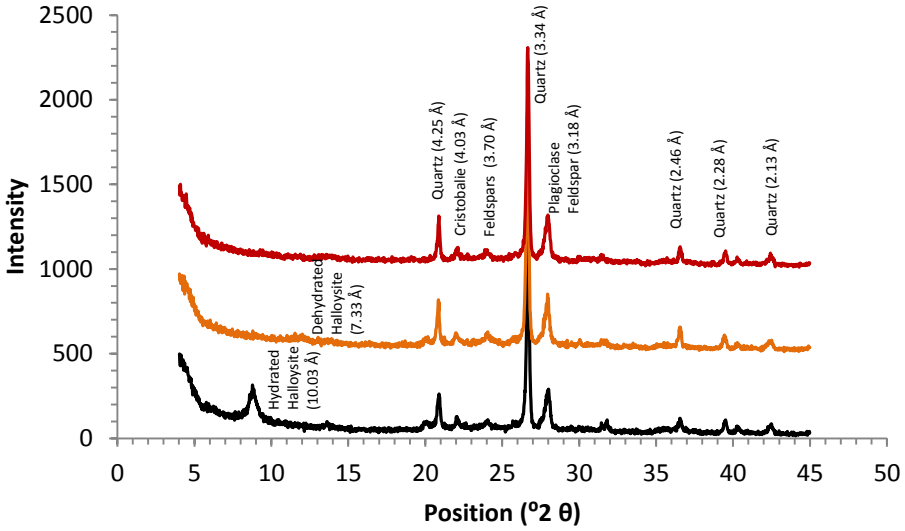

Figure 6.7: TPS1 unheated clay fraction sample diffractogram (black), heated to 110 ^{o}C (orange) and heated to 550 ^{0}C (red). Hydrated halloysite can be seen to peak at ~ 10 Å in the unheated sample, while the 110^{0}C heated sample indicates the dehydrated form of halloysite, where the interlayer water is removed and the peak collapsed to ~ 7 Å. Following 550 ^{0}C heating, the ~ 10 Å peak becomes X-ray amorphous, further confirming halloysite. Note each intensity data point for the 110 ^{0}C heated data set has been offset/increased by 500 points each while the 550 ^{0}C dataset has been offset by 1000 points to differentiate between scans.

6.2.1.3 **Pahoia Peninsula (PS1, PS2)**

The bulk sample analyses from PS1 and PS2 indicated a very similar mineralogical composition to that of both Omokoroa and Te Puna. The bulk sample mineralogies from PS1 and PS2 are summarised in Table 6.4.

Table 6.4: Mineralogy of both the PS1 and PS2 bulk sample scan. All clay, silt and sand size minerals are accounted for in these scans.

Sample	Mineralogy
PS1	Hydrated halloysite, dehydrated halloysite, quartz
PS2	Hydrated halloysite, dehydrated halloysite, quartz, biotite

The bulk sample indicated that halloysite is the dominant clay mineral in both PS1 and PS2, where it occurs in both its hydrated and dehydrated state (Figure 6.8, 6.9). Primary halloysite peaks were observed at ~ 10 Å for both samples and strongly in the 02, 11 band at ~ 4.44 Å. A small reflection with a high scatter at ~ 8 Å was observed in the bulk sample between the hydrated and dehydrated halloysite peak, which likely represented halloysite in a partially dehydrated state (Jock Churchman *pers. comm.* 2012). Reflections for kaolinite were observed in both PS1 and PS2 at the 002 (~ 3.55 Å) peak and the 003 (~ 2.34 Å) peak, but the primary 001 (~ 7 Å) peak was possibly masked by that for dehydrated halloysite. The asymmetric halloysite peak at ~ 4.43 Å suggested that the ~ 7 Å peak was in fact halloysite (Wyatt *et al.* 2010). However, considering the 002 and 003 peaks were present for kaolinite, formamide was added to both bulk samples to reach a definitive conclusion on the possibility of the ~ 7 Å peak being kaolinite (Figure 6.8, 6.9). The addition of formamide expanded the ~ 7 Å peak to ~ 10 Å, confirming that they were indeed dehydrated halloysite. The formamide-treated bulk sample also indicated there were no 002 and 003 peaks for kaolinite. Thus kaolinite is absent from the samples.

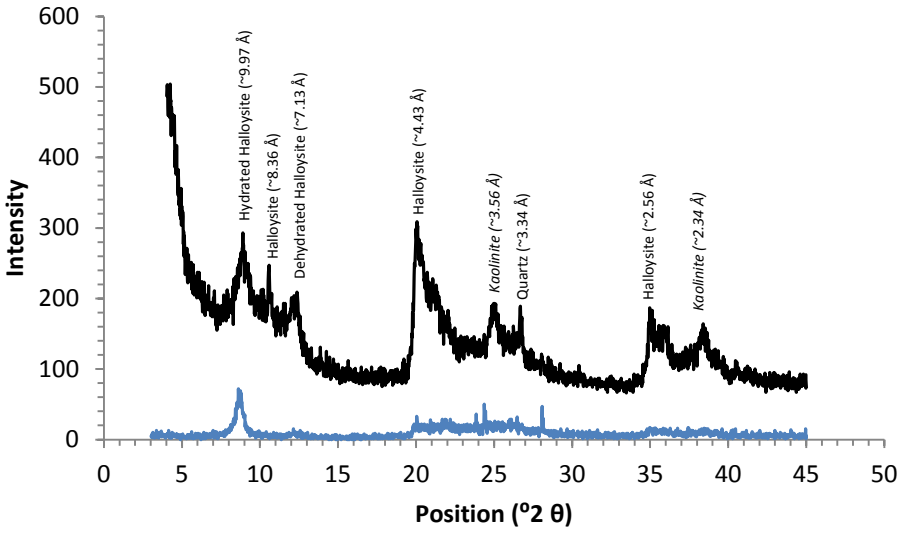

Figure 6.8: Bulk XRD diffractogram for PS1. The pre-formamide sample is represented by the black line while the formamide treated sample is indicated by the blue line. Peak descriptions in italics indicate interpretations before the addition of formamide.

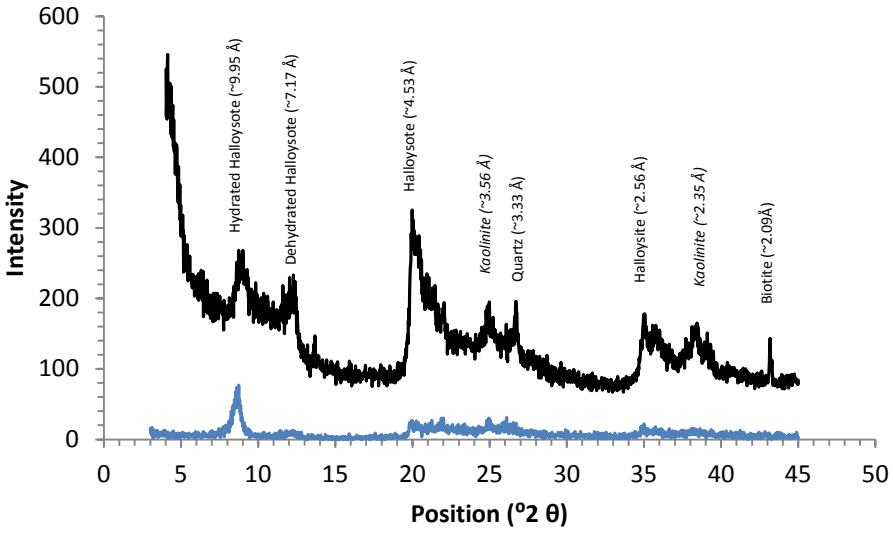

Figure 6.9: Bulk XRD diffractogram for PS1. The pre-formamide sample is represented by the black line while the formamide treated sample is indicated by the blue line. Peak descriptions in italics indicate interpretations before the addition of formamide.

Other minerals observed in the XRD diffractograms included plagioclase feldspar and quartz. PS2 also indicated that biotite was represented in the sample with a peak of 2.09 Å. Biotite has been previously reported in Te Puna Tephra from the Tauranga region (Arthurs 2010). While the ~ 10 Å reflection was observed to be that of the halloysite peak, ~ 10 Å is also the 001 peak for biotite. Graham *et al*. (1989), however, suggested that biotite does not always show a 001 peak when it is in relatively low abundance. Although PS1 did not contain biotite, the amount in PS2 was considered small. Thus the samples remain likely correlatives (as suggested in Chapter 4).

Analysis of the clay fraction indicated that halloysite, both in the hydrated and dehydrated form, were the main clay minerals in samples from both PS1 and PS2 (Table 6.5).

Table 6.5: Clay fraction mineralogical summary for PS1 and PS2 from Pahoia Peninsula. The samples include only minerals of clay size or smaller (< 2 µm).

Sample	Mineralogy
PS1	Hydrated halloysite, dehydrated halloysite, quartz, plagioclase feldspar, cristobalite
PS2	Hydrated halloysite, dehydrated halloysite, quartz, plagioclase feldspar, cristobalite

Kaolinite was not identified by its 002 or 003 peaks by XRD of bulk sample materials. The 001 peak was weakly identified at ~ 7 Å in both PS1 and PS2. However, considering they were attached as a shoulder to the ~ 10 Å peaks, they likely represent dehydrated halloysite ~ 7 Å peaks (Churchman *et al.* 1972; Wyatt 2009). The addition of formamide confirmed the presence of dehydrated halloysite instead of kaolinite because the ~ 7 Å shoulders in both PS1 and PS2 expanded to larger peaks at ~ 10 Å (Figure 6.10). Plagioclase feldspar, quartz and cristobalite were also recognised in the clay fractions.

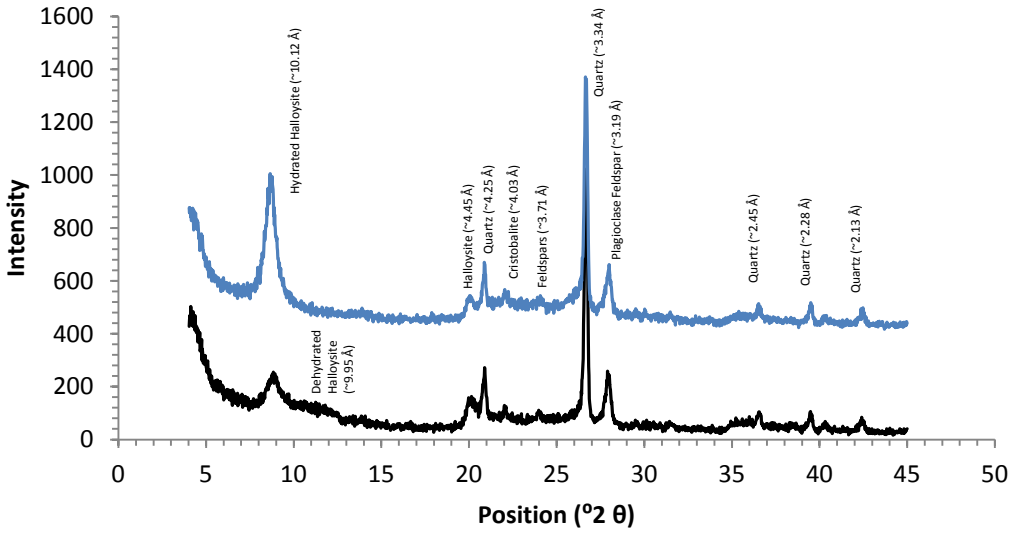

Figure 6.10: PS2 before the addition of formamide (black) and after formamide treatment (blue) for the clay fraction sample. The ~ 7 Å dehydrated halloysite 'shoulder' peak is observed in the pre-formamide scan. Upon the treatment of formamide the peak is seen to expand and shift to ~ 10 Å indicating the ~ 7 Å peak is d halloysite and not kaolinite. Note each intensity data point for the formamide-treated set has been offset/increased by 400 points each.

6.2.1.4 **Tauriko (TS1, TS2, TS3, TS4)**

The non-sensitive Tauriko samples were taken from Te Ranga Ignimbrite rather than the Te Puna Tephra, which was the geological unit sampled at Omokoroa, Te Puna, and Pahoia Peninsula (refer to Chapter 4). Despite this, similar minerals were encountered from the XRD tracings. All four sites were typically the same, with minor variations. Table 6.6 summarises the minerals observed in the bulk sample scans.

Table 6.6: Bulk mineralogy of TS1, TS2, TS3 and TS4. All clay, silt and sand size minerals are accounted for in these scans.

Sample	Mineralogy
TS1	Hydrated halloysite, dehydrated halloysite, feldspars, plagioclase feldspar, cristobalite
TS2	Hydrated halloysite, dehydrated halloysite, feldspars, quartz, cristobalite
TS3	Hydrated halloysite, dehydrated halloysite/kaolinite, plagioclase feldspar, feldspars
TS4	Hydrated halloysite, dehydrated halloysite, quartz, plagioclase feldspar

Halloysite and kaolinite were recognised in the bulk Tauriko samples as the dominant clay minerals present. Relative abundance of the clay minerals was quite low, however, with typically weak peaks arising (Figure 6.11, 6.12). All samples displayed a shoulder between the ~ 10 Å hydrated halloysite peak and the ~ 7 Å dehydrated position, masking the 001 kaolinite peak (Figure 6.11). 003 dehydrated halloysite peaks were observed at the ~ 2.35 Å position in TS1, TS2 and TS4. TS3 displayed a peak for kaolinite at the ~ 4.36 Å position, however the corresponding 001 broad peak of ~ 7.43 Å peak suggested dehydrated halloysite (Joussien *et al.* 2005). Considering the evidence is almost equivocal for both kaolinite and dehydrated halloysite in the bulk fraction, no firm distinction is made. The relative abundance of kaolinite, if any, would be very small nevertheless. Another feature distinguishing the sites was profile depth variation and similarities between the sites. Samples at TS1 and TS2, at ~ 17 m depth, contained more halloysite than the samples at TS3 and TS4, at ~ 23 m depth, which displayed weak halloysite reflections.

Of the non-clay minerals, plagioclase feldspar and quartz were present in the majority of samples. Feldspars were prominently observed in samples from TS1 with several recurring reflections (Figure 6.11). Cristobalite was observed in both TS1 and TS2 at ~ 4.04 Å and ~ 2.8 Å. Quartz was seen to dominate TS2 and TS4 while plagioclase feldspar was particularly abundant in TS3. Figure 6.11 presents the bulk XRD diffractogram for TS1, which was identical for TS2 (excluding the ~ 6 Å feldspar). Figure 6.12 indicates an XRD diffractogram for TS4, which was very similar to TS3, aside from subtle variation in peak intensity. All remaining Tauriko bulk sample XRD diffractograms can be found in Appendix 6.1.

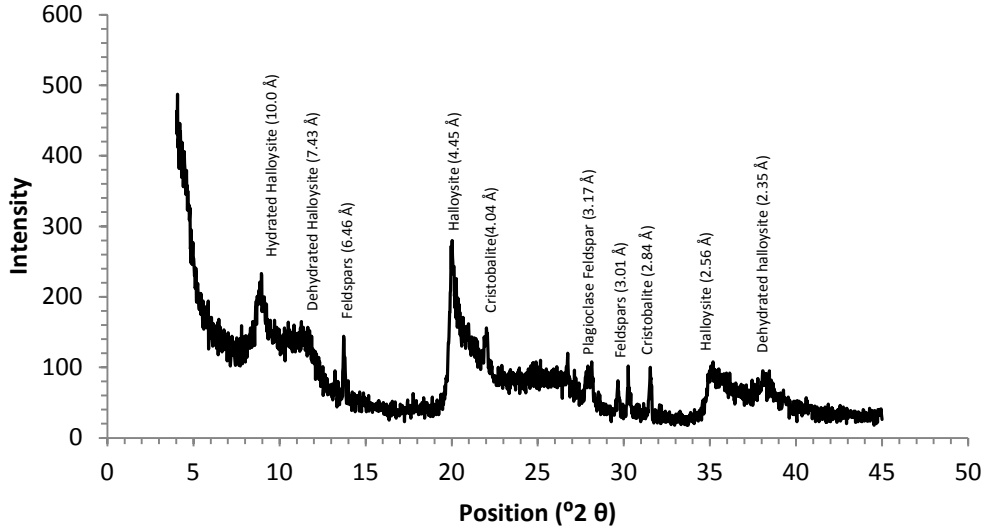

Figure 6.11: Bulk sample XRD diffractogram of TS1. TS2 was identical to TS1 excluding the ~ 6 Å feldspar. All clay, silt and sand size minerals are included in the analysis.

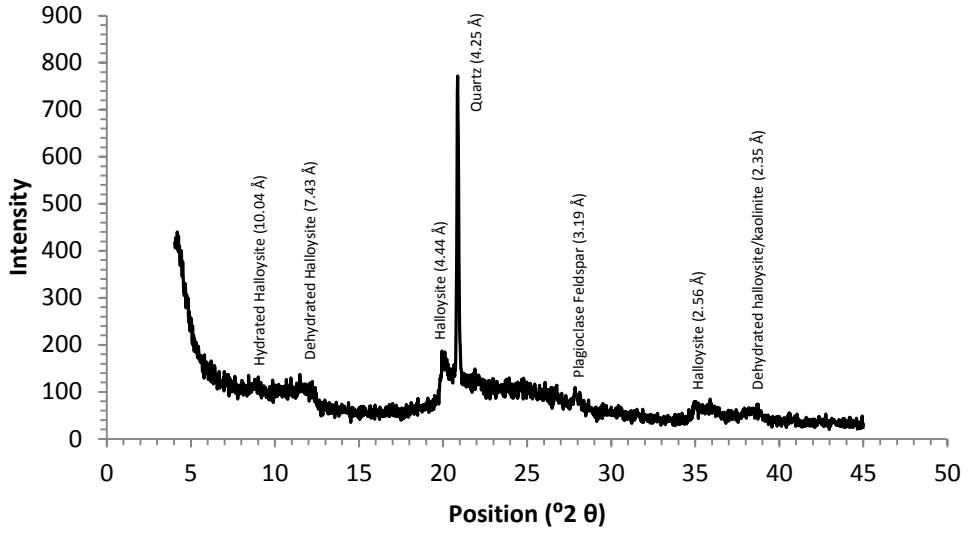

Figure 6.12: Bulk sample XRD diffractogram of TS3. TS4 displayed a very similar diffractogram, but the relative intensities of quartz and plagioclase feldspar subtly different. All clay, silt and sand size minerals are included in the analysis.

The clay fraction samples had similar minerals to those of the bulk samples (Table 6.7).

Table 6.7: Clay fraction mineralogical summary for TS1, TS2, TS3 and TS4 from Tauriko. The samples include only minerals of clay size or smaller (<2μm).

Sample	Mineralogy
TS1	Halloysite, feldspars, quartz, plagioclase feldspar, cristobalite
TS2	Halloysite, dehydrated halloysite , feldspars, quartz, plagioclase feldspar, cristobalite
TS3	Halloysite, dehydrated halloysite , feldspars, quartz, plagioclase feldspar
TS4	Halloysite, dehydrated halloysite, plagioclase feldspar, quartz

As with the bulk samples, halloysite was observed to be the most prominent clay mineral. Upon the application of formamide, the prevalence of kaolinite at ~ 7 Å in all samples was ruled out with each sample peak expanding to ~ 10 Å. Heating the samples to 110 ^{0}C and 550 ^{0}C further indicated that halloysite was present. Heating to 110 ^{0}C shifted the sample peaks to ~ 7 Å, suggesting the interlayer water held in the halloysite minerals was removed, while 550 ^{0}C heating removed the peaks all together. The mineral assemblages between

all sites were very similar. TS1 and TS2 had an identical mineral assemblage, both including cristobalite, while TS3 and TS4 were lacking that mineral.

6.2.1.5 **Rangataua Bay (RS1)**

Mineralogical analysis of samples from Rangataua Bay (RS1) indicated a very similar mineral composition to those from Omokoroa, Te Puna, Pahoia Peninsula and Tauriko (Table 6.8). Furthermore, the only significant difference between the bulk RS1 diffractogram and the clay size diffractogram was the increased intensity of the quartz in the clay size fraction which is likely due to the ceramic plate.

Table 6.8: Bulk and clay size sample mineralogy for RS1 from Rangataua Bay. No mineralogical difference was observed between the bulk sample scan and the clay size scan and so the analyses are given as a combination of results from both scans.

Sample	Mineralogy
RS1	Hydrated halloysite, plagioclase feldspar, quartz

RS1 displayed the most pronounced halloysite reflection from all samples studied. This is somewhat unsurprising given that RS1 had the highest clay content from particle size analysis (Chapter 5 Section 5.4). Both the bulk and clay fraction samples from RS1 showed a slight shoulder between the ~ 10 Å position of halloysite and the ~ 7 Å position, suggesting that a minor amount of dehydrated halloysite was present (Figure 6.13) (Churchman *et al.* 1972). Furthermore, upon the addition of formamide, the halloysite peak intensity increased and the shoulder disappeared, implying that the dehydrated halloysite had been expanded (Figure 6.13).

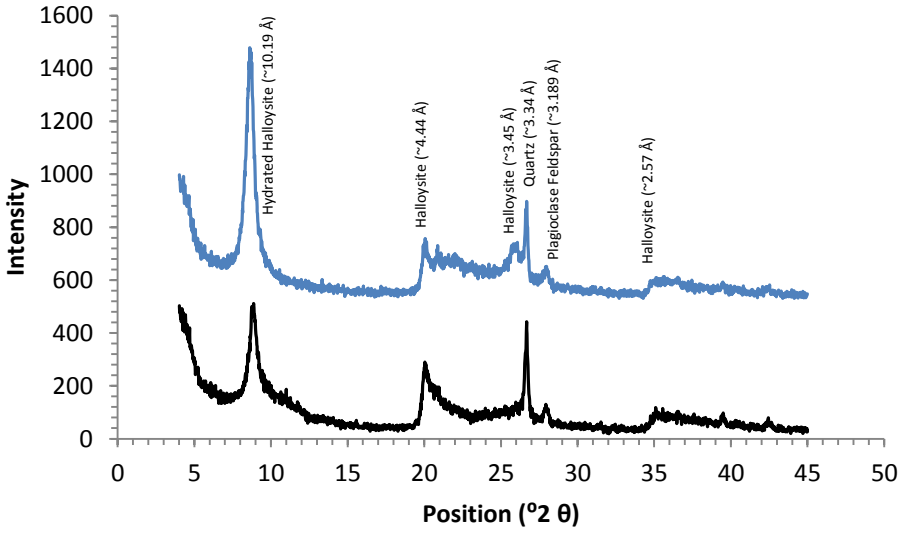

Figure 6.13: RS1 before the addition of formamide (black) and after formamide treatment (blue). The subtle ~ 7 Å dehydrated halloysite 'shoulder' peak is observed in the pre-formamide scan. Following treatment with formamide the peak is seen to expand and shift to ~ 10 Å indicating the ~ 7 Å peak was indeed halloysite and not kaolinite. Note each intensity data point for the formamide data set has been offset by 500 points each to differentiate the scans.

Non-clay minerals indicated that plagioclase feldspar and quartz were present in the clay fraction. Quartz was the second-most abundant mineral in the sample, displaying a pronounced peak at ~ 3.34 Å, while plagioclase feldspar was less pronounced and thus not as abundant.

6.2.1.6 X-ray diffraction summary

X-ray diffraction analysis of all samples indicated that a similar range of clay and non-clay minerals were present. Commonly, halloysite, quartz, plagioclase feldspar and cristobalite were observed. Halloysite was recognised in both its hydrated and dehydrated states, being positively identified following heating and the addition of formamide to the clay fractions. Kaolinite was rarely identified in the bulk fraction of the samples, where it could not be distinguished from dehydrated halloysite. Following the heating and addition of formamide to the samples, kaolinite in the clay fraction was ruled out, suggesting that even if some kaolinite was present in the bulk samples, it was typically in a low abundance.

6.2.2 Scanning electron microscope (SEM) observations

The morphology of clay minerals was investigated by scanning electron microscopy. Considering the main clay types identified in the XRD analyses were kaolin group minerals (halloysite and kaolinite), the morphologies were classified into four known groups: spheres, tubes, plates and books (Joussien *et al.,* 2005). For the SEM analysis, the classic clay size definition (< 2 µm) was not considered the key criterion for classifying between clay and non-clay minerals; rather, the known distinguishing shapes previously reported (Joussien *et al.* 2005; Wyatt 2009). Table 6.9 summarises the clay morphologies observed from SEM analyses of all samples from this study. All original SEM images are presented in Appendix 6.2.

Table 6.9: Clay mineral shapes observed following scanning electron microscopy (SEM). All samples represent morphologies observed in their intact state, with the exception of OLRO* which was already remoulded upon collection. Approximate length sizes of the clay morphologies are presented in parentheses. Gaps indicate such morphologies were not present in the sample

		Clay Morphology			
Location	**Sample**	**Spheres**	**Tubes**	**Plates**	**Books**
Omokoroa	OS1	(~150 nm)	(~400 nm)	(~600 nm)	
	OS2	(~190 nm)	(~350 nm)		
	OLRO*	(~260 nm)	(~100 nm)	(~500 nm)	(~9 µm)
Te Puna	TPS1	(~200 nm)	(~200 nm)	(~1750 nm)	
Pahoia Peninsula	PS1	(~200 nm)	(~700 nm)	(~30 µm)	(~1500 µm)
	PS2	(~200 nm)	(~450 nm)	(~2500 nm)	(~15 µm)
Tauriko	TS1	(~620 nm)	(~600 nm)		
	TS2	(~800 nm)	(~900 nm)		
	TS3	(~600 nm)			
	TS4	(~550 nm)			(~12 µm)
Rangataua Bay	RS1	(~600 nm)	(~750 nm)		

Spheroidal shapes were the most commonly observed formation. All samples, with the exception of TS2, had sphere morphologies present (Table 6.10). Typically, tubes are the most common form of halloysite, with spheres the next most common (Joussein *et al.* 2005). Alteration of halloysite is not common in morphology formation, as opposed to weathering by dissolution and

precipitation, however, when alteration does take place, this (tubes to spheres) is the common sequence (Delvaux *et al.* 1992; Papoulis *et al.* 2004). The following section describes the clay morphologies observed in the order of possible alteration and then finally book type morphologies.

6.2.2.1 **Spheroidal clay morphologies**

Spheroidal clays are typically associated with halloysite and allophanic minerals (Parfitt 2009; Churchman and Lowe 2012). Halloysite spheres are particularly common in weathered volcanic ashes and pumices (Parham 1969; Nagasawa and Miyasaki 1976; Tazaki 1979; Sudo *et al.* 1981; Churchman and Theng 1984; Ward and Roberts 1990). Distinguishing between halloysite and allophane is important considering their relative association with sensitivity, given that previous studies have aligned sensitivity with allophane (and imogolite) formation (Jacquet 1990), while others have promoted the importance of halloysite (Smalley *et al.* 1980; Keam 2008; Wyatt 2009; Arthurs 2010). Allophane was not expected in the soil samples because Wyatt (2009) had previously reported low or zero levels after acid-oxalate analysis of samples from the Tauranga region. Furthermore, van der Gaast *et al.* (1985) determined the diameter of allophane spherules to be approximately 4.0 nm. My SEM analysis indicated that all spherules were much larger than 4.0 nm making it unlikely that the spheres were allophanic. Halloysite spheres on the other hand have previously been widely reported widely in New Zealand and more locally in the Waikato-Bay of Plenty areas (Salter 1979; Smalley et al. 1980; Lowe and Percival 1993; Wyatt 2009; Arthurs 2010). Furthermore, spheroidal halloysite formation has been previously reported to appear in weathering products of volcanic glass, due to the fast dissolution rate and recrystallization from saturated environments (Adamo *et al.* 2001; Singer *et al.* 2004; Churchman and Lowe 2012). Based on the sample environments and known halloysite characteristics, it was concluded that the spherule particles were, as suggested by XRD, halloysite.

Spherical particles from this study ranged in size from 150 – 600 nm. Previously, spheroidal halloysite particles from New Zealand have been reported with diameters between 100 – 800 nm (Salter 1979; Smalley *et al.* 1980; Kirkman 1981; Shepherd 1984; Wyatt 2009), suggesting that the size of the spherical

particles found in this study are not uncommon. Spheroidal particles from Omokoroa were typically regular shaped, and consistently 150 – 260 nm in size (Figure 6.14). Spheres from the Te Puna sample were also very similar to those from Omokoroa, where ~ 200 nm sized particles were observed. Spherical particles from Pahoia Peninsula were also similar in size (~ 200 nm), but they were not as regularly shaped as those from Omokoroa or Te Puna (Figure 6.15).

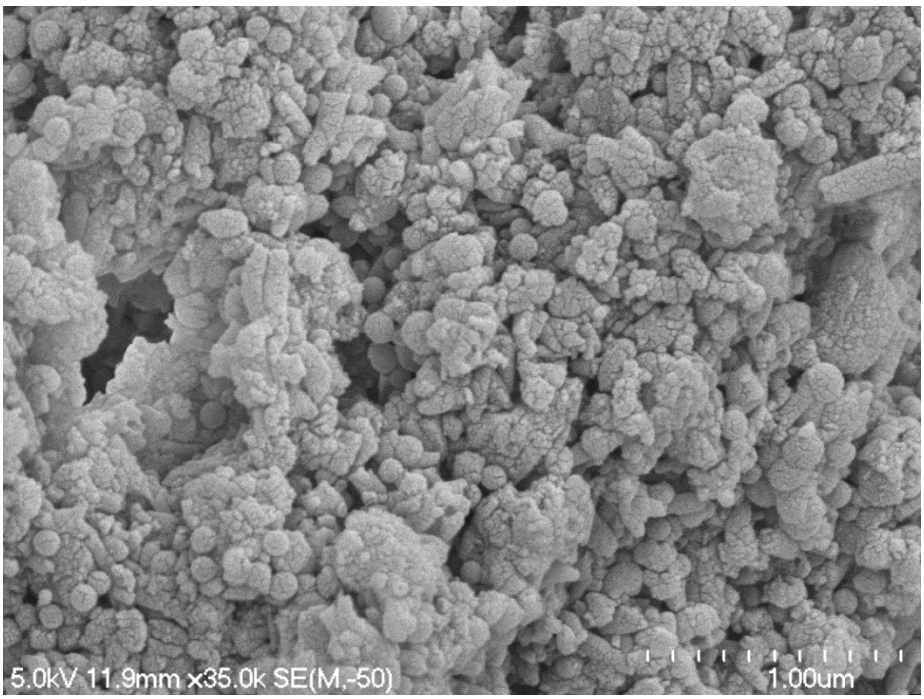

Figure 6.14: Assemblage of regularly shaped spherical particles from OS1. All spheres are approximately 150 – 200 nm in diameter.

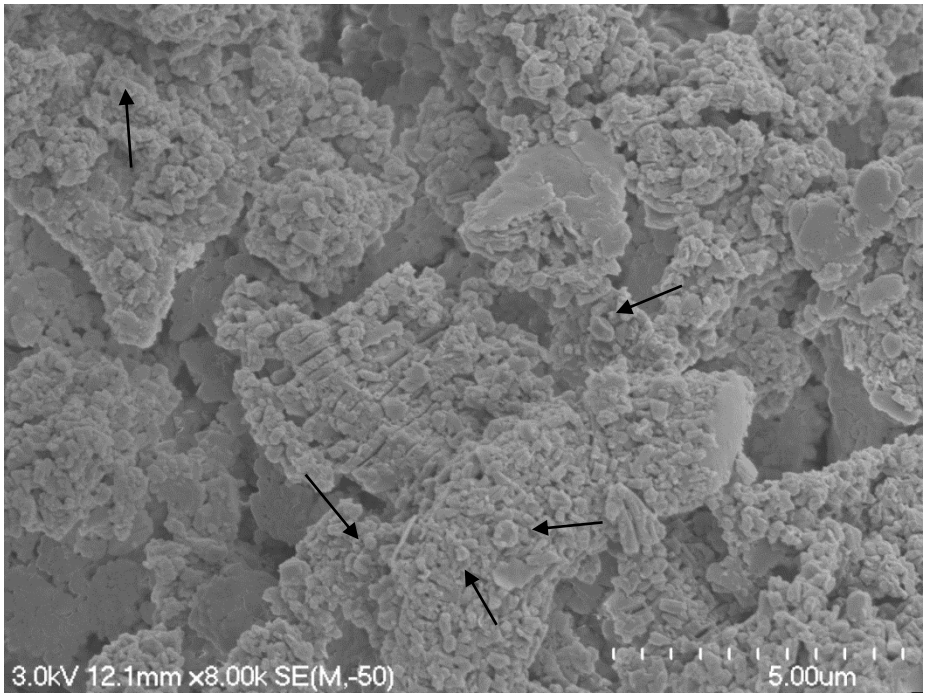

Figure 6.15: Irregularly shaped, yet similarly sized spherical particles from PS1 (indicated by the arrows). All spheres are approximately 200 nm in diameter.

For samples from Rangataua Bay and Tauriko, spherical particles were also observed. However, these displayed distinct differences in size and shape compared to those from Omokoroa, Te Puna and Pahoia Peninsula. The spheres were typically larger at ~ 550 – 800 nm in diameter (Figure 6.16). Furthermore, tubes could be seen to be emerging from the sides of the spheres (and tightly interacted with the spheres), potentially indicating the neo-formation of tubes as a subsequent stage of weathering reforms the clay particles.

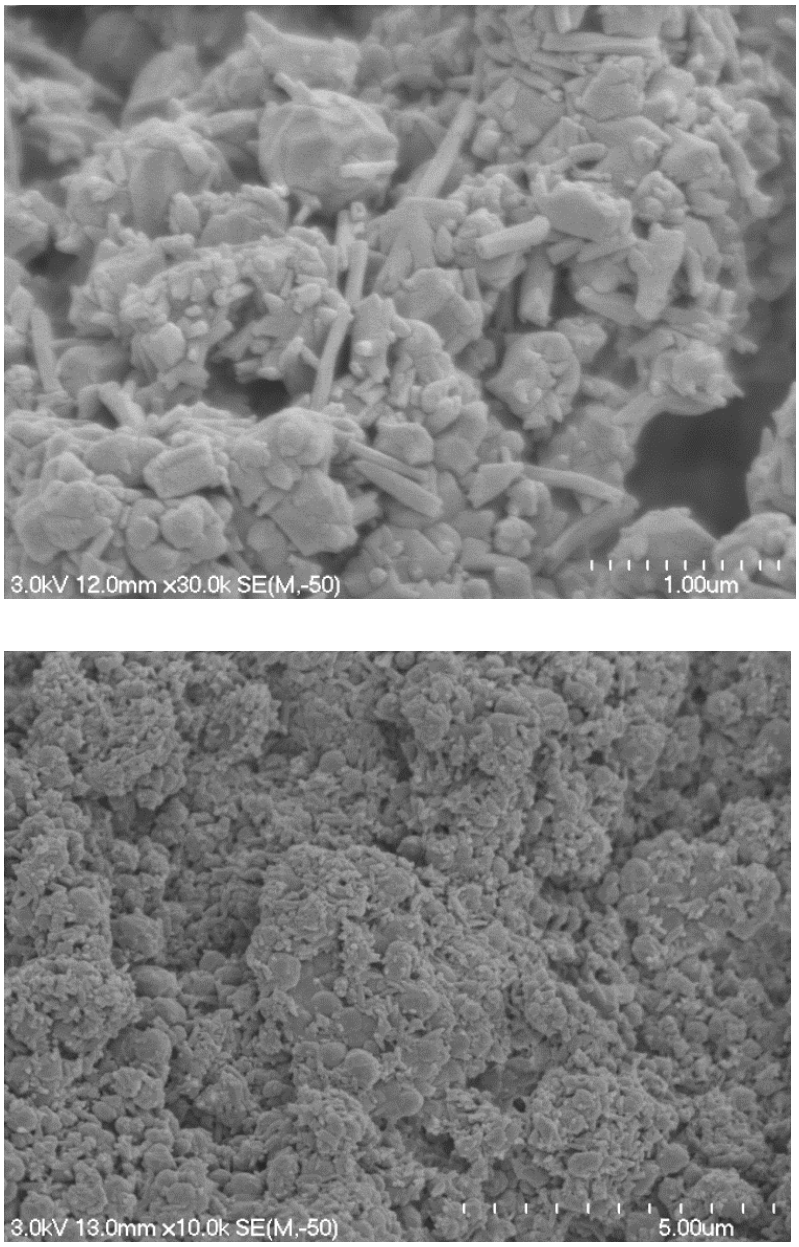

Figure 6.16: Large spheres from Tauriko (TS2) (top) and Rangataua Bay (RS1) (bottom). Similar sphere morphologies can be seen between the two samples. Tubes also appear to be "breaking out" of the samples, indicating the possible formation of the tubes after the spheres had developed.

6.2.2.2 **Tubular Clay Morphologies**

Tubular halloysite was also common (Table 6.10). Samples from all sites except TS3 and TS4 displayed tubular halloysite morphologies. Previous authors have indicated that tubes are the most common and recognisable halloysite clay morphology type (Joussien *et al.* 2005). Tubes from intact Omokoroa, Te Puna and Pahoia Peninsula samples were typically short and stubby, with sizes ranging between 200 – 900 nm in length, and 100 – 200 nm in diameter. Halloysite tubes

can vary in size from 0.02 µm to > 30 µm, with typical diameters between < 0.05 – 0.2 µm (Dixon and McKee 1974; Joussien *et al*. 2005), indicating that while the tubes observed in this study are not unique they do conform to the lower end of the length size scale. Interestingly the tubes were relatively wide. The widest tubes were observed in samples from OS1 and OS2 at ~ 150 nm. Furthermore, tubular morphologies were most abundant in OS1 and OS2, whereas PS1 and PS2 indicated relatively few tubes. The only naturally remoulded sample of OLRO displayed very short tubes, which had possibly been broken upon remoulding (Figure 6.17). Their hollow nature and barrel shape separated them from spheroidal morphologies.

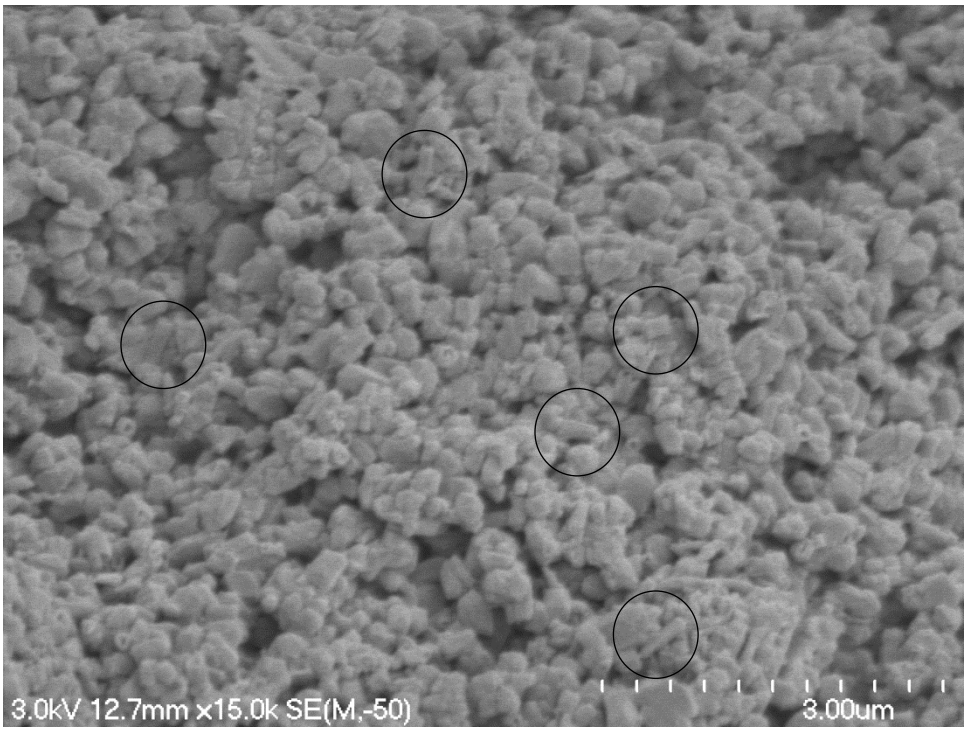

Figure 6.17: Naturally remoulded sample of OLRO. Very short tubes, which were likely derived from breakdown of larger tubes, are identified in the circles.

Samples from Tauriko and Rangataua Bay conversely tended to display long (~ 900 nm) and thin tubular morphologies in abundance (Figure 6.18). The tubes were generally tightly intermixed with the large spheres, and were aggregated together in a matted layering structure, similar to the felting described by Papoulis *et al.* (2004). No short, wide diameter tubes were observed in the Tauriko samples, however, a small portion of the tubular particles (which were aggregated with spheres) from RS1 were relatively short (~ 400 nm).

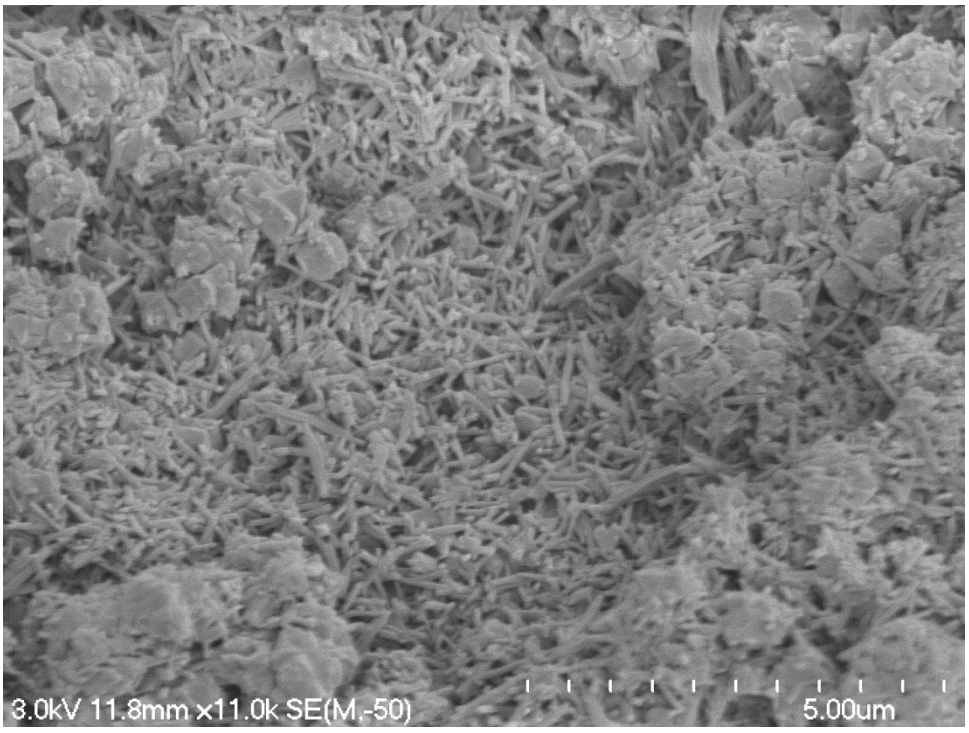

Figure 6.18: Tubular halloysite morphologies from TS2. The tubes can be seen to be ~ 900 nm in length.

6.2.2.3 **Plate Clay Morphologies**

Plate morphologies were most prominent in TPS1 (Figure 6.19), followed by PS1 and PS2, while they were least common in OS2 and the Tauriko and Rangataua Bay sites. Plate sizes ranged from ~ 500 nm width from the OLRO sample to ~ 30 µm width at Pahoia Peninsula. Plate sizes were difficult to gauge, however, as the boundaries were somewhat distorted by the positions of other overlapping plates. Notwithstanding this, the plates were still clearly identifiable from their thin and flat nature. The plates were mostly irregularly shaped and did not appear to display any particular type of ordering or sorting.

Plate clay morphologies are typically rare for halloysite formations. Important is the addition of Fe within the halloysite unit cell to account for the mismatch of the Si to Al sheets (see Chapter 2). Halloysite plates have, however, been recognised in weathered volcanic ash from the Tauranga region in previous studies (Wyatt 2009; Arthurs 2010), which are typically observed in small irregular shapes (Wyatt 2009) as observed in this study.

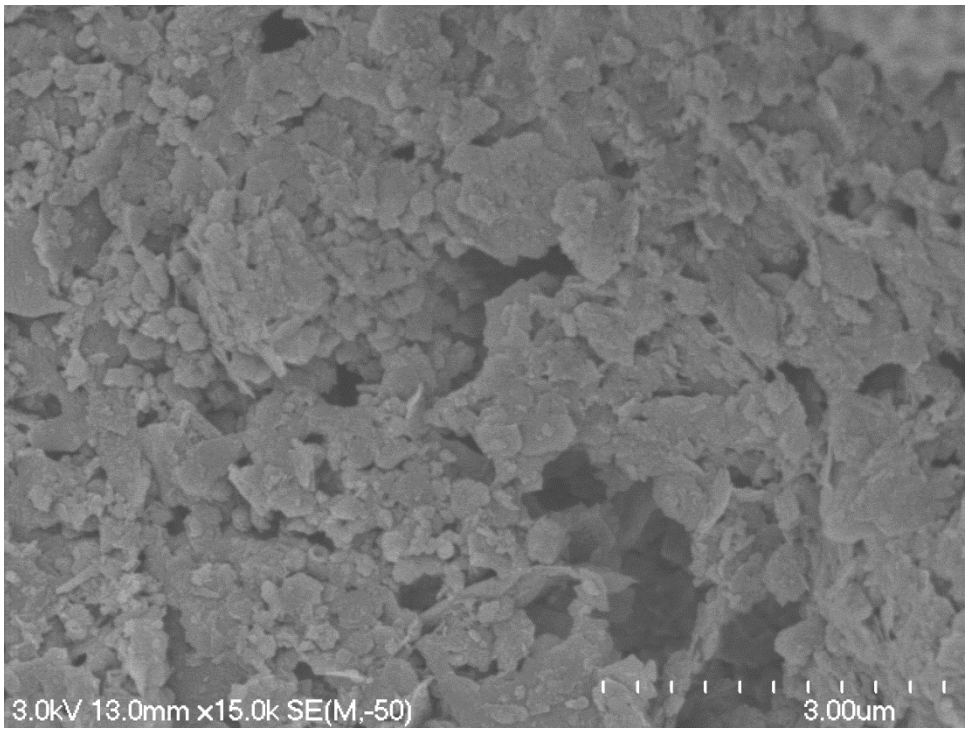

Figure 6.19: Flat plate morphologies from TPS1. The plates can be seen to dominate the structure, with some spheres and tubes also present.

6.2.2.4 **Book Clay Morphologies**

Vermiform or 'book' morphologies were the least common clay mineral observed. Books were only observed in 4 of the 11 samples analysed (OLRO, TPS1, PS1, PS2), but in those samples, they were commonly present. Books are stacked aggregations of plate morphologies which are typical forms of kaolinite clays (Jeong 1998). Kaolinite books have been reported to form from the weathering of mica, feldspar weathering or the weathering conversion of halloysite tubes to kaolinite plates (Keller 1977; Banfield and Eggleton 1988; Jeong 1998).

Book size varied between samples. OLRO indicated book platelet sizes of approximately 6 – 10 µm in length. Often the books were partially "submerged" at one end, meaning that defining size boundaries were difficult. OLRO books were always partially delaminated, with discernible gaps between the plates. Platelet cross dimensional size was typically 1.5 – 3 µm. Small spheres and very short tubes (~ 350 nm) were observed within some of the delaminated plates (Figure 6.20). The books from OLRO were determined to be halloysite on the basis of XRD of the clay fraction. XRD indicated that only halloysite was present, with no

kaolinite (because the ~ 7 Å shoulder disappeared following heating to 110^0 C). Halloysite has previously been reported in book type morphologies from Tauriko, Tauranga (Wyatt 2009). This identification at Omokoroa in naturally remoulded sensitive soil material is the first for the site.

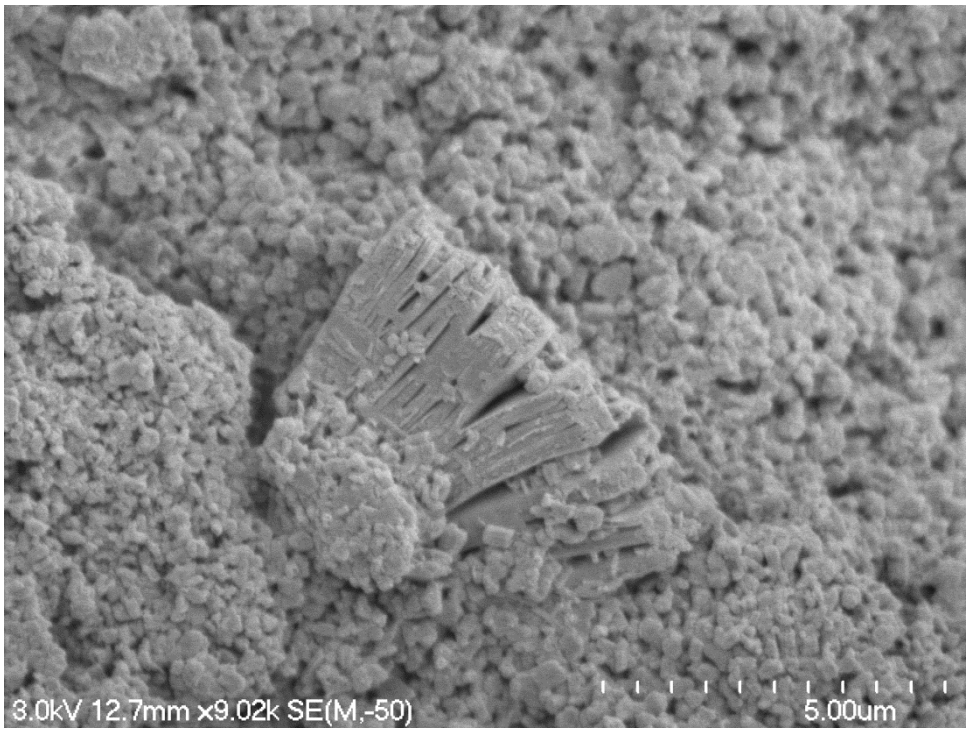

Figure 6.20: Halloysite book from the naturally remoulded sensitive soil of OLRO. Partial delamination between plates can be seen along with some spherical particles within the gaps.

Book vermiforms from Pahoia Peninsula displayed much larger, silt to sand size, forms (Figure 6.21, 6.22, 6.23). The larger book sizes were predominantly found in PS1, but some were also found in PS2. The large books of PS1 and PS2 ranged in size from ~ 15 µm to ~ 1.5 mm in length. PS2 generally contained a multitude of smaller books, of approximately ~ 2 µm width, and lengths of ~ 7 to ~ 9 µm (Figure 6.24). All of the book sizes present in both PS1 and PS2 were larger than the classic clay size definition of particle sizes smaller than 2 µm. This finding (of extremely large books) could mean that such books dropped out of suspension during the sedimentation process in preparing the XRD slides (see Chapter 3 Section 3.6.1) and so their abundance would be underestimated. The XRD of the clay fraction only was therefore insufficiently comprehensive, and so bulk XRD analysis was examined instead. The bulk fraction indicated that while a primary 001 peak of ~ 7 Å was present, the addition

of formamide resulted in the peak expanding to ~ 10 Å and hence showing the exceptionally large books to be halloysite (see Section 6.2.1.1.3).

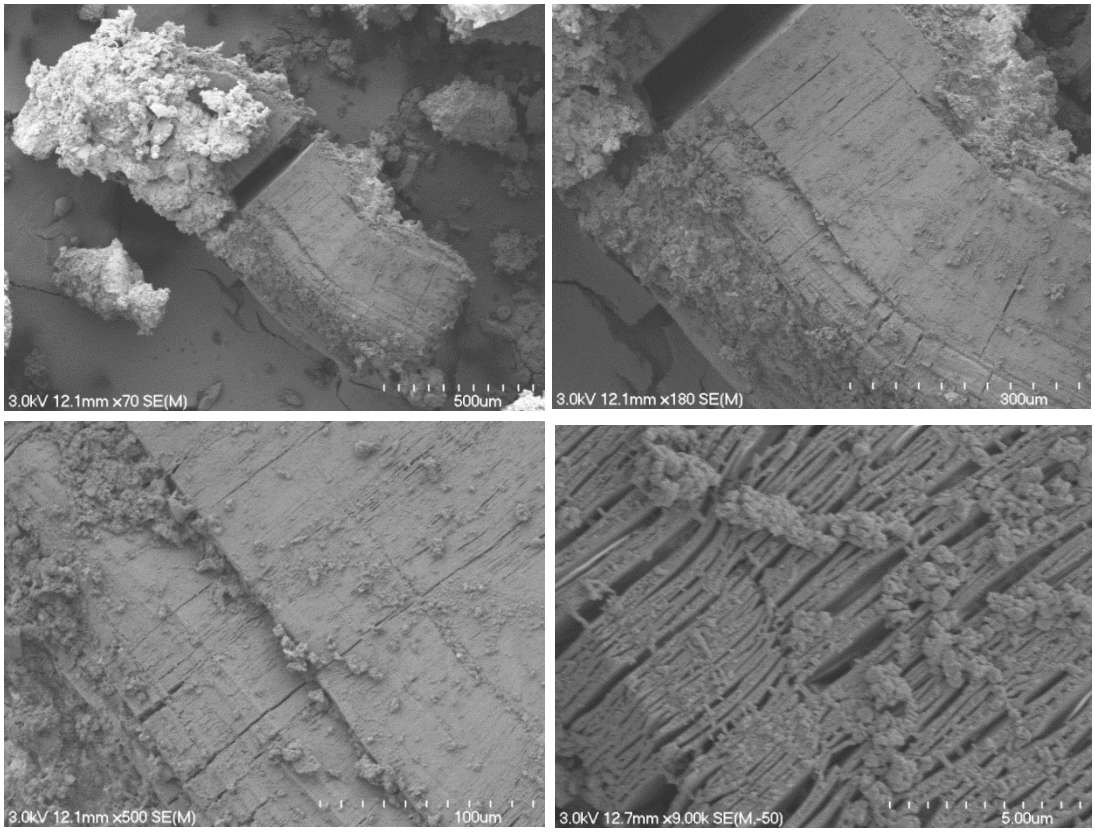

Figure 6.21: Large halloysite book material from PS1. The book is ~ 1.5 mm in length and can be clearly seen to be comprised of multiple thin plates or 'leaves'.

Figure 6.22: Large halloysite book from PS1.

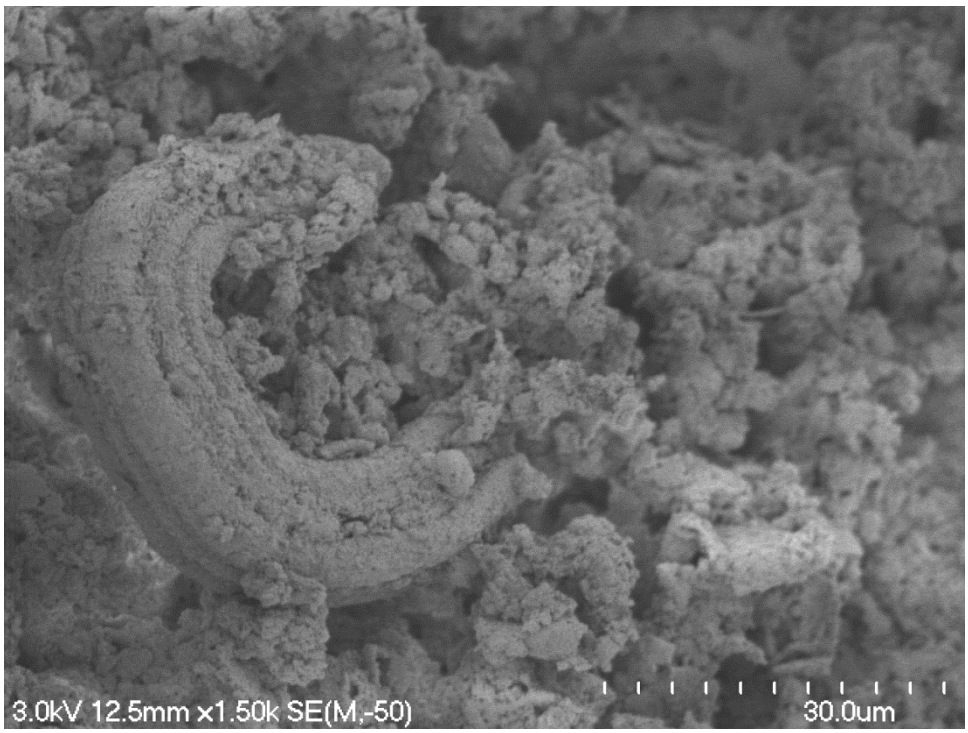

Figure 6.23: Large, highly curved halloysite book from PS1.

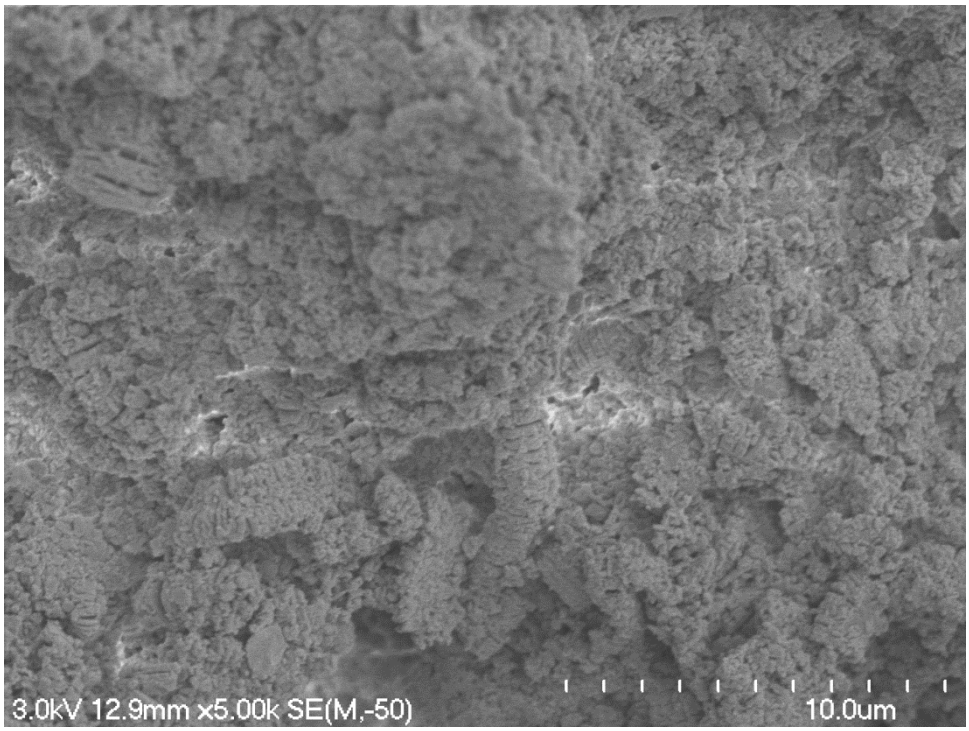

Figure 6.24: Multiple halloysite books from PS2. The books do not appear to be oriented in any specific way. Each book indicates some delamination between plates.

Energy dispersive X-ray (EDX) analysis was undertaken on the very large book materials from PS1 to characterise the clays and to identify the elements of the structures (Table 6.10). Considering the books were so large they provided good surface areas for analysis, promoting the reliability of the results. To further decrease error associated with the EDX analysis, 7 books were analysed from PS1. Important oxides essential for the identification of kaolin group minerals are the proportions of Al_2O_3, SiO_2 and Fe_2O_3 (Joussien *et al.* 2005). Other elements detected included Cl and Na, but these were in very low concentrations.

Table 6.10: Energy dispersive X-ray (EDX) analysis of the large books found in PS1.

	Book							
Compound	**1 (%)**	**2 (%)**	**3 (%)**	**4 (%)**	**5 (%)**	**6 (%)**	**7 (%)**	**Mean (%)**
Al_2O_3	37.01	29.09	13.26	25.95	21.59	17.04	26.05	**24.28 ± 3.21**
SiO_2	48.51	38.18	16.15	33.88	28.09	19.83	33.30	**31.13 ± 4.49**
Fe_2O_3	11.84	3.70	2.46	3.35	3.46	1.86	3.80	**4.35 ± 1.38**

The EDX analysis further confirmed the large books were indeed kaolin group minerals on the basis that the Si:Al ratio was approximately 1:1 which is

characteristic of kaolin material. Also interesting was the significant iron (Fe_2O_3) content. Iron content is suggested to be important for the morphology of halloysite clays (Joussien *et al*. 2005). High iron content has previously been attributed to halloysite in plate form (~ 4 wt. % - see Chapter 2), while tubes and sphere morphologies typically have low Fe contents (Joussien *et al*. 2005). Iron contents in the large books observed in PS1 indicated a mean value of 4.35% consistent with plate morphologies presented by Joussien *et al*. (2005). Two books, however, indicated relatively low iron content (Book 3, 6), indicating that iron concentration is not necessarily consistent across the samples, and the relative size of the book is not dictated by the iron, but rather just to facilitate the shape of the halloysite. Furthermore, it suggests that relatively low iron contents can still produce plate/book halloysite morphologies. Nevertheless, the presence of the significant iron content is also consistent with halloysite books found by Wyatt (2009), who showed book morphologies in his study to have a mean Fe_2O_3 content of 5.2%.

Accounting for both the XRD and EDX results, it appears conclusive that the books observed are indeed halloysite. Although large kaolinite books have been recognised before (Salter 1979; Shepherd 1984; Papoulis *et al.* 2004), halloysite books of this very large size (up to coarse sand, ~ 1.5 mm) have not previously been reported within international literature.

6.2.3 **Other materials**

Non-clay constituents often made up significant portions of the samples. Volcanic glass was most commonly observed (Figure 6.25). Each sample displayed some glass fragments, which ranged from ~ 20 µm to ~ 420 µm in length. Glass particles from all samples were easily identifiable from the bubble-wall (cuspate) and platy or vesicular morphologies (e.g. Lowe 2011). However, in many cases clay minerals blanketed the samples, suggesting that much more glass was potentially hidden below (Figure 6.26).The aggregation and close association of clay materials on the glass was not surprising, given that the weathering of glass enables spheroidal halloysite to form (Adamo *et al.* 2001). Figure 6.27 appears to indicate the neo-formation of small spheres from the weathering of glass within the spherical hollows. From the glass abundance which could be

distinguished, the most pronounced quantities were from the sites at Tauriko, where glass structures were frequently observed.

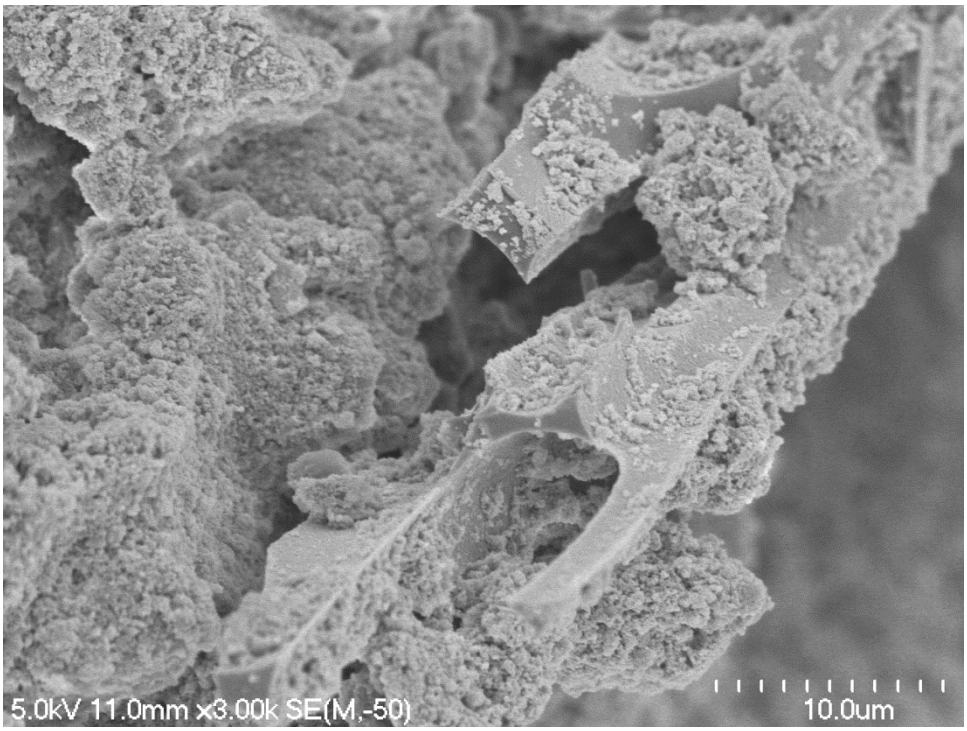

Figure 6.25: Long glass shard protruding from OS2.

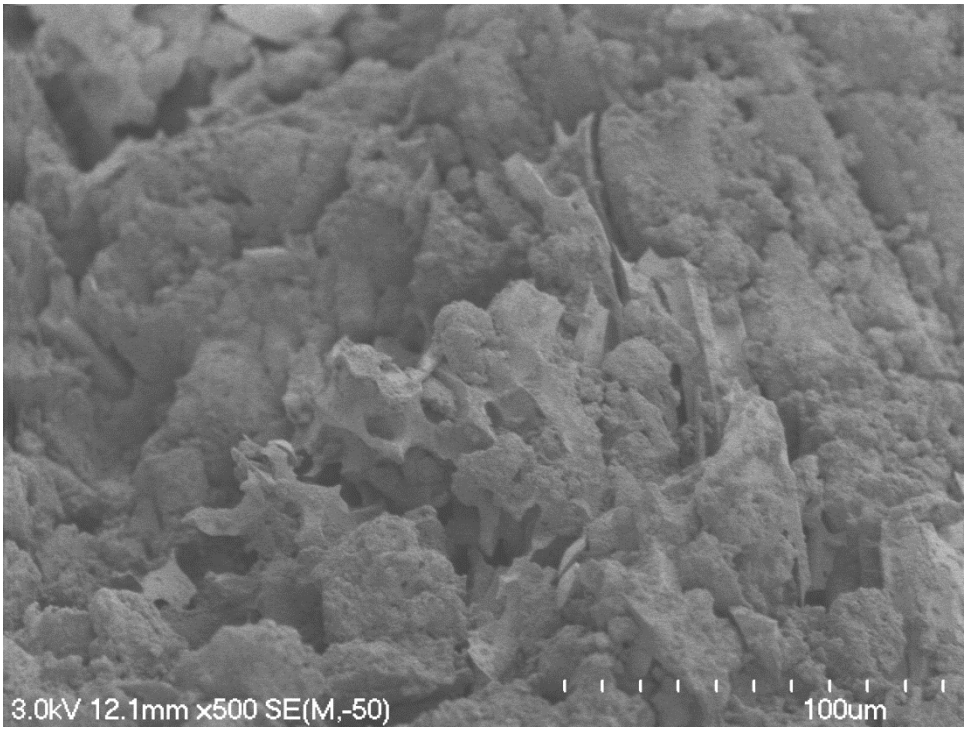

Figure 6.26: Large vesicular glass fragment from TPS1. Note that the glass shard is largely buried within the clay matrix which suggests it could be much bigger than can be seen.

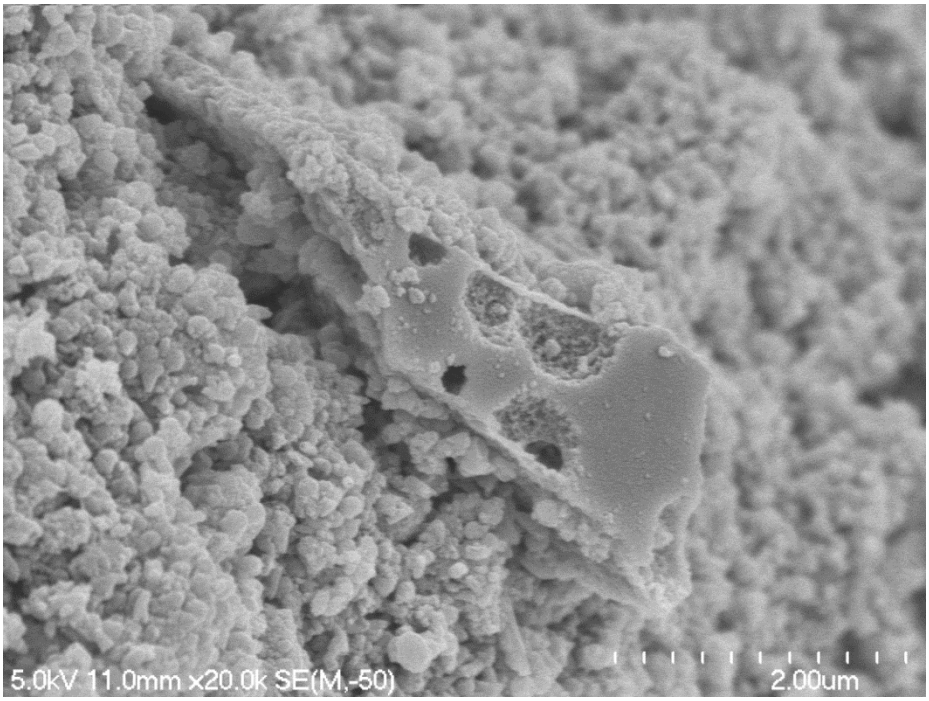

Figure 6.27: Glass fragment from OS2. Spherical particles, presumably halloysite, appear to be precipitating in the vesicles (hollows) which have been enlarged by dissolution processes (see Churchman and Lowe 2012).

Plagioclase feldspars were indicated in the XRD diffractograms to be continually present throughout the majority of samples. Plagioclase feldspar was also identified through SEM analysis (Figure 6.28). Feldspars were positively identified in the electron micrographs by their cleavage planes and big block-like shape. Plagioclase feldspars were generally large at ~ 1.5 mm in length and ~ 0.6 mm wide. Clay minerals also often coated the feldspars.

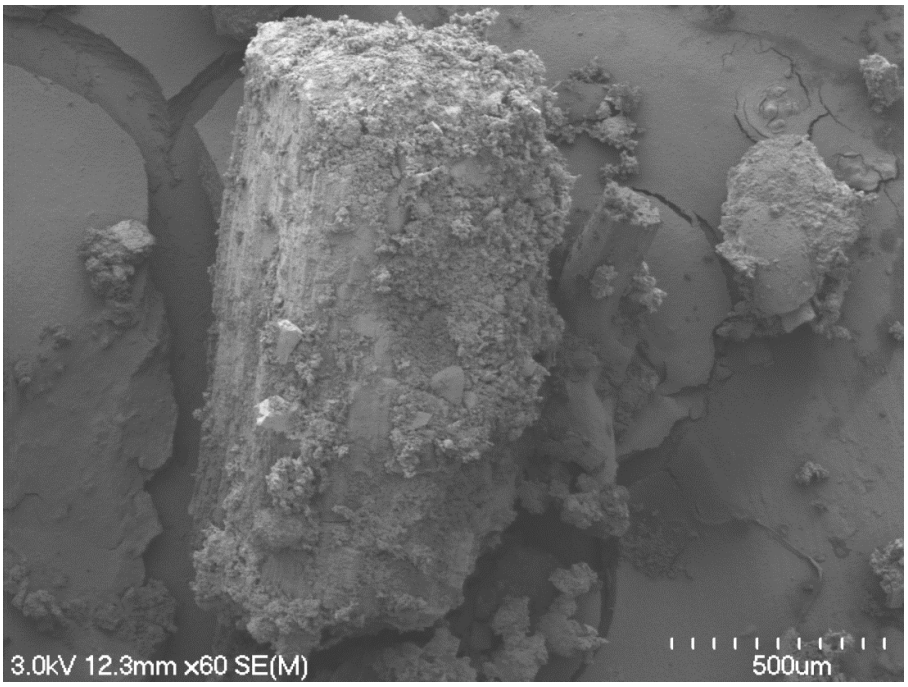

Figure 6.28: Plagioclase feldspar from PS1. Parallel cleavage planes are clearly discernible along the long axis (top to bottom) of the particle.

Biotite was recognised by XRD only in PS2. However, biotite was identified by SEM in OLRO, where it was characterised by its distinguishing hexagonal shape (Figure 6.29). The biotite displayed uniform stacking as laminar aggregates and displayed excellent basal cleavage which is typical in biotite (Bishop *et al.* 1999). The mineral was quite large at ~ 200 µm in diameter.

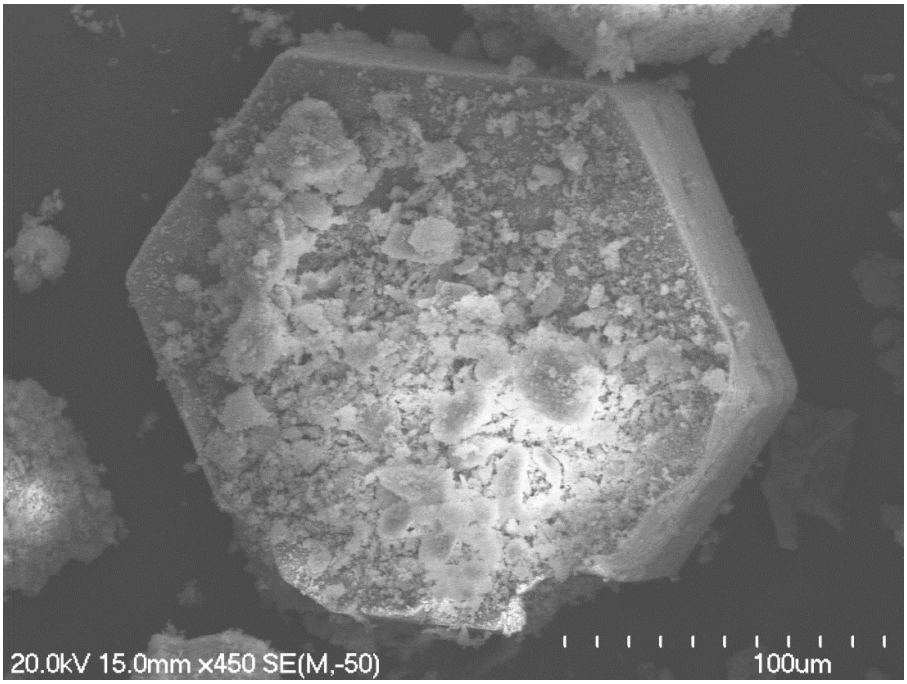

Figure 6.29: Large hexagonal grain, presumed to be biotite, from OLRO.

Interestingly, a diatom frustule was observed in sensitive material from Omokoroa (Figure 6.30). It was small, ~ 2.5 µm in width and ~ 1.5 µm in length, and appeared weathered. The diatom is important as it further indicated that the sensitive material at Omokoroa was deposited and reworked in a lacustrine environment as previously speculated (Briggs *et al*. 1996; Keam 2008; Arthurs 2010). Diatoms were, however, very sparse with only one found in OS1.

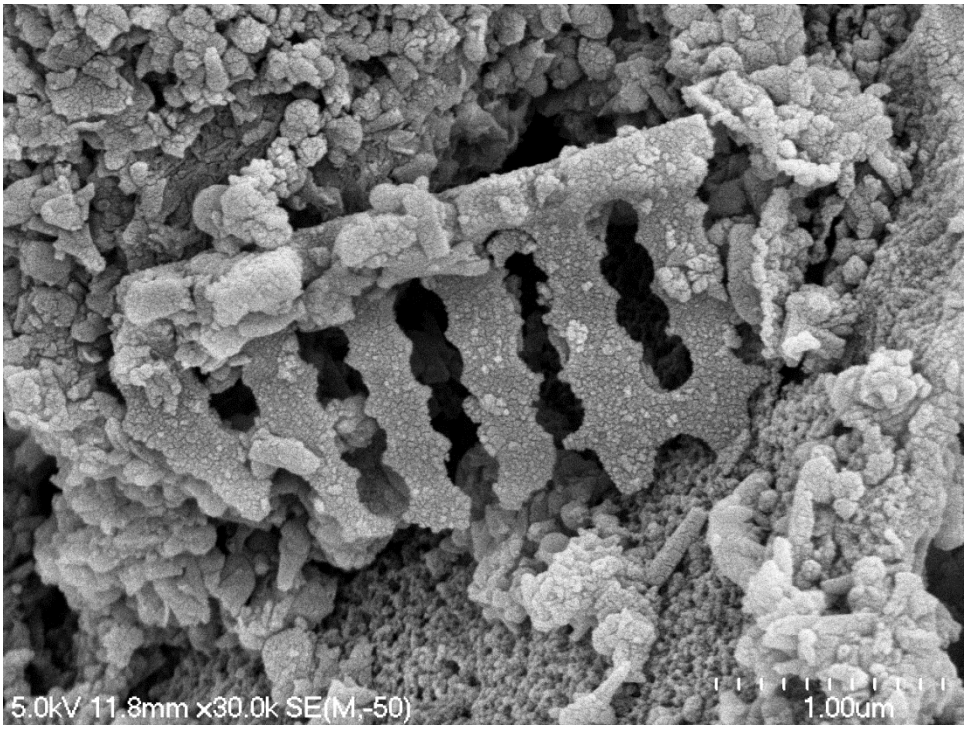

Figure 6.30: Diatom observed in OS1.

6.3 **Microstructure**

Microstructure refers to the combined properties of a soil fabric and interparticle forces (Mitchell and Soga 2005). Soil fabric, in this context, is the geometrical arrangement of particles, particle groups and pore spaces in a particular soil (soil is referred to here in the engineering sense rather than pedological sense) (Grabowska-Olszewska *et al.* 1984). The microstructural constitution of soil materials is critical to understanding their mechanical behaviour (Sergeyev *et al.* 1980; Selby 1993) and can be undertaken by SEM analysis. Considering the complex behaviour between the peak/intact to remoulded state for sensitive soils, it is imperative to understand the microstructure to characterise such behaviour and why it occurs.

6.3.1 **Classification scheme**

The microstructural classification of soils has previously been divided into sedimentary derived and pyroclastic derived materials. The sedimentary basis for microstructural classification for clay, silt and sand materials has been used both in New Zealand and internationally, establishing it as a widely employed scheme

(Collins and McGown 1974; Sergeyev *et al.*1980; Grabowska-Olszewska *et al.* 1984; Huppert 1988; Selby 1993). These sedimentary structural classifications are based around the initial workings of Terzaghi (1925) and Casagrande (1932) who coined the terms honeycomb and matrix clay, respectively, to describe interactions between clay particles. Lambe (1953) pressed the importance of electrochemical environments in the development of face-to-face, edge-to-edge, and edge-to-face connections between clay minerals whereas Collins and McGown (1974) proposed the identification of clay minerals 'assembling' to form connectors, aggregations or particle matrices between larger silt and sand grains. 'Connectors' are classified as assemblages that have formed between silt and sand grains, which often vary in size, whereas 'aggregations' are assemblages which effectively act as individual units within a soil microfabric. 'Particle matrices' are defined as assemblages that form the background microfabric that can act as a binder to other grains within the microfabric (Figure 6.31).

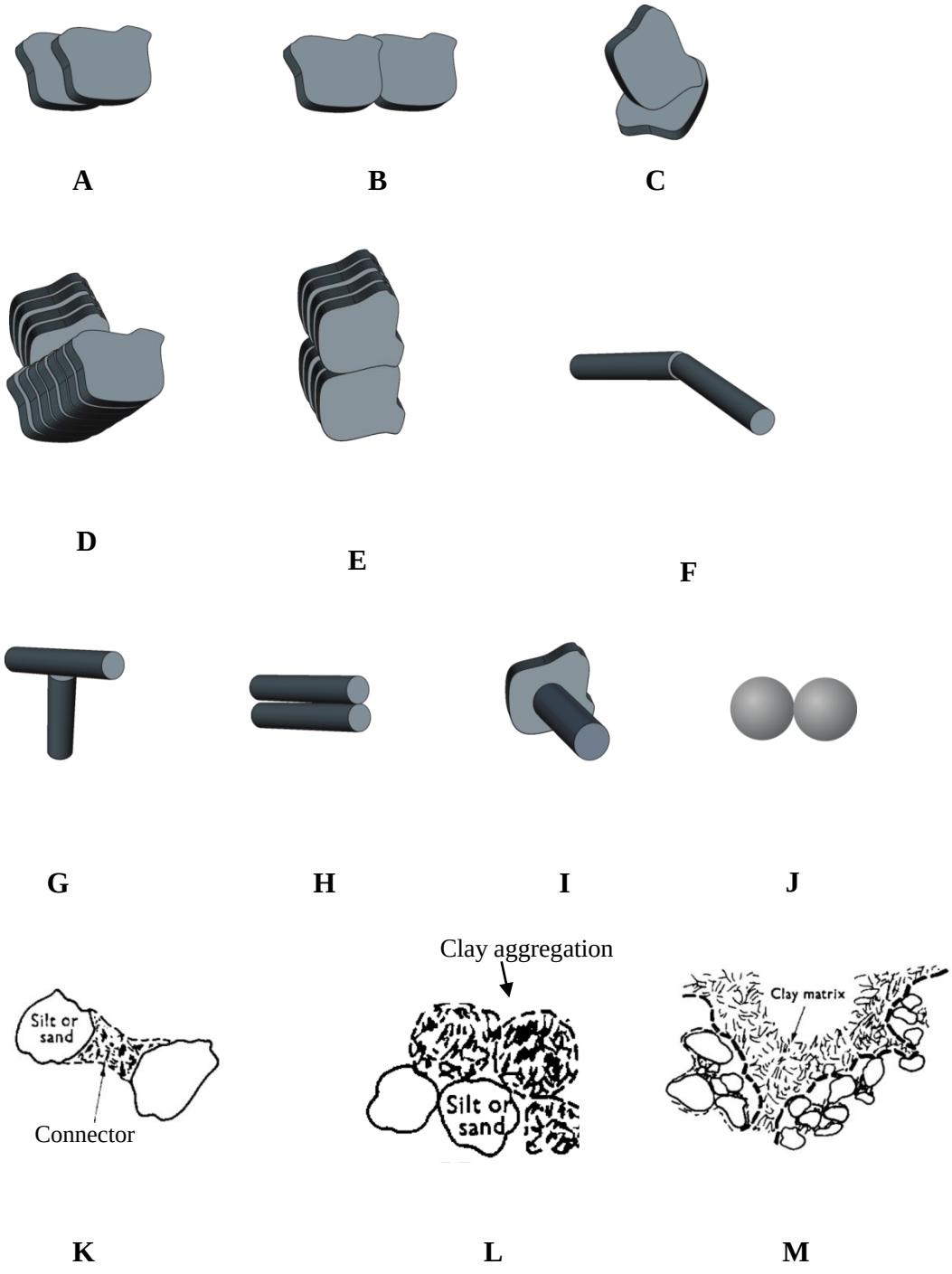

Figure 6.31: Individual clay mineral interactions identified by Lambe (1953) and particle assemblages characterised by Collins and McGown (1974). (A) face to face plate interaction, (B) edge to edge plate interaction, (C) face to edge plate interaction, (D) face to edge book interaction, (E) edge to edge book interaction, (F) edge to edge tube interaction, (G) edge to face tube interaction, (H) face to face tube interaction**,** (I) edge to face book/tube interaction, (J) edge to edge sphere interaction, (K) connectors, (L) aggregations, (M) particle matrices.

Microstructural classification was further developed by Sergeyev *et al.* (1980) and Grabowska-Olszewska *et al.* (1984) who built on the terms honeycomb, skeletal, matrix, turbulent and laminar to describe the interactions of silt and sand grains with clay particles in a soil structure. These terms have been frequently used for sedimentary soils and are defined in Table 6.11 and illustrated in Figure 6.32.

Table 6.11: Microstructural classification for sedimentary soils based on Sergeyev *et al.* (1980) and Grabowska-Olszewska *et al.* (1984)

Structure type	Definition
Honeycomb	This structure is characterised by the presence of open isometric cells from 2-3 μm to 10-12 μm in size (Sergeyev 1980). Furthermore, the cell walls consist of micro aggregates in the form of face to face and face to edge contacts (Figure 6.32a).
Skeletal	Skeletal structure is identified as a loosely uniform porous skeleton primarily composed of silt grains (Grabowska-Olszewska *et al.* 1984). The clay in the structure is non-uniformly arranged and is not continuous (Figure 6.32b).
Matrix	This structure is characterised by a continuous unoriented clay matrix which consists of silt and sand grains in an irregular arrangement (Grabowska-Olszewska *et al.* 1984). The clay within the structure is aggregated where contacts are face to face, face to edge and edge to edge (Sergeyev 1980) (Figure6.32c).
Turbulent	This feature is established by clay microaggregates forming in a well oriented structure along a bedding plane. The silt and sand grains are closely enveloped together. Clay microaggregate interaction is generally in a face to face manner with little to no face to edge structure (Sergeyev 1980) (Figure6.32d).
Laminar	Laminar structure has a well sorted and strongly bedded structure. As with turbulent structure, clay microaggregate assemblages are generally in face to face contact and rarely in face to edge contact (Sergeyev 1980) (Figure6.32e).

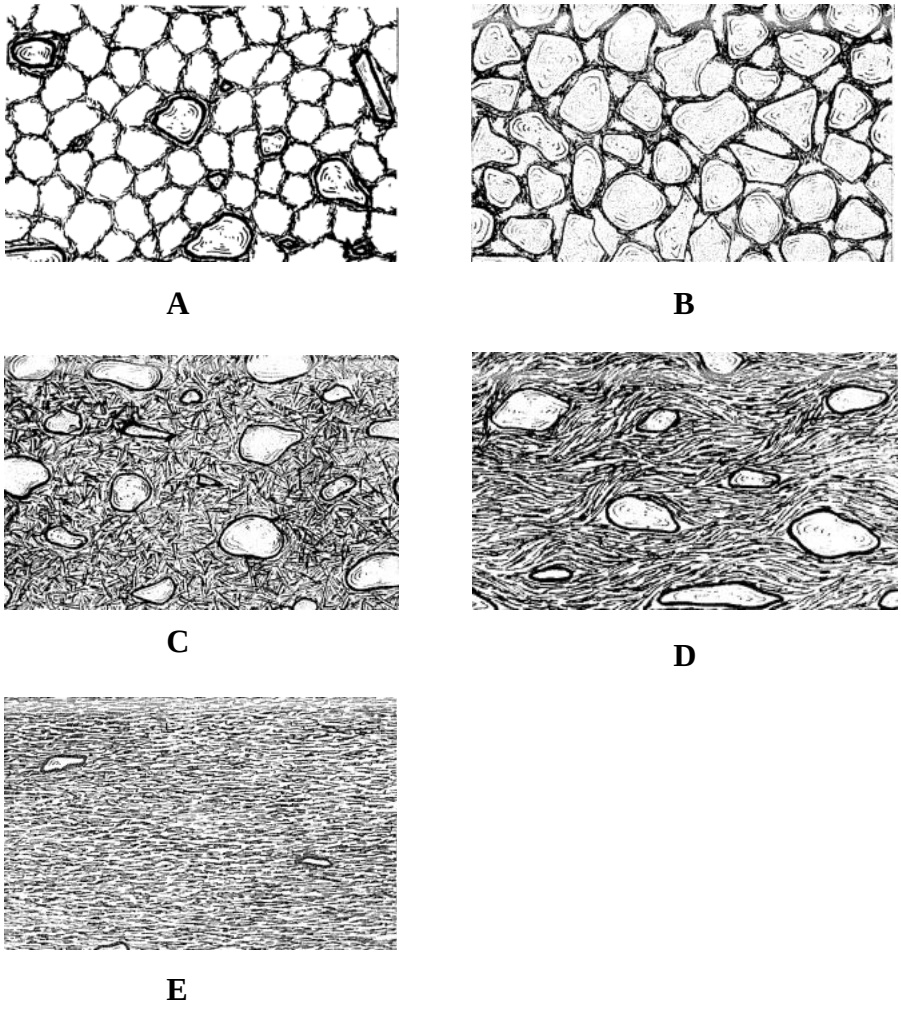

Figure 6.32: Microstructural classification based on sedimentary soils. (A) Honeycomb, (B) skeletal, (C) matrix, (D) turbulent, (E) laminar. Adapted from Sergeyev *et al.* (1980).

In comparison, pyroclastic-derived soil microstructural definitions are somewhat less widely recognised, stemming from the identification and characterisation of microstructures in weathered (welded to non-welded) ignimbrite (Carr 1981; Moon 1993). Moon (1993) suggested the use of sedimentary terminology was deemed inappropriate for non-welded ignimbrite studies considering the sedimentary schemes were based on the interactions of clays and their surrounding materials, while non-welded ignimbrites studied generally contained no clay, rendering the previous classification schemes unhelpful.

Microstructure classification for New Zealand sensitive soils remains without an accepted protocol for description. Previous workers have employed both sedimentary soil based classification schemes (Cong 1992; Keam 2008) and

also pyroclastic-sedimentary based schemes (Wyatt 2009). Wyatt (2009) suggested that the use of a sedimentary classification system was potentially misleading for pyroclastic (also referred to as tephric where unconsolidated) soils. He suggested that consolidation conditions were not comparable between the soil materials and that classifying the volcanic materials under a sedimentary based system was impossible given the different constituents comprising the soils. Wyatt (2009) incorporated terminology based on ignimbrite descriptions (from Carr 1981), primarily in describing the unordered, undifferentiated material, which was common in the sensitive soils investigated, as groundmass. Groundmass was originally used to describe broken fragmentary material in pyroclastic materials, which contained little to no clay (Moon 1993). Issues arise with this terminology for classification as the materials being consulted have been seen through SEM imaging to contain significant clay mineral assemblages. The sedimentary classification scheme on the other hand does not take into account the large amount of glass and other volcanic constituents observed in the soil from SEM analysis prompting further classification issues.

The inconsistencies between the appropriate use of both the sedimentary based classification scheme and the pyroclastic-sedimentary classification scheme employed by Wyatt (2009) indicate that there is no clear approach which should be adopted for describing the geometrical arrangement of particles in pyroclastic sensitive soils. Arthurs (2010) recognised this classification adaptation issue, and again adopted the sedimentary based classification scheme as he suggested that those schemes more accurately portrayed the role and structure of clay within the soil. Arthurs (2010), however, suggested that defining contacts between particles remained an issue as the clay minerals present often do not lend themselves to the classic edge-to-edge, face-to-face and edge-to-face ideology derived from Lambe (1953), given that the particles were rounded. Previous workers have accepted that where spherical shaped particles are united, the bond was in a face-to-face orientation (Wyatt 2009). Arthurs (2010) rejected that classification and instead developed new terms such as bundled (for multiple tubular morphologies in consistent orientation), lattice (for tubular morphologies in random orientation), and globular microaggregates (for aggregated spheroidal clays). In reviewing these terms for this study, the use of the classification from Lambe (1953) still provided an acceptable means of judgement, however where purely spheroidal

particles were observed, the contacts were considered edge to edge, as the surface area making contact is akin to the minimal connection of two edges. Although tubular morphologies were also rounded, they were not proportionately sized and therefore the side portions of the tubes were considered faces, whereas the edges were located at the ends of the tubes.

With consideration of all of the arguments outlined by previous workers, the use of the sedimentary classification scheme adapted from several workers (Lambe 1953; Collins and McGown 1974; Sergeyev *et al.* 1980; Grabowska-Olszewska *et al.* 1984; Huppert 1986) was the most appropriate. Initially dominant clay morphologies were identified, and then their particle interaction was determined, i.e. face-to-face, edge-to-face, edge-to-edge. The clay interaction with surrounding material was then identified, as was the microstructural classification based on Sergeyev (1980) and Grabowska-Olszewska *et al.* (1984). Finally the porosity of the material was classified according to Huppert (1986). Differing from the classification schemes identified is the presence of volcanic material within the soils, meaning the employed approach is a sedimentary-pyroclastic hybrid scheme. The ability of the sedimentary-based scheme to adequately account for clay mineral assemblages is critical, and is the primary reason for the use of this scheme over the scheme employed by Carr (1981) and Moon (1993) for pyroclastic materials. Furthermore, the sedimentary based scheme allows for the comparison with other soils, both from different authigenic environments and also from those studies completed in New Zealand. Using the sedimentary based scheme does not introduce any new descriptors and so I aim to reduce confusion in understanding the soil microstructure, principally when comparing the findings of different studies. The flow chart in Figure 6.33 gives the order of classification for microstructural identification in this study.

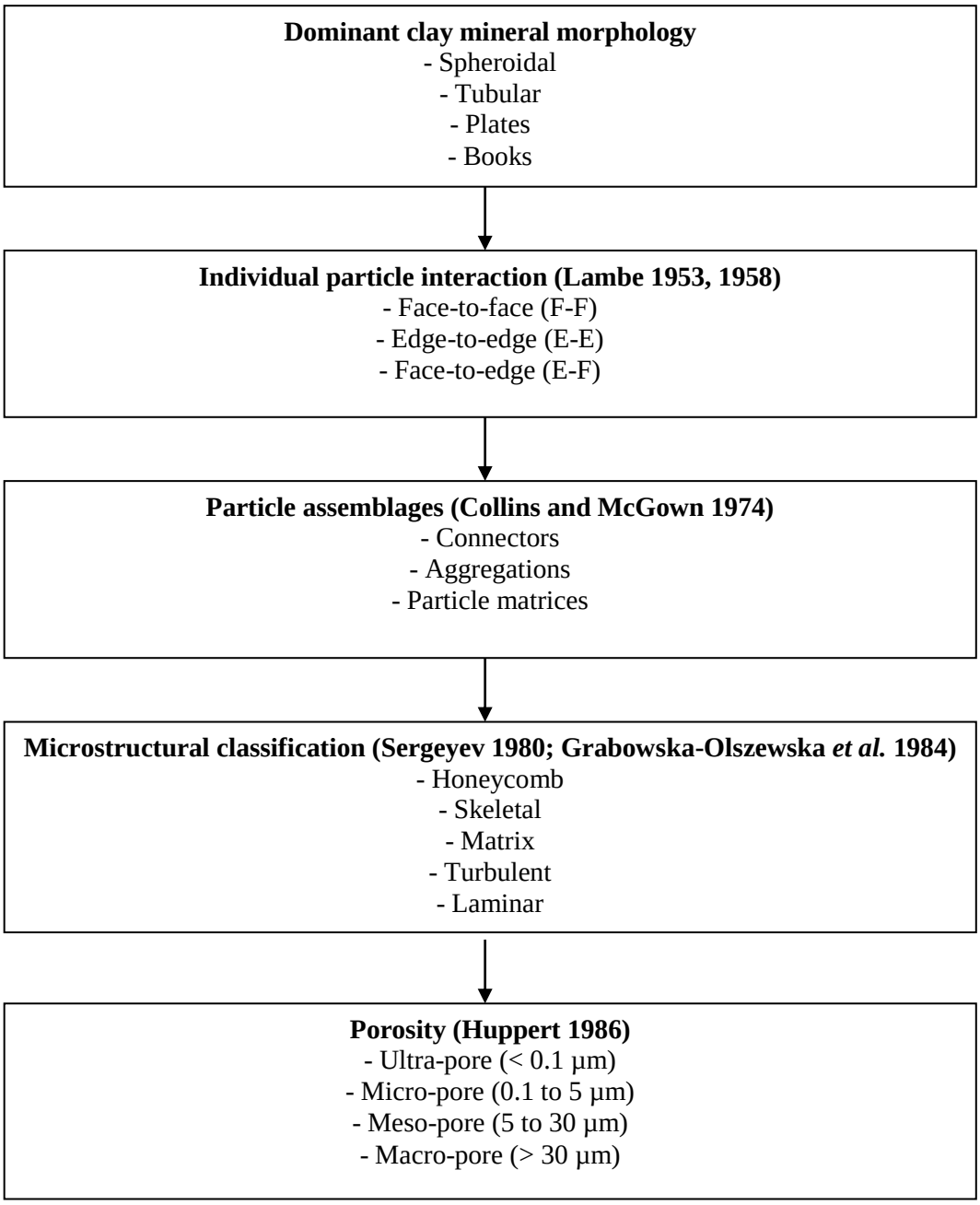

Figure 6.33: Flow chart utilised to identify microstructure for the sensitive soils from this study.

6.3.2 **Microstructural Characteristics**

The microstructures of samples were described in a systematic order for each sample.

6.3.2.1 **Omokoroa**

The two intact samples from Omokoroa (OS1, OS2) exhibited similar microstructural properties. Initially, dominant clay morphologies included spheroidal and tubular forms, with OS1 also containing plates (see section 6.2.2). Pumice was also common within the sample. Particle interactions were primarily in an edge to edge orientation, followed in occurrence by face to edge, with face to face aggregations less commonly identified (Figure 6.34, 6.35).

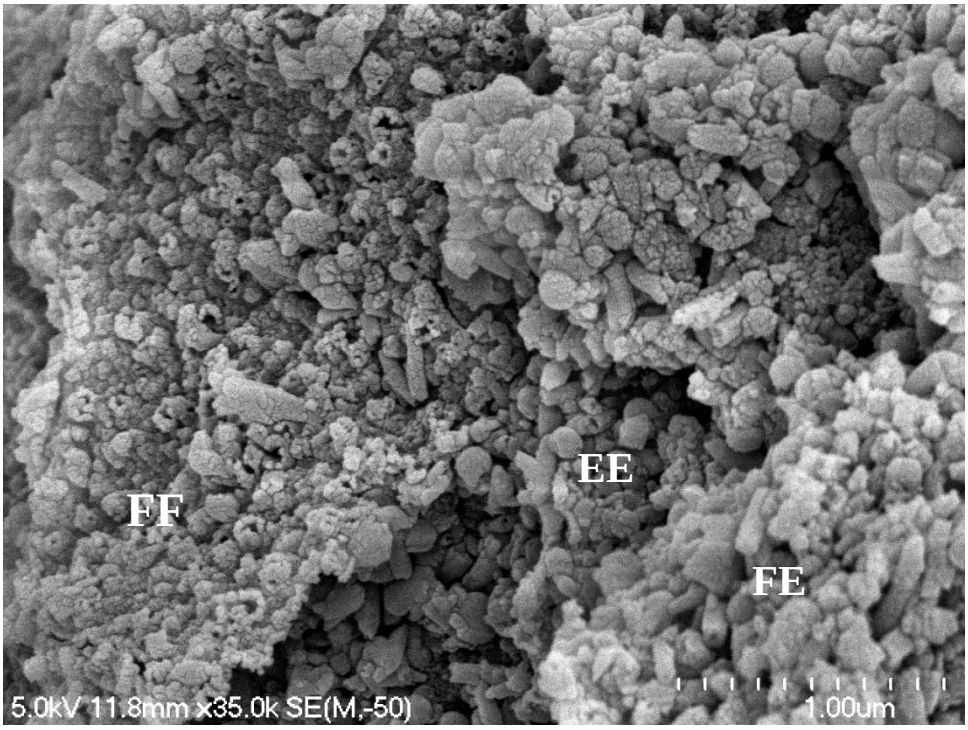

Figure 6.34: Edge to edge (EE), face to edge (FE) and face to face (FF) contacts in OS1. Multiple tube ends can be seen in the left of the image, of which are all facing in a similar orientation indicating face to face tubular particle interaction. Small tubular particles at the bottom right of the image can be seen to be forming face to edge interactions. Meanwhile spheroidal contacts are producing edge to edge contacts in the centre of the image.

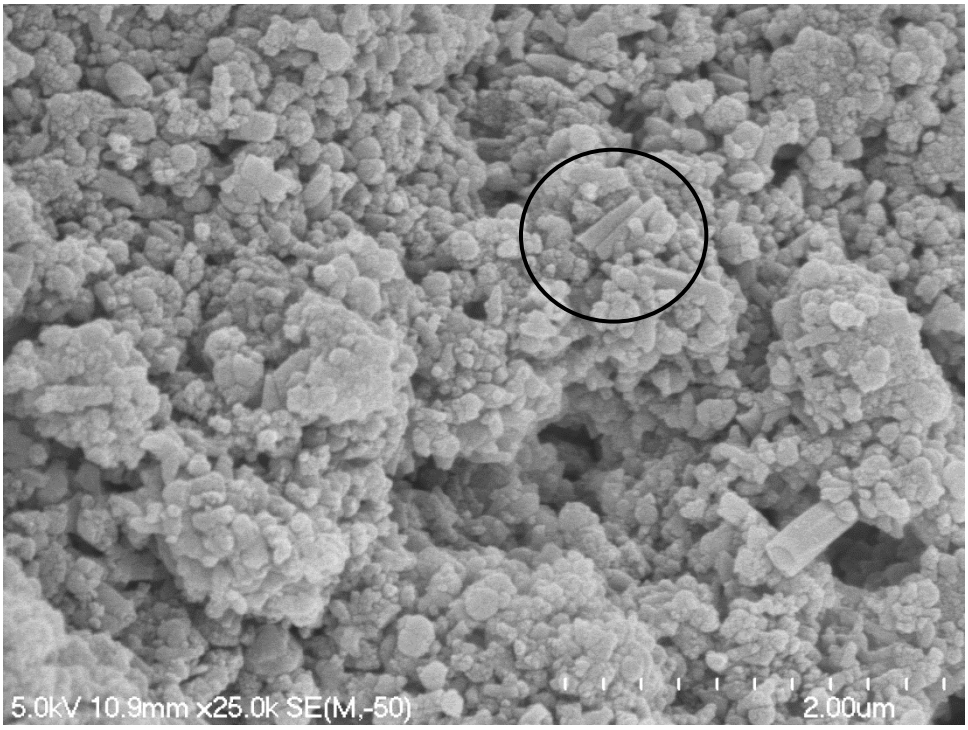

Figure 6.35: Particle assemblages from OS2**.** Primarily aggregations of spherical edge to edge interactions and also tubular face to face interactions can be observed (circled).

Particle assemblages were typically observed as particle matrices. Larger pumice grains were generally embedded within the particle matrices (Figure 6.36, 6.37). The position of pumice and vesicular glass within the background of particle matrices does not seem unsurprising considering the weathering of these materials likely formed the clay minerals present. The particle matrices generally coated sand and silt grains fairly comprehensively. Considering that the clay minerals were so abundant, the particle size analysis (see Chapter 5) which suggested relatively low proportions of clay (< 11 %) did not seem to be consistent with the SEM observations. It is possible that before the particle size analysis some of the clay particle assemblages were not completely disaggregated from the silt and sand grains meaning clay proportions were underestimated at Omokoroa. Although this disaggregation may have been an issue for particle analysis, a reasonable assessment of the microstructure is still believed to be achievable from the sample analysed.

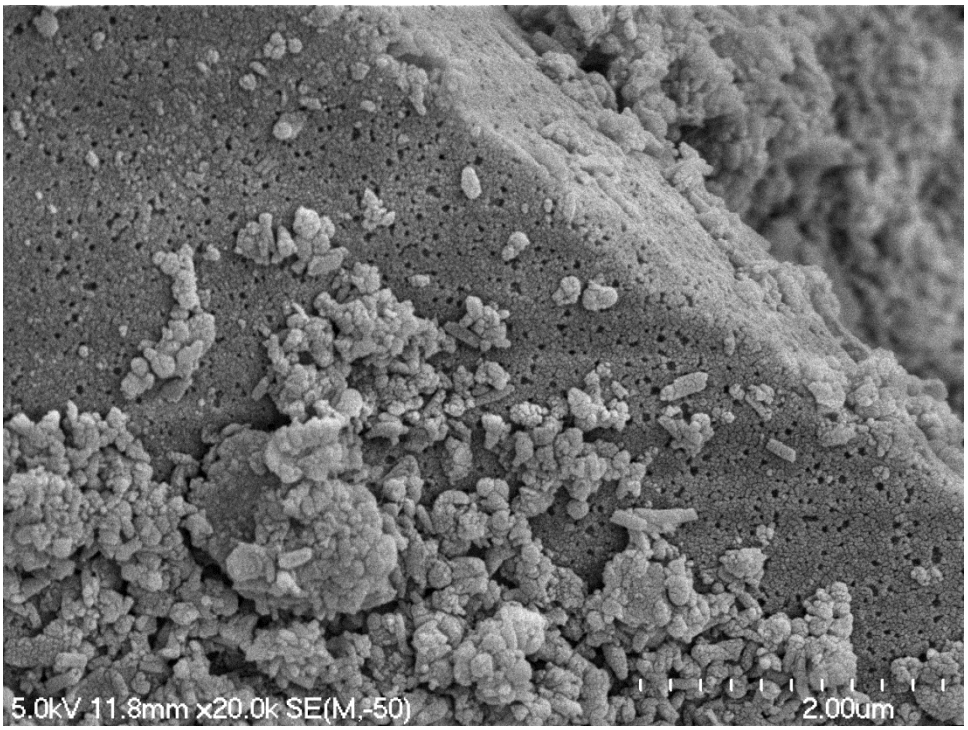

Figure 6.36: Pumice grain embedded within the particle matrices of OS1.

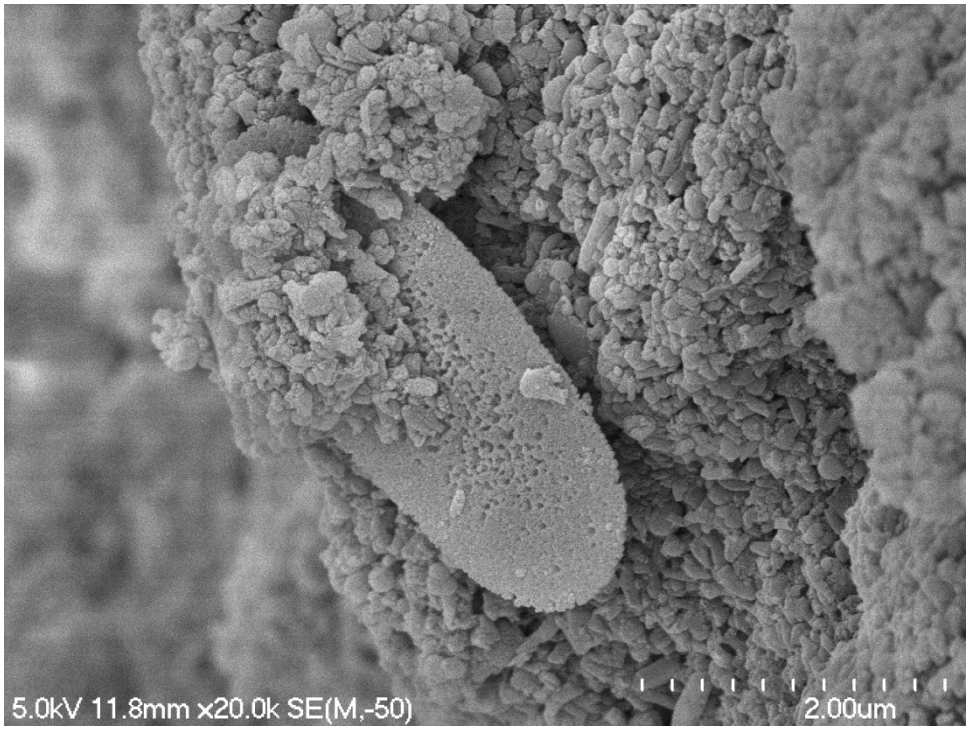

Figure 6.37: Highly weathered pumice fragment from OS1 partially submerged by particle matrices.

Microstructural classification for both OS1 and OS2 from Omokoroa was classified as a matrix-skeletal formation. The structure was partially continuous and the clay materials were generally unorientated. The material contained regular inclusions of silt and sand grains (Figure 6.38) and, as mentioned earlier, the clay was aggregated in face-to-face, face-to-edge and most commonly edge-to-edge contacts. The clay particles have been established as primarily halloysite from XRD analysis (see section 6.2.1.1.1). The skeletal classification was based on the high porosity (> 65 %) determined in Chapter 5 and the pore spaces observed from SEM imaging.

Pore spaces were relatively abundant in both OS1 and OS2. The average pore size was ~ 0.2 µm in diameter, classifying them as micropores while some ultrapores were also observed (0.1 µm) (Figure 6.39). Furthermore, the pore spaces were generally not uniformly shaped because of the differing formation of tubular, spheroidal and plate-like clay morphologies and their interaction with one another. Larger pore spaces of mesopore size were typically observed within weathered pumice and glass deposits (Figure 6.40)

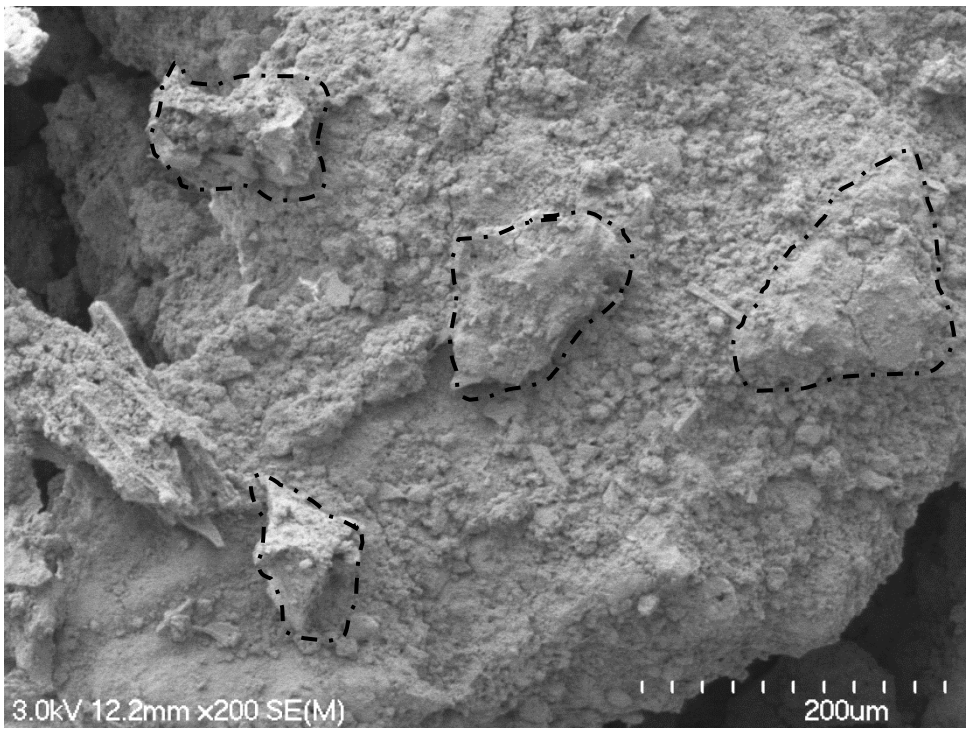

Figure 6.38: Regular sand and silt inclusions from OS1. Sand and silt sized particles are outlined indicating their close spatial relationship.

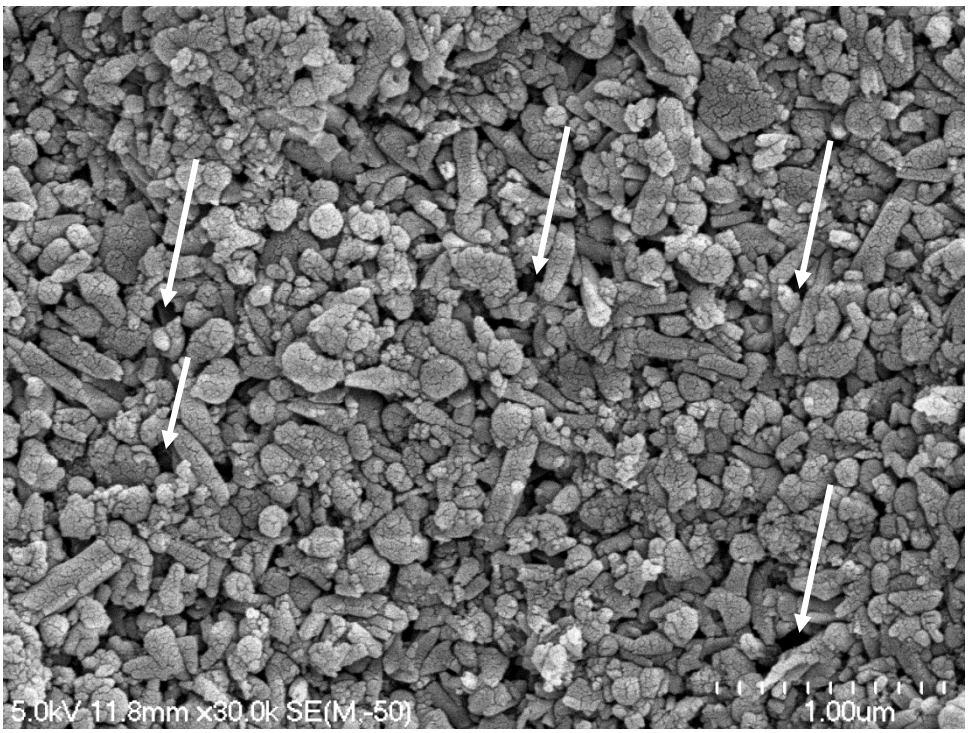

Figure 6.39: Abundance of small micropores from OS1 (indicated by arrows). The pore spaces can be frequently seen throughout the sample.

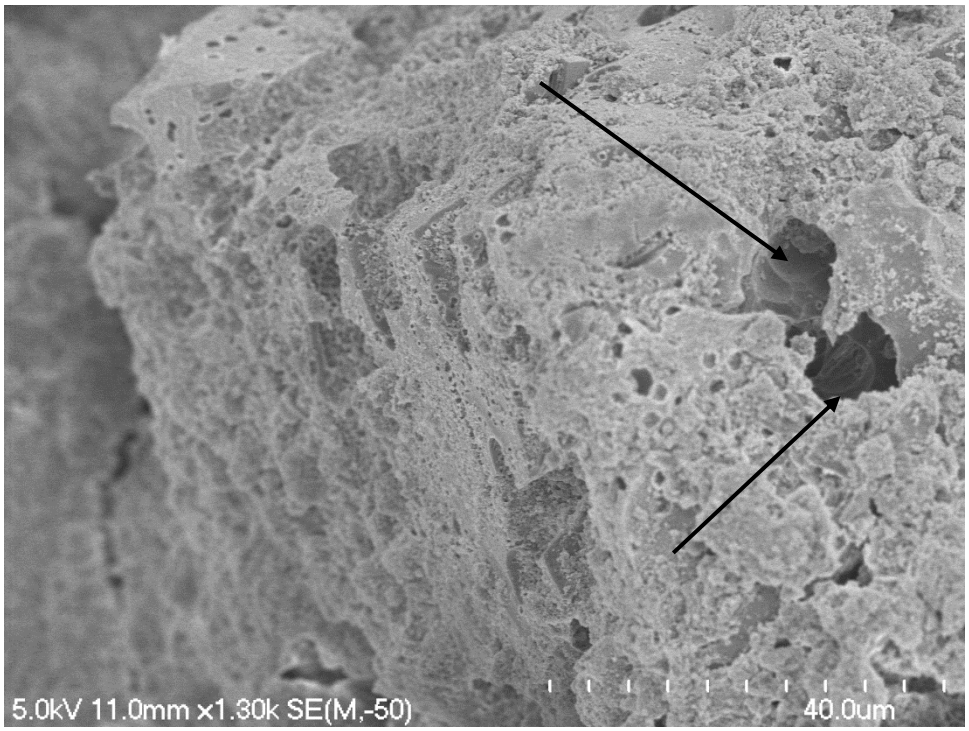

Figure 6.40: Weathered pumice grain from OS2. Large vesicles can be seen, which contribute to the high porosity of the sample (indicated by the arrows).

6.3.2.1.1 **Impact of remoulding at Omokoroa**

6.3.2.1.1.1 OS1 and OS2

Remoulding OS1 and OS2 indicated the presence of individual plates and very small or broken tubular forms of halloysite. The intact samples contained halloysite tubes of ~ 400 – 600 nm in length, but following remoulding, tubes were observed to be < 300 nm in length (Figure 6.41). This tube shortening was also seen in the OLRO sample. As with the intact samples, both OS1 and OS2 displayed an abundance of ultra and micropores in their remoulded states.

Remoulded OS1 appeared structurally similar to its intact state with many pores visible. OS2, however, displayed a partially homogenous structure with edge-to-edge plate connections (Figure 6.42). The remoulded form seemed to represent a laminar type structure as opposed to the matrix-skeletal structure present in the intact state. The plates appeared to have settled in this orientation following the likely suspension of clay particles when water was released from the pores upon remoulding. In comparison with OLRO, the remoulding process used to analyse these samples appears to produce similar disturbed structures as in a naturally remoulded sample.

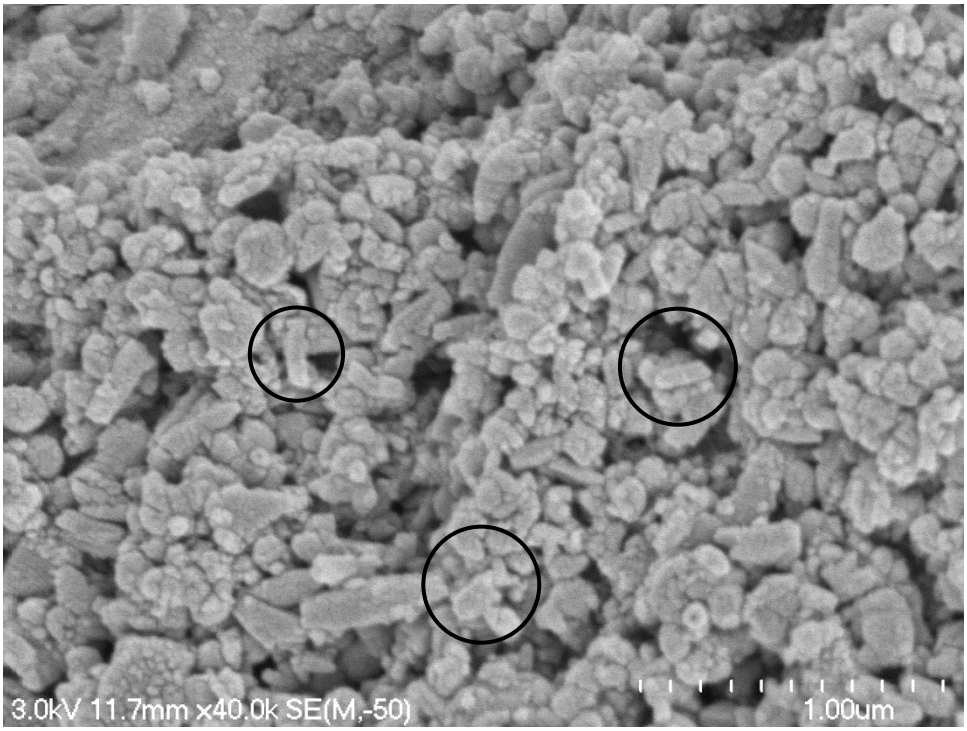

Figure 6.41: Remoulded OS1 structure. Tubes appear shorter than the intact state. Ultrapores and micropores are still abundant throughout the sample.

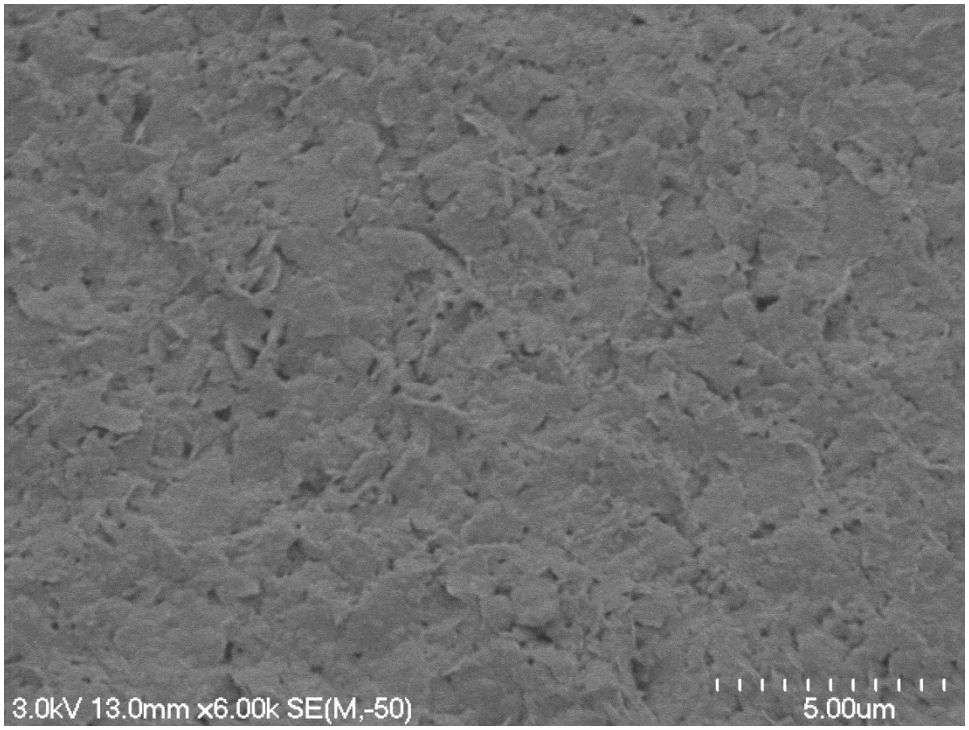

Figure 6.42: OS2 indicating plate type morphologies connecting via edge to edge interactions to form a laminar type structure upon remoulding.

6.3.2.1.1.2 OLRO

The naturally remoulded sample of OLRO was analysed separately from the forcibly remoulded OS1 and OS2 samples to establish the variation between the modes of remoulding. Initially OLRO displayed halloysite plate and book type morphologies along with both spheres and tubes (section 6.2.1.1.1). In contrast to the intact samples, the tubes appeared to be much shorter, while individual plates were found to be scattered within areas of clay mass (Figure 6.43). The small tubes and plates could possibly have been broken down from larger tubes and books, respectively, by remoulding. Clay particle interactions were edge-to-edge between the spheroidal particles, whereas face-to-face interactions were typical for the stacked plate aggregates forming books in OLRO.

Connector contacts were observed in OLRO, where books formed bridge type contacts between grains (Figure 6.44). Such connectors were infrequent yet do indicate that some books can survive natural remoulding and fluidisation. Particle matrices were also common throughout the sample, where spheroidal particles often formed an unoriented clay mass around larger grains. The structure appeared to be more consistent with a matrix formation, where the silt and sand

grains were irregularly arranged within the soil mass. Micropores are also characteristic of a matrix classification (Sergeyev *et al*. 1980), and were the most common pore size observed in the OLRO sample (Figure 6.43). The pores were positioned frequently throughout the structure, while pores larger than ~ 5 µm were infrequent.

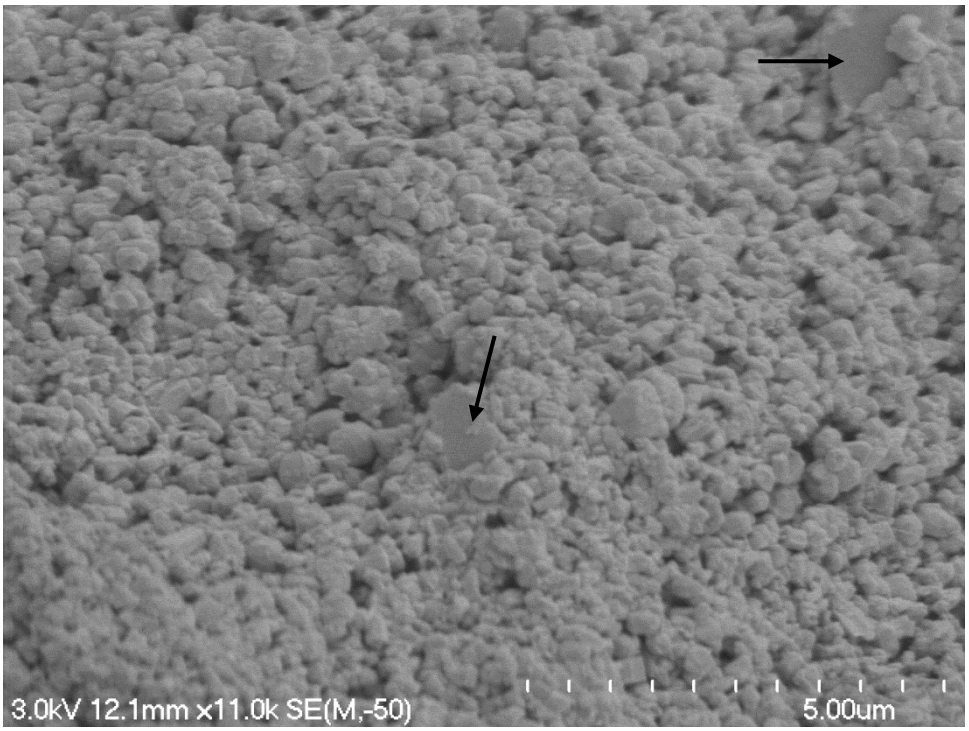

Figure 6.43: Naturally remoulded structure of OLRO. Individual plates (indicated by the arrows) are scattered throughout the sample, while much shorter tubes are also present.

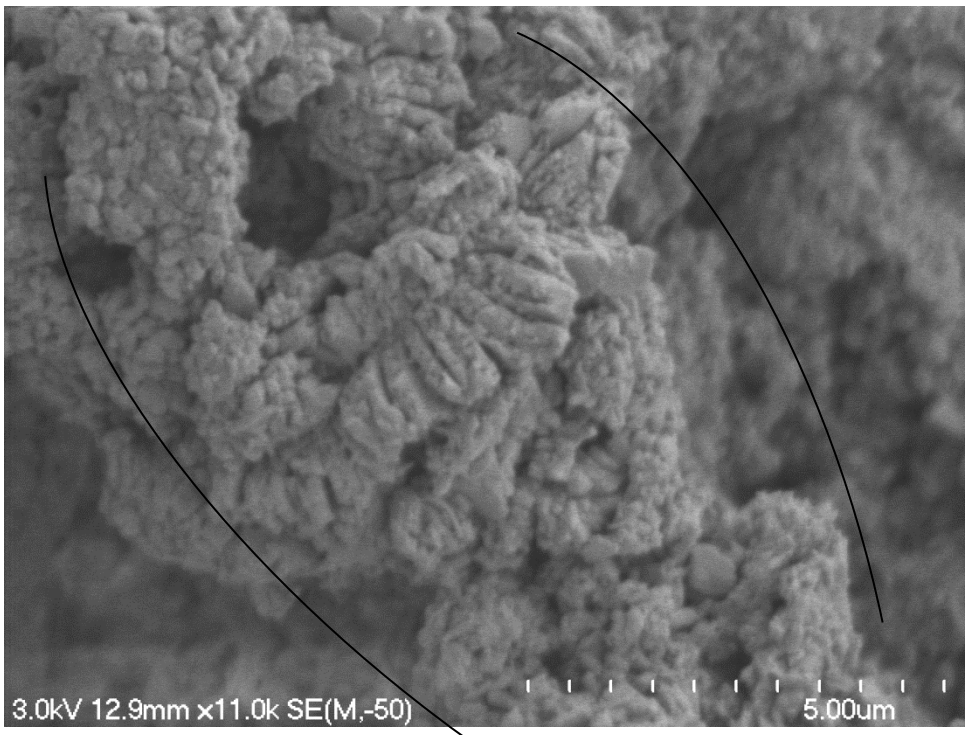

Figure 6.44: Books aggregating in face to face and edge to edge contacts to form a bridge/connector between larger silt particles in OLRQ.

6.3.2.2 **Te Puna**

The TPS1 microstructure was dominated primarily by plates, tubular and spheroidal halloysite clay morphologies (see section 6.2.1.1.2 and 6.2.2). Primarily face to edge and edge to edge particle interactions were observed (Figure 6.45).

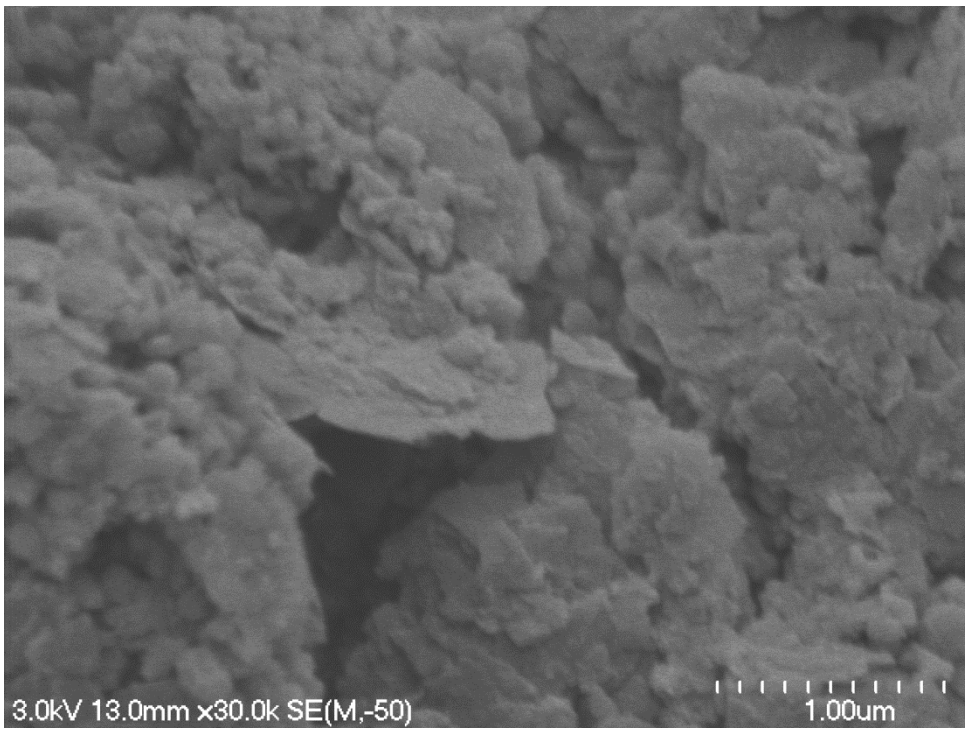

Figure 6.45: Plate morphologies forming edge to edge interactions in TPS1.

Particle assemblages were in the form of aggregations (Figure 6.46) and particle matrices. Aggregations of clay were typically positioned on larger grains, but boundaries of the assemblages were clearly identifiable, and hence were defined as individual acting units. Particle matrices were also a major constituent with embedded sand and silt grains within this background material. Aggregations comprised ~ 15 % of the soil while the remaining ~ 85 % was observed to be silt and sand embedded within particle matrices.

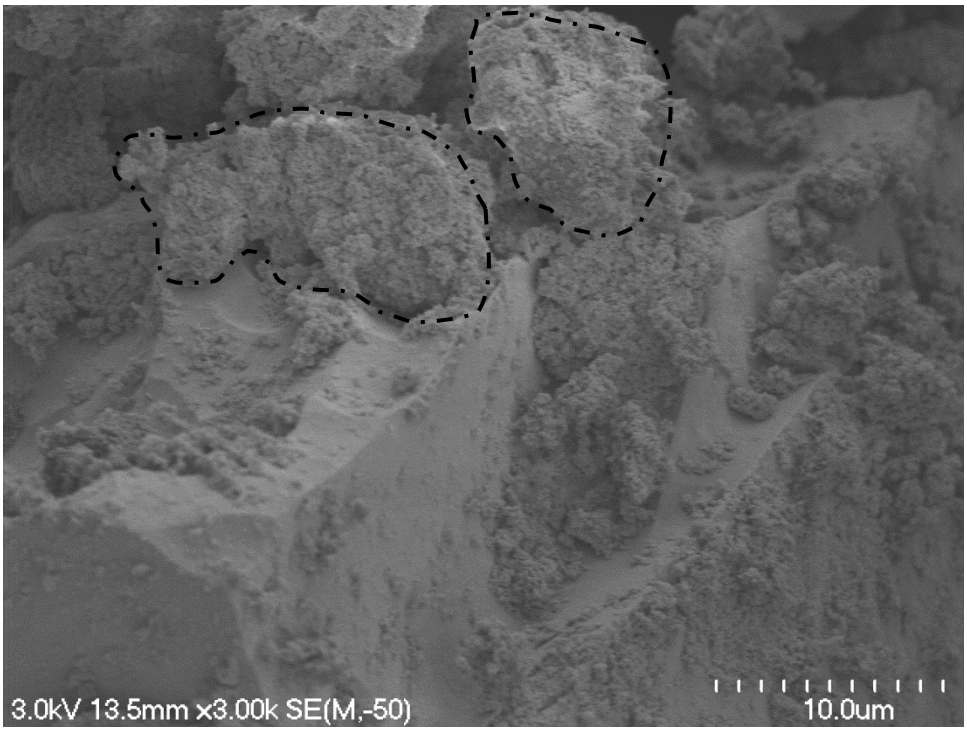

Figure 6.46: Clay aggregations effectively forming individual units in TPS1.

The microstructural classification is considered matrix-turbulent. The predominance of the plate morphologies form in a uniform orientation enveloping the silt and sand grains, and suggest a turbulent structure (Figure 6.47). In other areas of the sample, tubular and spherical, particles formed a randomly orientated structure where the silt grains appeared to be situated more irregularly giving rise to the partial matrix classification.

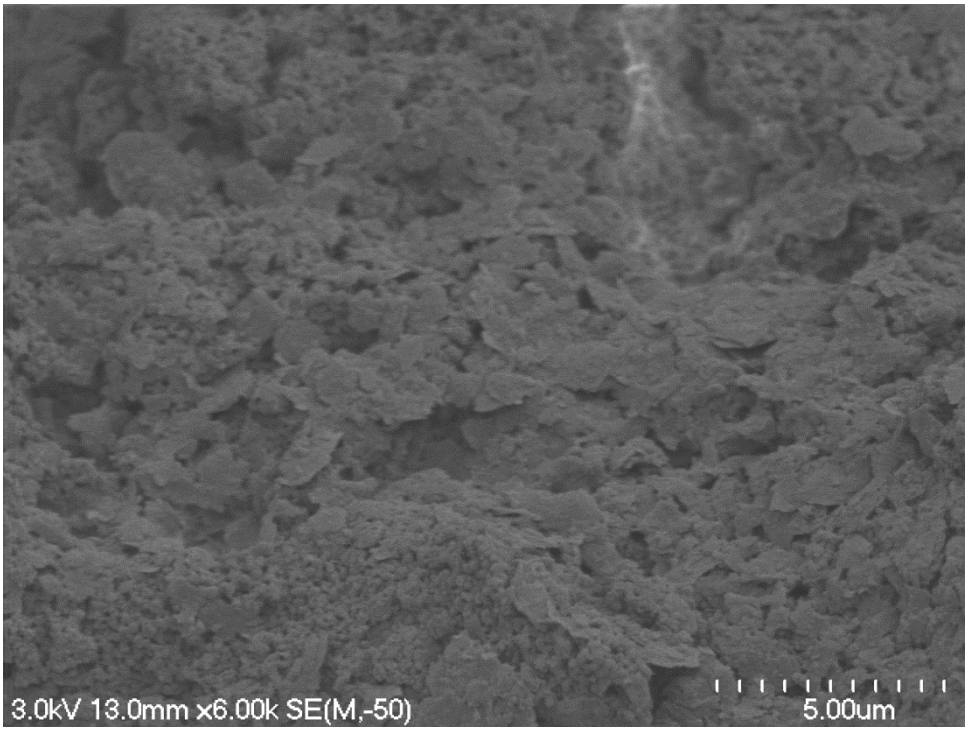

Figure 6.47: Plate morphologies forming a turbulent-matrix microstructure in TPS1.

The pore spaces in the clay fraction of the sample were typically 0.5 µm – 2 µm in size, meaning they are micropores. The pores were relatively common throughout the sample, confirming the high porosity as recorded in Chapter 5. Pore spaces were most prevalent where multiple edge-to-edge plate connections were formed. Furthermore, the pores generally had an elongated shape rather than a typical spherical shape where multiple plates were aggregated. Volcanic glass in the sample provided some rounded weathered vesicles which were the largest pore spaces observed at ~ 15 µm in diameter.

6.3.2.2.1 **Impact of remoulding**

The remoulded structure of TPS1 revealed few plates remained in the structure, suggesting they had been broken down into small remnants. Furthermore, spherical type clay formations seemed to dominate the structure which was previously not seen in the intact sample. These spheres were difficult to differentiate from reduced tubular forms, but it appears likely that the tubes previously observed in the intact sample were broken down into sphere sized portions. The volcanic glass constituents within the soil also appeared to have also been broken into smaller fragments upon remoulding (Figure 6.48), which was

common through the whole sample, illustrating the destructive nature of the remoulding process on embedded material within the matrix.

Figure 6.48: Broken glass fragment within the TPS1 matrix as a result of remoulding.

6.3.2.3 **Pahoia Peninsula**

The Pahoia Peninsula samples (PS1 and PS2) both indicated halloysite clay morphologies in all four recognised forms: spheres, tubes, plates and books (see section 6.2.1.1.3 and 6.2.2). Primarily, individual clay particle contacts were observed to be in face-to-face, face-to-edge and edge-to-edge orientation. Face-to-face contacts were typically observed between plates to form books, while the spherical and tubular particles were mainly in edge-to-edge and edge-to-face placement.

Considering the books observed in PS1 and PS2 were so large (see Section 6.2.2.4), they almost always acted as aggregations in their interaction with surrounding material within the soil matrix (Figure 6.49). Smaller sized material was classified as particle matrices given that the assemblages formed a background microfabric, in which larger silt and sand particles were embedded. Similar to OLRO, smaller book material (~ 5 µm) in PS2 was also observed to

provide connector interactions between clay assemblages and some larger silt grains. The small books were usually concentrated and formed edge-to-edge contacts between one another to form the connectors.

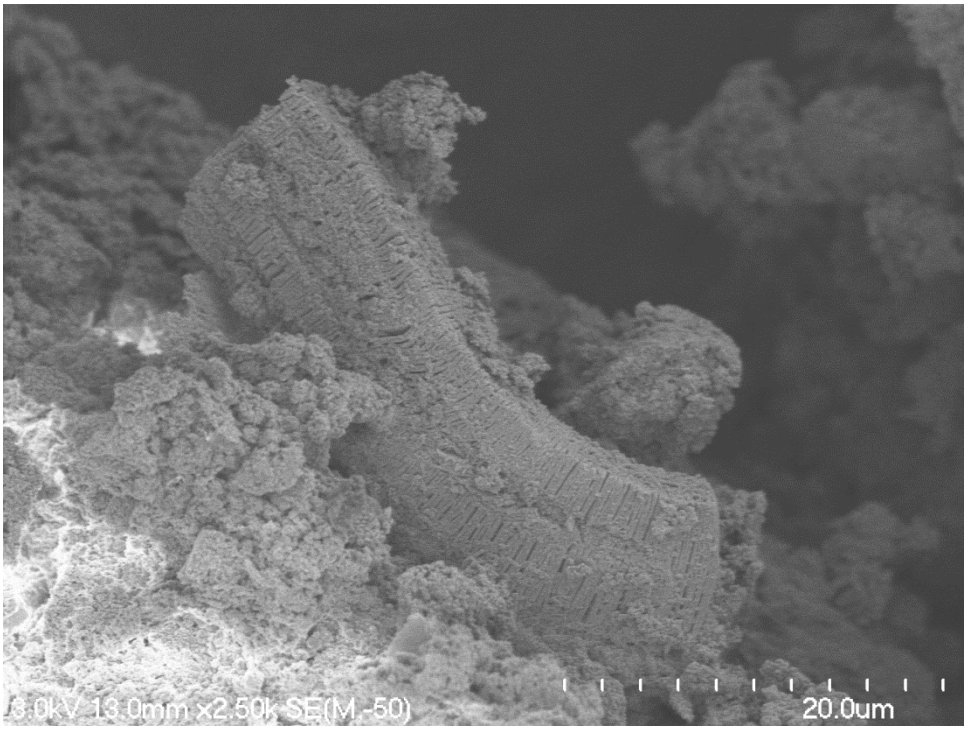

Figure 6.49: Large book material from PS1 acting as a sole aggregation with minimal embedding and appearing loosely connected to the surrounding material.

The microstructural classification of PS1 and PS2 appeared very similar and could be grouped as matrix-skeletal (Table 6.12). Much of the smaller material (spheres and tubular clay forms) tended to form an unoriented clay mass suggesting a matrix formation, whereas the smaller books usually provided some structured aggregation, forming a skeletal type framework. Furthermore, the orientation of the books is generally not structured in a particular pattern (Figure 6.50), showing this site to be primarily a matrix microstructure.

The porous nature of the sample (~ 61 – 64 %, see Chapter 5 section 5.3), however, does support the importance of the skeletal formation of the microstructure. The significant accumulation of ~ 5 µm books in PS2 promoted a fairly open structure with pore sizes of ~ 2 – 3 µm, which were bigger in comparison to Omokoroa and Te Puna (Figure 6.50). The pore sizes in the smaller

spheroidal and tubular constituent of the sample were similar to those at Omokoroa and Te Puna, typically of micropore size ranging from ~ 0.5 to 1.5 µm.

Figure 6.50: Contacts and interaction of book material from PS2 producing big pore spaces as indicated by the circle.

6.3.2.3.1 **Impact of remoulding**

Remoulding of both samples from Pahoia Peninsula indicated the destruction of the books, producing many more singular plate morphologies (Figure 6.51). As with Omokoroa and Te Puna, the sample characteristically still appeared porous. Furthermore, the broken books and plates appeared to promote a skeletal type structure. Tubular clay forms were observed to have broken down similar to that seen in the OLRO sample (Figure 6.52).

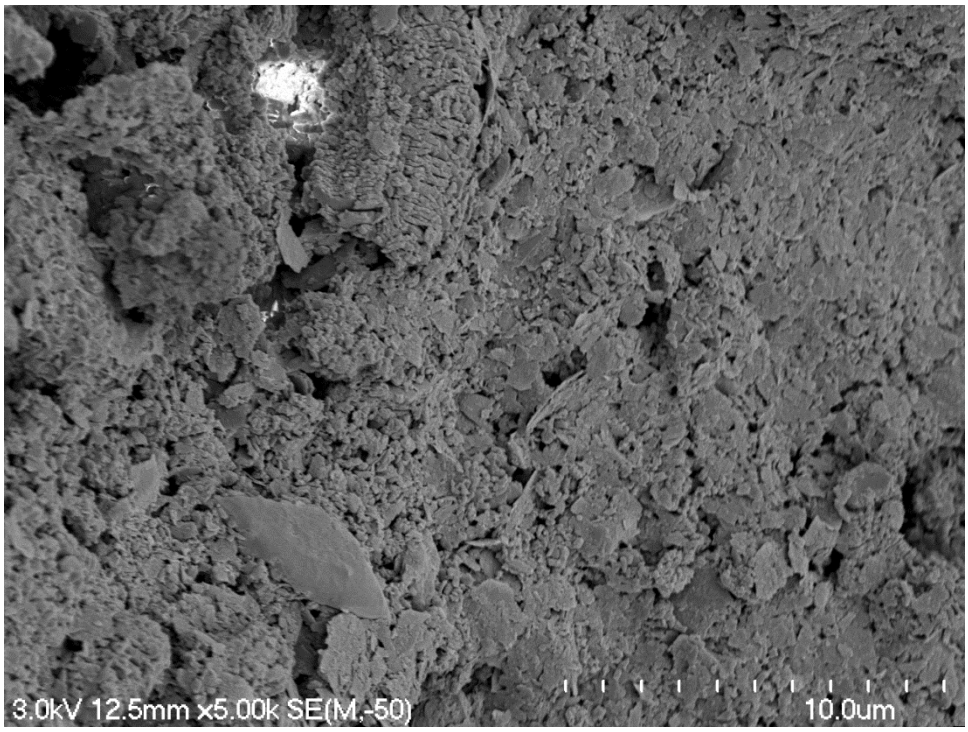

Figure 6.51: Remoulded PS2 indicating single plate morphologies arising from disturbed books.

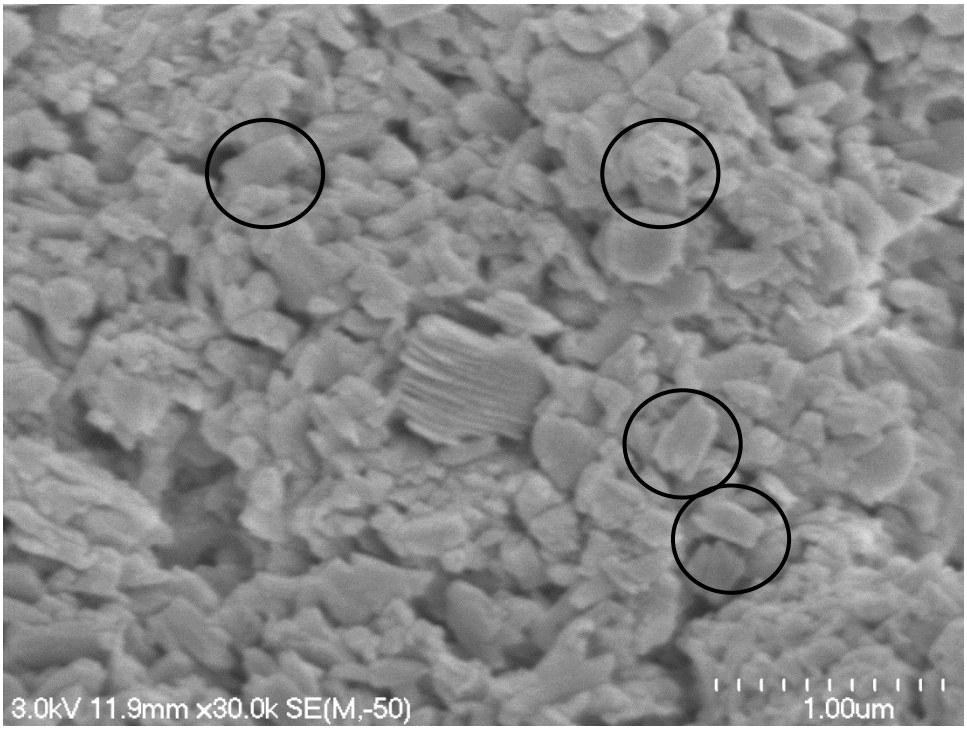

Figure 6.52: Remoulded PS2 displaying smaller broken tube morphologies throughout the sample.

6.3.2.4 **Tauriko**

The microstructures of all the Tauriko samples were very similar and thus all four samples (TS1, TS2, TS3, and TS4) were defined as one group. The primary clay mineral, halloysite (see section 6.2.1.2.1), could be seen in tubular, spherical and, in TS4, book morphologies. Individual particle interactions were face-to-face and edge-to-edge. TS2 indicated a lattice like arrangement, similar to that previously described by Arthurs (2010), where numerous tubes amassed on top of one another (Figure 6.53).

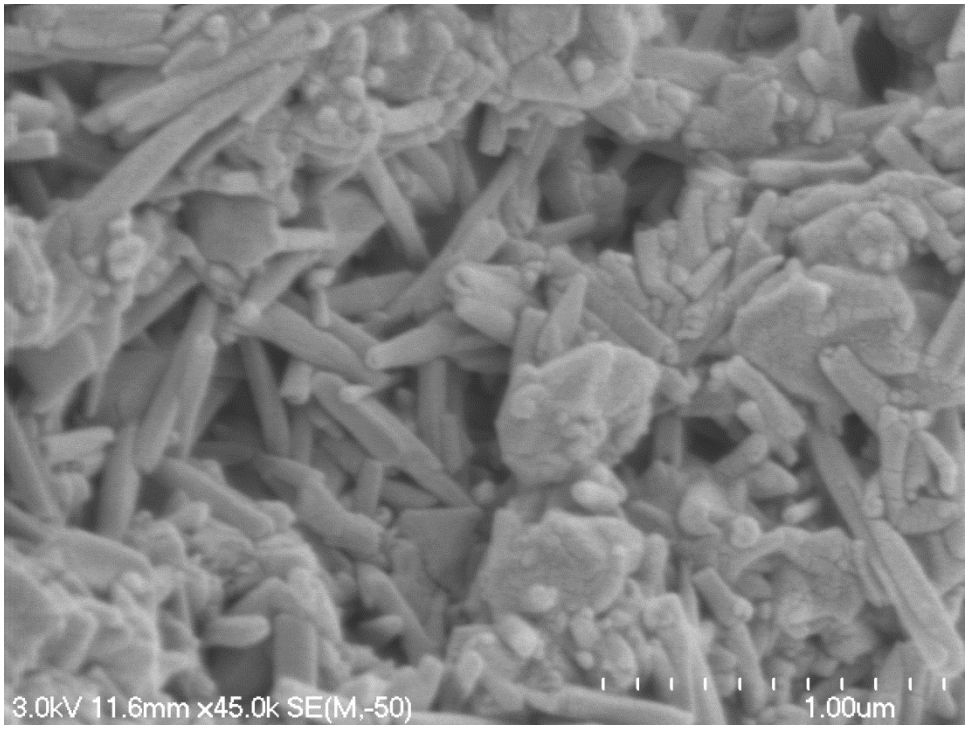

Figure 6.53: Tubes and spheres comprising the clay constituent of TS2.

The interaction of these clay minerals with surrounding particles was typically in the form of particle matrices and few connectors. Dissimilar to the sensitive samples, the Tauriko material displayed a large proportion of exposed volcanic glass and other sand sized grains. While some clay connectors could be seen assembled between larger grains, the clay fraction was much less dominant and many grains were seen to 'act' individually. Within the clay matrix, shorter distances between sand and silt sized grains were apparent, with the larger grains positioned in a closer approximation and abundance than that observed in the sensitive samples (Figure 6.54 and 6.55). Furthermore, TS3 displayed clearly

discernible boundaries between some individual grains indicating some aggregations were present.

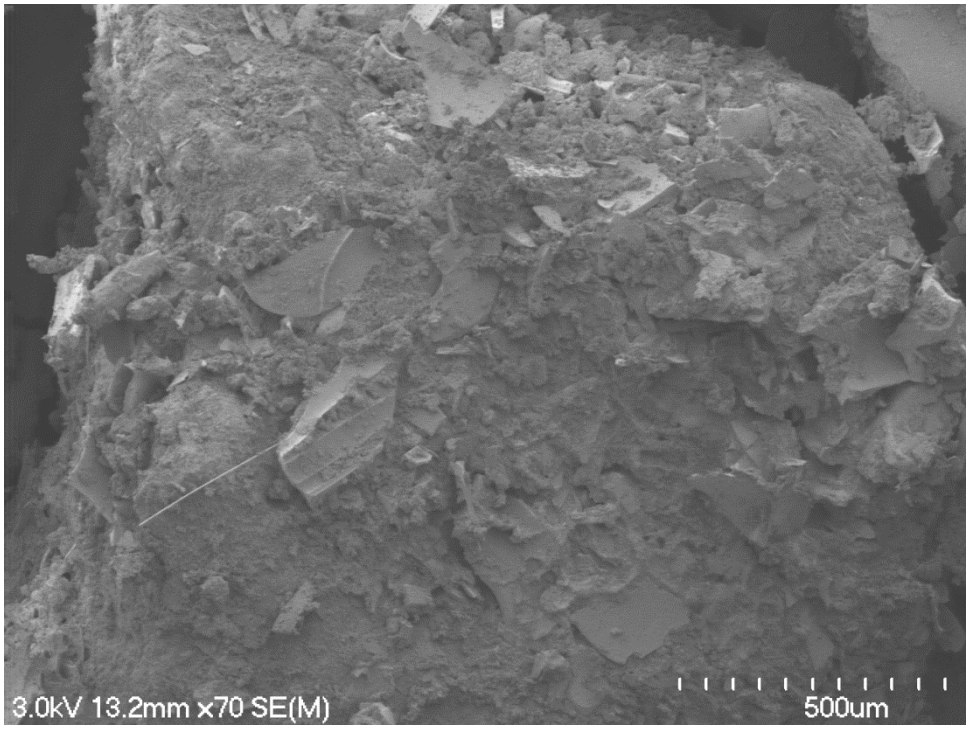

Figure 6.54: Microstructure of TS4. A large quantity of sand and silt size material can be seen, while the proportion of clay is much less than that from the sensitive samples.

All of the Tauriko samples were considered to have a matrix microstructure. No clear orientation of the clay materials was apparent, and so did not lend itself to any other classification. Where spherical clay particles were present, they tended to be tightly amassed with tubular morphologies, which typically filled space between spheres in a medium to well sorted arrangement. A difference from the sensitive samples was the larger size of these particles and seemingly tight interaction with the tubular forms of halloysite present.

The Tauriko sample indicated quite a high porosity, with many open pores viewed throughout the SEM. The pore spaces were generally between sand and silt sized material. Pore sizes ranged from micropore (~ 0.4 µm) to the majority at macropore size (~ 70 µm) (Figure 6.55) The observed high porosity may indicate that the sample was free draining, with little clay to absorb any water applied to the sample (Figure 6.55). Field observations indicated that the sample was dry, even ~ 1 m back into the profile, further suggesting that this was the likely situation (Chapter 4).

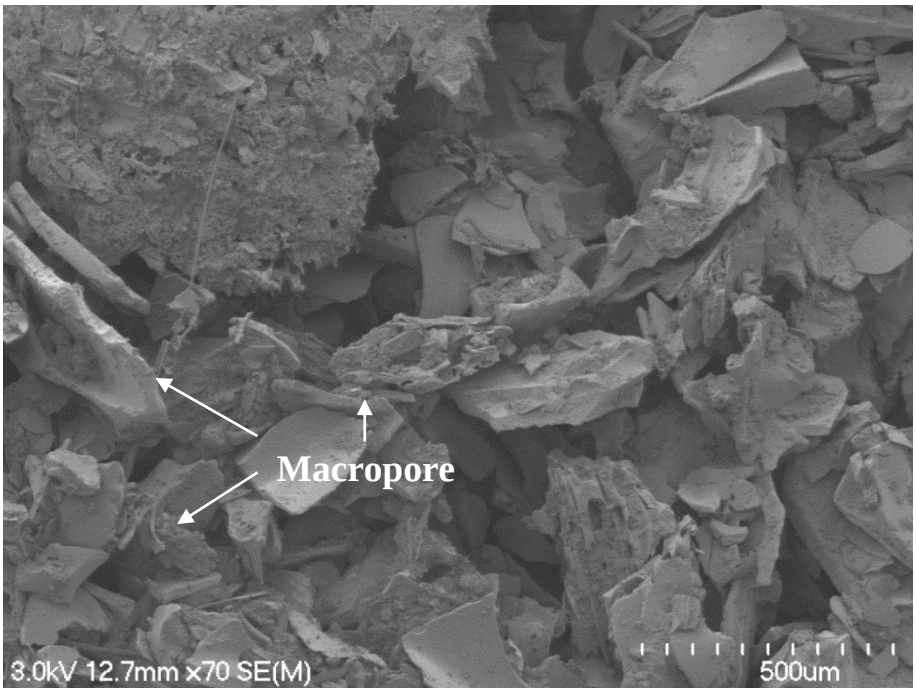

Figure 6.55: Abundance of individual sand and silt sized particles from TS3. Abundant cuspate and vesicular glass shards are evident.

6.3.2.5 **Rangataua Bay**

The Rangataua Bay (RS1) sample displayed a consistent formation of halloysite spheres and tubes within the clay dominated structure (Figure 6.56). The contacts were primarily in an edge-to-edge orientation for the spherical clays, while some of the tubes displayed face-to-face and face-to-edge contacts.

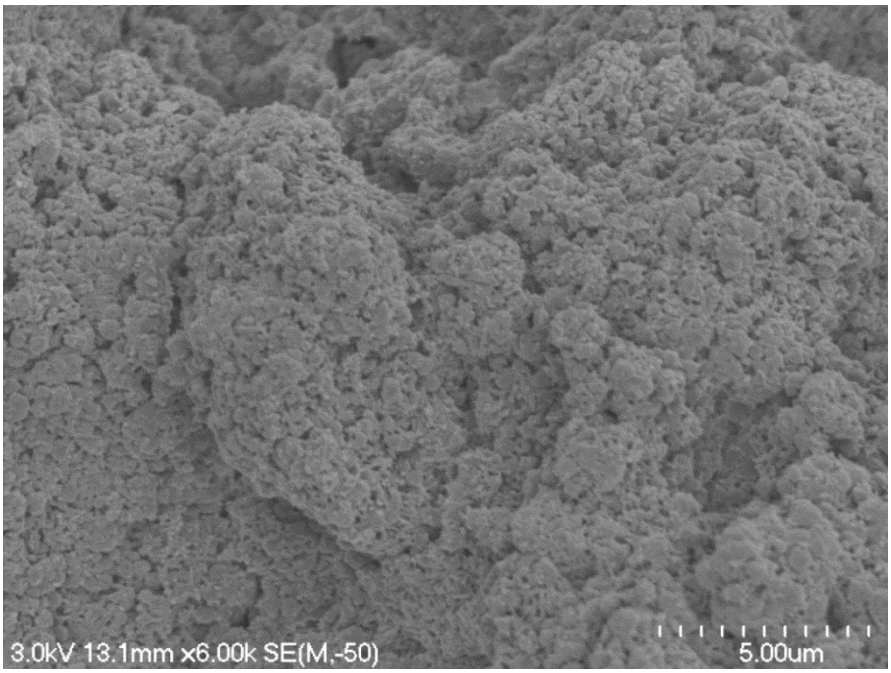

Figure 6.56: Halloysite spheres can be seen to dominate the soil matrix in RS1.

The clay particles appeared to extensively cover the silt and minor sand fraction contained within the sample. No immediate connectors were observed, however, the spherical clay minerals were observed to form bridge-like properties suggesting connector type interactions could form. Particle matrices were primarily seen to have quartz and other small grains embedded within the structure (Figure 6.57).

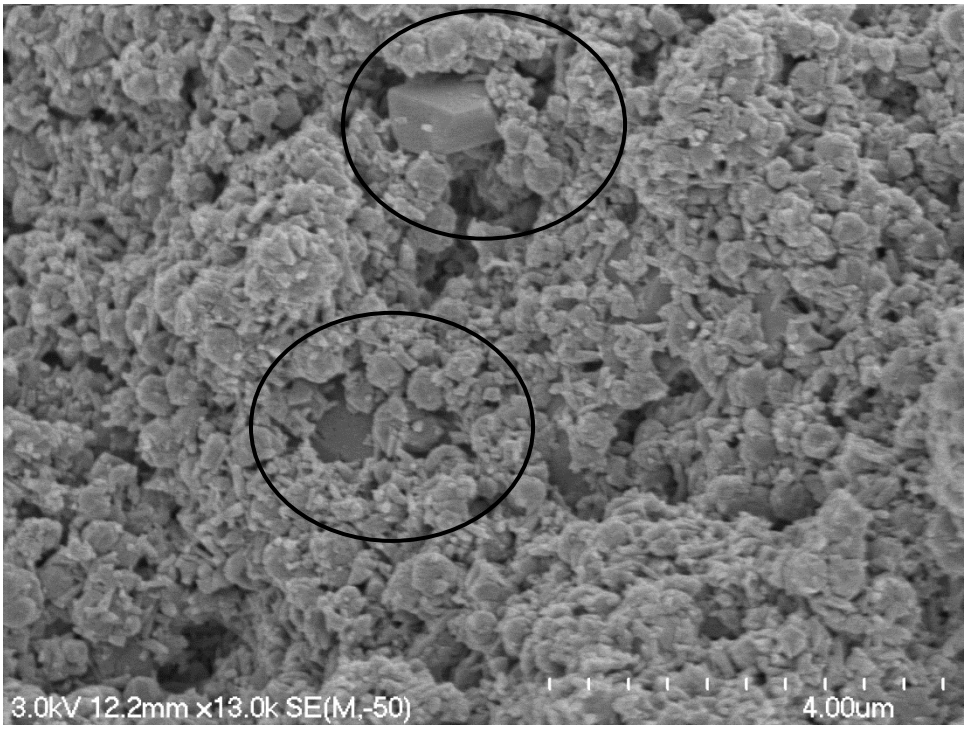

Figure 6.57: Small quartz grains embedded within particle matrices of PS1.

RS1 did not indicate a particular orientation of particles within the matrix, whereas larger granular particles were generally intermixed within the clay mass. On this basis, the microstructure was considered matrix. The spherical particles did seem tightly packed, where the tubular morphologies were tightly packed and well sorted between the spheres producing a dense packing arrangement. Some small pore spaces were positioned throughout the sample, however, did not extend deeply. This was reflected by the medium to low moisture content (~ 46 %) and porosity (~ 51 %) of the sample. Pore spaces were of micropore size (~ 0.6 µm) and were relatively consistent given the constant edge to edge contact of the spherical particles.

6.3.2.5.1 **Impact of remoulding**

The soil material from Rangataua Bay was thoroughly remoulded in an attempt to identify key structural differences between the remoulded sensitive samples and a remoulded non-sensitive sample. Distinctly, the remoulded RS1 sample only displayed minor structural deformation following disturbance (Figure 6.58). Connections between the spherical grains can still be seen, suggesting that the bonds are strong and do not easily detach following remoulding. Furthermore, the individual sphere structures themselves did not appear to break up or alter significantly. The structure does indicate that some larger pore spaces (0.8 – 1.0 µm) have opened up and are more frequent within the sample (Figure 6.59). The lack of moisture within the sample to begin with, however, appears to have reduced any possible fluidisation potential upon remoulding.

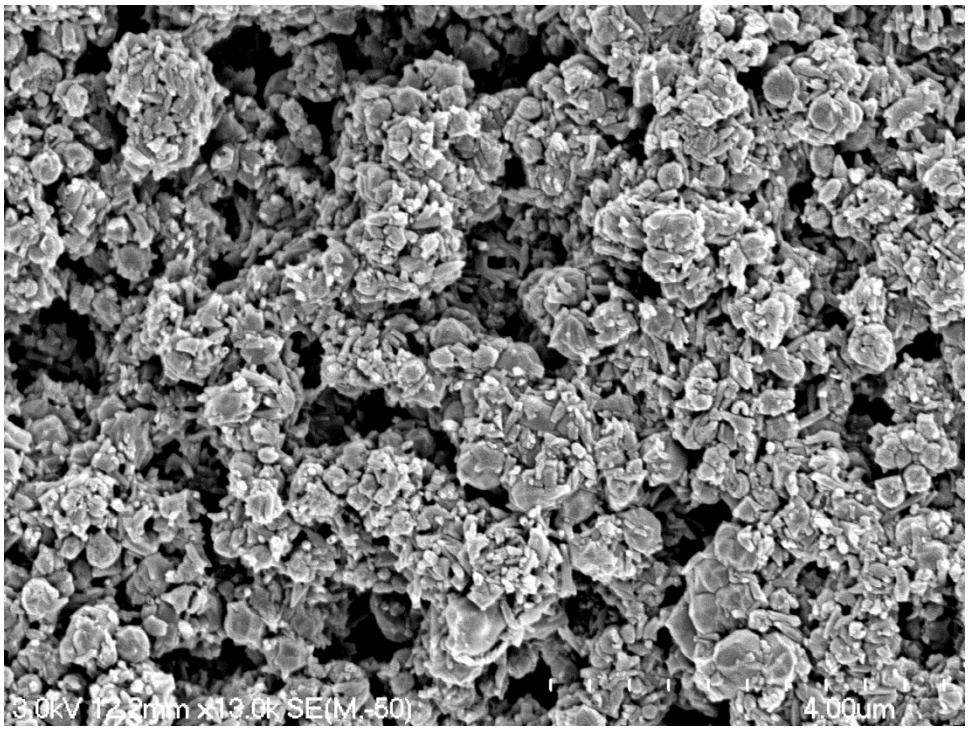

Figure 6.58: Remoulded RS1 indicated that strong bonds between spherical particles still exist even following thorough remoulding.

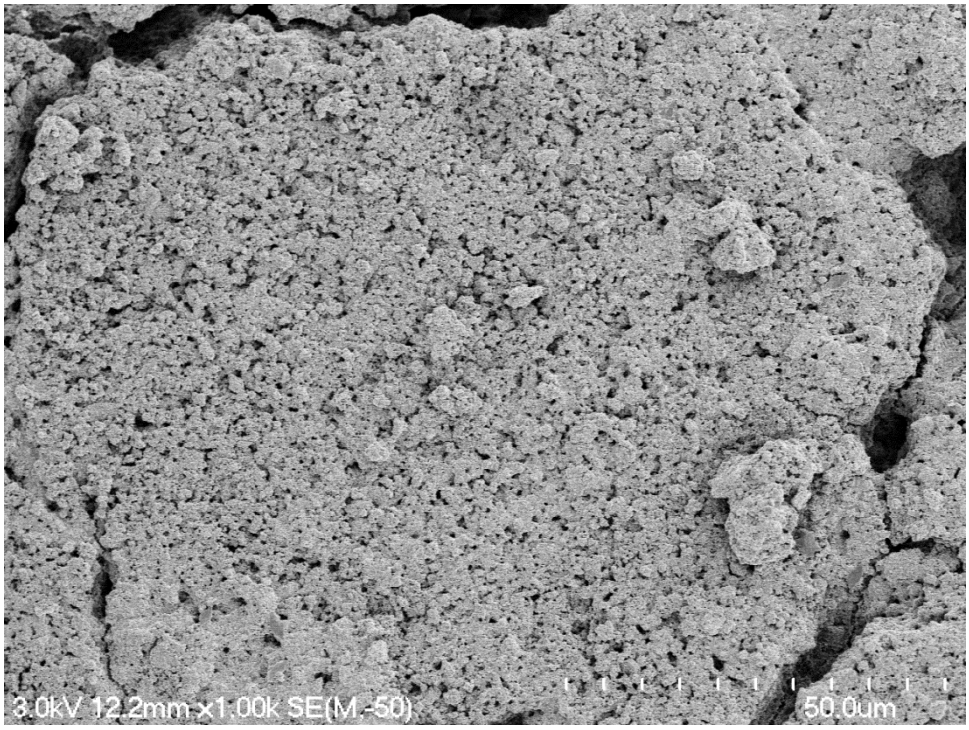

Figure 6.59: Pores can still be seen in the remoulded RS1 sample suggesting a partially open structure following remoulding.

6.3.3 Summary of Microstructural Characteristics

Microstructural trends and characteristics between all sites have been tabulated for comparison (Table 6.12). The results indicate that samples from all sites displayed some form of matrix type microstructure. Honeycomb and laminar microstructures were not observed at all, while only TPS1 indicated some form of turbulent microstructure. Particle interactions at all sites were in the form of face to face and almost always edge to edge contact with the exception of TPS1. Particle matrices were the most common form of particle assemblage within all samples, whereas aggregations were somewhat rarer. Porosity was generally observed in the form of micro-pores at all sites, although larger sized pores were generally observed in the samples from Tauriko.

Table 6.12: Summary microstructural characteristics from all samples examined in this study.

	Microstructure					Individual Particle Interaction			Particle Assemblages			Porosity			
Sample	**Honeycomb**	**Skeletal**	**Matrix**	**Turbulent**	**Laminar**	**Face to face**	**Edge to edge**	**Face to edge**	**Connectors**	**Aggregations**	**Particle matrices**	**Ultra-pore**	**Micro-pore**	**Meso-pore**	**Macro-pore**
OS1	-	●	●	-	-	●	●	●	-	-	●	●	●	-	-
OS2	-	●	●	-	-	●	●	●	-	-	●	●	●	-	-
OLRO	-	-	●	-	-	●	●	-	●	-	●	-	●	-	-
TPS1	-	-	●	●	-	●	-	●	-	●	●	-	●	-	●
PS1	-	●	●	-	-	●	●	●	●	●	●	-	●	-	- -
PS2	-	●	●	-	-	●	●	●	●	●	●	-	●	-	
TS1	-	-	●	-	-	●	●	-	●	-	●	-	●	●	●
TS2	-	-	●	-	-	●	●	-	●	-	●	-	●	●	●
TS3	-	-	●	-	-	●	●	-	●	-	●	-	●	●	●
TS4	-	-	●	-	-	●	●	-	●	-	●	-	●	●	●
RS1	-	-	●	-	-	●	●	●	-	-	●	-	●	-	-

6.4 **Summary**

Mineralogical and microstructural analyses of 11 samples from Omokoroa, Te Puna, Pahoia Peninsula, Tauriko and Rangataua Bay were undertaken. XRD revealed that all samples had a typical composition dominated by halloysite (both 1.0 nm and 0.7 nm forms) together with quartz, plagioclase feldspar, cristobalite, and glass shards and pumice grains. SEM investigation confirmed the prevalence of halloysite, which was manifest as spheres, tubes, and plates, and books including very large halloysite books, up to coarse sand size, previously undocumented. SEM analysis revealed that vesicular and cuspate glass and pumice fragments comprised the majority of non-clay material in most samples.

Microstructural characterisation indicated that most samples conformed to a matrix-skeletal type classification. The exceptions were TPS1 from Te Puna which had a matrix-tubulent structure and all samples from Tauriko and Rangataua Bay which had a matrix structure. The process of remoulding generally indicated the destruction of some plates, books and tubes, while structures generally remained porous.

Chapter 7

STATISTICAL ANALYSIS

7.1 Introduction

A statistical analysis was undertaken to determine relationships between measured soil properties in an attempt to predict and characterise the sensitivity of weathered rhyolitic materials. Non-sensitive materials were not used in the analysis, given that the properties of sensitive materials are of most interest and no calculated value of sensitivity could be attained for those materials. Without sensitivity values, the relationship of any other parameters with the sensitive material equivalent could not be statistically quantified. The following chapter describes the relationships between a range of measured variables (from Chapters 4, 5 and 6) and their role in helping to identify characteristics of sensitivity. Primarily, linear regression was used to analyse the regression and correlation characteristics. Where appropriate data was available, previous studies analysing sensitivity in the Tauranga region (Keam 2008; Wyatt 2009; Arthurs 2010) were also used in characterisation.

7.2 Data analysed

Initially, data regarding geomechanical parameters and petrography observations both from this study and others was collated (Table 7.1). It should be noted that one sample site (Otumoetai S3) from Wyatt (2009) was omitted from the analysis. Inspection of the results suggested that sensitivity of the sample was possibly overestimated and inaccurate; reasons for this judgement are further discussed in Chapter 8.

Sensitivity was measured in Chapters 4 and 5 by both laboratory and field shear vanes, however for this statistical analysis only the field shear vane was included as it was comparable with other studies.

Table 7.1: Summary table of the data used in the statistical analysis. The data includes both sensitive and non-sensitive sites from the Tauranga region. Data is included from this study, Arthurs (2010), Wyatt (2009) and Keam (2008). THV indicates that the soil was too hard for shear vane penetration, while NP suggests that the soil was non-plastic (according to the NZS 4402) and NCS indicates that the soil was not cohesive.

		Field Shear Vane			Soil Properties						Atterberg Limits					Particle Size			Yield Stress	Triaxial (Consolidated, Undrained)		Minerals				
	Sample	Mean Peak Strength (kPa)	Mean Remoulded Strength (kPa)	Mean Sensitivity	Moisture Content (%)	Wet Bulk Density (kgm^{-3})	Dry Bulk Density (kgm^{-3})	Particle Density (kg/m^3)	Porosity (%)	Voids Ratio	Liquid Limit (%)	Plastic Limit (%)	Plasticity Index (%)	Liquidity Index (%)	Activity	Clay (%)	Silt (%)	Sand (%)	Yield Stress	Effective Cohesion	Effective Friction angle	Halloyiste	Kaolinite	Cristobailte	Plagioclase Feldspar	Quartz
This study (2012)	**OS1**	92	8	11	84.0	1535.0	834.24	2410.0	65.38	1.89	72.30	45.66	26.6	1.44	2.59	10.29	49.11	40.60	213.4	8.0	37.0	Yes	No	Yes	Yes	Yes
	OS2	74	5	15	89.3	1475.0	779.19	2420.0	67.80	2.11	73.57	51.47	22.1	1.71	10.21	2.2	73.4	24.4	214.7	16.0	28.0	Yes	No	Yes	Yes	Yes
	OLRO	-	-	-	42.4	-	-	2550.0	-	-	39.90	24.09	15.8	1.16	1.47	10.7	26.9	62.3	253.4	-	-	Yes	Yes	No	Yes	Yes
	TPS1	122	12	11	108.8	1436.3	687.7	2220.0	69.02	2.23	89.36	45.74	43.6	1.45	14.74	2.96	76.1	20.9	219.9	16.0	41.0	Yes	No	Yes	Yes	Yes
	PS1	69	6	11	67.5	1633.4	975.1	2530.0	61.46	1.59	52.86	34.28	18.6	1.79	3.74	4.97	84.6	10.4	181.5	15.0	32.0	Yes	No	Yes	Yes	Yes
	PS2	67	8	9	70.0	1618.9	952.2	2610.0	63.51	1.74	53.64	35.76	17.9	1.91	2.65	6.75	69.5	23.7	154.0	10.0	36.0	Yes	No	Yes	Yes	Yes
	RS1	THV	THV	THV	46.3	1721.0	1176.6	2390.0	50.77	1.03	52.65	37.13	15.5	0.59	0.51	30.4	59.5	10.0	-	-	-	Yes	No	No	Yes	Yes
	TS1	NCS	NCS	NCS	31.6	1289.8	980.02	2372.2	58.69	1.42	39.41	NP	NP	-	-	5.05	22.5	72.4	-	-	-	Yes	Yes	Yes	Yes	No
	TS2	NCS	NCS	NCS	23.4	1346.9	1091.67	2348.4	53.51	1.15	44.37	NP	NP	-	-	4.35	24.6	70.9	-	-	-	Yes	Yes	Yes	No	Yes
	TS3	NCS	NCS	NCS	23.3	1124.8	912.62	2258.4	59.59	1.47	59.39	NP	NP	-	-	2.40	14.1	83.4	-	-	-	Yes	Yes	No	Yes	Yes
	TS4	NCS	NCS	NCS	26.1	1133.8	899.34	2219.3	59.48	1.47	58.10	NP	NP	-	-	3.25	17.4	79.3	-	-	-	Yes	Yes	No	Yes	Yes
Arthurs (2010)	**Omokoroa**	112	11	10	80.1	1500.6	839.7	-	56.0	-	69.7	40.7	29.1	1.30	-	-	-	-	-	52.0	29.0	Yes	Yes	No	Yes	Yes
	Otumoetai	-	-	-	99.8	1470.5	737.5	-	33.3	-	98.0	66.0	32.0	0.50	-	-	-	-	-	52.0	31.0	Yes	Yes	No	Yes	Yes
	Te Puna	53	4	13	100.7	1413.3	675.0	-	33.0	-	93.0	52.0	40.0	1.20	-	-	-	-	-	14.0	37.0	Yes	Yes	No	Yes	Yes
	Pahoia Peninsula	161	11	15	57.6	1557.1	985.8	-	36.0	-	51.0	33.0	18.0	1.51	-	-	-	-	-	36.0	23.5	Yes	Yes	No	Yes	Yes
Wyatt (2009)	**Tauriko S1**	58	6	10	115.0	1280.0	656.0	2532.0	74.1	2.9	81.3	56.9	24.4	2.39	4.3	5.7	81.2	13.1	-	11.8	27.3	Yes	No	No	Yes	Yes
	Tauriko S2	45	2	23	109.0	1273.0	589.0	2591.0	77.3	3.4	72.7	46.7	26.0	2.41	3.6	7.2	82.9	9.9	-	-	-	Yes	No	No	Yes	Yes
	Tauriko S3	151	34	4	64.0	1581.0	966.0	2542.0	62.0	1.6	52.0	38.7	13.2	1.88	1.6	8.3	80.4	11.3	-	24.0	31.1	Yes	No	No	Yes	Yes
	Otumoetai S1	101	13	8	104.0	1358.0	656.0	2636.0	75.1	3.0	90.0	47.3	42.7	1.33	4.3	10.0	65.4	24.5	-	34.5	25.7	Yes	No	Yes	No	Yes
	Otumoetai S2	125	15	8	69.0	1497.0	893.0	2664.0	66.5	2.0	57.4	32.4	25.0	1.46	3.9	6.4	40.6	52.9	-	4.7	38.5	Yes	No	No	No	Yes
	Otumoetai S4	72	14	5	86.0	1407.0	743.0	2686.0	72.3	2.6	73.0	36.8	36.2	1.35	18.3	2.0	51.2	46.9	-	13.7	28.5	Yes	Yes	No	No	Yes
Keam (2008)	**Omokoroa**	102	10	11	67.0	1886.7	1195.7	-	59.3	-	60.5	46.5	14.0	3.44	-	-	-	-	-	18.9	52.9	Yes	Yes	Yes	Yes	Yes

7.3 Correlation and parameter determination

A correlation matrix of 20 potential parameters (all data from Table 7.1, excluding the non-quantified mineralogy determinations) measured in this study was derived (Table 7.2). The correlation matrix identified which parameters provided suitable correlations for further plotted analysis. Only linear regression coefficients were analysed as opposed to logarithmic and exponential relationships, as the small dataset available to this study meant that such complex relationships would not likely be determined with any realistic confidence (Moore and McCabe 2003). Correlation analyses are useful indicators of the strength of a linear relationship between parameters and determining how predictable one parameter is from another (Watts and Halliwell 1996). Correlation coefficients (R) of + 0.90 to + 1.00 and - 0.90 to - 1.00 were categorised as very strong correlations, while coefficients of + 0.75 to + 0.89 and - 0.75 to - 0.89 represented a strong correlation. These divisions were based on the work of Beattie (1990) and Bell (2007). Beattie (1990), based off the work of Moon (1989), previously incorporated R values as low as 0.70 under a strong classification, which was also adapted by Bell (2007), however this tended to include unreliable relationships upon further plotted analysis. Considering this, an arbitrary cut-off point for correlation of R = 0.75 is used in this study, which is above the commonly used R value of 0.70 typically used for environmental and geotechnical analysis (Bell 2007).

The presence of a high correlation between two variables, however, does not automatically imply one directly results in the other's occurrence (Bell 2007). Several variables that displayed correlation coefficients of strong and very strong values were analysed further by plotting the variables as scatterplots based on this matrix. The construction of scatterplots helped to identify outliers and clusters which meant that artificially high correlation coefficients could be discarded. Values that were closely related in calculation, i.e. porosity and void ratio, were typically not treated separately in their relationship with other parameters. Therefore any correlations above + 0.75 or – 0.75 that are not plotted in this chapter are because they were influenced by the biasing factors aforementioned.

Table 7.2: Linear correlation matrix from 20 parameters used to characterise sensitivity. The correlation matrix is only of the data derived from this study. Values between +0.90 to +1.00 and -0.90 to -1.00 were categorised as very strong correlations, while coefficients of +0.75 to +0.89 and -0.75 to -0.89 represented a strong correlation.

	Mean peak strength	Mean sensitivity	Moisture content	Wet bulk density	Dry bulk density	Particle density	Porosity	Voids ratio	Liquid limit	Plastic limit	Plasticity index	Liquidity index	Activity	Clay	Silt	Sand	Yield stress	Effective cohesion	Effective friction angle	Mean remoulded strength
Mean peak strength	1.00																			
Mean sensitivity	-0.03	1.00																		
Moisture content	0.90	0.33	1.00																	
Wet bulk density	-0.76	-0.54	-0.96	1.00																
Dry Bulk density	-0.75	-0.46	-0.95	0.95	1.00															
Particle density	-0.93	-0.33	-0.96	0.90	0.87	1.00														
Porosity	0.56	0.46	0.84	-0.86	-0.96	-0.69	1.00													
Voids ratio	0.59	0.46	0.85	-0.87	-0.96	-0.72	1.00	1.00												
Liquid limit	0.89	0.37	0.99	-0.97	-0.91	-0.97	0.77	0.78	1.00											
Plastic limit	0.44	0.75	0.73	-0.88	-0.74	-0.67	0.66	0.66	0.79	1.00										
Plasticity index	0.99	0.02	0.93	-0.80	-0.82	-0.94	0.65	0.68	0.91	0.45	1.00									
Liquidity index	-0.51	-0.02	-0.36	0.36	0.10	0.48	0.16	0.14	-0.49	-0.44	-0.41	1.00								
Activity	0.70	0.46	0.89	-0.87	-0.97	-0.83	0.95	0.96	0.83	0.60	0.78	0.07	1.00							
Clay	-0.13	-0.55	-0.41	0.45	0.65	0.34	-0.77	-0.77	-0.31	-0.28	-0.25	-0.61	-0.78	1.00						
Silt	-0.14	0.13	-0.07	0.13	-0.14	0.06	0.27	0.28	-0.19	-0.34	-0.04	0.81	0.37	-0.79	1.00					
Sand	0.21	0.00	0.21	-0.29	-0.02	-0.17	-0.10	-0.11	0.33	0.50	0.13	-0.80	-0.21	0.66	-0.98	1.00				
Yield stress	0.66	0.60	0.75	-0.82	-0.64	-0.83	0.43	0.45	0.84	0.84	0.63	-0.72	0.54	-0.09	-0.36	0.47	1.00			
Effective cohesion	0.19	0.56	0.40	-0.41	-0.59	-0.41	0.64	0.66	0.31	0.22	0.30	0.50	0.75	-0.95	0.83	-0.72	0.19	1.00		
Effective friction angle	0.75	-0.68	0.44	-0.22	-0.24	-0.46	0.10	0.12	0.42	-0.13	0.71	-0.41	0.19	0.32	-0.28	0.24	0.11	-0.30	1.00	
Mean remoulded strength	0.89	-0.46	0.67	-0.46	-0.52	-0.67	0.39	0.40	0.63	0.06	0.88	-0.34	0.49	0.03	-0.11	0.13	0.26	-0.01	0.95	1.00

7.4 Linear regression relationships

7.4.1 Shear strength (peak strength, remoulded strength, effective cohesion and friction angle)

Shear strength characteristics are perhaps the most fundamental aspects in characterising sensitivity. The factors that influence the peak and remoulded shear strengths inherently influence the value of sensitivity and so understanding these interactions is critical. From the correlation matrix, nine useful correlation relationships were established:

- Mean peak strength and mean remoulded strength (7.4.1.1)
- Mean peak strength and particle density (7.4.1.2)
- Mean peak strength and bulk density (wet and dry) (7.4.1.2)
- Mean peak strength and moisture content (7.4.1.3)
- Mean peak strength and liquid limit (7.4.1.3)
- Mean peak strength and plasticity index (7.4.1.5)
- Mean peak strength and activity (7.4.1.5)
- Mean remoulded strength and effective friction angle (7.4.1.4)
- Effective cohesion and clay content (7.4.1.5)

7.4.1.1 Peak and remoulded strength

The relationship between mean peak and mean remoulded strength is characterised by a positive linear trend (R = 0.89) (Figure 7.1). Adding data based on two previous studies into sensitivity in the Tauranga region (Wyatt 2009; Arthurs 2010) indicates a similar result where the relationship remains reasonably consistent (R = 0.70). Fundamentally, the relationship indicates that as peak strength increases, remoulded strength also increases. The rate of increase is slightly less for the regression based on the values from this study as opposed to the combination of all three studies, indicating that at the same peak strength values, remoulded strengths are lower, thus giving a higher mean sensitivity value. than previously seen in other studies.

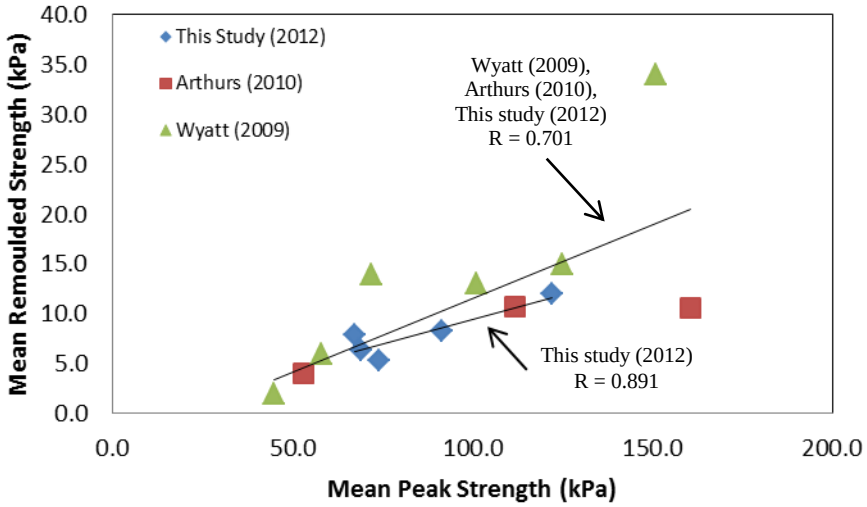

Figure 7.1: Correlation scatterplot between mean peak strength and mean remoulded strength for sensitive soils from the Tauranga region.

7.4.1.2 Peak strength and soil density

The regression model between mean peak strength and wet bulk density indicated a negative trending relationship (Figure 7.2). The relationship suggested that as wet bulk density increased, mean peak strength decreased. This correlation is primarily due to the weathered state of the soil materials. Lower density of rhyolitic tephra deposits suggests that more clay has been produced from the dissolution and precipitation of volcanic glass (McLaren and Cameron 1996). Hence, the clay minerals are expected exhibit greater cohesion (as opposed to frictional strength) and thus higher peak strength (Craig 1997). The trend was

generally consistent across the majority of samples, however the regression fit was severely undervalued due to one outlier from OS2 (producing a correlation coefficient of R = 0.76). While this trend is generally not confined to sensitive only material (Craig 1997), it indicates that peak strength of sensitive materials does behave in a similar manner to non-sensitive material as a result of wet bulk density variation. As expected, dry bulk density displays a near identical relationship as wet bulk density (R = 0.75).

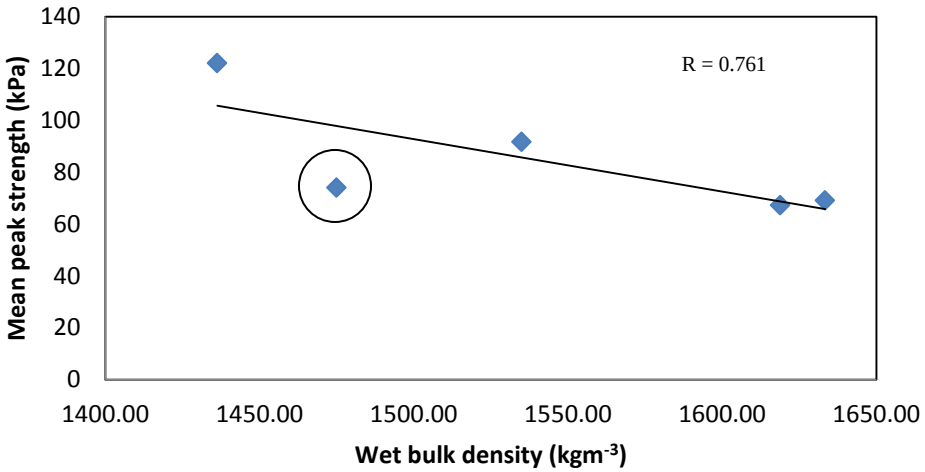

Figure 7.2: Scatterplot graph showing the correlation of mean peak strength and wet bulk density from only the sensitive material from this study. The main outlier of OS2 is circled.

Mean peak strength also indicated a strong correlation with particle density (R = 0.93) (Figure 7.3). The relationship was again negative trending, and showed that as particle density decreased, a simultaneous increase in peak strength was attained. The highest particle density and subsequent lowest mean peak strength was from PS1. Conversely, the highest mean peak strength was observed at TPS1 which had the lowest particle density of 2220 kg m^{-3}. While it would be typically expected that, in a cohesion dominated system, the lowest particle density (greatest clay component) would have the highest mean peak strength (Craig 1997), the relationship observed here would appear to be principally controlled by the morphology of the clay constituents. Primarily, the high peak strength of TPS1 is likely a result of the plate material observed in Chapter 6. It would be expected that plate morphologies display greater resistance to initial peak shear compared to other morphology types considering that plates can have larger face-to-face and face-to-edge contact and do not move easily past one another upon shearing.

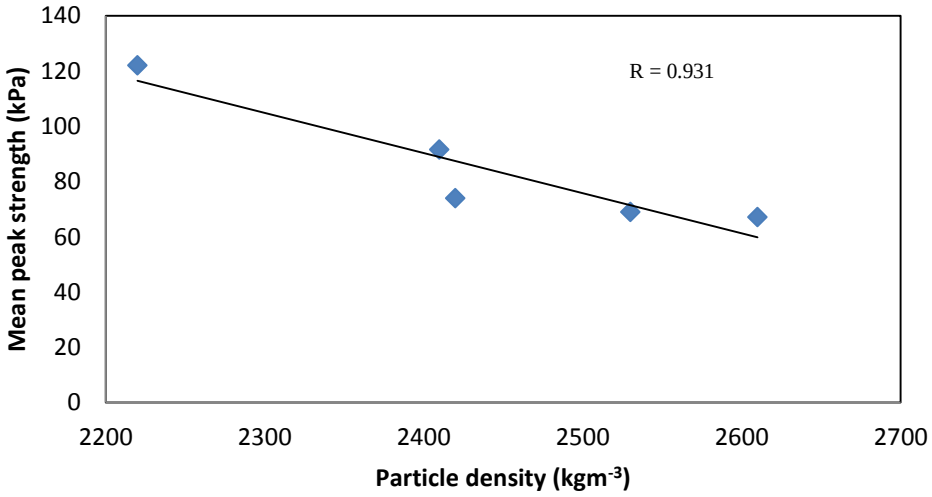

Figure 7.3: Scatterplot relationship showing the negative correlation between particle density and mean peak strength from sensitive soils from the Tauranga region.

7.4.1.3 Mean peak strength, moisture content and liquid limit

The mean peak strength relationship with moisture content indicated opposing correlations between the data from this study and three previous studies from the Tauranga region (Keam 2008; Wyatt 2009; Arthurs 2010). A strong positive correlation (R = 0.93) between mean peak strength and moisture content existed for the sensitive samples analysed from this study, while a negative trending relationship occurred when all studies were analysed together (R = 0.55) (Figure 7.4). The positive relationship from the results of this study is primarily because of TPS1 which had a high peak strength yet also comparatively high moisture content. It would appear that the presence of plate morphology halloysite clay forming a partially flocculated structure in conjunction with regular spheres and tubes (see Chapter 6), allowed for the higher moisture contents to develop. As mentioned earlier, the plate morphologies were expected to provide a greater frictional resistance to shearing as the particle size provides greater surface area. Such plate features likely promote the development of a higher mean peak strength. When removing TPS1, a reduction in peak strength with moisture content across all studies is apparent. Considering the relative variability between different samples, it could be established that moisture content values above ~ 60 % are required for sensitivity, however, variation above such levels is not critical in peak strength determination for sensitive deposits. Furthermore, clay microstructure appears to be important, where if all samples were composed of a

similar structure, a consistent decrease in peak strength with moisture content might be expected. Where particle morphology variation is apparent, deviations from this trend should be expected given that particle morphologies such as books and plates tend to flocculate a soil structure leading to larger pore spaces and possibly a high moisture content.

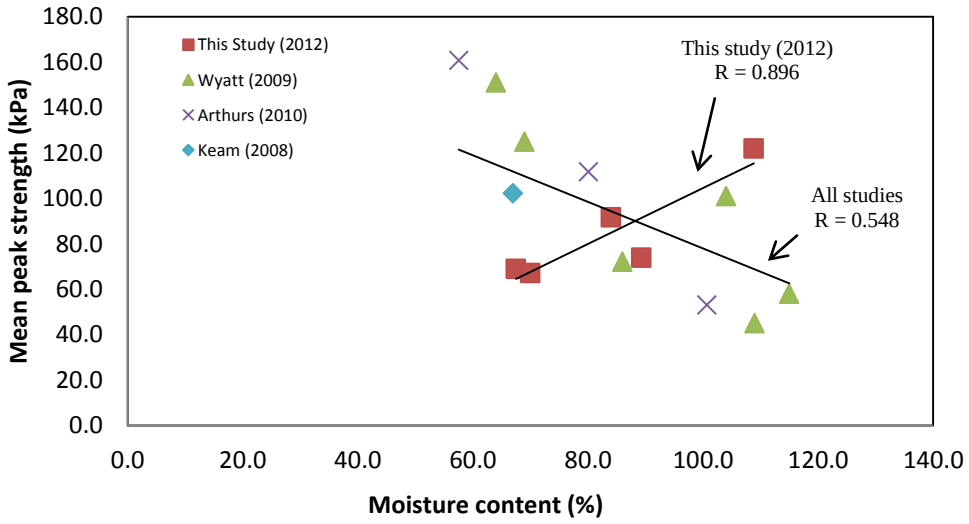

Figure 7.4: Contrasting correlation relationship between moisture content and mean peak strength for sensitive soils from the Tauranga region. The results from this study indicate a positive correlation, while with the addition of multiple studies, a negative relationship is produced.

Mean peak strength also displayed a similar relationship with liquid limit, where a strong correlation (R = 0.89) was observed for the samples from this study. However, in comparing the data with those from previous studies, the regression reduces dramatically (R = 0.17) (Figure 7.5). This indicates that the use of the liquid limit solely (as a single Atterberg parameter in isolation) as a predictor for sensitivity is not appropriate due to its unreliable relationship with mean peak strength between studies.

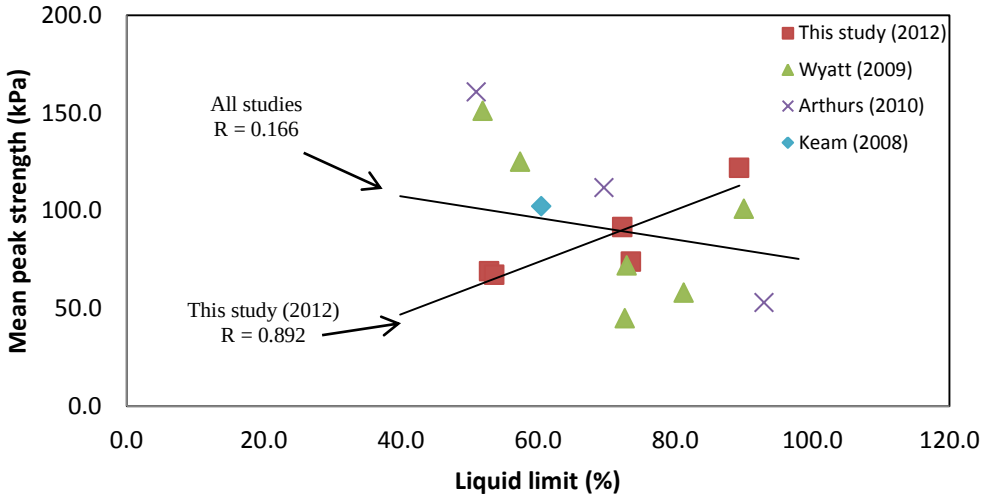

Figure 7.5: Scatterplot correlation between mean peak strength and the liquid limit for the sensitive samples from both this study and others from the Tauranga region.

7.4.1.4 Mean remoulded strength and effective friction angle

In correlating the effective friction angle with mean remoulded strength from the sensitive materials analysed in this study (Figure 7.6), a strong positive linear relationship is produced (R = 0.95). The plot shows that as the effective friction angle increases, the mean remoulded strength also increases. This relationship suggests that soil materials with low peak friction angles also have low remoulded strength, meaning that they may be particularly prone to sensitive failure.

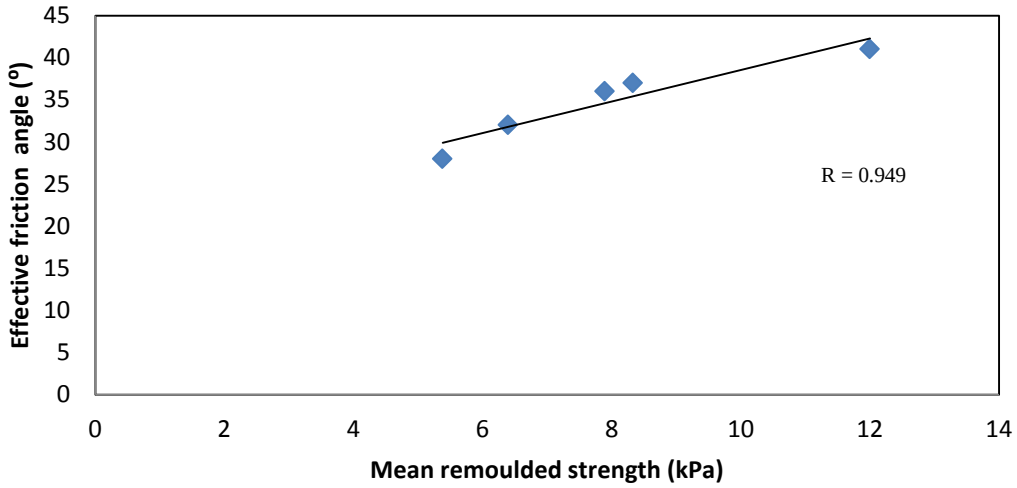

Figure 7.6: Correlation relationship between effective friction and mean remoulded strength for sensitive samples from this study.

7.4.1.5 Mean peak strength, activity, plasticity index, effective cohesion and clay content

Mean peak strength indicated a strong positive correlation with plasticity index for the sensitive samples from this study (Figure 7.7). Such a strong relationship would typically be expected, given that for a plasticity index to increase, either the liquid limit must decrease, the plastic limit increase, or both. Hence, as the range that a soil remains in plastic state increases, a greater peak strength would be expected because of the greater cohesion associated with the soil plasticity (Gratchev *et al.* 2006). Given the plasticity index is partially derived from the liquid limit, the positive correlation with only the data from this study is expected following the relationship seen in Figure 7.8. When analysing multiple study data for the same correlation (Keam 2008; Wyatt 2009; Arthurs 2010), however, the correlation disappears (R = 0.15) and the points become scattered, suggesting plasticity index is not a reliable predictor for mean peak strength for sensitive soils from the Tauranga region. Furthermore, the majority of plasticity indices for the sensitive material for all studies were < 30 %, while some peak strengths for material were recorded up to 160 kPa, suggesting that high peak strengths could still develop from low plasticity indices in sensitive material. This relationship would indicate that the clay mineralogy and morphology within the microstructure are dominating factors (Gratchev *et al.* 2006) as opposed to the clay particle component or cohesive properties. Activity variation also indicated an expected positive correlation as a function of the plasticity index relationship, however, it was not considered strong (R < 0.75) (Figure 7.8).

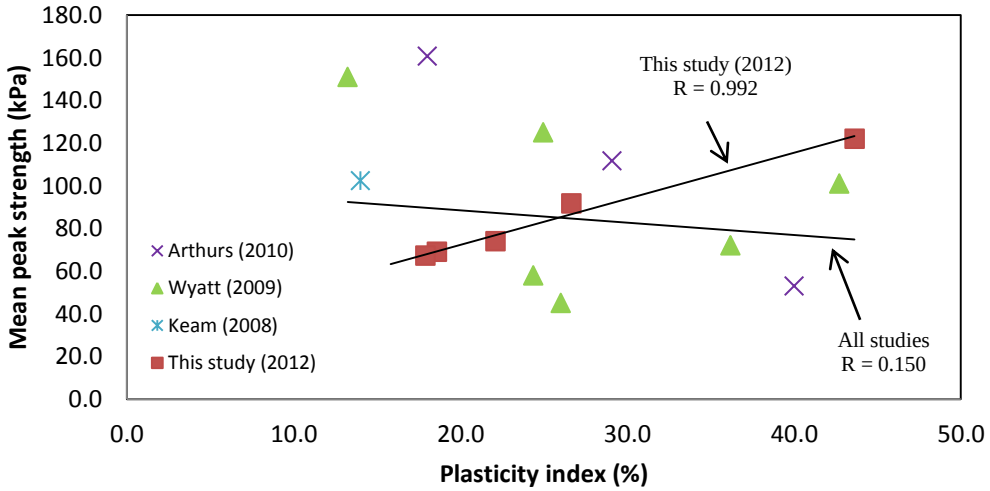

Figure 7.7: Scatterplot between plasticity index and mean peak strength indicating a positive linear relationship for samples from this study. When multiple study datata is added the relationship becomes negative trending.

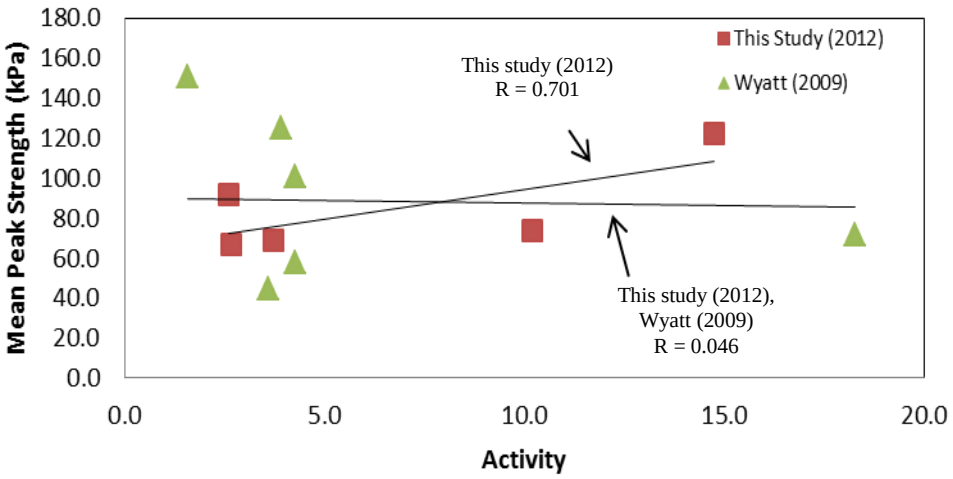

Figure 7.8: Scatterplot correlation between mean peak strength and the Activity for the sensitive samples from both this study and Wyatt (2009).

The negative relationship of effective cohesion and clay content is surprising (Figure 7.9). Typically, effective cohesion is expected to increase with clay content (Selby 1993; Craig 1997), however, this was not observed for the sensitive materials. Based on this evidence, the cohesion exhibited by the clay materials from the sensitive material therefore does not act to promote cohesive behaviour, suggesting small increases in clay content (below ~ 11 %) do not reduce sensitivity potential. This would indicate that the influence of clay morphology interaction within the microstructure is again a critical factor, rather than the relative amount of clay.

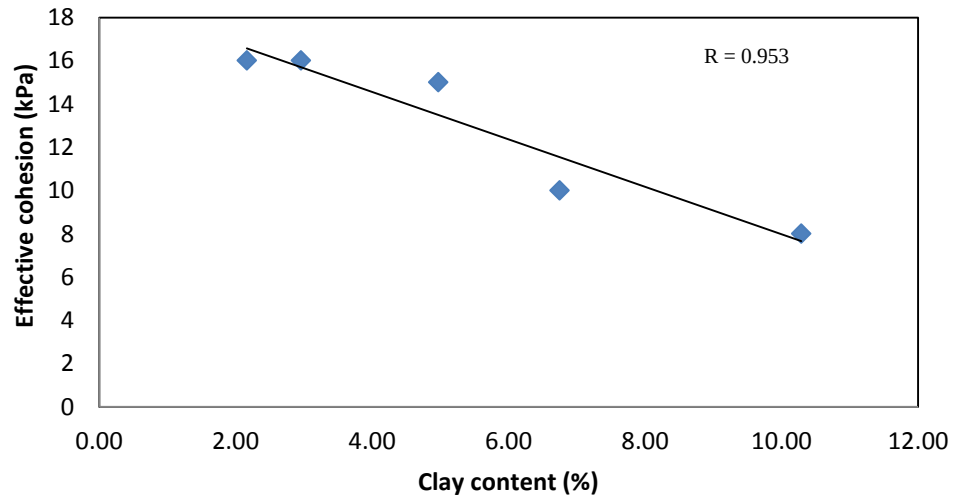

Figure 7.9: Scatterplot correlation between particle size of the clay fraction and effective cohesion for the sensitive samples from this study.

7.4.2 Moisture content, bulk density, porosity and void ratio

Moisture content has historically proven to be a key factor for sensitivity (Jacquet 1990; Rankka *et al.* 2004; Mitchell and Soga 2005). Previous studies investigating sensitivity in the Tauranga region have identified high moisture contents within the sensitive material encountered (Gulliver and Houghton 1980; Wesley 2007; Keam 2008; Wyatt 2009; Arthurs 2010). Furthermore, as a mechanism for sensitivity, the release of considerable moisture stored within the soil microstructure is paramount in promoting fluidised behaviour upon remoulding. The relationship of moisture content to wet bulk density, void ratio and porosity therefore provide suitable predictors for identifying whether a soil may be prone to sensitive behaviour. Relationships between these parameters and moisture content are presented in Figures 7.10 – 7.12.

7.4.2.1 Moisture content, porosity and void Ratio

Porosity and void ratio both expectedly produced a positive correlation with moisture content (R = 0.76 and 0.81 respectively) (Figures 7.10, 7.11). Porosity and void ratio are interrelated and both impact the available moisture content, given that a more porous sample with a greater void ratio can hold more water within available voids, hence giving a positive correlation with moisture content. This feature is particularly important in characterising sensitivity as the ability for a sensitive soil to become very wet to saturated, often well in excess of the liquid limit, is a characteristic of not only sensitivity encountered in Tauranga, but also internationally (Skempton and Northey1952; Mitchell and Soga 2005; Wesley 2007; Wyatt 2009).

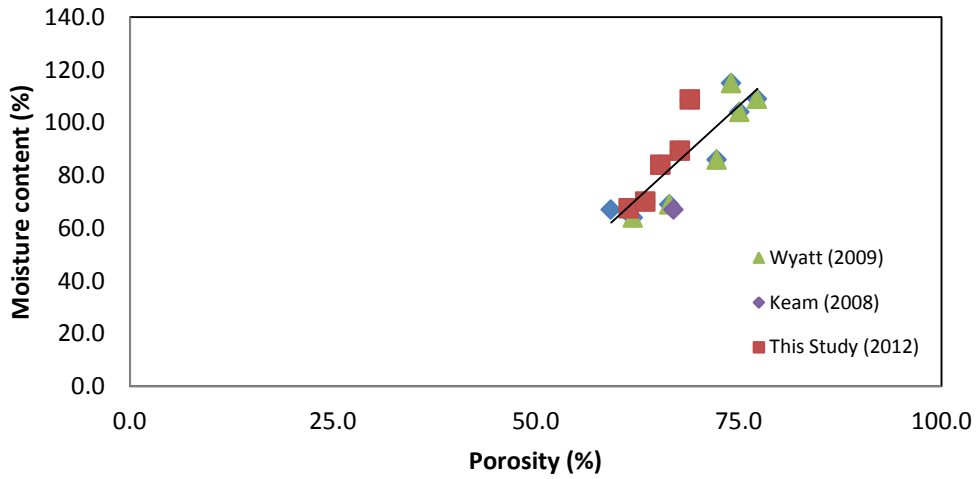

Figure 7.10: Scatterplot indicating a positive linear correlation between porosity and moisture content for sensitive material from the Tauranga region.

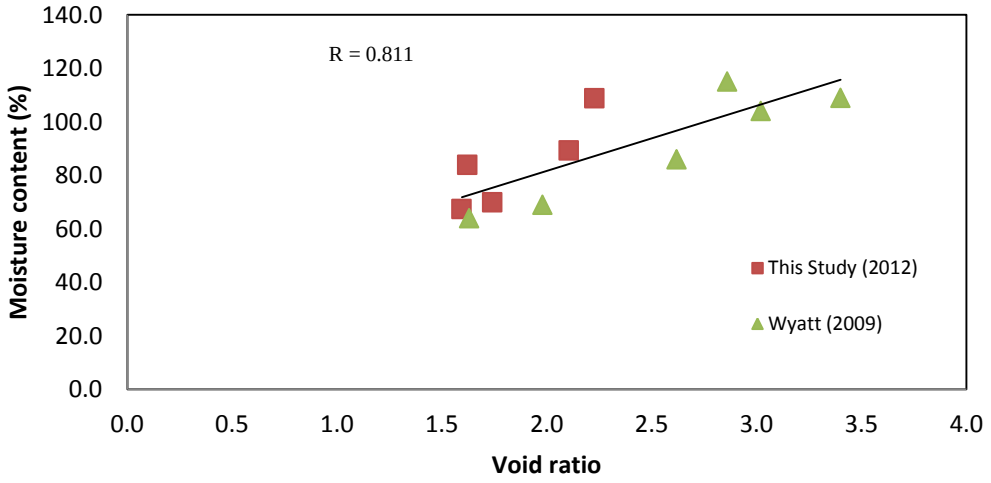

Figure 7.11: Scatterplot graph showing the correlation between void ratio and moisture content from this study and Wyatt (2009).

7.4.2.2 Moisture content, wet bulk density and liquid limit

Moisture content indicated a negative trending correlation with wet bulk density (Figure 7.12). This relationship is expected given that bulk density represents the measure of soil mass per unit volume, meaning those samples with lower moisture content have a higher bulk density due to the reduced amount of pores within the sample. The liquid limit also displayed an expected trend with moisture content, with a strong positive correlation from the sensitive samples

from this study (Figure 7.13). The trend indicates that as the moisture content increases, the clay minerals in the sample adsorb water to their structure leading to the slight increase in liquid limit with moisture content. Halloysite clays are typically low swelling clays (Selby 1993), yet still support interlayer water, which is consistent with the moderate to low slope gradient of the relationship. When incorporating the results of Keam (2008), Wyatt (2009) and Arthurs (2010), the correlation coefficient is consistent, indicating this trend is common with sensitivity throughout the Tauranga region.

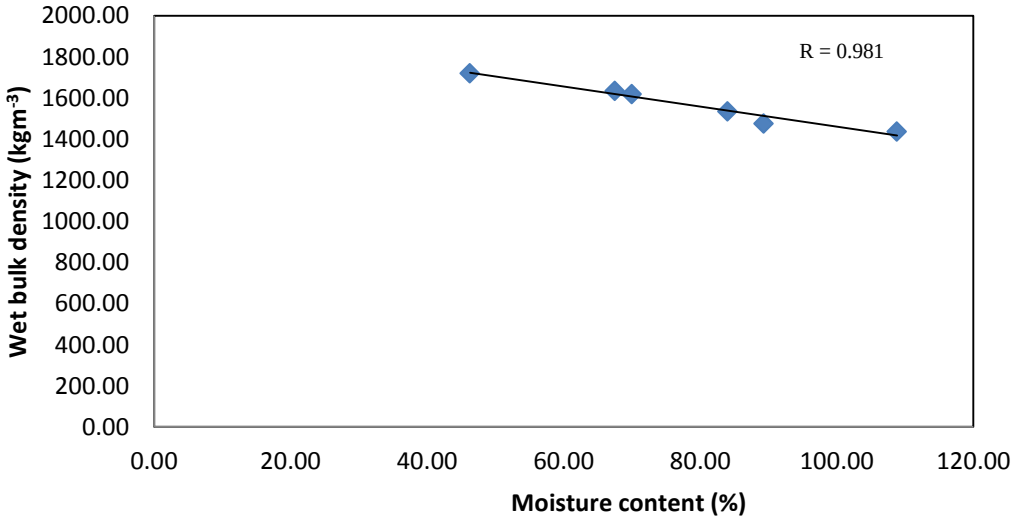

Figure 7.12: Scatterplot correlation graph between moisture content and wet bulk density for the sensitive material from this study.

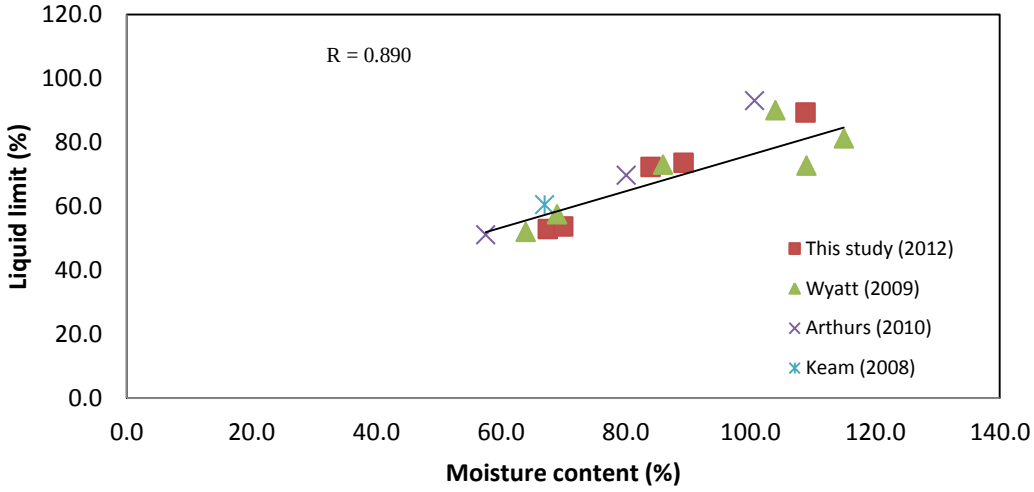

Figure 7.13: Scatterplot graph showing the correlation between moisture content and liquid limit from multiple studies in the Tauranga region.

7.4.2.3 Moisture content and plasticity index

The correlations of activity and plasticity index with moisture content similarly produced an expected positive relationship (Figure 7.14). Again, given that activity is a function of the plasticity index, the similar positive linear relationship between both factors with moisture content is expected. In terms of the plasticity index, as the value increases, the range of moisture at which the soil remains plastic is also higher. The increase of plasticity index with moisture content is expected, given that as the moisture content increases, the halloysite clays adsorb more water to their surface and possibly within the structure (similar to Figure 7.13) . Given that this trend is not specifically identifiable for sensitive material, it does not appear to act as a good predictor for sensitive materials.

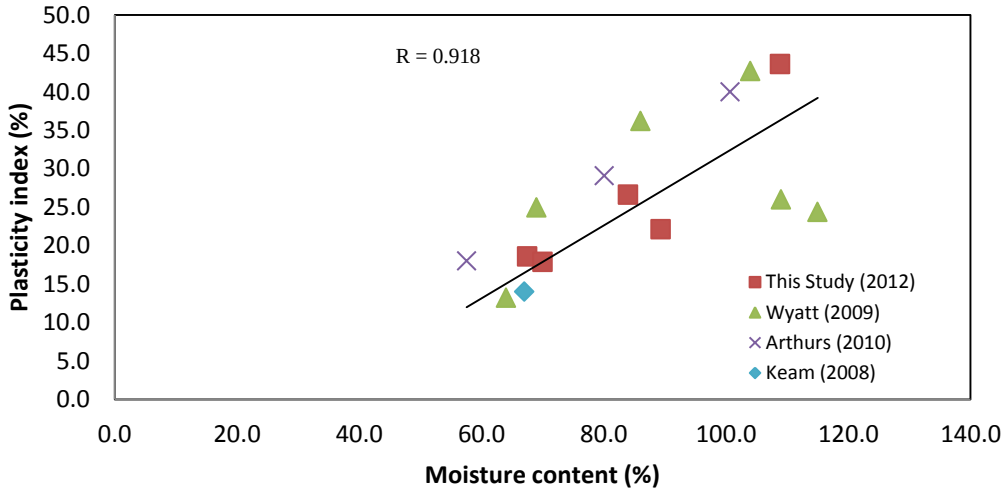

Figure 7.14: Scatterplot graph showing the correlation between moisture content and plasticity index for sensitive materials from the Tauranga region.

7.4.3 Particle density and size

Particle density showed strong relationships with mean peak strength (as mentioned in Section 7.3.1.1.2), liquidity index (Figure 7.16), moisture content (Figure 7.17), wet bulk density (Figure 7.18), activity (Figure 7.17) and yield stress (Figure 7.18). Surprisingly, it did not correlate well with any of the particle size measurements ($R < 0.34$), indicating that one single particle size class range does not have a distinguishing effect on the particle density outcome for sensitive soils from this study.

7.4.3.1 Particle density and liquidity index

Liquidity index is positively correlated with particle density (R = 0.86) (Figure 7.15). As particle density increases, the liquidity index also responds with an increasing trend. The trend was relatively flat with a range of only 0.56 between all liquidity indices. The slightly increasing trend does, however, indicate that particles of a lower particle density (such as clay) tend to promote a lower liquidity index, which would correspond with a lower sensitivity (Skempton and Northey 1952; Wyatt 2009). No such trend was apparent between the actual sensitivity of the material and particle size. The relationship between particle density and liquidity index may alternatively be an indicator of the degree of weathering that each sample has been subjected to. As minerals are weathered from primary to secondary states a reduction in particle density is expected due to the increase of interlayer space within the clay lattice. Hence it could be suggested that as the samples become more weathered, the liquidity index decreases, however, the very slight incline in slope indicates that the relationship is relatively inconsequential.

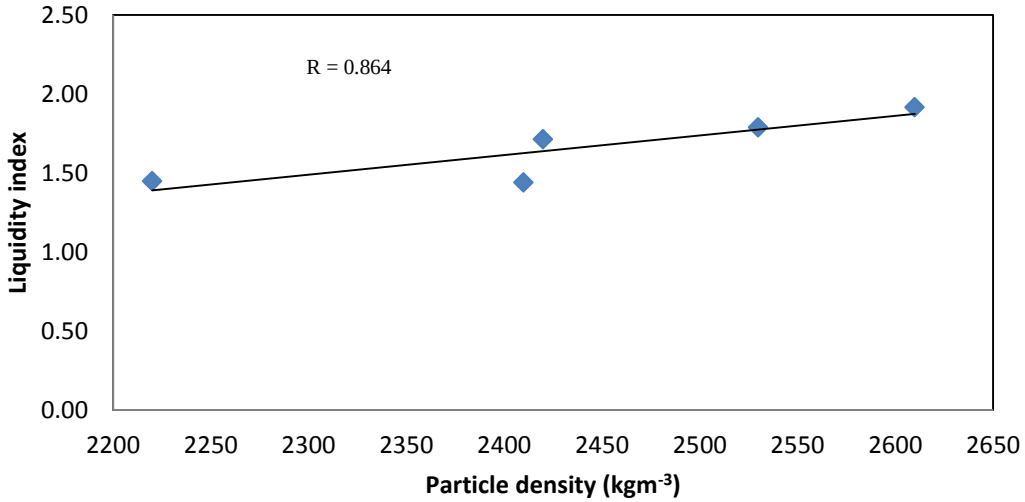

Figure 7.15: Correlation scatterplot between particle density and liquidity index.

7.4.3.2 Particle density, moisture content and wet bulk density

Two closely related parameters to liquidity index, which display opposing relationships with particle density, are moisture content and bulk density. Moisture content variation displays a consistent negative correlation with particle density (R = 0.96) (Figure 7.16). Sensitive samples with the lowest moisture

contents (PS1 and PS2) have the highest particle density, while the sample with the highest moisture content has the lowest particle density (TPS1). These results are likely a consequence of the microstructural properties, where TPS1 which had a partially flocculated plate structure could hold the highest moisture content, yet pumice and volcanic glass weathered enough to produce the lowest particle density. PS1 and PS2 which had few plates, but some books, displayed the highest particle density, yet held the lowest moisture content. The higher particle density indicates the PS1 and PS2 units are not as weathered as TPS1. The high silt content (~ 76 – 84 %) suggested that more glass and pumice existed as silt sized material in the samples.

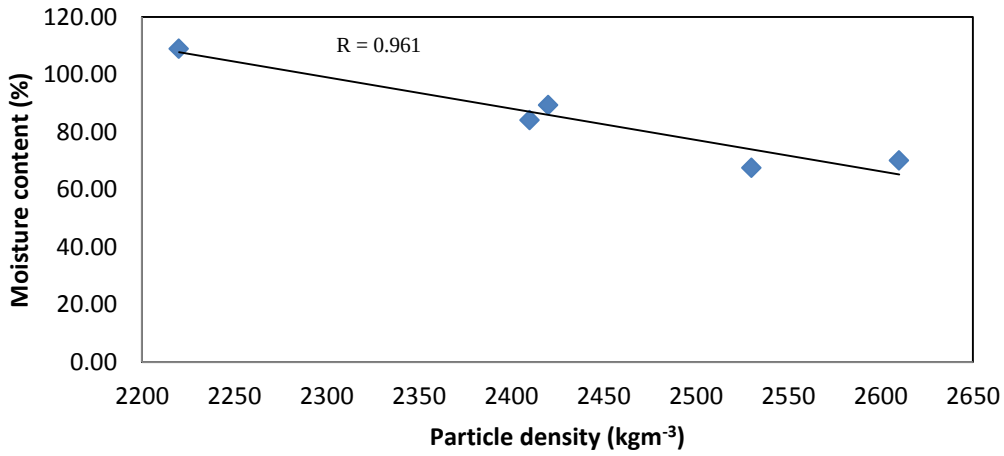

Figure 7.16: Scatterplot correlation between particle density and moisture content.

Wet bulk density conversely, indicates a positive relationship with particle density (Figure 7.17). This relationship is expected given that the bulk density is related to the mass of the soil and the volume of the soil, where the greater volume of the sample occupied by water will result in a lower overall bulk density. The morphologies of the clay particles observed in Chapter 6 appear to be the dominant control. TPS1, with a partially flocculated plate structure and regular, small-sized spheres and tubes, indicates that this type of packing arrangement supports a higher amount of moisture within the sample. The structure of PS1 and PS2, conversely, do not support as much moisture and therefore give the two highest wet bulk densities.

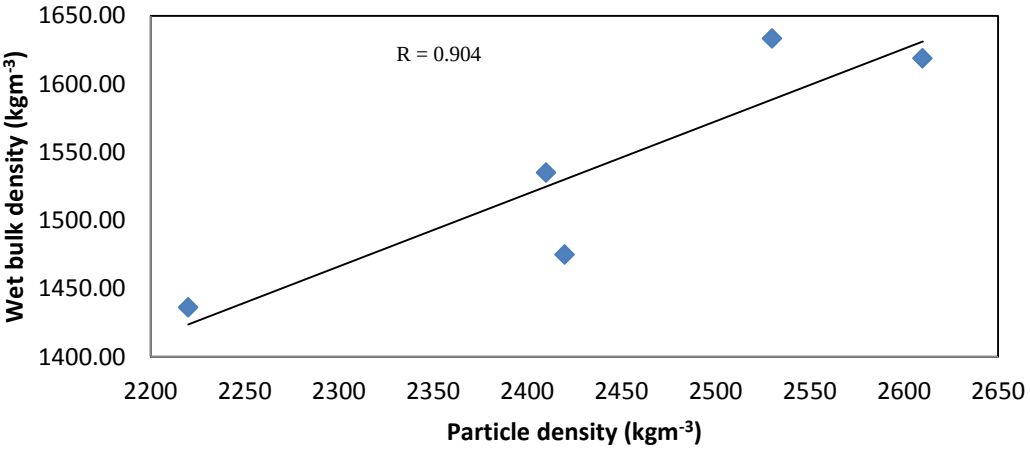

Figure 7.17: Scatterplot correlation between particle density and wet bulk density.

7.4.3.3 **Particle density and activity**

Particle density indicated a negative correlation with activity (Figure 7.18). This relationship is expected given that low particle densities generally represent a greater clay fraction in the sample which is correlated with low activity. All samples from this study were dominated by halloysite (see Chapter 6) which is typically recognised as a low activity clay mineral (Egashira and Ohtsubo 1982). With the addition of the results from Wyatt (2009), however, it becomes clear that the relationship is not as consistent as data from the present study would suggest (R = 0.24) indicating that particle density and activity do not offer a reliable relationship for the characterisation of sensitivity. Furthermore, the particle size results (see Chapter 5) indicate that the sensitive materials typically have low clay fractions. The inconsistency of particle size with particle density and the expected correlation of particle density with activity may indicate that the particle size analysis was not accurate.

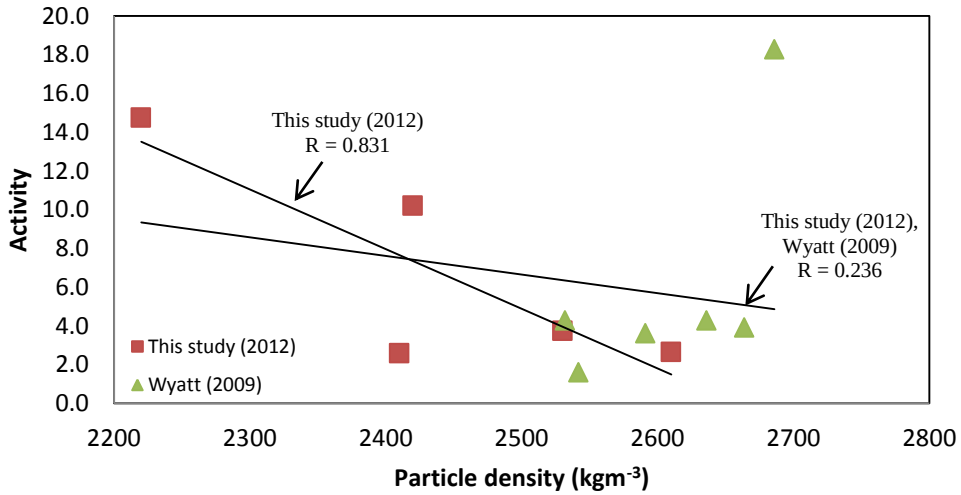

Figure 7.18: Scatterplot correlation between particle density and activity for data from both this study (2012) and Wyatt (2009).

7.4.3.4 Particle density and yield stress

Yield stress at natural pH was negatively correlated with particle density (Figure 7.19). As the particle density of each sample increases, the yield stress decreases. The behaviour of this negative correlation suggests that where the particle density is lower (or clay mineral content may be higher) the yield stress for a sample increases. This could indicate that the yield stress is instead influenced by the progression of weathering within sensitive materials, where more highly weathered samples with lower particle densities (and thus higher clay contents) exhibit greater yield stress values. In comparing the data with the particle size determinations, however, PS1 and PS2 indicated clay fraction sizes of ~ 4.97 % and ~ 6.75 % respectively, while OS2 and TPS1 only indicated < 3 % clay mineral content and yet had higher yield stress values. This may, again, be the result of incorrect particle size determinations.

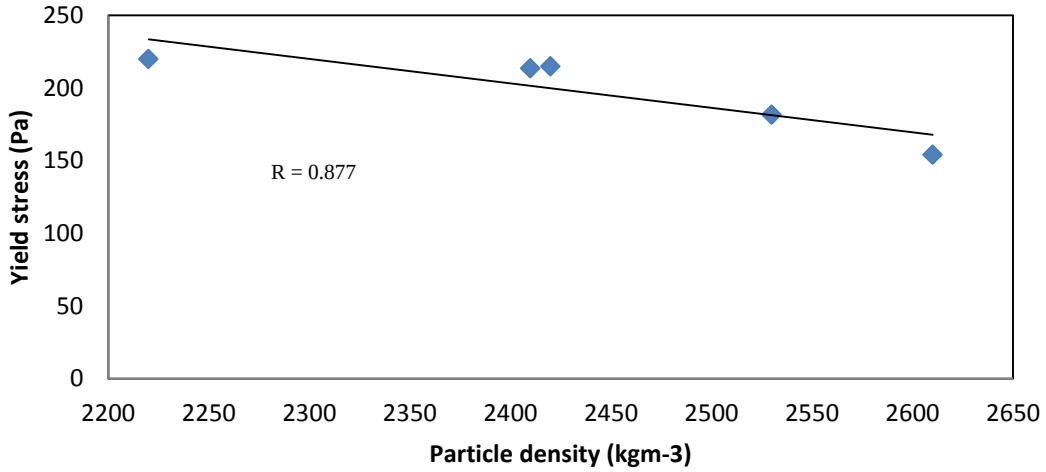

Figure 7.19: Scatterplot correlation between particle density and yield stress.

7.4.4 **Sensitivity**

In analysing sensitivity, the correlation matrix revealed that plastic limit gave the only strong relationship (R = 0.75), while no very strong relationships were present. In reviewing the relationship between plastic limit and sensitivity with data from Keam (2008), Wyatt (2009) and Arthurs (2010), the relationship was diminished (R = 0.19), suggesting that plastic limit is not a suitable predictor for sensitivity and so this relationship was not further explored. The lack of other relationships was unexpected, particularly due to the assertion of a relationship between sensitivity and liquidity index from Wyatt (2009). Liquidity index was again plotted with sensitivity to establish whether the lack of relationship was affected by skewed outliers or whether the combined relationship with other studies revealed a relationship (Figure 7.20). The relationship was very weak (R = 0.194) and not considered strong under the boundaries defined earlier. This suggests that although a high liquidity index may be important for the establishment of sensitivity, its relative value does not influence the magnitude of sensitivity.

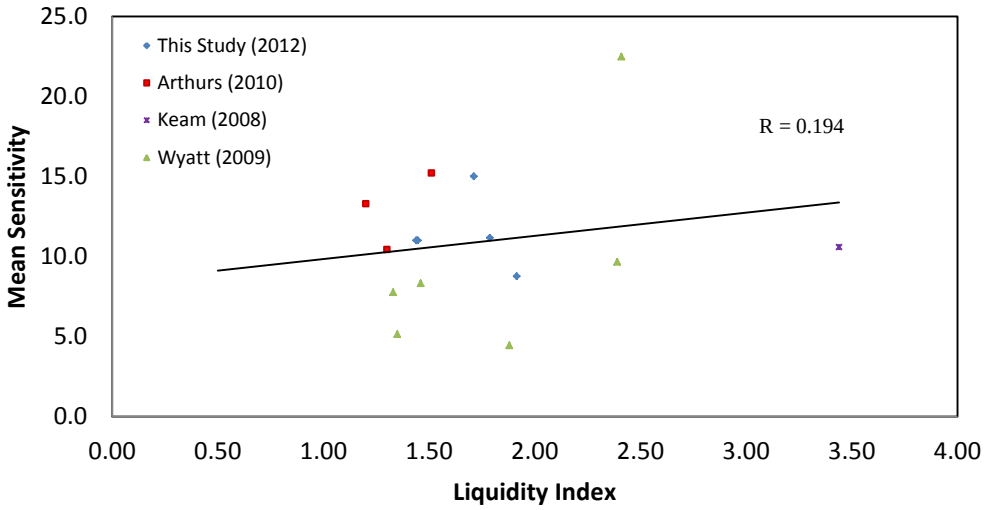

Figure 7.20: Scatterplot correlation between mean sensitivity and liquidity index for data from Keam (2008), Wyatt (2009), Arthurs (2010) and this study (2012)

Given the multiple strong correlations between particle density and other parameters of sensitive materials described earlier, the relationship between particle density and sensitivity was further analysed. A potentially viable regression relationship between particle density and sensitivity was attained when data from Wyatt (2009) was incorporated into the relationship, however, one of the samples from Wyatt (2009) was omitted (Figure 7.21). This was done as the point is primarily defined by its exceptionally low remoulded strength, skewing sensitivity to be very high (~ 22). The sample has a remoulded strength of 2 kPa, whereas the next lowest remoulded strength is 5.4 kPa. At such low remoulded strengths, very small (~ 1 kPa) differences can have an important impact considering the sensitivity ratio is weighted evenly between peak and remoulded strength. This ratio weighting issue means that soils which record extremely low remoulded strengths may not be adequately represented because the precision of the shear vane instrument (see Chapter 8 for further discussion). Thus the true sensitivity of the material may not be realised. Including this point in the analysis meant the regression coefficient was markedly reduced (R = 0.29) and the value of the fit was inconclusive.

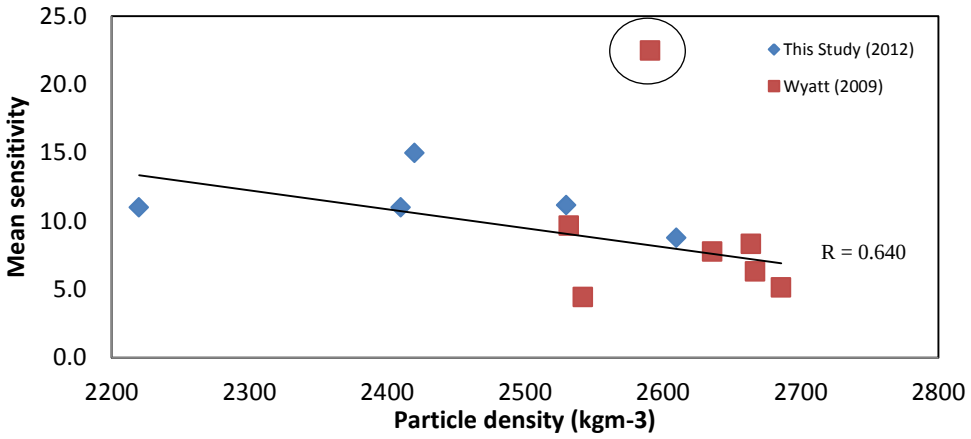

Figure 7.21: Scatterplot correlation between mean sensitivity and particle density from Wyatt (2009) and this study indicating a weak negative relationship. The omitted sample from Wyatt (2009) is circled.

The value of particle density as a predictor for sensitivity has not previously been explored. Clay particle interactions have previously been identified as key contributors to the development of sensitivity (Jacquet 1990; Wyatt 2009; Arthurs 2010). The weathering of primary minerals to clay particles and the resulting particle density variation, therefore may provide a contribution in understanding the development of sensitivity in rhyoltic soils. The relationship between sensitivity and particle density displays a moderate negative correlation (R = 0.64) between the two parameters from both this study and Wyatt (2009). Although the relationship is only weakly defined, the correlation is still apparent.

The relationship describes that as particle density increases, sensitivity decreases. Furthermore, this relationship indicates the importance of particle density in relation to sensitivity, and was the only variable that offered a suitable predictor for sensitivity when analysing more than one study. The relationship primarily indicates that as a soil mass is increasingly weathered (where more halloysite is formed along with other secondary minerals, reducing particle density) sensitivity is higher. Meanwhile, where a soil mass is less weathered, the sensitivity is lower. This could suggest that sensitivity, particularly high sensitivities, are typically born out of weathered tephra deposits, while less weathered materials may not exhibit such high states of sensitivity. The non-sensitive nature of RS1 may refute this claim, on the basis of the high halloysite content of the sample (see Chapter 6). Therefore the stage of weathering of the sample only indicates that enough clay is likely present for sensitive development

to occur, not necessarily that it will occur, as other factors (i.e. clay particle interaction within the microstructure – see Chapter 6) play an important role in determining the sensitive development. The presence of a non-sensitive sample with low particle density from the Tauranga region, however, does not necessarily diminish the usefulness of the negative correlation of particle density with mean sensitivity as it still provides some potential predictability for the magnitude of sensitivity within a particular range of particle densities. However with consideration of RS1, the relationship should be treated with caution for physically varying deposits.

7.4.4.1 **Non-regression related statistical analysis**

Regression analysis was not appropriate for all data analyses explored in the possible prediction of sensitivity. In particular, mineralogy is not quantifiable so other tools were required to draw out any potential indicators of sensitivity.

A frequency histogram of measured sensitivity values shows that mean sensitivity in the Tauranga region from this study and three previous studies (Keam 2008; Wyatt 2009; Arthurs 2010) was most frequently within the range of 10 to 12 on the sensitivity scale with the majority spread between 6 and 12 (Figure 7.22). This relationship indicates that the general sensitivity classification for the Tauranga region is extra sensitive. Only at one location was mean sensitivity considered on the scale as exhibiting behaviour similar to that of ‘quick’ clay, which was reported by Wyatt (2009) in Tauriko, Tauranga.

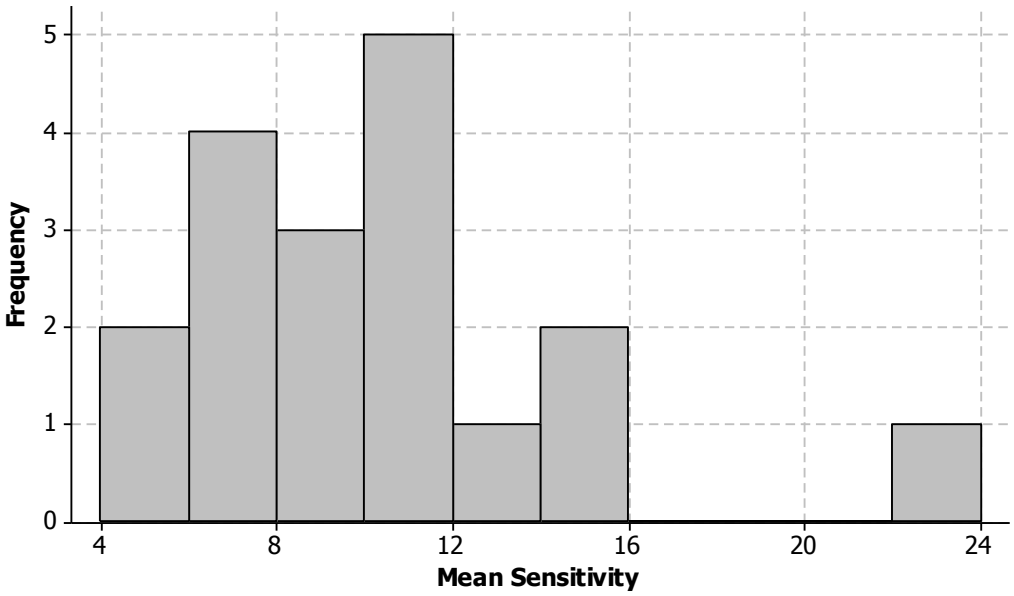

Figure 7.22: Histogram plot of the frequency of sensitivity in the Tauranga region from Keam (2008), Wyatt (2009), Arthurs (2010) and this study indicating sensitivities between 10 and 12 are most commonly observed in the region.

Statistically correlating sensitive sample mineralogy encountered in the Tauranga region indicates that halloysite and quartz were always present in the sensitive material (Figures 7.23 – 7.27). This would suggest that halloysite is a necessary precursor to development of sensitivity in rhyolitic tephra from the Tauranga region. The Ranagtaua Bay (RS1) sample clearly shows, however, that the mere presence of halloysite does not ensure sensitive behaviour. Kaolinite was typically absent from sensitive material. Only two samples from Wyatt (2009) indicated kaolinite was present in the sensitive samples, while the remaining majority showed that no kaolinite was in fact present in any of the samples. Both the studies by Arthurs (2010) and Keam (2008) were omitted from the kaolinite analysis as no distinction between halloysite and kaolinite was made during mineral identification. Cristobalite varied in presence in sensitive materials from the Tauranga region, while plagioclase feldspar was commonly identified.

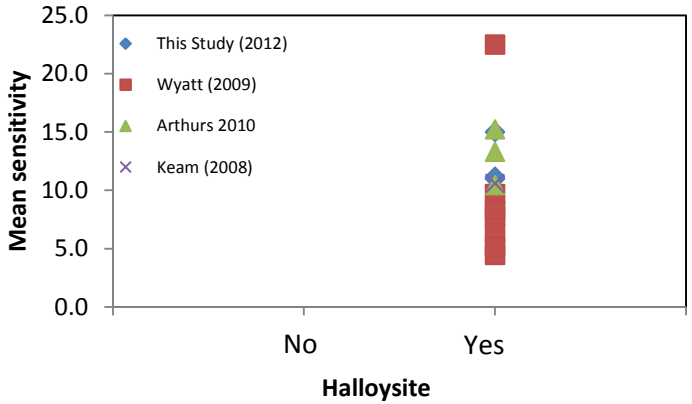

Figure 7.23: Mean sensitivity association with halloysite from multiple studies from the Tauranga region. 'Yes' denotes that he mineral was present in the sample, while 'No' indicates that it was not.

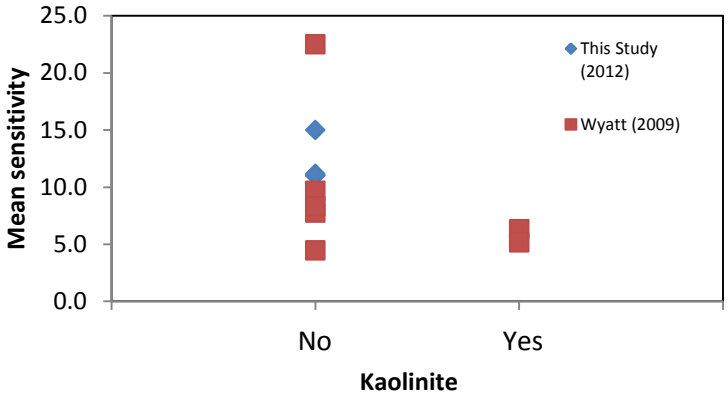

Figure 7.24: Mean sensitivity association with kaolinite from Wyatt (2009) and this study. Keam (2008) and Arthurs (2010) were not included as no distinction of kaolinite compared to dehydrated halloysite was established in their studies. 'Yes' denotes that he mineral was present in the sample, while 'No' indicates that it was not.

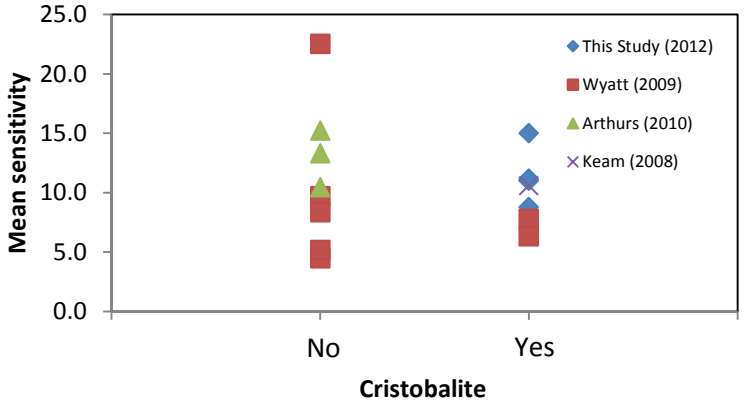

Figure 7.25: Mean sensitivity association with cristobalite from multiple studies from the Tauranga region. 'Yes' denotes that he mineral was present in the sample, while 'No' indicates that it was not.

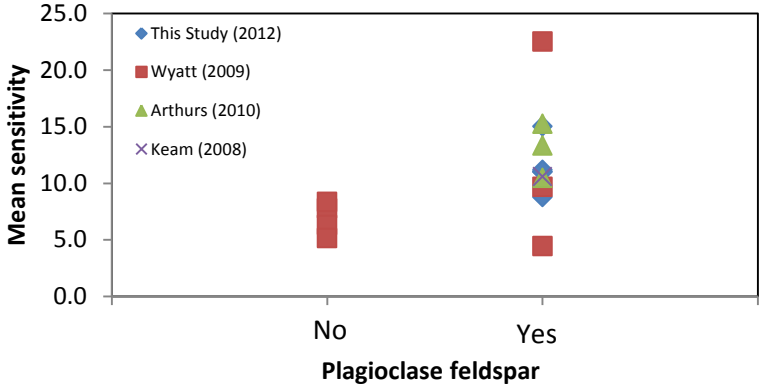

Figure 7.26: Mean sensitivity association with plagioclase feldspar from multiple studies from the Tauranga region. 'Yes' denotes that he mineral was present in the sample, while 'No' indicates that it was not.

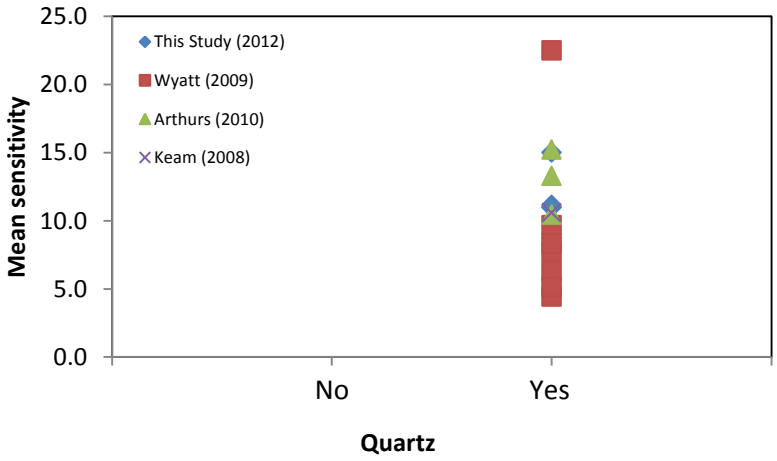

Figure 7.27: Mean sensitivity association with quartz from multiple studies from the Tauranga region. 'Yes' denotes that he mineral was present in the sample, while 'No' indicates that it was not.

7.5 Statistical conclusions

From the analyses undertaken, some conclusions can be drawn regarding the applicability of several soil characterisation parameters and their potential to predict sensitivity. Initially, the relationship between shear strength and various other soil parameters described in Section 7.4.1 typically displayed expected relationships that did not differentiate sensitive materials. The relationship between remoulded strength and the effective friction angle, however, was interesting, indicating that as friction angle is reduced, the remoulded strength is also reduced, possibly indicating an increase in soil sensitivity. Another factor related to the triaxial testing of the samples was the effective cohesion and its relationship with clay content. Typically cohesion would be expected to increase with the measured clay content. However, as the opposite behaviour is apparent for the sensitive material from this study, it is suggested that small variations in clay content below ~ 11 % do not reduce sensitivity. Moreover, the clay content itself is not likely the most important factor, but rather the microstructural interaction of the clay materials with each other and surrounding particles.

Another interesting statistical relationship was between particle density and the various soil characteristics, but primarily its relationship with sensitivity. Typically, particle density would increase as the magnitude of sensitivity

decreased, possibly suggesting that as rhyolitic soil profiles in the Tauranga region become more weathered, the sensitivity of the soil increases.

Sensitivity values were most commonly between values of 10 and 12 across various studies in the Tauranga region, indicating that the classification of rhyolitic sensitive soils in the Tauranga region as 'extra sensitive' is justified.

Relationships between mean sensitivity and various clay and non-clay minerals indicated that the presence of halloysite was a necessary condition for sensitivity in these materials. No noteworthy relationship existed between the degree of sensitivity and any of the minerals, as the range of sensitivity varied highly, with no clear distinction between the presence or lack of a particular mineral in the degree of sensitivity.

Chapter 8

DISCUSSION

8.1 Introduction

All field, geomechanical, petrographic and statistical investigations used in analysing the structural breakdown of sensitive soil deposits are discussed in this chapter. Initially, the origins of sensitive and non-sensitive materials are discussed, and a hypothesis about the formation of large halloysite books is presented. The microstructural properties inherent in the breakdown of sensitive and non-sensitive soils will then be discussed as well as the geomechanical analysis of the materials studied. A critique of the classification and measurement of sensitivity will be presented, while also proposing the likely process of development of sensitive behaviour in rhyolitic sensitive material.

8.2 Origins of deposits and associated weathered materials

8.2.1 Sensitive material

The sensitive material analysed in this study is primarily of tephra-fall origin, either from locally derived eruptive units within the Tauranga Basin, or distal equivalents of widespread, unidentified pyroclastic materials derived from the Taupo Volcanic Zone (TVZ) (Whitbread-Edwards 1994; Briggs *et al*. 2005), or both. The high abundance of glass, feldspars and pumice indicates the rhyolitic (silica-rich) origin of the volcanic deposits (Briggs *et al.* 2005). It is suggested on the basis of stratigraphic position and correlation with the findings of Arthurs (2010) that the sensitive units from all site locations represent the Te Puna pyroclastic tephra deposits, intercalated with Matua Subgroup silts and sands. Briggs *et al.* (1996) suggested that the outcrops of the Te Puna Ignimbrite are confined to the vicinity of the Tauranga Harbour indicating that the Te Puna

Ignimbrite eruptive sequence was sourced locally. The Tauranga region comprises a complex array of geologic units, which in conjunction with various paleoerosion events and topographic unevenness, has meant that the distribution and thickness of the Te Puna tephra-fall beds and ignimbrite is not consistent in all areas throughout the Tauranga region. Hence, prediction of sensitivity based on the Te Puna Tephra unit cannot be confidently assigned over the entire region, but rather only sporadically. The following section will describe the deposits at locations where sensitive materials were identified. .

8.2.1.1 **Omokoroa**

The two samples of *in-situ* sensitive materials from Omokoroa (OS1 and OS2) were extracted from a weathered tephra unit lying immediately above a firm clay layer (Chapter 4). This firm clay-rich layer likely represents the Te Puna Ignimbrite (0.93 Ma) described by Briggs *et al*. (1996; 2005), suggesting the sensitive layer above it is associated with the Te Puna Tephra. The rhyolitic nature of the sensitive deposit is further evidenced by rhyolitic rock fragments observed through SEM imaging, particularly the abundant pumice and siliceous glass fragments.

The lignite basement also alludes to the depositional environment into which the pyroclastic deposit flowed. The presence of the lignite suggests that the area was likely a wetland swamp or estuarine environment prior to the original deposition. Furthermore, the Te Puna Tephra material itself has notably been reworked following emplacement, with the presence of diatom species observed during scanning electron microscopy (SEM) imaging (Chapter 6). Glass shard evidence also supports the theory of the material being reworked. The glass was usually small, and while it was angular, it did appear to have been broken down and reduced, suggesting more than one mode of transport (Eden 1996).

The condition of both OS1 and OS2 indicate that considerable weathering has taken place, primarily from the large amount of clay minerals observed through SEM analysis. A high proportion of halloysite clay minerals formed in rhyolitic materials is indicative of an increased stage of soil weathering (Bakker *et al.* 1996). This stage of weathering suggests that the deposit was near the surface for a long period at some point during the past. Other major constituent features

such as pumice and volcanic glass have clearly been weathered as their surfaces were typically covered with a lot of clay minerals which suggests that considerable weathering had taken place (Aomine and Wada 1962). With consideration to the very wet nature of the deposits, the state of weathering (observed in the SEM analysis) is unsurprising, given that glass deposits are highly susceptible to solution weathering and subsequent formation of clay minerals (Wada 1987; Churchman and Lowe 2012). The glass fragments observed in OS1 and OS2 were typically small and thin, and the least abundant from all sensitive samples. The small sizes of the glass shards suggest that the weathering environment at Omokoroa was the most intense in comparison to the other samples analysed.

One sample of sensitive material (OLRO) was collected from a landslide runout zone at Omokoroa. The properties of the OLRO sample were more difficult to characterise, primarily because the sample had already been remoulded, reworked and was not located near its original position in the profile upon collection. This also meant that other characteristic features such as moisture content, shear strength and particle size could not be used in identifying the deposition history of the material. Notwithstanding these issues, the material could still be characterised on the basis of field observations, XRD and SEM imaging. The sample colour was very similar to that of OS1, and also had a similar clayey SILT composition. Considering that no other material that was recognised above or below the Te Puna Tephra in stratigraphic position appeared to have these characteristics, the sample was again considered to be rhyolitic in composition and likely associated with the Te Puna Tephra intercalated with Matua Subgroup sediments. XRD also indicated a very similar mineral assemblage to OS1 and OS2, further suggesting a strong correlation in deposition material.

SEM observations suggest that primarily small sized, partially broken clay minerals dominate the structure of OLRO. Glass fragments and larger sized silt grains were sparse. The lack of this size material and the large mass of clay sized material observed would intuitively suggest that significant weathering has indeed taken place, with the dissolution of the glass material in the sample (Aomine and Wada 1962). The possibility does remain, however, that the larger sized material actually settled through the depositional layer, leaving the smaller size material at

the top of the runout layer. This could happen when water in the sample is high enough upon deposition that the grains sediment with time following deposition, and so there is a tendency for the fine grained material to remain at the top of the layer, while coarser material settles towards the bottom (Jock Churchman *pers comm.* 2012). This would suggest that glass and other silt to sand sized fragments would not tend to be seen in the material that was collected considering that the material was not sampled according to depth and only a small (thought to be representative) sample was taken for SEM analysis. Considering the apparent similarities to OS1, nevertheless, the material was thought to again be in a similar stage of weathering at the time of failure.

8.2.1.2 **Te Puna**

The material collected from Te Puna (TPS1) also appeared to be similar to that obtained from Omokoroa. The similar colour and position below the Hamilton Ash and Pahoia Tephras again suggest the material to be tephra fallout associated with the Te Puna Ignimbrite sequence. The Te Puna Ignimbrite was not visible, leaving the possibility open that the unit may have been an unassociated tephra deposit. The material again appeared to have been reworked, with no visible bedding present.

SEM analysis revealed large glass fragments in comparison with OS1 and OS2, with thin walled vesicles suggesting that the sample had been weatherd promoting the formation of clay minerals, however, not to the same extent as that which occurred at Omokoroa. It is also inferred that the level of reworking of this material has not been as intense, on the basis that the glass has not been broken into many small fragments, but rather larger portions of glass are seen in the sample (Eden 1996). The depositional environment at Te Puna also appears to be under less consolidation than that at Omokoroa, and thus the sampled material is inherently more porous. Only thin deposits of later materials (~ 2.2 m of overlying material at present) provide consolidation loads giving a high void ratio of 2.23 and thus highest porosity of ~ 69 % compared to deposits at other sensitive sites analysed. The high porosity may suggest that as the voids hold more water and there is a lack of MnO_2 concretions, a more intense drying period is required to produce MnO_2 concretions as observed at the other sensitive sites.

TPS1 indicated a pink reaction when the α α'-dipyridyl Childs' Test was applied, suggesting that ferrous iron was not completely incorporated in the formation of clay minerals and has remained in the soil solution. The formation of plate morphologies from TPS1 suggest that some iron was incorporated into the halloysite structure to 'flatten out' the crystal structure with enough iron remaining to form the reaction. The relatively small sizes of the plates also indicate that the iron likely inhibited larger growth of the plates following formation. The soil was therefore under reducing conditions which was further confirmed by its low chroma (white) colour (Buol *et al.* 2003).

8.2.1.3 **Pahoia Peninsula**

The two samples from Pahoia Peninsula (PS1 and PS2) were again suspected to be tephra fallout deposits from the Te Puna Ignimbrite eruptive sequence. Based on the position of the unit below Pahoia Tephras, the presence of pumice and rhyolitic glass features, and the correlation suggested by Arthurs (2010), this source was again assumed. PS1 and PS2 were very similar in appearance and in all soil properties tested, making it acceptable to assume that they were distal correlatives of the same unit. Both units were considered to be reworked due to the small glass textures throughout the sample (Eden 1966). PS1 showed the presence of small silt lenses, which were likely produced from the weathering of pumice clasts within the soil material (Aomine and Wada 1962).

Observations from Childs' Test suggested a very weak reaction which could not be distinguished from the soil background colour, indicating that very small or no ferrous iron was present in the soil. This was confirmed by the large halloysite books in the sample, which would not have likely formed in the presence of high iron content in solution following the books initial formation (book formation was likely in a much smaller state – discussed further in Section 8.2.3.1).

8.2.2 **Non-sensitive material**

Non-sensitive material was sampled in a similar stratigraphic location to the sensitive material. Both non-sensitive units were considered to be different

from the tephra units associated with the Te Puna Ignimbrite eruptive sequence, considering they were located much closer to the overlying Hamilton Ash sequence (0.35-0.1 Ma; Briggs *et al*. 1996). An abundance of volcanic glass and pumice again indicate the rhyolitic origin of the material at both locations.

8.2.2.1 **Tauriko**

The Tauriko deposit was considerably different from all others studied. The material was very thick and massive, and primarily characterised by its high sand content and relatively low silt and clay constituents. This material was therefore characterised as a pyroclastic flow deposit, most likely the Te Ranga Ignimbrite (0.27 Ma; Briggs *et al*. 2005). The ignimbrite was non-welded and pumice rich, but it had a low moisture content which resulted in a less weathered state than was previously observed at the sensitive locations. Manganese concretions did suggest that the material was wet at some point, however, the well-draining nature of the sample currently suggests that the material was, and likely still is, in an oxidising regime (moisture content < 32%). Many glass shard textures were recognised from SEM observations, while a significant amount of quartz was also present as indicated by XRD. The quartz was well rounded, suggesting that it could have possibly been partially reworked or deposited in a shallow subaqueous environment as suggested by Briggs *et al*. (2005). This would also explain the massive, non-bedded properties of the ignimbrite.

The material was not cohesive, and could not be remoulded at the *in-situ* moisture content, and therefore could not be given a sensitivity value. However, because the material did not smear or become fluidised upon remoulding, it was considered non-sensitive according to the Milne *et al.* (1995) test for sensitivity.

8.2.2.2 **Rangataua Bay**

The Rangataua Bay deposit did not have the same depositional record as that from any of the other sites studied. The material was fine grained, stiff, and had a comparably high clay content (> 30 %). The unit contained few manganese concretions, suggesting that at some point through the depositional history the material had been saturated for long enough, with subsequent drying and then oxidation to form MnO_2 concretions (Vepraskas 1994).

The location of the Hamilton Ash sequence immediately above the sampled unit, suggests that the material is likely associated with the Te Ranga Ignimbrite (~ 0.27 Ma; Briggs *et al.* 2005). The presence of glass shards and feldspars confirms that the unit is of tephric origin and so is suspected of being an undifferentiated tephra deposit associated with the Te Ranga Ignimbrite.

The material also appeared to be highly weathered, with little glass being observed through SEM analysis. Consistent throughout the sample was the abundance of halloysite clay material, suggesting that the majority of glass in the material had been weathered to clay.

8.2.3 **Clay Mineral Development**

Clay mineral development was profound throughout the majority of the sensitive samples, as well as the non-sensitive material sampled from Rangataua Bay, regardless of particle size determinations. The Tauriko samples also indicated some clay development, but clays did not blanket the samples in the substantive manner that was observed in the other materials, which is consistent with the lack of cohesion observed.

The main clay formed in all samples was halloysite. X-ray diffraction of sensitive samples both before and after the addition of formamide indicated that, with the possible exception of OLRO and TS3 (which contained equivocal evidence for dehydrated halloysite and kaolinite), no other clay species were present in the samples. The lack of kaolinite in the samples was unexpected, considering previous authors had found small amounts of kaolinite in sensitive tephra from the Tauranga region (Wyatt 2009; Arthurs 2010). This absence of kaolinite is likely due to the very wet nature of the sensitive material during the

clay mineral formation from solution. Churchman *et al*. (2010) suggested that halloysite is favoured where soil solutions are wet, likely due to the absorption of interlayer water within the halloysite structure (Churchman and Carr 1975), while the formation of kaolinite is favoured where drying occurs. The absence of kaolinite does, however, indicate that it is not a precursor to the development of sensitivity in volcanic tephras from the Tauranga region. In the non-sensitive material halloysite was again dominant, however minor kaolinite was observed in the bulk fraction from Tauriko (TS3). This would suggest that even though the soil material is significantly drier than the sensitive material in its current form, during early clay mineral formation, the soil material was wet, but had subsequently dried, leading to the primary formation of halloysite, with the minor recrystalisation of kaolinite with drying (Churchman *et al.* 2010).This interpretation is further supported by the presence of manganese concretions at Tauriko, which as previously mentioned, indicates that the profile was at one time sufficiently saturated and subsequently dehydrated (or repeated cyclic wet-dry periods) which would lead to manganese reduction to the MnO_2 state it was observed in (Vepraskas 1994). In all samples allophane was not considered to be an essential constituent that needed quantifying into clay mineral formations in sensitive tephra from the Tauranga region, on the basis of the analysis undertaken by Wyatt (2009) (see Chapter 2). SEM analysis similarly did not indicate any spherules of 3 – 5 nm nor were any imogolite fibres observed and so the formation of allophane was not evident. Furthermore, the highly siliceous environment means that halloysite is favoured over allophane in clay mineral formation and so the presence of allophane should be minimal in this environment. Halloysite is considered to be thermodynamically more stable than imogolite at high silica activity (Percival 1985; Lowe 1995; Churchman and Lowe, 2012) which appears to be the likely situation in this study.

The stratigraphic position of units within the Tauranga region appears to be an essential factor in the development and present occurrence of halloysite as the dominant clay mineral over kaolinite and allophane. All of the sensitive units were very wet and were overlain by several rhyolitic units (Briggs *et al.* 1996; 2005). This overburden material provides a satisfactory environment for silica to be redissolved into solution (Lowe and Percival 1993) and then leached through the profile to the Te Puna Tephra. The position of the weathered Te Puna

Ignimbrite then becomes critical to the pooling of water at the level of the Te Puna Tephra and thus concentrating the high level of silica that has leached through. Such poor drainage is described by the low hydraulic conductivity of the Te Puna Ignimbrite. This is inferred because clay materials near saturation (as observed for the Te Puna Ignimbrite at Omokoroa – see Chapter 4) have low hydraulic conductivity especially compared to sandy soils (Selby 1993). The low hydraulic conductivity means that the ease with which the soil pores permit water movement is significantly reduced, and so water permeating through layers above that unit is impeded from leaching further through the profile (Selby 1993). Therefore, the combination of the highly siliceous units that overly the only-slowly permeable Te Puna Ignimbrite promotes a wet, silica-rich halloysite favourable environment (Churchman *et al.* 2010). Halloysite formation from impeded drainage has been previously reported in the Tauranga region and also other areas in the central North Island of New Zealand, suggesting that halloysite is the favoured clay mineral under these circumstances (Bakker *et al.* 1996; Wyatt 2009). Bakker *et al.* (1996) described soil profiles Naike and Patumahoe as having impeded drainage from clay illuviation at the bottom of the units, which promoted halloysite formation. Wyatt (2009) also suggested that the increased clay fraction of units below sensitive material at Otumoetai, Tauranga, reduced Si loss and encouraged halloysite formation in the sensitive material he studied. The most obvious example of these formations in this study was at Omokoroa, where the Te Puna Ignimbrite was exposed immediately below the Te Puna Tephra (see Chapter 4) which undoubtedly hindered further drainage as water and silica leached through the profile.

Wyatt (2009) has similarly reported the presence of impermeable layers beneath the sensitive units, suggesting that the position of such impermeable layers may be essential in the formation of sensitive rhyolitic material.

At the non-sensitive locations, no impermeable clay layer could be seen to be situated below the sampled material which suggests that during dry regimes or seasonally dry periods the material is easily drained and remains with a low moisture content. The dry period, however, must not have been for an extended period because halloysite remains at the site, rather than conversion to kaolinite.

8.2.3.1 Halloysite morphologies and their formation

Halloysite spheres followed by tubes were the most common morphologies identified in this study (see Chapter 6). Joussein *et al*. (2005) suggested that tubular halloysite is the most common form of halloysite, but two other morphologies were also encountered: plates and books. Plates were typical of the sensitive materials, but were not found in any of the non-sensitive samples. Variations in size were also apparent, with the sensitive samples containing predominantly small spherical particles (~ 150–200 µm in diameter), while the non-sensitive material typically contained larger spheres (~ 550–800 µm in diameter). The variability of halloysite sphere size has previously been suggested to be because halloysite spheres consist of many layers (Dixon and McKee 1974; Kirkman 1977; Joussein *et al*. 2005). Similarly, spheres from both non-sensitive sample locations (particularly RS1) displayed partial amalgamation with tubes, which promotes a much tighter packing of these two morphologies.

The most intriguing morphology was the occurrence of halloysite books at PS1. Previously book morphologies were thought to be confined to kaolinite (Joussein *et al.* 2005), but more recently halloysite book morphologies have been discovered (Wyatt 2009; Wyatt *et al.* 2010). In my study, the identification of very large halloysite books of silt to sand size (~ 60 µm– ~1500 µm) is novel – such large halloysite books have not been previously reported.

The formation of the halloysite books could be the result of several processes. Soils with both halloysite and kaolinite have previously shown the formation of kaolinite books (Jeong 1998). One potential mechanism for the formation of large kaolinite books is the process of the alteration or kaolinization of biotite which has been described by multiple authors (Wilson 1967; Ojanuga 1973; Salter 1979; Graham *et al.*, 1989). The kaolinization of biotite involves the progressive alteration of biotite (or other micaeous mineral) to kaolinite (Dong *et al.* 1998). Ojanuga (1973) indicated that the direct weathering of biotite to kaolinite was found to occur under humid tropical climates, whereas under temperate conditions biotite weathered to vermiculite. Banfield and Eggleton (1988) also showed that biotite weathers to vermiculite, but suggested that vermiculite can be further altered to kaolinite in the form of large particles. In New Zealand, Salter (1979) identified large, sand-sized kaolinite books in the

very strongly weathered Kauroa Ash Formation and attributed them to be the weathering product of vermicular materials altered from biotite weathering. Fanning *et al.* (1989) more generally suggested that biotite became kaolinized by various mechanisms including dissolution of biotite and recrystallization of kaolinite at linear boundaries (e.g. Ahn and Peacor 1987). At Welch Road near Orini, Shepherd (1984) suggested that sand-sized golden platy minerals in weathered Hamilton Ash beds were K-depleted micaceous kaolinite intergrades that formed by initial crystallisation of a kaolinite-mica intergrade (in approximately equal proportions) from solution followed by the hydrolysis of the mica (likely biotite) to form micaceous kaolinite (Lowe and Percival 1993; Churchman and Lowe, 2012).

The formation of 1:1 kaolin minerals from 2:1 micas such as biotite, however, does not appear to be the most likely situation to have occurred. The primary reason for this is because the formation of the books is almost identical to the original shape of mica, which would require transformation of the biotite (Papoulis *et al.* 2004) rather than dissolution followed by neogenesis of the halloysite books. The transformation of biotite in this situation is considered highly unlikely because for this to transpire, a series of processes must occur with consideration to the structure of biotite. Initially, potassium must be removed from the structure by acidification or chelation to break down the structure towards kaolinite (Jock Churchman *pers comm.* 2012). The acidification would be effective in removing the potassium, but it would also likely remove aluminium from the system, meaning kaolinite would not be able to form. Chelation would also have a similar affect to acidification, as chelating agents such as citrate also have a tendency to remove aluminium, suggesting that a complete transformation from biotite to kaolinite is not likely to be feasible (Jock Churchman *pers comm.* 2012). A partial transformation may be possible, although this would not remove the potassium from the structure, meaning complete kaolinite transformation is not possible. The dissolution and recrystalisation of biotite to kaolinite is the only other possible mechanism for the formation of kaolin books from micas. The process requires the silica and aluminium from the mica to dissolve and re-combine and precipitate to form the kaolin mineral. However, in this case it would appear very unlikely that the complete dissolution of the silica and aluminium would recrystalise in a very similar shape to the

original biotite, which the shapes of the books in this study appear to be. So on the basis of this evidence, the books are unlikely to be the result of the kaolinization of biotite.

The role of biotite in the samples could, however, be rather in the facilitation of halloysite tubes than the interaction of biotite layers with halloysite spheres. Papoulis *et al.* (2004) suggested that spheres of halloysite, which form on layers of biotite, exchange cations with biotite and enable the alteration of biotite layers sufficiently to form tubular halloysite. This could in turn result in the amalgamation of halloysite particles to form plates and thus amass to produce the large book morphologies (similar to the mode of formation suggested by Wyatt *et al.* 2010). Considering the lack of biotite observed from both XRD analysis and in the SEM images (see Chapter 6), however, the role of biotite is not considered to be a crucial factor in the formation of the halloysite books observed in this study.

Another mode of formation could be the dissolution and precipitation or solid-state transformation of halloysite to form book morphologies. Halloysite books, as the resulting formation from such weathering processes however, have been rarely characterised. Typically kaolinite has historically prevailed where the two species coexist, yet the process of the formation of books could offer a potential avenue for the formation of the large halloysite books. Figure 8.1 A–D summarises some previous attempts at explaining the formation of kaolinite and halloysite books. One such example was from Jeong (1998) who characterised the formation of kaolinite books from halloysite tubes from a weathered soil profile in Korea. The halloysite tubes were suggested to amalgamate to form plates. However, in plate form, halloysite becomes unstable and subsequently transforms to kaolinite (Jeong 1998; Figure 8.1a). Papoulis *et al.* (2004) also observed similar transitions in clay fractions from weathering profiles in Greece. They observed the "felting" of halloysite tubes into planar masses of halloysite, which ultimately converted to stable kaolinite (Figure 8.1b). Wyatt *et al.* (2010) similarly suggested that felting to form plates was possible in the formation of halloysite books from Tauriko in Tauranga. These authors suggested that the felting of halloysite tubes produced pure halloysite plates, which upon 'coalescence' produced halloysite books without any coexistence between kaolinite and halloysite, meaning no transformation to kaolinite (Figure 8.1c). The most recent study of the formation

of kaolinite books from halloysite was that of Inoue *et al.* (2012) who proposed that following halloysite formation and subsequent dehydration, kaolinite nucleates on the edges of the tubular halloysite. The kaolinite is then suggested to consume the precursor halloysite in a "cannibalistic manner", forming elongated psuedomorphic aggregates of kaolinite (Inoue *et al*. 2012; Figure 8.1d).

While these hypotheses do offer the possibility of halloysite book formation in an unstable state, they do not necessarily lend themselves to all of the observed sample conditions and the significant size of the books encountered in this study. Initially, the size of the books suggests a relatively 'pure' environment, in which the halloysite particles can grow into particularly large sizes. Typically, when crystals such as kaolin minerals are formed in 'clean' environments without the presence of other major elements, the formation of crystals is large and unconstrained (Churchman *et al.* 2010). Meanwhile 'dirty' environments (commonly in pedological soils) which contain significant portions of elements such as Fe tend to constrain the formation of minerals, meaning they are typically small in size (Churchman *et al.* 2010; Churchman and Lowe, 2012). For example, Churchman and Theng (1984) showed that halloysite morphologies from Matauri Bay, which typically has much less Fe_2O_3 than other locations around the North Island of New Zealand, were a much larger size than any other samples studied. This observation would be suggested as the intuitive case for the large halloysite books found, but EDX analyses of the books suggested otherwise (see Chapter 6). The books typically contained iron contents of ~ 4.35 % (as Fe_2O_3), contradicting the idea of the pure environment in the formation of the large halloysite books. Furthermore, iron appears to be extremely important in the shape of the books, given that the isomorphous substitution of Fe^{3+} for Al^{3+} in the octahedral sheet decreases layer curvature, meaning that as iron is incorporated into the halloysite unit cell, tubular and spheroidal formations unroll and flatten to form flat plate-type morphologies (Joussein *et al.* 2005; see Chapter 2). This substitution means that while iron may be important in dictating crystal size formation, it is not the sole determinant and its presence in the early stages of halloysite formation is essential for plate formation. The iron must, however, be used up or converted to an insoluble form for the crystals to grow larger.

Notwithstanding the role of environmental purity in the formation of the books, other constraints must also be taken into account, primarily time,

thermodynamics and physical environment (essentially kinetics). Initially, time is not seen as an issue or constraint in the formation of the crystals. The material is thought to be the Te Puna Tephra which has an approximate age of 0.93 Ma (Briggs *et al.* 2005) which provides plenty of time for crystal formation. It is likely that the process of Ostwald ripening, which suggests that given enough time small crystals will evolve into large crystals in a relatively pure environment (Churchman and Lowe 2012), took place, increasing the size of the books. Next, thermodynamics would typically suggest that halloysite is thermodynamically less stable than kaolinite, meaning that kaolinite is favoured (Jeong 1998; Papoulis *et al.* 2004). As mentioned previously, however, Churchman *et al.* (2010) identified that halloysite is favoured where the soil profile is saturated, while if drying occurs the formation of kaolinite is favoured, indicating that the very wet to saturated conditions of the profiles from this study are critical to the formation of halloysite and its persistence (i.e., without transforming to kaolinite). An open physical environment is suggested, again not restricting the possible size of the books during formation. All samples indicated a significant proportion of pumice, which, given the large vesicles, would provide a large, open environment for large crystal formation. Furthermore, Adamo *et al.* (2001) previously reported the formation of halloysite within pumice vesicles in rhyolitic deposits from Italy, suggesting the suitability of pumice as a 'template' for halloysite formation is adequate.

Based on this evidence a process of large halloysite plate formation can be established. The highly siliceous, fragmented rhyolitic materials, typically dominated by glass and pumice fragments with high surface areas, and thus very easily weathered (Churchman and Lowe 2012), are in a very wet environment which promotes the formation of halloysite spheres (the high dissolved Si concentrations would also preclude the formation of allophane). With subsequent rhyolitic volcanic eruptions, more pyroclastic material is deposited onto the profile which would weather rapidly to provide a new source of Si in soil solution to leach downwards, adding more silica to the profile. Following this, the halloysite spheres reform as tubes through either coalescence or dissolution and precipitation with time (insufficient evidence to be definitive). Meanwhile, the progressive weathering of glass (which contains Fe as a major element), feldspars and ferromagnesian minerals enriches the profile with iron. This readily available

soluble iron is subsequently incorporated into the halloysite unit cell, where Fe substitutes for Al in the octahedral sheet, leading to sheet unrolling (see Chapter 2) and thus promoting the formation of the plates. At this point the iron has either been all bound to the halloysite octahedral sheets or is insoluble, leaving a relatively clean environment. The removal of the Fe is corroborated by Childs' Test at PS1 (where the large halloysite books were discovered), which did not indicate any distinguishable colour development, suggesting that only relatively small amounts of insoluble iron were likely present in the profile (see Chapter 4). This clean environment and onset of Ostwald ripening encourages large halloysite plates to form.

At this stage, the coalescence of these plates is required to form large books. This coalescence appears to be the result of the partial dehydration of the profile, which promotes shrinkage between the plates and thus the amalgamation of the plates to form large books (Wyatt *et al.* 2010). The drying stage is clearly evidenced by the scattered, fine MnO_2 concretions, showing that reduction followed by oxidation of the profile has occurred, as seen at PS1 and PS2 where the large books were observed. Considering the MnO_2 was not particularly concentrated in the profile (~ 10 %, see Chapter 4), only partial (relatively short-lived) dehydration is suspected. This is important as with full dehydration, kaolinite would be thermodynamically favoured, but only partial dehydration does not appear to have been sufficient to promote the transformation. Such a dehydration stage could have resulted from dry glacial climates (marine oxygen isotope stages 2, 6, 8) (Kohn *et al.* 1992). This process of partial dehydration appears to be critical for the formation of the books. At TPS1, where no manganese concretions were observed, many plates were seen, however, no books were found whatsoever, supporting the hypothesis that no drying had occurred to enable the plates to coalesce into books. Similarly, the timing at which the drying occurred is also critical. At OS1 and OS2 where the abundance of manganese concretions was similar to that at PS1 (~ 5 %–10 %), no books were observed. This would suggest that the partial dehydration of the material occurred before the formation of plates and so no books were formed.

Following the partial dehydration of the profile and the formation of the books, the profile appears to get very wet again to the position it is in today, which as Churchman *et al.* (2010) suggest, preserved halloysite rather than

permitting kaolinite transformation. If drying had continued to occur followed by plate coalescence, then it is likely that kaolinite books would be formed in a similar manner to the findings of Jeong (1998) and Papoulis *et al.* (2004). Figure 8.1e summarises the processes likely to have occurred for the formation of the large halloysite books observed in this study.

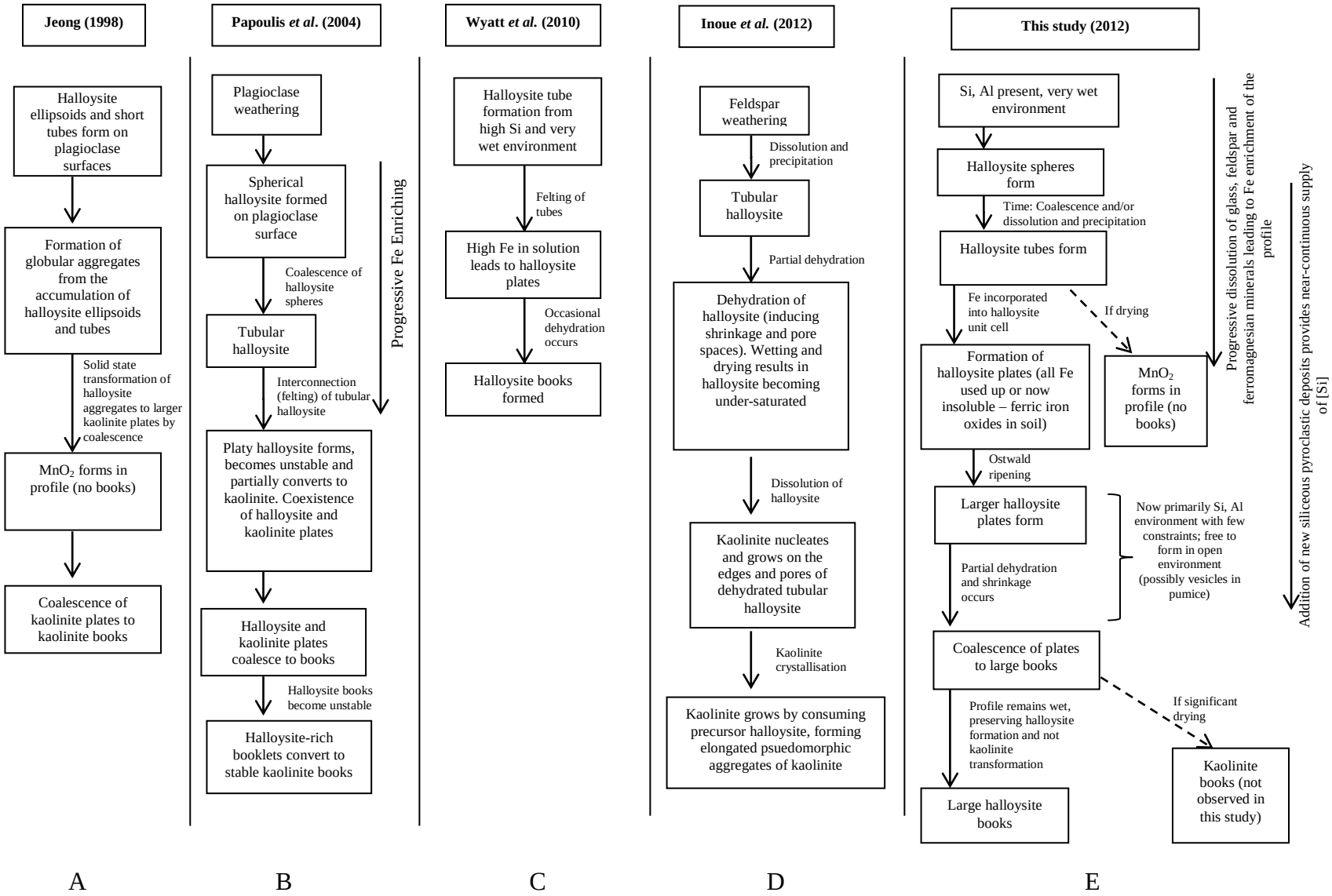

Figure 8.1: Process of kaolin group mineral book formations from five studies, including this study (E).

8.3 Peak to remoulded strength variation

The variation between peak and remoulded strength is the most fundamental aspect in defining the sensitivity of soils. The following section describes the microstructural properties and geomechanical properties from both the peak and remoulded soil states in analysing what makes the soils either prone or resistant to development of sensitivity.

8.3.1 Microstructural properties

The analysis of the microstructural properties of the sensitive soils offers the most important information and comprehensive assessment of the structural changes between the peak and remoulded state (Wesley 1974; Jacquet 1990). Furthermore, both sensitive and non-sensitive material could be directly compared and analysed in all aspects, which could not be achieved from the geomechanical testing. The following section discusses the peak undisturbed state and remoulded state characteristics from both the sensitive and non-sensitive material encountered in this study.

8.3.1.1 Sensitive

8.3.1.1.1 Undisturbed state

The primary particle shape that was very common across all sensitive samples was the spherical halloysite formation (see Chapter 6). Also common were small, yet relatively thick tubes which were approximately 3–4 times the size of the spheres. Joussien *et al.* (2005) described halloysite tubes forming within a wide range of sizes between 0.02 µm to > 30 µm in length. Typically in the sensitive material, lengths of only ~ 200–400 nm (note unit) were realised. This relatively regular sizing between the spheres and tubes is thought to be critical in the formation of sensitive material. The varied shapes, yet regular sizes, promote many micropores within the sample, where pore spaces are increased because of the regular sizing of the particles. This uniformity produces a low density of packing (Figure 8.2). The formation of this low density of packing appears ‘loose’, where there is only small surface area contact between sphere particle edges and tube faces, allowing for the high proportion of micropores and

a high void ratio. A low density of packing that produces high porosity and void ratio, which allows for a liquidity index of > 1 to be achieved, is critical for the formation of sensitive material both within New Zealand and internationally (Skempton and Northey 1952; Bjerrum 1954; Torrance 1992; Mitchell and Soga 2005; Wyatt 2009). The high liquidity index allows the soil to become fluidised upon remoulding and drastically reduces the remoulded strength leading to the classification as extra sensitive.

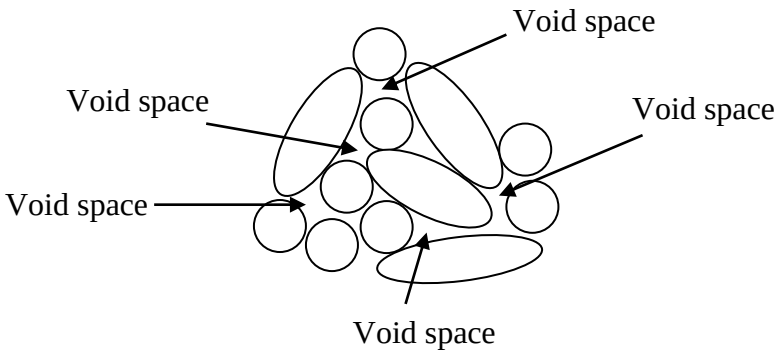

Figure 8.2: Simplified diagram of the interrelationship of comparatively similarly sized spheres and short wide tubes producing a low density of packing. This formation produces many voids and thus high porosity considerable moisture content to build within the sample. This formation was observed in the sensitive samples from this study.

The formation of these halloysite clay particles and their relationship with the remaining non-clay constituents in the sample typically formed an open matrix-skeletal structure, with the exception of TPS1, in which the abundance of plates produced a matrix-turbulent microstructure. The formation of a matrix-skeletal microstructure was important for imparting initial high peak strength along with significant moisture held within the structure to again facilitate a liquidity index > 1. Primarily, the connectors and bridges of the partially skeletal soils were critical for maintaining an open structure, allowing significant moisture to be withheld in the structure and also for the potential to break down upon remoulding. Previously, sensitive soils sourced from various rhyolitic deposits from the North Island of New Zealand have been classified as either skeletal-matrix or matrix-skeletal, identifying these formations as a recognised feature of sensitivity (Cong 1992; Keam 2008; Wyatt 2009; Arthurs 2010). The partially turbulent microstructure from TPS1 did sit outside this trend, but this microstructure allowed for more face to edge interactions between plate halloysite morphologies, which, along with the similarly small sized spheres and tubes

within the matrix component, provided for a highly porous structure. This structure allowed for very high moisture contents to build within the sample, in excess of 100% (see Chapter 5). This type of structure was more in line with what has previously been observed in glaciomarine sensitive deposits (Selby 1993; Mitchell and Soga 2005), indicating that this structural type does have some importance for sensitivity. In agreement with this study, however, a turbulent or partially turbulent microstructure is relatively rare in sensitive rhyolitic deposits from New Zealand (Cong 1992; Keam 2008; Wyatt 2009; Arthurs 2010).

8.3.1.1.2 **Remoulded state**

The remoulded condition of the sensitive soil material typically indicated a similar breakdown in structure between all samples. Initially, bridges and connectors which were present in the undisturbed state were broken down and no longer evident. Furthermore, the tubular morphologies appeared broken and reduced in size, indicating the effect of the remoulding. Books and plates within the samples were also significantly reduced in size, where the books were replaced by either much smaller, damaged books or by individual plates in no particular arrangement. In this sense, they appeared to have been mobilised upon remoulding (consistent with the flow characteristics of the soil) and flattened to remain on top of the sample as the grains settled (Figure 8.3). These observations are consistent with those on the naturally remoulded sensitive sample of OLRO. OLRO primarily comprised small spheres and broken tubular forms of halloysite of a similar size. Furthermore, a similar non-orientated structure was also apparent in OLRO, with the few books present appearing small and likely damaged upon remoulding. Overall, the structure of all of the sensitive material appeared to be completely destroyed, and particle interactions were minimised, indicating that upon remoulding the grains were effectively acting as individual aggregates or particles, which were entrained in the significant amount of water that was released from the pores upon remoulding. The high moisture content was the most important factor for reducing the soil strength and thus determining this material as sensitive.

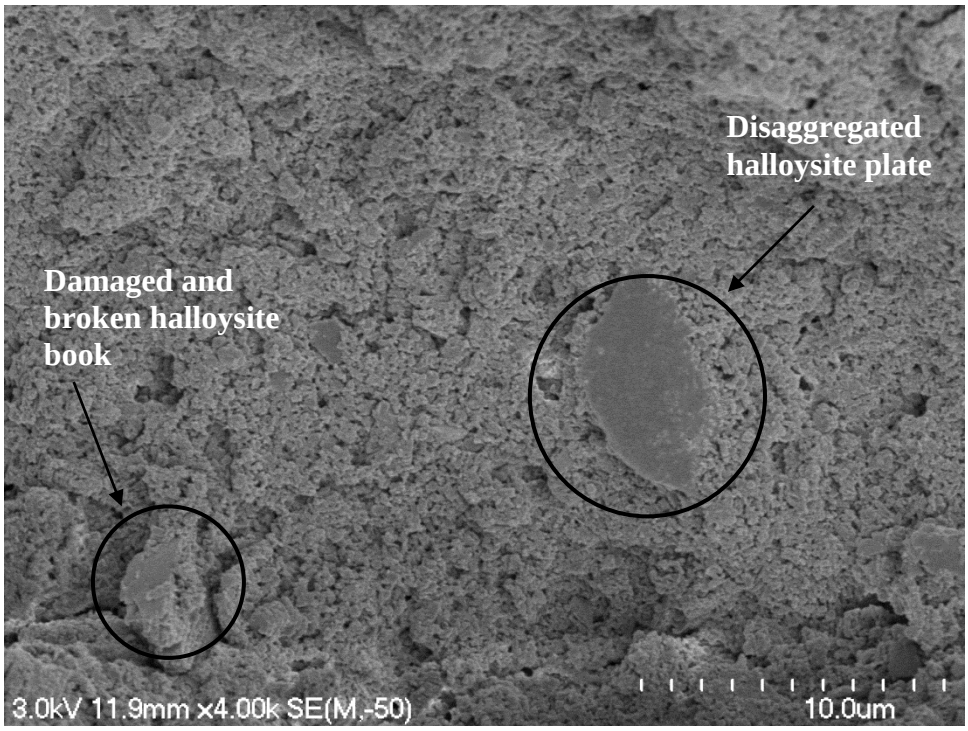

Figure 8.3: Remoulded material from PS2. Individual platelets can be seen on top of the sample, while the smaller spherical and broken down tubular morphologies have settled below. Broken and damaged book morphologies can also be seen, which do not have a the same defined shape as was previously seen in the peak strength state of the material

8.3.1.2 Non-Sensitive

8.3.1.2.1 Undisturbed state

Characteristically, the non-sensitive material analysed in this study indicated some clear and seemingly significant differences in clay particle interaction from the sensitive material. Primarily, the non-sensitive material was comprised of both spheroidal and tubular clay morphologies, but the spheres were typically larger (~ 600–800 µm; see Chapter 6) than those in the sensitive material, while the tubular morphologies were much longer and thinner (~ 600–900 µm; see Chapter 6). The tube sizes encountered were in the upper size range for the tube halloysite morphologies identified by Joussien *et al.* (2005). While the tubes were longer than those observed in the sensitive material, relative to the sphere sizes from the non-sensitive material, the tubes were similar in size. The diameter widths of the tubes (from the non-sensitive material), provide the distinction from the sensitive material, given they are much thinner than the spheres, while in the sensitive material the tubes are stubby and are relatively

wide, comparable to the spheres. These big spheres and long thin tubes (compared to the sensitive material) appear to be very important in non-sensitive development. Where the spheres interact with each other, pore spaces would typically exist within the voids that they create. Given the size of the spheres, however, the size of the voids is larger, however fewer void spaces exist, meaning the potential moisture content up build in the clay fraction is limited to those spaces.

The role of the tubes is also important. Typically the long thin tubes 'fill' the gaps between the large spheres, reducing the available pore space and giving a more tightly interacting clay structure, where the halloysite appears to be closely packed. Consequently, this mix provides a higher density of packing of the clay material. These characteristics were both common from RS1 which contained significant clay levels (> 30 %; see Chapter 5) as well as all samples from Tauriko which contained low clay levels (~ 2.4 %–5.1 %; see Chapter 5). This indicates that the characteristics of non-sensitivity are common across more than just one sample material source. The size relationship of various clay morphologies has previously been recognised as a contributor to soil strength. Craig (2004) suggested that high proportions of tubular and spheroidal clays typically increase the remoulded shear strength of a soil. This statement actually appears to be size dependent, given that from this study, such behaviour is apparent for irregular, large sized halloysite clay particles. In the situation where the sizes are small and comparatively similar, however, void ratios are increased and liquidity indexes are higher, therefore producing a lower remoulded strength. Consequently, the shapes and interactions between the irregular sizes reduces the opportunity for high moisture contents through reduced pore space, which in turn increases the remoulded strength, reducing sensitivity (Figure 8.4).

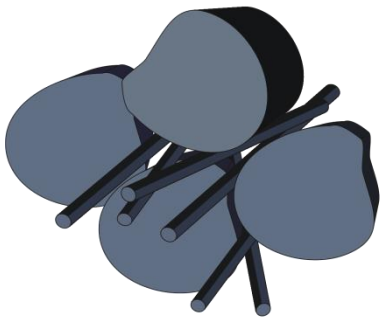

Figure 8.4: Simplified diagram of the interrelationship between irregular tubular and spherical halloysite clay morphologies promoting a high density of packing. Such packing reduces void space and thus the potential for moisture to build within the sample.

8.3.1.2.2 **Remoulded state**

The remoulded structure of the non-sensitive material generally showed very little disturbance following remoulding (see Chapter 6). The position of the tubes intermixed tightly with the spheres was commonly visible following disturbance and the particles appeared to be oriented in the same way as before the remoulding had taken place. This feature indicated that the sphere and tube interactions were tight and could resist disruption without disaggregating.

Pore spaces could still be seen throughout the samples, but they were typically not deep and the moisture content of the samples (< 47 %) indicated that they did not hold substantial levels of water. Even if all water in RS1, for example, was mobilised, the soil would not exhibit flow properties because the liquid limit was higher than the moisture content, meaning that the soil would remain in a plastic state and not enough water would be available for the transformation of the soil to a liquid state. Of the water that is held within the sample, the clay interactions that remain after the remoulding process indicate that even upon structural disturbance, the bonds are strong enough for the clay particles to not act as individual aggregates. These bonds are likely electrostatic bonds between sphere edges and tubular halloysite formations. The water within the sample is important for allowing cohesion between the clay particles and the ions in the water, yet also at a low enough level to not produce fluidised soil behaviour. Put simply, if the moisture content of this sample exceeded the soil liquid limit and the soil became fluidised upon remoulding, the reduction in strength would be assumed to be great enough for this type of soil to be

considered highly sensitive. In the case of RS1, however, the high clay content and irregular clay particle shapes and sizes reduce pore space, inhibiting such moisture contents, while in the Tauriko samples, the large proportion of sand promotes a well drained environment that does not allow for considerably high moisture contents to build up. Wyatt (2009) also suggested that irregular clay particle sizes and shapes, as seen in both samples from Rangataua Bay and Tauriko, are more likely to interlock when sheared and so the frictional strength of the soil materials is enhanced purely by these shapes, again reducing the potential for a large reduction in soil strength and thus highly sensitive behaviour.

8.3.2 Geomechanical properties

8.3.2.1 Undisturbed strength

Intact or peak strength of the sensitive materials was characterised primarily by the Atterberg limits of the soil, triaxial shear strength, field and laboratory shear vane strengths and density properties. The following section discusses the peak strength geomechanical properties for each sensitive and non-sensitive sample. Relationships between the variables are also discussed.

8.3.2.1.1 Soil density void ratio and porosity (activity, void ratio, porosity, bulk density, particle density)

Soil density characteristics indicated some distinct differences between the sensitive soil and the non-sensitive soil in its peak strength state. The sensitive material typically had low dry bulk densities which, with the exception of PS1 and PS2, were lower than the non-sensitive material. Arthurs (2010) previously characterised sensitive pyroclastic soils from the North Island as having low dry bulk densities, consistent with the sensitive material from this study. Wet bulk density varied more greatly. SEM observations indicated that the sensitive samples were very porous with many micropores throughout the sample. This high microporosity in turn increased the void ratio, driving the wet bulk density up, while the dry bulk density is still low.

Of the non-sensitive samples the higher bulk density in RS1 was consistent with the SEM observations, where clay particles were tightly packed with few

pores visible, increasing the overall bulk density of the sample. This high bulk density was consistent also with the particle size measurements which indicated that the clay fraction was highest in the sample, and while this is typically attributed to lowering the bulk density of a soil (due to many small pores being present) (McLaren and Cameron 1996), the tight packing of the clays observed in the SEM observations confirm the reduction of pore space compared with that of the sensitive samples. Non-sensitive Tauriko samples indicated low wet bulk densities, with small reductions in their dry bulk density which was primarily due to their very low moisture content (< 32%). Furthermore, samples from Tauriko also exhibited tightly packed clay particles in the clay fraction. However, the clay fraction was observed to be very low and so did not have much impact on the bulk density. This tight packing of the clay particles was different from that of the sensitive materials.

Like bulk density, void ratios and porosities of the studied material typically separated the soils into sensitive and non-sensitive. All porosities for the sensitive material were > 61 % while the non-sensitive material was always < 60 %. McLaren and Cameron (1996) previously characterised a range of New Zealand soils as having a porosity range between ~ 30 % and ~ 60 %, indicating that sensitive materials have, on average, typically higher porosity than most New Zealand soils. This potentially provides a useful indicator for sensitivity in New Zealand soils. Void ratio unsurprisingly followed a similar pattern to porosity, categorising sensitive material as those which have void ratios > 1.48, whereas non-sensitive material was consistently below 1.48. Such high porosities and void ratios are consistent with materials analysed by Wyatt (2009) who also noted that sensitive material porosities and void ratios were above the values given. Keam (2008) alternatively identified that sensitive material from his study had porosities of > 55 % indicating that some overlap may exist between sensitive and non-sensitive material for porosity variation. This overlap would suggest that sensitive material cannot be solely characterised by a specific porosity range, but high porosities of > 60 % are a typical feature of sensitive rhyolitic material along with void ratios above 1.48. These high values are primarily are promoted by the mode of deposition of the materials and the subsequent large proportion of micropores present within the sample structures. Initially the fallout nature of pyroclastic deposition allows for a high void ratio as irregular volcanic glass textures settle

(Rogers 1995), followed by the diagenesis of pumice fragments to produce many pores within the sample (Torrance 1992). Secondly, within the sensitive material from this study, micropores are consistently present, as regularly shaped particles provide many pores where they adjoin, whereas in non-sensitive material the irregularly sized particles induce less pore space as they are more efficiently sorted.

Typically as the sensitivity decreased the particle density increased (see Chapter 7). This relationship is consistent with the dissolution and precipitation of the halloysite clay particles, suggesting that as more primary minerals are dissolved and secondary minerals are formed, such as clay particles producing a lower particle density, the sensitivity increases. This higher sensitivity could be expected given that halloysite is commonly seen throughout the sensitive material. Furthermore, this relationship was maintained with the addition of the data from Wyatt (2009).The non-sensitivity of RS1, however, may contradict this relationship, on the basis of the high halloysite content of the sample. Therefore particle density cannot be used as a reliable predictive factor in the forecast of the magnitude of sensitivity. The increase in particle density may alternatively be coincidentally related to the sensitivity by virtue of the size of pumiceous materials in the samples. SEM analysis revealed pumice in much of the sensitive material, which may suggest that the decrease in sensitivity with the subtle increase in particle density may be a result of smaller size of pumice clasts in those samples. Typically as pumice is weathered and reduces in size, the amount of vesicles is reduced and particle density increases marginally (McLaren and Cameron 1996). This could be possible for the rhyolitic deposits examined both in this study and by Wyatt (2009).

8.3.2.1.2 **Atterberg limits, moisture content and activity**

The most characteristic feature of the Atterberg limits was the relationship between the moisture content and liquid limit, and the formation of high liquidity indices (> 1). All sensitive samples exhibited moisture contents well above the liquid limit for each sample, indicating that after remoulding the remoulded soil will behave as a liquid without the addition of further water (Rankka *et al.* 2004). This feature is characteristic of sensitive soils both within New Zealand and elsewhere (Skempton and Northey 1952; Smalley *et al.* 1980; Torrance 1983;

Rankka *et al.* 2004; Mitchell and Soga 2005; Wesley 2007; Wyatt 2009; Arthurs 2010; Tonkin and Taylor 2011), and so does not appear to be surprising for the sensitive material encountered in this study. Nevertheless, it remains an important feature.

The liquid limits, however, appear to differ in formation between sensitive fine-grained pyroclastic derived materials and the post-glacial derived sensitive clays typically encountered internationally. Salt leaching in glaciomarine derived clays is considered very important as it decreases the liquid limit by decreasing electrolyte concentration and causing an increase in the clay double layer thickness (see Chapter 2). The increase in the clay double layer in turn increases the interparticle repulsion, reducing the remoulded strength of the soil and producing high sensitivities (Skempton and Northey 1952; Mitchell and Soga 2005). Considering salt leaching is not a factor in the pyroclastic-derived sensitive soils from New Zealand, the high sensitivity is not necessarily derived from a particularly low liquid limit as observed internationally. Rather, in some cases the liquid limit is high (~ 89 % at TPS1). Instead, the critical factor is the high void ratio within the sensitive material facilitating very high moisture contents, which exceed the liquid limit (producing liquidity indexes > 1). The occurrence of many voids due to the abundance of similarly sized spherical and tubular forms of halloysite in the samples promotes the high porosities and therefore high moisture contents. The very small dominant clay particle sizes (~ 150–400 nm, see Chapter 6), allow pore water to be easily retained within the microstructure of the soil (because the pore sizes are so small and abundant), allowing moisture contents to build to high levels.

Another important feature in relation to the liquid limit is the presence of low activity clays (Torrance 1983; Mitchell and Soga 2005). Torrance (1983) suggests that high activity clays inhibit the development of high sensitivity due to swelling, increasing the soil liquid limit, while low activity clays have the opposite effect. The samples from this study were dominated by halloysite clay, which is typically identified as a low activity clay mineral (Joussien *et al.* 2005). The activity determinations for the sensitive material, however, typically indicated that the soil was of high activity (1.47 – 14.74, see Chapter 5), rather than the low (< 1) activity expected for halloysite (Selby 1993). These activity values,

however, are highly reliant on the clay size particle percentage determined from the particle size measurements (see Chapter 3). Under the SEM it appeared that the clay fraction of the samples was significantly higher than the ~ 2 – 11 % determined for the samples, suggesting that the soil was not adequately dispersed for particle size measurement. Similar measured particle size discrepancies were described by Wyatt (2009) for sensitive material from the Tauranga region using the same particle size determination method. On the basis that the particle size determination may be inaccurate because of the incomplete dispersion of clay particles, SEM images of samples dispersed with sodium hexametaphosphate were examined (Figure 8.5, 8.6). The clay particles still appeared to be aggregated, implying that a true realisation of the particle size using sodium hexametaphosphate is not entirely appropriate. This likely explains why the Malvern particle sizer method and the pipette method (see Chapter 3) gave similar results. On this basis, the assertion of halloysite, and therefore the soil material from this study, as low activity material is accepted.

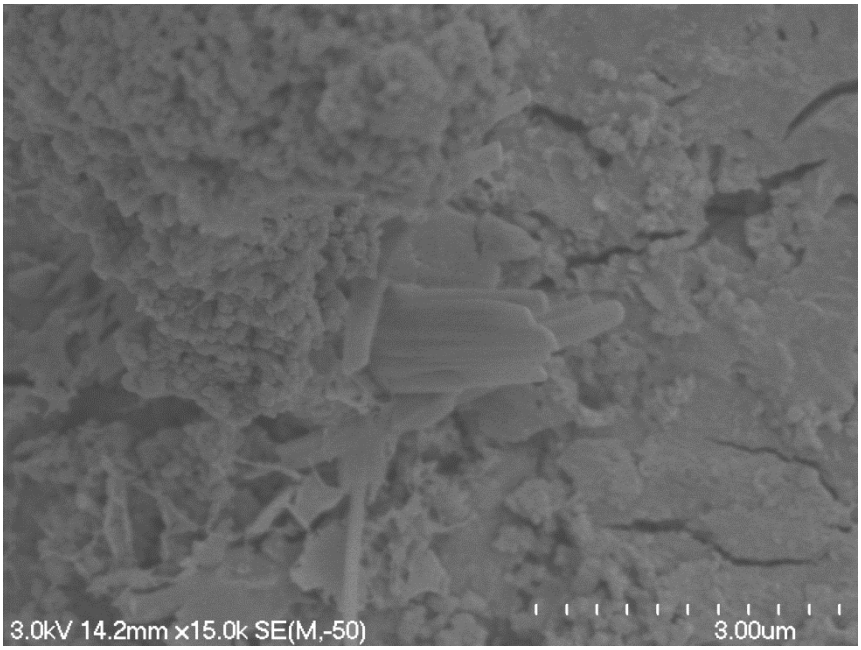

Figure 8.5: Clay particles from TPS1 following sodium hexametaphosphate treatment for particle dispersal. The aggregates still appear to form aggregations and do not appear to have been completely dispersed following treatment.

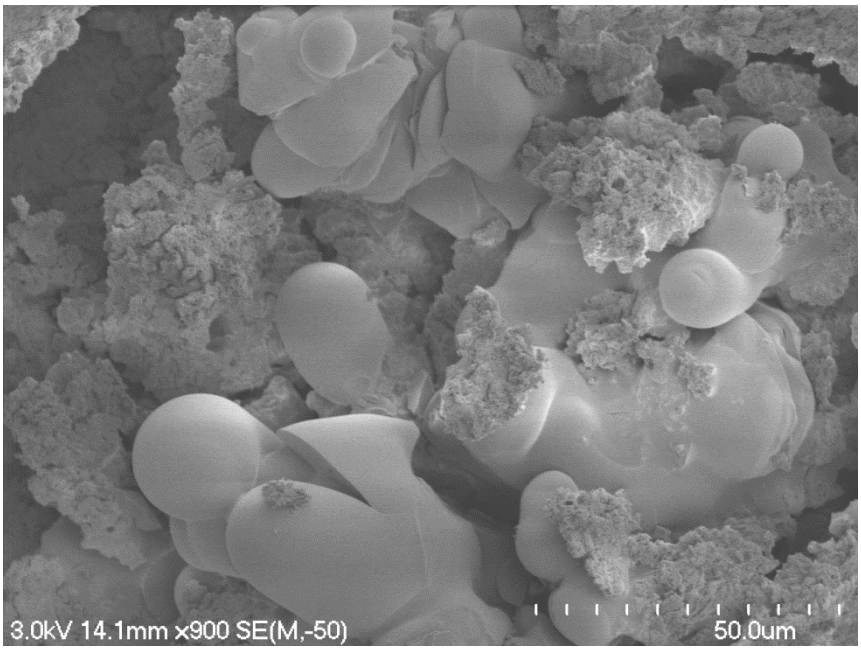

Figure 8.6: Clay particles following sodium hexametaphosphate treatment for particle dispersal. Blocky aggregates of small clay particles can be seen. The very rounded large globules are likely the sodium hexametaphosphate that was left in the soil solution when the samples were dried for SEM analysis.

It could be assumed, therefore, that the presence of halloysite to promote a dominantly low activity soil material (which consequently assumes a low liquid limit and subsequently a low remoulded strength) promotes higher sensitivity. This assumption is, however, contradicted by the non-sensitive material, particularly at Rangataua Bay which had a high clay content, and was comprised only of halloysite indicating a low activity. RS1 did not become fluidised upon remoulding and therefore did not have a low remoulded strength as may have been assumed on the basis of the low activity. However, the high density of particle packing as observed from the SEM (see Chapter 6, Section 6.2.3.5) determinations indicate that the morphologies and size of the halloysite particles are important in promoting the high moisture content and thus the formation of high liquidity indexes, rather than just solely the presence of the low activity halloysite mineral. In other words, the types of halloysite morphology are more important than just the presence of low activity halloysite. A simple statement suggesting that the low activity of halloysite clay promotes lower liquid limits and thus high sensitivity, cannot be generalised for sensitive rhyolitic deposits from the Tauranga region.

8.3.2.1.3 **Triaxial**

Triaxial test results did not vary greatly between the sensitive samples analysed; this consistency was in keeping with the results of Wyatt (2009), and well within the broad ranges reported by other authors analysing sensitivity in the Tauranga region (Keam 2008; Wyatt 2009; Arthurs 2010). While the previous results from multiple studies may suggest sensitivity does not conform to any particular friction angle or cohesion, the results from this study do yield some potential conclusions. Initially, as mentioned in Chapter 5, the material behaviour resembles that of a clayey SILT to SILT material evidenced by the low cohesion and moderate to high friction angle achieved by all samples. Wesley (2010) stated that soils with higher friction angles tend to suggest soil behaviour that lies below the A-line in the Plasticity chart (see Chapter 5), which is consistent with findings in this study. The moderate to high friction angles also suggest that the sensitive material can maintain steep slope angles before collapsing which is critical to the fact that sensitive soils can remain stable for very long periods of time before failing catastrophically.

The cohesion and friction angle did not vary significantly between the tests indicating little difference in soil materials between the consolidated drained test and the consolidated undrained test in OS1. The primary difference observed was in the stress versus strain behaviour during the compression stage, where the deviator stress rarely reached a maximum before 20 % strain in the consolidated drained test. Meanwhile, the consolidated undrained tests consistently reached maximum deviator stress before the 20 % strain boundary (typically between 2 – 8 % strain). Primarily this was because of the effect of the drained environment for the drained test. The drained environment allows the pore water pressure to dissipate during compression and thus results in negative pore pressure, while undrained tests promote positive pore pressures, pushing the grains apart during compression (Head 1998). Furthermore, the failure at low strains (as observed in the undrained testing) is typical for sensitive soils. Mitchell and Soga (2005) suggest the amount of strain at the point of failure decreases with increasing sensitivity. Keam (2008) previously attributed the sensitive failure at Bramley Drive, Omokoroa, to excess pore water pressure build up. Wesley (2007) similarly advocated this explanation, meaning that a consolidated undrained test more accurately characterises the soil conditions pre-failure as pore water pressure does not adequately dissipate based on case histories of sensitive material in the Tauranga region.

Effective stress paths of the sensitive material typically did not indicate a tendency towards over-consolidated (dilation) or normally consolidated (compaction) characteristics. Wyatt (2009) previously attributed compaction characteristics to the majority of the sensitive material that he analysed. Mitchell and Soga (2005) also suggested that the strain required to cause failure in glaciomarine sensitive material increases with increasing dilatation, but the behaviour is highly dependable on the depositional characteristics of the soil/material. They suggest that considering the undisturbed structure of sensitive material is affected by many factors (such as overburden stress, stratigraphic position and depositional environment), the volume changes under pressure are a function of the soil structure (Mitchell and Soga 2005). Therefore, neither compaction nor dilation behaviour upon failure is dominant for sensitive rhyolitic soils. In this sense, the development of sensitive rhyolitic soils does not require a specific deposition depth or high overburden effective stress (i.e. they do not have

to be exposed to a higher consolidation stress above what they are currently at to exhibit sensitive behaviour).

A characteristic porous open structure of sensitive material (similar to that observed in this study) is thought to be critical for failure (Houston 1967; Mitchell and Soga 2005). Mitchell and Soga (2005) suggested that the loss in shear strength in glaciomarine quick clay was because of soil disturbance accompanied by a simultaneous large increase in pore pressure and decrease of effective stress to almost zero. Similar pore water pressure changes (facilitated by the porous microstructure) were observed in all sensitive samples analysed in this study. The high natural moisture content means that full saturation within the samples is easily attained (e.g. from high rainfall event) which induces failure, resulting in significant strength reduction and thus high sensitivity (Mitchell and Soga 2005).

8.3.2.1.4 **Shear Vane**

Peak vane shear strength was highly variable between sensitive samples and also between the field and laboratory shear vane methods (see Chapter 5, Section 5.5). The vane shear strength did not correlate with the clay content, as may have been expected, given clay content usually exhibits cohesion (Selby 1993). The highest peak vane shear strength was consistent between methods, both recorded at TPS1 (122 kPa for field shear vane and 80 kPa for laboratory shear vane). This appears to correlate with the plate-like halloysite clays present in the sample along with the tubular and spherical shapes observed through the SEM. Samples with the greatest abundance of plates are more likely to intertwine upon shearing. Wyatt (2009) previously identified that irregular, individual particle shapes (such as plates) increase frictional strength and are more likely to interlock (increasing peak strength) when sheared. Furthermore, the silt sized material within the turbulent-matrix microstructure increased the frictional resistance. This relationship was supported by the triaxial determinations which indicated that the deviator stress required for failure was consistently higher in TPS1 than that observed in any other sample, at all three confining pressures (50, 100, 150 kPa).

The lowest shear vane strength varied between methods. The Pahoia Peninsula samples had the lowest field strengths (< 70 kPa), while the laboratory

shear vane indicated that PS2 had the second highest peak strength (57 kPa). PS1, however, had the second lowest mean peak shear strength with the laboratory shear vane (26 kPa). Considering that three of the four mean peak strengths determined from Pahoia Peninsula were either the lowest or second lowest mean peak strength, the soil was concluded to have the lowest mean peak strength. This was somewhat surprising, given that the halloysite book morphologies were thought to promote a higher interaction between particles and provide a larger surface area to assist with cementation (as suggested by Wyatt 2009). It appeared, however, that the books instead promoted bridge type connections throughout the sample, which increased the amount of larger sized voids, and in turn reduced the peak strength.

8.3.2.2 **Remoulded Strength**

The remoulded geomechanical properties of the sensitive materials were primarily characterised by the viscosity characteristics, yield stress variation and remoulded strength measurement by the field and laboratory shear vane.

8.3.2.2.1 **Yield stress variation**

The most important feature of the analysis of yield stress for characterising the behaviour of the remoulded strength of the sensitive samples was its relationship with pH. Yield stress variation with pH typically decreased as pH increased (excluding OLRO) from its natural position. Changes in yield stress with reduced pH were not always consistent between samples. The decrease in yield stress observed at higher pH for all samples, excluding OLRO, was the likely result of the change in halloysite particle charge with pH adjustment. In studying the flow characteristics of halloysite, Theng and Wells (1995) observed that increasing pH generally decreased the viscosity (and thus yield stress) of the suspensions. Such behaviour has been attributed to an increase of negative charge on the particle edges as pH increases, which in turn repels the negative basal surface charge of the other halloysite particles, resulting in the dispersion of the particles (Michaels and Bolger 1964; Theng and Wells 1995). This dispersion appears to explain the (in some cases large) decrease in yield stress with increasing pH. Such behaviour has also been characterised by Nuntiya and Prasanphan (2006) who described the rheological behaviour of kaolin

suspensions. They consequently suggested that where a sample had lower pH, the magnitude of positive charges increased on the edges of the kaolin group material, thus attracting the clay minerals and producing higher yield stresses and greater remoulded strength. Nuntiya and Prasanphan (2006) also indicated, however, that the face-to-edge interactions formed by decreasing pH would form a house-of-cards type structure, increasing flocculation and possibly increasing the potential to hold more moisture within the structure.

The impact of a flocculated structure is negative for sensitivity. Although the strength of the clay particle interactions would be increased from the reduced pH (if such interactions were to form in a peak strength state), the moisture content would be increased even further, which could reduce remoulded strength, thus increasing the potential sensitivity of the material (Bentley 1979). An increase in yield stress at lower pH was only apparent for OS1, OS2, PS1 and PS2, while conversely TPS1 decreased with both increasing and decreasing pH. OLRO was the only sample to initially increase with pH before declining at pH ~ 8 (see Chapter 5). Theng and Wells (1995) suggested that the increase of yield stress with pH could possibly be because the surface charge characteristics do not have as great an effect on spheroidal particles. This could be the case for OLRO which SEM analysis confirmed a high abundance of spheroidal particles. TPS1, also indicated that yield stress did not increase as pH was lowered below its natural position. In addition to the spherical particles within the structure, TPS1 also contained many plate-like particles, meaning a increase with lowered pH might have been expected. Carroll (1959) suggested that the addition of sodium hydroxide can actually partially decompose halloysite, which may suggest that the formation of more very small particles occurred, through plate decomposition, leaving primarily spheroidal morphologies and thus reducing the impact of the surface charge characteristics as Wells and Theng (1995) suggested.

Some authors, however, have introduced another possibility regarding inconsistent halloysite particle behaviour, primarily as a result of the effect of pH with ionic strength (Williams and Williams 1982; Chang *et al.* 1993). Chang *et al.* (1993) proffered that as particle suspensions are increasingly more basic, the viscosity is reduced because of the increased negative charge on the particle edges as discussed earlier. At acidic pHs, however, the addition of HCl increases the

ionic strength. This increase of ionic strength interferes with the electric double layer of the particle faces, which has the effect of reducing the edge-to-edge interactions, decreasing the viscosity as well. This reduction of edge-to-edge interactions may also explain the negative trending behaviour of TPS1 at both sides of the natural (~ 6.2) pH. The behaviour of OLRO which decreases in yield stress at lower pHs, yet increases subtly at pH ~ 7, followed by a decrease at pH 8 (see Chapter 5), could be the result of both processes identified. Initially the low interaction between spheroidal particles, as Theng and Wells (1995) suggested, allows for the subtle yield stress increase at pH ~ 7, but as pH increases the particles do start to repel one another. At lower pHs the ionic strength increases, and reduces the edge to edge interactions aforementioned. It is not clear from this study why the ionic behaviour with the electric double layer is variable between samples. Further measurements including the position of the soil isoelectric point would need to be determined to deduce what impact this has (Yong *et al.* 1979; Theng and Wells 1995).

8.3.2.2.1.1 Comparison with international sensitive soils

In comparing these remoulded characteristics with international sensitive soils, there is not a strong correlation between the results. No research of this nature into sensitive rhyolitic soils could be found in the literature, and so comparisons with glaciomarine derived sensitive clays were the only suitable comparison. Previous research has indicated that sensitive Leda clays increase in yield stress with pH to a peak of ~ 6 – 6.5, before it declines at high pH (~ 8) (Bentley 1979; Yong *et al*. 1979). This behaviour was similar to that observed at OLRO, however, the critical pH with maximum yield stress was much more apparent in the international samples. Bentley (1979) and Yong *et al.* (1979) both suggested that increasing yield stress with pH is a result of the change in the solubility of the cementing material that increased the bridging effect between peds and other grains within the matrix. In their study, the pH increase obviously had a critical stage before the bonds were reduced, decreasing the yield stress at pH ~ 7.5. Explaining the difference between the variation observed in the sensitive material from this study and the international studies appears to lie within the clay mineral type and formation. Sensitive Leda clay is typically comprised of illite and chlorite clay minerals (Gillott 1971; Bentley and Smalley 1979), while the sensitive material investigated from this study has been

conclusively identified as halloysite (see Chapter 6). Of most importance is the interaction between halloysite clay particles. Given that increasing pH with sodium hydroxide tends to induce halloysite particle repulsion, increasing pH is unlikely to have a positive impact of yield stress compared with the international glaciomarine clays as suggested by Bentley (1979).

8.3.2.2.1.2 Shear stress curve characteristics

In analysing the shear stress with shear rate characteristics, Theng and Wells (1995) identified that steep gradients represented the presence of blocky aggregates within the sample (see Chapter 5). Typically PS1 and PS2 were observed to have the highest shear stress gradients. SEM analysis revealed that the large halloysite books of PS1, along with the close aggregation of some books in PS2, formed blocky aggregates. Blocky aggregates are suggested to offer greater resistance to flow, while small spherical particles, as observed in OS1 and OS2, slide past each other with ease (Theng and Wells 1995). These features are important in characterising the flow behaviour of the halloysite dominated samples because the blocky aggregates impact the flow characteristics, meaning that the remoulded material will not flow as far (Theng and Wells 1995). The reduced flow characteristics of some sensitive materials are important as it means smaller runout lobes may be expected (reducing the hazard area of slopes prone to sensitive failures) for materials that contain large halloysite books.

8.3.2.2.2 Shear Vane

Remoulded shear vane characteristics were consistent for both the field and laboratory shear vane methods, suggesting that the remoulded strength could be quantified for the sensitive material. OS1, TPS1 and PS2 all indicated mean remoulded strengths of ~ 8 – 12 kPa, while PS1 and OS2 were between 2 kPa and 6 kPa. The high remoulded strength of TPS1 was expected given the abundance of plate-like halloysite clays which increase the frictional resistance to shearing. Following remoulding, the plates that were not completely destroyed allowed for a slight increase in remoulded strength (Wyatt 2009). The lowest mean remoulded strength was recorded at PS1, which was surprising given the large book aggregates observed during SEM analysis. These books were seen to be broken upon remoulding, and so provided little resistance within the structure in

determining the remoulded strength. OS2 also had a very low remoulded strength, which was expected given the abundance of halloysite spheres. Smalley *et al.* (1980) previously suggested that small halloysite spheres offered very little resistance upon remoulding, instead simply rolling over each other when in suspension due to their lack of long range interparticle forces.

The remoulded strengths of all materials from this study were typically lower than those encountered by Jacquet (1990) who showed an average remoulded strength of ~ 11 ± 2 kPa across all sampling sites tested. Wyatt (2009) suggested that sensitivity from Otumoetai and Tauriko was the product of low remoulded strength giving high sensitivity values. This finding appears consistent for the results of this study, which indicated that subtle low variations in remoulded strength typically produced extra sensitive material, rather than the sensitivity being a result of high peak strengths.

8.3.3 **Sensitivity classification**

As previously described in Chapter 3, the method of remoulding for determining sensitivity with a shear vane does not appear to completely represent the true remoulded strength of a soil.

Wyatt (2009) attempted to rectify this limitation by completely immersing the shear vane within physically remoulded soil which revealed that remoulded strength was typically higher by ~ 23 % upon repeating sensitivity measurements on the same material (see Chapter 3). While ~ 23 % is only a very small variation between such low remoulded values these small variations have a significant impact in relation to the calculation of sensitivity by an evenly weighted ratio of undrained peak strength to undrained remoulded strength.

The even weighting of the sensitivity ratio is a primary issue in the classification of sensitivity. In the context of sensitive rhyolitic tephra from New Zealand, multiple studies have indicated low remoulded strengths, typically below 15 kPa, with the majority less than 10 kPa (Gulliver and Houghton 1980; Jacquet 1990; Wyatt 2009; Arthurs 2010). Typically what is observed is that the highest sensitivities are where the remoulded strength is so low. The issue lies in that when the denominator of the equation is less than 10 kPa, each 1 kPa has a large

impact, especially where the denominator is less than 5. For example, if the peak strength is 40 kPa and the remoulded strength is 2, then the sensitivity is 20. However if the remoulded strength is only 2 kPa higher at 4 kPa then the sensitivity is 10, markedly lower. This example demonstrates that subtle variations in remoulded strength can have considerable bearings on the outcome of the sensitivity quantification, while only at slightly higher remoulded strength values the influence is markedly less. Additionally, at such low remoulded strengths, the accuracy of the field shear vane is diminished where the small graduations and operator effects are likely to have as much of an impact. Furthermore, by evenly weighting the sensitivity ratio the remoulded strength is always going to have the most influence over the sensitivity value, especially where very subtle changes in remoulded strength are apparent. At high remoulded strengths of > 10 kPa, the influence of small 1–2 kPa differences has much less of an impact on the sensitivity ratio. In this sense, the sensitivity ratio may not be entirely appropriate for the very low remoulded strength values achieved in rhyolitic tephra derived sensitive soils.

Importantly also is the user discrimination in determining what is sensitive by means of physical behaviour. The shear vane test can indicate that samples that do not flow upon remoulding or have a sufficient enough moisture content to promote > 1 liquidity indexes are classified as extra sensitive to quick (e.g. Jacquet 1990). Quick clay behaviour suggests some form of fluidisation upon remoulding as it generally applies to the northern hemisphere glaciomarine sensitive material (Rankka *et al*. 2004). Eden (1966) identified such an issue in evaluating sensitive clay from glaciomarine environments, suggesting that the vane is only appropriate for soft saturated clay, while hard to stiff material that was not saturated was not suitable for the vane (as observed at Rangataua Bay). Attempting to determine sensitivity from materials that are not wet to saturated can result in a misguided ‘false’ sensitivity determination. Such a misinterpretation of sensitivity was most apparent from the study of Wyatt (2009). A sample was chosen which clearly did not flow upon remoulding and had a very high remoulded strength of 36 kPa. The sample could be remoulded into a shape, held its own structure and did not release water upon remoulding. Furthermore, the moisture content was below the liquid limit, suggesting that it would not remould into a liquid state. While a soil is not required to flow upon remoulding

for it to be sensitive (Mitchell and Soga 2005) the water does promote very low remoulded strengths and so high moisture contents are common for sensitive materials, especially in the Tauranga area (Gulliver and Houghton; Wesley 2007; Keam 2008; Wyatt 2009; Arthurs 2010). On the basis of the photo evidence, a sensitivity value of 8 (classified as 'extra sensitive') is not comparable to the extra sensitive materials from this study. Based on this, the importance of the Milne *et al.* (1995) field test to accompany the shear vane test in determining sensitivity is critical to ensure that the quantified shear vane values match the field conditions.

8.3.4 Summary of undisturbed to remoulded strength characteristics of rhyolitic sensitive soil

Undisturbed sensitive material was dominated by small regularly sized spheres and small wide tubes that did not pack efficiently together. This lack of packing promotes a high void ratio and porosity. Such conditions facilitated high moisture contents, and therefore liquidity indices > 1. Furthermore, connector contacts between larger silt grains in the microstructure also provided large voids for moisture storage, and weak connectors that could be easily broken. The release of moisture upon remoulding is characteristic of sensitive materials in facilitating a low remoulded strength and thus high sensitivity.

Non-sensitive material was primarily characterised by comparatively larger spheres (than the sensitive material), tightly intermixed with comparatively long and thin tubes. This particle interaction produces less opportunity for void space, reducing moisture content in the clay fraction. Porosity was always lower than 60 % and liquidity indices were always lower than 1. The microstructure was a continuous matrix, where larger silt sized material would be tightly packed within the tubular and spherical particle interactions. Following remoulding the clay particle interactions were still intact with little structural disturbance obvious, indicating that the tight particle interactions were significantly stronger than the sensitive material.

Table 8.1 summarises the variation in peak undisturbed strength to remoulded strength for both the sensitive and non-sensitive material.

Table 8.1: Comparison of undisturbed/peak strength to remoulded strength changes between sensitive and non-sensitive materials from this study.

Sensitive		**Non-sensitive**	
Undisturbed/peak strength	**Remoulded Strength**	**Undisturbed/peak strength**	**Remoulded Strength**
• Halloysite clay minerals • Small spheres and short, wide tubes resulting in a low density of packing. • Porosity > 61 %, high void ratio > 1.5 • Low cohesion • High moisture content, liquidity index > 1 • Matrix-skeletal microstructure	• Moisture released from microstructure • Low remoulded strength • Partially broken tubes, books, plates and connectors • Microstructure becomes continuous • Large books possibly reduce the runout zone in failed state	• Large spheres, long, thin tubes resulting in high density of packing • Porosity < 60 % • Low moisture content, liquidity index < 1 • Matrix microstructure	• Minimal water release on remoulding • Tubes, spheres interactions remain following remoulding. No substantial change to the structure upon disturbance

In comparing these general summary properties of the sensitive materials from this study with Jacquet (1990) (andesitic sensitive materials from New Plymouth – see Chapter 2), the formation and characteristics of sensitivity appear to be quite different. Jacquet (1990) found that materials of a higher clay fraction (21 – 56 %) appeared to result in plastic failure following remoulding. Liquidity indices were less than 1 yet the soils still had high moisture contents (up to 108 %). The nature of sensitivity in the samples from his study were characterised by very high peak strength as opposed to a low remoulded strength. The opposite results were observed in this study, where the release of significant moisture upon remoulding facilitated the large loss in shear strength and promoted failure in materials that did not necessarily yield large peak strength. The variation in microstructure therefore appears to provide the critical reasoning for this sensitivity behaviour variation. The key difference was that Jacquet (1990) found large portions of allophane in the microstructure, with halloysite less dominant. Wyatt (2009) suggested that allophane within sensitive material would tend to increase the remoulded strength and reduce sensitivity. This may be a reason for the plastic failure and inability of the materials to support liquidity indexes greater

than 1 from Jacquet's study. The allophane spherules and imogolite fibres do not produce the same open voids as the regular small halloysite spheres and stubby tubes, and so the propensity to flow and produce a very low remoulded strength is reduced. As a conclusion, it appears that sensitivity cannot be generalised in formation between volcanic ash materials from around New Zealand, but are case dependent as to their clay mineralogy and subsequent microstructure formation.

8.4 Development of sensitivity in rhyolitic tephra

The sensitive nature of the samples from this study was primarily controlled by the ability of the soil to maintain a high moisture content above the liquid limit (liquidity indices > 1) along with a weakly arranged halloysitic structure containing regularly sized spheres and tubes.

Initially, a key contributor to the development of sensitivity is the mode of deposition for the materials and how these affect the formation of sensitivity. Sensitivity of samples from this study appears to require materials derived from fallout tephra, where the loose packing that results allows for the development of a high void ratio (Torrance 1992). The high void ratio allows for a significant amount of moisture to be contained within the deposit, further enhancing diagenesis and weathering of primary minerals to generate secondary clay minerals. At Omokoroa, it appeared that the material had been reworked following initial deposition. Reworking of tephra material does not appear to compact the packing of the material, but rather, allows for high void ratios within the profile and as a result further increases the saturation potential. Arthurs (2010) previously suggested that some form of reworking was required for sensitivity in the samples he studied from the Tauranga region. He did suggest, however, that the reworking was not advanced enough to the stage where denser mineral grains were more highly concentrated compared with volcanic glass and pumice (Arthurs 2010). Such a level of reworking is suggested to decrease sensitivity as the structure would become less delicate and also fewer clay minerals would be weathered from the glass, reducing sensitivity potential (Arthurs 2010). Wyatt (2009) previously suggested that sensitive material from Otumoetai (with the exception of one sample) and Tauriko, Tauranga had not experienced reworking,

indicating that reworking is not always necessary for the development of sensitivity, but is common in the Tauranga region.

The next primary control in the development of sensitivity in rhyolitic derived materials, is their weathering and subsequent synthesis of clay minerals and their interaction within the microstructure. Initially, the wet to saturated deposit facilitates the dissolution and precipitation of the siliceous rhyolitic glass material to form halloysite in predominantly spheroidal and tubular forms, while some plates and books are also formed. The formation of halloysite is important, given that as a typically low activity clay mineral, the plasticity of the clay is low promoting a low liquid limit (Torrance 1983). While the formation of halloysite is not the primary contributor to sensitivity (Jacquet 1990; Wyatt 2009), it is important for providing the necessary conditions for sensitivity to develop. In the situation where the halloysite forms small, similarly sized tubes and spheres, a low density of packing is produced, facilitating the high void ratios and subsequent high porosity within the sample. The high porosity allows for a high moisture content, which again facilitates halloysite formation over any other type of mineral, forming a circular relationship where halloysite is continually formed. Only a significantly long drying event would break this loop, where the halloysite would likely be transformed to thermodynamically stable kaolinite (Churchman *et al.* 2010). Furthermore, the high level of water able to be held within the pores as a result of the packing allows for liquidity indices > 1 significantly reducing the soil strength as the soil becomes fluidised upon remoulding. Where halloysite forms in a variety of irregular sizes, primarily large spheres and thin tubular morphologies, the voids are reduced in the sample, particle interaction forms in a tighter arrangement, moisture content is reduced below the liquid limit and therefore the soil remoulded strength is not reduced enough as a primary requirement for sensitive development.

These halloysite clay formations must also form in a matrix-skeletal or flocculated matrix-turbulent structure. These structures also allow for large voids with high porosities, while also producing weak face-to-edge and edge-to-edge contacts between particles that can easily be destroyed upon remoulding, allowing clay aggregates to become suspended in flow. The skeletal and turbulent microstructure formations are primarily important because they form bridges and weak edge-to-edge particle interactions between larger silt grains, which can

easily be destroyed upon remoulding allowing those larger silt sized grains to become disaggregated and fluidised. It must be recognised, however, that it is the matrix microstructure formation of similar small sized halloysite spheres and tubes that dominate the sensitive materials.

In summary, sensitivity of rhyolitic tephra is the product of a several-step process. Initially silica-rich fallout tephra is deposited and, irrespective of whether it is reworked or not, forms a loosely packed material comprising mainly small-grained particles of glass and pumice (and subordinate crystals and rock fragments), which are easily weatherable. Wet to saturated conditions, with high concentrations of silica in soil solution, must then dominate, allowing the formation of halloysite (not allophane nor kaolinite). If the halloysite forms in regular spheres and tubes, the low density of packing and high void ratios facilitate high moisture contents to develop in the presence of low liquid limits, ultimately producing liquidity indexes > 1. The microstructure must contain easily broken bridges and connectors consistent with a matrix-skeletal formation or a flocculated partially turbulent formation. Upon remoulding, the combination of these factors allow for the release of significant water stored in the pores reducing soil strength significantly where individual particles and small aggregates act individually and flow in a fluidised behaviour leading to high sensitivity. Figure 8.7 conceptually characterises the interacting processes in the formation of sensitivity of rhyolitic tephra from the Tauranga region.

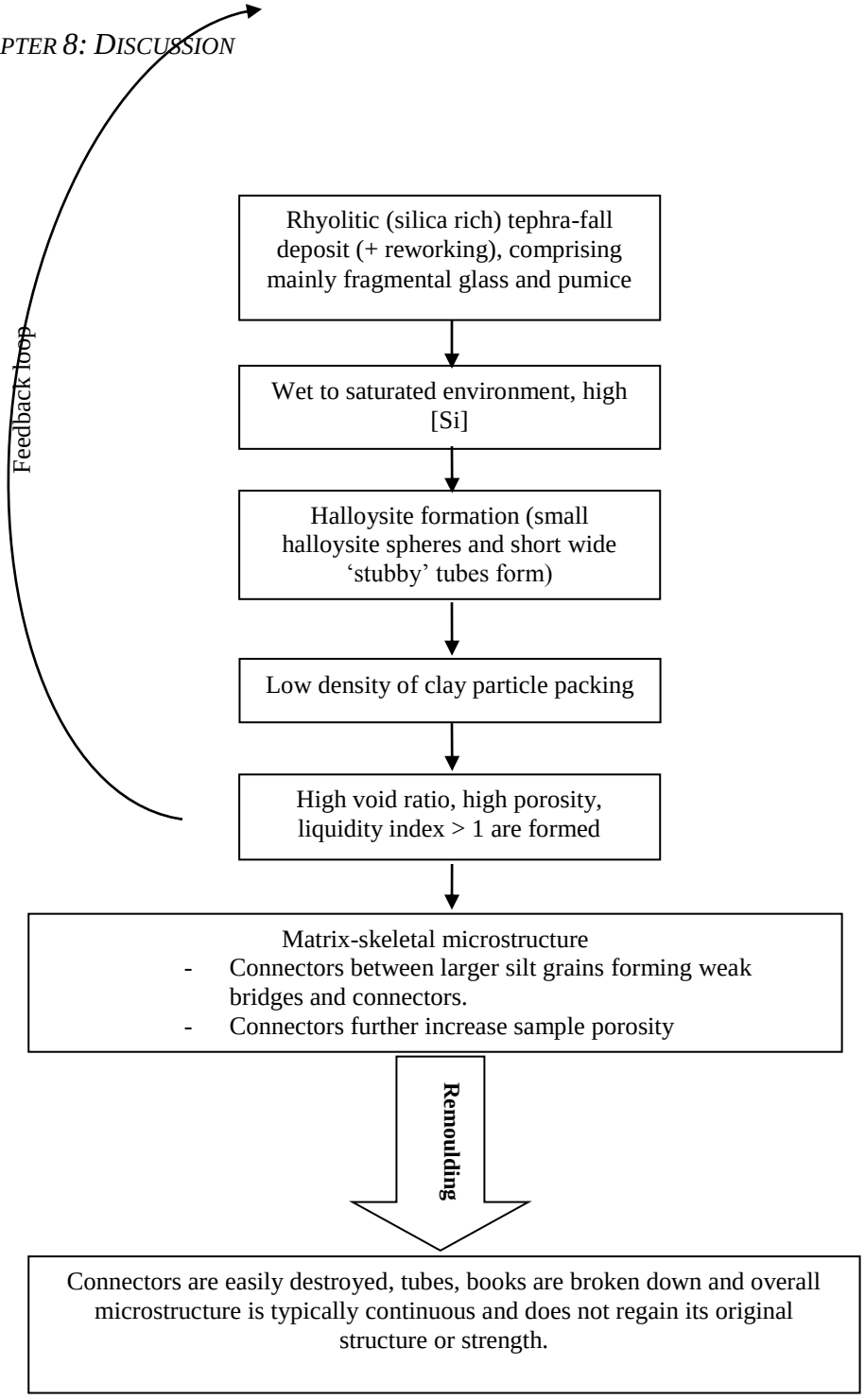

Figure 8.7: Conceptual diagram of the interacting processes involved in the sensitive development of rhyolitic tephra from the Tauranga region. Of note is the circular feedback relationship facilitating the formation of small halloysite spheres and short wide tubes from the continuously wet environment, which further promotes high void ratios and the storage of moisture, leading back to the wet environment and further halloysite formation.

8.5 **Summary**

The geomechanical and microstructural properties of both the undisturbed and remoulded state of sensitive rhyolitic material have been analysed. All sensitive soil material was of tephric origin and likely associated with the Te Puna Ignimbrite. Non-sensitive material was of both ignimbrite and tephra fall derived materials. All soil materials contained halloysite, with very large silt to sand sized, previously undocumented books forming in PS1. The formation of these books was likely the result of Fe enriching of the halloysite unit cell to facilitate plate development followed by Ostwald ripening and coalescence.

Sensitive material was comprised of predominantly small halloysite spheres and comparatively short and wide tubular morphologies in a matrix-skeletal microstructure. These morphologies inefficiently packed together (low density of packing) providing high void ratios and porosities, ultimately leading to high moisture contents exceeding the soil liquid limit. Following remoulding, skeletal connectors between large grains were destroyed, along with the break down of tube and book morphologies, indicating the microstructure interactions were weak and easily separated upon remoulding.

Non-sensitive material, on the other hand, was comprised of larger spheres and long and thin halloysite tubes in a matrix microstructure. The tube and sphere arrangement were much more efficiently packed, reducing pore space in the clay fraction of the sample, ultimately denying the opportunity for very high moisture contents to develop and ensuring liquidity indexes were always below 1.

The sensitivity of samples was facilitated by the ability of the soils to maintain high moisture content, producing liquidity indexes > 1. Such high moisture contents leading to low remoulded strengths and fluidised behaviour was common for all sensitive materials. These high moisture contents were a product of the aforementioned inefficient packing of similar small sized spheres and short stubby tubular formations of halloysite.

Chapter 9

CONCLUSIONS

9.1 Summary of research findings

The nature of soil sensitivity within the Tauranga region has been examined with particular regard to the microstructural and geomechanical characteristics of both the undisturbed state and remoulded state of sensitive and non-sensitive pyroclastic deposits. Materials at five sites were analysed. The primary aim of this thesis was to investigate the structural difference between intact and remoulded strength states of sensitive rhyolitic material, principally in comparison with non-sensitive soil samples. Five objectives were set to achieve that aim, and the following chapter summarises the research findings of these objectives and documents the outcomes and conclusions drawn.

9.1.1 Field observations

Field geological observations indicated that the sensitive material was likely associated with the Te Puna Tephra (~ 0.93 Ma) which is not believed to be a correlative of the Kidnappers Ignimbrite (~ 1 Ma) as previously suggested by Arthurs (2010). Opposite paleomagnetisation of the Te Puna and Kidnappers Ignimbrite provided decisive evidence for this conclusion.

The Te Puna Tephra was observed to outcrop at several coastal sites, but it was not visible at the inland Tauriko site. Briggs *et al.* (1996) showed that the Tauranga region is underlain by a complex sequence of materials of secondary and primary volcanic and pyroclastic origin that varies in both thickness and spatial distribution. On this basis, the availability of the Te Puna Tephra and therefore potential sensitive deposits cannot be generalised over the entire region, but rather its distribution and influence can only be identified sporadically.

9.1.2 **Geomechanical properties**

The sensitive materials from this study were typically characterised as 'extra sensitive' where mean sensitivity values across all sites ranged from 9 to 15 for the *in-situ* field shear vane test. The laboratory shear vane supported these measurements and showed that all sites were extra sensitive with the exception of OS2 which was considered sensitive. *In-situ* peak strength analysis was highly variable across all sites (31–156 kPa), whereas *in-situ* remoulded strengths followed a similar variation between sites but were much lower (3–19 kPa). Shear strength analysis from the laboratory shear vane was also highly variable, but also gave much lower peak strength results than the field shear vane, between 20 to 83 kPa, while the remoulded strength was also slightly lower than the field shear vane determinations (2–14 kPa). Non-sensitive materials were classified according to the Milne *et al.* (1995) field test. The samples varied between cohesive and non-cohesive, yet also exhibited properties associated with non-sensitive materials.

Wet bulk densities in comparison with the dry bulk densities were typically much higher for the sensitive material than the non-sensitive material. Wet bulk densities for the sensitive material ranged between ~ 1436 kg m^{-3} and ~ 1633 kg m^{-3}, whereas the non-sensitive material was between ~ 1124 kg m^{-3} and ~ 1721 kg m^{-3}. The dry bulk density for the sensitive material, however, was typically very low, between ~ 687 kg m^{-3} and ~ 952 kg m^{-3}, while the non-sensitive material was higher at ~ 900 kg m^{-3} to ~ 1176 kg m^{-3}. Such low dry bulk densities from the sensitive material in comparison with the non-sensitive material indicate that the sensitive samples contained many more voids and thus had a higher porosity. Porosity for the sensitive material was always greater than ~ 61 %, but non-sensitive values were always less than ~ 60 %. These high porosities and voids allow for significant moisture to be held within the sensitive samples, facilitating a low remoulded strength from fluidised behaviour upon remoulding.

Moisture contents were characteristically high for the *in-situ* sensitive materials (~ 68 % – ~ 109 %), whereas non-sensitive material had lower moisture contents (~ 23–46 %). TPS1 had the highest moisture content. It was primarily a consequence of the partially flocculated microstructure produced by interactions

between halloysite plates, and also because of the high vesicularity of the pumice within the sample. The non-sensitive materials typically had low moisture contents because fewer small voids were available for moisture storage from Rangataua Bay, although the high sand proportion of the Tauriko samples allowed large pores and effective drainage.

Particle density values were typically higher for the sensitive material from this study (2220–2610 kgm^{-3}) than that of the non-sensitive material (2219–2390 kgm^{-3}). Particle density from the sensitive sites was moderately correlated with mean sensitivity (R = 0.64), suggesting a decrease in the magnitude of sensitivity as particle density increased. The weathered non-sensitive sample from Rangataua Bay also had a low particle density, given the sample had a high halloysite concentration. However, the tightly packed microstructure reduced the sensitivity. Therefore, the relationship between particle density and sensitivity does not consistently provide a suitable correlation for predicting sensitivity in the Tauranga area.

The liquid limit broadly distinguished sensitive material (~ 40 to ~ 89 %), from non-sensitive material (~ 39 to ~ 59 %). The relationship between the liquid limit and moisture content was critical in determining a key difference between the liquidity index for both the sensitive and non-sensitive material: the sensitive material always had moisture contents higher than their respective liquid limits, giving liquidity indices > 1, which indicates that the material will become fluidised upon remoulding. The release of the water held is crucial to the drastic loss in strength upon remoulding and thus the high sensitivity of the materials. Conversely, the non-sensitive material always had liquidity indexes < 1, and so did not become fluidised upon remoulding and did not have a sufficient reduction in strength to be considered sensitive.

Plasticity indices ranged between ~ 16 % and ~ 44 % for both sensitive and non-sensitive material, which was comparable with indices from other studies investigating sensitivity from the Tauranga region. All sensitive samples excluding the naturally remoulded OLRO sample and the non-plastic Tauriko samples (which were not plotted) plotted below the A-line on the Plasticity chart. Such characteristics indicate that the sample materials for sensitive soils behave as

highly compressed silts with limited cohesion, which is also common for halloysite bearing materials. This behaviour was comparable to the findings of previous studies from New Zealand on soil sensitivity.

Particle size analysis indicated that relatively low levels of clay and typically high silt concentrations were present in the sensitive material, showing that potentially only low levels of clay are required to facilitate sensitive behaviour in predominantly silt material of pyroclastic origins.

Triaxial testing revealed effective cohesion values for sensitive materials were usually consistent and only varied between ~ 8 kPa and ~ 16 kPa. Effective friction angles were similarly consistent, ranging from ~ 28 ^{0} to ~ 41 ^{0}. Strain softening was also common for sensitive material, suggesting positive pore pressures weakened the material following failure. Post-failure characteristics indicated that shear failure was dominant for over-consolidated samples, while intermediate and barrel failure was common for normal consolidation. The results did not identify any other individual factors for defining sensitivity.

Viscometry analysis was used to characterise the remoulded behaviour of the sensitive rhyolitic materials. Sensitive material analysed in this study was observed to be notably more viscous than quick clay material described in international publications. The result was unsurprising given the larger silt component and minor to moderate sand component of the materials. Analysis of yield stress variation with pH revealed that yield stress typically decreased as pH was increased, especially between pH ~ 7 to ~ 8. An increase of negative charges on the edges of the halloysite clay particles is attributed to causing this behaviour, where the negative charge will repel the negative basal surface charge of the halloysite. The response to the pH change was not effective for spherical particles and so the results were not consistent between all samples. The samples bearing halloysite books generally had the greatest response to pH.

9.1.3 **Petrography**

All samples from this study were characterised by a very similar petrographical make up, regardless of their sensitive or non-sensitive

characteristics. The deposits were composed of halloysite, both in hydrated and dehydrated states, together with volcanic glass fragments, pumice grains, and cristobalite, plagioclase feldspar, and quartz. The occurrence of these minerals and other materials in the Tauranga region has been previously widely described and, considering the rhyolitic environment, the presence of these materials was expected. An abundance of halloysite was facilitated by the rhyolitic (i.e. silica-rich) origin of the pyroclastic deposits, a significant level of moisture within the profile during clay-mineral formation, and abundant time. The dissolution of volcanic glass and glassy pumice fragments, and felsic minerals, meant that abundant silica was available in solution, leading to halloysite formation rather than allophane because it is more stable thermodynamically in these conditions (Churchman and Lowe 2012). The formation of halloysite rather than kaolinite was primarily controlled by the saturated environment during formation, whereas, if considerable drying had taken place, kaolinite would have likely formed instead (Churchman *et al*. 2010).

Halloysite morphologies were, from most to least common, spherical, tubular, plate-like, and in books. The books are unique in that some are very large, from ~ 60 µm to ~ 1500 µm in size, which have not previously been recognised. XRD, EDX and SEM analyses confirmed that the books were halloysite. The formation of the large books likely occurred following the formation of halloysite plates (from the incorporation of iron, derived from the dissolution of glass and felsic and probably ferromagnesian minerals, into the halloysite unit cell). After which Ostwald ripening and partial dehydration promoted the large size and coalescence of the plates to form large books.

The contribution of the books towards promoting sensitive behaviour is not considered to be significant given their inconsistent occurrence throughout the selected sensitive samples. It is suggested however, that the books may decrease the distance over which the material would flow following remoulding.

Highly sensitive microstructures were typically composed of small spherical particles, and also small, wide tubular halloysite in a matrix-skeletal microstructure. The small sphere sizes and short, stubby tubes formed a low density of packing with many micro and ultra-pores throughout the samples,

promoting the high porosity recorded from geomechanical testing. Following disturbance, tubes, plates and books were broken and the structure was typically very continuous.

The non-sensitive samples were comprised of much longer, yet thin tubular formations along with larger spheres. While the larger spheres may have helped promote larger pore spaces, the thin long tubes, tended to fill those spaces and promote a high density of packing. The porosity therefore, was much lower, and the particle interactions much tighter and efficiently sorted. The remoulding process did not cause a noticeable difference from the peak strength state, indicating that the tightly packed structure was not easily disturbed upon remoulding.

The primary difference, between the sensitive and non-sensitive material, therefore, was the density of packing of the clay particles within the microstructure. The sensitive material had a loosely packed, porous structure resultant upon the similar sized and shaped halloysite particles, whereas the non-sensitive material had large, irregularly shaped halloysite particles that packed a lot more efficiently. Therefore, in the non-sensitive material, the amount of pore space was decreased and the particle interaction was increased meaning that the potential for large strength decrease upon remoulding was reduced.

9.1.4 Structural changes of sensitive soils and development of sensitivity

Initially, it could be concluded that the structural changes between the undisturbed and remoulded strength of sensitive material, which promoted sensitive behaviour, was the release of high moisture content within the structure which led to the fluidised sensitive behaviour of the soils upon remoulding. The non-sensitive material indicated tight inter-particle interactions that did not appear to disaggregate following remoulding. The clay particle interactions forming the microstructure were still tight, whereas the sensitive material comprised broken books, plates and a large reduction in the connectors present. The breakdown of larger aggregations in the sensitive material facilitated the ability of the materials

to become entrained within the high moisture available, and thus a large reduction in strength was achieved in comparison with that of the non-sensitive material.

The development of soil sensitivity, therefore, was facilitated by the microstructural characteristics of the sensitive materials. These microstructural characteristics were first initiated by the compositional and depositional mechanism of the geological materials. Initially the rhyolitic pyroclastic materials were deposited as tephra fallout, which, being unconsolidated (fragmental) and pumiceous, promotes initial high void ratios. The subsequent deposition of younger rhyolitic pyroclastic fall and flow materials, in conjunction with a largely wet environment, promotes the movement of silica in solution through the sdeposits. The silica leaching is slow because of the low hydraulic conductivity of the weathered Te Puna Ignimbrite which allows for a silica-rich environment to promote the formation of halloysite.

Primarily, the formation of halloysite spheres of similar size and comparatively small, stubby halloysite tubes is critical for the formation of sensitive soil behaviour. The dominance of these particular morphologies promotes a low density of packing which encourages a high void ratio and porosity, through an abundance of small pores. This microporosity allows the moisture content to build to significantly high levels, exceeding the liquid limit, producing liquidity indices > 1. The formation of these high liquidity indexes is critical to the formation of a low remoulded strength, allowing for high sensitivities to develop.

9.2 Suggestions for future work

Possible future research analysing sensitive rhyolitic soils could involve the following suggestions:

- Establish a calculation for sensitivity based on the peak and remoulded strength which is not equally weighted. Such a weighted index would potentially remove some of the error in quantifying sensitivity where remoulded strength is particularly low, and peak strength is highly variable.

- Determine whether the Te Puna Tephra can be correlated over larger spatial variations in the Tauranga region. Considering the expanding population and subdivision of inland areas, coastal localities provide the greatest ease of access, but this does not answer how the question about the spatial distribution of Te Puna Ignimbrite and associated tephra deposits in the inland locations. Bore logs around the region could be taken to establish whether sensitivity is based at a consistent depth and stratigraphic position to understand the sensitivity of the Te Puna Tephra continuously.

- Determine whether soil sensitivity in the Tauranga region is only associated with the Te Puna Ignimbrite and not the Te Ranga Ignimbrite.

- Undertake a viscometric assessment of sensitive materials from elsewhere in New Zealand (e.g. Taranaki region) to determine how they differ in their remoulded state to rhyolitic materials.

- Form an adjusted sensitivity scale so that there is a physical distinction between sensitive soil materials that flow upon remoulding and sensitive materials that do not flow. Although fluidised soil behaviour may contribute to a higher sensitivity value, it is possible the definition of sensitivity covers behaviour types too broadly. This means that materials that physically behave differently are not adequately distinguished by definition.

REFERENCES

Adamo, P.; Violante, P.; Wilson, M.J. 2001: Tubular and spheroidal halloysite in pyroclastic deposits in the area of the Roccamonfina Volcano (southern Italy). *Geoderma 99:* 295 – 316.

Ahn J.H.; Peacor D.R. 1987: Kaolinitization of biotite: TEM data and implications for an alteration mechanism. *American Mineralogist 72:* 353 – 356.

Aomine, S.; Wada, K. 1962: Differential weathering of volcanic ash and pumice, resulting in formation of hydrated halloysite. *American Mineralogist 47:* 1024 – 1048.

Arthurs, J. M. 2010: *The nature of sensitivity in rhyolitic pyroclastic soils from New Zealand.* Unpublished MSc Thesis, University of Auckland, Auckland, New Zealand.

ASTM D2573 2008: *Standard test method for field shear vane test in cohesive soil*. Philadelphia: American Society for Testing Materials

Aves, M. 1973: *Investigation on brown ash. Progress report as at 9 November 1973.* Ministry of Works. Unpublished memorandum.

Bailey, S.W. 1990: Halloysite – A critical assessment. *Sciences Geologiques 86:* 89 – 98.

Bakker, L.; Lowe, D.J.; Jongmans, A.G. 1996: A micromorphological study of pedogenic processes in an evolutionary soil sequence formed in late Quaternary rhyolitic tephra deposits, North Island, New Zealand. *Quaternary International 34 – 36:* 249 – 261.

Banfield, J.F.; Eggleton, R.A. 1988: Transmission electron microscope study of biotite weathering. *Clays and Clay Minerals 36 (1):* 47 – 60.

Beattie, A.G. 1990: *Petrological controls on the geomechanical behaviour of coal measure soft rock, Waikato, New Zealand.* Unpublished MSc Thesis. University of Waikato, Hamilton, New Zealand.

Bell. J.E. 2007: *Towards a better understanding of costal cliff erosion in Waitemata Group Rock; Auckland, New Zealand.* Unpublished MSc Thesis. University of Waikato, Hamilton, New Zealand.

Bell, D.; Richards, L.; Thomson, R. 2001: Relic slip verification study Tauranga District Council environs. Tauranga District Council, Report 485.

Bentley, S.P 1979: Viscometric assessment of remoulded sensitive clays. *Canadian Geotechnical Journal 16:* 414 – 419.

Bentley, S.P.; Smalley, I.J. 1979: Mineralogy of a Leda/Champlain clay from Gloucester (Ottawa, Ontario). *Engineering Geology 14:* 209 – 217.

Bird, G.A. 1981: *The Nature and causes of coastal landsliding on the Maungatapu Peninsula.* Unpublished MSc Thesis. University of Waikato, Hamilton, New Zealand.

Birkeland, P.W. 1999: *Soils and geomorphology (3rd ed.).* Oxford University Press, New York.

Birrell, K.S. 1951: Some physical properties of New Zealand volcanic ash soils. In Black M.A. (ed.), *Royal Society of New Zealand, Report of the 7th Science Congress, Christchurch, 1951.* Royal Society of New Zealand, Wellington. 208 – 216.

Bishop, A.W.; Henkel, D.J. 1962: *The measurement of soil properties in the triaxial test.* Edward Arnold (Publishers) Ltd, London.

Bishop, A.C.; Woolley, A.R.; Hamilton, R. 1999: *Philip's minerals, rocks and fossils*. George Philip (Publishers), London.

Bjerrum, L. 1954: Geotechnical properties of Norwegian marine clays. *Geotechnique 4:* 49 – 69.

Borja-Baeza, R.C.; Esteban-Chávez, O.; Marcos-López, J.; Peña-Garnica, R.J.; Alcántara-Ayala, I. 2006: Slope Instability on Pyroclastic Deposits: Landslide Distribution and Risk Mapping in Zacapoaxtla, Sierra Norte De Puebla, Mexico. *Journal of Mountain Science 3 (1):* 1 – 19.

Briggs, R.M.; Hall, G.J.; Harmsworth, G.R.; Hollis, A.G.; Houghton, B.F.; Hughes, G.R.; Morgan, M.D.; Whitbread-Edwards, A.R. 1996: *Geology of the Tauranga Area – Sheet U14 1:50 000.* Department of Earth Sciences, University of Waikato Occasional Report 22.

Briggs, R.M.; Houghton, B.F.; McWilliams, M.; Wilson, C.J.N. 2005: 40Ar/39Ar ages of silicic volcanic rocks in the Tauranga-Kaimai area, New Zealand: dating the transition between volcanism in the Coromandel Arc and the Taupo Volcanic Zone. *New Zealand Journal of Geology & Geophysics 48:* 459 – 469.

Briggs, R.M.; Lowe, D.J.; Esler, W.R.; Smith, R.T.; Henry, M.A.C.; Wehrmann, H.; Manning, D.A. 2006: *Geology of the Maketu area, Bay of Plenty, North Island, New Zealand – Sheet V14 1:50 000.* Department of Earth Sciences, University of Waikato, Occassional Report 26.

Brindley, G.W.; Brown, G. 1980: *Crystal structure of clay minerals and their x-ray identification.* Mineralogical Society Monograph 5. Mineralogical Society, London.

British Standard 1377 (BS1377) 1990: *Methods of test for soils for civil engineering purposes.* British Standards Authority, London.

Brookfield. 2012: *More solutions to sticky problems*. Brookfield Engineering Labs Incorporated, Middleboro, USA.

Budhu, M.; Mahajan, S.P. 2008: Shear viscosity of clays to compute viscous resistance. Paper presented at the 12th International Conference of International Association for Computer Methods and Advances in Geomechanics, India.

Bullen, R.O.; Campbell, P.L. 1972: *Housing earthworks: New Plymouth.* Ministry of Works. New Plymouth Residency. Unpublished Memoranda dated 21 June 1972 and 28 September 1972.

Buol S.W.; Southard, R.J.; Graham, R.C.; McDaniel, P.A. 2003: *Soil Genesis and Classification (5th ed.).* Iowa State Press, Ames, Iowa.

Burns, D.A.; Cowbourne, A.J. 2003: Engineering geological aspects of the Ruahihi Power Scheme, Tauranga. In S. Crawford, P. Bauton and S. Hargraves (eds.), *Geotechnics on the Volcanic Edge.* Institute of Professional Engineers, New Zealand, Tauranga. 71 – 80.

Campbell, P.L. 1972: Notes of the visit by Messrs Western, Robinson and Dr Northy in November 1972. Ministry of Works. New Plymouth Residency. Unpublished memorandum dated 11 December 1972.

Campbell, D.J. 1975: Liquid limit determination of arable topsoils using a drop-cone penetrometer. *Journal of Soil Science 26 (3).*

Campbell, D.J. 1976: Plastic limit determination using a drop-cone penetrometer. *Journal of Soil Science 27:* 295 – 300.

Carr, R.G. 1981: A scanning electron microscope study of post-depositional changes in the Matahina Ignimbrite, North Island, New Zealand. *New Zealand Journal of Geology & Geophysics 24:* 429 – 434.

Carroll, D. 1959: Ion exchange in clays and other minerals. *Bulletin of the Geological Society of America 70:* 749 – 780.

Casagrande, A. 1932: Research on the Atterberg limits of soils. *Public Roads,*

13: 121-136.

Chang, S.H.; Ryan, M.E.; Gupta, R.K. 1993: The Effect of pH, Ionic Strength, and Temperature on the Rheology and Stability of Aqueous Clay Suspensions.
Rheological Acta 32: 263 – 269.

Childs, C.W. 1981: Field tests for ferrous iron and ferric-organic complexes (on exchange sites or in water-soluble forms) in soils. *Australian Journal of Soil Research 19:* 175 – 180.

Churchman, G.J. 1990: Relevance of different intercalation tests for distinguishing halloysite from kaolinite in soils. *Clays and Clay Minerals 38 (6):* 591 – 599.

Churchman, G.J. 2000: The alteration and formation of soil minerals by weathering. In M. E. Summer (ed.), *Handbook of soil science.* CRC press, Boca Raton, Florida. F3 – F76.

Churchman, G.J.; Carr, R.M. 1975: The definition and nomenclature of halloysites. *Clays and Clay Minerals 23:* 382 – 388.

Churchman G.J.; Lowe D.J. 2012: Alteration, Formation, and Occurrence of Minerals in Soils. In Huang, P.M.; Li, Y.; Sumner, M.E. (eds.), *Handbook of Soil Sciences (2nd ed.). Vol. 1: Properties and Processes*. CRC Press, Taylor & Francis, Boca Raton, Florida. 20.1 – 20.72.

Churchman, G.J.; Theng, B.K.G. 1984: Interactions of halloysite with amides; minerological factors affecting complex formation. *Clay Minerals 19 (2):* 61 – 176.

Churchman, G.J.; Aldridge, L.P.; Carr, R.M. 1972: The relationship between the hydrated and dehydrated states of an halloysite. *Clays and Clay Minerals 20:* 241 – 246.

Churchman, G.J.; Whitton, J.S.; Claridge, G.C.; Theng, B.K. 1984: Intercalation method using formamide for differentiating Halloysite from Kaolinite. *Clays and Clay minerals 32 (4):* 241 – 248.

Churchman, G.J.; Pontifex, I.R.; McClure, S.G. 2010: Factors influencing the formation and characteristics of halloysites or kaolinites in granitic and tuffaceous saprolites in Hong Kong. *Clays and Clay Minerals 58 (2):* 220 – 237.

Civil Defence 2010: *Quick Evacuation Maps Western Bay of Plenty District Te Puna*. Western Bay of Plenty District Council.

Civil Defence 2010: *Quick Evacuation Maps Western Bay of Plenty District Omokoroa*. Western Bay of Plenty District Council.

Collins, K.; McGown, A. 1974: The form and function of microfabric features in a variety of natural soils. *Geotechnique 24 (2):* 223 – 254.

Cong, S. 1992: *Engineering geology of rhyolitic silts in the upper Waitemata Harbour, Auckland, New Zealand.* Unpublished MSc Thesis. University of Auckland, Auckland, New Zealand.

Craig, R.F. 1997: *Soil Mechanics*, E & FN Spon, London, United Kingdom.

Craig, R.F. 2004: *Craig's Soil Mechanics*, Spoon Press, London, United Kingdom.

De Vita, P.; Agrello, D.; Ambrosino, F. 2006: Landslide susceptibility assessment in ash-fall pyroclastic deposits surrounding Mount Somma-Vesuvius: Application of geophysical surveys for soil thickness mapping. *Journal of Applied Geophysics 59:* 126 – 139.

Delvaux, B.; Tessier, D.; Herbillon, J.A.; Burtin, G.; Jaunet, A.; Vielvoye, L. 1992: Morphology, texture, and microstructure of halloysitic soil clays as related to weathering and exchangeable cation. *Clays and Clay Minerals 40 (4):* 446 - 456.

Dixon, J. B.; McKee, T. R. 1974: Spherical halloysite formation in a volcanic soil of Mexico. *Transactions, 10th International Congress of Soil Science (7):* 115-124.

Dong, H.; Peacor, D.R.; Murphy, S.F. 1998: TEM study of progressive alteration of igneous biotite to kaolinite throughout a weathered soil profile. *Geochimica et Cosmochimica Acta 62 (11):* 1881 – 1887.

Eden, D.N.; Froggatt, P.C.; Zheng, H.; Machida, H. 1996: Volcanic glass found in late Quaternary Chinese loess: a pointer for future studies? *Quaternary International 34-36:* 107-111.

Edgers, L.; Karlsrud, K. 1985: Viscous analysis of submarine flows. Proceedings of the 4th International Conference on the behaviour of offshore structures, Delft. *Developments in Marine Technology 2:* 773 - 784.

Egashira, K.; Ohtsubo, M. 1982: Smectite in marine quick clays of Japan. *Clays and Clay Minerals 30:* 275 – 280.

Ekosse, G.I.E.; 2010: Kaolin deposits and occurrences in Africa: geology, mineralogy and utilization. *Applied Clay Science 50:* 212 – 236.

Eshel, G.; Levy, G.J.; Mingelgrin, U.; Singer, M.J. 2004: Critical Evaluation of the Use of Laser Diffraction for Particle-Size Distribution Analysis. *Soil Science Society of America Journal 68 (3):* 736 – 743.

Etame, J.; Gerard, M.; Suh, C.E.; Bilong, P. 2009: Halloysite neoformation during the weathering of nephelinitic rocks under humid tropical conditions at Mt Etinde, Cameroon. *Geoderma 154:* 59 – 68.

Fanning, D.S.; Keramidas, V.Z.; El-Desoky, M.A. 1989: Micas. In Dixon J.B.;

Weed, S.B. (eds.), *Minerals in soil environments*, Soil Science Society of America, Madison, Wisconsin. 551 – 624.

Fell, R.; Glastonbury, J.; Hunter, G. 2007: Rapid landslides: the importance of understanding mechanisms and rupture surface mechanics. *The Eighth Glossop Lecture.*

Fieldes, M. 1955: Clay mineralogy of New Zealand soils. Allophane and related mineral colloids. *New Zealand Journal of Science and Technology B36:* 140 – 154.

Fratta, D.; Aguettant, J.; Roussel-Smith, L. 2007: *Introduction to soil mechanics laboratory testing.* Taylor & Francis, Boca Raton, Florida.

Fullarton, D.H. 1978: Taranaki brown ash as an engineering material. *Ministry of Works and Development. Central Laboratories. Report No. 2 – 78/2.*

Gillott, J.E. 1971: Mineralogy of Leda clay. *Canadian Mineralogist* 10: 797 – 811.

Gillott, J.E. 1979: Fabric, composition and properties of sensitive soils from Canada, Alaska and Norway. *Engineering Geology 14:* 149 – 172.

Goldschmidt, V.M. 1926: Undersokelser over lersedimenter. *Nordisk jordbrugsforskning, NOS (4 – 7):* 434 – 445.

Goldstein, J.; Newbury, D.; Joy, D.; Lyman, C.; Echlin, P.; Lifshin, E.; Sawyer, L.; Michael, J. 2003: *Scanning Electron Microscopy and X-Ray Microanalysis (3rd ed.).* Kluwer Academic, Plenum Publishers, New York.

Google Earth 2012: Various map images. *Google Earth 2012*. Retrieved from 10/10/2012 www.google.com.

Grabowska-Olszewska, B.; Osipov, V.; Sokolov, V. 1984: *Atlas of the microstructure of clay soils.* Panstwowe Wydamnictwo Naukowe, Warszawa.

Gradwell, M.W.; Birrell, K.S. 1954: Physical properties of certain volcanic clays. N.Z. Journal of Science and Technology B36: 108 – 122.

Graham, R.C.; Weed, S.B.; Bowen, L.H.; Buol, S.W. 1989: Weathering of iron-bearing minerals in soils and saprolite on the North Carolina Blue Ridge front: I. sand-size primary minerals. *Clays and Clay Minerals 37 (1):* 19 – 28.

Gratchev, I.B.; Sassa, K.; Fukuoka, H. 2006: How reliable is the plasticity index for estimating the liquefaction potential of clayey sands. *Journal of Geotechical and Geoenvironmental Engineering 132:* 124 – 127.

Gregersen, O. 1981: The quick clay slide in Rissa, Norway. *Proceedings of the ICSMFE,* Stockholm. 421 – 426.

Gulliver, C.P.; Houghton, B.F. 1980: *Omokoroa Point Land Stability Investigation.* Unpublished Report 4487/2, Tonkin and Taylor.

Harmsworth, G.R. 1983: *Quaternary stratigraphy of the Tauranga Basin.* Unpublished MSc Thesis. University of Waikato, Hamilton, New Zealand.

Head, K.H. 1992: *Manual of soil laboratory testing; volume 1: Soil classification and compaction tests.* Pentech Press, London.

Head, K.H. 1998: *Manual of soil laboratory testing; volume 3: Effective stress tests*. John Wiley and Sons. West Sussex.

Hodder, A.P.W.; Green, B.E.; Lowe, D.J. 1990: A two-stage model for the formation of clay minerals from tephra-derived volcanic glass. *Clay Minerals 25:* 313 – 327.

Houghton, B.F.; Hegan, B.D. 1980: *A preliminary assessment of geological factors influencing slope stability and landslipping in and around Tauranga City*. New Zealand Geological Survey, Lower Hutt.

Houghton, B.F.; Wilson, C.J.N.; McWilliams, M.O.; Lanphere, M.A.; Weaver, S.D.; Briggs, R.M.; Pringle, M.S. 1995: Chronology and dynamics of a large silicic magmatic system: Central Taupo Volcanic Zone, New Zealand. *Geology 23*, 13 – 16.

Houston, W.N. 1967: *Formation mechanisms and property interrelationships in sensitive clays*. Unpublished PhD thesis, University of California, Berkeley.

Huppert, F. 1986: *Petrology of soft tertiary rocks and its relationship to geomechanical behaviour, Central North Island, New Zealand*. Unpublished PhD Thesis. University of Auckland, Auckland, New Zealand.

Huppert, F. 1988: Influence of microfabric on geomechanical behaviour of tertiary fine grained sedimentary rocks from Central North Island, New Zealand. *Bulletin of the International Association of Engineering Geology 38:* 83 – 94.

Inoue, A.; Utada, M.; Hatta, T. 2012: Halloysite-to-kaolinite transformation by dissolution and recrystallization during weathering of crystalline rocks. *Clay Minerals 47:* 373 – 390.

Jacquet, D. 1987: *Bibliography on the physical and engineering properties of volcanic soils in New Zealand*. New Zealand Soil Bureau bibliographic report, Lower Hutt.

Jacquet, D. 1990: Sensitivity to remoulding of some volcanic ash soils in New Zealand. *Engineering Geology 28:* 1 – 25.

Jeong, G. Y. 1998: Formation of vermicular kaolinite from halloysite aggregates in the weathering of plagioclase. *Clays and Clay Minerals 46 (3):* 270 – 79.

Jones, R.M. 2003: Particle size analysis by laser diffraction: ISO 13320, standard operating procedures, and Mie theory. *American Laboratory, January 2003*. 44 – 47.

Joussein, E., Petit, S.; Churchman, J.; Theng, B.; Righi, D.; Delvaux, B. 2005: Halloysite clay minerals – A review. *Clay Minerals 40 (4):* 383 – 426.

Kaufhold, S.; Ufer, K.; Kaufhold, A.; Stucki, J.W.; Anastácio, A.S.; Jahn, R.; Dohrmann, R. 2010: Quantification of allophane from Ecuador. *Clays and Clay Minerals 58 (5):* 707 – 716.

Keam, M.J. 2008: *Engineering geology and mass movement on the Omokoroa peninsula, Bay of Plenty, New Zealand*. Unpublished MSc Thesis, University of Auckland, Auckland, New Zealand.

Kear, D.; Schofield, J.C. 1978: *Geology of Ngaruawahia subdivision*. New Zealand Geological Survey Bulletin 88.

Keller, W.D. 1977: Scan electron micrographs of kaolins collected from diverse environments of origin – IV Georgia kaolin and kaolinizing source rocks. *Clays and Clay Minerals 25:* 311 – 345.

Kirkman, J.H. 1977: Possible structure of halloysite disks and cylinders observed in some New Zealand rhyolitic tephras. *Clay Minerals 12:* 199 – 215.

Kirkman, J.H. 1981: Morphology and structure of halloysite in New Zealand tephras. *Clays and Clay Minerals 29 (1):* 1 – 9.

Kirkman, J.H.; Pullar, W.A. 1978: Halloysite in late Pleistocene rhyolitic tephra beds near Opotiki, coastal Bay of Plenty, North Island, New Zealand. *Australian Journal of Soil Research 16:* 1 – 8.

Kohn, B.P.; Pillans, B.; McGlone, M.S. 1992: Zircon fission-track age for middle Pleistocene Rangitawa Tephra, New Zealand – stratigraphic and paleoclimatic significance. *Palaeogeography Palaeoclimatology Palaeoecology 95 (1 – 2):* 73 – 94.

Lambe, T. W. 1953: The structure of inorganic soils. *Proceedings of the*

American Society of Civil Engineers 79, 315

Lancellotta, R. 1995: *Geotechnical engineering*. A.A. Balkema Publishers, Rotterdam, Netherlands.

Lee, R.E. 1993: *Scanning Electron Microscopy and X-Ray Microanalysis.* PTR Prentice Hall, Englewood Cliffs, New Jersey.

Lefebvre, G. 1996, Soft Sensitive Clay. In Turner A.K.; Schuster R.L. (eds.), *Landslides investigations and mitigation*. Special Report 247. Transportation Research Board. National Research Council. 607 – 617.

Liebling, R.S.; Kerr, P.F. 1965: Observations on quick clay. *Geological Society of America Bulletin 76 (8):* 853 – 878.

Locat, J.; Demers, D. 1988: Viscosity, yield stress, remoulded strength, and liquidity index relationships for sensitive clays. *Canadian Geotechnical Journal 25:* 799 – 806.

Locat, J.; Kurfurst, P.; Berube, M.A.; Chagnon, J.Y.; Gelinas, P. 1988: *Viscosimetric properties of a Beaufort Sea sediment*. Geological Survey of Canada, open file 1708.

Locat, A.; Leroueil, S.; Bernander, S.; Demers, D.; Jostad, H.P.; Ouehb, L. 2011: Progressive failures in eastern Canadian and Scandinavian sensitive clays. *Canadian Geotechnical Journal 48:* 1696 – 1712.

Loizeau, J.L.; Arbouille, D.; Santiago, S.; Vernet, J.P. 1994: Evaluation of a wide range laser diffraction grain size analyser for use with sediments. *Sedimentology 41:* 353 – 361.

Lowe, D.J. 1986: Controls on the rates of weathering of clay mineral genesis in airfall tephra: A review and New Zealand case study. In Colman, S.M.; Dethier, D.P. (eds.), *Rates of chemical weathering of rocks and minerals*. Academic Press. Orlando, Florida. 265 – 330.

Lowe, D.J. 1995: Teaching clays: from ashes to allophane. In Churchman, G.J.; Fitzpatrick, R.W.; Eggleton, R.A. (eds.), *Clays controlling the environment.* Proceedings of the 10th International clay conference 1996 vol 2 Oral papers. CSIRO Publishing Melbourne.

Lowe, D.J.; Nelson, C.S. 1983: *Guide to the Nature and methods of analysis of tephras from the South Auckland Region, New Zealand*. Department of Earth Sciences, University of Waikato Occasional Report 11.

Lowe, D.J.; Percival, H.J. 1993: Clay mineralogy of the tephras and associated paleosols and soils, and hydrothermal deposits, North Island. *Guide book for the New Zealand Pre Conference field trip F.1.* 10th International Clay Conference. Adelaide, Australia.

Lowe, D.J.; Tippett, M.J.; Kamp, P.J.J.; Liddell, I.J.; Briggs, R.M.; Horrocks, J.L. 2001: Ages on weathered plio pleistocene tephra sequences, Western North Island New Zealand. *Les Dossiers de l`Archeo-Logis 1:* 45 – 60.

McCave, I.N.; Bryant, R.J.; Cook, H.F.; Coughanowr, C.A. 1986: Evaluation of a laser-diffraction-size analyser for use with natural sediments. *Journal of Sedimentary Research 56 (4):* 561 – 564.

McLaren, R.G.; Cameron, K.C. 1996: *Soil science*. Oxford University Press, Auckland.

Michaels, A.S.; Bolger, J.C. 1964: Particle interactions in aqueous kaolinite dispersions. *I & EC Fundamentals 3 (1).*

Milne, J.D.G.; Clayden, B.; Singleton, P.L.; Wilson, A.D. 1995: *Soil description handbook.* Manaaki Whenua Press, Lincoln, Canterbury.

Mirabella, A.; Egli, M.; Raimondi S.; Giaccai, D. 2005: Origin of clay minerals in soils on pyroclastic deposits in the Island of Lipari (Italy). *Clays and Clay Minerals 53 (4):* 409 – 421.

Mitchell, J.K.; Soga, K. 2005: *Fundamentals of soil behaviour*. John Wiley & Sons, Hoboken, NJ.

Mizota, C.; Itoh, M. 1993: Volcanic origin of a cristobalite in the Te Ngae tephric loess from North Island, New Zealand. *Clays and Clay Minerals 41:* 755 – 756.

Mizota, C.; Toh, N.; Matsuhisa, Y. 1987. Origin of cristobalite in soils derived from volcanic ash in temperate and tropical regions. *Geoderma 39:* 323 – 330.

Moller, P.C.F.; Mewis, J.; Bonn, D. 2006: Yield stress and thixotropy: on the difficulty of measuring yield stresses in practice. *Soft Matter 2:* 274 – 283.

Moon, V.G. 1989: *Relationships between the geomechanics and petrography of ignimbrite.* Unpublished PhD Thesis, University of Waikato, Hamilton, New Zealand.

Moon, V.G. 1993: Microstructural controls on the geomechanical behaviour of ignimbrite. *Engineering Geology 35 (1 – 2):* 19 – 31.

Moore, D.S.; McCabe, G.P. 2003: *Introduction to the Practice of Statistics (4th ed.).* W.H. Freeman and Co., New York.

Nagasawa and Miyasaki 1976: Mineralogical properties of halloysite as related to its genesis. *Proceedings of the International Clay Conference Mexico City,* 257-265.

Nanzyo, M. 2002: Unique properties of volcanic ash soils. *Global Environmental Research 6:* 99 – 112.

New Zealand Geotechnical Society (NZGS) 2001: *Guideline for hand held shear vane test.* New Zealand Geotechnical Society.

New Zealand Geotechnical Society (NZGS) 2005: *Guidelines for the field classification and description of soil and rock for engineering purposes*. New Zealand Geotechnical Society.

New Zealand Standard (NZS) 4402 1986: *Methods of testing soil for civil engineering purposes*. The soil testing committee, (44/3), of the building and civil engineering division committee, (30/-) Standards Association of New Zealand. Wellington.

Nuntiya, A.; Prasanphan, S. 2006: The rheological behavior of kaolin suspensions. *Chiang Mai Journal of Science 33 (3):* 271 – 281.

Oborn, L.E.; Northey, R.D.; Beetham, R.D.; Brown, I.R. 1982: *Engineering geological factors, related to collapse of Ruahihi canal*. Department of Scientific and Industrial Research, Wellington, New Zealand.

Ohtsubo, M.; Takayama, M.; Egashira, K. 1982: Marine quick clays from Ariake Bay area, Japan. *Soils and Foundations 22 (4):* 71 – 80.

Ojanuga, A. G. 1973: Weathering of biotite in soils of a humid tropical climate. *Soil Science Society of America 37 (4):* 644 – 646.

Oliver, R.C. 1997: *A geotechnical characterisation of volcanic soils in relation to coastal landsliding on the Maungatapu peninsula, Tauranga, New Zealand*. Unpublished MSc Thesis, University of Canterbury, Christchurch, New Zealand.

Pain, C.F. 1975: Some tephra deposits in the South-West Waikato area, North Island, New Zealand. *New Zealand Journal of Geology and Geophysics 18 (4):* 541 – 550.

Papoulis, D.; Tsolis-Katagas, P.; Katagas, C. 2004: Progressive stages in the formation of kaolin minerals of different morphologies in the weathering of plagioclase. *Clays and Clay Minerals 52 (3):* 275 – 286.

Parfitt, R.L. 1990: Allophane in New Zealand – a Review. *Australian Journal of Soil Research 28 (3):* 343 – 360.

Parfitt, R.L. 2009: Allophane and imogolite: role in soil biogeochemical processes. *Clay Minerals 44:* 135 – 155.

Parfitt, R.L.; Saigusa, M.; Cowie, J.D. 1984: Allophane and halloysite formation in a volcanic ash bed under different moisture conditions. *Soil Science 138 (5):* 360 – 364.

Parham, W.E. 1969: *Halloysite-rich tropical weathering products of Hong Kong.* In Proceedings of the International Clay Conference, Tokyo, Vol 1.

Percival, H.J. 1985: *Soil solutions, minerals, and equilibria*. New Zealand Soil Bureau Scientific Report 69.

Perlow, M.; Richards, A.F. 1977: Influence of shear velocity on vane shear strength. *Journal of the Geotechnical Engineering Division 103 (1):* 19 – 32.

Powrie, W. 2004: *Soil Mechanics: Concepts and Applications (2nd ed.).* Spon Press, London and New York.

Prebble, W.M. 1983: Investigations in an Active Volcanic Terrain. *Proceedings of the Symposium Engineering for Dams and Canals*. Institute of Professional Engineers New Zealand. 17.1 – 17.15.

Prebble, W.M. 1986: Geotechnical problems in the Taupo Volcanic Zone. *Volcanic hazard assessment in New Zealand*. New Zealand Geological Survey Record 10. 65 – 80.

Prevost, J.H.; Hoeg, K. 1975: Soil mechanics and plasticity analysis of strain softening. *Geotechnique 25 (2):* 279 – 297.

Pusch, R. 1970: Microstructural changes in soft quick clay at failure. *Canadian Geotechnical Journal 7:* 1 – 7.

Quinn, P.E.; Hutchinson, D.J.; Diederichs, M.S.; Rowe, R.K. 2011: Characteristics of large landslides in sensitive clay in relation to susceptibility, hazard, and risk. *Canadian Geotechnical Journal 48:* 1212 – 1232.

Rankka, K.; Andersson-Skold, Y.; Hulten, C.; Larsson, R.; Leroux, V.; Dahlin, T. 2004: *Quick clay in Sweden*. Swedish Geotechnical institute, Report 65.

Rogers, C.D.F. 1995: Types and distribution of collapsible soils. In Derbyshire, E.; Smalley I.J. (eds.), *Genesis and properties of collapsible soils*. Kluwer Academic Publishers, Netherlands. 1 – 18.

Salter, R.T. 1979: *A Pedological Study of the Kauroa Ash formation at Woodstock.* Unpublished MSc Thesis, University of Waikato, Hamilton, New Zealand.

Selby, M.J. 1993: *Hillslope materials and processes*. Oxford University Press, Oxford.

Sergeyev, Y.M.; Grabowska-Olszewska, B.; Osipov, V.; Sokolov, V.; Kolomenski, Y.N. 1980: The classification and microstructure of clay soils. *Journal of Microscopy 120 (3):* 237 – 260.

Shepherd, T.G. 1984: *A pedological study of the Hamilton Ash group at Welches Road, Mangawara, North Hamilton*. Unpublished MSc Thesis, University of Waikato, Hamilton, New Zealand.

Sherwood, D.T.; Ryley, M.D. 1970: An investigation of a cone-penetrometer method for the determination of the liquid limit. *Geotechnique 20:* 203 – 8.

Singer, J.K.; Anderson J.B.; Ledbetter, M.T.; McCave, I.N.; Jones, K.P.N.; Wright, R. 1988: An assessment of analytical techniques for the size analysis of fine-grained sediments. *Journal of Sedimentary Petrology 58 (3):* 534 – 543.

Singer, A.; Zarei, M.; Lange, F.M.; Stahr, K. 2004: Halloysite characteristics and formation in the northern Golan Heights. *Geoderma 123:* 279 – 295.

Skempton, A.W.; Northey, R.D. 1952: The sensitivity of clays. *Geotechnique 3 (1):* 30 – 53.

Smalley, I.J. 1971: Nature of quick clays. *Nature 231:* 310.

Smalley, I.J.R.; Ross, C.W.; Whitton, J.S. 1980: Clays from New Zealand support the inactive particle theory of soil sensitivity. *Nature 288:* 576 – 577.

Sperazza, M.; Moore, J.N.; Hendrix, M.S. 2004: High-resolution particle size analysis of naturally occurring very fine-grained sediment through laser diffractionometry. *Journal of Sedimentary Research 74 (5):* 736 – 743.

Sudo, T.; Shimoda, S.; Yotsumoto, H.; Aita, S. 1981: Electron micrographs of clay minerals. *Developments in Sedimentology 31*.

Tadros, T.F. 2010: *Rheology of dispersions: principles and applications*. Wiley-VCH, Hoboken, NJ.

Tavenas, F. 1984: Landslides in Canadian sensitive clays – a state-of-the-art. *Proceedings of the 4th International Symposium on Landslides, Toronto, Ontario.* University of Toronto Press, Toronto, Ontario. Vol. 1: 141 – 153.

Tazaki, K. 1979: Micromorphology of halloysites produced by weathering of plagioclase in volcanic ash. In Mortland, M.M.; Farmer, V.C. (eds.), Proceedings of the 6th International Clay Conference 1978. *Developments in Sedimentology 27:* 415 – 422.

Terzaghi, K. 1925: *Erdbaumechanik auf Bodenphysikalischer Grundlage Deuticke.* Vienna.

Theng, B.K.G.; Wells, N. 1995: The flow characteristics of halloysite suspension. *Clay Minerals 30:* 99 – 106.

Theng, B.K.G.; Russell, M.; Churchman, G.J.; Parfitt, R.L. 1982: Surface properties of allophane, halloysite and imoglite. *Clays and Clay Minerals 30 (2):* 143 – 149.

Tonkin & Taylor 2011: *Landslip assessment - Ruamoana Place, Omokoroa.* Unpublished Report 851378.150, Tonkin and Taylor.

Tonkin & Taylor 2011: *Bramley Drive landslip hazard assessment.* Unpublished Report 851378.150, Tonkin and Taylor.

Torrance, J.K. 1978: Post-depositional changes in the pore-water chemistry of the sensitive marine clays of the Ottawa area, eastern Canada. *Engineering Geology 14:* 135 – 147.

Torrance, J.K. 1983: Towards a general model of quick clay development. *Sedimentology 30 (4):* 547 – 555.

Torrance, J.K. 1987: Quick Clays. In M.G. Anderson and K.S. Richards (eds.), *Slope Stability: Geotechnical Engineering and Geomorphology*. John Wiley and Sons, Ltd, Chichester. 447 – 473.

Torrance, J.K. 1992: Discussion on sensitivity to remoulding of some volcanic ash soils in New Zealand, by D. Jacquet. *Engineering Geology 32 (1 – 2):* 101 – 105.

Towner, D. 1973: An examination of the fall-cone method for the determination of some strength properties of remoulded agricultural soils. *Journal of Soil Science 24 (4):* 470 – 479.

van der Gaast S.J.; Wada K.; Wada S.I.; Kakuto Y. 1985: Small-angle X-ray powder diffraction, morphology and structure of allophane and imogolite.
Clays and Clay Minerals 33: 237 – 243.

Vepraskas, M.J. 1994: *Redoximorphic features for identifying aquic conditions*. North Carolina Agricultural Research Service, North Carolina State University, Technical Bulletin 301.

Vickers, B. 1978: *Laboratory work in civil engineering, soil mechanics*. Granada Publishing, London, Great Britain.

VJ Tech. 2011: *Laboratory vane apparatus user manual*. Issue v1.01. VJ Tech, United Kingdom

Wada, K. 1987: Minerals formed and mineral formation from volcanic ash by weathering. *Chemical Geology 60:* 17 – 28.

Wada, K. 1989: Allophane and imogolite. In Dixon J.B.; Weed, S.B. (eds.), *Minerals in soil environments*, Soil Science Society of America Madison, Wisconsin. 1051 – 1087.

Walker, G.P.L. 1979: A volcanic ash generated by explosions where ignimbrite entered the sea. *Nature 281:* 784 – 837.

Wallace, R.C. 1991: New Zealand theses in earth sciences. The mineralogy of the Tokomaru silt loam and the occurrence of cristobalite and tridymite in selected North Island soils. *New Zealand Journal of Geology & Geophysics 34:* 113.

Waltham, T. 2002: *Foundations of Engineering Geology (2nd ed.).* Spon Press, New York.

Ward, T.W. 1967: Volcanic ash beds of the lower Waikato basin, North Island, New Zealand. *New Zealand Journal of Geology & Geophysics 10:* 1109 – 1135. Ward, C.R.; Roberts, F.I. 1990: Occurrence of spherical halloysite in bituminous coals of the Sydney Basin, Australia. *Clays and Clay Minerals 38 (5):* 501 – 506.

Watts, S.; Halliwell, L. 1996: *Essential environmental science methods and techniques*. Routledge, London.

Wells, N.; Childs, C.W. 1988: Flow behaviour of allophane and ferrihydrite under shearing forces. *Australian Journal of Soil Research 26:* 145 – 152.

Wells, N.; Theng, B.K.G. 1985: Factors affecting the flow behavior of soil allophane suspensions under low shear rates. *Journal of Colloid and Interface Science 104 (2).*

Wells, N.; Childs, C.W.; Downes, C.J. 1977: Silica springs, Tongariro National Park, New Zealand – analyses of the spring water and characterisation of the alumino-silicate deposit. *Geochimica et Cosmochimica Acta 41:* 1497 – 1506.

Wesley, L.D. 1968: *Hamilton Police Station soil investigation.* Ministry of Works. Central Laboratories. Report No. 298.

Wesley, L.D. 1973: Some basic engineering properties of halloysite and allophane clays in Java, Indonesia. *Geotechnique 23 (4):* 471 – 494.

Wesley, L.D. 1974: Tjipanundjang Dam in West Java, Indonesia. Proceedings of the American Society of Civil Engineers in Jacquet 1990. *Journal of Geotechnical Engineering Division*.

Wesley, L.D. 1977: Shear strength properties of halloysite and allophane clays in Java, Indonesia. *Geotechnique 27 (2):* 125 – 136.

Wesley, L.D. 2001: Consolidation behaviour of allophane clays. *Geotechnique 51 (10):* 901 – 904.

Wesley, L.D. 2003: Residual strength of clays and correlations using Atterberg limits. *Geotechnique 53:* 669 – 672.

Wesley, L.D. 2007: Slope behaviour in Otumoetai, Tauranga. New Zealand *Geomechanics News 74:* 63 – 75.

Wesley, L.D. 2010: *Geotechnical Engineering in Residual Soils*. Wiley, Hoboken, NJ.

Whitbread-Edwards, A.R. 1994: *Volcanic Geology of the Western Tauranga Basin.* Unpublished MSc Thesis. University of Waikato, Hamilton, New Zealand.

Whitton, J.S.; Churchman, G.J. 1987: *Standard methods for mineral analysis of soil survey samples for characterisation and classification*. New Zealand Soil Bureau Scientific Report 79.

Williams, D.J.A.; Williams, K.P. 1982: Colloid Stability and Rheology of Kaolinite Suspensions. *British Ceramic Transaction Journal 81:* 78 – 83.

Wilson, M.J. 1967: The clay mineralogy of some soils derived from a biotite-rich quartz-gabbro in the Strathdon area, Aberdeenshire. *Clay Miner 7:* 91 – 100.

Wilson, C.J.N.; Houghton, B.F.; Kamp, P.J.J.; McWilliams, M.O. 1995: An exceptionally widespread ignimbrite with implications for pyroclastic flow emplacement. *Nature 378:* 605 – 607.

Wilson, C.J.N.; McWilliams, M.O.; Lanphere, M.A.; Weaver, S.D.; Briggs, R.M.; Pringle, M.S. 2007: A multiple-approach radiometric age estimate for the Rotoiti and Earthquake Flat eruptions, New Zealand, with implications for the MIS4/3 boundary. *Quaternary Science Reviews 25:* 1861 – 1870.

Wires, K.C. 1984: The casagrande method versus the drop-cone penetrometer method for the determination of liquid limit. *Canadian Journal of Soil Science 64:* 297 – 300.

Wood, D.M. 1990: *Soil behaviour and critical state soil mechanics*. Cambridge University Press, NY.

Wyatt, J. 2009: *Sensitivity and clay mineralogy of weathered tephra-derived soil materials in the Tauranga region*. Unpublished MSc thesis, University of Waikato, Hamilton.

Wyatt, J.; Lowe, D.J.; Moon, V.G.; Churchman, G.J. 2010: *Discovery of halloysite books in a ~270,000 year-old buried tephra deposit in*

northern New Zealand. Extended abstracts presented at the 21st Australian Clay Minerals Conference Brisbane, Australia.

Yong, R.N.; Warkentin, B.P. 1966: *Introduction to soil behaviour*. Macmillan, NY.

Yong, R.N.; Sethi, A.J.; Booy, E.; Dascal, O. 1979: Basic characterization and effect of some chemicals on a sensitive clay from Outardes 2. *Engineering Geology. 14:* 83 – 107.

Appendix 4.1

Field peak shear vane strength, remoulded shear vane strength and calculated sensitivities are presented for all sensitive samples analysed in this study.

Omokoroa (OS1, OS2)

Sample	Peak Strength (Nm)	Peak Strength (kPa)	Remoulded Strength (Nm)	Remoulded Strength (kPa)	Sensitivity
OS1	68.0	106.2	6.0	9.4	11.3
OS1	64.0	100.0	7.0	10.9	9.1
OS1	58.0	90.6	5.0	7.8	11.6
OS1	57.0	89.0	4.0	6.2	14.3
OS1	50.0	78.1	5.0	7.8	10.0
Mean	59.4	92.8	5.4	8.4	11.3
std dev	6.9	10.8	1.1	1.8	1.9
std error	3.1	4.8	0.5	0.8	0.6

Sample	Peak Strength (Nm)	Peak Strength (kPa)	Remoulded Strength (Nm)	Remoulded Strength (kPa)	Sensitivity
OS2	70.0	109.3	4.0	6.2	17.5
OS2	60.0	93.7	5.0	7.8	12.0
OS2	55.0	85.9	5.0	7.8	11.0
OS2	42.0	65.6	3.0	4.7	14.0
OS2	34.0	53.1	4.0	6.2	8.5
OS2	44.0	68.7	2.0	3.1	22.0
OS2	36.0	56.2	2.0	3.1	18.0
OS2	45.0	70.3	4.0	6.2	11.3
OS2	40.0	62.5	2.0	3.1	20.0
Mean	47.3	73.9	3.4	5.4	14.9
std dev	11.9	18.6	1.2	1.9	4.6
std error	4.0	6.2	0.4	0.6	1.5

Te Puna (TPS1)

Sample	Peak Strength (Nm)	Peak shear strength (kPa)	Remoulded Strength (Nm)	Remoulded vane shear strength (kPa)	Sensitivity
TPS1	60.0	93.7	6.0	9.4	10.0
TPS1	66.0	103.1	6.0	9.4	11.0
TPS1	68.0	106.2	7.0	10.9	9.7
TPS1	86.0	134.3	9.0	14.1	9.6
TPS1	88.0	137.5	11.0	17.2	8.0
TPS1	76.0	118.7	7.0	10.9	10.9
TPS1	100.0	156.2	4.0	6.2	25.0
TPS1	86.0	134.3	8.0	12.5	10.8
TPS1	88.0	137.5	8.0	12.5	11.0
TPS1	72.0	112.5	11.0	17.2	6.5
TPS1	60.0	93.7	5.0	7.8	12.0
TPS1	90.0	140.6	12.0	18.7	7.5
Mean	78.3	122.4	7.8	12.2	11.0
Std Dev	13.1	20.5	2.5	3.9	4.7
Std Error	1.1	1.7	0.2	0.3	1.4

Pahoia Peninsula (PS1, PS2)

Sample	Peak Strength (Nm)	Peak Strength (kPa)	Remoulded Strength (Nm)	Remoulded Strength (kPa)	Sensitivity
PS1	45	70	4	6	11.25
PS1	47	73	5	8	9.40
PS1	47	73	5	8	9.40
PS1	44	69	5	8	8.80
PS1	43	67	6	9	7.17
PS1	42	66	4	6	10.50
PS1	49	77	5	8	9.80
PS1	45	70	4	6	11.25
PS1	48	75	5	8	9.60
PS1	44	69	4	6	11.00
PS1	42	66	4	6	10.50
PS1	39	61	4	6	9.75
PS1	48	75	4	6	12.00
PS1	47	73	3	5	15.67
PS1	43	67	3	5	14.33
PS1	46	72	3	5	15.33
PS1	43	67	4	6	10.75
PS1	30	47	3	5	10.00
PS1	40	62	4	6	10.00
PS1	50	78	4	6	12.50
PS1	46	72	3	5	15.33
Mean	44.2	69.0	4.1	6.4	11.2
St Dev	4.3	6.8	0.8	1.3	2.3
St Error	0.9	1.5	0.2	0.3	0.5

Sample	Peak Strength (Nm)	Peak Strength (kPa)	Remoulded Strength (Nm)	Remoulded Strength (kPa)	Sensitivity
PS2	52.0	81.2	5.0	7.8	10.4
PS2	50.0	78.1	6.0	9.4	8.3
PS2	42.0	65.6	4.0	6.2	10.5
PS2	52.0	81.2	6.0	9.4	8.7
PS2	44.0	68.7	5.0	7.8	8.8
PS2	44.0	68.7	4.0	6.2	11.0
PS2	52.0	81.2	6.0	9.4	8.7
PS2	42.0	65.6	6.0	9.4	7.0
PS2	44.0	68.7	5.0	7.8	8.8
PS2	38.0	59.4	4.0	6.2	9.5
PS2	52.0	81.2	5.0	7.8	10.4
PS2	50.0	78.1	4.0	6.2	12.5
PS2	48.0	75.0	4.0	6.2	12.0
PS2	52.0	81.2	5.0	7.8	10.4
PS2	45.0	70.3	5.0	7.8	9.0
Mean	47.1	73.6	4.9	7.7	9.2
St Dev	4.7	7.3	0.8	1.2	1.5
St Error	1.1	1.7	0.2	0.3	0.4

Appendix 5.4

The following presents the raw laboratory shear vane data from all sensitive samples analysed in this study.

Omokoroa (OS1, OS2)

Date	Sample	Peak strength maximum angular rotation of the torsion spring (degrees)	Torque (M)	Peak Strength (kPa)	Remoulded strength maximum angular rotation of the torsion spring (degrees)	Torque (M)	Remoulded Strength (kPa)	Sensitivity
26/04/2012	OS1 (Repitition1)	115.00	209.04	48.72	9.00	16.36	3.81	12.78
	OS1 (Repitition2)	49.00	89.07	20.76	6.00	10.91	2.54	8.17
	OS1 (Repitition3)	168.00	305.37	71.18	18.00	32.72	7.63	9.33
11/06/2012	OS1 (Repitition1)	160.00	290.83	67.79	18.00	32.72	7.63	8.89
	OS1 (Repitition2)	142.00	258.11	60.16	20.00	36.35	8.47	7.10
	OS1 (Repitition3)	163.00	296.29	69.06	15.00	27.27	6.36	10.87
Mean				56.28			6.07	9.52
St Dev				19.24			2.38	2.03
St Error				7.86			0.97	0.83

Date	Sample	Peak strength maximum angular rotation of the torsion spring (degrees)	Torque (M)	Peak Strength (kPa)	Remoulded strength maximum angular rotation of the torsion spring (degrees)	Torque (M)	Remoulded Strength (kPa)	Sensitivity
9/02/2012	OS2 (Repitition1)	40.00	101.68	23.70	7.00	17.79	4.15	5.71
	OS2 (Repitition2)	73.00	185.57	43.25	16.00	40.67	9.48	4.56
	OS2 (Repitition3)	47.00	119.47	27.85	8.00	20.34	4.74	5.88
2/03/2012	OS2 (Repitition1)	42.00	76.34	17.80	6.00	10.91	2.54	7.00
	OS2 (Repitition2)	54.00	98.16	22.88	7.00	12.72	2.97	7.71
	OS2 (Repitition3)	55.00	99.97	23.30	6.00	10.91	2.54	9.17
Mean				26.46			4.40	6.67
St Dev				8.83			2.64	1.64
St Error				3.60			1.08	0.67

Te Puna (TPS1)

Date	Sample	Peak strength maximum angular rotation of the torsion spring (degrees)	Torque (M)	Peak Strength (kPa)	Remoulded strength maximum angular rotation of the torsion spring (degrees)	Torque (M)	Remoulded Strength (kPa)	Sensitivity
26/04/2012	TPS1	183.0	332.6	77.5	14.0	25.4	5.9	13.1
	TPS1	196.0	356.3	83.0	15.0	27.3	6.4	13.1
	TPS1	190.0	345.4	80.5	34.0	61.8	14.4	5.6
Mean				80.4			8.9	10.6
St Dev				2.8			4.8	4.3
St Error				1.6			2.8	2.5

Pahoia Peninsula (PS1, PS2)

Date	Sample	Peak strength maximum angular rotation of the torsion spring (degrees)	Torque (M)	Peak Strength (kPa)	Remoulded strength maximum angular rotation of the torsion spring (degrees)	Torque (M)	Remoulded Strength (kPa)	Sensitivity
27/04/2012	PS1 (Repitition1)	53.0	96.3	22.5	4.5	8.2	1.9	11.8
	PS1 (Repitition2)	70.0	127.2	29.7	4.0	7.3	1.7	17.5
	PS1 (Repitition3)	59.0	107.2	25.0	5.5	10.0	2.3	10.7
Mean				25.7			2.0	13.3
St Dev				3.7			0.3	3.6
St Error				2.1			0.2	2.1

Date	Sample	Peak strength maximum angular rotation of the torsion spring (degrees)	Torque (M)	Peak Strength (kPa)	Remoulded strength maximum angular rotation of the torsion spring (degrees)	Torque (M)	Remoulded Strength (kPa)	Sensitivity
27/04/2012	PS2 (Repitition1)	91.0	231.3	53.9	5.0	12.7	3.0	18.2
	PS2 (Repitition2)	125.0	317.8	74.1	18.0	45.8	10.7	6.9
	PS2 (Repitition3)	75.0	190.7	44.4	20.0	50.8	11.9	3.8
Mean				57.5			8.5	9.6
St Dev				15.1			4.8	7.6
St Error				8.7			2.8	4.4

Appendix 6.1

Appendix 6.1 presents all of the X-ray diffractograms for both sensitive and non-sensitive material from this study.

OS1

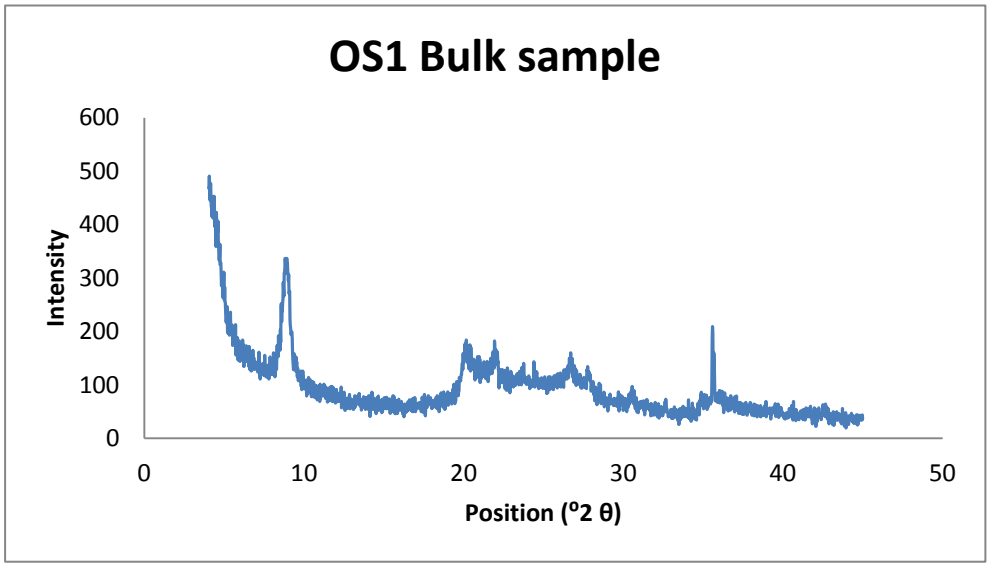

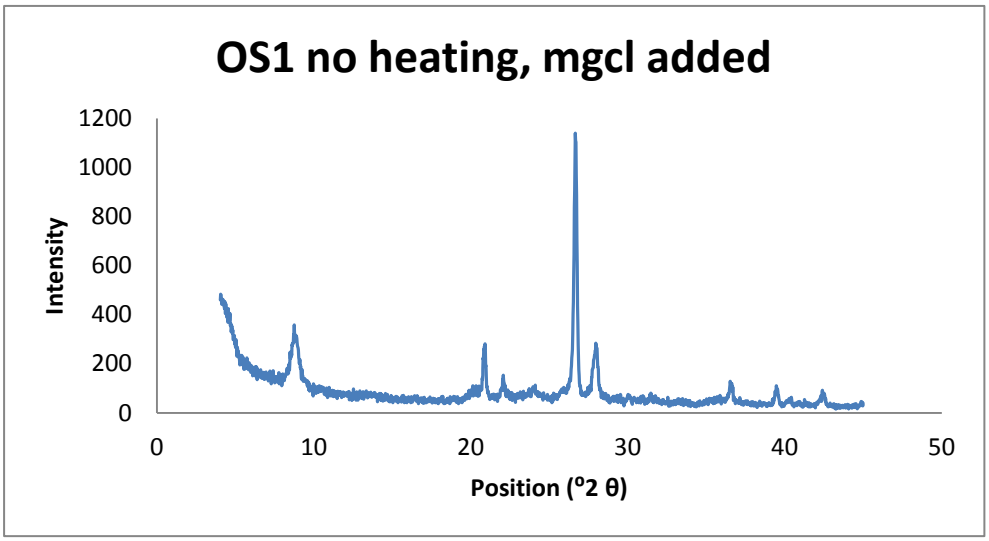

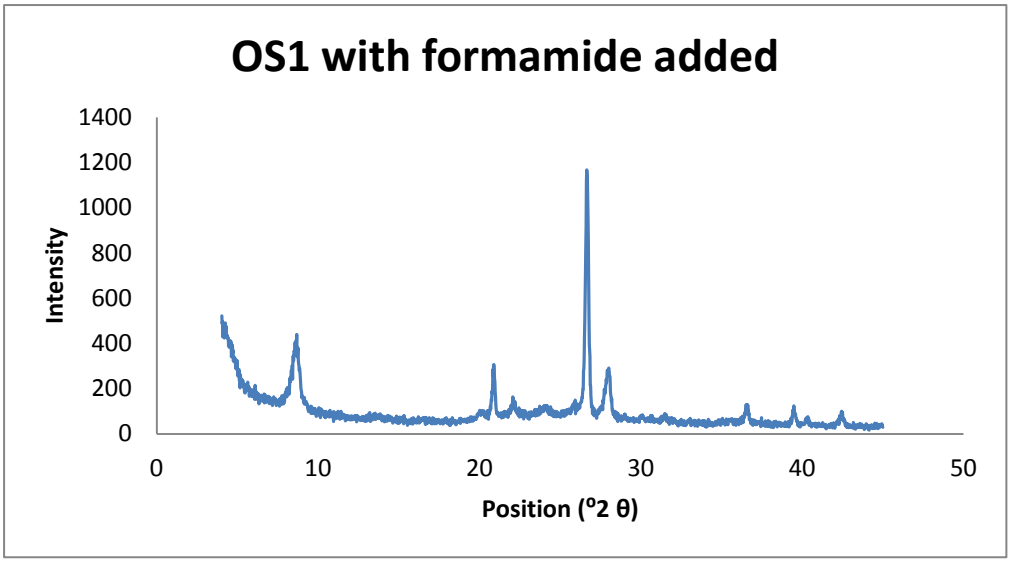
OS1 with formamide added
Intensity
1400
1200
1000
800
600
400
200
0
0
10
20
30
40
50
Position (°2 θ)

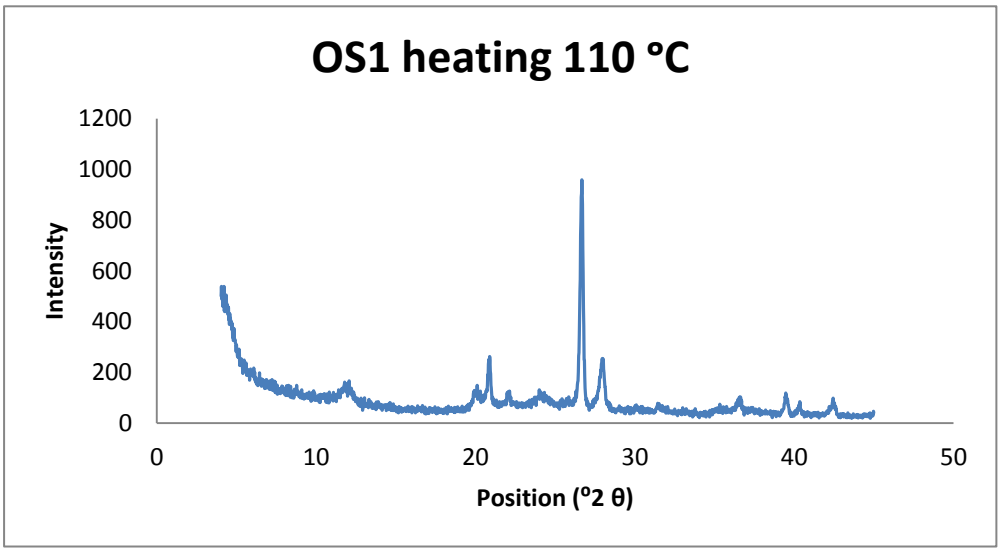
OS1 heating 110 °C
Intensity
1200
1000
800
600
400
200
0
0
10
20
30
40
50
Position (°2 θ)

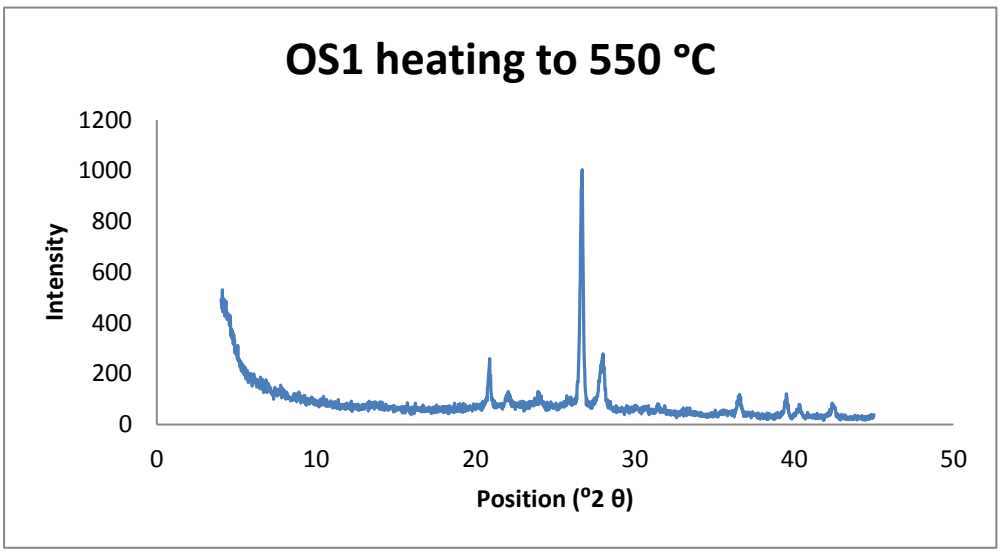
OS1 heating to 550 °C
Intensity
1200
1000
800
600
400
200
0
0
10
20
30
40
50
Position (°2 θ)

OS2

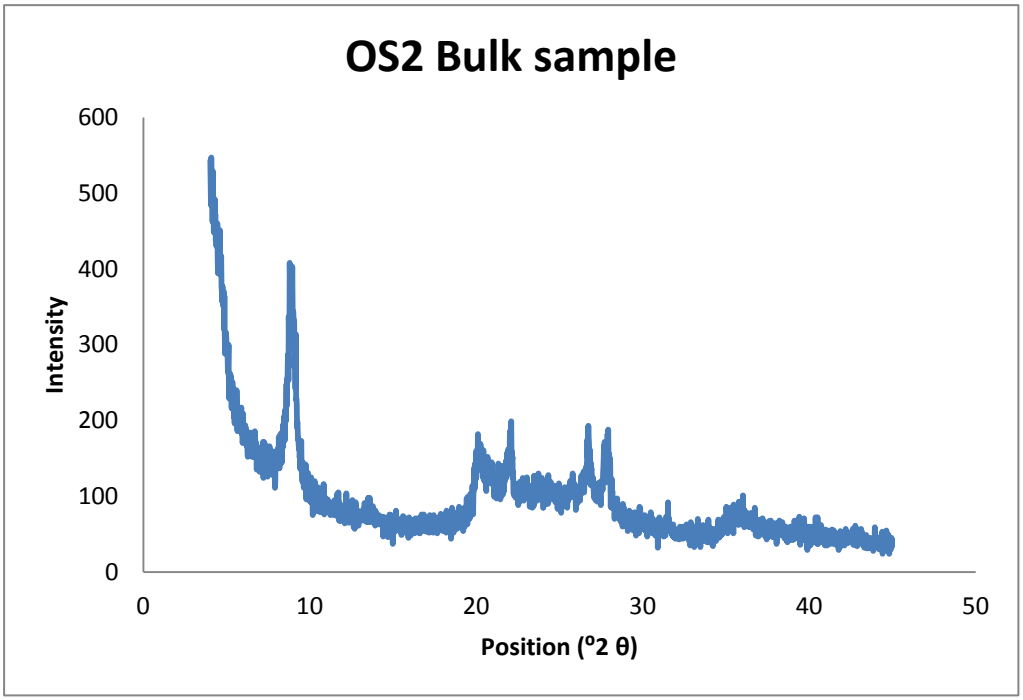
OS2 Bulk sample
600
500
400
300
200
100
0
Intensity
0
10
20
30
40
50
Position (°2 θ)

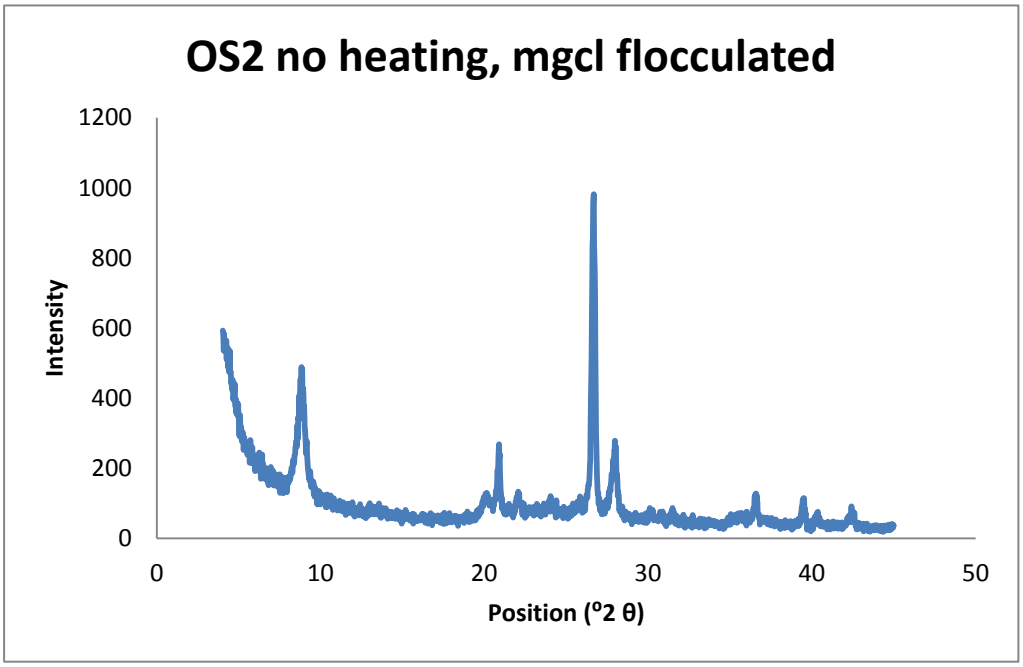
OS2 no heating, mgcl flocculated
1200
1000
800
600
400
200
0
Intensity
0
10
20
30
40
50
Position (°2 θ)

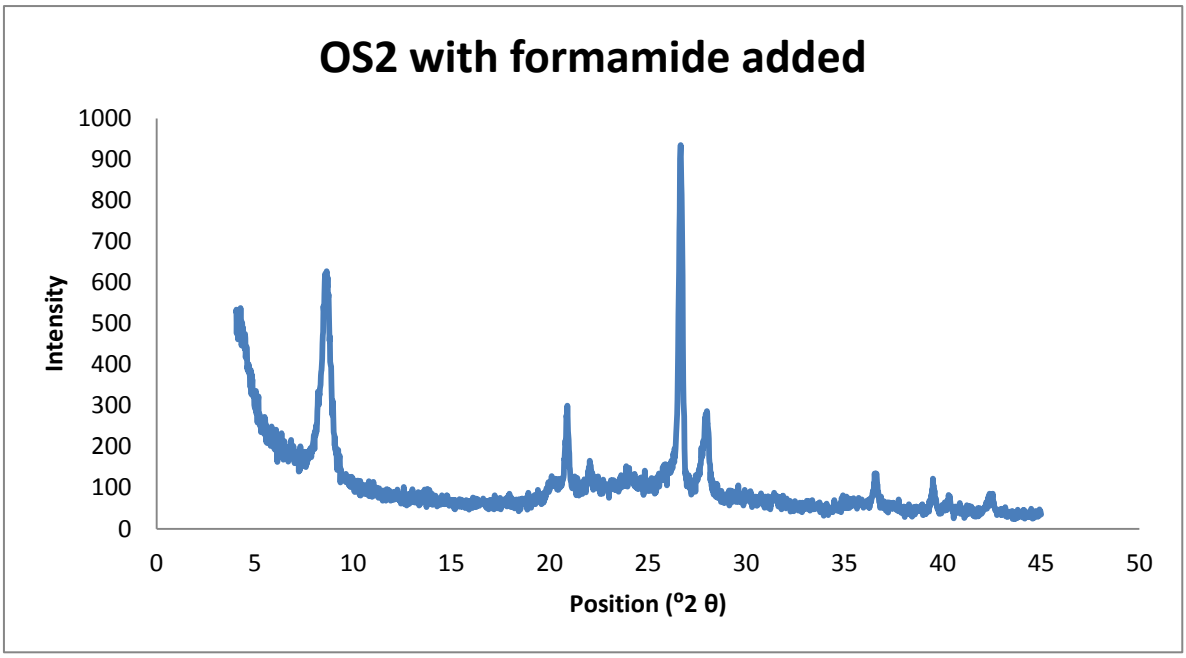
OS2 with formamide added
Intensity
1000
900
800
700
600
500
400
300
200
100
0
0
5
10
15
20
25
30
35
40
45
50
Position (°2 θ)

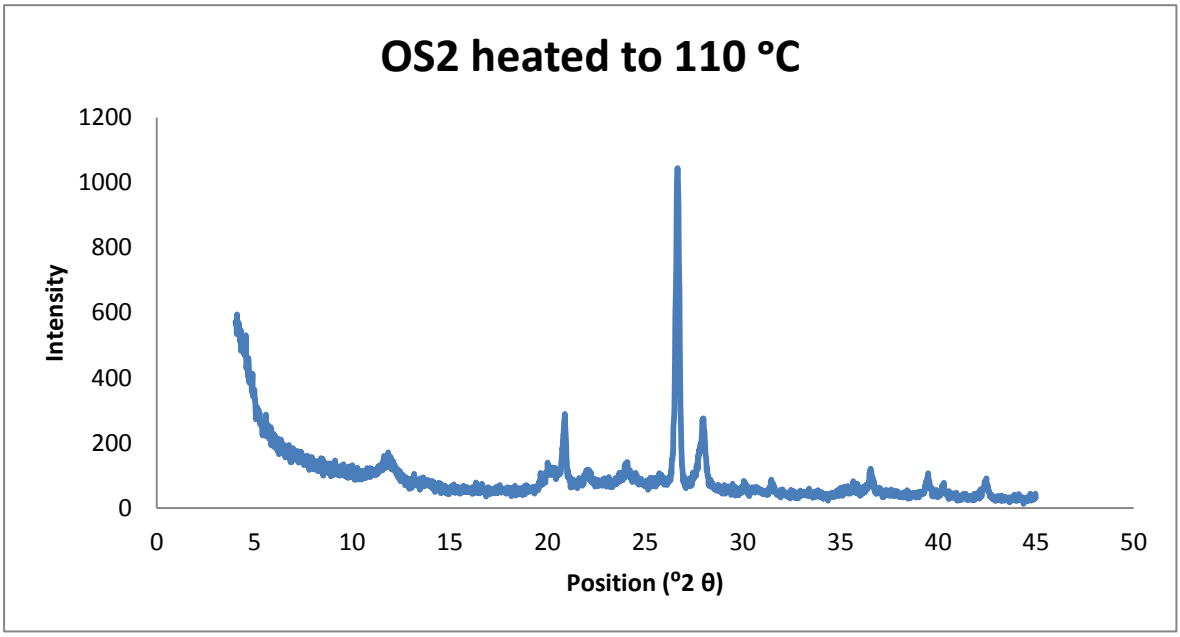
OS2 heated to 110 °C
Intensity
1200
1000
800
600
400
200
0
0
5
10
15
20
25
30
35
40
45
50
Position (°2 θ)

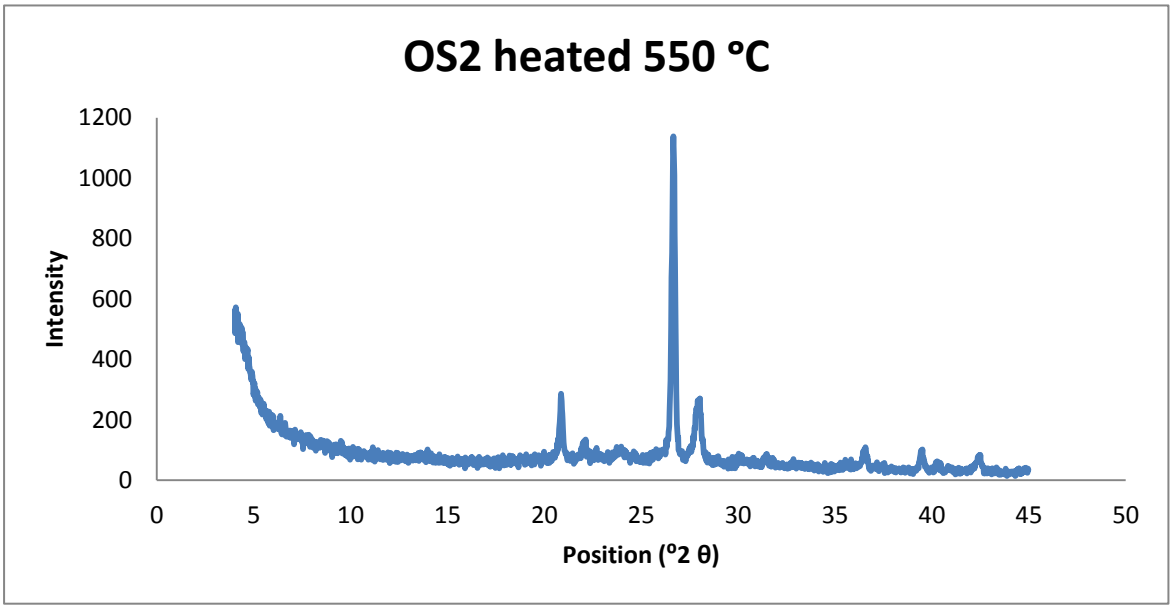
OS2 heated 550 °C
Intensity
1200
1000
800
600
400
200
0
0
5
10
15
20
25
30
35
40
45
50
Position (°2 θ)

OLRO

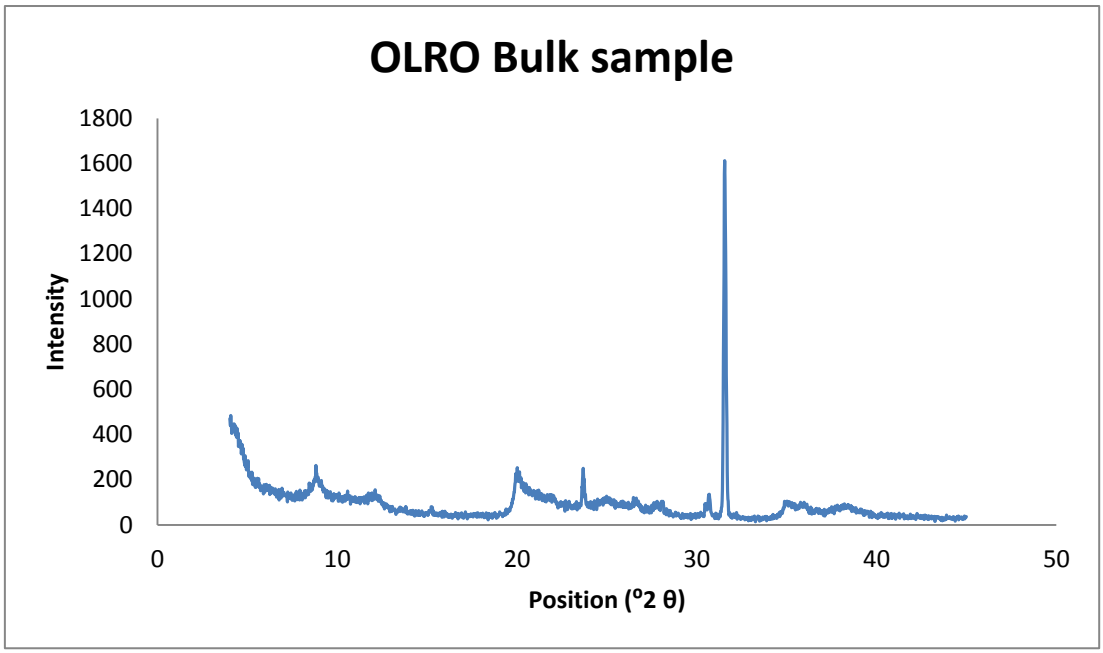
OLRO Bulk sample
Intensity
1800
1600
1400
1200
1000
800
600
400
200
0
0
10
20
30
40
50
Position (°2 θ)

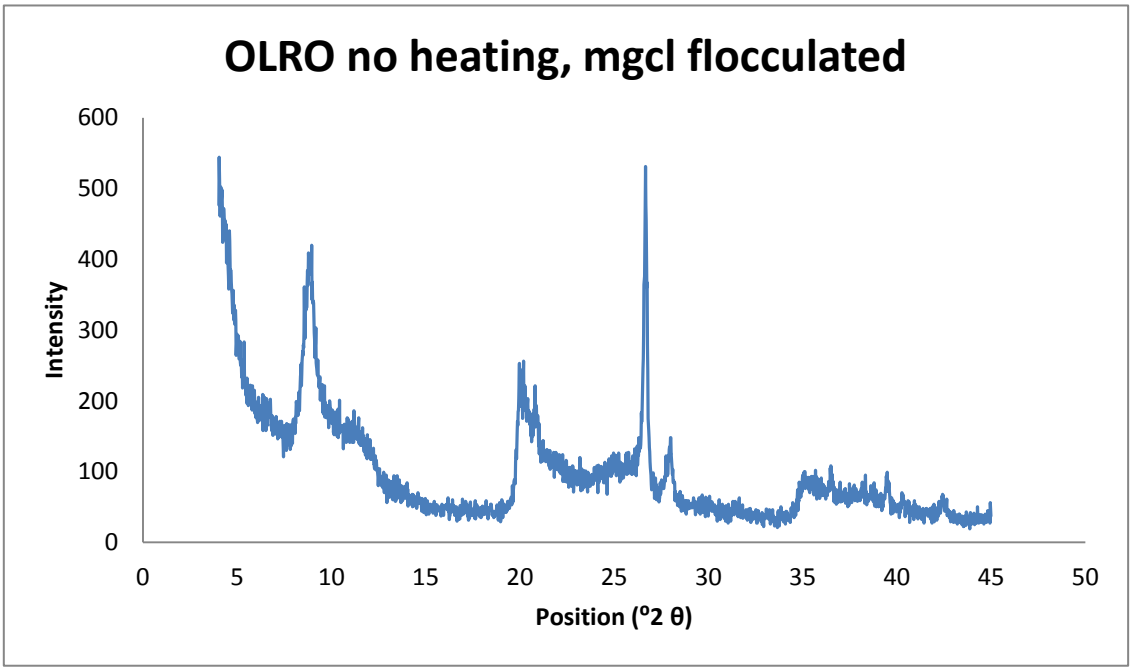
OLRO no heating, mgcl flocculated
Intensity
600
500
400
300
200
100
0
0
5
10
15
20
25
30
35
40
45
50
Position (°2 θ)

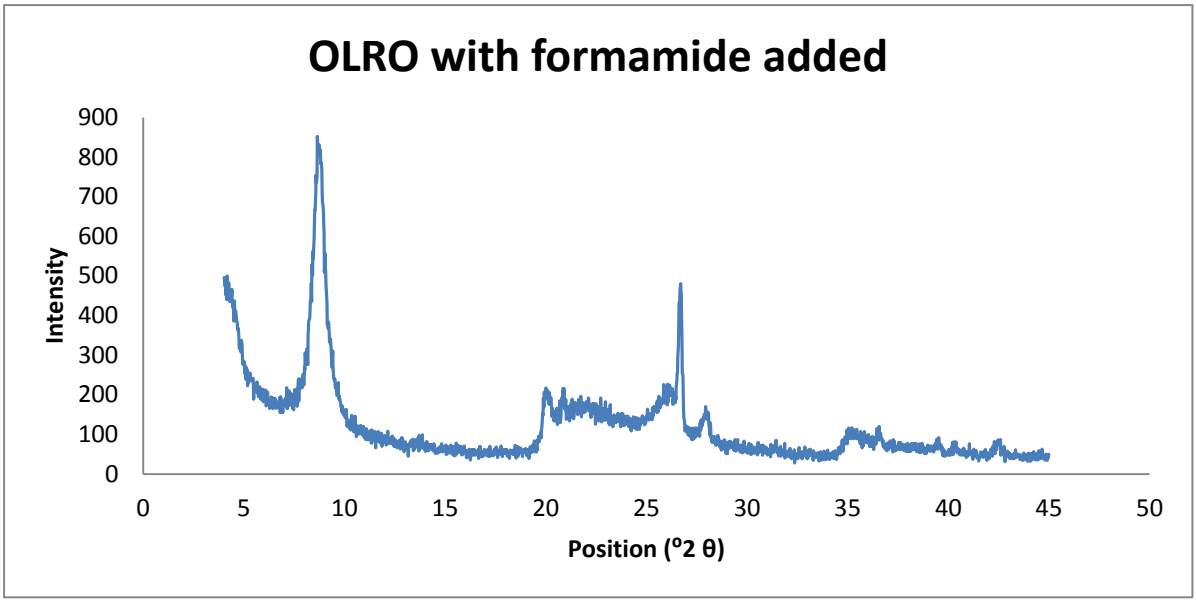
OLRO with formamide added
Intensity
900
800
700
600
500
400
300
200
100
0
0
5
10
15
20
25
30
35
40
45
50
Position (°2 θ)

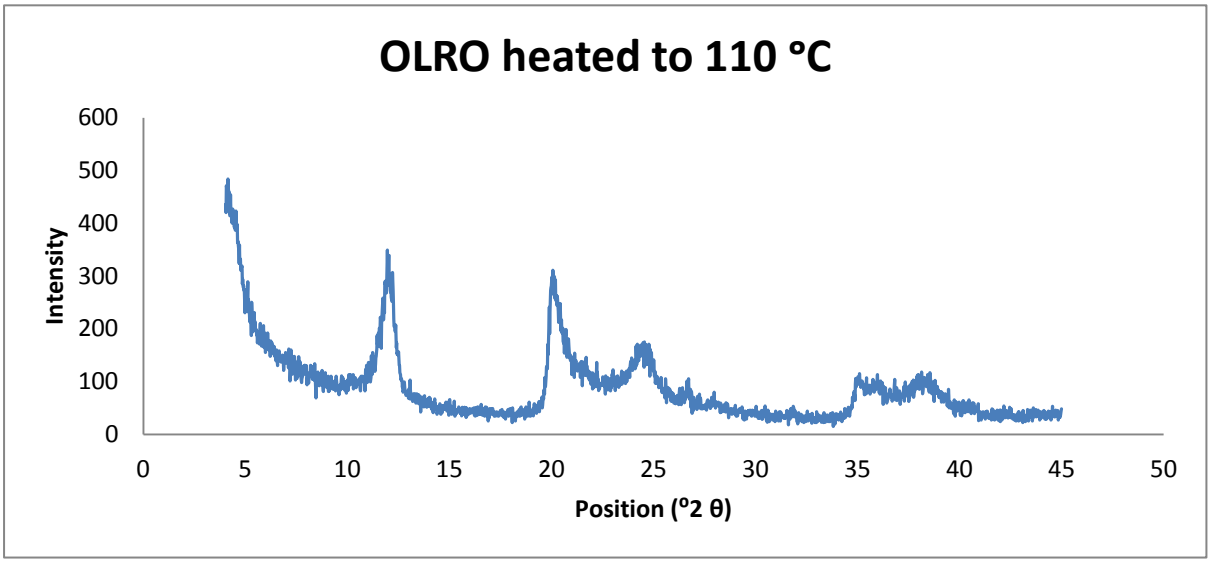
OLRO heated to 110 °C
Intensity
600
500
400
300
200
100
0
0
5
10
15
20
25
30
35
40
45
50
Position (°2 θ)

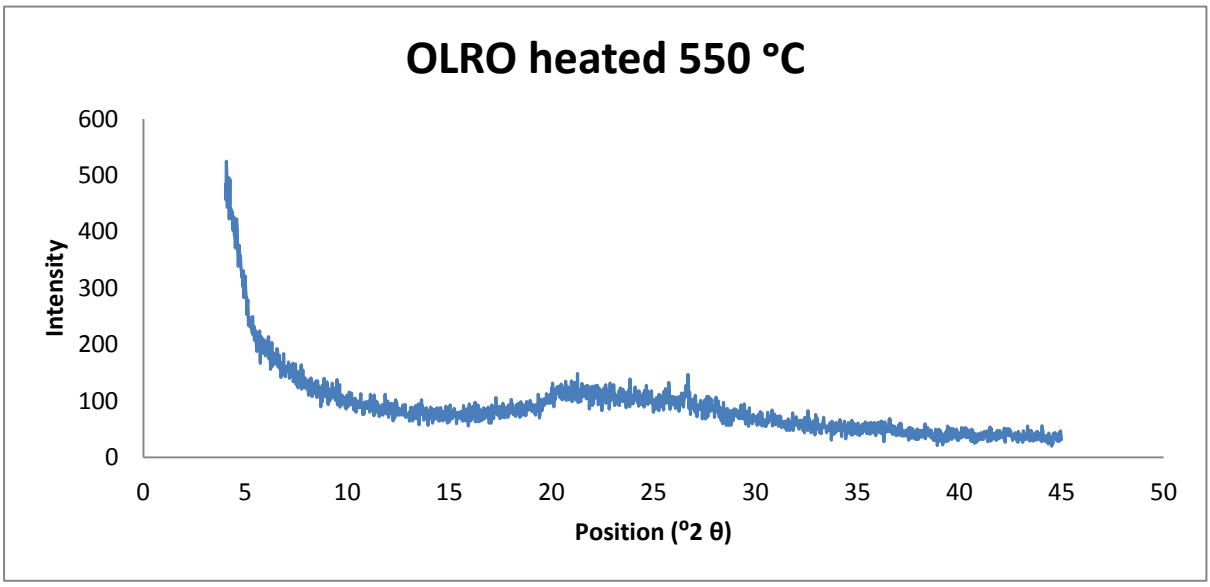
OLRO heated 550 °C
Intensity
600
500
400
300
200
100
0
0
5
10
15
20
25
30
35
40
45
50
Position (°2 θ)

TPS1

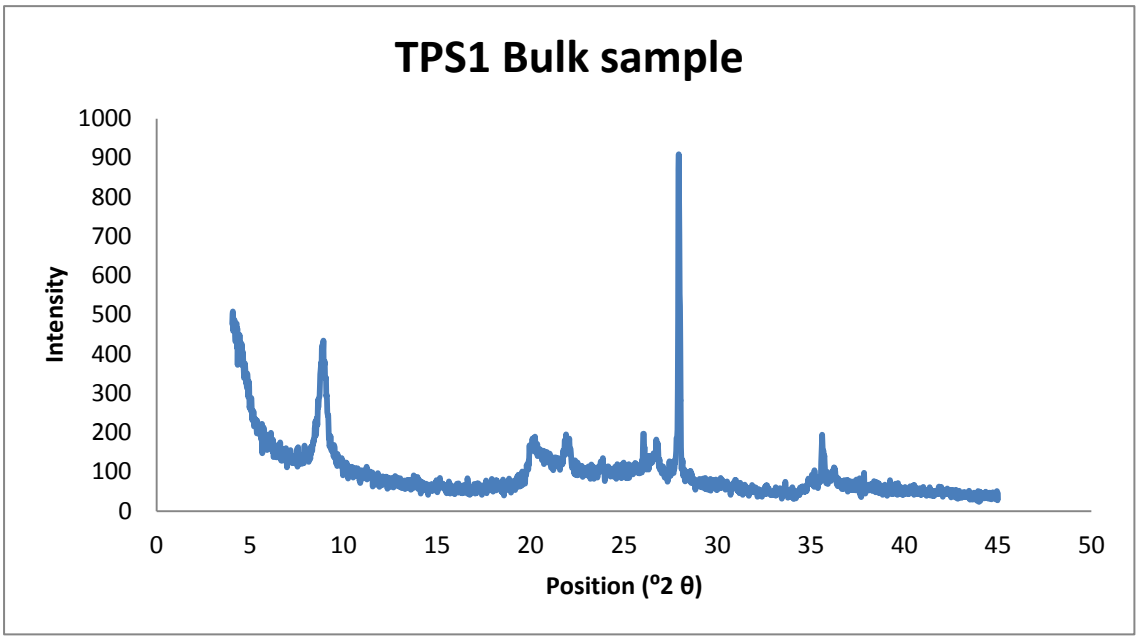
TPS1 Bulk sample
Intensity
1000
900
800
700
600
500
400
300
200
100
0
0
5
10
15
20
25
30
35
40
45
50
Position (°2 θ)

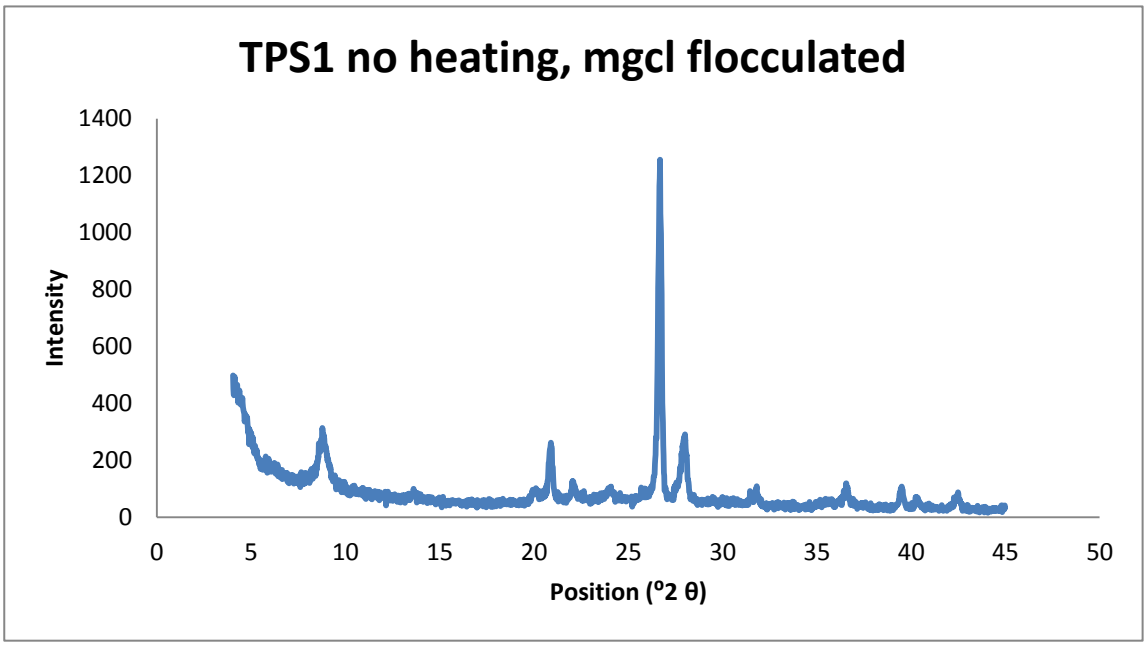
TPS1 no heating, mgcl flocculated
Intensity
1400
1200
1000
800
600
400
200
0
0
5
10
15
20
25
30
35
40
45
50
Position (°2 θ)

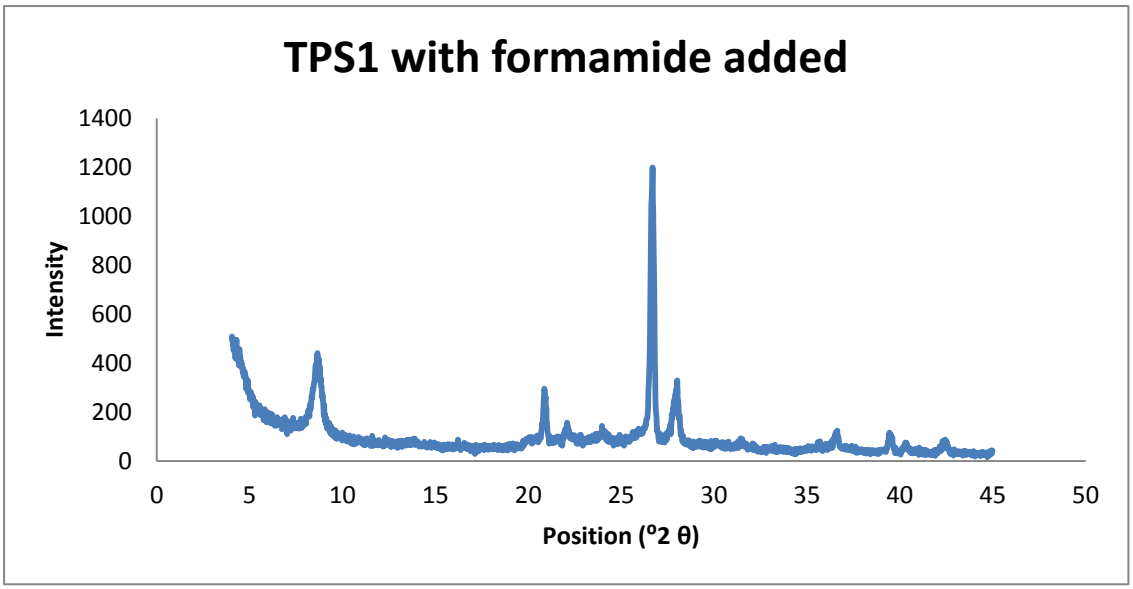
TPS1 with formamide added
Intensity
1400
1200
1000
800
600
400
200
0
0
5
10
15
20
25
30
35
40
45
50
Position (°2 θ)

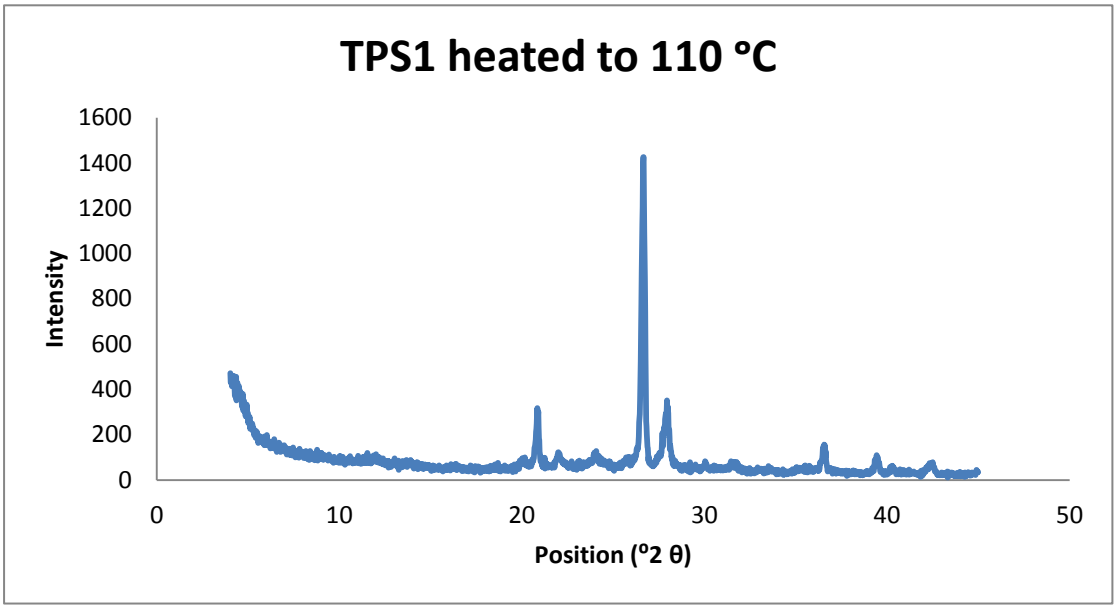
TPS1 heated to 110 °C
Intensity
1600
1400
1200
1000
800
600
400
200
0
0
10
20
30
40
50
Position (°2 θ)

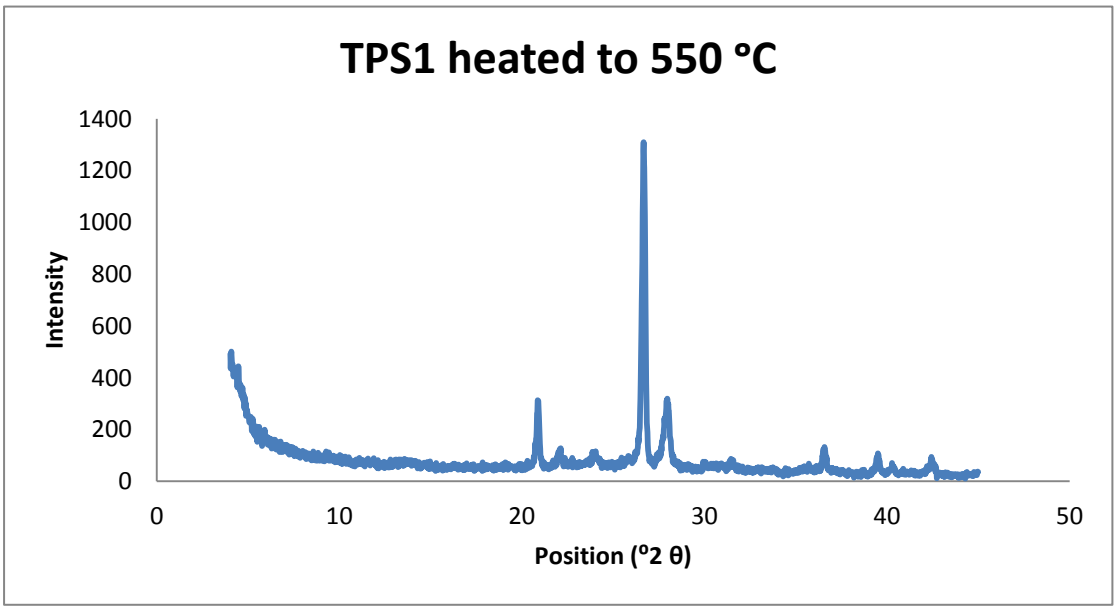
TPS1 heated to 550 °C
Intensity
1400
1200
1000
800
600
400
200
0
0
10
20
30
40
50
Position (°2 θ)

PS1

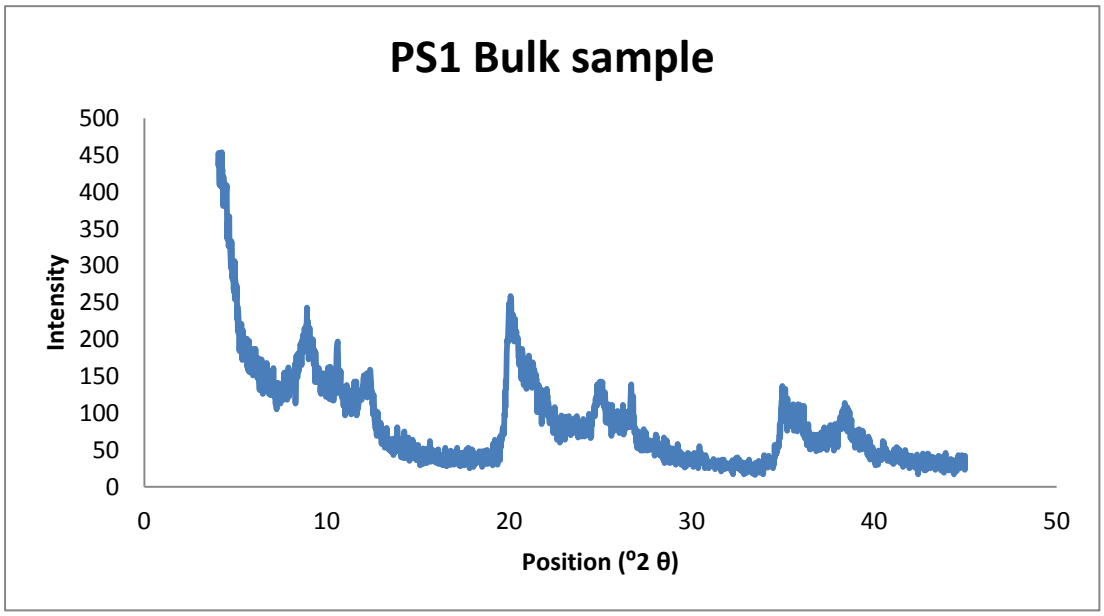
PS1 Bulk sample
Intensity
500
450
400
350
300
250
200
150
100
50
0
0
10
20
30
40
50
Position (°2 θ)

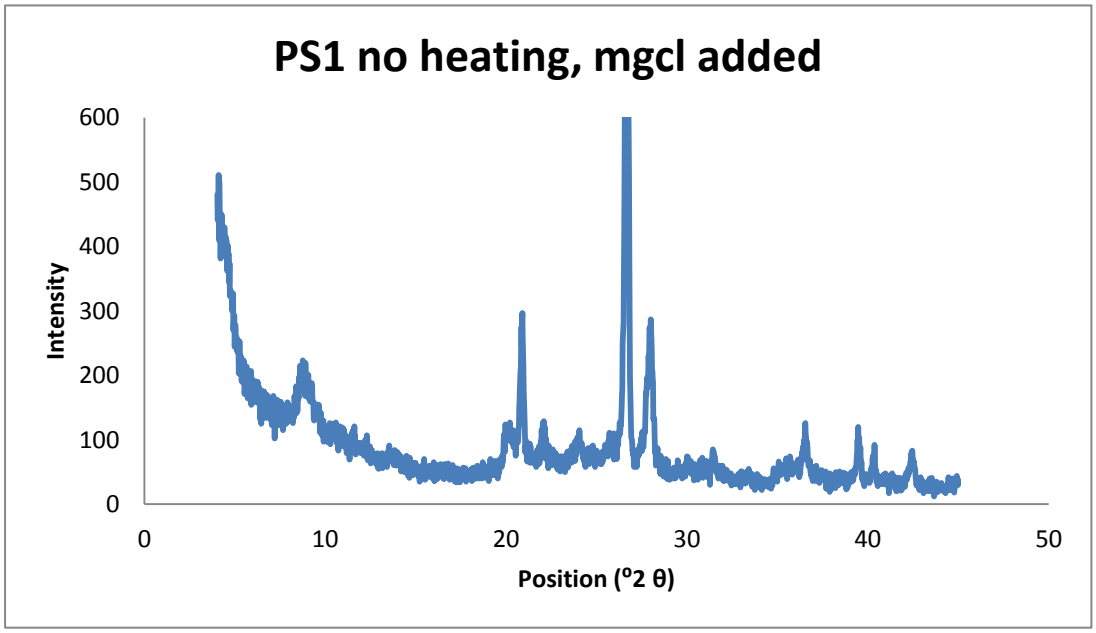
PS1 no heating, mgcl added
Intensity
600
500
400
300
200
100
0
0
10
20
30
40
50
Position (°2 θ)

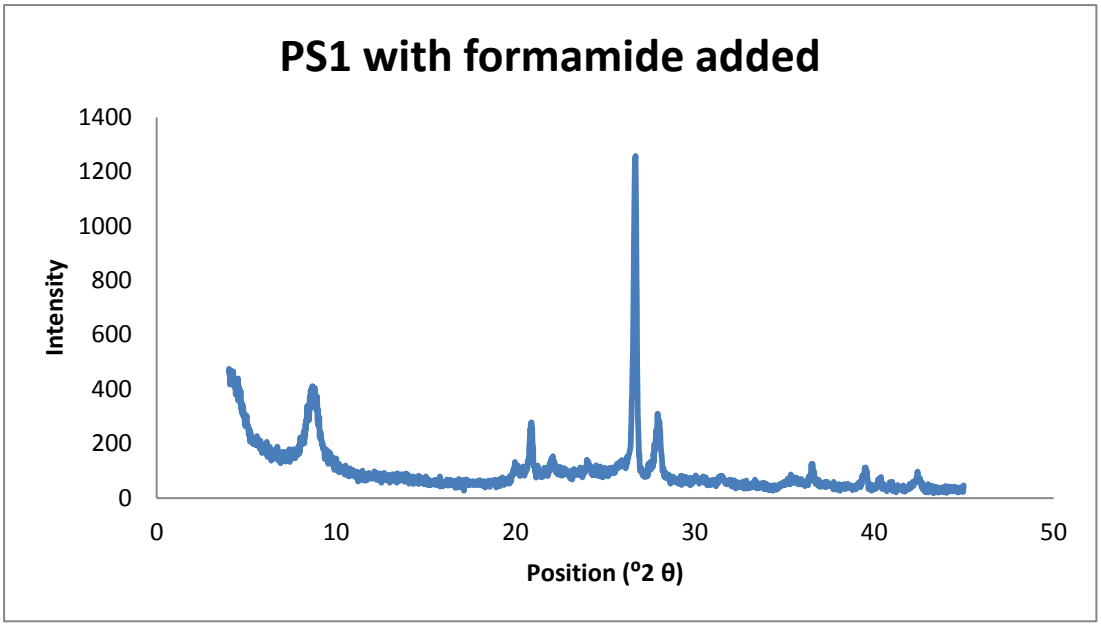
PS1 with formamide added
Intensity
1400
1200
1000
800
600
400
200
0
0
10
20
30
40
50
Position (°2 θ)

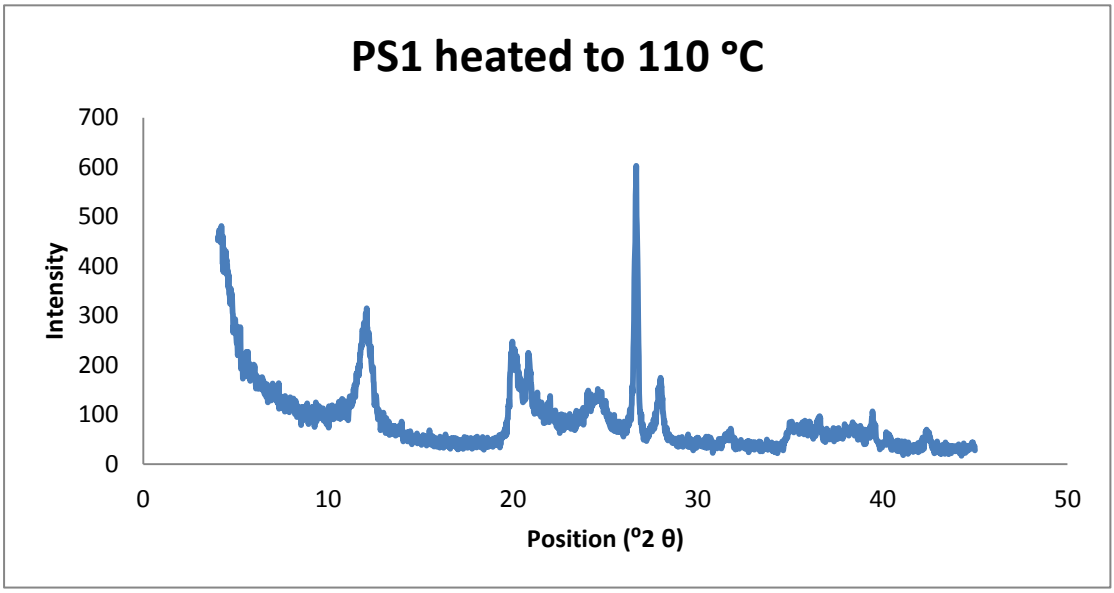
PS1 heated to 110 °C
Intensity
700
600
500
400
300
200
100
0
0
10
20
30
40
50
Position (°2 θ)

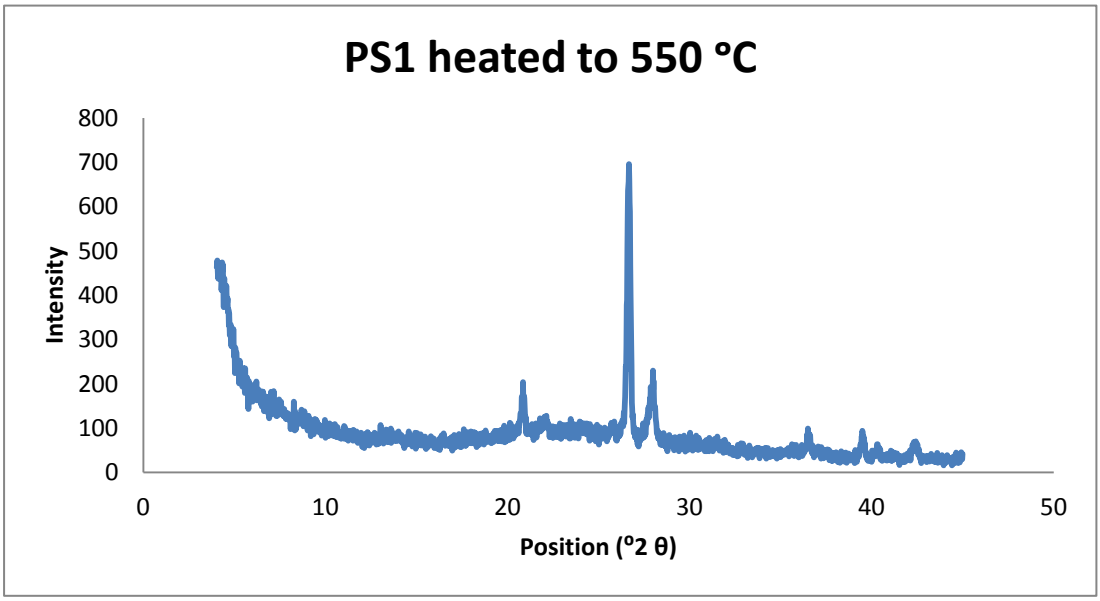
PS1 heated to 550 °C
Intensity
800
700
600
500
400
300
200
100
0
0
10
20
30
40
50
Position (°2 θ)

PS2

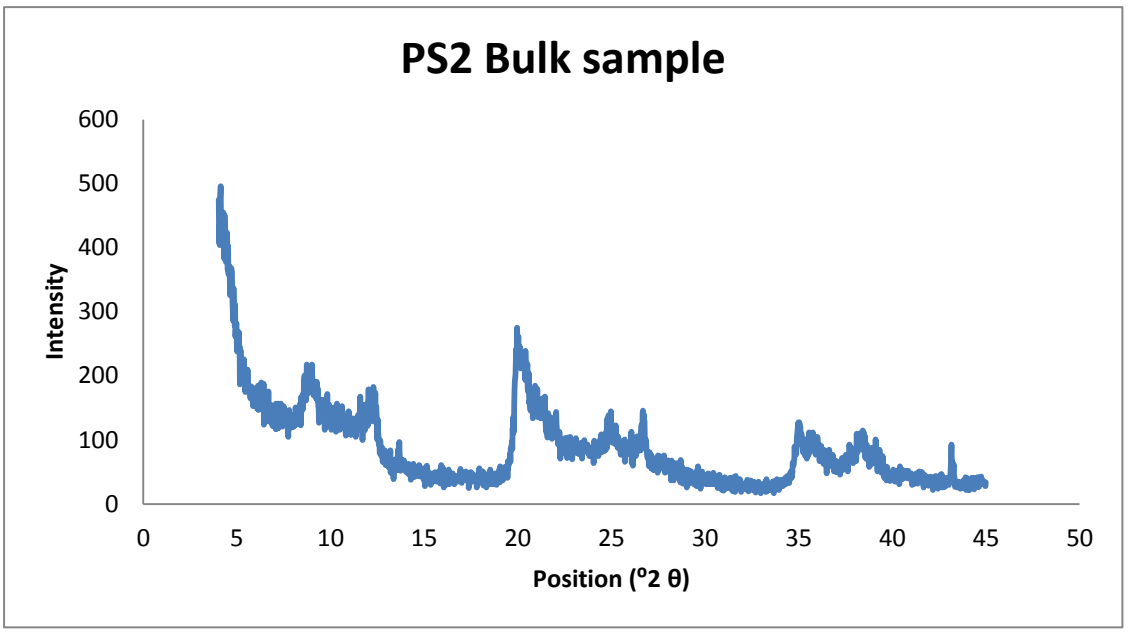
PS2 Bulk sample
Intensity
600
500
400
300
200
100
0
0
5
10
15
20
25
30
35
40
45
50
Position (°2 θ)

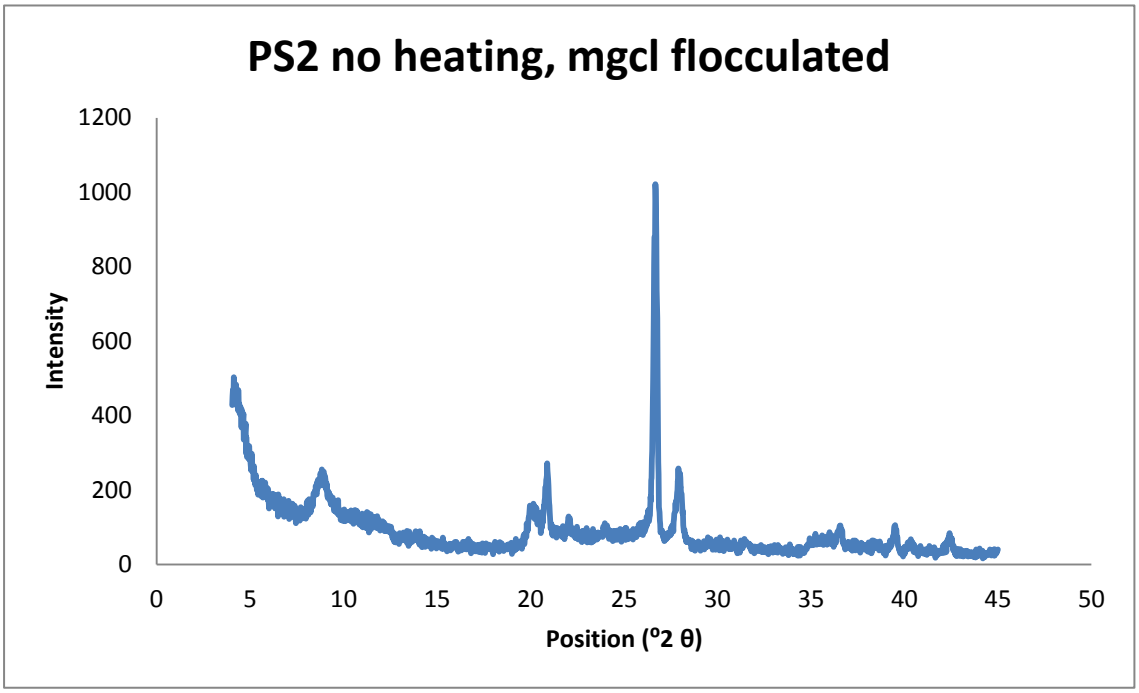
PS2 no heating, mgcl flocculated
Intensity
1200
1000
800
600
400
200
0
0
5
10
15
20
25
30
35
40
45
50
Position (°2 θ)

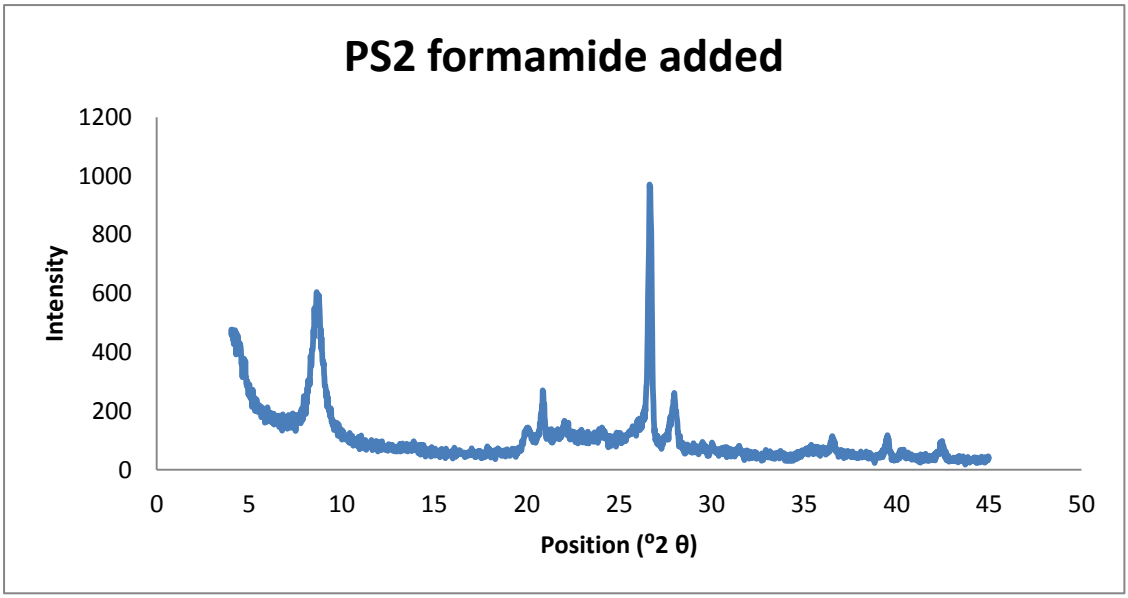
PS2 formamide added
Intensity
1200
1000
800
600
400
200
0
0
5
10
15
20
25
30
35
40
45
50
Position (°2 θ)

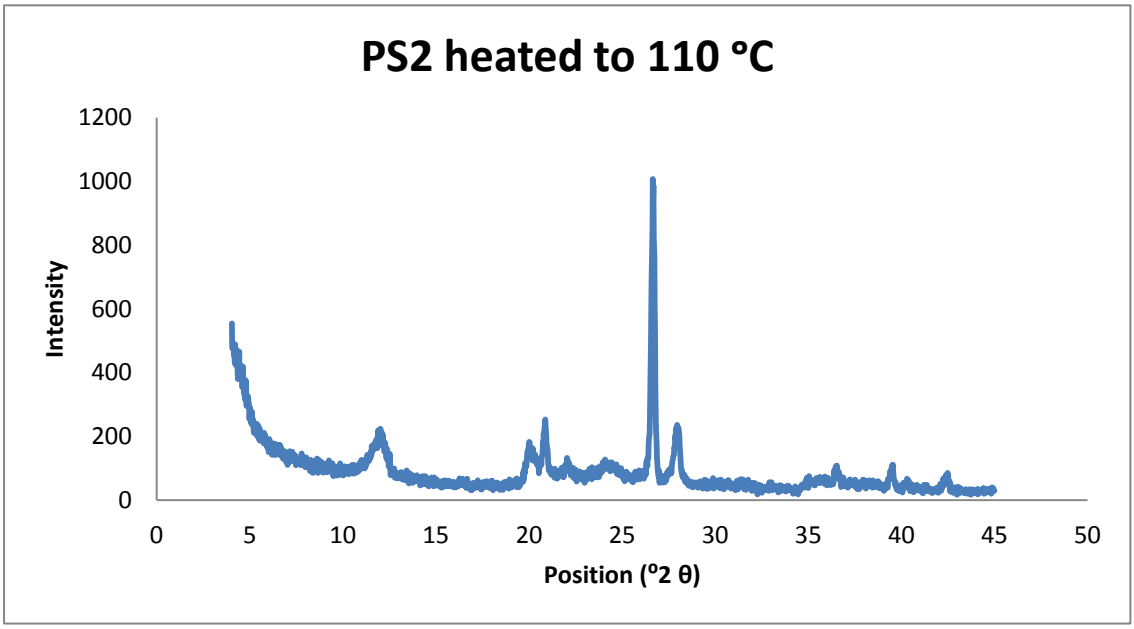
PS2 heated to 110 °C
Intensity
1200
1000
800
600
400
200
0
0
5
10
15
20
25
30
35
40
45
50
Position (°2 θ)

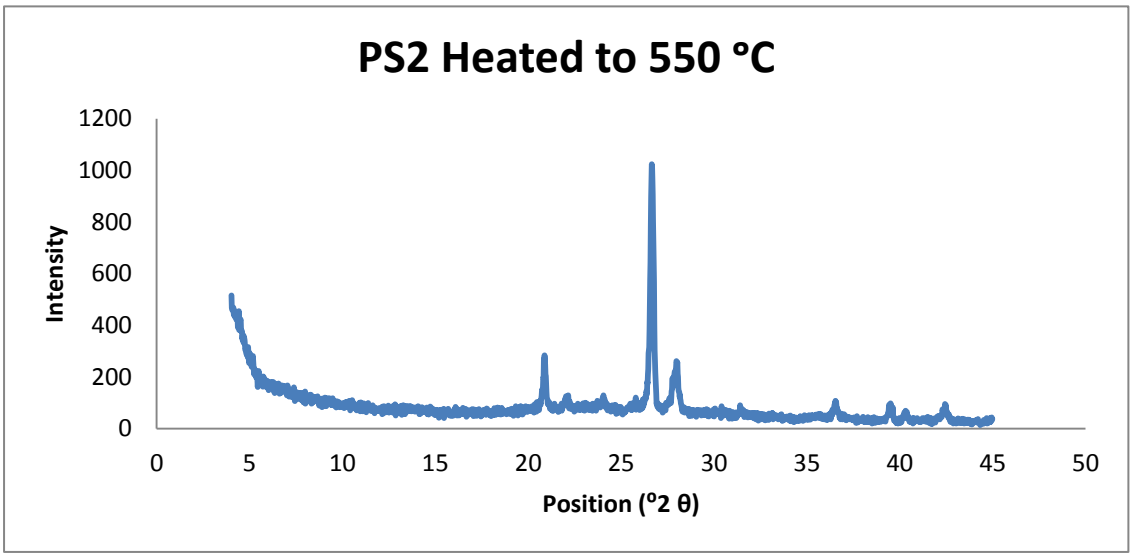
PS2 Heated to 550 °C
Intensity
1200
1000
800
600
400
200
0
0
5
10
15
20
25
30
35
40
45
50
Position (°2 θ)

TS1

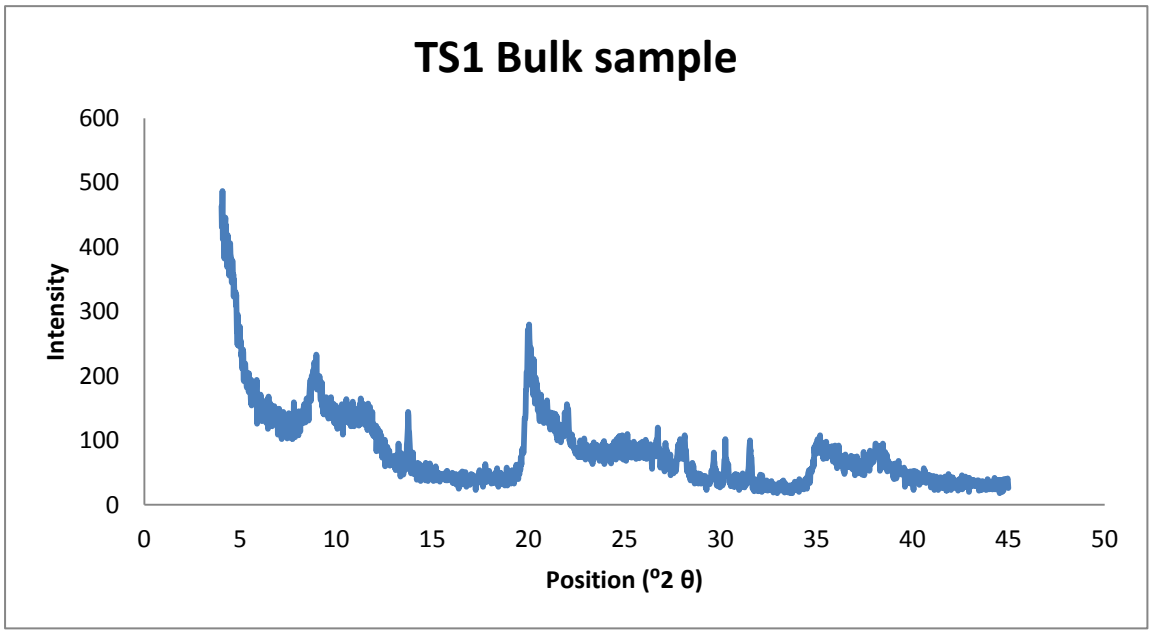
TS1 Bulk sample
Intensity
600
500
400
300
200
100
0
0
5
10
15
20
25
30
35
40
45
50
Position (°2 θ)

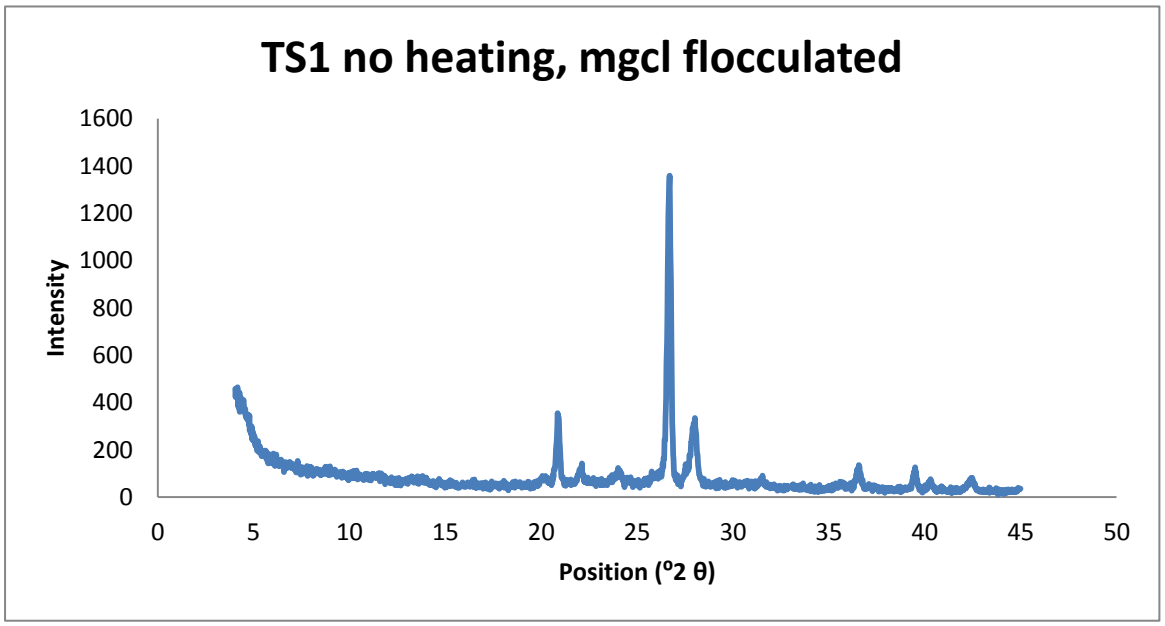
TS1 no heating, mgcl flocculated
Intensity
1600
1400
1200
1000
800
600
400
200
0
0
5
10
15
20
25
30
35
40
45
50
Position (°2 θ)

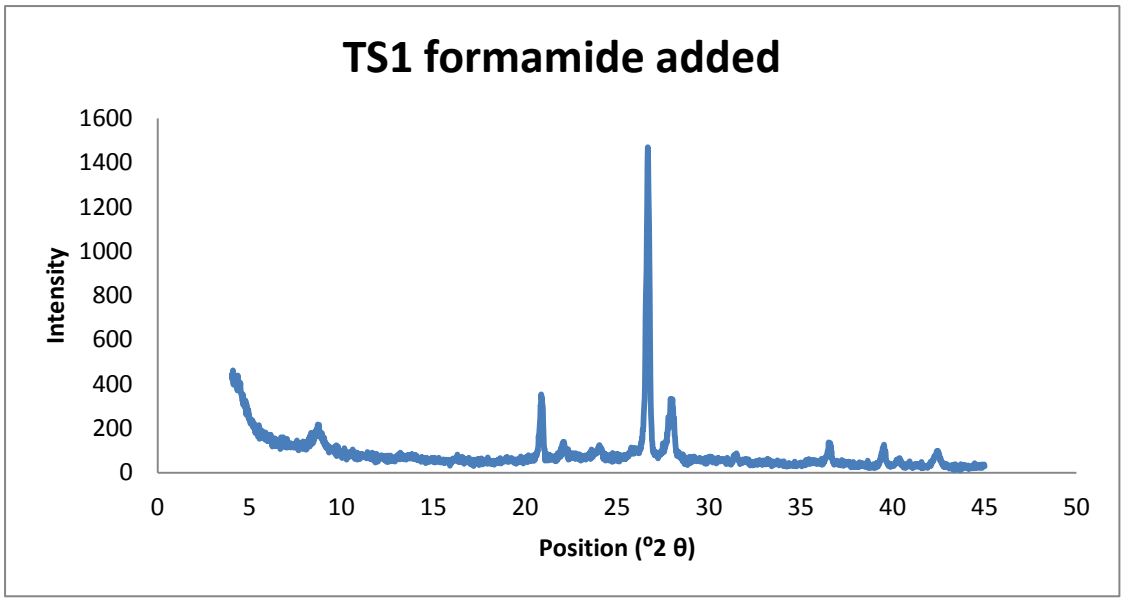
TS1 formamide added
Intensity
1600
1400
1200
1000
800
600
400
200
0
0
5
10
15
20
25
30
35
40
45
50
Position (°2 θ)

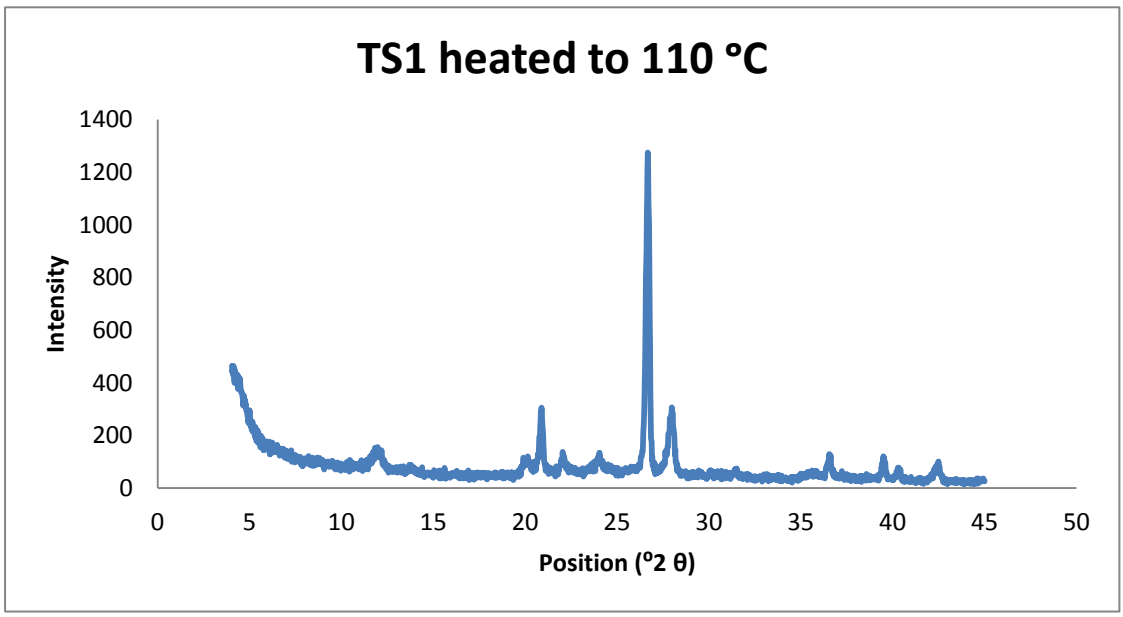
TS1 heated to 110 °C
Intensity
1400
1200
1000
800
600
400
200
0
0
5
10
15
20
25
30
35
40
45
50
Position (°2 θ)

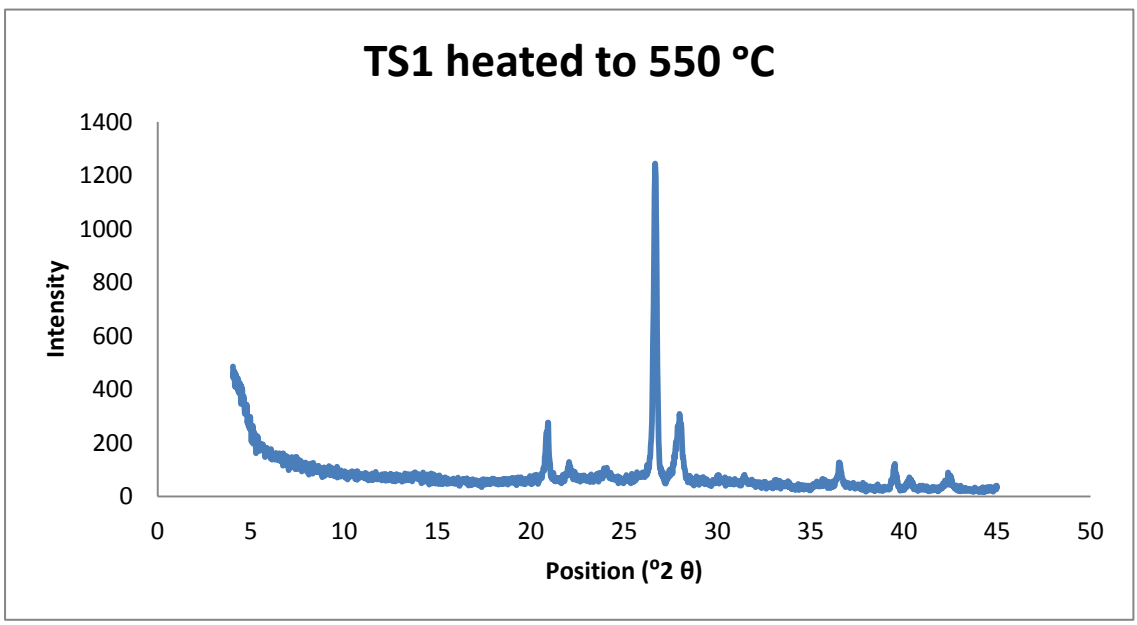
TS1 heated to 550 °C
Intensity
1400
1200
1000
800
600
400
200
0
0
5
10
15
20
25
30
35
40
45
50
Position (°2 θ)

TS2

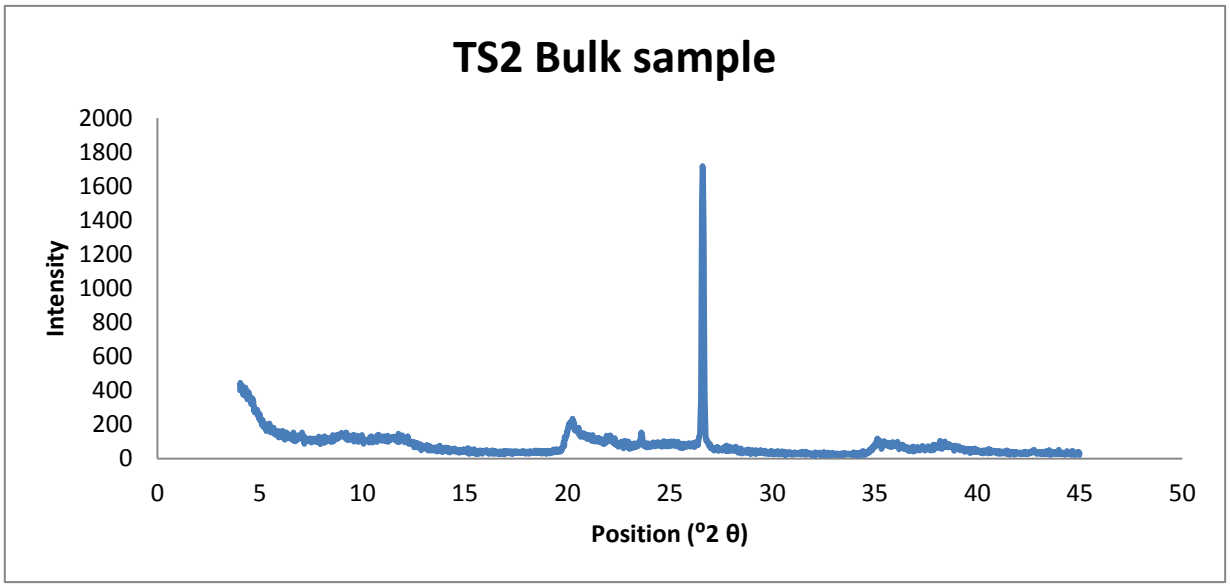
TS2 Bulk sample
Intensity
2000
1800
1600
1400
1200
1000
800
600
400
200
0
0
5
10
15
20
25
30
35
40
45
50
Position (°2 θ)

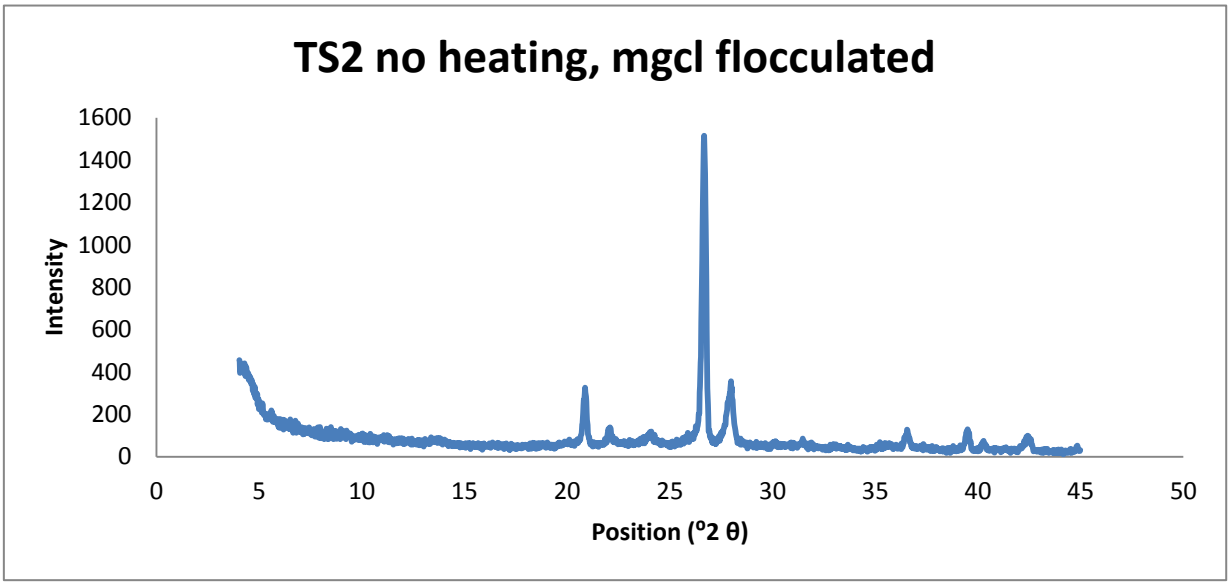
TS2 no heating, mgcl flocculated
Intensity
1600
1400
1200
1000
800
600
400
200
0
0
5
10
15
20
25
30
35
40
45
50
Position (°2 θ)

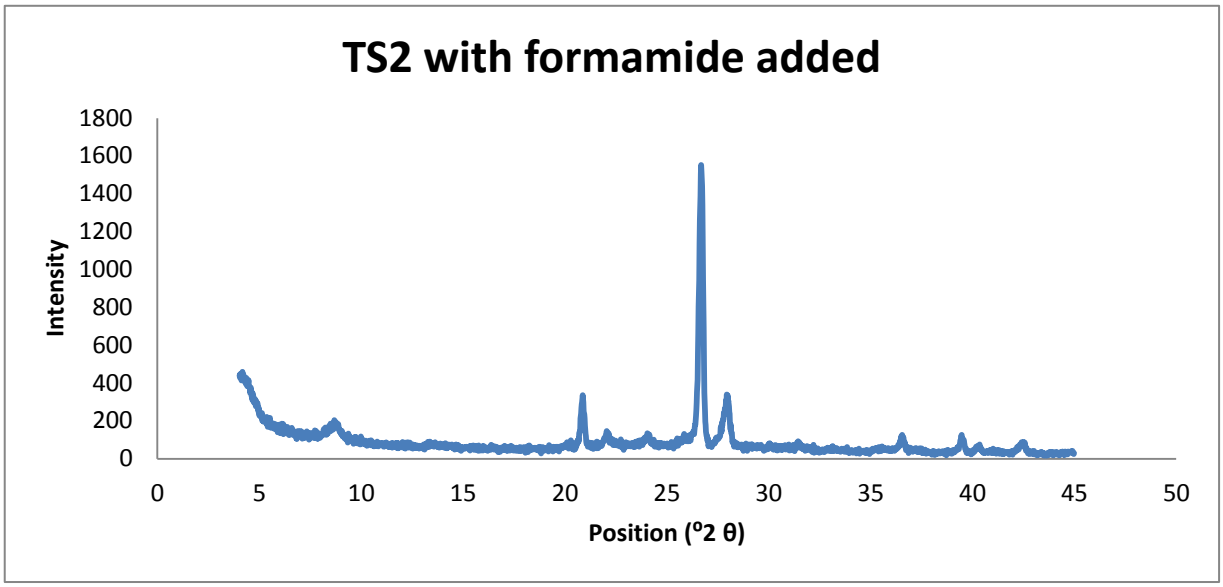
TS2 with formamide added
Intensity
1800
1600
1400
1200
1000
800
600
400
200
0
0
5
10
15
20
25
30
35
40
45
50
Position (°2 θ)

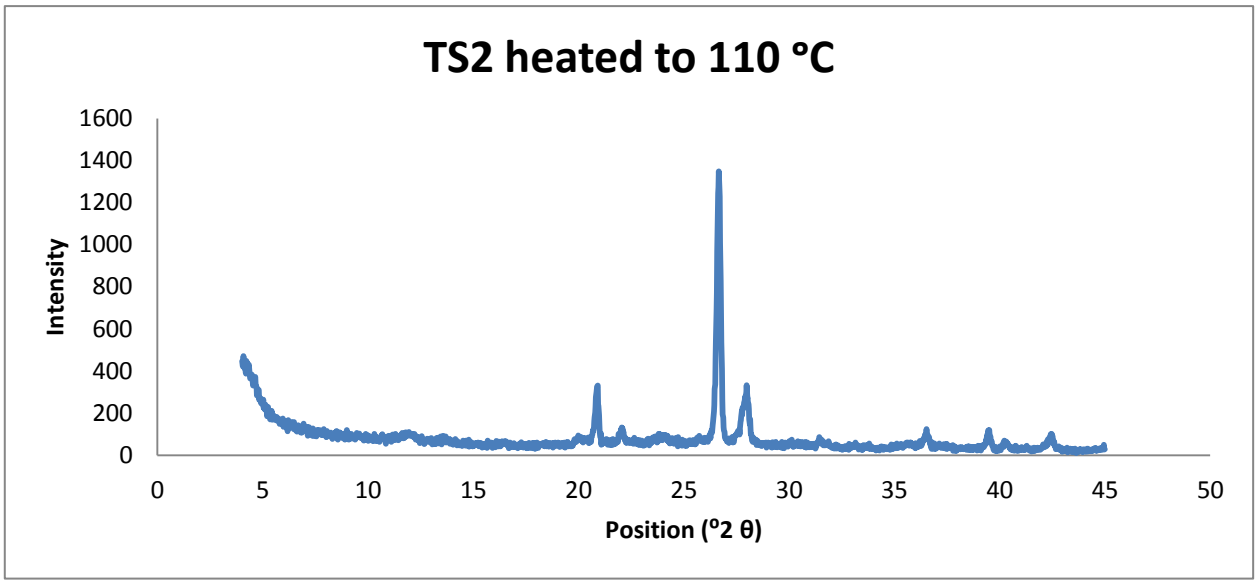
TS2 heated to 110 °C
Intensity
1600
1400
1200
1000
800
600
400
200
0
0
5
10
15
20
25
30
35
40
45
50
Position (°2 θ)

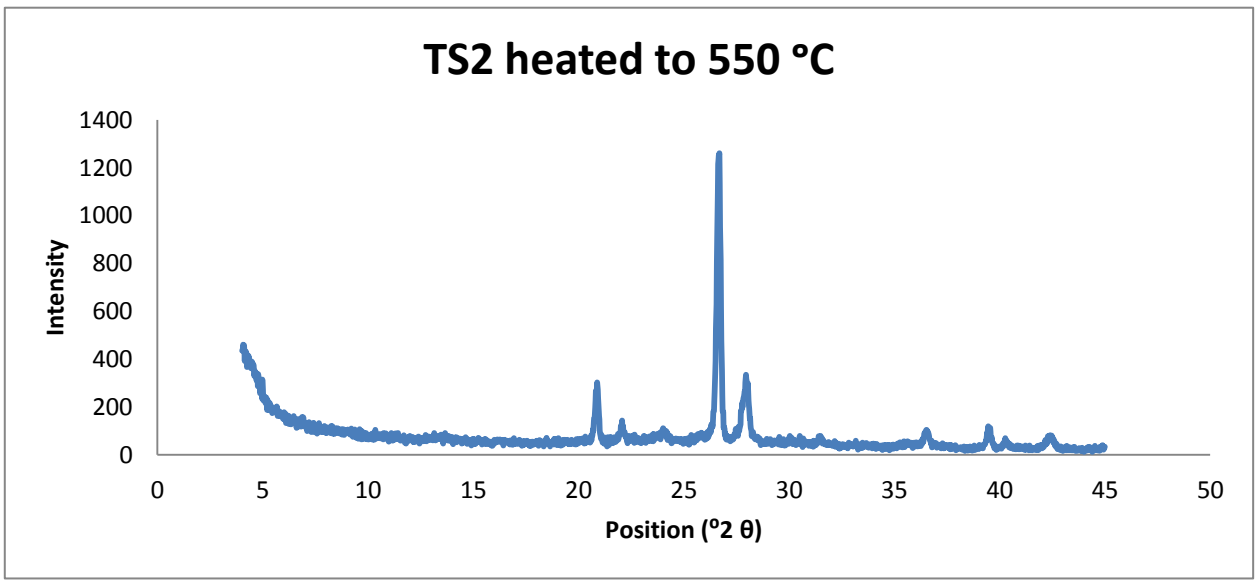
TS2 heated to 550 °C
Intensity
1400
1200
1000
800
600
400
200
0
0
5
10
15
20
25
30
35
40
45
50
Position (°2 θ)

TS3

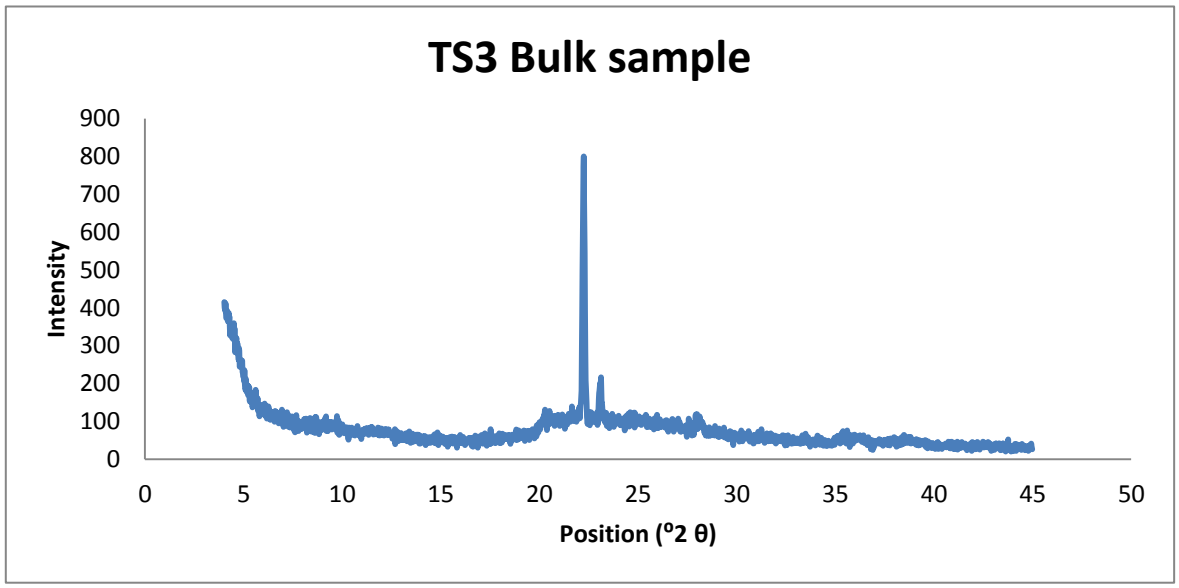
TS3 Bulk sample
Intensity
900
800
700
600
500
400
300
200
100
0
0
5
10
15
20
25
30
35
40
45
50
Position (°2 θ)

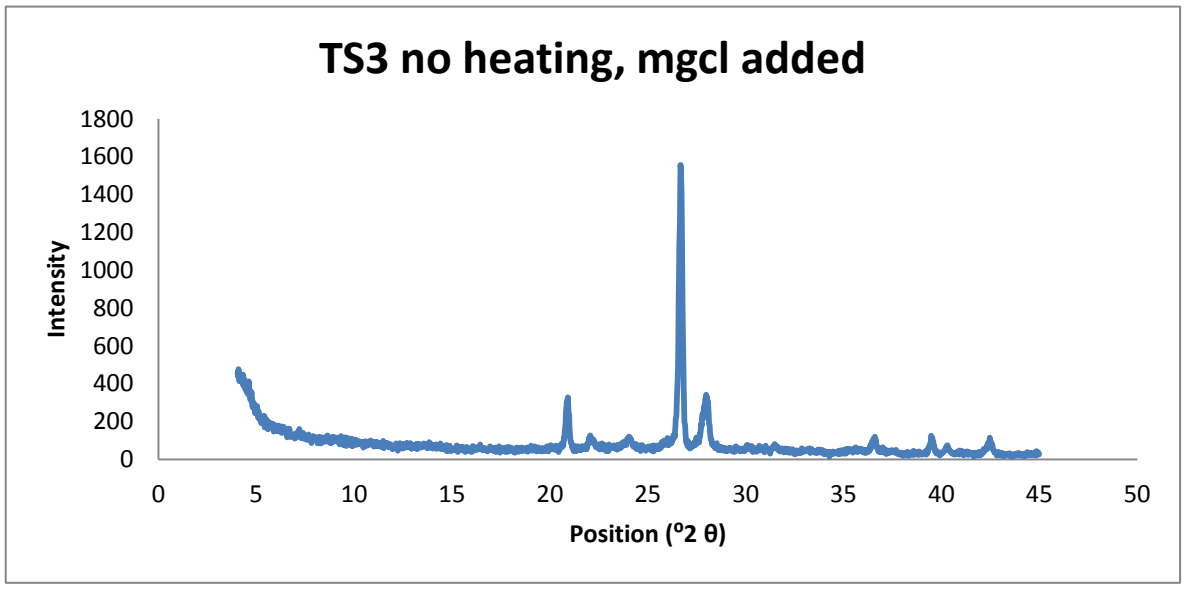
TS3 no heating, mgcl added
Intensity
1800
1600
1400
1200
1000
800
600
400
200
0
0
5
10
15
20
25
30
35
40
45
50
Position (°2 θ)

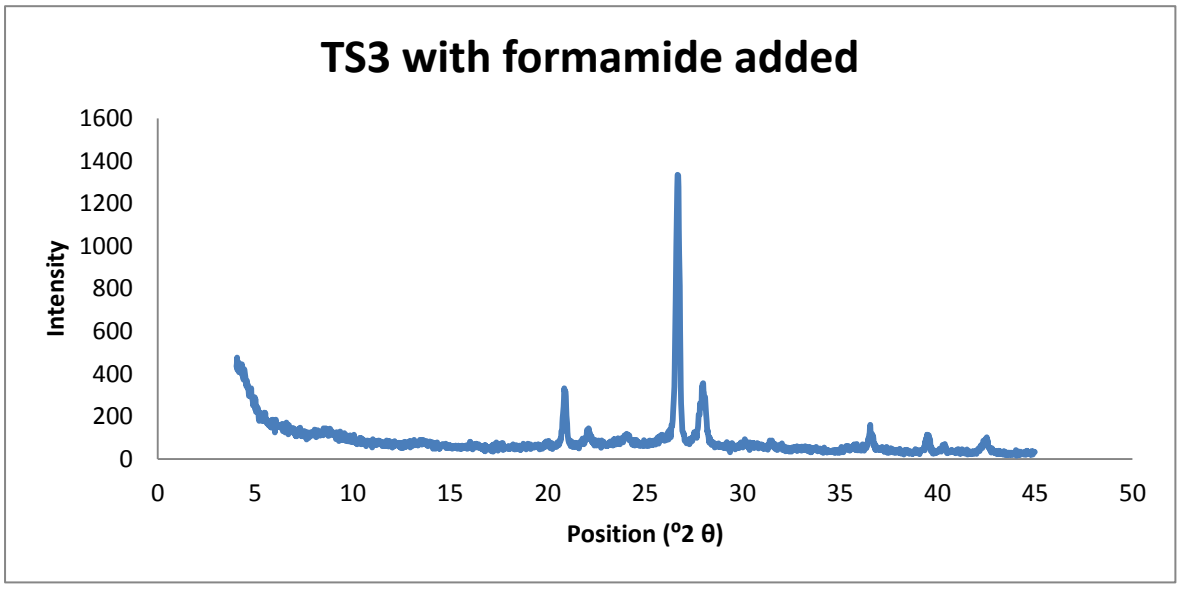
TS3 with formamide added
Intensity
1600
1400
1200
1000
800
600
400
200
0
0
5
10
15
20
25
30
35
40
45
50
Position (°2 θ)

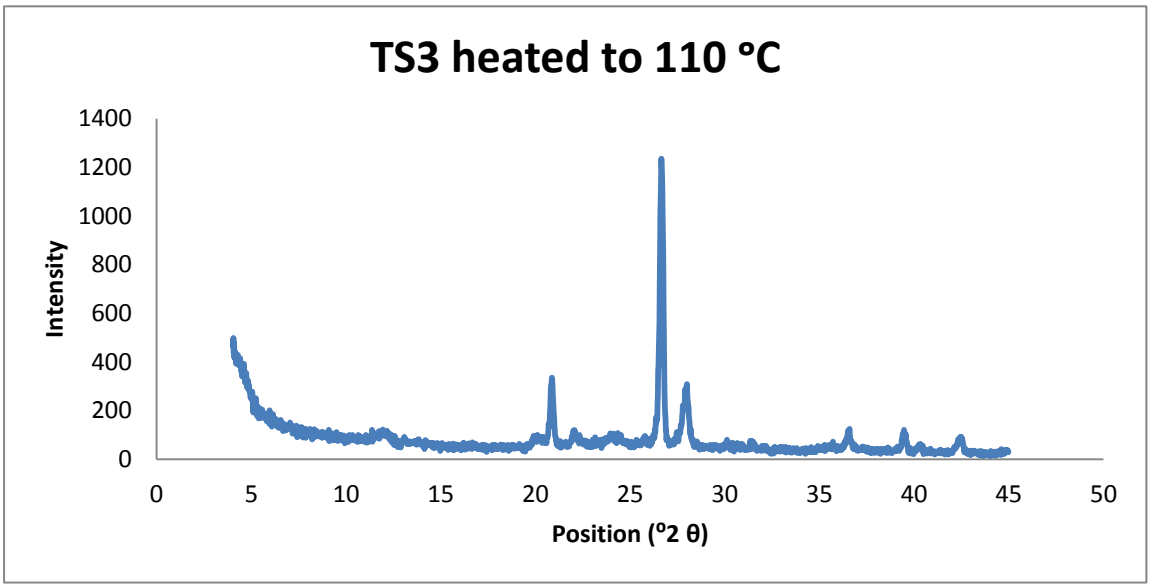
TS3 heated to 110 °C
Intensity
1400
1200
1000
800
600
400
200
0
0
5
10
15
20
25
30
35
40
45
50
Position (°2 θ)

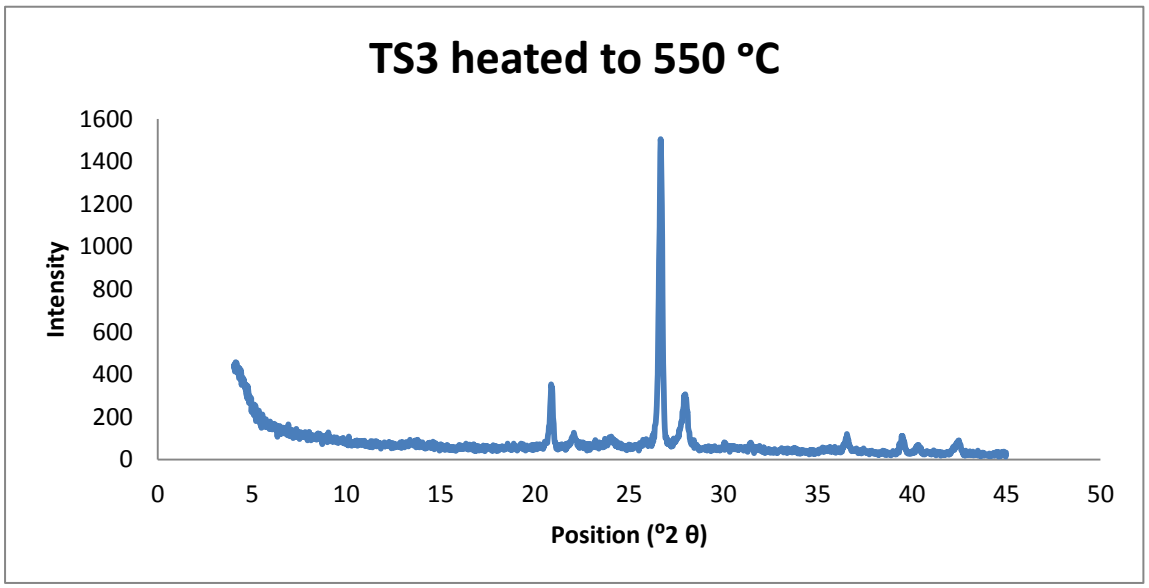
TS3 heated to 550 °C
Intensity
1600
1400
1200
1000
800
600
400
200
0
0
5
10
15
20
25
30
35
40
45
50
Position (°2 θ)

TS4

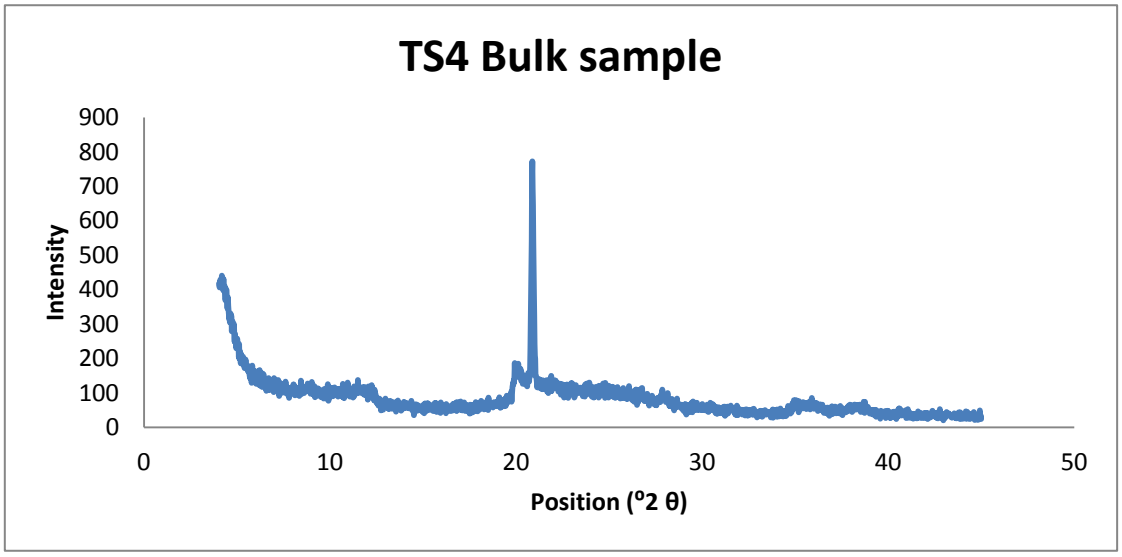
TS4 Bulk sample
Intensity
900
800
700
600
500
400
300
200
100
0
0
10
20
30
40
50
Position (°2 θ)

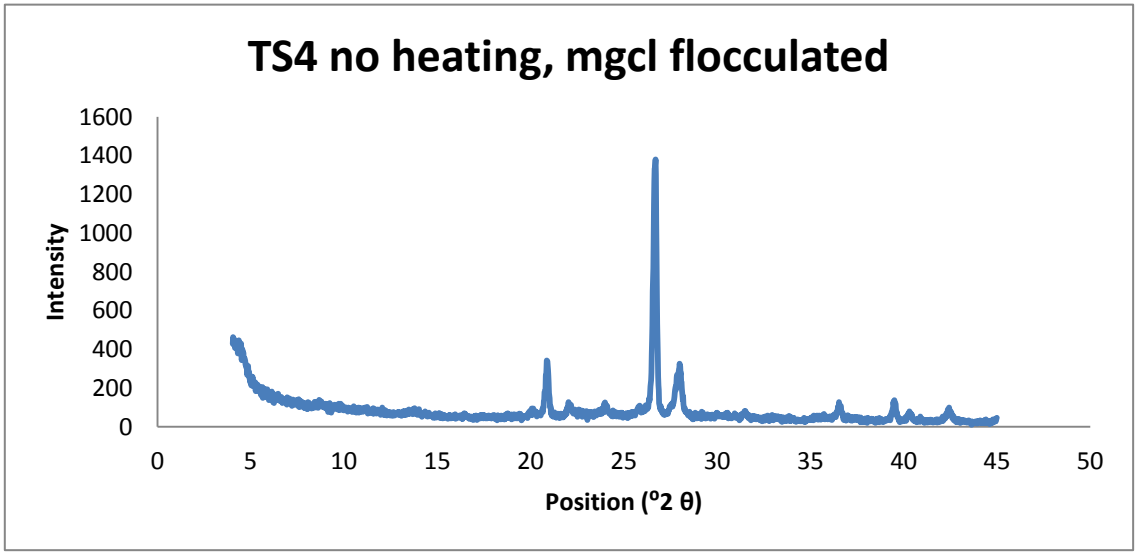
TS4 no heating, mgcl flocculated
Intensity
1600
1400
1200
1000
800
600
400
200
0
0
5
10
15
20
25
30
35
40
45
50
Position (°2 θ)

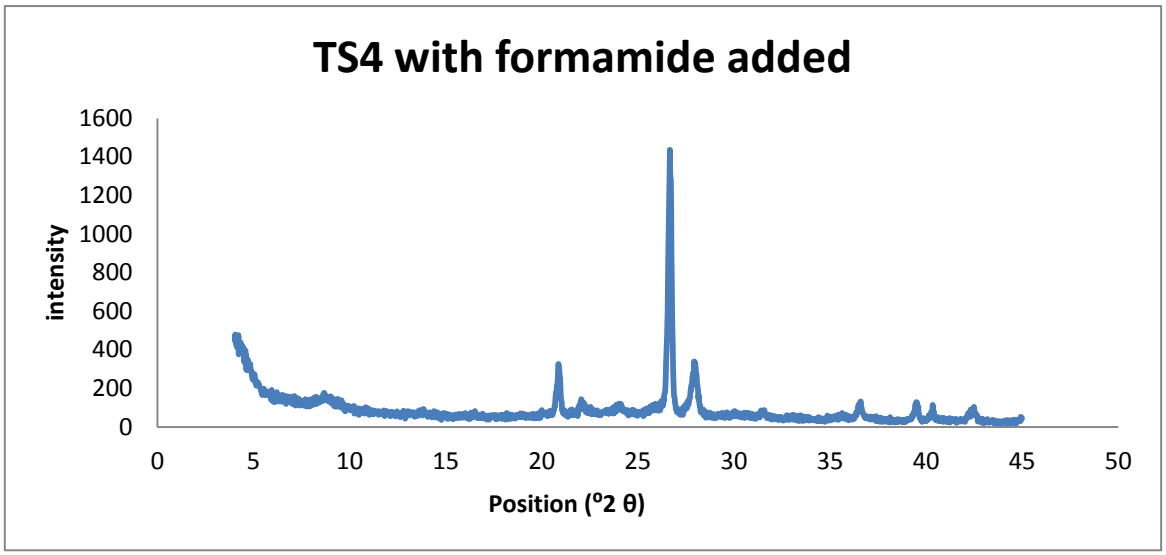
TS4 with formamide added
intensity
1600
1400
1200
1000
800
600
400
200
0
0
5
10
15
20
25
30
35
40
45
50
Position (°2 θ)

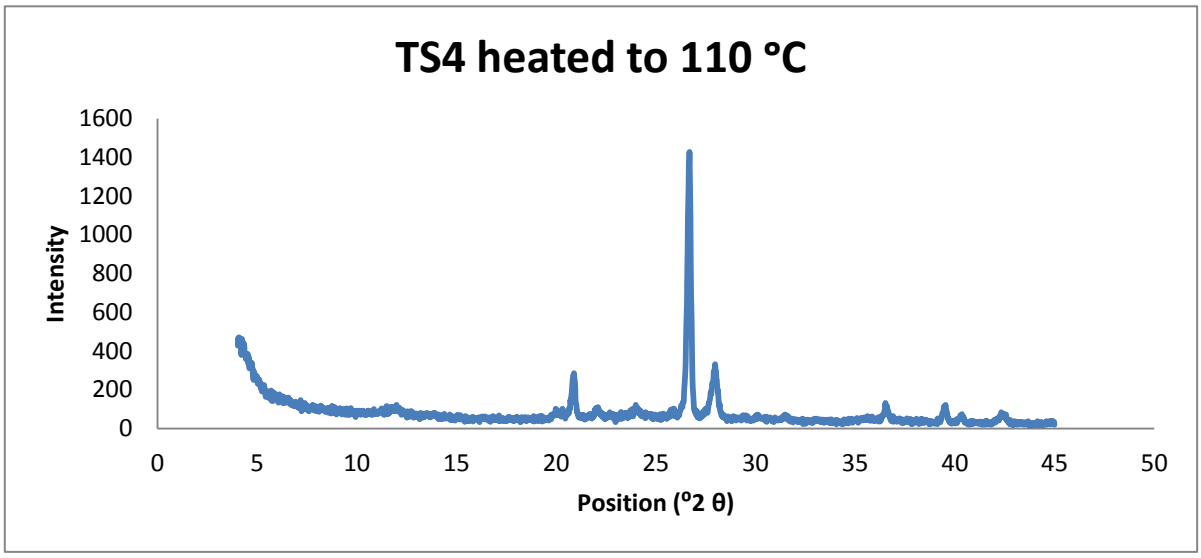
TS4 heated to 110 °C
Intensity
1600
1400
1200
1000
800
600
400
200
0
0
5
10
15
20
25
30
35
40
45
50
Position (°2 θ)

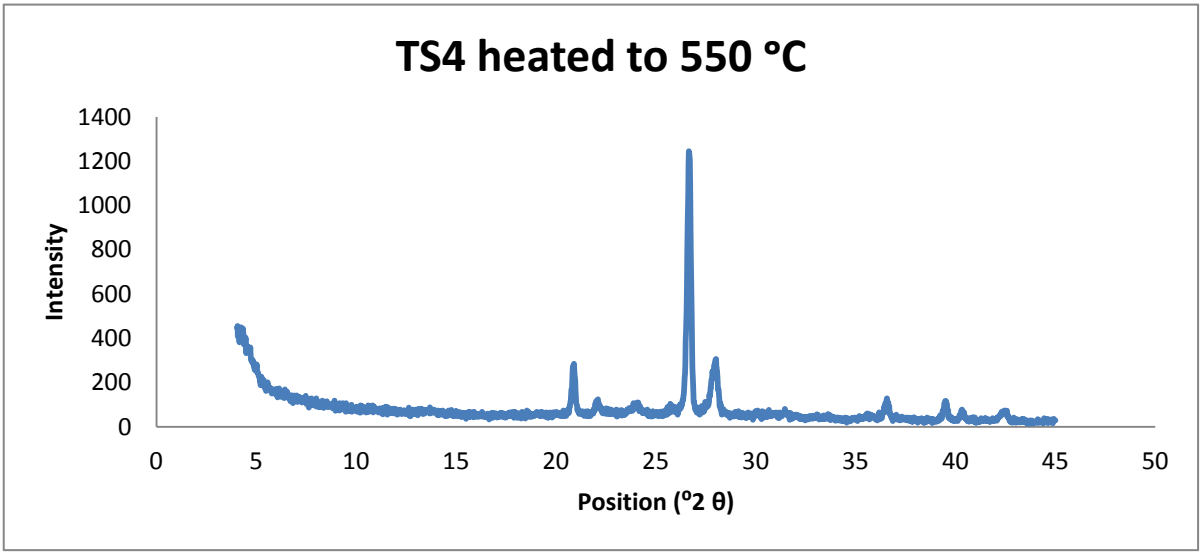
TS4 heated to 550 °C
Intensity
1400
1200
1000
800
600
400
200
0
0
5
10
15
20
25
30
35
40
45
50
Position (°2 θ)

RS1

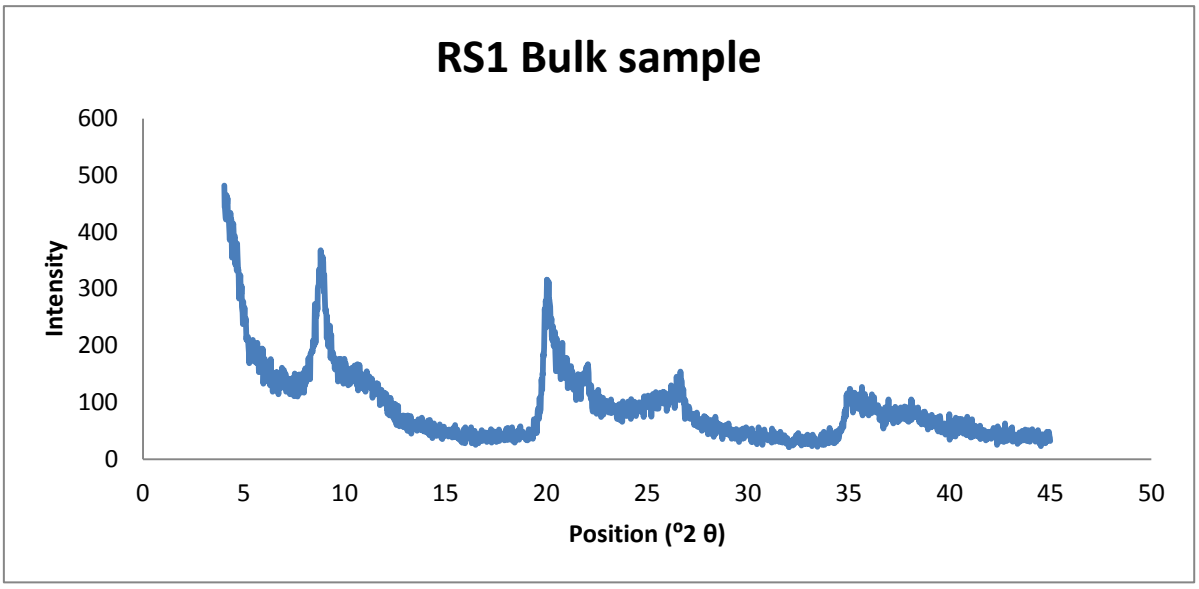
RS1 Bulk sample
Intensity
600
500
400
300
200
100
0
0
5
10
15
20
25
30
35
40
45
50
Position (°2 θ)

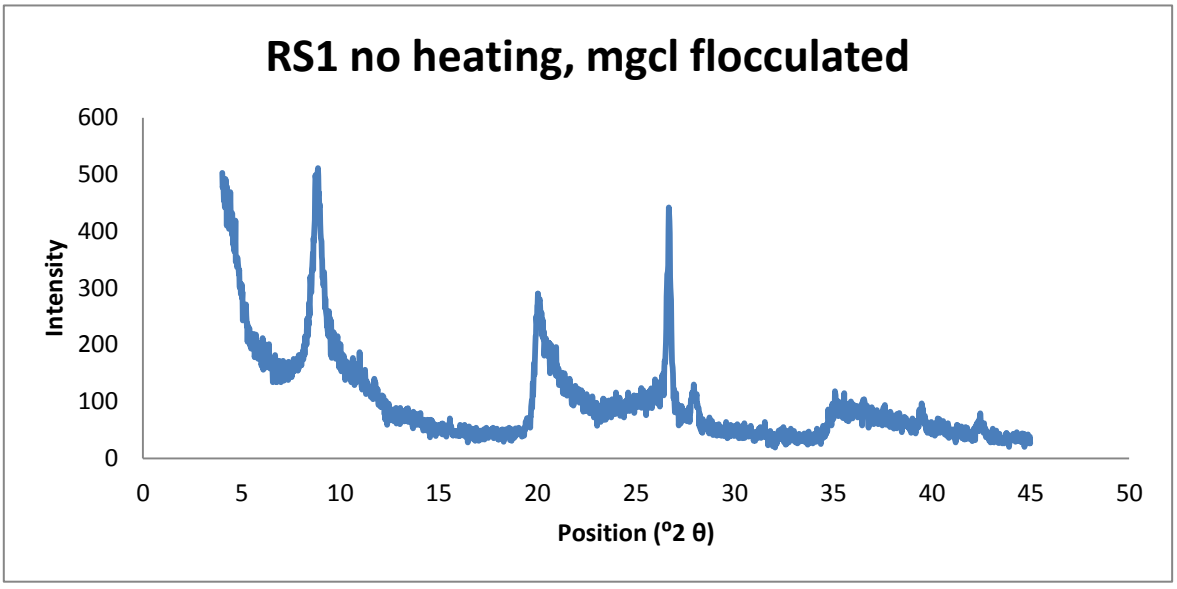
RS1 no heating, mgcl flocculated
Intensity
600
500
400
300
200
100
0
0
5
10
15
20
25
30
35
40
45
50
Position (°2 θ)

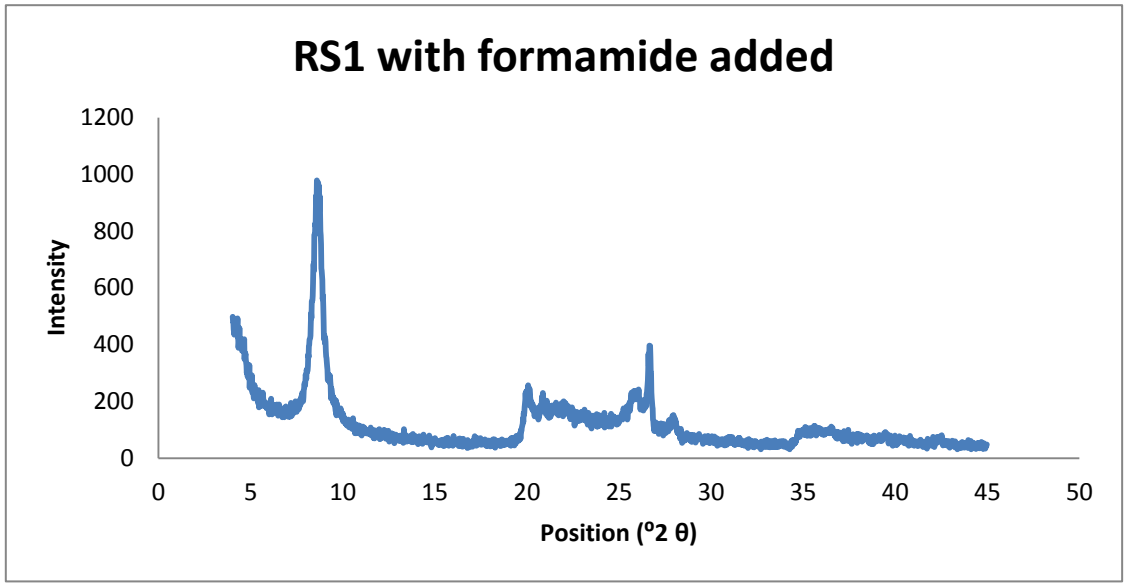
RS1 with formamide added
Intensity
1200
1000
800
600
400
200
0
0
5
10
15
20
25
30
35
40
45
50
Position (°2 θ)

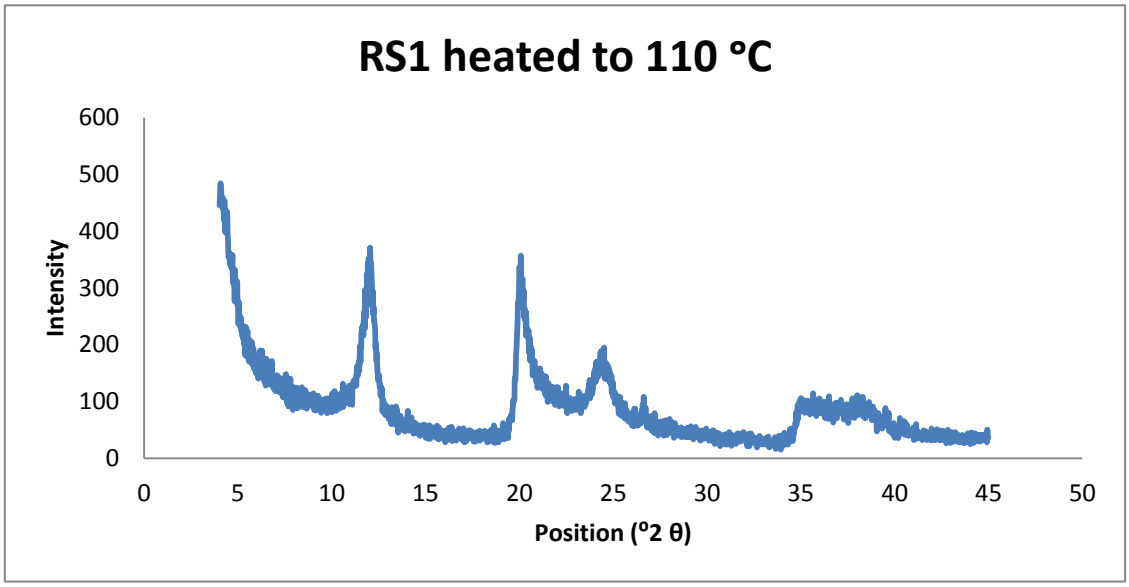
RS1 heated to 110 °C
Intensity
600
500
400
300
200
100
0
0
5
10
15
20
25
30
35
40
45
50
Position (°2 θ)

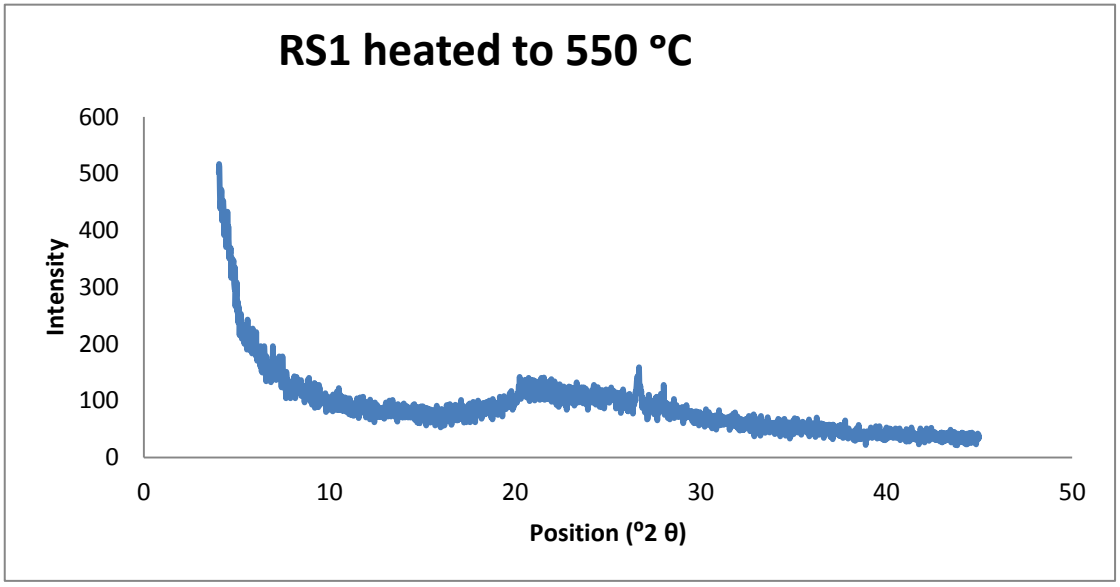
RS1 heated to 550 °C
Intensity
600
500
400
300
200
100
0
0
10
20
30
40
50
Position (°2 θ)

Appendix 6.2

The following appendix presents the SEM images taken from all samples in this study that were not presented in the main text (Chapters 6 and 8)

OS1 – Peak strength state

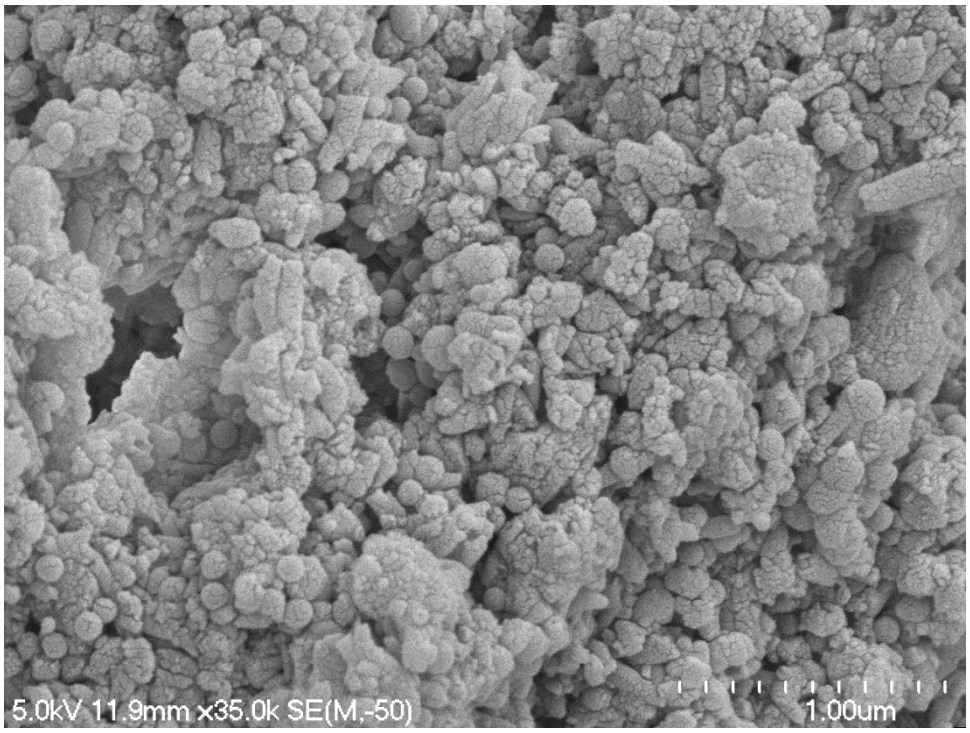

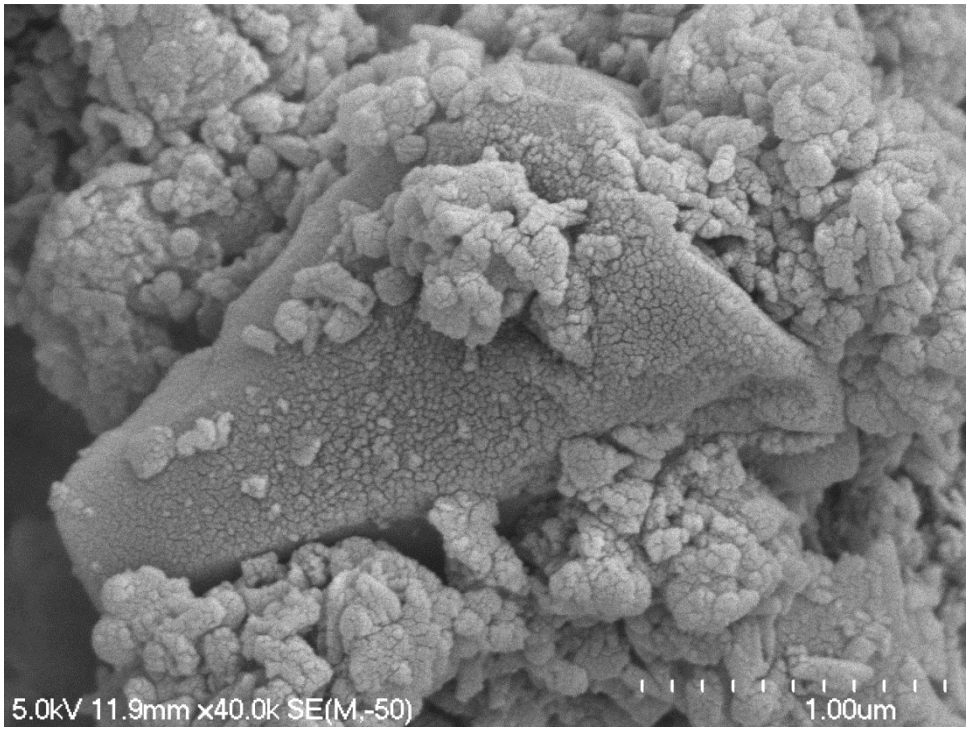

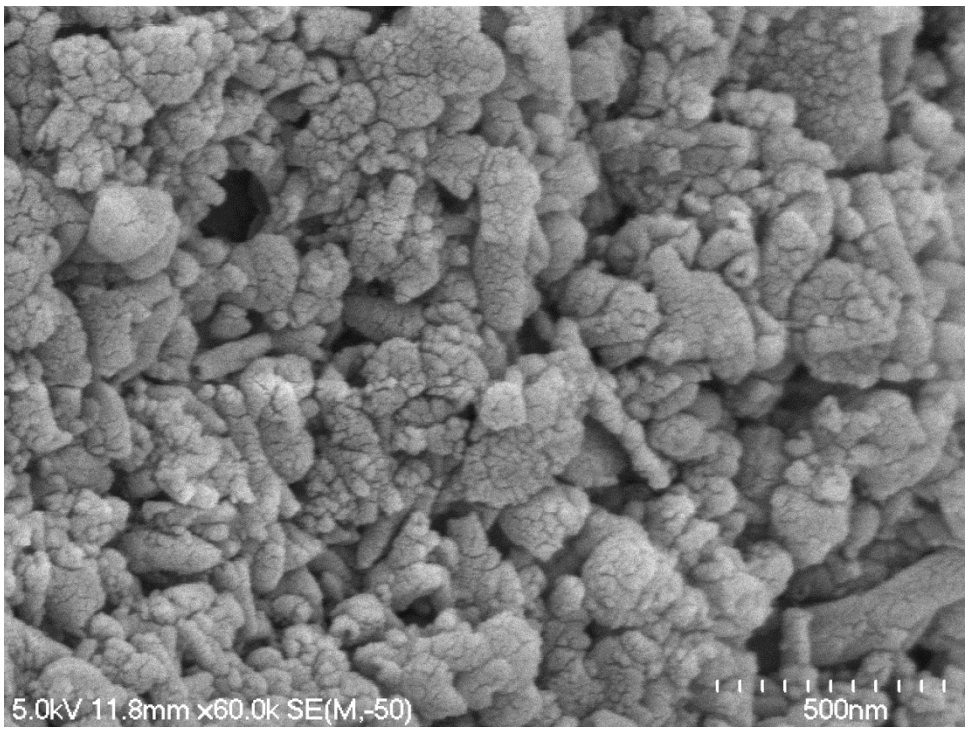
5.0kV 11.8mm x60.0k SE(M,-50)
500nm


5.0kV 11.9mm x90.0k SE(M,-50)
500nm

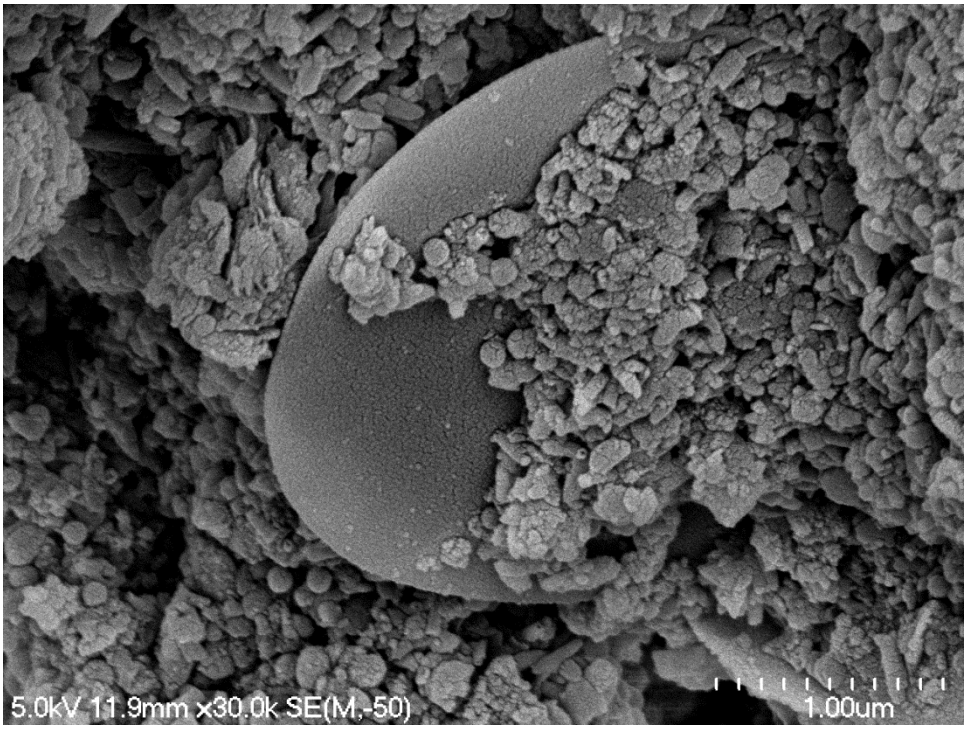
5.0kV 11.9mm x30.0k SE(M,-50)
1.00um


5.0kV 11.6mm x4.56k SE(M,-50)
10.0um

OS1 – Remoulded state

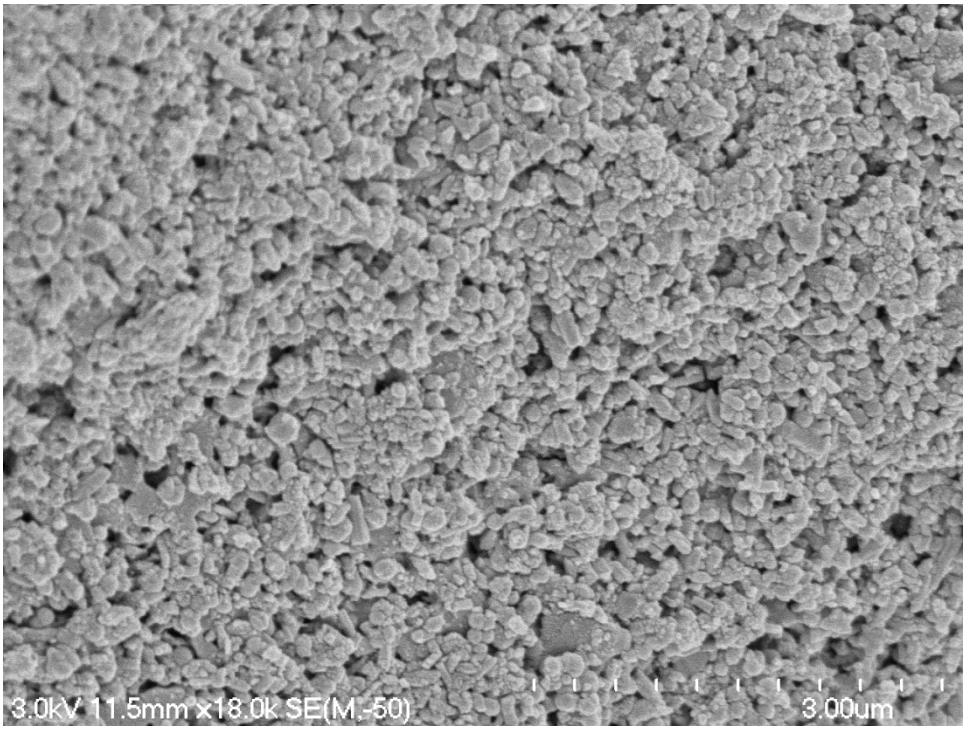

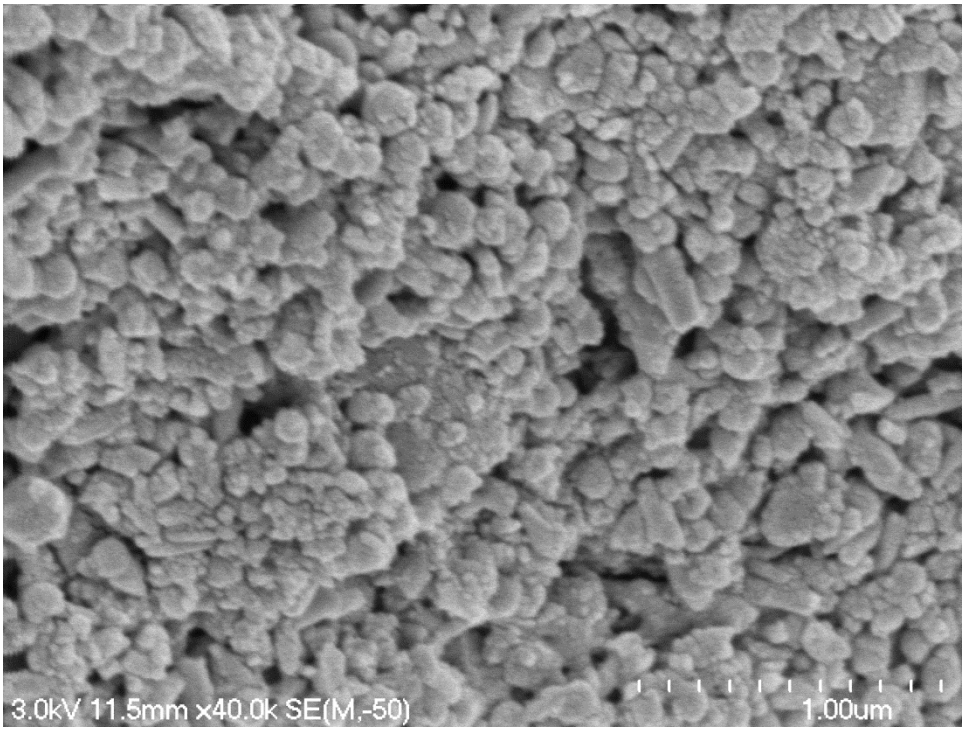

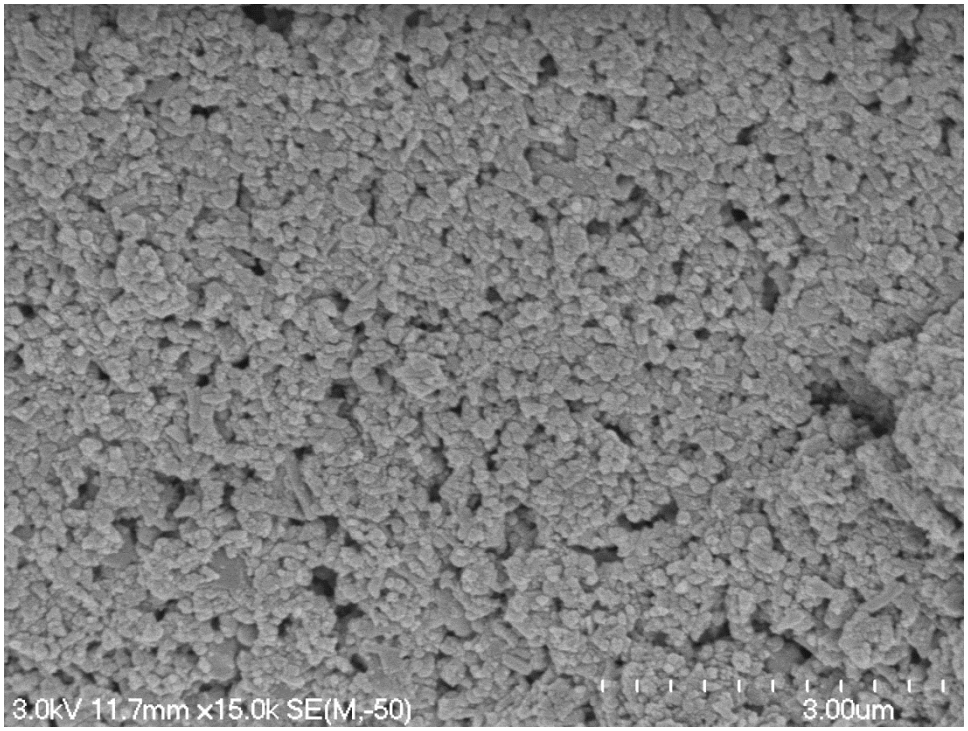
3.0kV 11.7mm x15.0k SE(M,-50)
3.00um

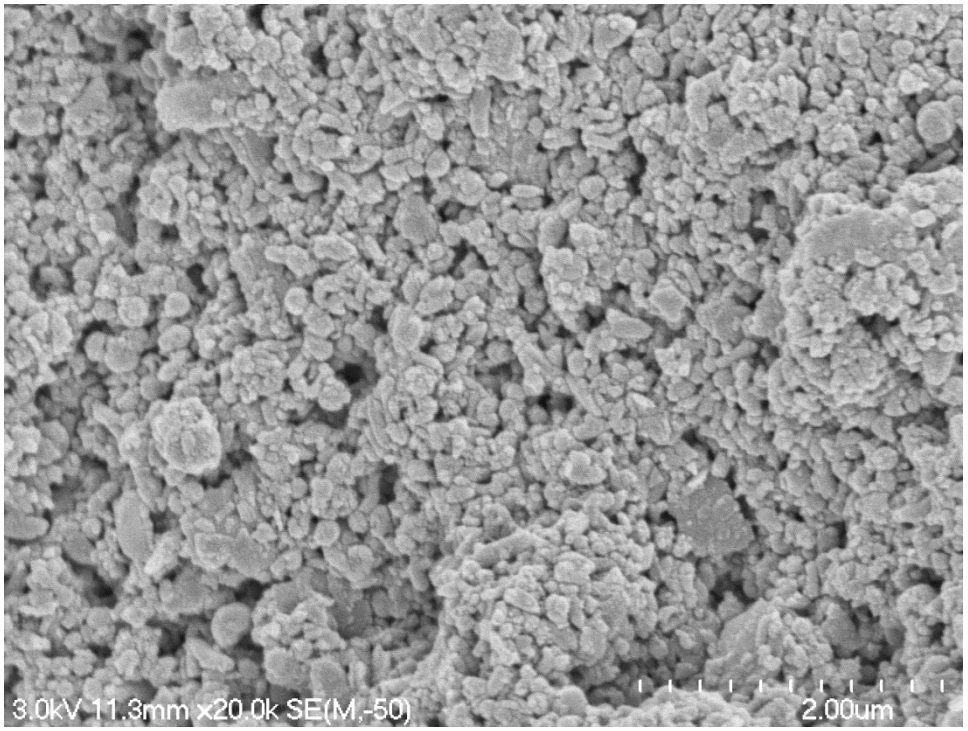
3.0kV 11.3mm x20.0k SE(M,-50)
2.00um

OS2 – Peak strength state

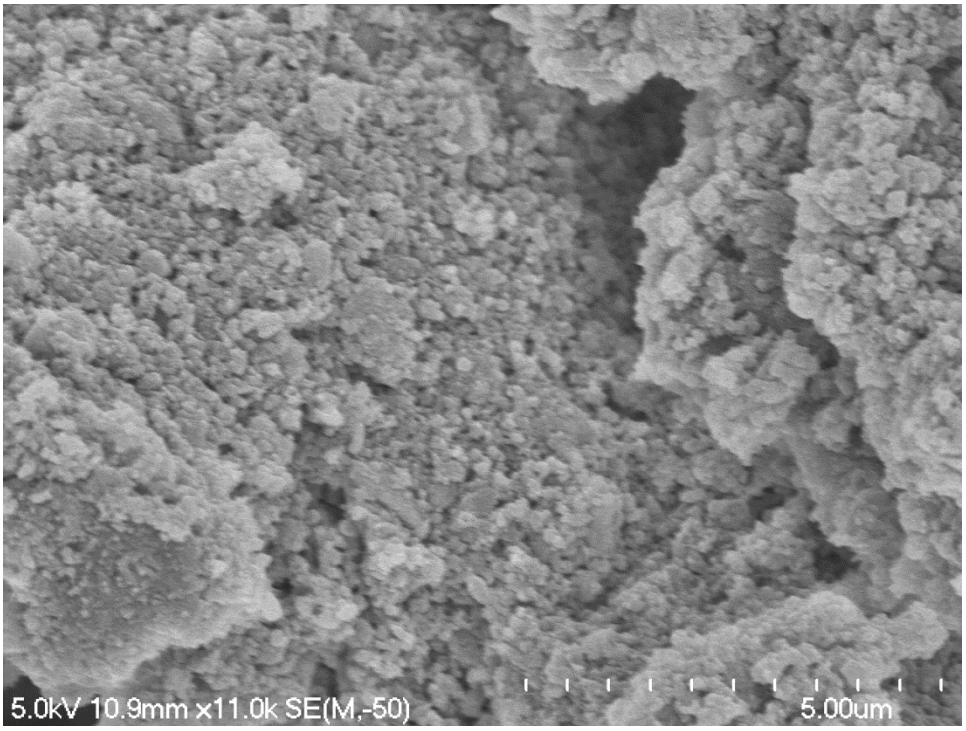

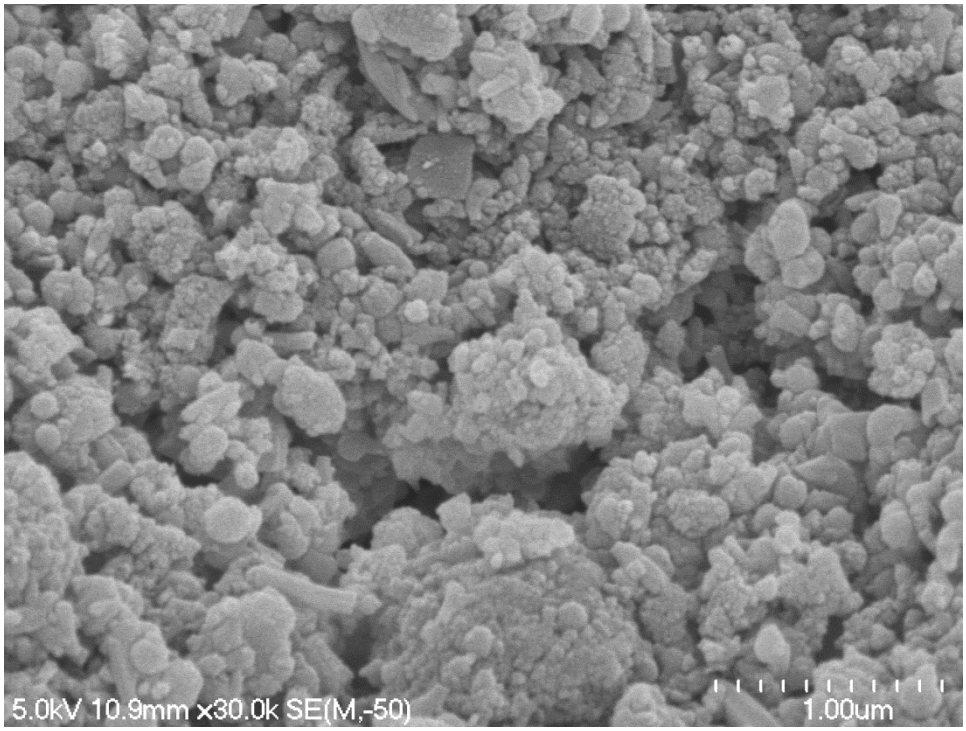

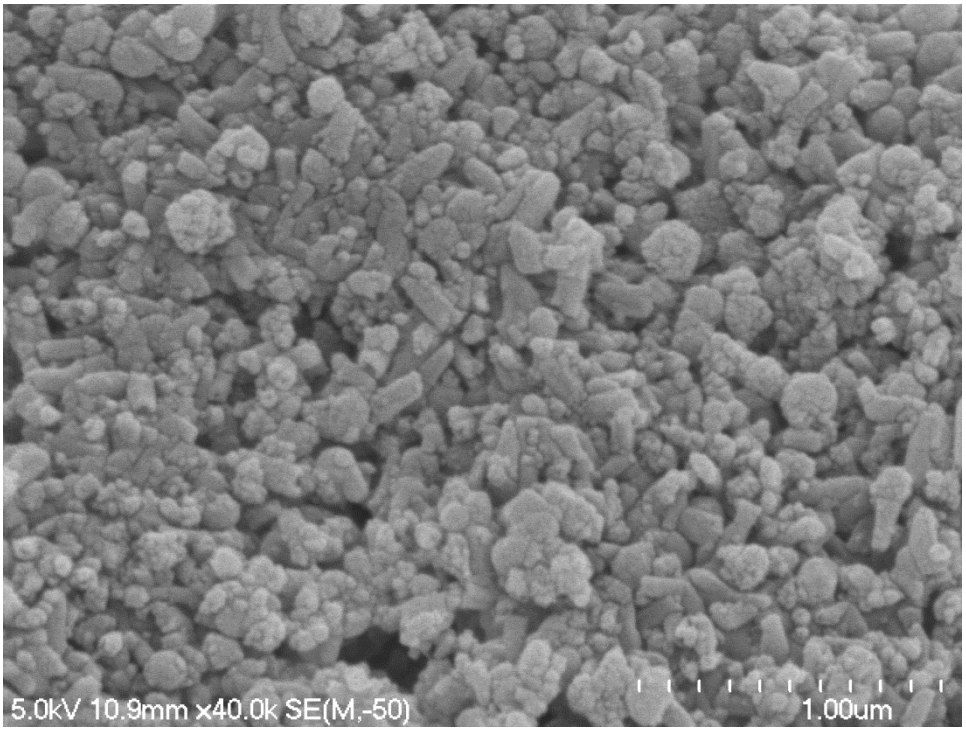
5.0kV 10.9mm x40.0k SE(M,-50)
1.00um

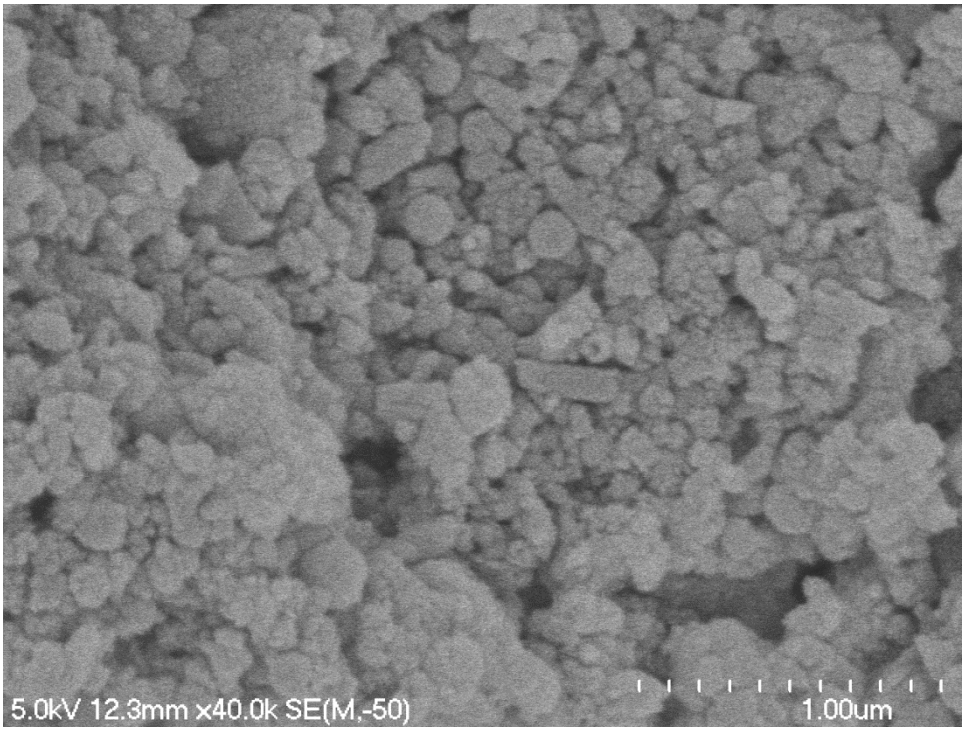
5.0kV 12.3mm x40.0k SE(M,-50)
1.00um

OS2 – remoulded state

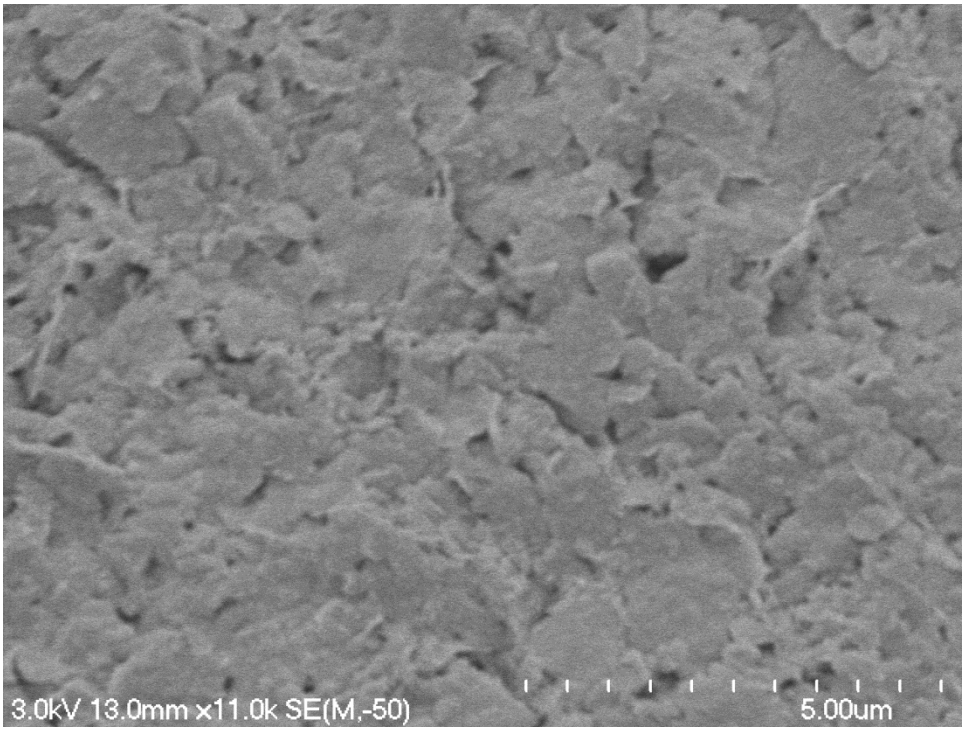

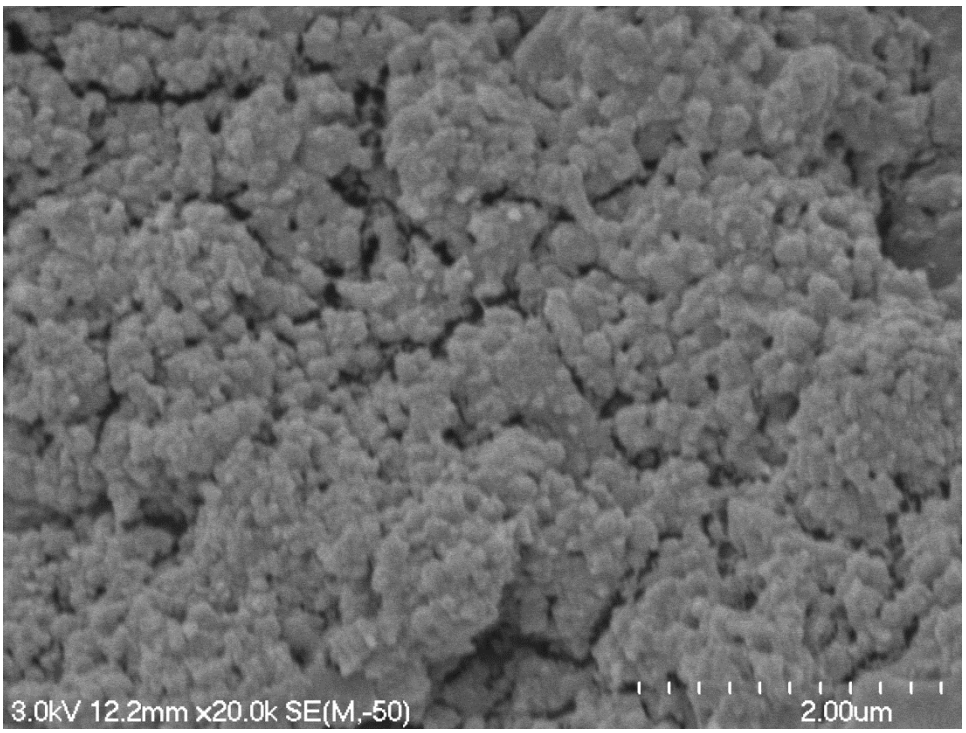

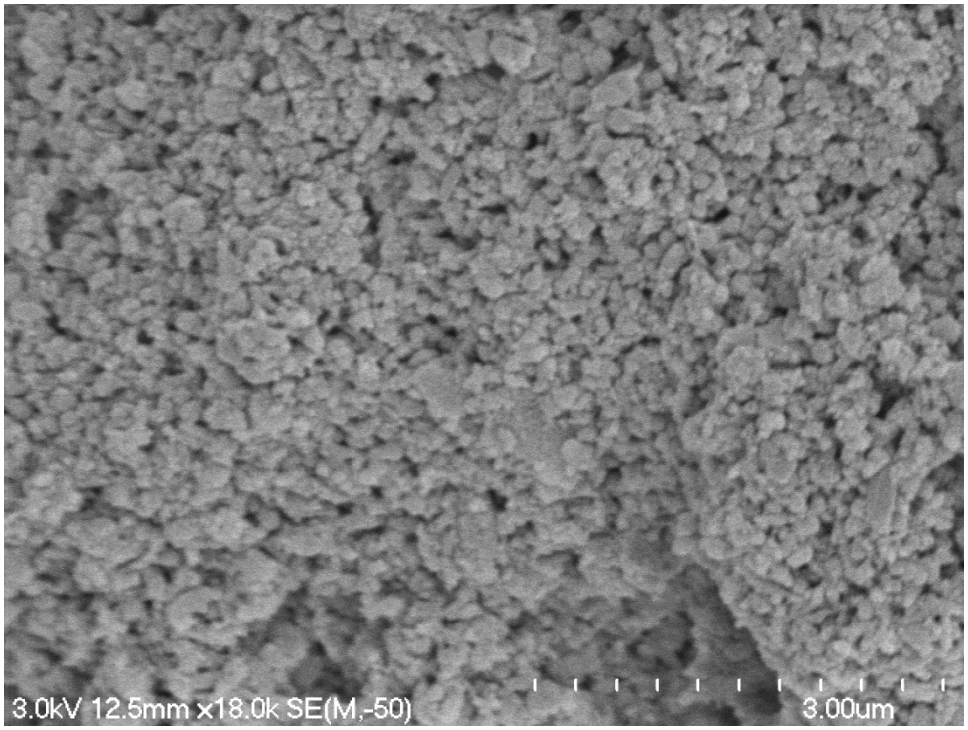
3.0kV 12.5mm x18.0k SE(M,-50)
3.00um

OLRO – remoulded

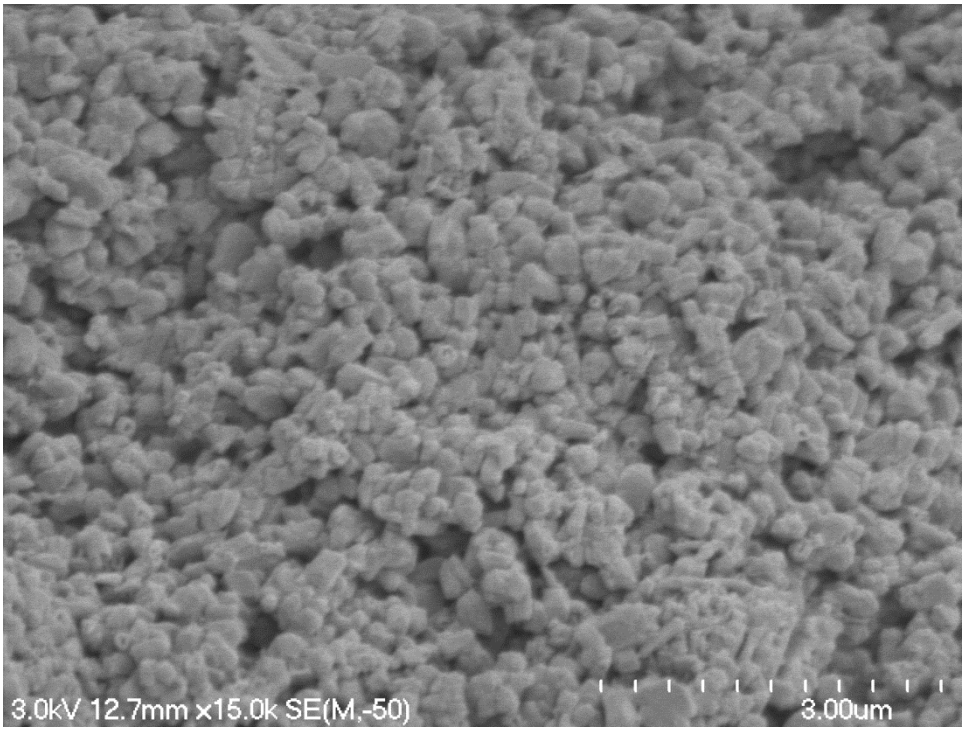

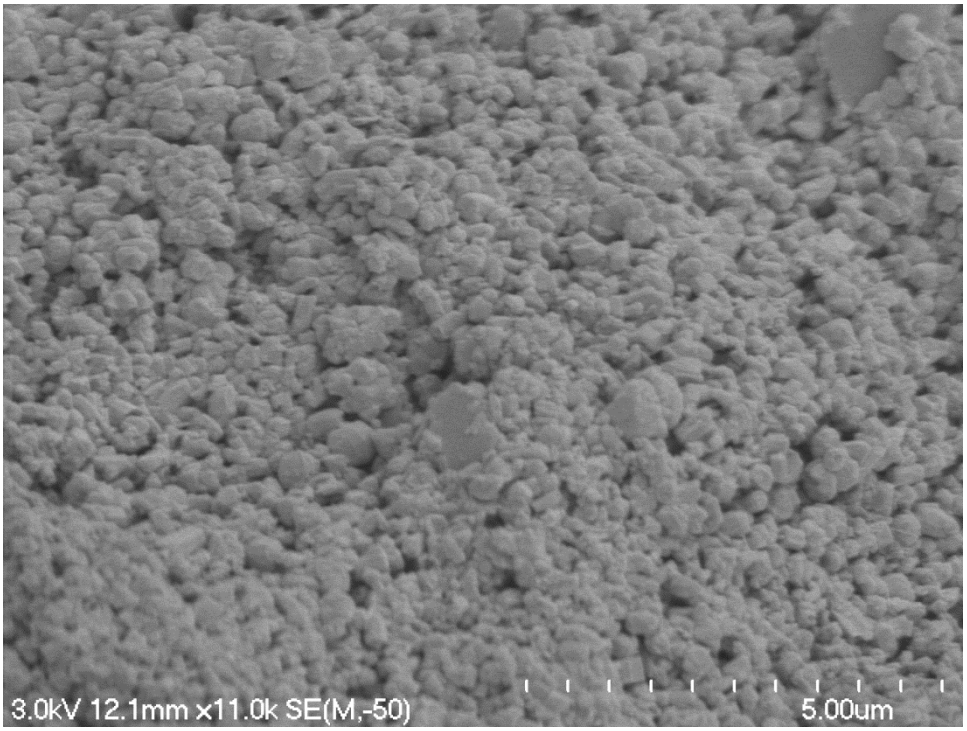

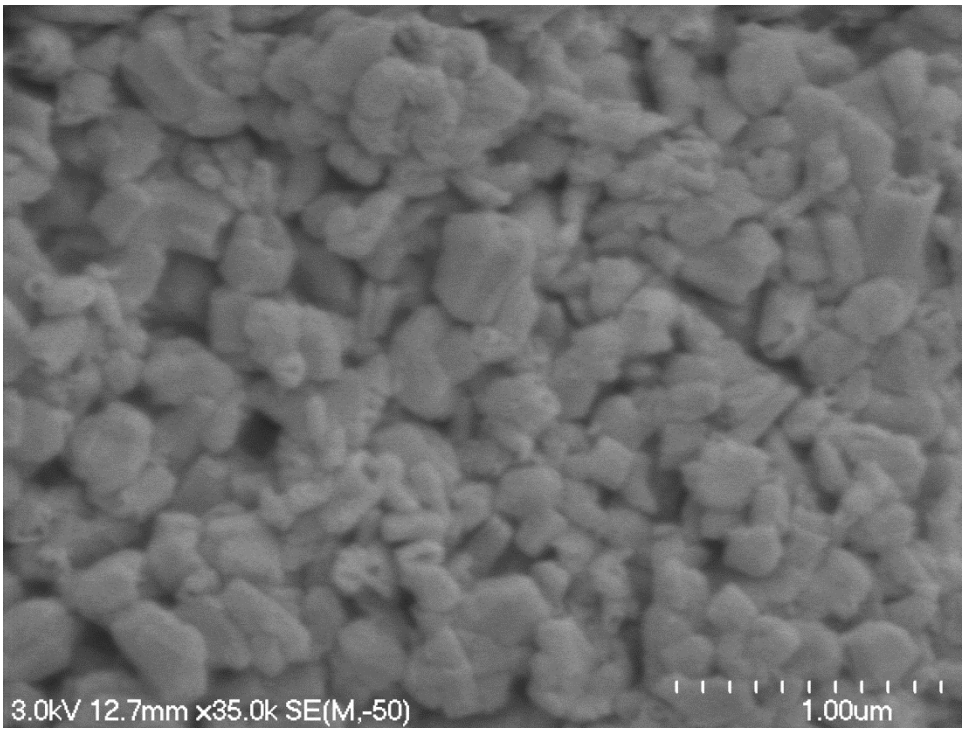
3.0kV 12.7mm x35.0k SE(M,-50)
1.00um

TPS1 - Peak strength

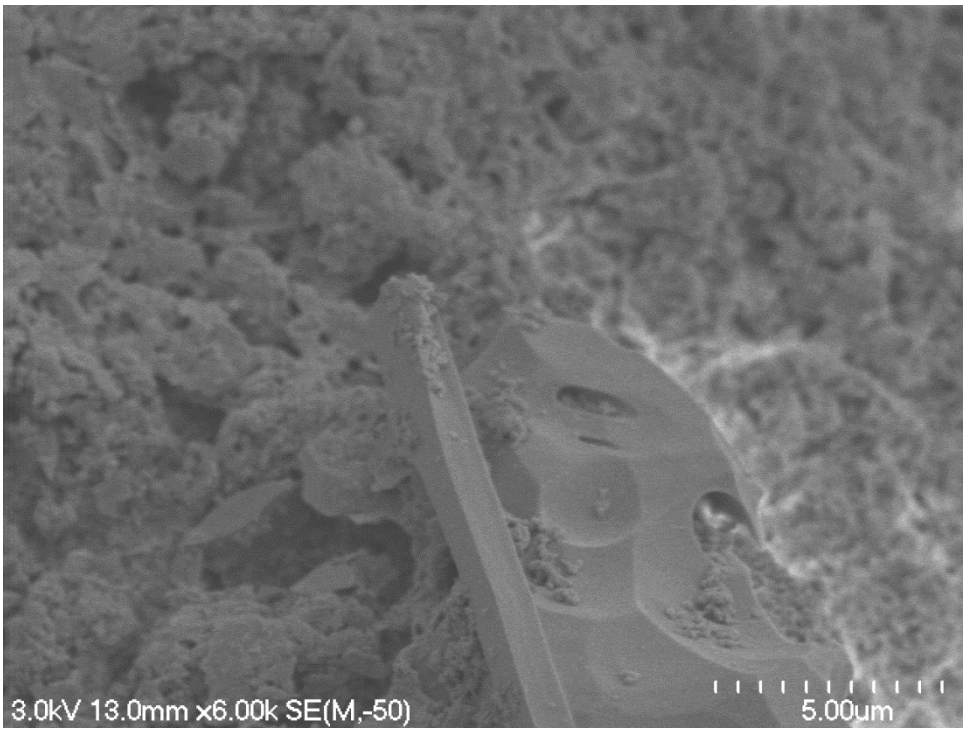

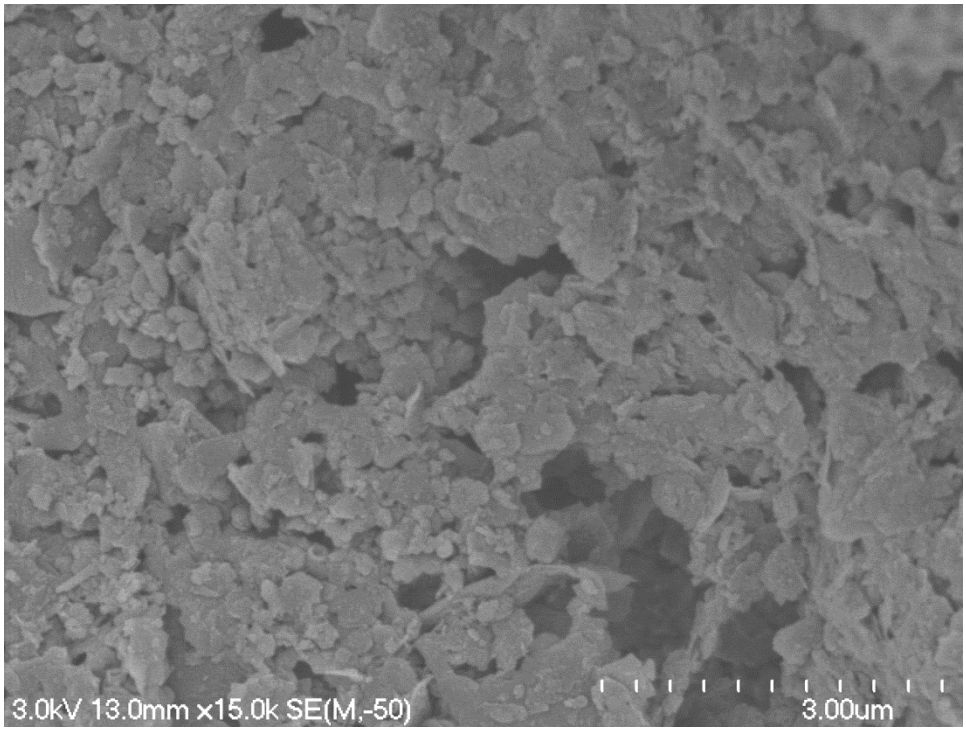

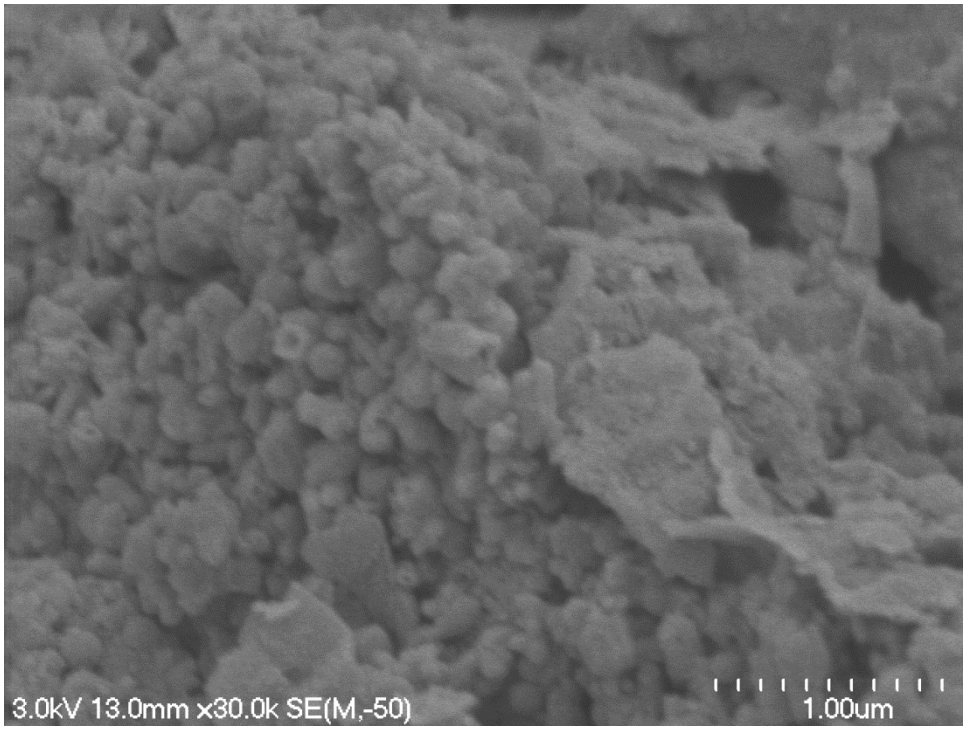
3.0kV 13.0mm x30.0k SE(M,-50)
1.00um

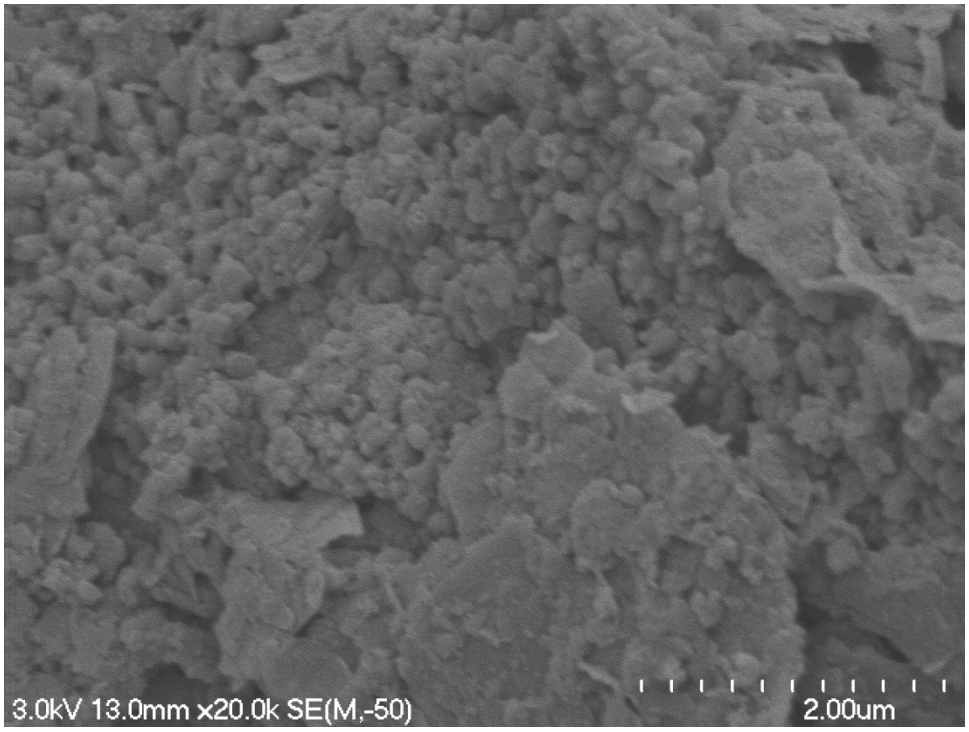
3.0kV 13.0mm x20.0k SE(M,-50)
2.00um

TPS1 – Remoulded strength state

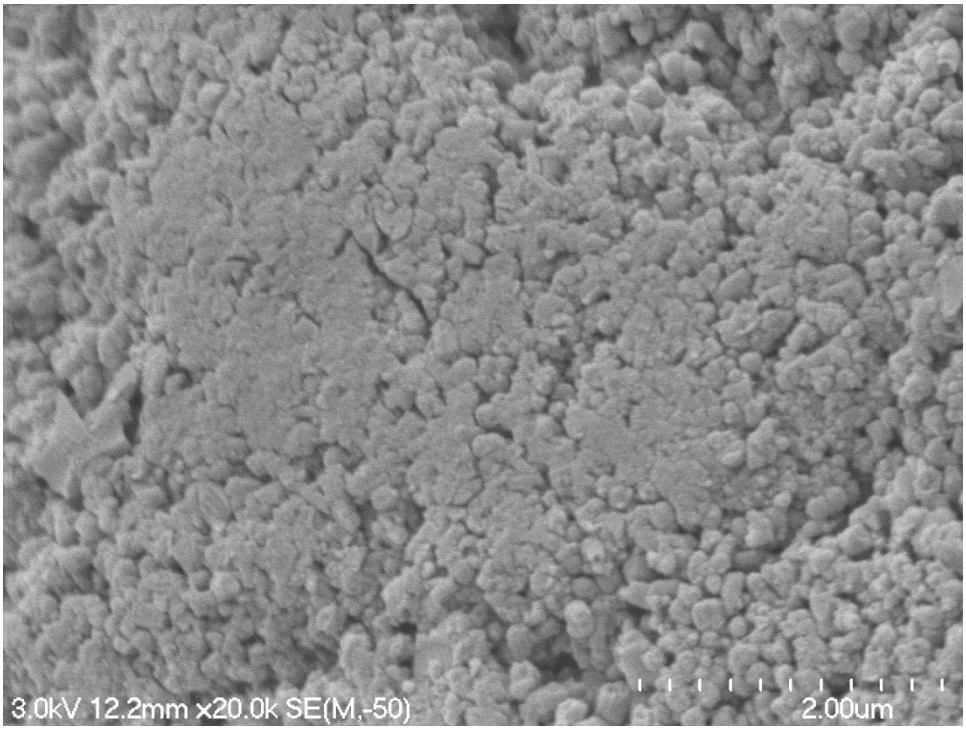

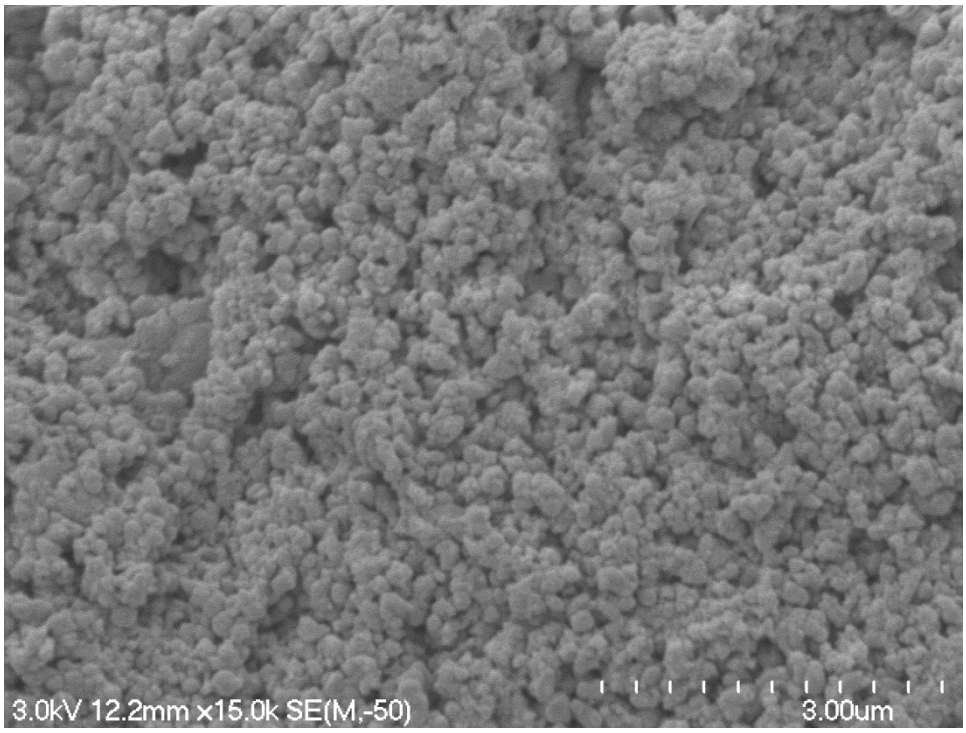

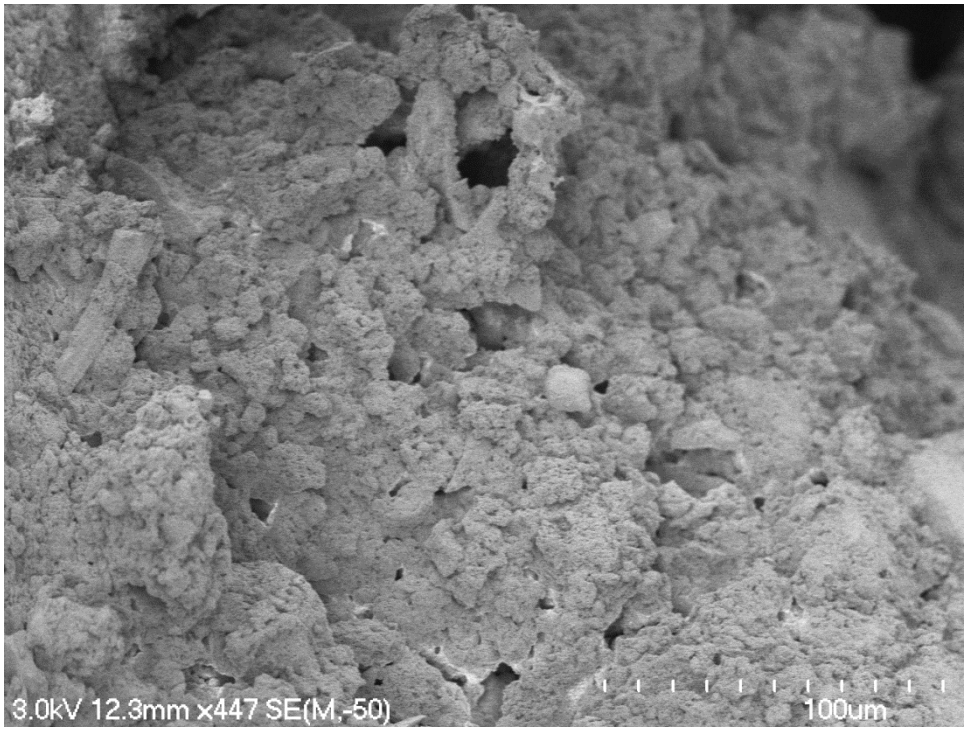
3.0kV 12.3mm x447 SE(M,-50)
100um

PS1 – peak strength state

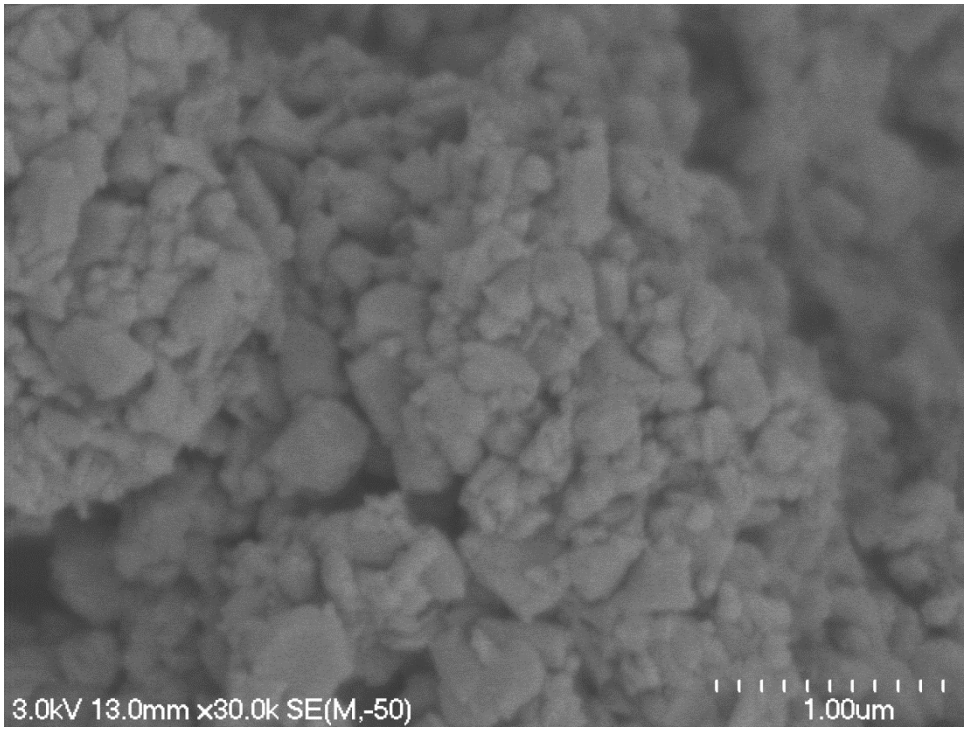

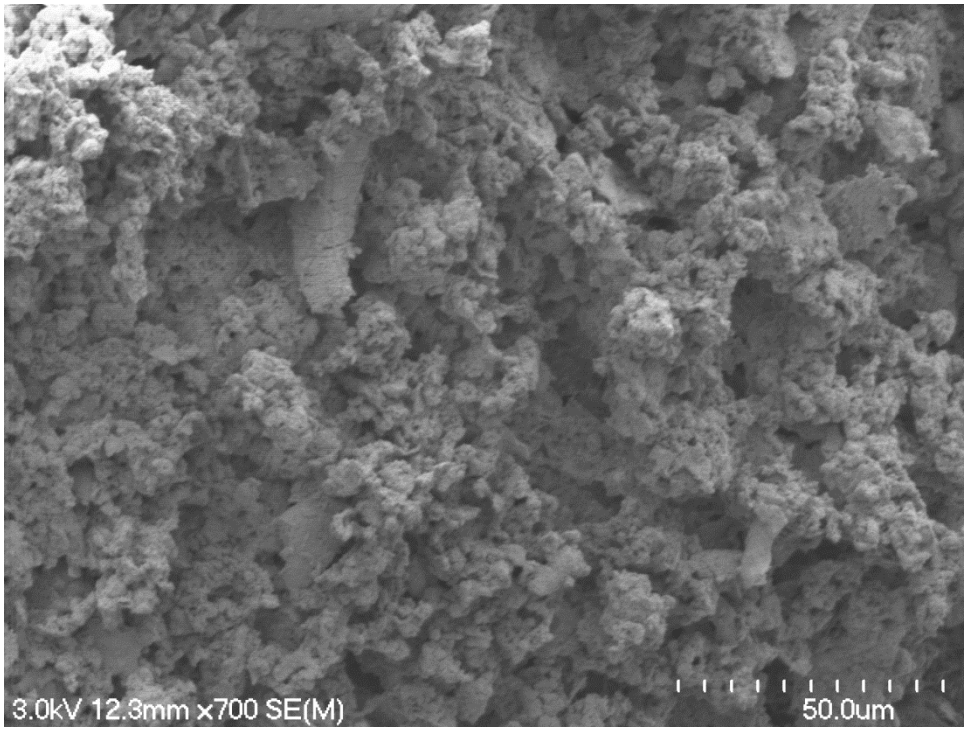

PS1 – remoulded strength state

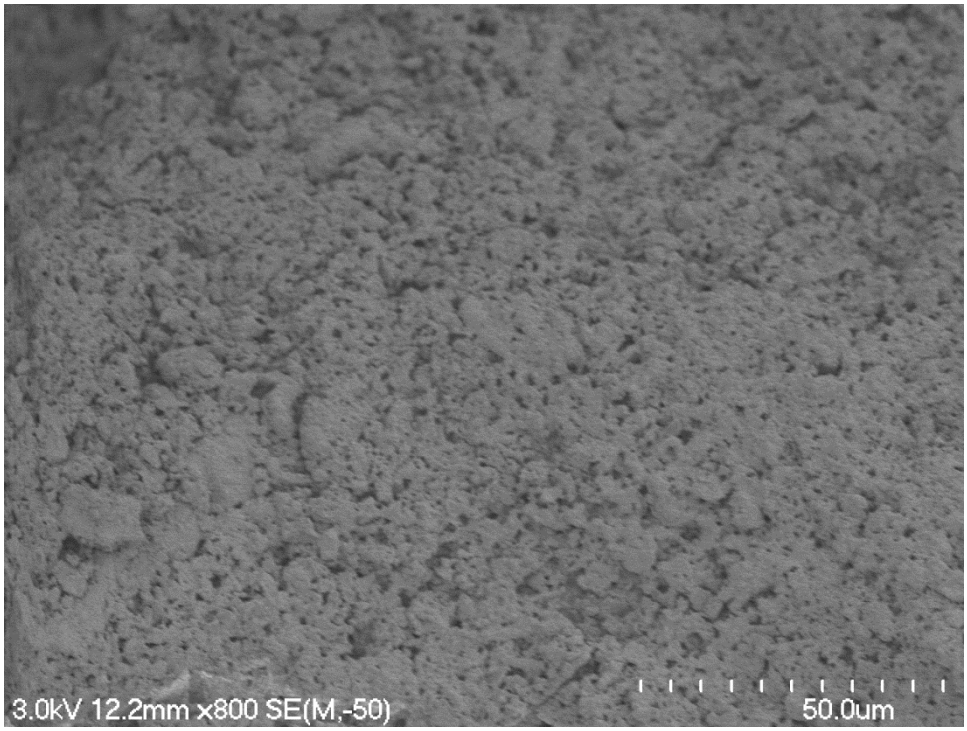

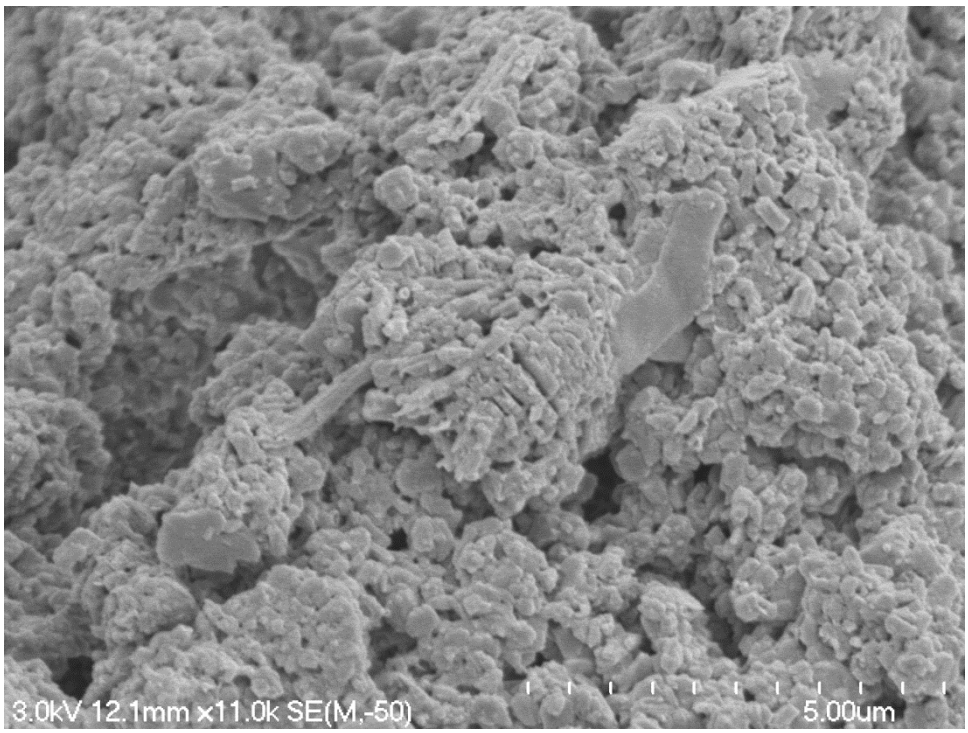

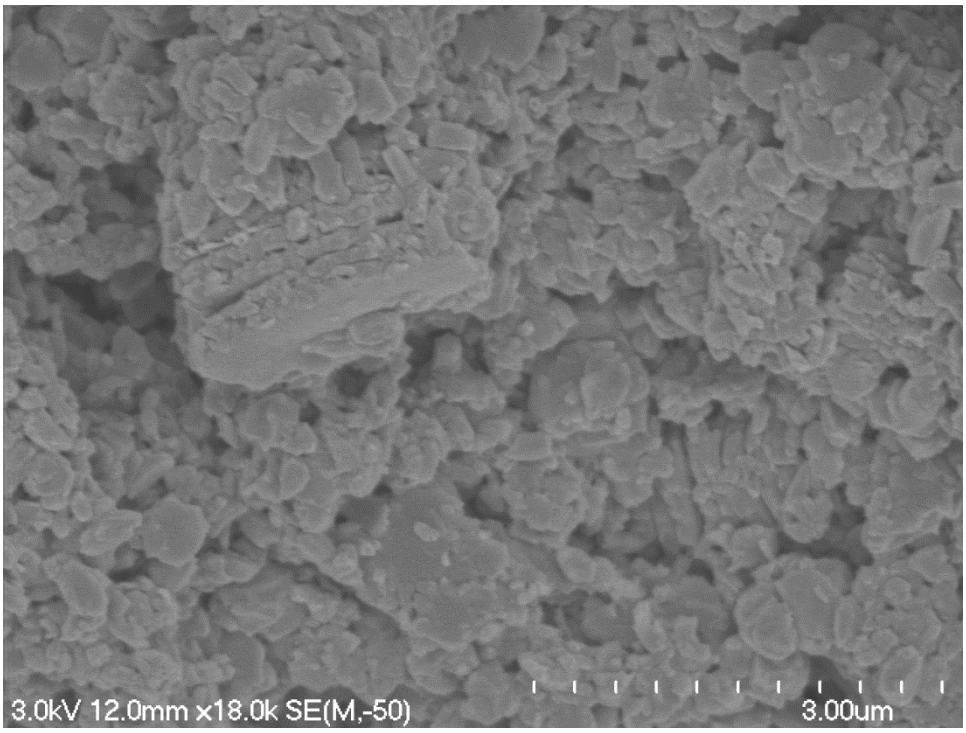
3.0kV 12.0mm x18.0k SE(M,-50)
3.00um

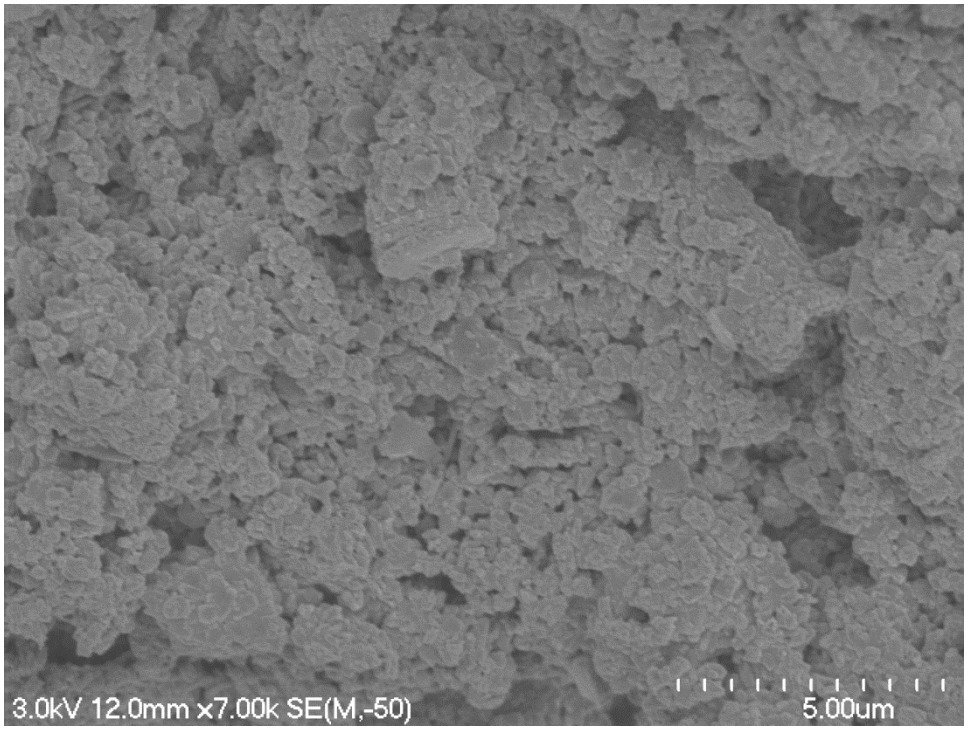
3.0kV 12.0mm x7.00k SE(M,-50)
5.00um

PS2 – Peak strength state

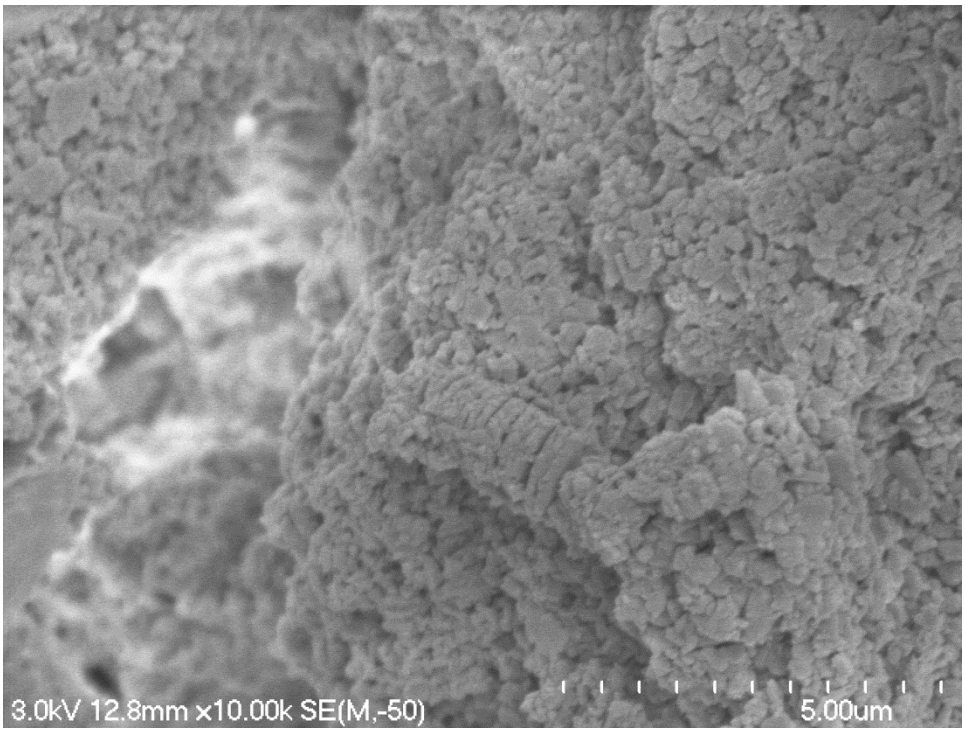

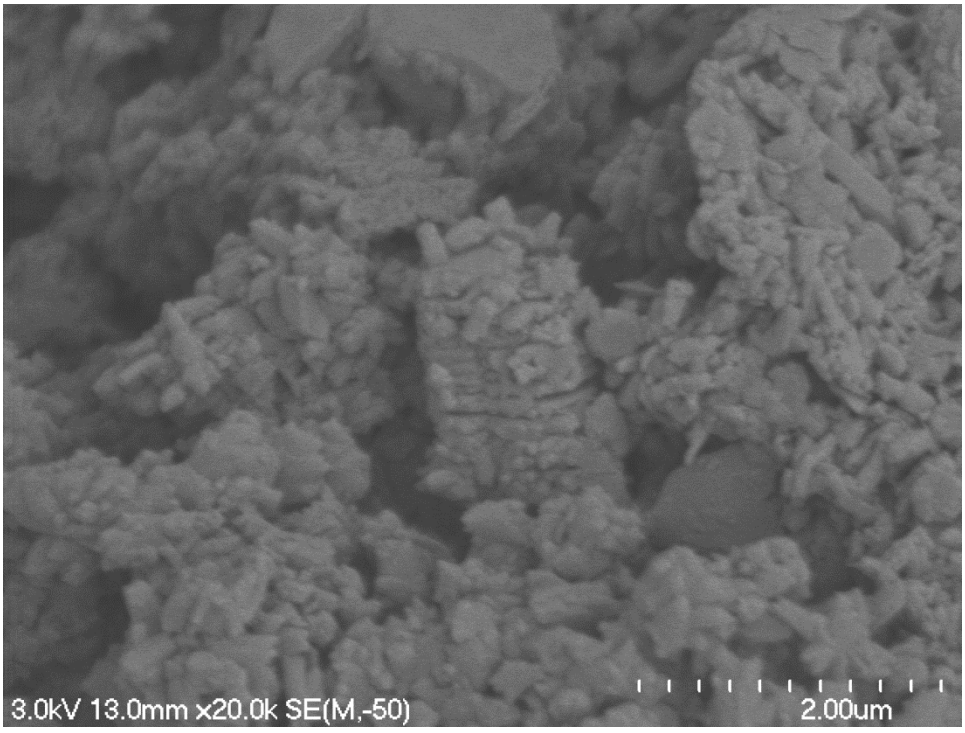

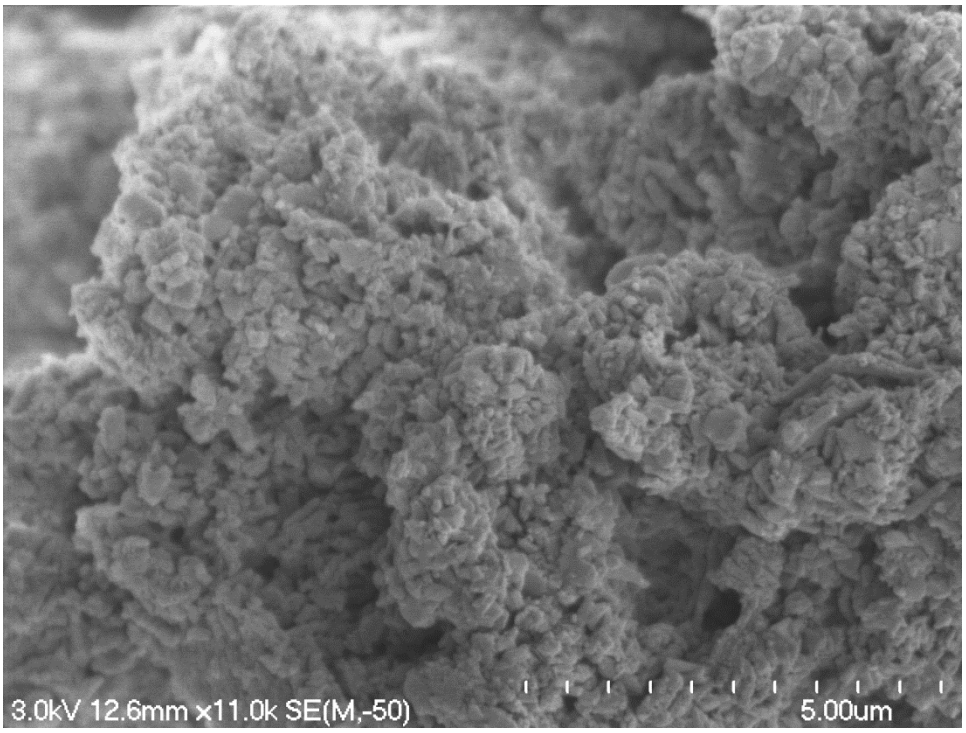
3.0kV 12.6mm x11.0k SE(M,-50)
5.00um

PS2 – remoulded state

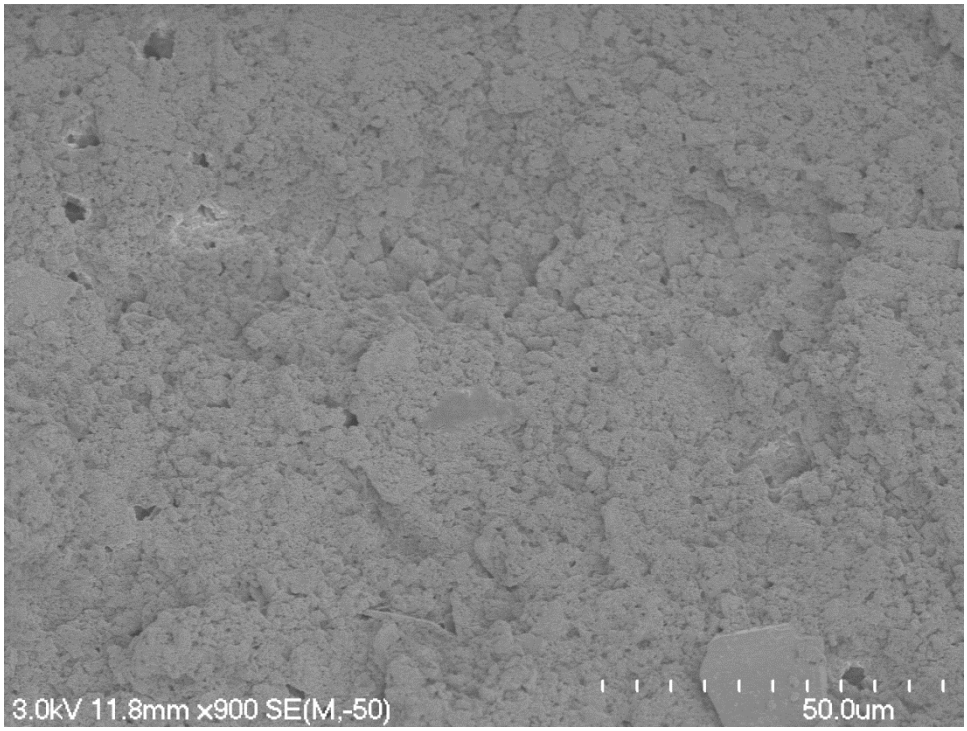

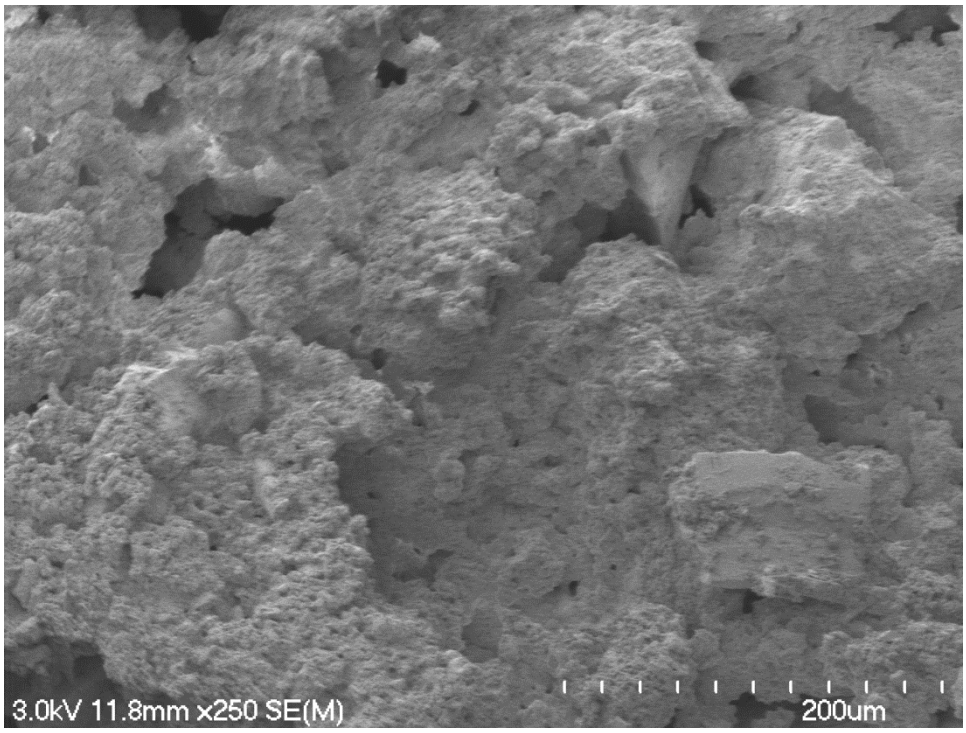

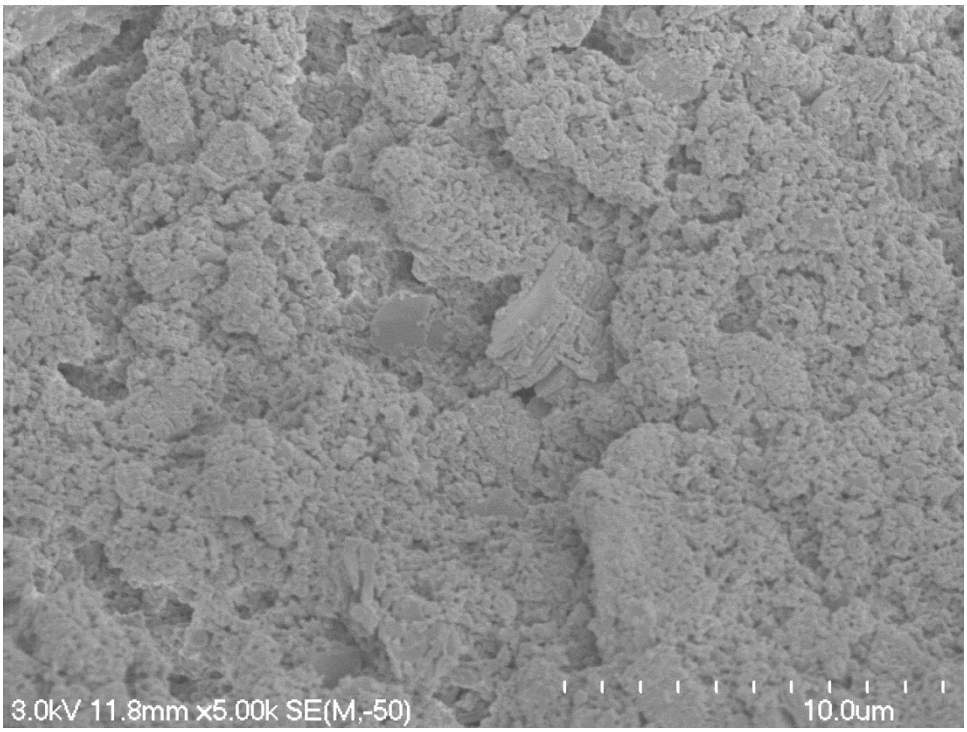
3.0kV 11.8mm x5.00k SE(M,-50)
10.0um

TS1 – Peak strength state

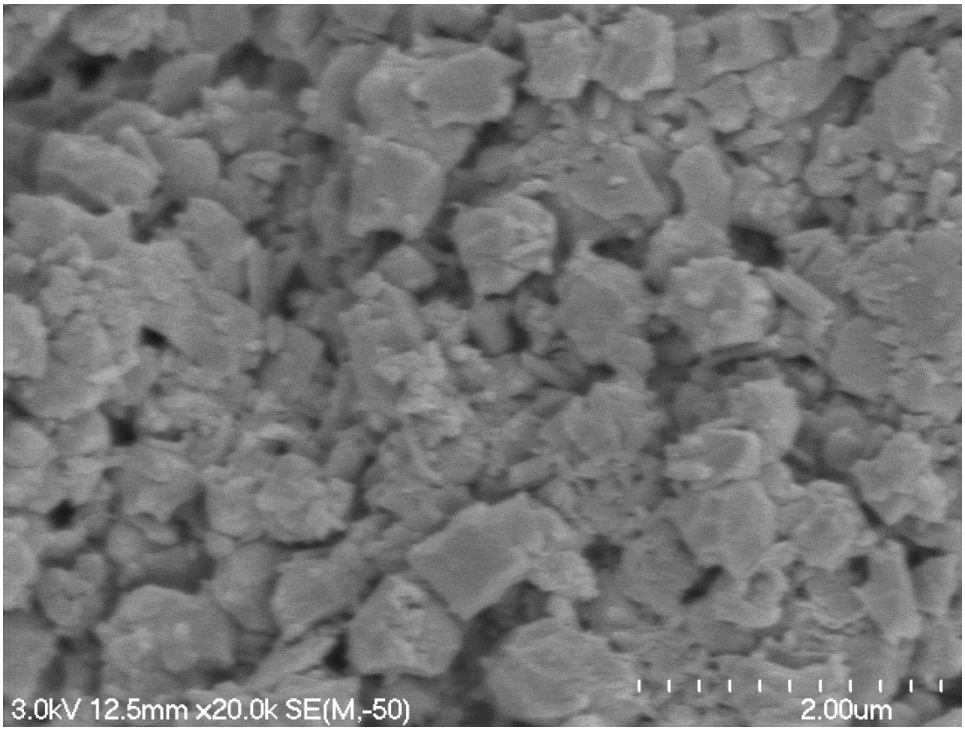

TS2 – Peak strength state

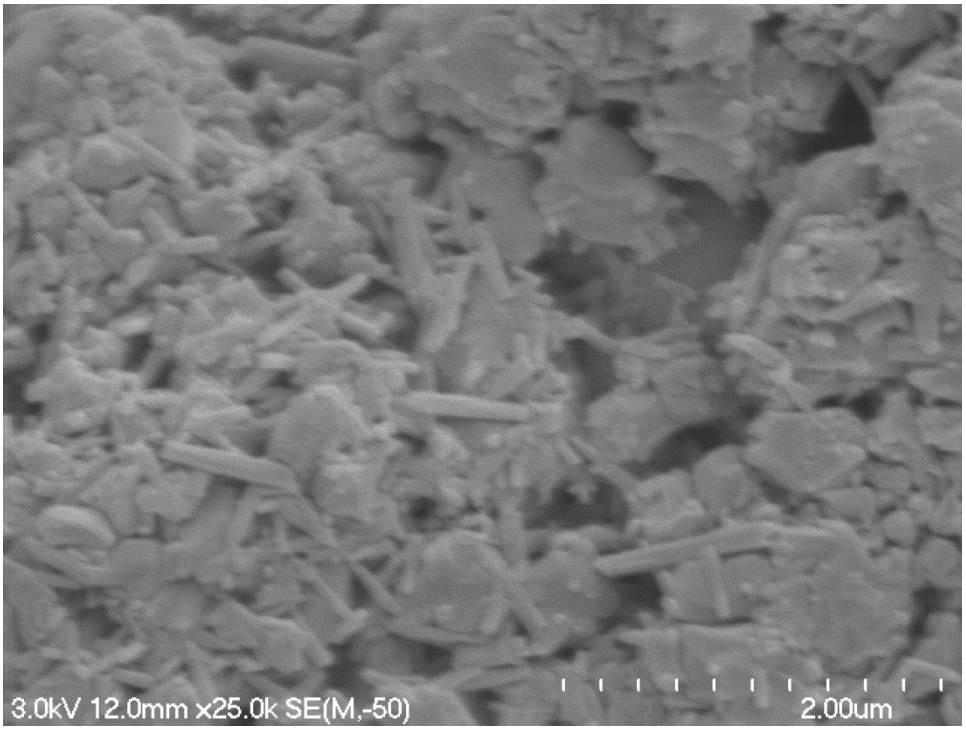

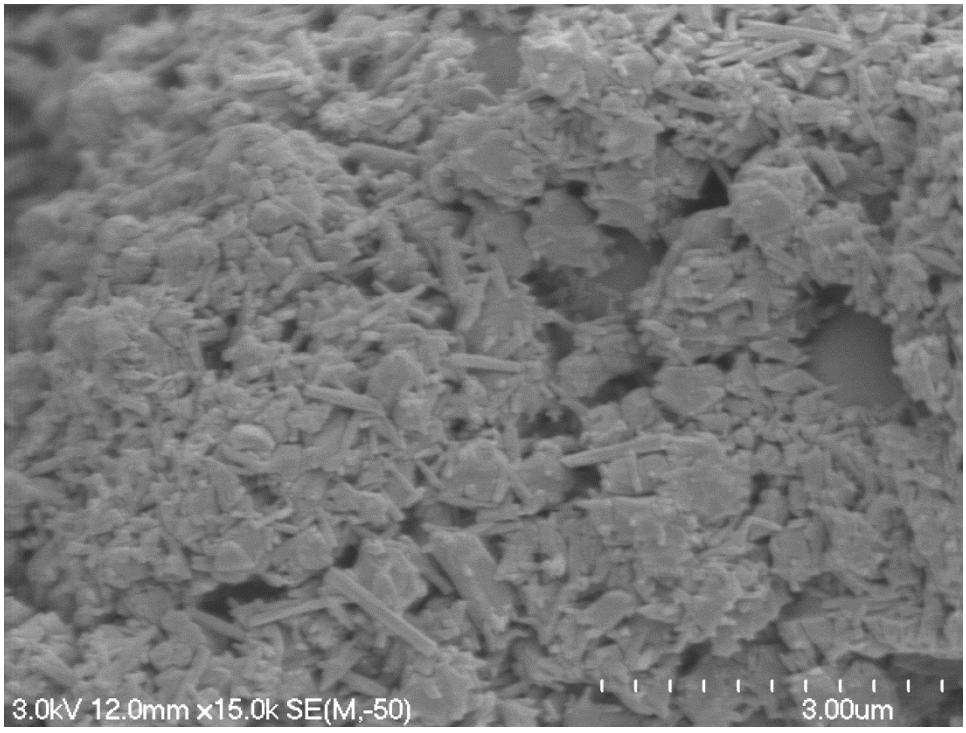

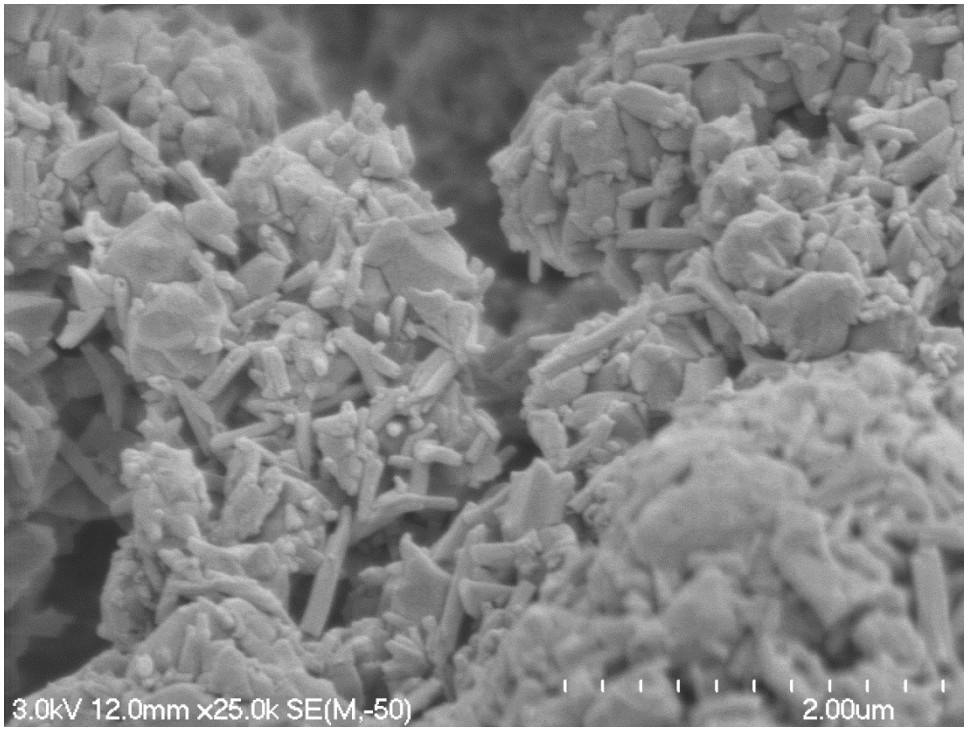
3.0kV 12.0mm x25.0k SE(M,-50)
2.00um

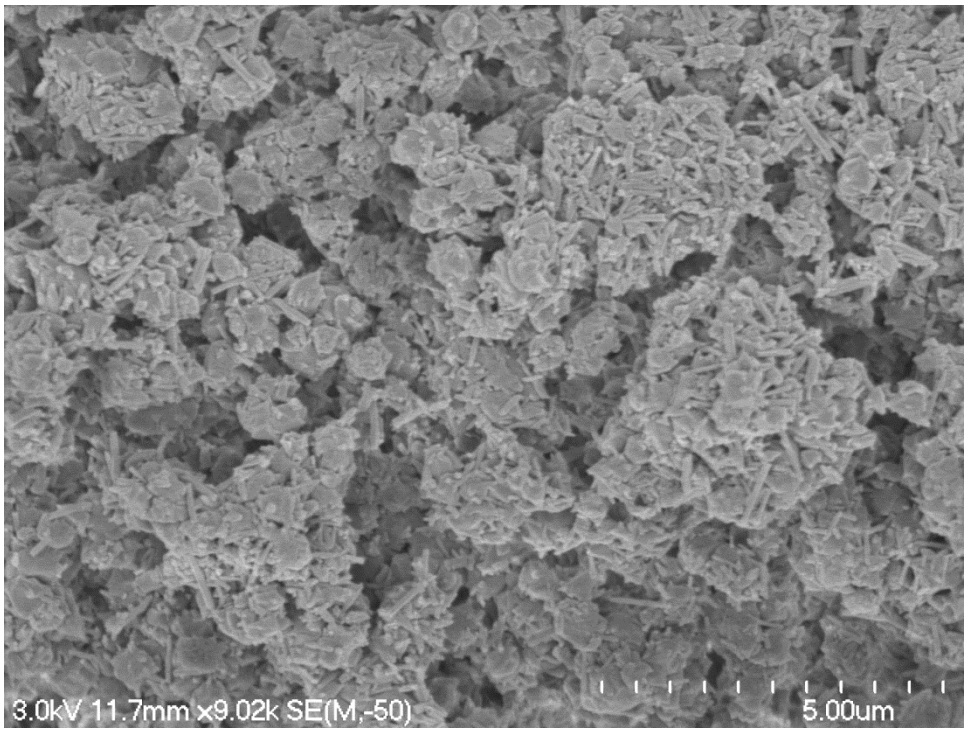
3.0kV 11.7mm x9.02k SE(M,-50)
5.00um

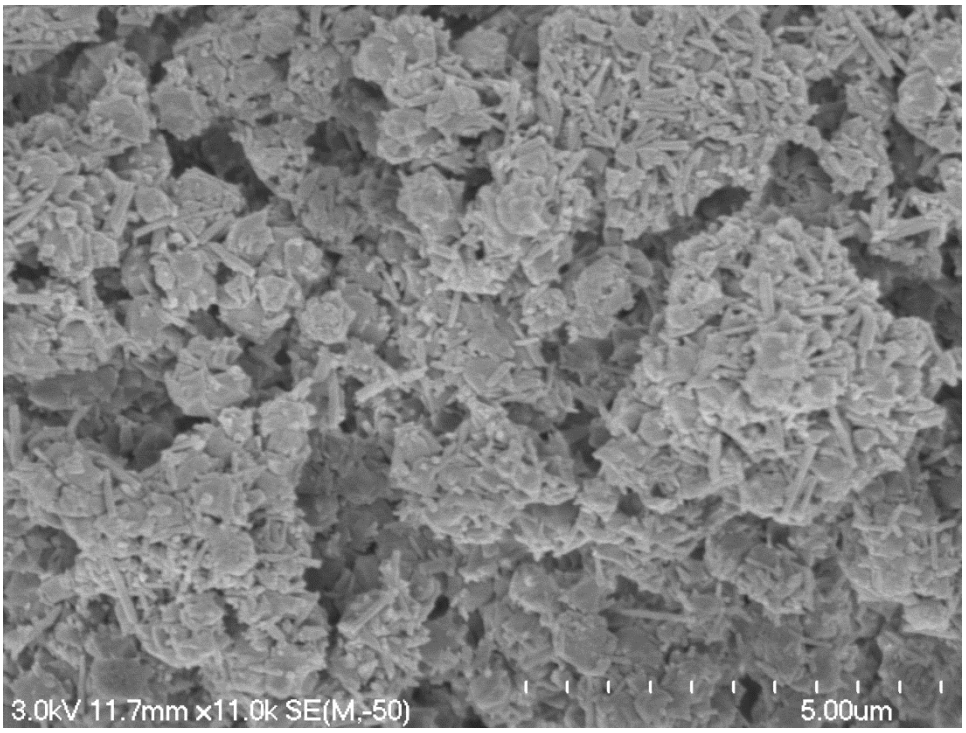
3.0kV 11.7mm x11.0k SE(M,-50)
5.00um

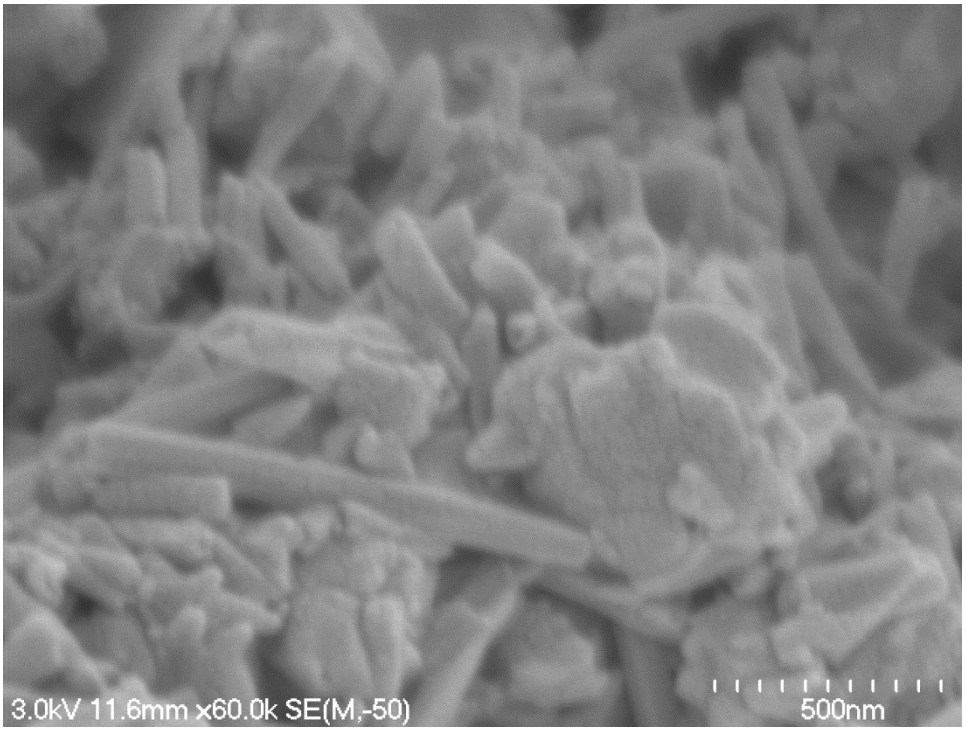
3.0kV 11.6mm x60.0k SE(M,-50)
500nm

TS3 – Peak strength state

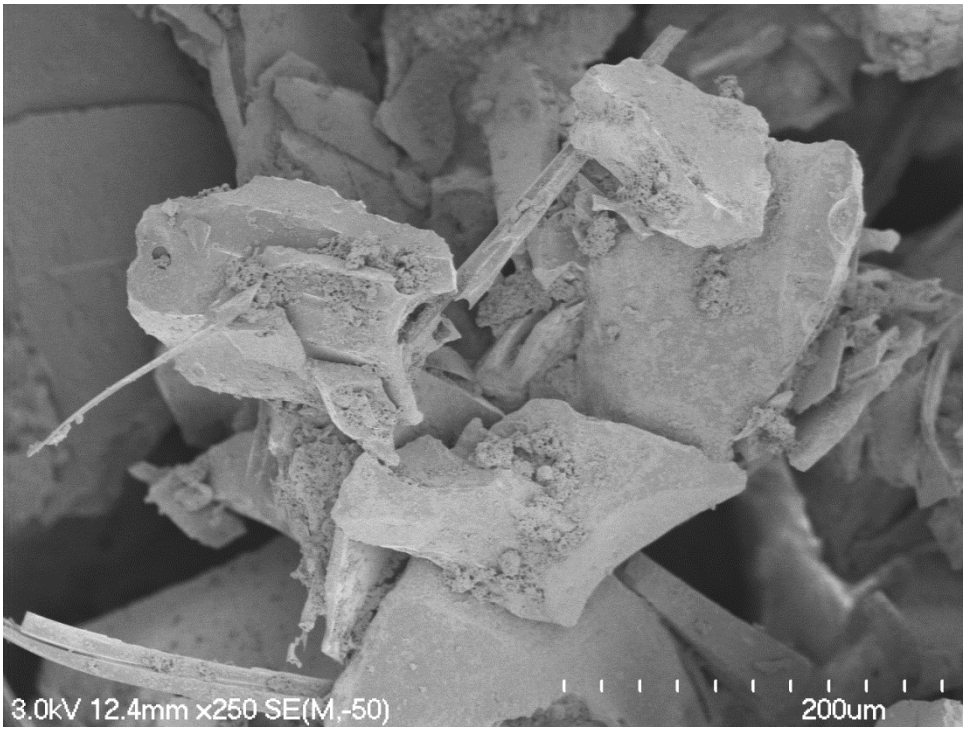


3.0kV 12.8mm x350 SE(M,-50)
100um

TS4 – Peak strength state

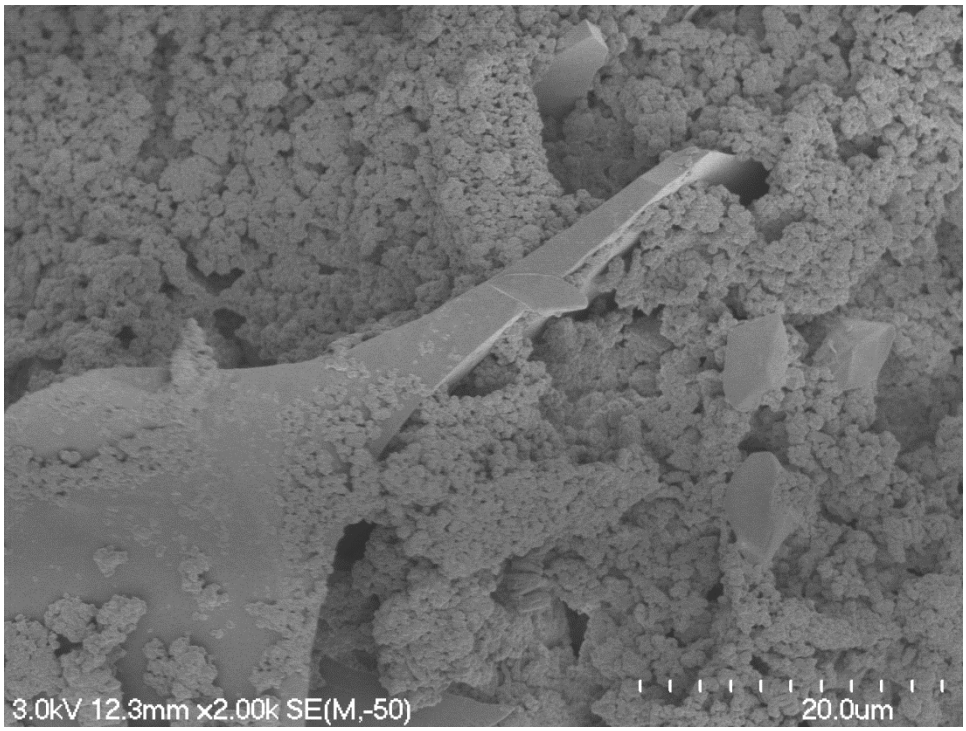

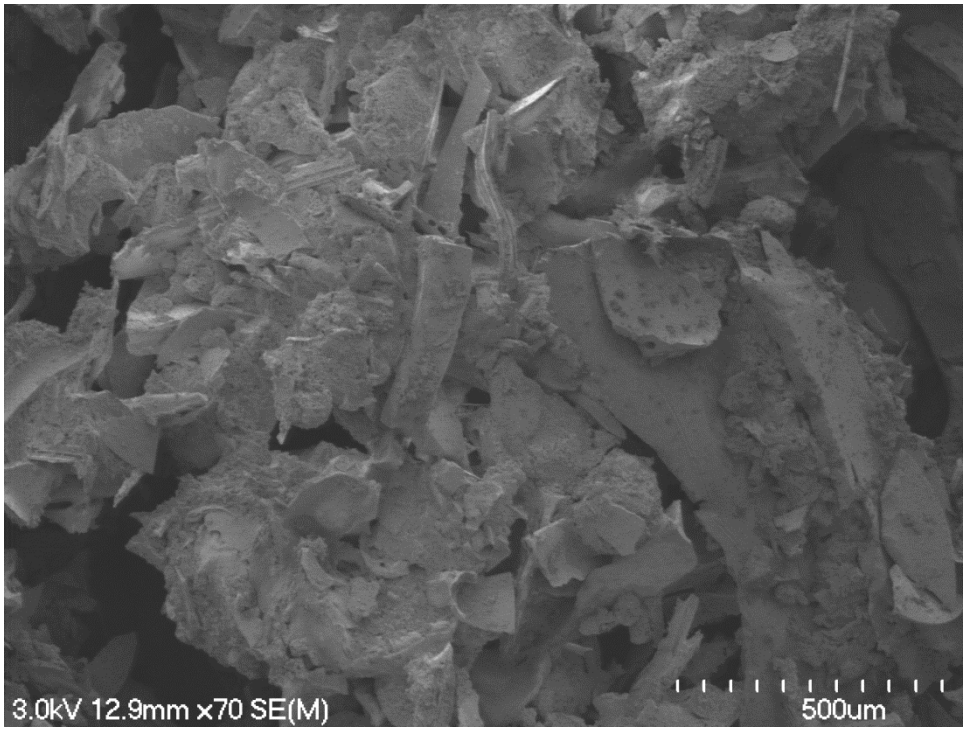

RS1 – Peak strength state

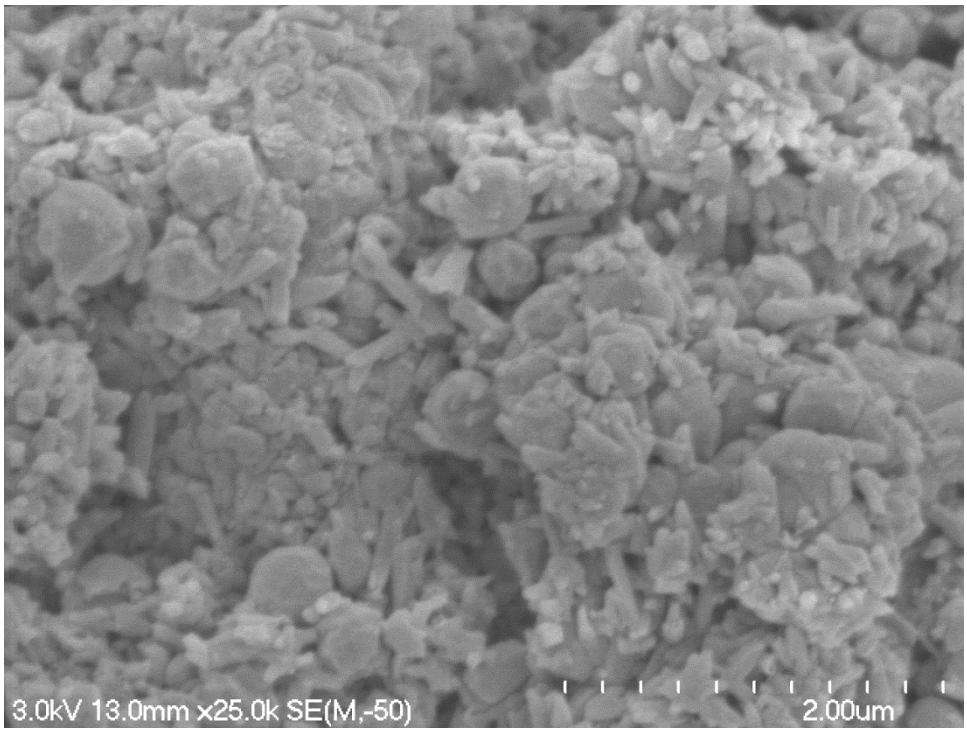

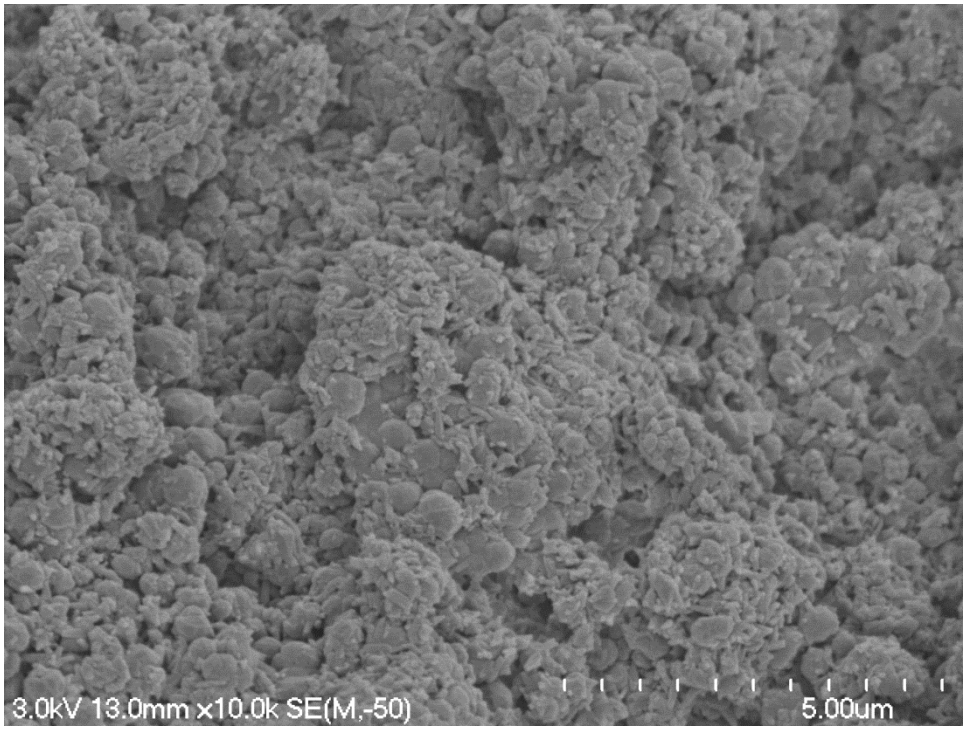

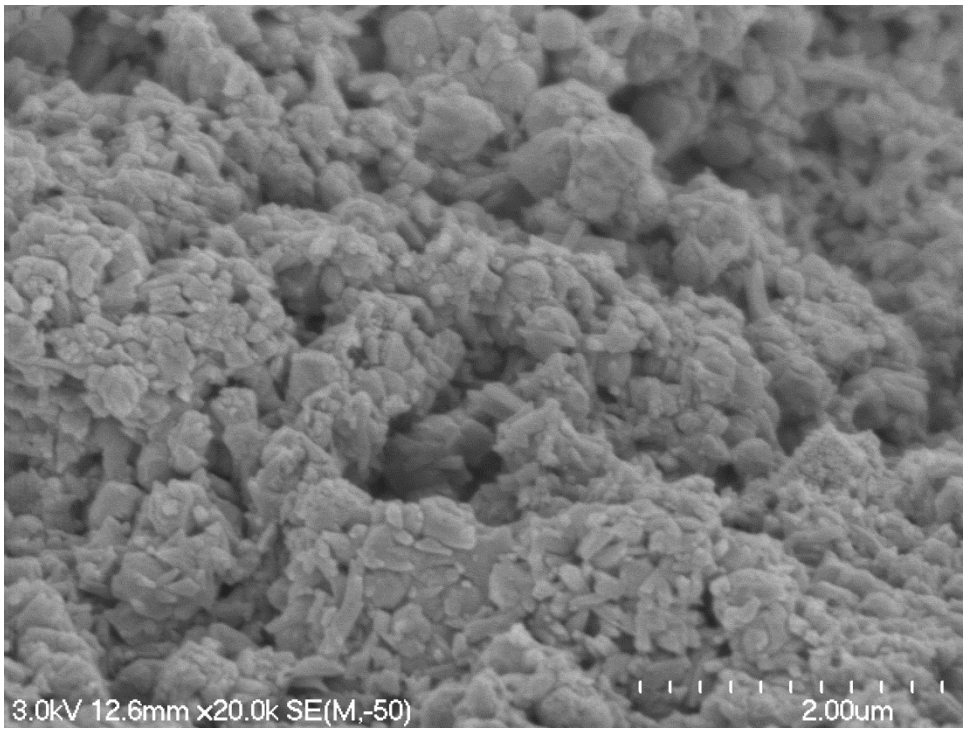
3.0kV 12.6mm x20.0k SE(M,-50)
2.00um

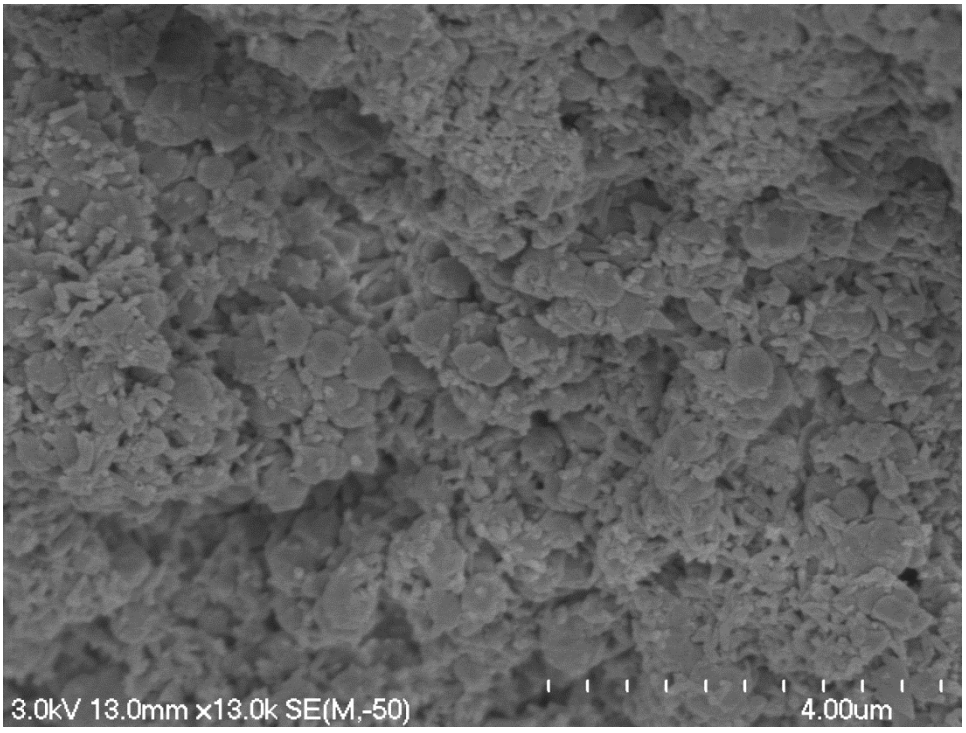
3.0kV 13.0mm x13.0k SE(M,-50)
4.00um

RS1 – remoulded state

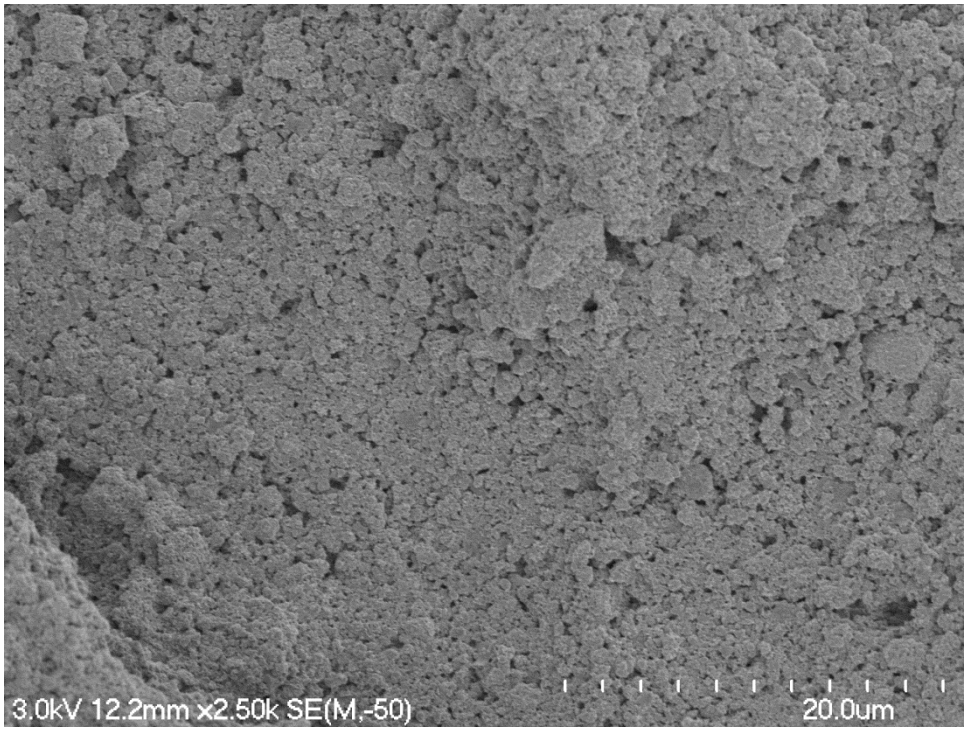

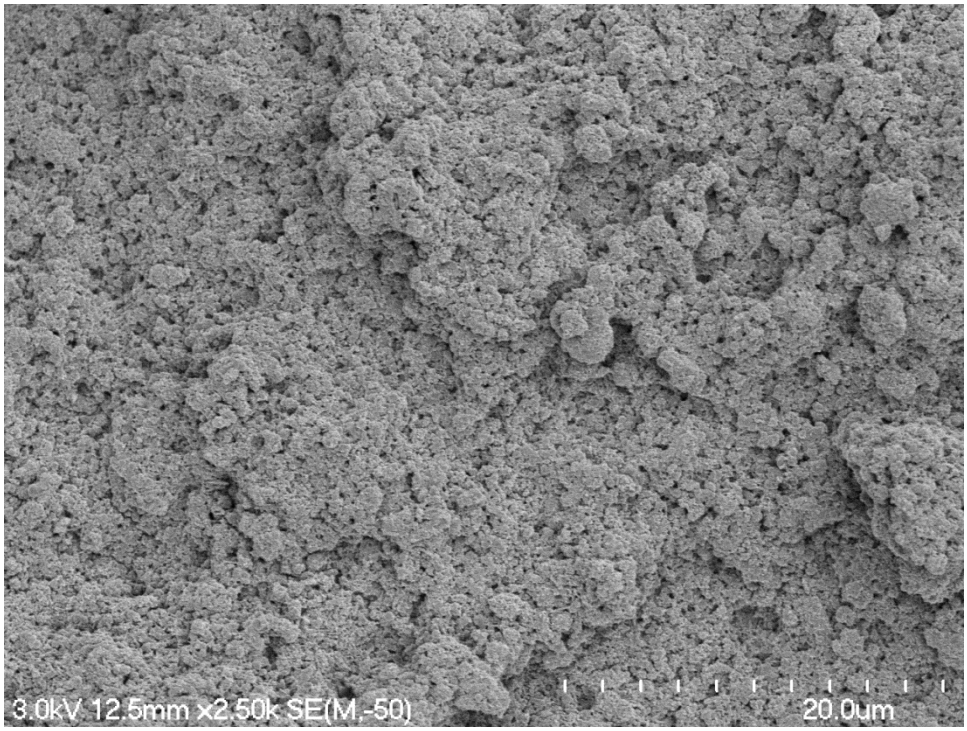

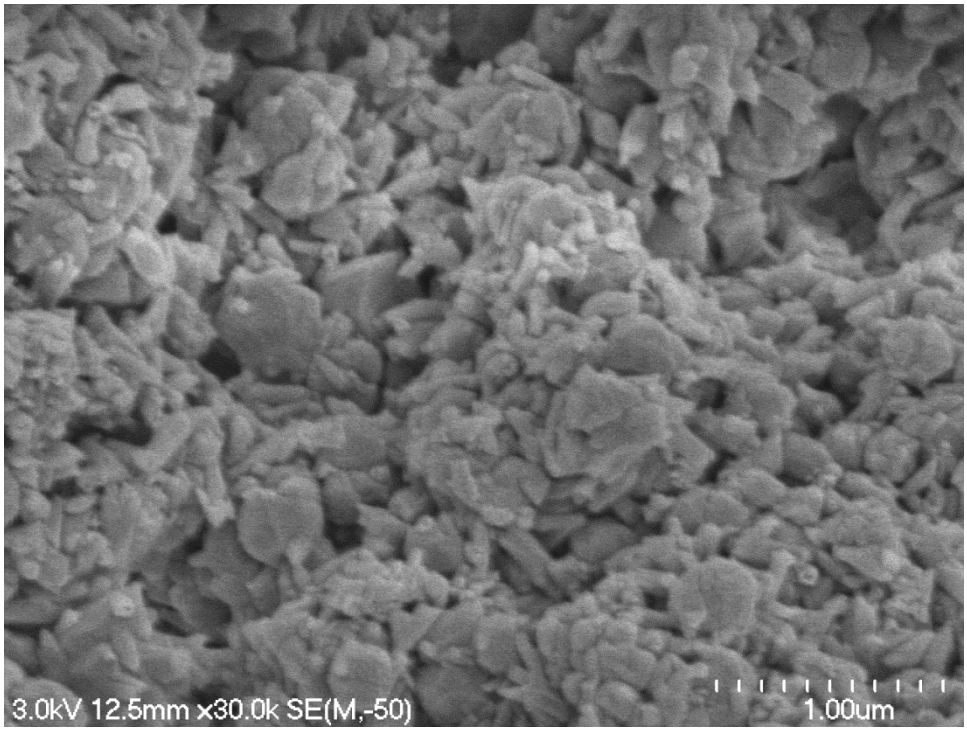
3.0kV 12.5mm x30.0k SE(M,-50)
1.00um